Scandium Cluster and Metallocene Chemistry

Inaugural-Dissertation

zur

Erlangung des Doktorgrades

der Mathematisch-Naturwissenschaftlichen Fakultät

der Universität zu Köln

vorgelegt von

Selvan Demir

aus Leonberg

Köln 2010

Berichterstatter:	Prof. Dr. Gerd Meyer
	Prof. William J. Evans PhD
	Prof. Dr. Peter Roesky
Tag der mündlichen Prüfung:	11.10.2010

Die vorliegende Arbeit wurde von September 2007 bis August 2010 am Institut für Anorganische Chemie der Universität zu Köln unter der Anleitung von Prof. Dr. Gerd Meyer sowie von Februar 2009 bis August 2009 und von Oktober 2009 bis März 2010 am Chemistry Department der University of California Irvine unter der Betreuung von Prof. William J. Evans PhD angefertigt.

Abstract

This thesis focuses on the synthesis and characterization of scandium compounds. One goal was to investigate the solution reactivity of $\{CSc_6\}I_{12}Sc$, which resulted in the isolation of a molecular scandium nitride, $[(C_5H_5)_2ScNSc(C_5H_5)(THF)]_2$, and a scandium propoxide complex, $[(C_5H_5)_2Sc(\mu\text{-OPr})]_2$.

Besides this, priority was given to the synthesis and characterization of the first scandium dinitrogen complex, $[(C_5Me_4H)_2Sc]_2(\mu\text{-}\eta^2\text{:}\eta^2\text{-}N_2)$, along with its precursor compounds: $(C_5Me_4H)_2ScCl(THF)$, $(C_5Me_4H)_2Sc(\eta^3\text{-}C_3H_5)$ and $[(C_5Me_4H)_2Sc]_2[(\mu\text{-Ph})BPh_3]$. The reduction of the latter complex with KC_8 under N_2 gave the elusive $[(C_5Me_4H)_2Sc]_2(\mu\text{-}\eta^2\text{:}\eta^2\text{-}N_2)$. Structure determination supported by DFT calculations revealed a coplanar arrangement of a bridging side-on bound dinitrogen unit and two scandium atoms. In one reaction, the dinitrogen complex co-crystallized with an oxide impurity as $\{[(C_5Me_4H)_2Sc]_2(\mu\text{-}\eta^2\text{:}\eta^2\text{-}N_2)[(C_5Me_4H)_2Sc]_2(\mu\text{-O})\}$.

Additionally, the borohydride complexes $(C_5Me_4R)_2M(BH_4)(THF)_x$ (M = Sc, Y; R = H, Me; x = 0, 1) were prepared. Yttrium borohydride complexes were investigated with respect to their dinitrogen activation capability, but were found to be inactive. Ligand based reactivity of $(C_5Me_4R)_2Sc(\eta^3\text{-}C_3H_5)$ (R = H, Me) occured with 9-BBN (9-borabicyclo[3.3.1]nonane) to form the corresponding $(C_5Me_4R)_2Sc(\mu\text{-H})_2BC_8H_{14}$ complexes, from which oxygen exposure (R = H) yielded $(C_5Me_4H)_2Sc(\mu\text{-O})BC_8H_{14}$.

Subsequent investigations focused on the reaction of $[(C_5Me_4H)_2Sc]_2[(\mu\text{-Ph})BPh_3]$ with KC_5Me_4H and gave $(\eta^5\text{-}C_5Me_4H)_2Sc(\eta^1\text{-}C_5Me_4H)$, which was structurally characterized and is the first example of an η^1-coordination mode for a $(C_5Me_4H)^-$ ligand bound to a rare-earth metal. This complex undergoes Sigma Bond Metathesis (SBM) reactivity towards diphenyldichalcogenides, PhEEPh (E = S, Se, Te), to produce $[(C_5Me_4H)_2ScSPh]_2$ and $(C_5Me_4H)_2ScEPh$ (E = Se, Te) complexes. The analogous products could be isolated and were fully characterized through the ligand based reactivity of $(C_5Me_4H)_2Sc(\eta^3\text{-}C_3H_5)$ and

PhEEPh reagents. These reactions also worked in the presence of THF to yield the solvated complexes $(C_5Me_4H)_2ScEPh(THF)$ (E = S, Se, Te). The reaction of $(C_5Me_4H)_2Sc(\eta^3\text{-}C_3H_5)$ with pySSpy produced the analogous $(C_5Me_4H)_2ScSpy$ complex. In addition, the formation of a scandium selenium cluster complex $[(C_5Me_4H)Sc]_3[SePh]_6$ was identified and reactivity studies with PhTeTePh additionally resulted in the isolation of a scandium tellurium cluster compound, $\{[(C_5Me_5)Sc]_4(\mu_3\text{-}Te)_4\}$.

The functionalization of N_2O via insertion into the metal carbon bond of allyl compounds, $(C_5Me_4R)_2M(\eta^3\text{-}C_3H_5)$ (M = Sc, Y, La, Sm; R = H, Me) formed $[(C_5Me_4R)_2M(\mu\text{-}\eta^1{:}\eta^2\text{-}ON{=}NC_3H_5)]_2$ complexes. The insertion of $^{i}PrN{=}C{=}N^{i}Pr$ into the Sc-C bond of $(C_5Me_4H)_2Sc(\eta^3\text{-}C_3H_5)$ gave $(C_5Me_4H)_2Sc[(^{i}Pr)NC(CH_2CH{=}CH_2)N(^{i}Pr)\text{-}\kappa^2N,N']$. Finally, although the desired products were not isolated from an attempted reaction of $(C_5Me_4H)_2Sc(\eta^3\text{-}C_3H_5)$ with diphenylhydrazine, a scandium hydroxo cluster complex $(C_5Me_4H)_5Sc_5(\mu_5\text{-}O)(\mu_3\text{-}OH)_4(\mu_2\text{-}OH)_4\cdot[(C_6H_5)NH]_2$ was isolated.

Inhalt

Die vorliegende Arbeit fokussiert auf die Synthese und Charakterisierung von Scandiumverbindungen. Ein Ziel war es, die Reaktivität von $\{CSc_6\}I_{12}Sc$ in Lösung zu untersuchen, das die Isolierung eines molekularen Scandiumnitrids, $[(C_5H_5)_2ScNSc(C_5H_5)(THF)]_2$, und eines Scandiumpropoxidkomplexes, $[(C_5H_5)_2Sc(\mu\text{-}OPr)]_2$, ergab.

Außerdem stand die Synthese und Analyse der ersten Scandiumdistickstoff-verbindung, $[(C_5Me_4H)_2Sc]_2(\mu\text{-}\eta^2\text{:}\eta^2\text{-}N_2)$, zusammen mit der Charakterisierung der Ausgangskomplexe: $(C_5Me_4H)_2ScCl(THF)$, $(C_5Me_4H)_2Sc(\eta^3\text{-}C_3H_8)$ und $[(C_5Me_4H)_2Sc]_2[(\mu\text{-}Ph)BPh_3]$, im Vordergrund. Die Reduktion des letztgenannten Komplexes mit KC_8 unter N_2 ergab das schwer zu isolierende und bislang unbekannte $[(C_5Me_4H)_2Sc]_2(\mu\text{-}\eta^2\text{:}\eta^2\text{-}N_2)$. Die Strukturbestimmung zeigte eine koplanare Anordnung der überbrückenden, seitlich gebundenen N_2-Einheit an die beiden Scandiumatome, welche durch DFT-Rechnungen unterstützt wird. In einer Reaktion cokristallisierte der Distickstoffkomplex mit einer Oxidverunreinigung in Form von $\{[(C_5Me_4H)_2Sc]_2(\mu\text{-}\eta^2\text{:}\eta^2\text{-}N_2)[(C_5Me_4H)_2Sc]_2(\mu\text{-}O)\}$.

Darüber hinaus wurden Borhydridkomplexe $(C_5Me_4R)_2M(BH_4)(THF)_x$ (M = Sc, Y; R = H, Me; x = 0, 1) hergestellt. Yttriumborhydridkomplexe wurden in Bezug auf ihre Fähigkeit N_2 zu aktivieren untersucht, wobei sich ihre Inaktivität demgegenüber herausstellte. Ligand-basierte Reaktivität von $(C_5Me_4R)_2Sc(\eta^3\text{-}C_3H_5)$ (R = H, Me) erfolgte mit 9-BBN (9-Borabicyclo[3.3.1]nonan), das die entsprechenden $(C_5Me_4R)_2Sc(\mu\text{-}H)_2BC_8H_{14}$-Komplexe hervorbrachte, aus welchen (R=H) mit Sauerstoff $(C_5Me_4H)_2Sc(\mu\text{-}O)BC_8H_{14}$ entstand.

Anschließende Untersuchungen umfassten die Reaktion von $[(C_5Me_4H)_2Sc]_2[(\mu\text{-}Ph)BPh_3]$ mit KC_5Me_4H, aus der sich $(\eta^5\text{-}C_5Me_4H)_2Sc(\eta^1\text{-}C_5Me_4H)$ ergab, welches strukturell charakterisiert wurde und das erste Beispiel eines über einen η^1-koordinierten Modus gebundenen $(C_5Me_4H)^-$-Liganden an ein Seltenerdmetall darstellt. Dieser Komplex zeigt Reaktivität im Sinne einer Sigma-Bindungs-Metathese (SBM) mit Diphenyldichalkogeniden,

PhEEPh (E=S,Se,Te) und ergibt Komplexe der Art $[(C_5Me_4H)_2ScSPh]_2$ sowie $(C_5Me_4H)_2ScEPh$ (E=Se,Te). Die analogen Produkte konnten über die Ligand-basierte Reaktivität von $(C_5Me_4H)_2Sc(\eta^3\text{-}C_3H_5)$ mit PhEEPh-Reagenzien isoliert und vollständig charakterisiert werden. Diese Reaktionen funktionierten ebenfalls in Gegenwart von THF und lieferten die solvatisierten Komplexe $(C_5Me_4H)_2ScEPh(THF)$ (E = S, Se, Te). Die Reaktion von $(C_5Me_4H)_2Sc(\eta^3\text{-}C_3H_5)$ mit pySSpy ergab $(C_5Me_4H)_2ScSpy$. Außerdem konnte der Scandium-Selen-Clusterkomplex $[(C_5Me_4H)Sc]_3[SePh]_6$ dargestellt werden und Reaktivitätsuntersuchungen mit PhTeTePh resultierten zusätzlich in der Isolierung einer Scandium-Tellur-Clusterverbindung, $\{[(C_5Me_5)Sc]_4(\mu_3\text{-}Te)_4\}$.

Die Funktionalisierung von N_2O durch die Insertion in die Metall-Kohlenstoffbindung von Allylverbindungen $(C_5Me_4R)_2M(\eta^3\text{-}C_3H_5)$ (M = Sc, Y, La, Sm; R = H, Me) bildete $[(C_5Me_4R)_2M(\mu\text{-}\eta^1\text{:}\eta^2\text{-}ON{=}NC_3H_5)]_2$-Komplexe. Die Insertion von $^iPrN{=}C{=}N^iPr$ in die Sc-C-Bindung ergab $(C_5Me_4H)_2Sc[(^iPr)NC(CH_2CH{=}CH_2)N(^iPr)\text{-}\kappa^2N,N']$. Schließlich, obwohl die erwünschten Produkte aus dem Versuch $(C_5Me_4H)_2Sc(\eta^3\text{-}C_3H_5)$ mit Diphenylhydrazin zur Reaktion zu bringen, ausblieben, wurde ein Scandiumhydroxocluster-komplex, $Sc_5(\mu_5\text{-}O)(\mu_3\text{-}OH)_4(\mu_2\text{-}OH)_4(C_5Me_4H)_5\cdot[(C_6H_5)NH]_2$, isoliert.

Table of Contents

Chapter 1

General Considerations

1.1 Scandium, Yttrium and the f-block Metals

Dmitri Mendeleev could not fill the space preceding yttrium in his original Periodic Table in 1869 for a metallic element of atomic mass 45, but he predicted an element specified as ekaboron.[1] In 1879, *Lars Fredrik Nilson* discovered a new element in the minerals euxenite and gadolinite from Scandinavia, produced scandium oxide and named the element scandium after the Latin word Scandia for Scandinavia.[2,3] It was *Per Teodor Cleve* who noticed the consistency between *Mendeleev's* prediction and *Nilsons* discovery and notified *Mendeleev*.[4] However, it was not until 1937 that the element itself was successfully isolated by electrolysis of a eutectic mixture of KCl, LiCl and $ScCl_3$ at 700-800 °C.[5] This soft and silvery metal is in fact fairly abundant, Table 1.1, but since it is evenly distributed in the earth's crust in the rare ore thortveitite ($Sc_2Si_2O_7$), and is difficult to extract and purify, it is more expensive than the majority of the transition metals. The largest amount of scandium is isolated from uranium extraction as one of the byproducts.

Although scandium has no important applications, the chemistry of scandium is very interesting and often challenging since it is the smallest transition metal with the electron configuration [Ar] $4s^2$ $3d^1$. It is often unclear whether its chemistry will resemble that of the later lanthanides or the group 3 metals.

Below scandium in group 3 of the periodic table are listed yttrium and the lanthanides, which are altogether with scandium generally considered as the "rare earth" elements implying that those are "rare" in the earth's crust. In fact, all sixteen elements are more abundant than for instance mercury or gold. Among them only promethium has no natural abundance, since all of its isotopes are radioactive. Table 1.1 gives the natural abundance of the rare earth elements in the earth's crust compared to other common metals.[6]

Table 1.1. Abundance of the "Rare-Earth" Metals in the Earth's Crust compared to Other Metals (ppm).[6]

aluminium	79600	erbium	2.1
iron	43200	ytterbium	2.0
titanium	4010	uranium	1.7
manganese	716	europium	1.3
zirconium	203	tantalum	1.1
cerium	60	tungsten	1.0
nickel	56	holmium	0.80
lanthanum	30	terbium	0.65
neodymium	27	lutetium	0.35
copper	25	thulium	0.30
yttrium	24	silver	0.07
scandium	16	mercury	0.04
lead	14.8	gold	0.0025
praseodymium	6.7	palladium	0.0004
samarium	5.3	platinum	0.0004
gadolinium	4.0	ruthenium	0.0001
dysprosium	3.8	iridium	0.0005

1.2 Size of the Rare Earth Ions

Lanthanides. Lanthanide complexes usually show coordination numbers from 8 to 10 due to their large sizes. The f-orbitals of the lanthanide elements have a limited radial extension compared to *d*-orbitals of the transition metals as proved by theoretical, magnetic, synthetic, spectroscopic and structural as well as reactivity investigations.[7-14] As opposed to yttrium and scandium, the lanthanides have f-orbitals which do not extend past the xenon core, Figure 1.1,[15] and therefore they cannot provide the needed metal-ligand orbital overlap to form a covalent bond. As the interactions between lanthanide metals and ligands are considered to be electrostatic, the bonding for the lanthanides is commonly more of an ionic nature. Since f-orbitals are of diffuse nature, an effective shield of the increasing nuclear

charge from La to Lu cannot be fulfilled by an increasing f-electron count. As a consequence, the ionic radii of the lanthanides decrease from La to Lu gradually by approximately 0.01 Å. The term lanthanide contraction describes this decrease in ionic radii of the lanthanides. Figure 1.2 gives the ionic radii for eight-coordinate trivalent rare earth elements.[16]

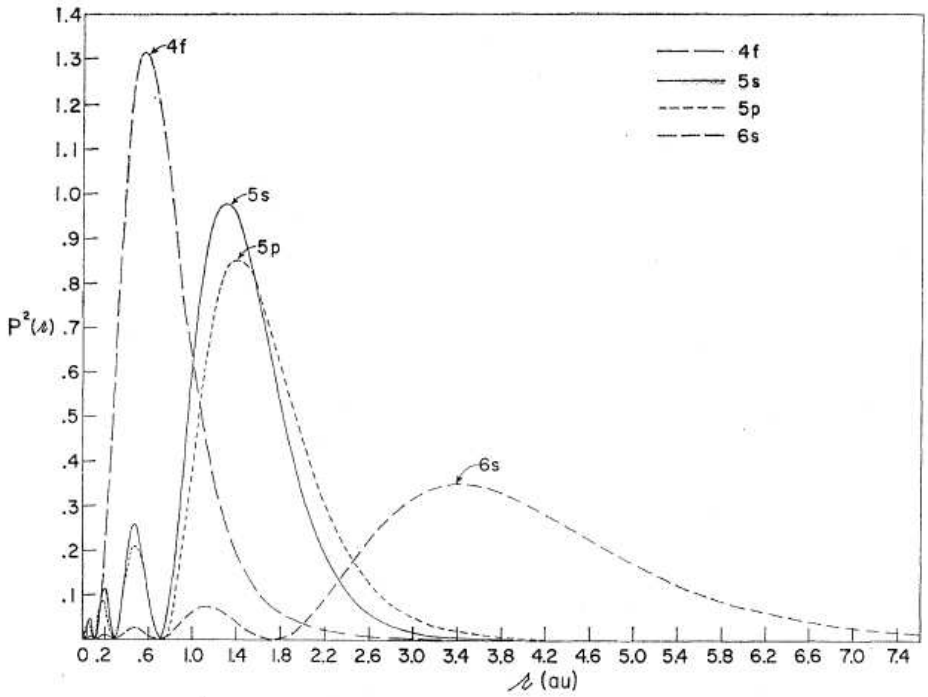

Figure 1.1. The distribution of the 4f, 5s, 5p and 6s electrons for trivalent gadolinium are presented as a function of radial distance.[15]

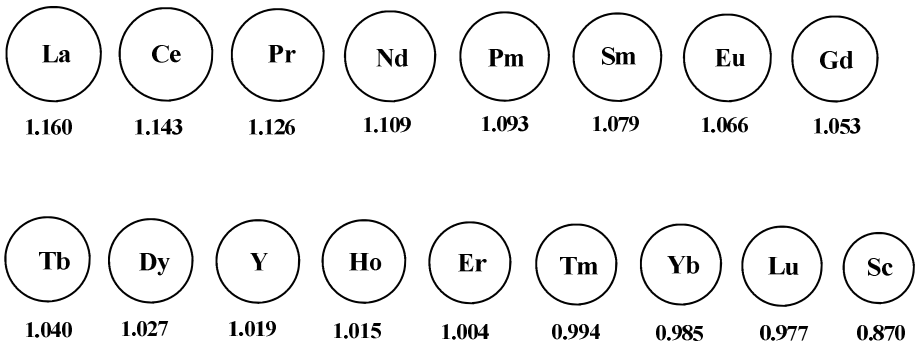

Figure 1.2 Ionic radii (Å) for eight-coordinate trivalent rare earth elements.[16]

Yttrium. Yttrium is often considered similar to the lanthanides due to its ionic radius which is in between that of dysprosium and holmium and its easily accessible trivalent oxidation state, Y^{3+}, with a d^0f^0 configuration. This can be compared to the f^n configuration of the trivalent lanthanides. Both represent closed shell ions which valence electrons do not extend past their nobel gas cores, Kr and Xe. Consequently, yttrium is expected to react in a similar way to the late lanthanides which is consistent with experimental results.

Scandium. Referring to the size of trivalent rare-earth elements the smallest ionic radius belongs to trivalent scandium. As shown in Figure 1.2, the ionic radius for eight-coordinate trivalent scandium is already about 0.1 Å smaller than that of lutetium. Coordination numbers for scandium range from 3 to 9, in which the sixfold coordination is the most common. The Shannon radius of six coordinate scandium is 0.745 Å, much smaller than six coordinated trivalent lutetium, 0.861 Å.[16]

1.3 Oxidation states of the Rare Earth Elements

The transition metals can access various oxidation states in organometallic complexes. In contrast, the rare earth elements show a more limited range of oxidation states with the most stable being +3, since the fourth ionization energy is larger than the sum of the first, second and third ionization energies. Indeed, the fourth ionization energy is so large that it cannot be compensated for by forming a new chemical bond.[10] The only exception in solution chemistry is the Ce^{3+}/Ce^{4+} redox couple, which due to the low fourth ionization energy, makes the accessibility of the Ce^{4+} ion possible as it possesses a more stable closed shell electronic configuration, $[Xe]4f^0$. Consequently, Ce^{4+} compounds are strong oxidizing agents.[17-19]

All observed oxidation states of rare earth metals in crystallographically unambiguously identified molecular complexes are shown in Figure 1.3.

Sc +3														
+1														
Y +3														
	+4													
La +3	**Ce** +3	**Pr** +3	**Nd** +3	**Pm** (rad.)	**Sm** +3	**Eu** +3	**Gd** +3	**Tb** +3	**Dy** +3	**Ho** +3	**Er** +3	**Tm** +3	**Yb** +3	**Lu** +3
+2	+2		+2		+2	+2	0		+2	0		+2	+2	

Figure 1.3. Oxidation states of rare earth metals observed in structurally characterized molecular complexes.

Divalent europium, samarium as well as ytterbium have been known for over 80 years.[20] Recently, accessible divalent oxidation states for metals such as thulium,[21] dysprosium[22] and neodymium[23] have been discovered. Predictably, the isolation of molecular divalent species containing the latter three ions was extremely challenging (described in detail on page 6). Very recently, the first two examples of divalent lanthanum complexes, namely $[K([18]c\text{-}6)(Et_2O)][LaCp''_3]$ and $[K([2.2.2]crypt)][LaCp''_3]$ [where Cp" = η^5-1,3-$(SiMe_3)_2C_5H_3$] could be synthesized.[24]

After the molecular structure of a formal Sc(I) containing scandium complex, $[\{\eta^5\text{-}P_3C_2{}^tBu_2)Sc\}_2(\mu\text{-}\eta^6{:}\eta^6\text{-}P_3C_3{}^tBu_3)]$ has been reported,[25a] another low-valent scandium species $[\{Sc(P_3C_2tBu_2)_2\}_2]$ has been obtained from the reaction of $[Sc(P_3C_2tBu_2)_3]$ with KC_8 in 2003 and has been structurally authenticated.[25b]

Even several lanthanide complexes containing formally Ln(0) has been successfully synthesized.[26] For instance, the reaction of Gd vapor with 1,3,5-tri-*t*-butyl-benzene formed $[(Gd(\eta\text{-}{}^tBu_3C_6H_3)_2]$.[26a]

1.4 Divalent Rare-Earth Metal Reduction Chemistry

Predictably, divalent rare earth compounds are very reactive, making them excellent reductants which have been applied in organometallic as well as in organic chemistry. The first soluble organometallic divalent samarium compound was isolated in 1981 as the solvated complex $(C_5Me_5)_2Sm(THF)_2$.[27] Shortly after this discovery, the unsolvated analog $(C_5Me_5)_2Sm$ was prepared which possesses an unexpected bent structure.[28,29] Both of these divalent samarium compounds show extensive reductive chemistry, which led to the first example of a lanthanide dinitrogen complex prepared from the reaction of the unsolvated samarium complex with dinitrogen eq 1.1.[30]

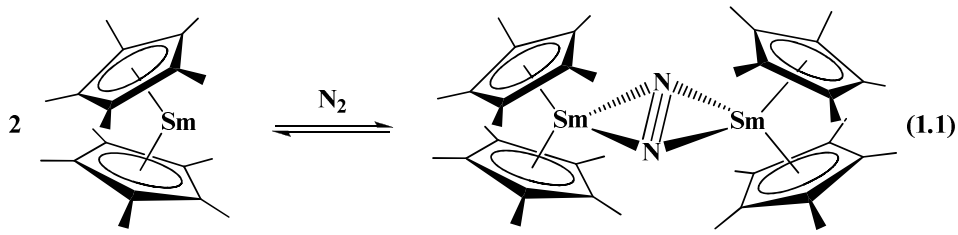

Another outstanding example is the reaction of the solvated samarium complex with diphenylacetylene and CO to give a tetracyclic hydrocarbon, eq (1.2).[31,32]

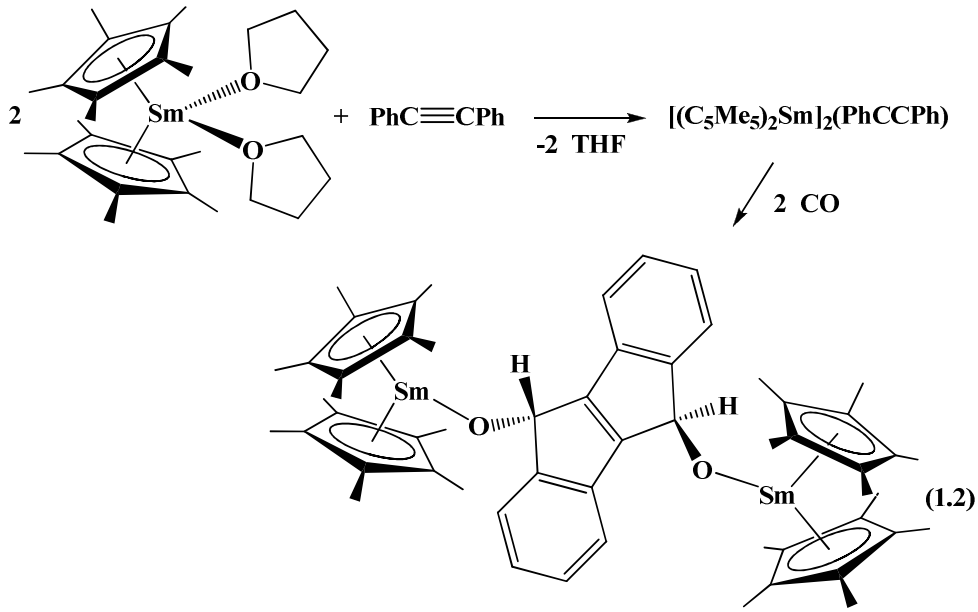

The first molecular Tm^{2+} compound was isolated by the *Bochkarev* and *Evans* group as $TmI_2(DME)_3$[21] from a freshly prepared sample, by using the *Bochkarev* method,[33] and

characterized by X-ray crystallography. The redox potential for Tm^{2+}/Tm^{3+} (−2.3 V)[34] shows that it is even more reducing than the redox couple Sm^{2+}/Sm^{3+} (−1.55 V).[34] For that reason, it was hard to isolate a metallocene complex of Tm^{2+} analogous to $(C_5Me_5)_2Sm$ and attempted syntheses under dinitrogen resulted in the first thulium dinitrogen complex, $[(C_5Me_5)_2Tm]_2(\mu\text{-}\eta^2{:}\eta^2\text{-}N_2)$,[35] since the possible metallocene intermediate must yield a species reactive enough to be able to reduce dinitrogen.[36] Similar observations of dinitrogen reduction were made by modifiying the ligand to the less-donating cyclopentadienyl group $(C_5H_4SiMe_3)^-$.[35] In order to isolate the first divalent thulium metallocene complex, the analogous reaction was performed under argon, but the product of the reaction of TmI_2 with KC_5Me_5 in Et_2O revealed that Tm^{2+} was reactive enough to activate the solvent diethylether to form ethoxide and oxide complexes.[35] A breakthrough came when the ligand set was changed from $(C_5Me_5)^-$ to $[C_5H_3(SiMe_3)_2]^-$ to give the first crystallographically identified Tm^{2+} metallocene, $[C_5H_3(SiMe_3)_2]_2Tm(THF)$, eq 1.3.[37]

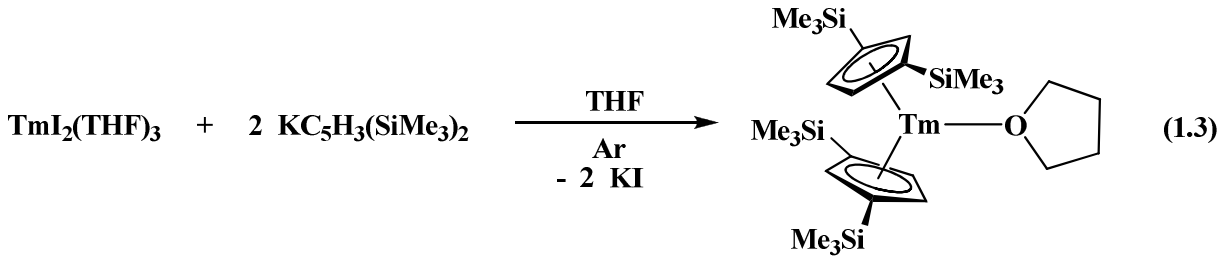

In a similar fashion to the preparation of Tm^{2+} complexes, the first molecular Dy^{2+} complex was realized as $DyI_2(DME)_3$.[37] X-ray crystallography revealed unambiguously the existence of both linear and bent DyI_2 units in a single crystal, which itself is isomorphous to the samarium analog.[38] DyI_2 is capable of reducing dinitrogen as well to form in the presence of $[C_5H_3(SiMe_3)_2]^-$ the dinitrogen complex, $\{[C_5H_3(SiMe_3)_2]_2Dy\}_2(\mu\text{-}\eta^2{:}\eta^2\text{-}N_2)$.[37]

However, because of its redox potential (Dy^{2+}/Dy^{3+} = −2.5)[34] Dy^{2+} can even reduce substrates with high reduction potentials like naphthalene (−2.60 V vs. SCE)[39], which after hydrolysis yields dihydronaphthalene.[22] The big advantage of this reduction is that it can be

done in an ether solution with a soluble molecular Dy^{2+} species. Normally this kind of reaction is only possible via a Birch reduction where alkali metal is used in liquid ammonia.[40] The first THF stabilized divalent neodymium complex was isolated as $NdI_2(THF)_5$.[23] The redox potential for Nd^{2+}/Nd^{3+} is −2.6 V vs. NHE.[34]

1.5 Trivalent Lanthanide Reduction

A breakthrough came with the exploration of routes to access divalent-like reduction chemistry with trivalent lanthanide compounds. For the first time, this new reductive chemistry could be applied with all of the lanthanides.

The first sterically crowded $(C_5Me_5)_3M$ complex was isolated in 1991 as $(C_5Me_5)_3Sm$ from the reduction of cyclooctatetraene with $(C_5Me_5)_2Sm$ to give the unprecedented products $(C_5Me_5)_3Sm$ and $(C_8H_8)Sm(C_5Me_5)$, eq 1.4.[41]

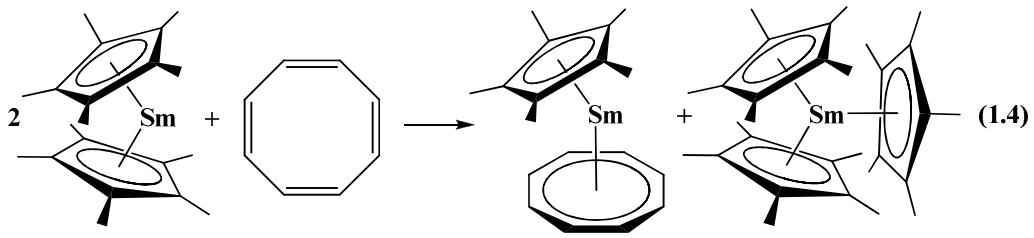

Thus, it had been discovered that the three large $(C_5Me_5)^-$ rings around Sm^{3+} form the very crowded complex $(C_5Me_5)_3Sm$, which had been assumed by many groups to not be possible to form, since it was estimated that the cone angle of a (C_5Me_5) ring is 142°.[42-44] Hence, three of these angles would exceed the limit of 360°. However, the steric crowding in $(C_5Me_5)_3Sm$ causes longer Sm-C(C_5Me_5) distances compared to previously reported Sm^{3+} complexes of $(C_5Me_5)^-$, as shown in Table 1.2. Thus, the required angle for the metal-centroid bond in $(C_5Me_5)_3Sm$ can be achieved by moving the ligand further away from the metal center, Scheme 1.1.

Table 1.2. Sm-C(C_5Me_5) distances in $(C_5Me_5)_3Sm$ (**a**) and other Sm^{3+} complexes of $(C_5Me_5)^-$ (**b**).

	Sm-C(C_5Me_5) distances (Å)
distances in **a**	2.782(2), 2.817(2), 2.910(3)
average in **a**	2.82(5)
typical averages in **b**	2.71(2)-2.75(2)
range of averages in **b**	2.68(1)-2.80(1)

Scheme 1.1. Change of the cone angle from 142° for normal metal-ligand distances to a cone angle of 120° by moving the ring further away from the metal core to enable the formation of $(C_5Me_5)_3Sm$.

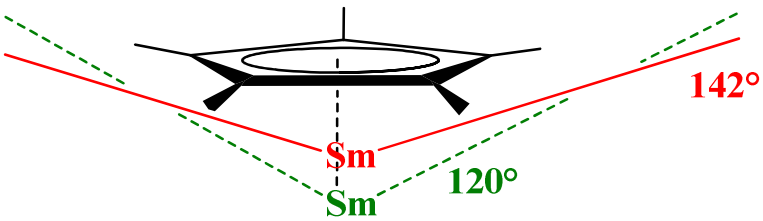

It could be conceivable that substrates cannot approach the metal because of the steric crowding in $(C_5Me_5)_3Sm$. However, the steric crowding in $(C_5Me_5)_3Sm$ causes a remarkably high reactivity of this complex towards numerous substrates, see section 1.6.[36,45]

Surprisingly, $(C_5Me_5)_3Sm$ can behave like a one electron reductant. Since samarium has not an accessible 4+ oxidation state, the reductive power in the $(C_5Me_5)_3Sm$ complex must derive from the $(C_5Me_5)^-$ ligands by offering one electron from one of the $(C_5Me_5)^-$ ligands to give half an equivalent of pentamethylcyclopentadienyl dimer, $(C_5Me_5)_2$, eq 1.5.

$$\mathbf{(C_5Me_5)^- \longrightarrow 0.5\ (C_5Me_5)_2 + 1\ e^-} \qquad \mathbf{(1.5)}$$

As the sterically crowded arrangement of bulky ligands to the metal atom initiated this reduction, such reactions are best described as sterically induced reductions (SIR). Thus, it can generally be distinguished between two different reduction types, Scheme 1.2, exemplified by divalent $(C_5Me_5)_2Sm$ and trivalent $(C_5Me_5)_3Sm$.

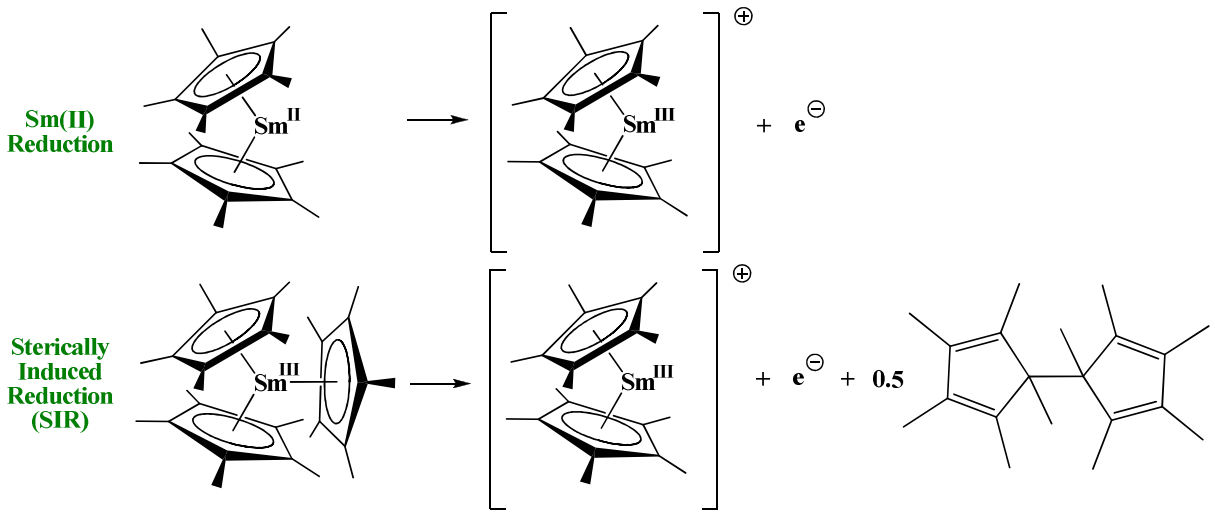

Scheme 1.2. Comparison of Divalent Sm(II) Reduction vs Sterically Induced Reduction (SIR).

1.6 Observed Reactivity Modes with $(C_5Me_5)_3M$ Complexes

As indicated above, all of the known $(C_5Me_5)_3M$ complexes show an unexpected $(C_5Me_5)^-$ reactivity. Depending on the substrate, it can be distinguished between various general modes of observed reactivity. As described above, one type of reaction is SIR, eq 1.6.[62]

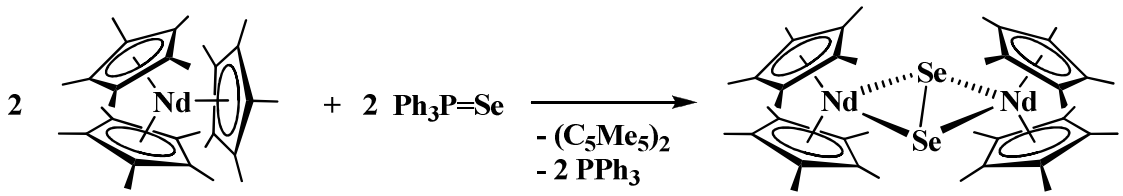

(1.6)

Another mode involves η^1-like $(C_5Me_5)^-$ reactivity where numerous reactions like hydrogenolysis, insertion of CO,[45] eq 1.7, CO_2,[46] and CS_2,[47] eq 1.8, into the M-C(C_5Me_5) bond, ring-opening of THF,[46] and olefin polymerization,[48] occur.

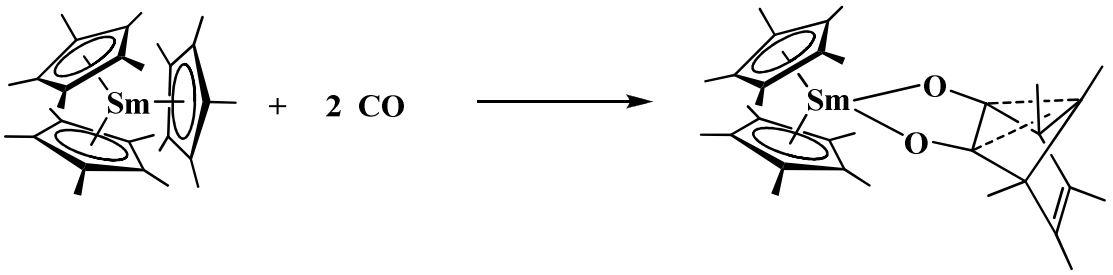

(1.7)

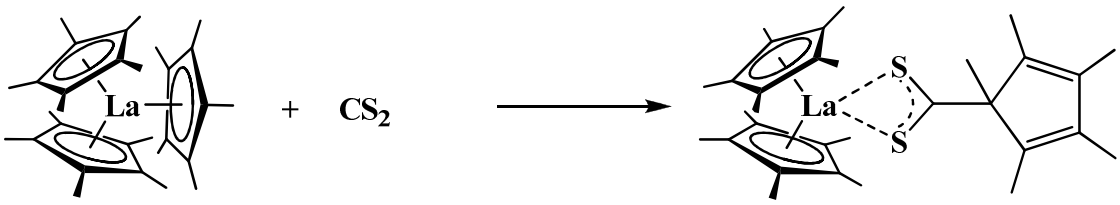

(1.8)

The third general reaction mode describes the substitution of a pentahapto η^5-$(C_5Me_5)^-$ ligand by a ligand of lower hapticity, e.q. $[N(SiMe_3)_2]^-$,[47,49] exemplified in eq 1.9.

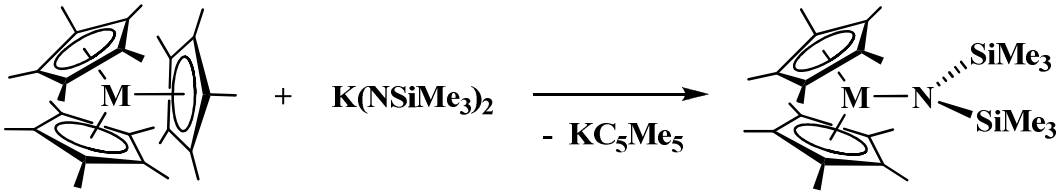

(1.9)

M = La, U

The fourth known reaction type involves the formation of base adducts $(C_5Me_5)_3ML$[50-52] and $(C_5Me_5)_3ML_2$[47,52] (where L = CO, N_2, RNC, RCN) from $(C_5Me_5)_3M$ complexes, eq 1.10.

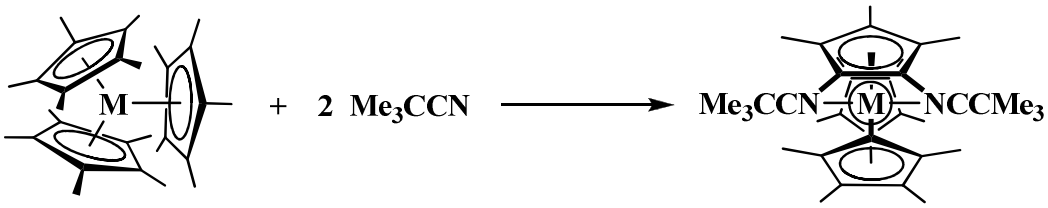

(1.10)

M = La, Ce, Pr

The majority of these reactions form single products in relatively high yields. In contrast, it has been reported that reactions of $(C_5Me_5)_3M$ with alkyl and aryl halides are more

complicated and result in various byproducts, eq 1.11, generated through a combination of nucleophilic displacement, radical reactions and reduction to form $(C_5Me_5)_2$.[46] The latter is the typical byproduct observed in SIR reactions, eq 1.5.

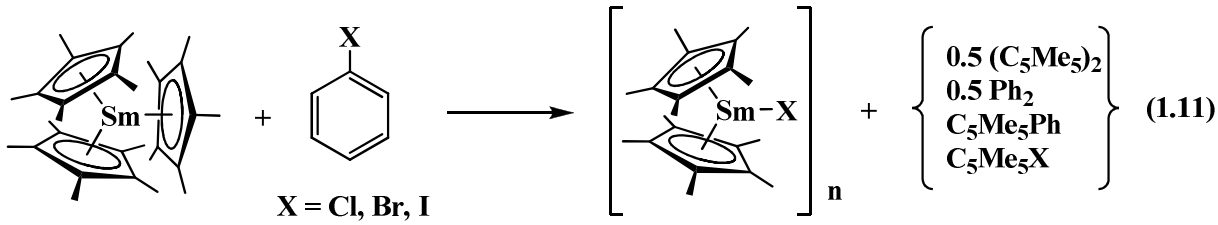

(1.11)

More recently it has been found that $(C_5Me_5)_3M$ as well as the nitrile adducts $(C_5Me_5)_3M(NCCMe_3)x$ show SBM reactivity with PhSSPh.[53] For instance, the organometallic product of the reactions of $(C_5Me_5)_3La$ with PhEEPh (E = S, Se, Te) is shown in eq 1.12. Whilst the (E = S, Se) analogues gave C_5Me_5EPh as the major and $(C_5Me_5)_2$ as the minor byproduct, the analogous reactions with PhTeTePh provided $(C_5Me_5)_2$ as the only byproduct.

The application of PhEEPh substrates has often been explored in reductive f-element chemistry[54-57] due to their broad range of reduction potentials: −1. 75 V,[58] −1.2 V,[58] and −1.06 V[59] *vs.* SCE for E = S, Se, and Te, respectively, and also because of the often crystalline nature of the $(EPh)^-$ containing complexes.

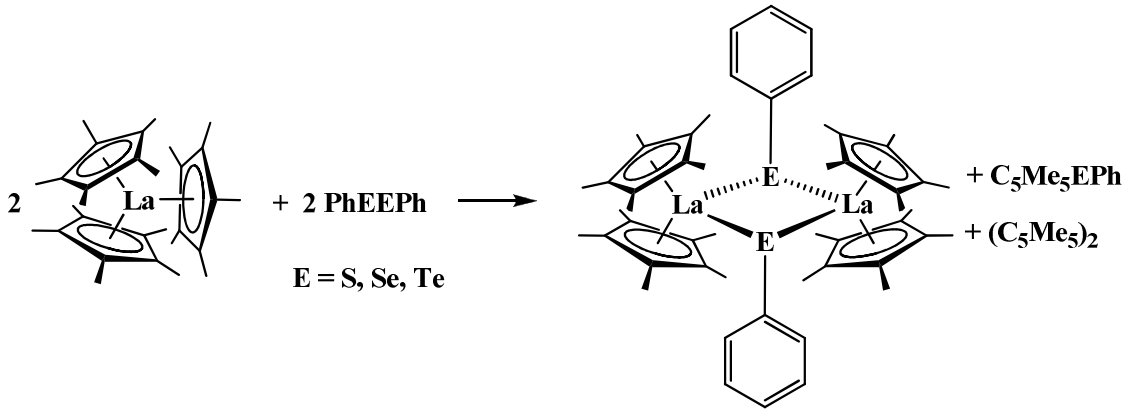

(1.12)

One explanation for the generation of the observed byproducts C_5Me_5EPh in these reactions could be sigma bond metathesis (SBM).[60] This reaction pathway would require the

η^1-$(C_5Me_5)^-$ bonding mode to be accessible for these complexes, Scheme 1.4. A reported example for this mode of SBM yields the products MeER and $[(C_5H_4{}^tBu)_2Ln(\mu\text{-}ER)]_2$ from the reaction of $(C_5H_4{}^tBu)_2Ln(\mu\text{-}Me)]_2$ (Ln = Y, Lu) with REER (E = S, Se; R = Ph, ^{n}Bu, ^{t}Bu, CH_2Ph).[61]

Scheme 1.4. Sigma Bond Metathesis (SBM) Mechanism via a Postulated η^1-$(C_5Me_5)^-$ ligand.

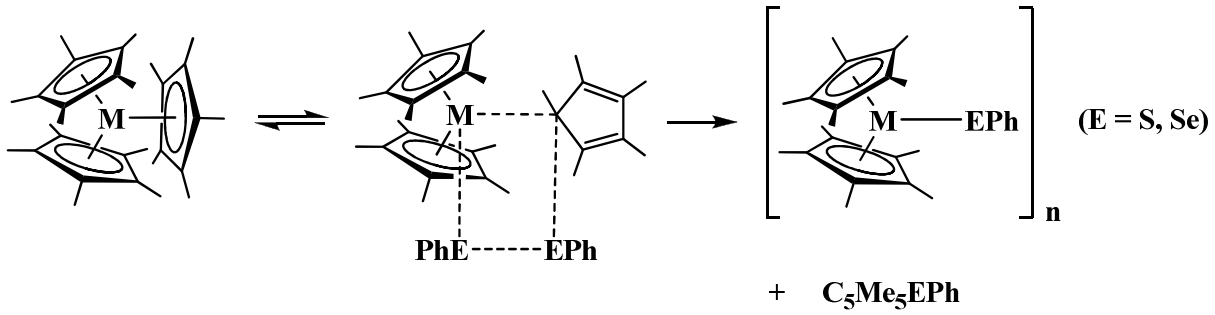

An alternative way to obtain these C_5Me_5EPh byproducts could be via a radical pathway. For this, a $(C_5Me_5)^-$ ligand would have to provide an electron to generate a $C_5Me_5{}^{\cdot}$ radical,[36,46,53,62-64] which is trapped by PhSSPh, Scheme 1.5.

Scheme 1.5. Generation of a $C_5Me_5{}^{\cdot}$ Radical and Subsequent Trapping by PhSSPh.

$$(C_5Me_5)^- \longrightarrow (C_5Me_5)^{\bullet} + e^-$$

$$(C_5Me_5)^{\bullet} + 0.5\ PhSSPh \longrightarrow C_5Me_5SPh$$

This reaction pathway is plausible since PhSSPh is known to act as a radical trapping reagent.[65] In order to test this conceivable route, a mixture of $(C_5Me_5)_2$ and PhSSPh was heated up, as it is known that cracking $(C_5Me_5)_2$ generates two $(C_5Me_5)^{\cdot}$ radicals.[53,66] However, this reaction gave only the $(C_5Me_5)_2$ disproportionation products, C_5Me_5H and tetramethylfulvene, and unreacted PhSSPh. The formation of C_5Me_5SPh was not observed. Additionally, the thermal stability of pure C_5Me_5SPh was tested: it showed no decomposition when heated up to 110 °C in toluene. This suggests that the most likely pathway to form

C_5Me_5EPh is via sigma bond metathesis,[53] although crystallographic evidence for an η^1-$(C_5Me_5)^-$ ligand is still not reported.

The reaction of PhTeTePh with $(C_5Me_5)_3M$ gave $(C_5Me_5)_2$ as the only byproduct. This would be consistent with SIR, but it might also be that C_5Me_5TePh has been formed via SBM first and subsequently decomposed to $(C_5Me_5)_2$ and PhTeTePh. The formation of C_5Me_5TePh was probed by combining PhTeTePh and LiC_5Me_5, but no reaction was observed.[53]

1.7 Divalent-like Reduction Chemistry Obtained Through Alkali-Metal Reduction of Trivalent Lanthanide Complexes

Divalent-like reduction chemistry was also observed by reduction of trivalent lanthanide complexes with alkali metals. These so-called LnZ_3/M and LnZ_2Z' reactions (Z = $[N(SiMe_3)_2]$ or C_5Me_4R (R = H or Me); Z' = BPh_4; M = Na, K or KC_8) yield $[Z_2Ln(THF)]_2(\mu\text{-}\eta^2\text{:}\eta^2\text{-}N_2)$ in the presence of N_2 and THF.[67-69] Hence, this route displays another way to access analogs of $[(C_5Me_5)_2Sm]_2(\mu\text{-}\eta^2\text{:}\eta^2\text{-}N_2)$ shown in eq 1.1. Remarkably, this "LnZ_2" chemistry accessible via Scheme 1.6 works also with lanthanides for which no divalent state has so far been isolated in solution.

Scheme 1.6. Divalent-like "LnZ_2" chemistry with reduction of an appropriate substrate.

$$\mathbf{2\ LnZ_3\ (\text{or } 2\ LnZ_2Z')\ +\ 2\ M\ +\ substrate \longrightarrow \{Z_2Ln\}_2[substrate]\ +\ 2\ MZ}$$

$$\mathbf{2\ LnZ_3\ (\text{or } 2\ LnZ_2Z')\ +\ 2\ M \xrightarrow[-\ 2\ MZ]{} \text{"}LnZ_2\text{"} \longrightarrow 2\ \{LnZ_2\}^+\ +\ 2\ e^-}$$

$$\mathbf{substrate\ +\ 2\ e^- \longrightarrow [substrate]^{2-}}$$

Z/Z' = Monoanionic Ligand; M = Na, K or KC_8

Following the discovery of the convenient access of reduced dinitrogen complexes, it was discovered that these are excellent reductants in their own right, as the N_2^{2-} ligand of the complex provides two electrons, Scheme 1.7

Scheme 1.7. Reduced dinitrogen complexes are excellent reductants.

$$(N_2)^{2-} \longrightarrow N_2 + 2\,e^-$$
$$\text{substrate} + 2\,e^- \longrightarrow [\text{substrate}]^{2-}$$

For instance, dinitrogen complexes are capable of reducing phenazine which is a fairly easy reducible substrate (−0.36 V vs. SCE),[70] eq 1.13. In the past years, numerous bimetallic reduced phenazine complexes have been isolated showing distinguishable binding modes of lanthanide to the substrate depending on the metal size, compare for example $[(C_5Me_4H)_2La](\mu\text{-}\eta^4{:}\eta^2\text{-}C_{12}H_8N_2)(La(THF)(C_5Me_4H)_2$ with $[(C_5Me_4H)_2Lu](\mu\text{-}\eta^3{:}\eta^3\text{-}C_{12}H_8N_2)(Lu(THF)(C_5Me_4H)_2$.[71]

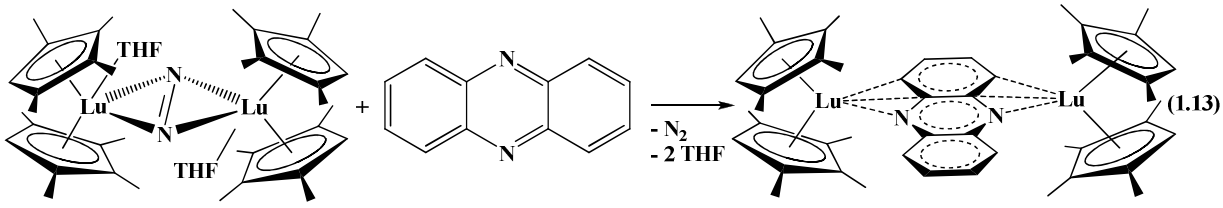

Another appropriate substrate for the application of the "LnZ_2" reactivity is anthracene that possesses reduction potentials of −1.98 and −2.44 V vs. SCE.[39] However, the use of anthracene instead of phenazine changes the reductive reactivity of the lanthanide dinitrogen compounds significantly. Whereas $[(C_5Me_4H)_2La(THF)]_2(\mu\text{-}\eta^2{:}\eta^2\text{-}N_2)$ shows reactivity with anthracene, there was no reaction observed in an analogues reaction with $[(C_5Me_4H)_2Lu(THF)]_2(\mu\text{-}\eta^2{:}\eta^2\text{-}N_2)$, even with heating to 75 °C for 24 h.[71]

Furthermore, reduced dinitrogen complexes are capable of reducing small molecules like CO_2, that has a reported reduction potential of −2.21 V vs SCE in dimethylformamide,[72] which would yield an oxalate derivate.[71] A second example of a small molecule activation is the reaction of $[(C_5Me_5)_2La]_2(\mu\text{-}\eta^2\text{:}\eta^2\text{-}N_2)$ with CO to yield a ketene carboxylate, namely $\{[(C_5Me_5)_2La]_2[\mu\text{-}\eta^4\text{-}O_2C\text{-}C{=}C{=}O](THF)\}_2$.[73] Another route for the synthesis of the same type of ketene carboxylate lanthanide complex is the reaction of $[(C_5Me_5)_2Sm](THF)_2$ with 6 eq of CO.[74] The synthesis routes for each of these products are combined in eq 1.14.

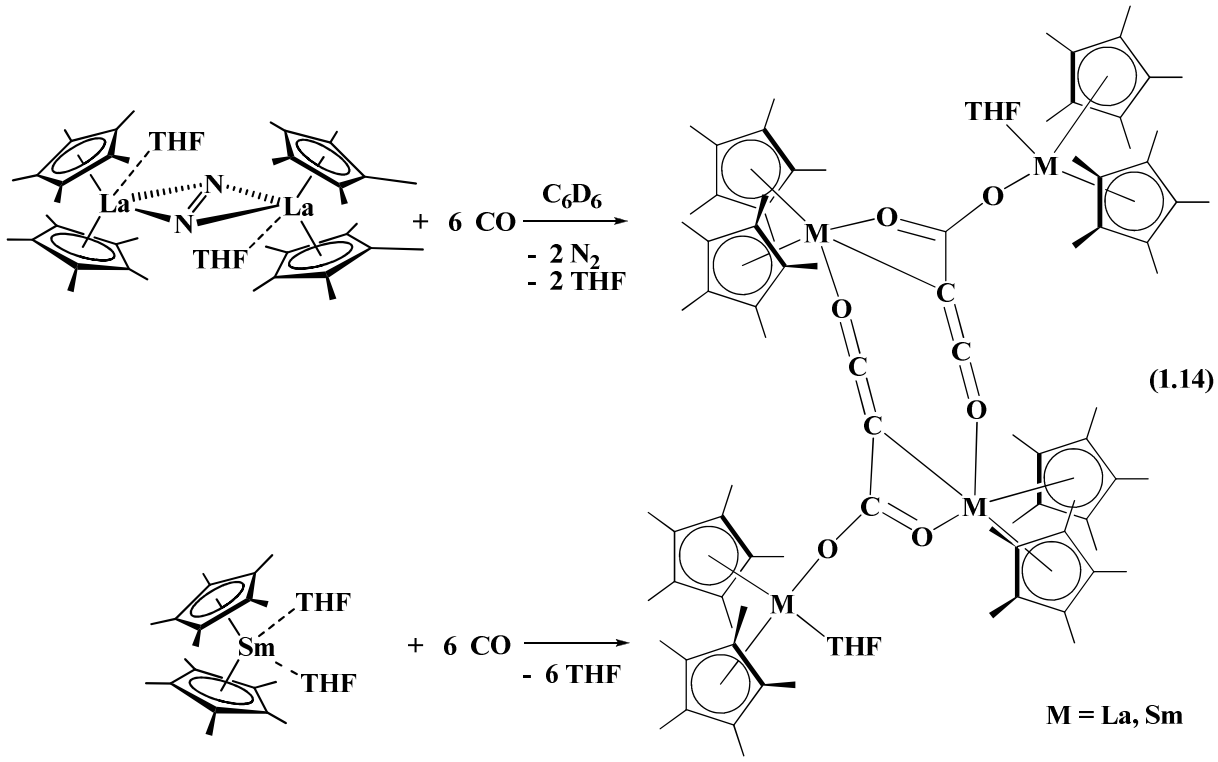

(1.14)

Although several substrates react with lanthanide dinitrogen complexes via "LnZ_2" reactivity, for some substrates there are limits of this divalent-like reactivity. For instance, $[(C_5Me_5)_2Ln]_2(\mu\text{-}\eta^2\text{:}\eta^2\text{-}N_2)$ with Ln = Lu, La are not able to reduce naphthalene that has a reduction potential of -2.60 V vs SCE.[39,71]

1.8 Organoscandium Compounds Compared to Organolanthanide Compounds

Organoscandium chemistry resembles in some respects the chemistry of the later lanthanides. For instance, the cyclopentadienyl complexes of scandium and lutetium, namely

$ScCp_3$[75] and $LuCp_3$,[76] show both mixed η^1- and η^5-coordination.[77] However, the size difference between scandium and the later lanthanides seems to affect some reactions which provide products with subtle differences. For instance, the bis(pentamethylcyclopentadienyl) complexes of scandium and lutetium possess different structures: $(C_5Me_5)_2ScMe$[60] is a monomer and $[(C_5Me_5)_2Lu(\mu\text{-}Me)Lu(C_5Me_5)_2(Me)]$[78] is an asymmetric dimer. Another example would be the difference in synthesis of the THF coordinated tris(phenyl) compounds. Interestingly, both synthesis routes and the structure of the scandium vs the lanthanide product is different. While the twofold THF coordinated tris(phenyl)scandium $ScPh_3(THF)_2$ is being produced by a salt metathesis reaction,[79] the tri-coordinated THF tris(phenyl)lanthanide compounds $LnPh_3(THF)_3$ (Ln = Ho, Er, Tm, Lu) require a redox reaction.[80]

1.9 Scandium Halides

All four trivalent scandium halides, ScF_3 (VF_3 structure),[81] $ScCl_3$ ($CrCl_3$ structure),[81] $ScBr_3$ (BiI_3 structure),[81] ScI_3 (BiI_3 structure),[81] in which the coordination number of the metal is six, are fairly stable compounds due to the preferred trivalent oxidation state of the metal.

However, through solid state synthesis techniques numerous well-defined scandium halide compounds consisting of low valent scandium are obtainable. These are generally prepared by the reduction of the respective trivalent halide with scandium metal at high temperatures. For instance, the reaction of scandium with $ScCl_3$ produces, depending on the temperature as well as the stoichiometry, Sc_2Cl_3[82] and Sc_7Cl_{10}.[83] The reduced sesqui scandium sesquibromide Sc_2Br_3 was obtained in an analogous reaction with $ScBr_3$.[82] The only known binary scandium iodide, namely $Sc_{0.89}I_2$, can be obtained from the reduction of ScI_3 with excess scandium metal at 750 °C in sealed tantalum or niobium ampoules. This compound crystallizes in a CdI_2-type structure and the X-ray structure revealed that there is an under-occupancy of scandium present. Conductivity measurements, supported also by EPR spectroscopy, showed that $Sc_{0.9}I_2$ is metallic above 100 K and an insulator below 100

K.[84] Through the phase transition at low temperature, the electrons are trapped in localized 3d orbitals. Hence, $Sc_{0.9}I_2$ = Sc_8I_{18} = $(Sc^{2+})_6(Sc^{3+})_2(I^-)_{18}$ becomes a mixed-valent compound owing to distinct and assignable electron configurations.

1.10 Rare-Earth Metal Cluster Compounds

The term 'metal atom cluster' typically refers to a group of two or more metal atoms in which there are direct bonds between the metal atoms.[85] Rare earth metals in low oxidation states form clusters with their remaining valence electrons and are typically stabilized by a halide sphere. Depending on the arrangement of the halogen atoms, it can be distinguished between the $[M_6X_8]$ and $[M_6X_{12}]$ cluster types, Figure 1.4. In a $[M_6X_8]$ unit the eight halogen atoms are located above the eight faces of the octahedron, thus the metal-metal bonds represent as two-center-two-electron bonds the 12 edges of the octahedron. In contrast, in the $[M_6X_{12}]$ unit the 12 halogen atoms are placed above all edges of the octahedron, hence the metal-metal bonds are located as three-center-two-electrons on the surfaces of the metal octahedron.

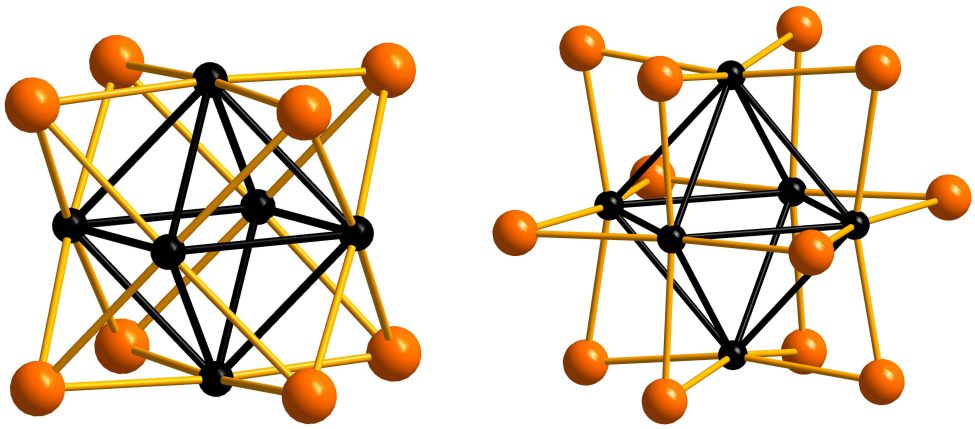

Figure 1.4 $[M_6X_8]$ cluster unit $[M_6X_{12}]$ cluster unit

With a few exceptions, rare earth (M) clusters *need* to sequester an endohedral atom Z to make up for the paucity of electrons of these group 3 elements. Therefore, isolated clusters are rare and cluster condensation is a common picture. Appropriate endohedral atoms are for

example carbon, boron or late transition metals from all three periods, Mn-Cu, Ru-Pd, Re-Au.[86] Figure 1.6 and 1.7 show examples for typical condensated clusters complexes.

$M_7X_{12}Z$ cluster compounds show a huge variety of compounds including Sc, Y and the rare earth metals, La, Ce, Pr, Gd, Tb, Dy, Ho, Er and Lu which form interstitially stabilized isolated octahedral clusters $\{M_6Z\}$.[87-98] The $\{M_6Z\}$ cluster is capped by 18 halide atoms, 12 halides above each edge of the octahedron and six above the corners. A seventh rare-earth metal atom links the $\{M_6Z\}X_{18}$ units into infinite chains. The chains are linked by X^{i-a} bridges resulting in $M\{M_6Z\}X_6{}^{i}X_{6/2}{}^{i-a}X_{6/2}{}^{a-i}$. Figure 1.5 shows the structure of $Sc_7Cl_{12}B$ as an example of an isolated cluster complex.

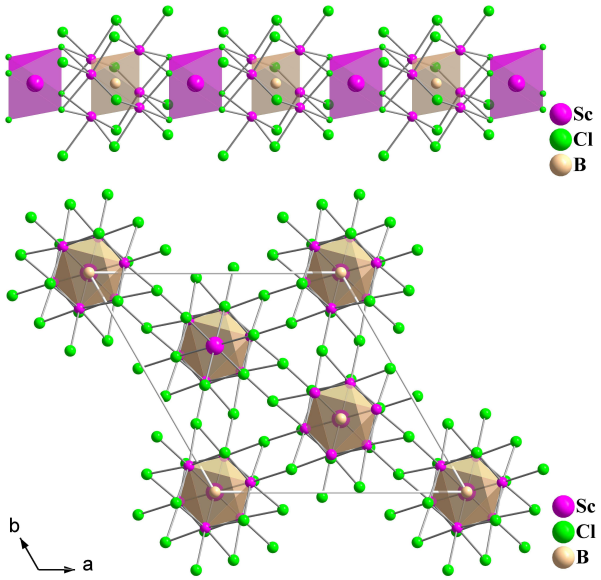

Figure 1.5. Structure of $Sc_7Cl_{12}B$ Part of the infinite chains (top) and their connection via i-a/a-i bridges according to $Sc\{Sc_6B\}Cl_6{}^{i}\,Cl_{6/2}{}^{i-a}\,Cl_{6/2}{}^{a-i}$ (bottom).

The R_4X_5Z series is known e.g. for La_4I_5Ru and Pr_4I_5Z, (Z = Co,[99] Ru,[99] Os,[99] Ni,[86]), Y_4I_5C,[100] and Gd_4I_5Z, (Z = C or Si).[101] Interstitial-atom-centered rare earth metal octahedra form infinite trans-edge chains, with all vacant edges bridged by halides. Another two halides on top of each apical octahedral position link the octahedral chains via I^{a-i} connections. A

further link between the chains is by an I^{i-i} connection. Figure 1.6 (a) shows Pr_4I_5Ru as an example for a typical condensated cluster complex.

A remarkable cluster compound is $Sc_{24}C_{10}I_{30}$, in which twenty scandium atoms build a T3-Supertetrahedron with all Sc_4 tetrahedron centered by a carbon atom, Figure 1.6 (b).[102] The carbon atoms are in the shape of a T2-Supertetrahedron and the octahedral cavities are filled with a T1-Sc_4-tetrahedron. The iodide atoms form a concave truncated T4-supertetrahedron shell, so that the molecular structure of $Sc_{24}C_{10}I_{30}$ can be described as T1 + T2 + T3 + T4*. Interatomic Sc-C distances are within the range of 2.01 and 2.42 Å, whereas the Sc-C distances are 2.28 and 2.33Å in $Sc\{Sc_6C\}I_{12}$[97] with isolated Sc-octahedra.

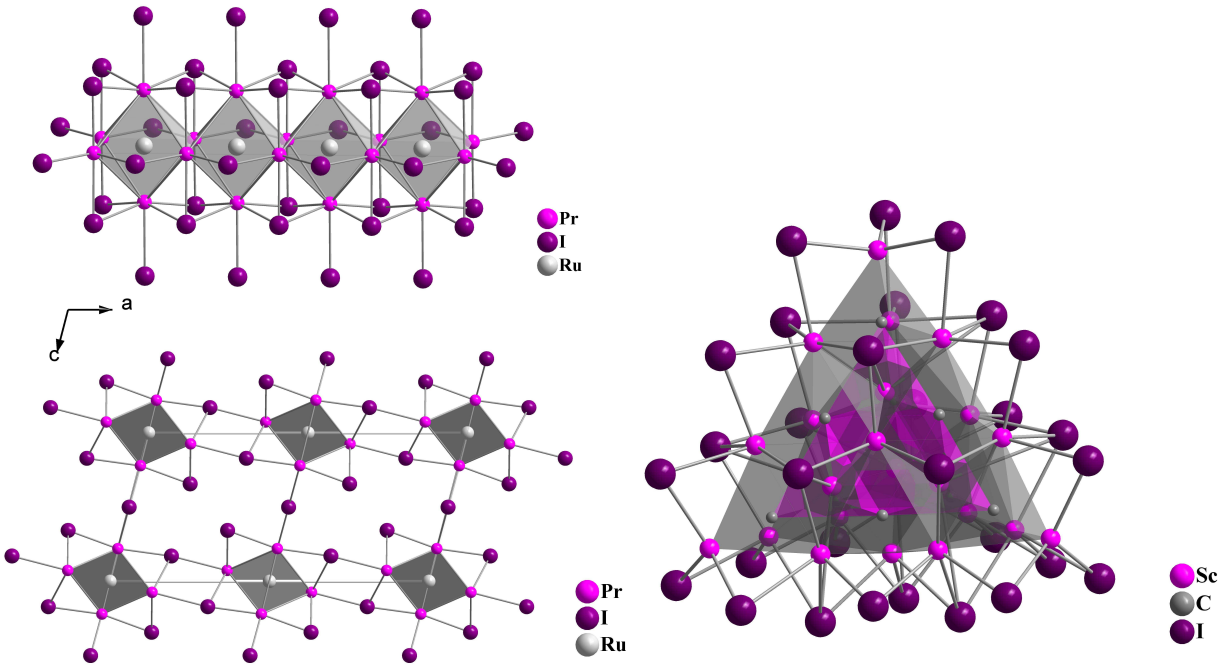

(a) (b)

Figure 1.6. (a) Crystal structure of Pr_4I_5Ru. Part of the infinite chains (top) and their connection via i-i/i-a/a-i bridges according to $[\{RuPr_4\}I^{i}_{4/2}I^{i-i}_{4/4}I^{i-a}_{4/3}I^{a-i}_{2/3}]$ (bottom).[99] (b) Molecular structure of $Sc_{24}C_{10}I_{30}$.[102]

Additionally there are structures with cluster chains linked by isolated rare earth metal atoms, e.g. Sc_5Cl_8Z (Z=C, N),[103] Figure 1.7 (a), and $Sc_7Cl_{10}C_2$,[104] Figure 1.7 (b). In Sc_5Cl_8Z single chains of octahedra are formed while $Sc_7Cl_{10}C_2$ is more condensed to double chains.

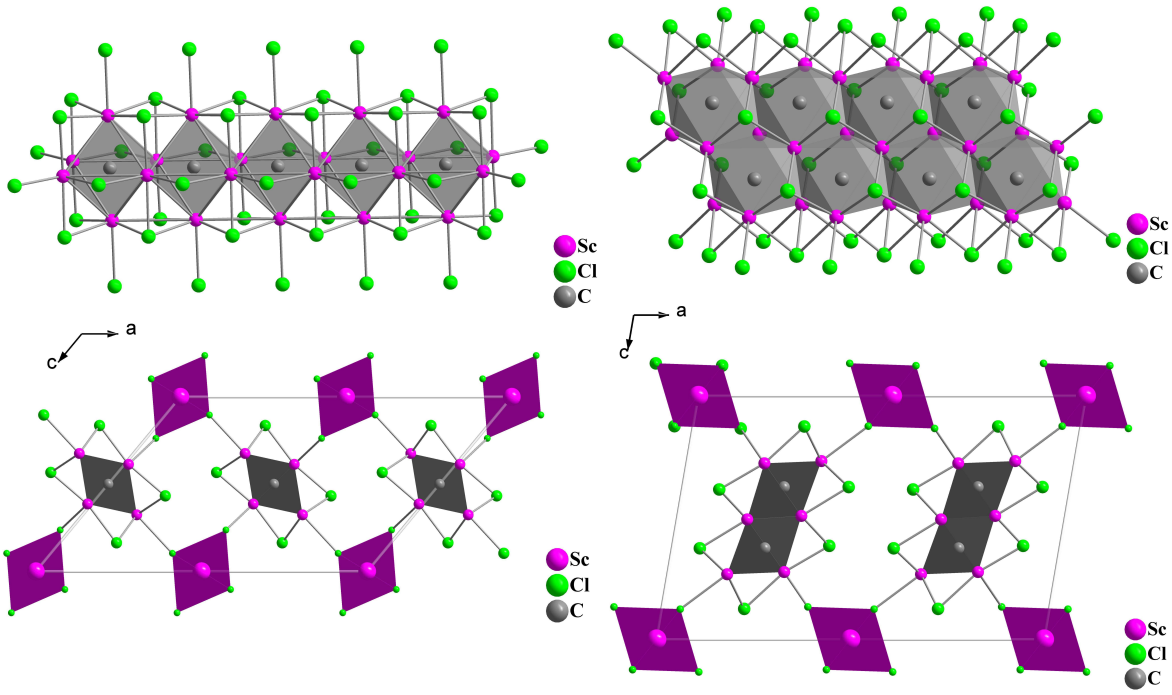

(a) (b)

Figure 1.7. (a) Crystal structure of Sc_5Cl_8C. Part of the infinite chains (top) and their connection via i-i/i-a/a-i bridges according to $Sc\{Sc_4C\}Cl_{8/2}{}^{i}Cl_{2/3}{}^{i\text{-}a}Cl_{6/3}{}^{a\text{-}i}$ (bottom). (b) Structure of $Sc_7Cl_{10}C_2$. Part of the infinite chains (top) and their connection via i-i/i-a/a-i bridges (bottom).

The exception to the centered rare earth clusters are the sequihalides M_2X_3 (e.g. M = Sc, Y; X=Cl, Br)[83,105] as well as M_7Cl_{10} (M=Sc,[83] Er,[106]) which evidently do not require an interstitial atom, Figure 1.8 (a) and (b). The first lanthanide compound with an oxidation number less than +2 was Gd_2Cl_3.[94] The sequihalides contain chains of trans edge linked octahedra. The $\{M_6\}$ octahedra are capped by eight halide atoms to form M_6X_8 cluster.

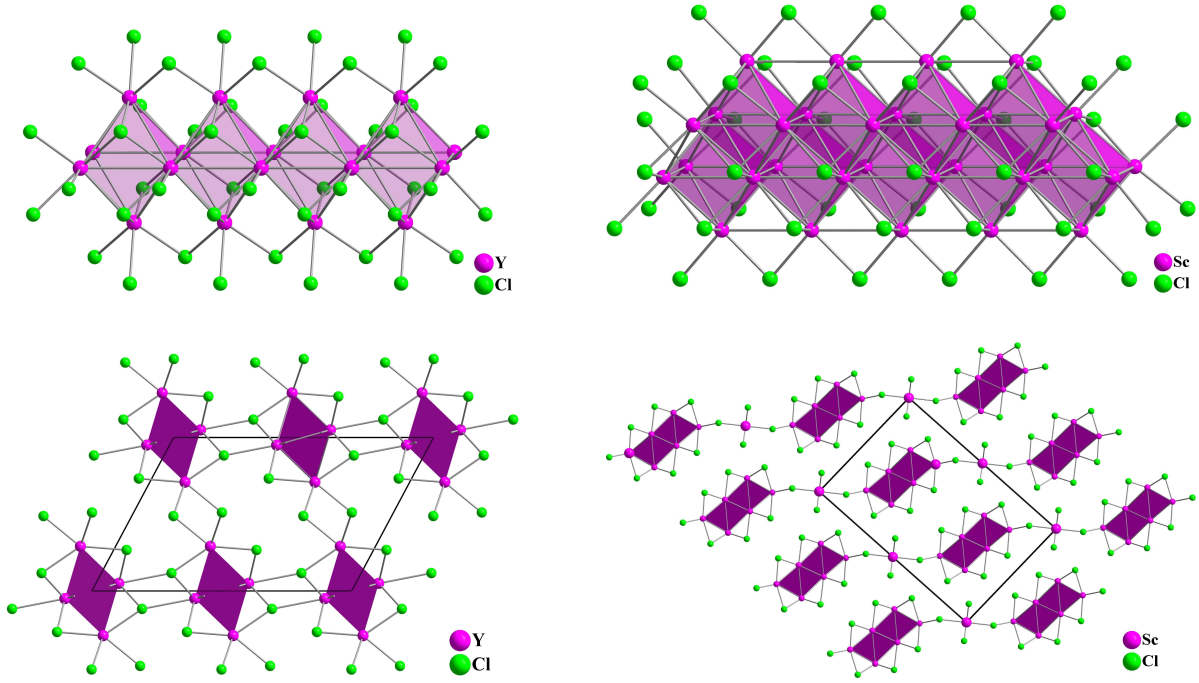

Figure 1.8. (a) Crystal structure of Y_2Cl_3. Part of the infinite chains (top) and their connection via i-i/i-a/a-i bridges (bottom). (b) Crystal structure of Sc_7Cl_{10}. Part of the infinite chains (top) and their connection via i-i/i-a/a-i bridges (bottom).

Another way to combat the electron deficiency of the third group metals is through the use of a third element such as an alkali metal to build up ternary halides, for example $CsSc_{1-x}Cl_3$. These phases crystallize with the hexagonal perovskite type of structure ($BaNiO_3$).[107,108]

1.11 Molecular Metal Atom Cluster Complexes

Decades ago, *Cotton* et al. succeeded in making various molecular metal atom cluster compounds consisting of transition metals. For instance, they could stabilize discrete trinuclear complexes of niobium,[109] and shortly after that they observed self-assembly of octahedral metal atom clusters of zirconium, niobium and tantalum.[110] The “modus operandi” in these syntheses was the reduction of a suitable transition metal complex with sodium amalgam in an appropriate solvent.

Around the same time, the synthesis of metal cluster compounds available through solid state chemistry was studied extensively. On this account, the idea arose to do solution chemistry with these metal cluster complexes. For instance, several hexazirconium chloride and bromide cluster complexes could be dissolved and characterized in polar solvents such as acetonitrile, methanol and pyridine or in ionic liquids [for example by use of a mixture of $AlCl_3$ and 1-ethyl-3-methylimidazolium-chloride ($AlCl_3$/ImCl)].[111] Later on, the dissolution of hexazirconium iodide cluster compounds was successful through the use of deoxygenated water.[112] To date, there is still an interest in the research of these zirconium cluster compounds. The reason for this is that through solid state synthesis there are plenty of [{ZZr_6}X_{12}] (Z=endohedral atom; X= halide) complexes particularly with a huge variety of endohedral atoms available,[113] which promises a plethora of possibilities in the solution chemistry as well as properties of excised zirconium clusters. In addition, even solid niobium cluster compounds are still interesting research objects, as exemplified with the recent isolation of crown ether stabilized niobium alcoholate cluster compounds with an octahedral arrangement of niobium atoms.[114]

Although a lot of investigations have been reported on transition metal cluster complexes, there is nothing known concerning the chemistry of rare earth metal cluster compounds in solution or the excision of a metal rich fragment out of these solids via solution chemistry. In general, it is expected that the excision of rare earth metal clusters should be more difficult to realize due to their extreme electron deficiency compared to transition metal clusters. Also, the assumption is that isolated rare earth metal cluster compounds should be easier to excise because of their fewer linkages within the structure compared to condensed rare earth metal cluster complexes.

1.12 Dissertation Outline

In light of the prevalence of solid rare earth metal cluster complexes, the incentive is given to investigate these in solution chemistry. The goal is to achieve a molecular rare earth metal cluster complex for which an example is not yet known. In order to achieve this objective, the electron deficiency of the rare earth metals is an additional challenge and the assumption is that such a goal is probably easier to attain by using solids with isolated metal clusters rather than condensed metal cluster compounds. On this account, $\{CSc_6\}I_{12}Sc$ was chosen for this research. Scandium was also desirable since low-valent molecular scandium species were obtainable via organometallic synthesis. $\{CSc_6\}I_{12}Sc$ reacted with potassium cyclopentadienide to form, under a nitrogen atmosphere, an unprecedented molecular scandium nitride complex. In addition, a scandium propoxide complex has been isolated from the analogous reaction conducted under an argon atmosphere (Chapter 2). In view of the expansion of divalent-like reactivity to the majority of the trivalent lanthanide systems, the question arose whether the extension of divalent-like reactivity to the smallest trivalent transition metal scandium is possible. In light of the exceedingly small size of scandium, it is not predictable if reaction modes will be comparable to the larger lanthanides. Hence, reactions could provide scandium compounds possessing unusual structural features and/or reactivity characteristics. To this end, reduced dinitrogen chemistry was extended to scandium to yield the first example of a scandium dinitrogen complex, namely $[(C_5Me_4H)_2Sc]_2(\mu\text{-}\eta^2\text{:}\eta^2\text{-}N_2)$. This complex shows a co-planar arrangement of a bridging side-on bound dinitrogen unit between the two scandium atoms, analogous to the lanthanide dinitrogen complexes. This is unusual in that it is unsolvated and because the four $(C_5Me_4H)^-$ rings define a square plane rather than a tetrahedron (Chapter 3). Valuable precursors for the preparation of lanthanide dinitrogen complexes are tetraphenylborate salts whose synthesis requires multiple steps. Therefore, borohydride rare earth metal complexes were prepared via one-pot-synthesis procedures and investigated with regard to dinitrogen activation, which

unfortunately did not occur (Chapter 4). Furthermore, scandium borane chemistry was explored yielding the 9-BBN substituted scandocene complexes $(C_5Me_4R)_2Sc(\mu\text{-}H)_2BC_8H_{14}$ (R = H, Me). Oxygen contamination of $(C_5Me_4R)_2Sc(\mu\text{-}H)_2BC_8H_{14}$ formed $(C_5Me_4R)_2Sc(\mu\text{-}O)BC_8H_{14}$ (Chapter 5). Tetraphenylborate salt complexes of general formula $(C_5R_5)_2M(BPh_4)$ (R = H, Me), however, are not only useful precursors for the activation of dinitrogen. In fact, they are excellent starting materials for the synthesis of highly reactive alkyl complexes, nitride as well as azide compounds and $(C_5Me_4R)_3M$ complexes (R = H, Me). Particularly, the latter tris(pentamethylcyclopentadienyl) and tris(tetramethylcyclopentadienyl) lanthanide complexes all show pentahapto coordination of the $(C_5Me_4R)^-$ ligands, which are of interest due to their high reactivity towards various substrates. For instance, one of the remarkable reaction modes of the tris(pentamethylcyclopentadienyl) complexes is sterically induced reduction (SIR). The postulated mechanism of many of these reactions requires a monohapto coordination of one of the penta/tetramethylcyclopentadienyl rings to the metal center for which no crystallographic or spectroscopic evidence has been reported so far. Despite this challenge, $(C_5Me_4H)_3Sc$ was prepared from the corresponding tetraphenylborate scandium cation and KC_5Me_4H (Chapter 6). X-ray crystallography revealed the solid state structure to be $(\eta^5\text{-}C_5Me_4H)_2Sc(\eta^1\text{-}C_5Me_4H)$. This was a spectacular result since this isolated compound represents the first example of a monohapto coordination of a tetramethylcyclopentadienyl ligand to a rare earth metal. Consequently, this supports the postulated monohapto coordination of a $(C_5Me_4R)^-$ ligand to the metal center for the reactions with lanthanide complexes. Obviously, metal size plays an important role: the change from the slightly bigger metal lutetium to the smaller scandium enables the generation of the elusive $(\eta^5\text{-}C_5Me_4H)_2M(\eta^1\text{-}C_5Me_4H)$. Furthermore, first reactivity tests with this complex were undertaken (Chapter 7). It can undergo sigma bond metathesis reactions with diphenyldichalcogenides PhEEPh (E = S, Se, Te). The same type of reaction was achieved by

the use of $(C_5Me_4H)_2Sc(\eta^3\text{-}C_3H_5)$. Depending on the presence of coordinating solvents, THF coordinated and non-coordinated products could be synthesized. Interestingly, one of the products, $(C_5Me_4H)_2ScSePh(THF)$, seems to rearrange with loss of coordinated THF to form an unprecedented scandium selenium cluster, $[(C_5Me_4H)Sc]_3[SePh]_3$, proven by X-ray crystallography (Chapter 7). Extending the ligand based reactivity of allyl complexes to $(C_5Me_5)_2Sc(\eta^3\text{-}C_3H_5)$ that possesses the bigger $(C_5Me_5)^-$ ligand set, included its synthesis and reaction with diphenylditelluride to yield an unexpected scandium tellurium cluster, $\{[(C_5Me_5)Sc]_4(\mu_3\text{-}Te)_4\}$ (Chapter 8).

One common decomposition product in lanthanide metallocene chemistry arises through the formation of an oxide complex of formula $[(C_5Me_4R)_2Ln]_2(\mu\text{-}O)$ (R = H, Me). Although the structural characterization of these complexes is important, spectroscopic identification also plays an important role, in particular via NMR spectroscopy. For this reason, efforts have been made to prepare the scandium oxide, which in only one case was co-crystallized with the scandium dinitrogen complex (Chapter 2). One of the attempts to generate such an oxide complex involves the use of nitrous oxide. Due to its weak σ donating and π accepting capabilities, laughing gas is commonly thought a poor ligand to transition metals. Surprisingly, N_2O inserted into the metal carbon bond of the allyl ligand of $(C_5Me_5)_2Sc(\eta^3\text{-}C_3H_5)$. This functionalization of nitrous oxide was extended to yttrium and lanthanide allyl complexes (Chapter 9). Other substrates can also insert into the scandium allyl-carbon bond such as carbodiimides, to give a scandium amidinate complex (Chapter 10). Hence, $(C_5Me_5)_2Sc(\eta^3\text{-}C_3H_5)$ has been proven to be an excellent precursor for various reactions. In one attempt to react it with 1,2-diphenylhydrazine, oxygen/water impurities formed an unexpected scandium hydroxo cluster, the core of which resembles the structural feature of lanthanide propoxides (Chapter 11).

Thus, the research comes to full circle: the solid state cluster chemistry initiated the solution chemistry and now the solution chemistry is making new cluster complexes.

1.13 References

(1) D. Mendelejeff, Zeitschrift für Chemie 12, 405-6 (1869). Reprinted in David M. Knight, ed., Classical Scientific Papers--Chemistry, Second Series, 1970; translation from German by Carmen Giunta.
(2) Nilson, L. F. *Comptes Rendus*, **1879**, *88*, 642-647.
(3) Nilson, L. F. *Berichte der deutschen chemischen Gesellschaft*, **1879**, *12*, 554-557.
(4) Cleve, P. T. *Comptes Rendus*, **1879**, *89*, 419-422.
(5) Fischer, W.; Brünger, K.; Grieneisen, H. *Z. Anorg. Allg. Chem.* **1937**, *231*, 54-62.
(6) Wedepohl, K. H. *Geochim. Cosmochim. Acta* **1995**, *59*, 1217-1232.
(7) Freeman, A. J.; Watson, R. E. *Phys. Rev.* **1962**, *127*, 2058.
(8) Dieke, G. H. *In Spectra and Energy Levels of Rare Earth Ions in Crystals*; Crosswhite, H. M. Crosswhite, H., Eds.; Wiley, New York, **1968**.
(9) Emeleus, H. J.; Sharpe, A. G.; *Modern Aspects of Inorganic Chemistry*, 4th ed.; Wiley: New York, 1999.
(10) Kaltsoyannis, N.; Scott, P. *The f-elements*; Oxford University Press: New York, 1999.
(11) Marks, T. J.; Ernst, R. D. *In Comprehensive Organometallic Chemistry*; Wilkinson, G.; Stone, F. G. A., Abel, E. W., Eds.; Pergamon: Oxford, U. K., 1982, Chapter 2.
(12) Schumann, H.; Meese-Marktscheffel, J. A.; Esser, L. *Chem. Rev.* **1995**, *95*, 865.
(13) Evans, W. J. *Polyhedron* **1987**, *6*, 803.
(14) Evans, W. J. *In The Chemistry of the Metal-Carbon Bond*; Hartley, F. R.; Patai, S.; Eds.; Wiley: New York, 1982; Chapter 12.
(15) Freeman, A. J.; Watson, R. E. *Phys. Rev.* **1962**, *127*, 2058-2075.
(16) Shannon, R. D. *Acta Cryst*. **1976**, *A32*, 751-767.
(17) Nair, V.; Balagopal, L.; Rajan, R.; Matthew, J. *Acc. Chem. Res.* **2004**, *37*, 21.
(18) Nair, V.; Deepthi, A. *Chem. Rev.* **2007**, *107*, 1862.
(19) Das, A. K. *Coord. Chem. Rev.* **2001**, *213*, 307.
(20) Meyer, G. *Chem. Rev.* **1988**, *88*, 93-107.
(21) Bochkarev, M. N.; Fedushkin, I. L.; Fagin, A. A.; Petrovskaya, T. V.; Ziller, J. W.; Broomhard-Dillard, R. N. R.; Evans, W. J. *Angew. Chem. Int. Ed. Engl.* **1997**, *36*, 113.
(22) Evans, W. J.; Allen, N. T.; Ziller, J. W. *J. Am. Chem. Soc.* **2000**, *122*, 11749-11750.
(23) Bochkarev, M. N.; Fedushkin, I. L.; Dechert, S.; Fagin, A. A.; Schumann, H. *Angew. Chem. Int. Ed.* **2001**, *40*, 3176.
(24) Hitchcock, P. B.; Lappert, M. F.; Maron, Laurent; Protchenko, A. V. *Angew. Chem. Int. Ed.* **2008**, *47*, 1488-1491.
(25) (a) Arnold, P. L.; Cloke, F. G. N.; Hitchcock, P. B.; Nixon, J. F. *J. Am. Chem. Soc.* **1996**, *118*, 7630-7631. (b) Clentsmith, G. K. B.; Cloke, F. G. N.; Green, J. C.; H., J.; Hitchcock, P. B.; Nixon, J. F. *Angew. Chem.* **2003**, *115*, 1068-1071.
(26) (a) Brennan, J. G.; Cloke, F. G. N.; Sameh; A. A.; Zalkin, A. *J. Chem. Soc., Chem. Commun.*, **1987**, 1668-1669. (b) Cloke, F. G. N. *Chem. Soc. Rev.* **1993**, *22*, 17 - 24. (c) Anderson, D. M.; Cloke, F. G. N.; Cox, P. A.; Edelstein, N.; Green. J. C.; Pang. T.; Sameh, A. A.; Shalimoff. G. *J. Chem.* Soc., *Chem. Commun.* **1989**, 53. (d) Arnold, P. L.; Cloke, F. G. N.; Hitchcock, P. B. *Chem. Commun.* **1997**, 481-482.
(27) (a) Evans, W. J.; Bloom, I; Hunter, W. E.; Atwood, J. L. *J. Am. Chem. Soc.* **1981**, *103*, 6507-6508. (b) Evans, W. J.; Grate, J. W.; Choi, H. W.; Bloom, I.; Hunter, W. E.; Atwood, J. L. *J. Am. Chem. Soc.* **1985**, *107*, 941-946.
(28) Evans, W. J.; Hughes, L. A.; Hanusa, T. P. *J. Am. Chem. Soc.* **1984**, *106*, 4270.
(29) Evans, W. J.; Hughes, L. A.; Hanusa, T. P. *Organometallics* **1986**, *5*, 1285.
(30) Evans, W. J.; Ulibarri, T. A. ; Ziller, J. W. *J. Am. Chem. Soc.* **1988**, *110*, 6877.
(31) Evans, W. J.; Hughes, L. A. Drummond, D. K.; Zhang, H.; Atwood, J. L. *J. Am. Chem. Soc.* **1986**, *108*, 1722.
(32) Evans, W. J.; Giarikos, D. G.; Robledo, C. B.; Leong, V. S.; Ziller, J. W. *Organometallics* **2001**, *20*, 5648.
(33) Bochkarev, M. N.; Fagin, A. A. *Chem. Eur. J.* **1999**, *5*, 2990.
(34) Morss, L. R. *Chem. Rev.* **1976**, *76*, 827.
(35) Evans, W. J.; Allen, N. T.; Ziller, J. W. *J. Am. Chem. Soc.* **2001**, *123*, 7927.
(36) Evans, W. J. *Inorg. Chem.* **2007**, *46*, 3435-3449.
(37) Evans, W. J.; Allen, N. T.; Ziller, J. W. *Angew. Chem. Int. Ed.* **2002**, *41*, 359-361.
(38) Evans, W. J.; Broomhall-Dillard, R. N. R.; Ziller, J. W. *Polyhedron* **1998**, *17*, 3361.
(39) de Boer, E. *Adv. Organomet. Chem.* **1964**, *2*, 115.
(40) Rabideau, P. W.; Marcinow, *Z. Org. React.* **1992**, *42*, 1.
(41) Evans, W. J.; Gonzales, S. L.; Ziller, J. W. *J. Am. Chem. Soc.* **1991**, *113*, 7423.
(42) White, D.; Taverner, B. C.; Leach, P. G. L.; Coville, N. J. *J. Comput. Chem.* **1993**, *14*, 1042.
(43) Stahl, L.; Ernst, R. D. *J. Am. Chem. Soc.* **1987**, *109*, 5673.
(44) Lubben, T. V.; Wolczanski, P. T. *J. Am. Chem. Soc.* **1987**, *109*, 424.

(45) Evans, W. J.; Forrestal, K. J.; Ziller, J. W. *J. Am. Chem. Soc.* **1995**, *117*, 12635-12636.
(46) Evans, W. J.; Perotti, J. M.; Kozimor, S. A.; Champagne, T. M.; Davis, B. L.; Nyce, G. W.; Fujimoto, C. H.; Clark, R. D.; Johnston, M. A.; Ziller, J. W. *Organometallics* **2005**, *24*, 3916-3931.
(47) Evans, W. J.; Mueller, T. J.; Ziller, J. W. *J. Am. Chem. Soc.* **2009**, *131*, 2678-2686.
(48) Evans, W. J.; Forrestal, K. J.; Ziller, J. W. *Angew. Chem. Int. Ed. Engl.* **1997**, *36*, 774-776.
(49) Evans, W. J.; Kozimor, S. A.; Ziller, J. W.; Kaltsoyannis, N. *J. Am. Chem. Soc.* **2004**, *126*, 14533-14547.
(50) Evans, W. J.; Kozimor, S. A.; Ziller, J. W. *J. Am. Chem. Soc.* **2003**, *125*, 14264.
(51) Evans, W. J.; Kozimor, S. A.; Nyce, G. W.; Ziller, J. W. *J. Am. Chem. Soc.* **2003**, *125*, 13831.
(52) Evans, W. J.; Mueller, T. J. ; Ziller, J. W. *Chem. Eur. J.* **2010**, *16*, 964.
(53) Mueller, T. J.; Ziller, J. W.; Evans, W. J. *Dalton Trans.* **2010**, *39*, 6767-6773.
(54) a) Freedman, D.; Emge, T. J.; Brennan, J. G. *J. Am. Chem. Soc.* **1997**, *119*, 11112. b) Banarjee, S.; Huebner, L.; Romanelli, M. D.; Kumar, G. A.; Riman, R. E.; Emge, T. J.; Brennan, J. G. *J. Am. Chem. Soc.* **2005**, *127*, 15900.
(55) Mashima, K.; Nakayama, Y.; Shibahara, T.; Fukumoto, H.; Nakamura, A. *Inorg. Chem.* **1996**, *35*, 93.
(56) Hillier, A. C.; Liu, S.; Sella, A.; Elsegood, M. R. J. *Inorg. Chem.* **2000**, *39*, 2635.
(57) (a) Evans, W. J.; Miller, K. A.; Ziller, J. W. *Inorg. Chem.* **2005**, *44*, 4326. (b) Evans, W. J.; Takase, M. K.; Ziller, J. W.; DiPasquale, A. G.; Rheingold, A. L. *Organometallics* **2009**, *28*, 263.
(58) Bradburry, J. R.; Masters, A. F.; McDonell, A. C.; Brunette, A. A.; Bond, A. M.; Wedd, A. G. *J. Am. Chem. Soc.* **1981**, *103*, 1959.
(59) Liftman, V.; Albeck, M. *Electrochim. Acta* **1984**, *29*, 95.
(60) Thompson, M. E.; Baxter, S. M.; Bulls, A. R.; Burger, B. J.; Nolan, M. C.; Santasiero, B. D.; Schaefer, W. P.; Bercaw, J. E. *J. Am. Chem. Soc.* **1987**, *109*, 203-219.
(61) Beletskaya, I. P.; Voskoboynikov, A. Z.; Shestakova, A. K.; Yanovsky, A. I.; Fukin, G. K.; Zacharov, L. N.; Struchkov, Y. T.; Schumann, H. *J. Organomet. Chem.* **1994**, *468*, 121.
(62) Evans, W. J.; Nyce, G. W.; Clark, R. D.; Doedens, R. J.; Ziller, J. W. *Angew. Chem. Int. Ed.* **1999**, *38*, 1801.
(63) Evans, W. J.; Davis, B. L. *Chem. Rev.* **2002**, *102*, 2119.
(64) Evans, W. J.; Davis, B. L.; Champagne, T. M.; Ziller, J. W. *Proc. Natl. Acad. Sci. U. S. A.* **2006**, *103*, 12678.
(65) a) Lin, X.; Stien, D.; Weinreb, S. M. *Tetrahedron Lett.* **2000**, *41*, 2333. b) Booker-Milburn, K. I.; Barker, A.; Brailsford, W.; Cox, B.; Mansley, T. E. *Tetrahedron* **1998**, *54*, 15321. c) Milburn, K. I.; Jones, J. L.; Sibley, G. E. M.; Cox, R.; Meadows, J. *Org. Lett.* **2003**, *5*, 1107.
(66) Davies, A. G.; Lusztyk, J. *J. Chem. Soc., Perkin Trans. 2*, **1981**, *4*, 692.
(67) Evans, W. J.; Lee, D. S.; Rego, D. B.; Perotti, J. M.; Kozimor, S. A.; Moore, E. K.; Ziller, J. W. *J. Am. Chem. Soc.* **2004**, *126*, 14574-14582.
(68) Evans, W. J.; Lee, D. S.; Johnston, M. A.; Ziller, J. W. *Organometallics* **2005**, 24, 6393-6397.
(69) Evans, W. J.; Lee, D. S.; Lie, C.; Ziller, J. W. *Angew. Chem., Int. Ed.* **2004**, *43*, 5517-5519.
(70) Nechaeva, O. N.; Pushkareva, *Z. V. Zh. Obshch. Khim.* **1958**, *28*, 2693.
(71) Evans, W. J.; Lorenz, S. L.; Ziller, J. W. *Inorg. Chem.* **2009**, *48*, 2001-2009.
(72) Lamy, E.; Nadjo, L.; Saveant, J. M. *Electroanal. Chem.* **1977**, 78, 403.
(73) Evans, W. J.; Lee, D. S.; Ziller, J. W.; Kaltsoyannis, N. *J. Am. Chem. Soc.* **2006**, *128*, 14176-14184.
(74) Evans, W. J.; Grate, J. W.; Hughes, L. A.; Zhang, H.; Atwood, J. L. *J. Am. Chem. Soc.* **1985**, *107*, 3728-3730.
(75) Atwood, J. L.; Smith, K. D. *J. Am. Chem. Soc.* **1973**, *95*, 1488-1491.
(76) Eggers, S. H.; Schultze, H.; Kopf, J.; Fischer, R. D. *Angew. Chem. Int. Ed.* **1986**, *25*, 656.
(77) Cotton, S. *Lanthanide and Actinide Chemistry*, Wiley, **2006**, 114.
(78) Evans, W. J.; Perotti, J. M.; Ziller, J. W. J. Am. Chem. Soc. 2005, 127, 3894-3909.
(79) Putzer, M. A.; Bartholomew, G. P. *Z. Anorg. Allg. Chem.* **1999**, *625*, 1777-1778.
(80) Bochkarev, L. N.; Stepantseva, T. A.; Zakharov, L. N.; Fukin, G. K.; Yanovsky, A. I.; Struchkov, Y. T. *Organometallics* **1995**, *14*, 2127-2129.
(81) Holleman, A. F.; Wiberg, E. *Lehrbuch der Anorganischen Chemie*, de Gruyter, 102. Auflage, Berlin, 2007.
(82) McCollum, B. C.; Camp, M. J.; Corbett, J. D. *Inorg. Chem.* **1973**, *12*, 778.
(83) Poeppelmeier, K. R.; Corbett, J. D. *Inorg. Chem.* **1977**, *16*, 1107.
(84) a) McCollum, B. C.; Dudis, D. S.; Lachgar, A.; Corbett, J. D. *Inorg. Chem.* **1990**, *29*, 2030-2032. b) Meyer, G.; Gerlitzki, N.; Hammerich, S. *J. Alloys Compd.* **2004**, *380*, 71-78. c) Meyer, G.; Jongen, L.; Mudring, A.-V.; Möller, A. *Inorganic Chemistry in Focus* (Eds.: Meyer, G.; Naumann, D.; Wesemann, L.), Wiley-VCH, Weinheim, **2005**, vol. 2, 105–120.
(85) Cotton, F. A.; Wilkinson, G. *Advanced Inorganic Chemistry*, Wiley-Interscience, New York,1988.
(86) Park, Y.; Martin, J. D.; Corbett, *J. D. J. Solid State Chem.* **1997**, *129*, 277-286.
(87) Hughbanks, T.; Corbett, J. D. *Inorg. Chem.* **1988**, 27, 2022–2026.
(88) Payne, M. W.; Corbett, J. D. *Inorg. Chem.* **1990**,29, 2246–2251.
(89) Corbett, J. D. *Rev. Chim. Miner.* **1973**, *10*, 239–257.

(90) Corbett, J. D. *J. Chem. Soc. Dalton Trans.* **1996**, 575–587.
(91) Corbett, J. D. *Inorg. Chem.* **2000**, *39*, 5178–5191.
(92) Corbett, J. D. *J. Alloys Compds* **2006**, *418*, 1–20.
(93) Meyer, G. &Wickleder, M. S. (2000). *Handbook on the Physics and Chemistry of Rare Earths*, edited by K. A. Gscheidner Jr. & L. Eyring, Vol. 28, Elsevier, Amsterdam, 53–129.
(94) Simon, A. *Angew. Chem. Int. Ed. Engl.* **1981**, *20*, 1–22.
(95) Simon, A.; Mattausch, Hj.; Miller, G. J.; Bauhofer, W.; Kremer, R. *Handbook on the Physics and Chemistry of Rare Earths*, edited by K. A. Gschneidner Jr. & L. Eyring, Vol. 15,. Elsevier, Amsterdam, 1991, 191–285.
(97) Wiglusz, R., Pantenburg, I.; Meyer, G. *Z. Anorg. Allg. Chem.* **2007**, *633*, 1317–1319.
(98) Dudis, D. S.; Corbett, J. D.; Hwu, S.-J. *Inorg. Chem.* **1986**, *25*, 3434-3438.
(99) Payne, M. W.; Dorhout, P. K.; Corbett, J. D. *Inorg. Chem.* **1991**, *30*, 1467 -1472. Corrections on page 3112.
(100) Kauzlarich, S. M.; Hughbanks, T.; Corbett, J. D.; Kalvins, P.; Shelton, R. N. *Inorg. Chem.* **1988**, *27*, 1791.
(101) Nagaki, D.; Simon, S.; Borrmann, H. *J. Less.-Common Met.* **1989**, *156*, 193.
(102) Jongen, L.; Mudring, A.V.; Meyer, G. *Angew. Chem., Int. Ed.* **2006**, *45*, 1886-1889.
(103) Hwu, S.-J.; Dudis, D. S.; Corbett, J. D. *Inorg. Chem.* **1987**, *26*, 469-473.
(104) Hwu, S.-J.; Corbett, J. D.; Poeppelmeier, K .R. *J. Solid State Chem.* **1985**, *57*, 43-58.
(105) Mattausch, H. J.; Hendricks, J. B.; Eger, R.; Corbett, J. D.; Simon, A. Inorg. Chem. **1980**, *19*, 2128-2132.
(106) Berroth, K.;Simon, A. *J. Less-Common Met.* **1980**, *76*, 41-54.
(107) Poeppelmeier, K. R.; Corbett, J. D.; McMullen, T. P.; Torgeson, D. R.; Barnes, R. G. *Inorg. Chem.* **1980**, *19*, 129.
(108) Corbett, J. D.; Meyer, G. *Inorg. Chem.* **1981**, *20*, 2627.
(109) Cotton, A. F.; Diebold, M. P; Roth, W. J. *J. Am. Chem. Soc.* **1987**, *109*, 2833-2834.
(110) Cotton, A. F.; Kibala, P. A.; Roth, W. J. *J. Am. Chem. Soc.* **1988**, *110*, 298-300.
(111) (a) Runyan, C. E., Jr.; Hughbanks, T. *J. Am. Chem. Soc.* **1994**, *116*, 7909-7910. (b) Tian, Y.; Hughbanks, T. *Inorg. Chem.* **1995**, *34*, 6250-6254. (c) Tian, Y.; Hughbanks, T. *Z. Anorg. Allg. Chem.* **1996**, *622*, 425-431. (c) Sun, D.; Hughbanks, T. *Inorg. Chem.* **1999**, *38*, 992-997. (d) Harris, J. D.; Hughbanks, T. *J. Am. Chem. Soc.* **1997**, *119*, 9449-9459. (e) Xie, X.; Hughbanks, T. *J. Am. Chem. Soc.* **1998**, *120*, 11391-11400.
(112) Xie, X.; Jones, J. N.; Hughbanks, T. *Inorg. Chem.* **2001**, *40*, 522-527.
(113) (a) Smith, J. D.; Corbett, J. D. *J. Am. Chem. Soc.* **1984**, *106*, 4618-4619. (b) Ziebarth, R. P.; Corbett, J. D. *J. Am. Chem. Soc*. 1985, 107, 4571-4573. (c) Smith, J. D.; Corbett, J. D. *J. Am. Chem. Soc.* **1985**, *108*, 5704-5711. (d) Smith, J. D.; Corbett, J. D. *J. Am. Chem. Soc.* **1986**, *108*, 1927-1934. (e) Hughbanks, T.; Rosenthal, G.; Corbett, J. D. *J. Am. Chem. Soc.* **1986**, *108*, 8389. (f) Ziebarth, R. P.; Corbett, J. D. *J. Am. Chem. Soc.* **1989**, *111*, 3272.
(114) Flemming, A.; Köckerling, M. *Angew. Chem., Int. Ed.* **2009**, *48*, 2605-2608.

Chapter 2

Reactivity of $Sc\{Sc_6C\}I_{12}$: Attempts to Excise $\{Sc_6C\}$ from the Solid State

2.0 Introduction

Long before it became clear where the rare earth elements would be placed in the periodic table of the elements, it was known that some of them could be reduced to the divalent state, namely europium, samarium, and ytterbium.[1] The solid-state chemistry community needed a few further decades to establish that there are pseudo-alkaline-earth halides with rare-earth elements M with electronic configurations of $[Xe]6s^0\mathbf{5d^0 4f^n}$ for M^{2+} (M = Nd, Eu, Sm, Dy, Tm, Yb). Moreover, the configuration crossover to $[Xe]6s^0\mathbf{5d^1 4f^{n-1}}$ offered hitherto unexpected possibilities as delocalization of the $5d^1$ electron into a band as in LaI_2 or the formation of (mostly octahedral) metal clusters for all the other rare earth elements.[2] For the solution/coordination chemistry community, it took much longer because chemistry even with the six $5d^0 4f^n$ elements mentioned above is highly unlikely in protic solvents (except maybe with Eu^{2+} with a reduction potential of –0.35 V) as well as in other solvents and with all ligands that are not stable against reduction. However, much progress has been made in recent years and new synthetic routes have been developed such that chemistry of rare-earth elements in oxidation states below +3 (mostly +2) is now well established for the magic six (Nd, Eu, Sm, Dy, Tm, Yb) and even with Sc, La and Ce.[3] Even complexes of higher nuclearity have been obtained, although, in a stricter sense, they may not be called cluster complexes.

With a few exceptions, rare earth metal clusters $\{M_x\}$ need to sequester an endohedral atom Z to make up for the electron deficiency of these group 3 elements. Due to this, condensed cluster complexes are more common than isolated clusters. One metal cluster compound type which appears for almost all of the rare earth elements (except those who require $5d^0 4f^n$ configuration, Eu, Yb, Sm, Tm) is the $M_7X_{12}Z = \{ZM_6\}X_{12}M$ type. By

experience, $\{CSc_6\}I_{12}Sc$ appears to be the most stable compound in the ternary system C/Sc/I which otherwise features cluster chains as in $\{(C_2)Sc_6\}I_{11}$ and $\{C_2)Sc_4\}I_6$ and the oligomeric T3-supertetrahedron $\{C_{10}Sc_{24}\}I_{30}Sc$.[4]

The interest is directed to molecular metal-rich fragments. Stabilization of a rare earth metal cluster, for example a carbon centered scandium octahedron $\{CSc_6\}$, by any kind of molecules could provide a previously unobserved molecular rare earth metal cluster. If a successful route was found, this synthetic route could be conceivable for the isolation of all missing molecular low-valent rare earth complexes by expanding this reaction to all of the lanthanides and yttrium. The challenging part though is the search for an appropriate ligand set to achieve this goal.

This chapter describes first attempts to establish rare earth clusters in solution and to establish new (organometallic) cluster complexes. Therefore, we have followed the route to excise clusters from solids and have chosen $\{CSc_6\}I_{12}Sc$, **1**, as our starting material.

2.1 Multigram Synthesis of the Solid $\{CSc_6\}I_{12}Sc$

In $\{CSc_6\}I_{12}Sc$, **1**, an endohedral carbon atom is surrounded by an octahedral scandium cluster and in the second coordination sphere by 12+6 iodide ligands; a seventh Sc atom occupies a "normal" octahedral hole provided by six I^- anions, which the simple *anti*-Werner-complex nomenclature,[2k] $\{CSc_6\}I_{12}Sc$, clearly exhibits. The $\{CSc_6\}$ cluster is actually surrounded by 18 iodide ligands of which 12 are involved in a-i and i-a connections, according to $[\{CSc_6\}I^{i}_{6}I^{i\text{-}a}_{6/2}I^{a\text{-}i}_{6/2}]Sc$, see Figure 2.1.1.

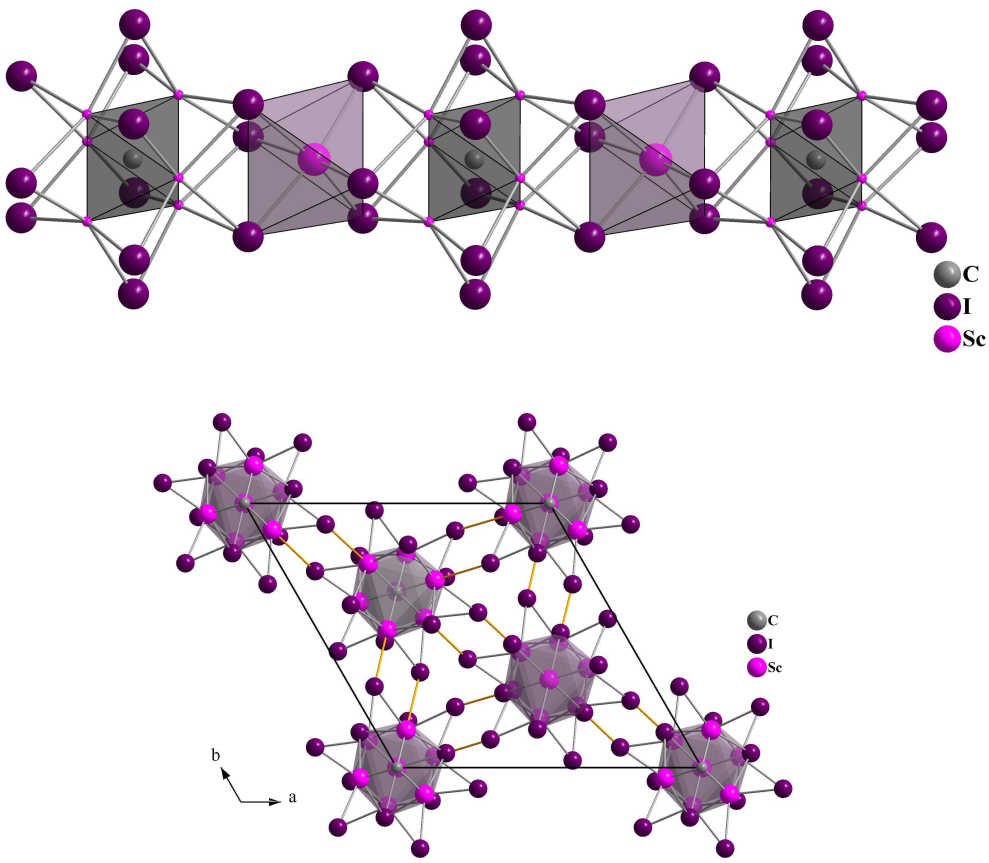

Figure 2.1.1. Crystal structure of $\{CSc_6\}I_{12}Sc$, **1**. Part of the chains ...$[\{CSc_6\}I_6]I_3ScI_3$... (top) and their connection via i-a/a-i bridges according to $[\{CSc_6\}I^{i}_{6}I^{i-a}_{6/2}I^{a-i}_{6/2}]Sc$ (bottom).

For a multi-gram synthesis of $\{CSc_6\}I_{12}Sc$, **1**, from carbon, scandium and scandium(III) iodide, ScI_3, an optimized synthetic route was established.[5] It depends strongly on the cooling rate from 850 °C, the reaction temperature, to ambient temperature. The faster the samples are quenched, the higher is the yield of $\{CSc_6\}I_{12}Sc$, **1**. The only (unavoidable) byproduct was scandium diiodide, $Sc_{0.89}I_2$, the only stable reduced scandium iodide in the binary system Sc/I.[6] Due to its pronounced crystal habit, it could be separated mechanically from the reaction mixture. Thus, pure samples of **1** were obtained as attested by the X-ray diffraction powder pattern as shown in Figure 2.1.2. It is compared with a powder pattern calculated from its own single crystal data[5,7] which perfectly match literature data.[4]

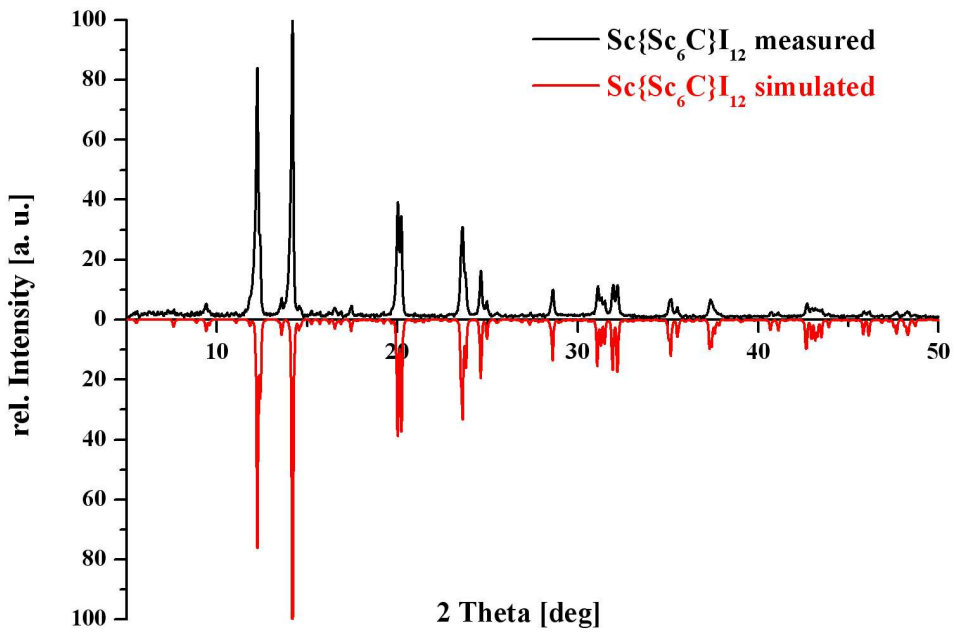

Figure 2.1.2. X-ray powder diffraction patterns of $\{CSc_6\}I_{12}Sc$, **1**. Top: measured with Mo-Kα radiation, bottom: calculated for Mo-Kα radiation with single crystal data.[4,7]

2.2 Attempts to Excise the $\{CSc_6\}$ Cluster from $\{CSc_6\}I_{12}Sc$ by the Use of Solvents

A series of dried solvents were tested in order to excise the $\{CSc_6\}$ cluster without destruction of the cluster as embedded in solid $\{CSc_6\}I_{12}Sc$. As expected, $\{CSc_6\}I_{12}Sc$ does not show any reactivity in nonpolar solvents like toluene, pentane or hexane. The use of protic solvents was avoided because previous experience has shown that rare earth cluster complexes are typically destroyed in such solvents. Even traces of water (moisture) leads to total decomposition yielding products such as $Sc(OH)_3$. However, $\{CSc_6\}I_{12}Sc$ dissolves in the polar solvents N,N-dimethyl-acetamide (DMA) or tetrahydrofuran (THF) and these solutions were investigated by ^{45}Sc NMR Spectroscopy.[5]

Solutions of **1** in DMA are EPR active. Two signals with axial symmetry (axially elongated, $g_{\parallel} > g_{\perp}$) were observed in glassy frozen solutions (at 110 K) at X band frequency with the following g values: $g_{1\parallel} = 3.10$ and $g_{1\perp} = 2.24$; $g_{2\parallel} = 2.46$ and $g_{2\perp} = 2.10$ (Figure 2.2.1). The two signals appear in an approximately 1:1 ratio and they do not reveal any hyperfine coupling to the ^{45}Sc isotope (nuclear spin $I = 7/2$, 100% natural abundance). Since

the nuclear spin of 7/2 would result in eight lines, the observed line width of about 200 G means that the (unresolved) hyperfine coupling constants do not exceed 25 G. Paramagnetic Sc^{2+} ($3d^1$) in solid matrices exhibits *g* values of 2.000 for ScO in argon at 4.2 K, *g* = 1.951 for $[ScF_8]^{6-}$ in CaF_2 (1.5 K) and *g* = 1.936 for $[ScF_8]^{6-}$ in SrF_2.[8] In $Sc_{0.89}I_2$, which is in fact $(Sc^{3+})_2(Sc^{2+})_6(I^-)_{18}$, an isotropic signal with no hyperfine structure is observed at *g* = 1.99 at temperatures below 100 K.[5c] Apart from these solid samples, there is also a report on the organometallic complex $[\{Sc(P_3C_2{}^tBu_2)_2\}_2]$ with an isotropic *g* value of 1.9823 and a ^{45}Sc hyperfine coupling constant of 37 G.[3f] In all these compounds, isolated Sc^{2+} species give rise to the EPR spectrum. For **1**, both signals exhibit *g* values above g_e = 2.0023 (the value of the free electron). While *g* values smaller than g_e are typical for isolated Sc^{2+} ions with marked spin-orbit coupling, *g* values larger than g_e point to species, which are characterized by a delocalized singly occupied molecular orbital (SOMO) and close-lying further unoccupied MOs.[8] This and the non-resolved hyperfine coupling are in line with the assumption that the two signals observed in DMA solution arise from scandium-cluster atoms. Whether two different $\{ZSc_x\}$ clusters are present in DMA solution, or one cluster with two different scandium sites, it cannot be decided from the EPR experiments. Indeed, in $\{CSc_6\}I_{12}Sc$ there are 13 cluster-based electrons available for intra-cluster bonding. In a localized picture, the MO scheme must contain a SOMO which is "delocalized" over the $\{CSc_6\}$ cluster.

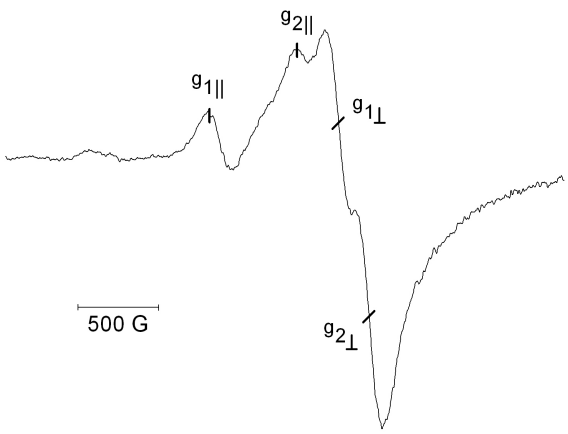

Figure 2.2.1. X-band EPR spectrum of the solution of **1** in glassy frozen DMA at 110 K.

EPR spectra of solutions of **1** in THF reveal signals very similar to those observed in the DMA solution. In glassy frozen solutions (at 110 K) at X-band frequency, two signals in a 1:1 ratio were observed with the following g values: $g_{1\parallel}$ = 3.11 and $g_{1\perp}$ = 2.24; $g_{2\parallel}$ = 2.47 and $g_{2\perp}$ = 2.10, Figure 2.2.2. Again, no hyperfine coupling to the ^{45}Sc isotope is observed.

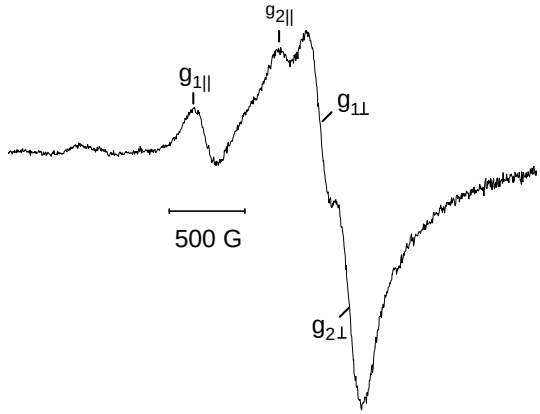

Figure 2.2.2. X-band EPR spectrum of the solution of **1** in glassy frozen THF at 110 K.

2.3 ^{45}Sc-MAS-NMR Spectrum of {CSc_6}I_{12}Sc

The ^{45}Sc-MAS-NMR spectrum of solid {CSc_6}I_{12}Sc shows only one peak centered at 434 ppm, Figure 2.3.1. From the width of the sideband manifold a quadrupole coupling constant of ca. 2 MHz is calculated. In the crystal structure of **1**, there are three crystallographically different scandium positions: while Sc2 and Sc3 are part of the {CSc_6} cluster core, Sc1 stands for the seventh scandium atom in {CSc_6}I_{12}*Sc*. Quadrupole coupling constants for all scandium positions were determined by quantum chemical calculations (WIEN2K).[9] These are 2.3 MHz for Sc1, 9.1 MHz for Sc2 and 7.0 MHz for Sc3. Only the calculated quadrupole coupling constant of 2.3 MHz matches the experimental value of 2 MHz. Thus, the cluster scandium atoms within **1** cannot be observed by solid-state ^{45}Sc-MAS-NMR spectroscopy. Either the corresponding peak(s) is (are) too broad to be observed or the paramagnetism of the 13-electron cluster unit {CSc_6} is responsible for the failure to obtain a ^{45}Sc-MAS-NMR spectrum for the cluster scandium atoms of **1**.

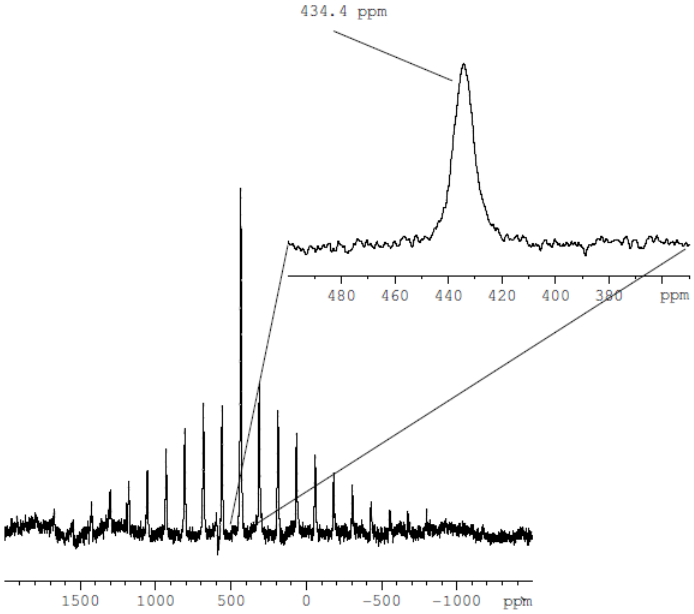

Figure 2.3.1. ^{45}Sc-MAS-NMR spectrum of solid $\{CSc_6\}I_{12}Sc$.

2.4 Attempts to Excise the $\{CSc_6\}$ Cluster from $\{CSc_6\}I_{12}Sc$ by its Reaction with KC_5H_5 in THF

For an excision of a $\{CSc_6\}$ cluster from $\{CSc_6\}I_{12}Sc$, ideally all iodides have to be removed. One way to do this might be a salt metathesis reaction by the use of 12 equiv. of an alkali metal ligand salt to remove the 12 iodide atoms, Figure 2.4.1. For charge equalization, the donating ligand should be a monoanionic ligand, which could drive the reaction to completion. The idea is that a monoanionic ligand can coordinate directly to one metal center, thus better filling the coordination sphere of the metal cluster. The stabilization of the metal rich fragment is thought to work better with a π-conjugated donating ligand set, such as aromatic systems.

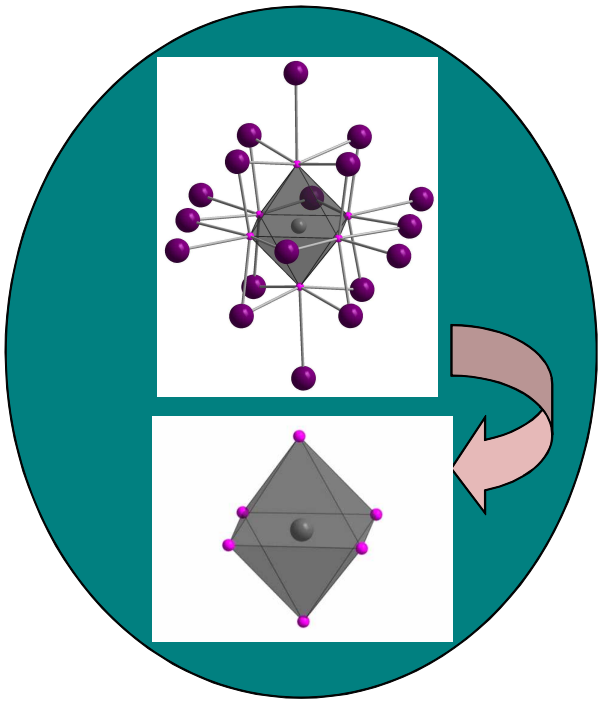

Figure 2.4.1. Excision of $\{CSc_6\}$.

Furthermore, it is thought that the use of small ligands, especially for a scandium cluster, is more appropriate. One promising ligand might be $(C_5H_5)^-$.

In this chapter, the reaction of $\{CSc_6\}I_{12}Sc$ with 12 equiv. of KCp to yield dark solutions is described. From the reaction conducted under a dinitrogen atmosphere, a scandium nitride, namely $[(C_5H_5)_2ScNSc(C_5H_5)(THF)]_2$, **2**, could be isolated. The analogous reaction under an argon atmosphere gave a dark solution from which a scandium propoxide complex, $[(C_5H_5)_2Sc]_2[\mu\text{-}O(C_3H_7)]_2$, **3**, was obtained.

Experimental

All manipulations were performed under nitrogen or argon with rigorous exclusion of air and water using glove-box, Schlenk, and vacuum line techniques. Solvents were sparged with UHP argon and dried over columns containing Q-5 and molecular sieves. Elemental analyses were performed on a Perkin Elmer 2400 Series II CHNS analyzer. $\{CSc_6\}I_{12}Sc$, **1**, was prepared according to literature.[4,5] KC_5H_5 was prepared according to literature.[10]

$[(C_5H_5)_2ScNSc(C_5H_5)(THF)]_2$, 2. In a nitrogen-filled glovebox, 12 equiv. of KC_5H_5 (0.072 g, 0.69 mmol) were slowly added to a stirred black slurry of $\{Sc_6C\}I_{12}Sc$, **1**, (0.107 g, 0.0579 mmol) in 20 mL of THF. After the mixture was stirred for 84 h, the solution was centrifuged to remove insoluble materials, presumably KI, and evaporated to dryness. The resulting pale redbrown powder was extracted with 2 mL of THF to give a dark red-brown solution that was cooled to -35 °C. Over the course of 2 days colorless material precipitated which was removed by centrifugation and filtration. The solution was concentrated and stored again at -35 °C. This purification cycle was repeated until no colorless material precipitated out of solution yielding an oily dark red-brown product. Dark orange crystals suitable for X-ray diffraction were obtained in an NMR tube from a concentrated THF-d_8 solution at 25 °C over the course of 2 weeks.

$[(C_5H_5)_2Sc]_2[\mu\text{-}O(C_3H_7)]_2$, 3. Following the procedure for **2**, in an argon-filled glovebox, KC_5H_5 (0.070 g, 0.67 mmol) and $\{Sc_6C\}I_{12}Sc$, **1**, (0.103 g, 0.0557 mmol) were combined in 18 mL of THF. Golden crystals suitable for X-ray diffraction were obtained in an NMR tube from a concentrated THF-d_8 solution at 25 °C over the course of 3 weeks.

X-Ray Crystallographic Data. X-Ray data collection parameters of **2** and **3** are summarized in Table 2.4.1. Details for X-ray data collection, structure, solution and refinement are given in the Appendix.

Results and Discussion

(a) Reaction of $\{CSc_6\}I_{12}Sc$ with KCp under Dinitrogen Atmosphere

The reaction of **1** with 12 equiv of KCp in THF under dinitrogen atmosphere shows after 3.5 days full consumption of **1** resulting in a red-brown solution. Out of this solution a scandium nitride complex, $[(C_5H_5)_2ScNSc(C_5H_5)(THF)]_2$, **2**, could be isolated, eq 2.4.1, Figure 2.4.2-2.4.4. The X-ray diffraction data showed the existence of four scandium atoms which are linked to each other by nitrogen atoms in the compound.

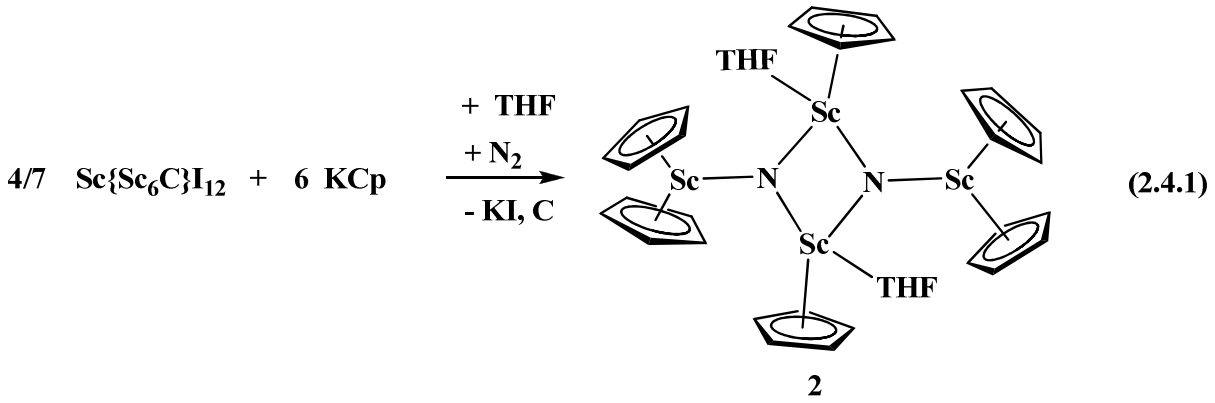

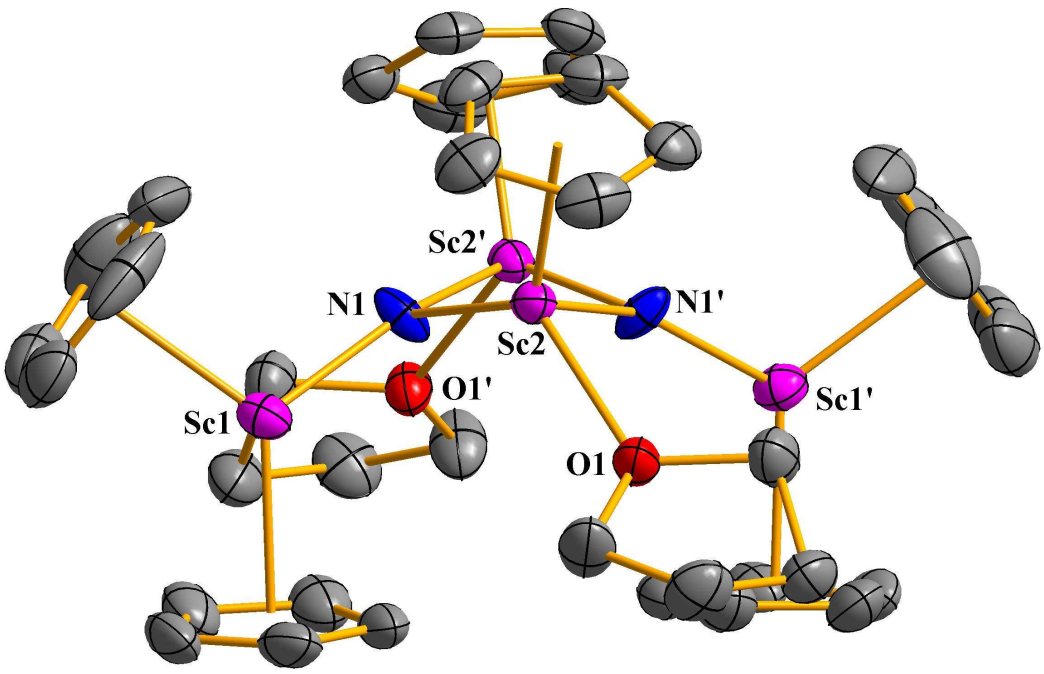

Figure 2.4.2. Thermal ellipsoid plots of $[(C_5H_5)_2ScNSc(C_5H_5)(THF)]_2$, **2**, drawn at the 50% probability level. Hydrogen atoms are omitted for clarity.

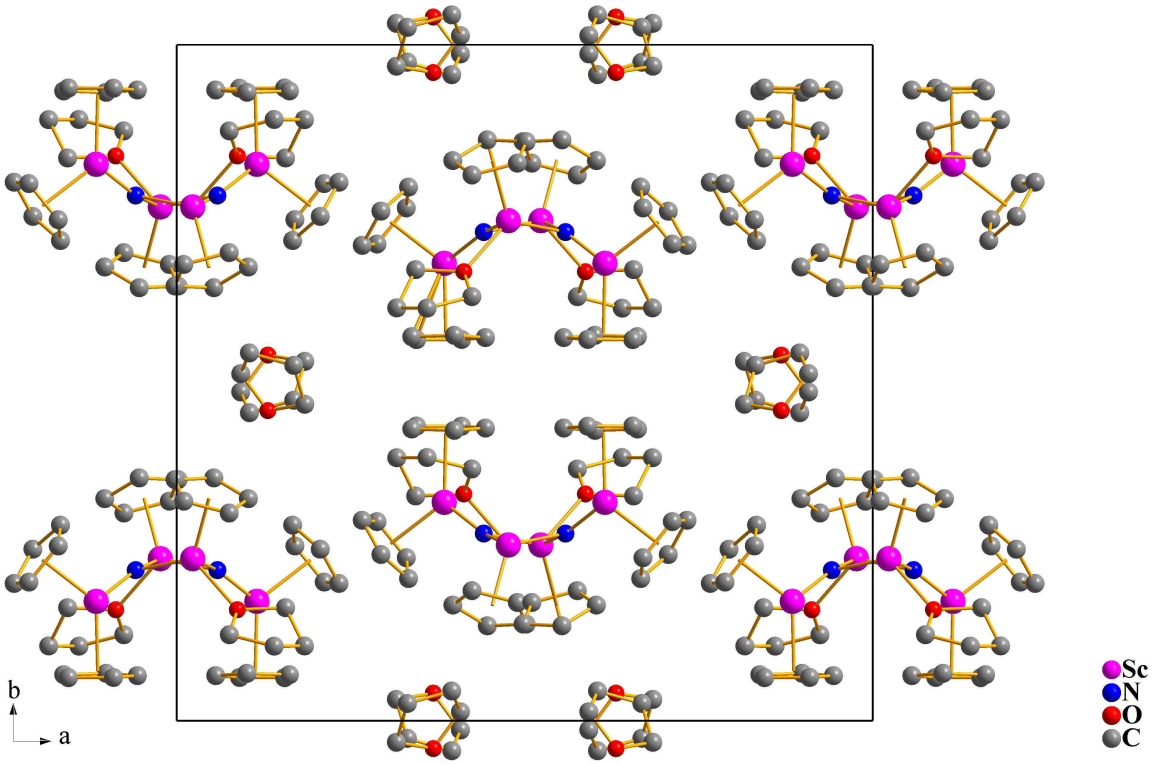

Figure 2.4.3. Crystal structure of $[(C_5H_5)_2ScNSc(C_5H_5)(THF)]_2$, **2**. View along the c-axis. Hydrogen atoms are omitted for clarity.

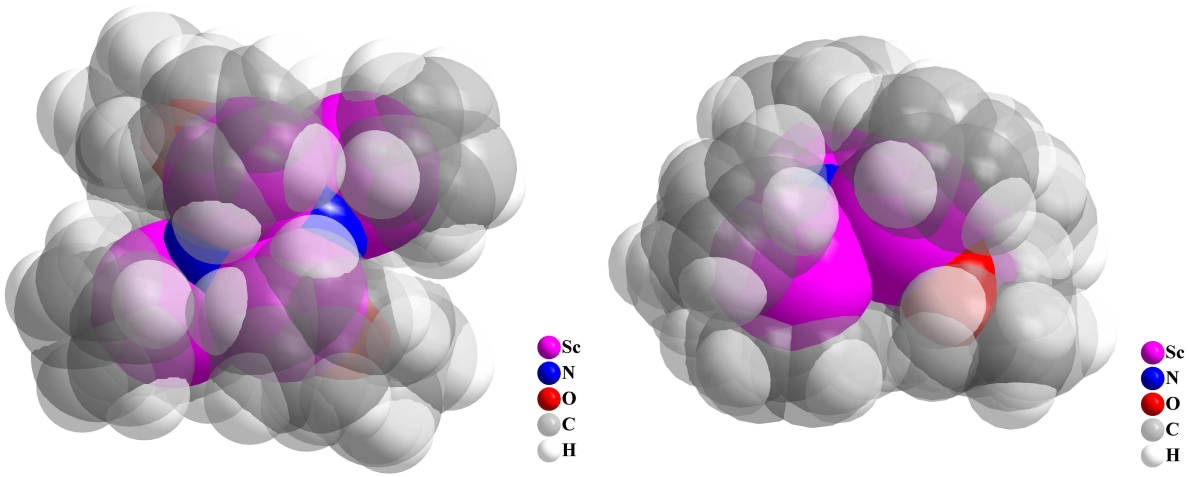

Figure 2.4.4. Two space-filling diagrams of $[(C_5H_5)_2ScNSc(C_5H_5)(THF)]_2$, **2**, with 50% transparency of carbon and hydrogen atoms.

Since it is often difficult to distinguish nitrogen and oxygen atoms from each other by X-ray crystallography, it might be conceivable that the defined nitrogen atoms in **2** could also be oxygen atoms. However, the elemental analysis of **2** showed a significant nitrogen percentage while none of the starting materials, **1** and KCp, contain nitrogen. If we assume that the entire redbrown product is **2**, then we would expect for elemental analysis C, 61.46; H, 6.24; N, 3.77, while we found C, 53.19; H, 6.10; N, 1.13. The self-evident huge discrepancy between the experimental and calculated EA values for nitrogen is due to the very difficult purification of **2**. The product is soluble in THF, however it is not soluble in a more nonpolar solvent such as toluene owing to the nature of the $(C_5H_5)^-$ ligand. However, all of the byproducts are also soluble in THF, making it difficult to separate them from the main product, which explains the discrepancy between theoretical and experimental values. A second hint for the existence of nitrogen in **2** is charge equalization. If **2** contains nitrogen, then the compound is neutral according to 6 $(C_5H_5)^-$, 2 N^{3-} and 4 Sc^{3+}. If we expect that instead of nitrogen atoms, there are oxygen atoms, then the entire molecule would have two delocalized electrons due to charge equalization: 6 $(C_5H_5)^-$, 2 O^{2-}, 2 e^- and 4 Sc^{3+}. A third indication for the existence of nitrogen in **2** is that **2** is EPR inactive. There are no similar

molecular scandium nitride complexes reported except the numerous encapsulated Sc_3N units in fullerenes.[11-18]

Table 2.4.1. X-ray Data Collection Parameters for $[(C_5H_5)_2ScNSc(C_5H_5)(THF)]_2$, **2**, and $[(C_5H_5)Sc]_2[\mu\text{-}O(C_3H_7)]_2$, **3**.

Complex	**2**	**3**
Empirical formula	$C_{38}H_{46}N_2O_2Sc_4$ • $2(C_4H_8O)$	$C_{26}H_{34}O_2Sc_2$
Fw	886.82	468.45
Temperature (K)	153(2)	98(2)
Crystal system	Orthorhombic	Tetragonal
Space group	*Pbcn*	$P4_22_12$
a (Å)	20.8031(16)	17.1961(6)
b (Å)	20.2022(16)	17.1961(6)
c (Å)	10.4370(8)	8.0473(3)
α (deg)	90	90
β (deg)	90	90
γ (deg)	90	90
Volume ($Å^3$)	4386.3(6)	2379.63(15)
Z	4	4
ρ_{calcd} (Mg/m^3)	1.343	1.308
μ (mm^{-1})	0.636	0.589
$R1\ [I > 2.0\sigma(I)]^a$	0.0612	0.0304
$wR2\ (all\ data)^a$	0.1815	0.0856

[a] Definitions: $wR2 = [\Sigma[w(F_o^2-F_c^2)^2] / \Sigma[w(F_o^2)^2]]^{1/2}$, $R1 = \Sigma||F_o|-|F_c|| / \Sigma|F_o|$

(b) Reaction of $\{CSc_6\}I_{12}Sc$ with KCp under Argon Atmosphere

The reaction of **1** with 12 equiv of KCp in THF under an argon atmosphere shows after 3.5 days full consumption of **2** resulting in a dark brown solution. Out of this reaction, a

dimeric scandium propoxide complex, namely $[(C_5H_5)Sc]_2[\mu\text{-}O(C_3H_7)]_2$, **3**, could be isolated, eq (2.4.2), Figure 2.4.5.

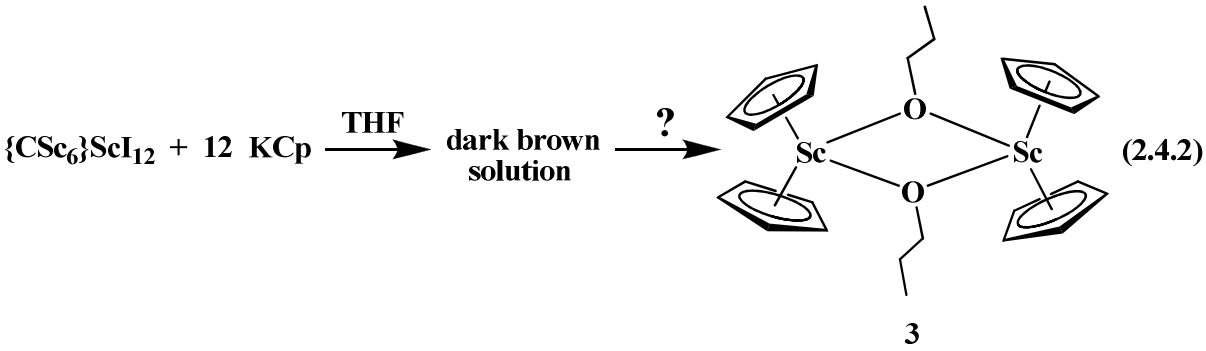

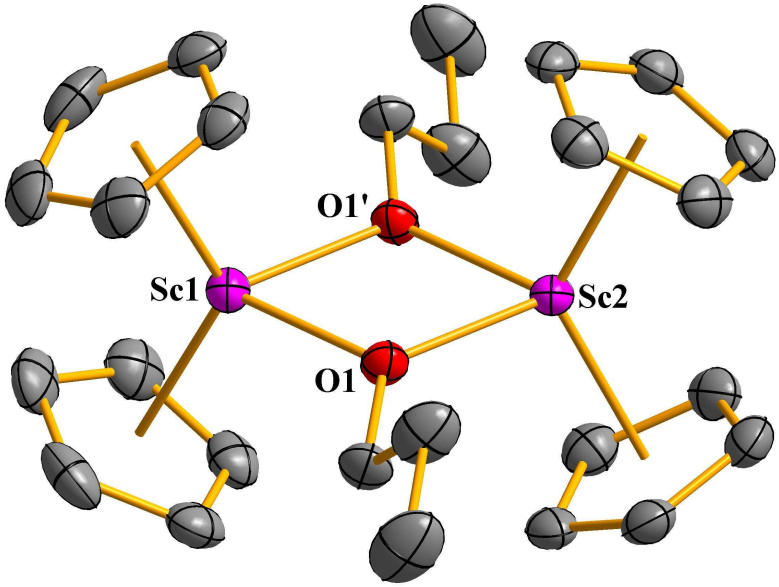

Figure 2.4.5. Thermal ellipsoid plot of $[(C_5H_5)_2Sc]_2[\mu\text{-}O(C_3H_7)]_2$, **3**, drawn at the 50% probability level. Hydrogen atoms are omitted for clarity.

A reaction obviously occurred between **2** and KCp under argon atmosphere. When the solvent was evaporated from the dark colored solution and analyzed by elemental analysis, no nitrogen was observed. One can assume that another reaction proceeded under argon compared with the reaction under dinitrogen. The isolation of $[(C_5H_5)Sc]_2[\mu\text{-}O(C_3H_7)]$, **3**, from this reaction was unprecedented. The existence of the propoxide ligand in **3** can not be explained. Since both starting materials, **2** and KCp, were pure according to elemental analysis (of KCp) and powder diffraction (of **2**), the propoxide ligands might have originated

from the solvent. However, a ring-opening of THF is unlikely since this would result in four carbons to give butoxide ligands.

Structural Studies

$[(C_5H_5)_2ScNSc(C_5H_5)(THF)]_2$, 2. For X-ray crystallography, a suitable crystal of $[(C_5H_5)_2ScNSc(C_5H_5)(THF)]_2$, **2**, was grown in a THF solution. Although the quality of the data is a little poor, the observed distances and angles are discussed in the following section, since this crystal is the only metal-rich fragment that could be obtained from all of the reactions carried out with **1**. Selected bond distances and angles are given in Table 2.4.2.

Table 2.4.2. Selected Bond Distances (Å) and Angles (deg) for $[(C_5H_5)_2ScNSc(C_5H_5)(THF)]_2$, **2**.

Cnt1-Sc1-Cnt2	128.2	Sc1-Cnt1	2.229
Cnt1-Sc(1)-N(1)	109.7	Sc1-Cnt2	2.225
Sc1-N1-Sc2'	153.55(16)	Sc2-Cnt3	2.216
Sc1-N1-Sc2	101.07(1)	Sc1-N1	1.997(3)
Sc2-N1-Sc2'	100.82(13)	Sc2-N1	2.094(3)
N1-Sc2'-Sc2	40.30(9)	Sc2-N1'	2.033(3)
N1-Sc2-Sc2'	38.39(8)	N1-N1'	2.5404(44)
N1-N1'-Sc2	53.086(103)	Sc1-Sc2	3.1584(11)
N1-Sc2-N1'	75.97(15)	Sc2-Sc2'	3.180(1)
		Sc1-Sc2'	3.9223(11)

The Sc_4N_2 core of **2** is compared with the Sc_3N core of $Sc_3N@C_{80}$, **4**,[11] and with the $\{Sc_6C\}$ unit of $Sc\{Sc_6C\}I_{12}$, **1**,[4,5] Table 2.4.3. The molecule was located about a two-fold rotation axis. The Sc-Sc distances are Sc1-Sc2 = 3.1585(10) Å and Sc2-Sc2' = 3.1800(14) Å which are shorter than the Sc-Sc distances in the $\{Sc_6C\}$ unit of $Sc\{Sc_6C\}I_{12}$, **1**,[4,5]: 3.323(2),

3.2380(18) and 3.231(2) Å (3.26 Å av.) and the Sc-Sc distances observed in the Sc_3N core of **4**: 3.2642(8), 3.5229(11) and 3.7146(11) Å. The latter Sc-Sc distance in **4** is remarkably longer than the other two. For comparison, the 3.9223(11) Å Sc1-Sc2' distance in **2** is also much longer. The Sc-N distances are Sc1-N1 = 1.997(3) Å, Sc2-N1 = 2.094(3) Å and Sc2-N1' = 2.033(3) Å and are comparable with the Sc-N distances of the Sc_3N portion of $Sc_3N@C_{80}$: Sc1-N = 2.014(2) Å, Sc2-N = 2.031(2) Å and Sc3-N = 2.041(2) Å.[11] The Sc_4N_2 portion of **2** is irregular as indicated by the Sc-N-Sc angles of Sc1-N1-Sc2' = 153.54(16)°, Sc1-N1-Sc2 = 101.07(1)° and Sc2-N1-Sc2' = 100.82(13)°, while the N-Sc-N angles in the Sc_3N part of $Sc_3N@C_{80}$ are greater: Sc1-N-Sc2 = 121.12(11)°, Sc1-N-Sc3 = 107.21(10)° and Sc2-N-Sc3 = 131.61(11)°. The angles of the rectangular portion N_2Sc_2 of **2** more closely resemble each other with N1-Sc2'-Sc2 = 40.30(9)° and N1-Sc2-Sc2' = 38.89(8)°, whereas the following angles in **2** are larger: N1-N1'-Sc2 = 53.086(10)° and N1-Sc2-N1' = 75.97(15) °.

The dihedral angle between the plane defined by Sc1, Sc2' and Sc2 atoms and the plane defined by Sc2', Sc2 and Sc1' atoms is 130.9°.

Table 2.4.3. Selected Bond Distances (Å) and Angles (deg) for the Sc_4N_2 Portion of $[(C_5H_5)_2ScNSc(C_5H_5)(THF)]_2$, **2**, the Sc_3N Portion of $Sc_3N@C_{80}$, **4**,[11] and the $\{Sc_6C\}$unit of $Sc\{Sc_6C\}I_{12}$, **1**.[5]

	2	**4**	**1**
(Sc)-(N)-(Sc)	153.55(16), 101.07(1), 100.82(13)	121.12(11), 107.21(10) 131.61(11)	-
(Sc)-(N)	1.997(3), 2.094(3), 2.033(3)	2.014(2), 2.031(2), 2.041(2)	-
(Sc)-(Sc)	3.1584(11), 3.180(1), 3.9223(11)	3.2642(8), 3.5229(11), 3.7146(11)	3.323(2), 3.2380(18), 3.231(2)

$[(C_5H_5)_2Sc]_2[\mu\text{-}O(C_3H_7)]_2$, 3. A suitable crystal for X-ray crystallography of $[(C_5H_5)_2Sc]_2[\mu\text{-}O(C_3H_7)]_2$, **3**, was obtained from a concentrated THF solution. Selected bond distances and angles are given in Table 2.4.4. The structure of **3** is compared to that of the compound $[(C_5H_5)_2Ti]_2[\mu\text{-}O(C_2H_5)]_2$, **5**,[19] that is the only directly related compound in literature, Table 2.4.5. An analogous propoxide has not been observed for any rare earth or transition metals. The metal oxygen bond distances are with 2.0936(12) and 2.0976(12) Å in **3**, about 0.2 Å longer than observed for the M-O bond distance in **5**: 2.0755(17) Å. The M-M bond distance in **3** is 3.3135(4) Å, thus slightly shorter than 3.3584(16) Å found for **4**. Although the structure of **3** consists of propoxide ligands and **5** contains ethoxide units, both complexes are similar. One similarity found for **3** and **5** is the metallocene part where the $(C_5H_5)^-$ are twisted relative to each other. Another structural feature which both compounds have in common is that the alkoxide chain is disordered in a similar way, Figure 2.4.6. The M-O-M bond distance in **3** is 104.48(5)°, slightly smaller than 108.01(6)° observed for **5**, Figure 2.4.4. The propoxide ligand in **3** shows regular C-C single bond distances within the range of 1.43(3) and 1.545(4) Å that is comparable to the 1.46(2) Å C-C alkyl bond distance in **5**.

Table 2.4.4. Selected Bond Distances (Å) and Angles (deg) for $[(C_5H_5)_2Sc]_2[\mu\text{-}O(C_3H_7)]_2$, **3**.

Cnt1-Sc1-Cnt1‘	127.1	Sc1-O1	2.0936(12)
Cnt2-Sc2-Cnt2’	126.4	Sc2-O1	2.0976(12)
Sc1-Cnt1	2.222	Sc1-Sc2	3.3135(4)
Sc2-Cnt2	2.220		

Table 2.4.5. Selected Bond Distances (Å) and Angles (deg) for $[(C_5H_5)_2Sc]_2[\mu\text{-}O(C_3H_7)]_2$, **3**, and $[(C_5H_5)_2Ti]_2[\mu\text{-}O(C_2H_5)]_2$, **5**.[19]

	3	**5**
(Cnt)-(M)-(Cnt)	127.1, 126.4	127.7
(Cnt)-(M)-(O)	112.9, 108.4, 107.8, 114.1	108.6, 113.3
(M)-(O)-(M)	104.480(52)	108.010(6)
(O)-(M)-(O)	75.603(46)	71.990(3)
(M)-(Cnt)	2.222, 2.220	2.1133
(M)-(O)	2.0936(12), 2.0976(12)	2.0755(17)
(M)-(M)	3.3135(4)	3.3584(16)
(O)-(C)	1.430(12), 1.440(3)	1.4787(88)
(C_f)-(C_s)*	1.43(3), 1.517(4)	1.4604(193)
(C_s)-(C_t)*	1.545(4), 1.54(2)	-
(O)- (C_f)-(C_s)	112.1(2), 106.9(15)	110.640(839)
(C_f)-(C_s)-(C_t)	110.7(3), 108.0(14)	-

*(C_f) : carbon attached to the oxygen of the propoxide ligand
(C_s): second carbon of the propoxide ligand
(C_t): terminal carbon of the propoxide ligand

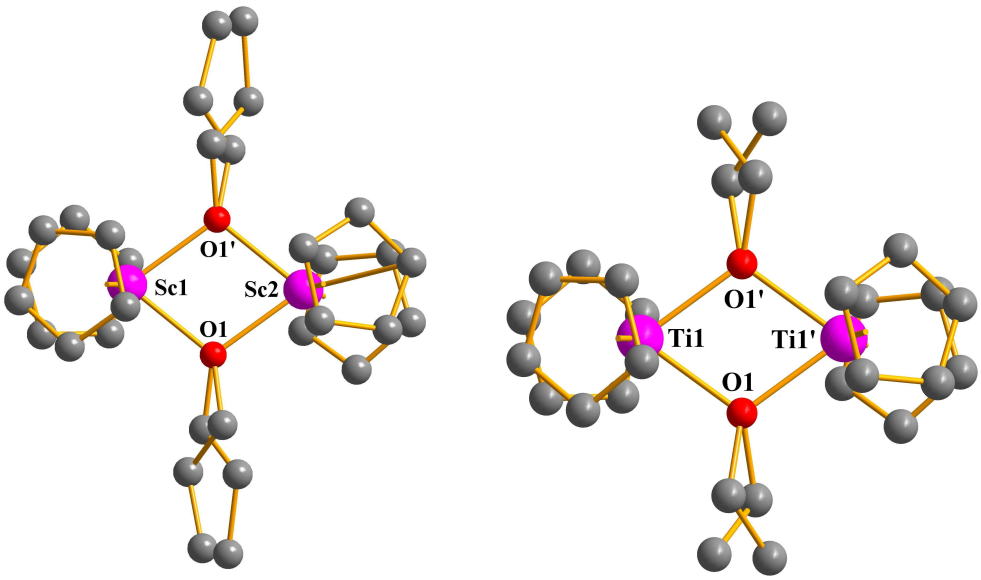

Figure 2.4.6. Structural similarities between $[(C_5H_5)_2Sc]_2[\mu\text{-}O(C_3H_7)]_2$, **3**, and $[(C_5H_5)Ti]_2[\mu\text{-}O(C_2H_5)]_2$, **5**. Hydrogen atoms are omitted for clarity.

Conclusion

$\{CSc_6\}I_{12}Sc$ reacts with potassium cyclopentadienide to yield dark colored products. From the reaction conducted under a dinitrogen atmosphere, a scandium nitride, $[(C_5H_5)_2ScNSc(C_5H_5)(THF)]_2$, **2**, could be isolated. From the analogous reaction under an argon atmosphere, an alkoxide product, $[(C_5H_5)Sc]_2[\mu\text{-}O(C_3H_7)]_2$, **3**, was crystallized. For both complexes, **2** and **3**, no isomorphous compounds were found in the literature.

2.5 Attempts to Excise the $\{CSc_6\}$ Cluster from $\{CSc_6\}I_{12}Sc$ by its Reaction with Different Ligands via Salt-Metathesis

$\{CSc_6\}I_{12}Sc$, **1**, has been reacted with several ligands. A series of salt metathesis reactions has been carried out where 12 equiv. of the ligand has been used in order to remove all 12 iodide ligands of the starting material. For this, ligands systems such as $(C_5MeH_4)^-$, $(C_5Me_4H)^-$ and $(C_5Me_5)^-$, which represent the larger analogues of KC_5H_5 (subchapter 2.4) have been chosen. Similar to the observed reactivity with KC_5H_5, the reaction of **1** with 12 equiv. of NaC_5MeH_4 under an argon atmosphere went within 3.5 days to completion yielding a brown-black solution. In contrast, the reaction of **1** with 12 equiv of KC_5Me_4H under a dinitrogen atmosphere gave only a yellow colored solution after 1 week of stirring. Similarly, the reaction of **1** with 12 equiv of KC_5Me_5 provided only a pale yellow solution after a one week reaction time. Longer reaction times did not affect the color or the completion of the last two reactions. Summing up these salt metathesis reactions, reactions of **1** go to completion with less bulky ligand systems like $(C_5H_5)^-$ and $(C_5MeH_4)^-$. The larger $(C_5Me_4H)^-$ and $(C_5Me_5)^-$ did not drive the reactions with **1** to completion. One reason for this might be that too large anions cannot get close enough to the scandium cluster unit in order to react with the iodide ligands of **1**. That means that bulkier ligand systems could prevent the desired reactions from occurring. This argument is supported by the fact that **1** reacts with $LiCH_2SiMe_3$ (in hexane) to yield a red solution, while **1** with the larger $LiCH(SiMe_3)_2$ (in

toluene) did not react at all. The following two reactions also support this assumption: Linear ligands like N_3^- from NaN_3 with **1** (in toluene) yielded a green-brown solution in three weeks, whereas aryloxide ligands such as $(OAR)^-$ via use of potassium 2,6-bis(*tert*-butyl)-4-methylphenoxide (KOAR) did not react at all with **1**. All of the described reactions of this section did not give crystallizable products. In conclusion, less bulky ligands seem to be more promising to initiate reactions with **1**.

2.6 Attempts to Excise the $\{CSc_6\}$ Cluster from $\{CSc_6\}I_{12}Sc$ by Oversaturation with Iodide

Another approach to the isolation of the desired molecular scandium cluster would be the oversaturation of the halide sphere of the octahedral metal fragment by halides. This goal could be achieved for zirconium clusters of the formula $[(ZZr_6)X_{12}]$ (Z = endohedral atom; X = halide) by the use of ionic liquids. For instance, $Zr_6Br_{14}Fe$ reacts with $ImCl/AlCl_3$ to give $(Im)_4[(Zr_6Fe)Cl_{18}]$.[20] Following the analogous reaction pathway, a similar reaction was carried out with $\{Sc_6C\}I_{12}Sc$ and 12 equiv. of BMIMI (1-butyl-3-methylimidazlium-iodide) that did not provide an isolable product. Attempts to work-up the reaction with MeCN, as reported in the Zr reactions, were not successful. Furthermore, it has been observed that $\{Sc_6C\}I_{12}Sc$ dissolves initially in MeCN, but subsequently reacts with the solvent itself,[5] for which reason it is not an appropriate solvent for work-up of the conducted reaction with the ionic liquid. However, the use of MeCN to isolate ionic liquid containing complexes (molecular zirconium compounds) is standard due to their excellent solubility in this solvent.

An alternative substrate to ionic liquids might be PNPI [Bis(triphenylphosphineiminium)iodide] which could fulfill the goal of overloading the scandium metal cluster with halides. PNPI is soluble in solvents such as CH_2Cl_2, acetone, and dimethylformamide,[21] and hardly soluble in solvents like THF. Since acetone is a coordinating solvent, and might destroy the metal atom cluster, the reaction of $\{Sc_6C\}I_{12}Sc$

with PNPI had been examined in dichloromethane as the solvent. This reaction was monitored by ^{45}Sc NMR spectroscopy, Figure 2.6.1. Although scandium possesses a quadrupole moment of $-0.22 \cdot 10^{-30}$ m^2 due to its I = 7/2 spin, it is qualified for ^{45}Sc NMR spectroscopy analysis due to the natural abundance of ^{45}Sc of 100 %.[22]

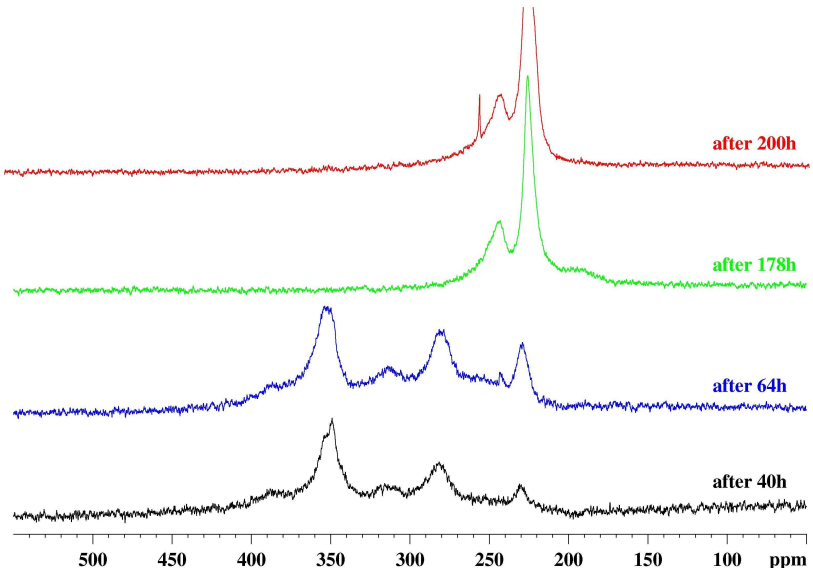

Figure 2.6.1. Control of the Reaction of $\{Sc_6C\}I_{12}Sc$ with PNPI in CH_2Cl_2 by ^{45}Sc-NMR spectroscopy.

A ^{45}Sc NMR spectrum was taken after each of the following reaction times: 40 h, 64 h, 178 h and 200 h. The presence of several peaks in the ^{45}Sc NMR spectra after 40 h and 64 h reaction time is a hint for either different scandium species next to each other in solution or the coordination of the PNPI molecule to the metal octahedron core. After 178 h reaction time, it seems like one main product has been formed together with only one byproduct. However, the ^{45}Sc-NMR spectrum after 200 h reaction time shows the formation of a peak at 249 ppm which can be unambiguously assigned to the ion $(ScCl_6)^-$. To sum this experiment up, $\{Sc_6C\}I_{12}Sc$ reacts with PNPI in CH_2Cl_2, however, either the solid $\{Sc_6C\}I_{12}Sc$ itself or the unknown formed product in solution starts to react with the solvent. In order to avoid this issue, a fast work-up would be necessary. However, the time difference of 22 h between

getting a reaction to completion (expecting only one or at the most 2 peaks in the ^{45}Sc NMR spectrum) and the start of a reaction with the solvent itself causes problems. First, the reaction starts with either the starting material or the generated compound with CH_2Cl_2 presumably before 22 h time difference. Second, the formed compound seems to be only soluble in CH_2Cl_2, which would prevent crystallization from another solvent.

2.7 Attempts to Excise the {CSc_6} Cluster from {CSc_6}I_{12}Sc by its Reaction with Nitriles

Reactions of **1** with nitriles in arene solvents were not supposed to be salt metathesis reactions. In fact, nitrile ligands were thought to fill up the coordination sphere of {CSc_6}I_{12}, consequently breaking the chain in **1**. This would require a removal of the trivalent scandium together with the cationic part of the nitrile, as an ionic pair.

Reactions of **1** were carried out with ^{t}butylnitrile and trimethylsilylcyanide (TMSCN). The reaction of Me_3CCN with **1** after 3 days gave a red color, however it did not go to completion after 17 d. In contrast, no reaction occurred with TMSCN and **1**.

2.8 References

(1) a) Matignon, C.; Cazes, E. C. *Ann. Chim. Phys.* **1906**, *8*, 417; b) Jantsch, G.; Grubitsch, H.; Hoffmann, F.; Alber, H. *Z. Anorg. Allg. Chem.* **1929**, *185*, 49-64; c) Klemm, W.; Bommer, H. *Z. Anorg. Allg. Chem.* **1937**, *231*, 138-171.

(2) a) Corbett, J. D. *Rev. Chim. Minérale* **1973**, *10*, 239; b) Corbett, J. D. *Acc. Chem. Res.* **1981**, *14*, 239-246; c) Simon, A. *Angew. Chem. Int. Ed.* **1981**, *20*, 1-22; *Angew. Chem.* **1981**, *93*, 23-44; d) Meyer, G. *Chem. Rev.* **1988**, *88*, 93–107; e) Simon, A.; Mattausch, H.-J.; Miller, G. J.; Bauhofer, W.; Kremer, R. K. in *Handbook on the Physics and Chemistry of Rare Earths* (Eds.: Gschneidner Jr., K. A.; Eyring, L.), North Holland Publ., Amsterdam, **1991**, Vol. 15, 191-285. f) Corbett, J. D. *J. Chem. Soc., Dalton Trans.* **1996**, *12*, 556; g) Corbett, J. D. *Inorg. Chem.* **2000**, *39*, 5178-5191; h) Meyer, G.; Wickleder, M. S. in *Handbook on the Physics and Chemistry of Rare Earths* (Eds.: Gschneidner Jr., K. A.; Eyring, L.), North Holland Publ., Amsterdam, **2000**, Vol. 28, 53-129; i) Simon, A.; Mattausch, H.-J.; Ryazanov, M.; Kremer, R. K. *Z. Anorg. Allg. Chem.* **2006**, *632*, 919-929; j) Meyer, G. *Z. Anorg. Allg. Chem.* **2007**, *633*, 2537-2552; k) Meyer, G. *Z. Anorg. Allg. Chem.* **2008**, *634*, 2729-2736; l) Corbett, J. D. *Inorg. Chem.* **2010**, *49*, 13-28.

(3) a) Bochkarev, M. N.; Fedushkin, I. L.; Fagin, A. A.; Petrovskaya, T. V.; Ziller, J. W.; Broomhall-Dillard, R. N. R.; Evans, W. J. *Angew. Chem.* **1997**, *109*, 123–124; *Angew. Chem. Int. Ed.* **1997**, *36*, 133–135; b) Evans, W. J. *Coord. Chem. Rev.* **2000**, *206*, 263–283; c) Evans, W. J.; Allen, N. T.; Ziller, J. W. *J. Am. Chem. Soc.* **2000**, *122*, 1749–1750; d) Bochkarev, M. N.; Fedushkin, I. L.; Dechert, S.; Fagin, A. A.; Schumann, H. *Angew. Chem.* **2001**, *113*, 3268–3270; *Angew. Chem. Int. Ed.* **2001**, *40*, 3176–3178; e) Jaroschik, F.; Nief, F.; Richard, L.; Le Goff, X.-F. *Organometallics* **2007**, *26*, 1123–1125; f) Clentsmith, G. K. B.; Cloke, F. G. N.; Green, J. C.; Hanks, J.; Hitchcock, P. B.; Nixon, J. F. *Angew. Chem. Int. Ed.* **2003**, *42*, 1038-1041; g) Evans, W. J. *Inorg. Chem.* **2007**, *46*, 3245-3449; h) Jaroschik, F.; Momin, A.; Nief, F.; Le Goff, X.-F.; Deacon, G. B. *Angew. Chem.* **2009**, *121*, 1137–1141; *Angew. Chem. Int. Ed.* **2009**, *48*, 1117–1121; i) Hitchcock, P.; Lappert, M. F.; Maron, L.; Protchenko, A. V. *Angew. Chem.* **2008**, *120*, 1510–1513; *Angew. Chem. Int. Ed.* **2008**, *47*, 1488–1491; j) Meyer,

G. *Angew. Chem.* **2008**, *120*, 5040–5042; *Angew. Chem. Int. Ed*. **2008**, *47*, 4962–4964; k) Evans, W. J. *J. Alloys Compd.* **2009**, *488*, 493-510; l) Meyer, G. *Angew. Chem*. **2010**, *122*, 3182-3184; *Angew. Chem. Int. Ed*. **2010**, *49*, 3116-3118.
(4) a) Dudis, D. S.; Corbett, J. D.; Hwu, S.-J. *Inorg. Chem.* **1986**, *25*, 3434-3438; b) Dudis, D. S.; Corbett, J. D.; *Inorg. Chem.* **1987**, *26*, 1933-1940; c) Jongen, L.; Mudring, A.-V.; Meyer, G. *Angew. Chem. Int. Ed. Engl.* **2006**, *45*, 1886-1889; *Angew. Chem.* **2006**, *118*, 1920-1923.
(5) Demir, S. Universität zu Köln, Diplomarbeit 2007.
(6) a) McCollum, B. C.; Corbett, J. D. *J. Chem. Soc., Chem. Commun.* **1968**, 1666; b) McCollum, B. C. ; Dudis, D. J. ; Lachgar, A. ; Corbett, J. D. *Inorg. Chem.* **1990**, *29*, 2030-2032; c) Meyer, G. ; Jongen, L. ; Mudring, A.-V. ; Möller, A. in *Inorg. Chem. in Focus* (Eds.: Meyer, G.; Naumann, D.; Wesemann, L.), Wiley-VCH, Weinheim, **2005**, *2*, pp. 105-120.
(7) Crystal Data for $\{CSc_6\}I_{12}Sc$, **1**: Trigonal, space group *R*3 (No. 146); *a* = 1472.06(16) pm, *b* = 985.00(10), γ = 120.00°, *V* = 1848.5(3)·10^6 pm^3; *Z* = 3; 2.61° < θ < 28.12°; Mo-Kα radiation (graphite monochromator, λ = 71.073 pm); T = 293(2) K; *F*(000) = 2367; μ = 16,829 mm^{-1}; 3444 reflections measured, 1792 unique, 1595 observed. R_{int} = 0.0523, *R1/wR2* = 0.0295/0.0699 [$I_0 > 2\sigma(I_0)$] and 0.0336/0.0711 [all data]; Goodness-of-fit on F^2 = 1.012.
(8) Goodman, B. A.; Raynor, J. B., ESR of Transition Metal Complexes, *Advances in Inorganic Chemistry and Radiochemistry* **13**, Academic Press, New York and London, **1970**, Vol. 13, 135-362.
(9) Blaha, P.; Schwarz, K.; Madsen, G. K. H.; Kvasnicka, D.; Luitz, J. *WIEN2k, An Augmented Plane WaVe + Local Orbitals Program for Calculating Crystal Properties*; Technical University: Wien, Austria, 2001.
(10) Panda, T. K.; Gamer, M. T.; Roesky, P. W. *Organometallics* **2003**, *22*, 877-878.
(11) Cai, T.; Xu, L.; Anderson, M. R.; Ge, Z. Zuo, T.; Wang, X.; Olmstead, M. M.; Balch, A. L.; Gibson, H. W.; Dorn, H. C. *J. Am. Chem. Soc.* **2006**, *128*, 8581-8589.
(12) Stevenson, S.; Rice, G.; Glass, T.; Harich, K.; Cromer, F.; Jordan, M.R.; Craft, J.; Hadju, E.; Bible, R.; Olmstead, M.M.; Maitra, K.; Fisher, A.J.; Balch, A.L.; H.C.Dorn *Nature* **1999**, *401*, 55.
(13) Olmstead, M.M.; Lee, H. M.; Duchamp, J.C.; Stevenson, S.; Marciu, D.; Dorn, H.C.; Balch,A.L. *Angew. Chem., Int. Ed.* **2003**, *42*, 900.
(14) Cai, T.; Xu, L.; Gibson, H. W.; Dorn, H. C.; Chancellor, C. J.; Olmstead, M. M.; Balch, A. L. *J. Am. Chem. Soc.* **2007**, *129*, 10795.
(15) Shu, C.; Slebodnick, C.; Xu, L.; Champion, H.; Fuhrer, T.; Cai, T.; Reid, J. E.; Fu, W.; Harich, K.; Dorn, H. C.; Gibson, H. W. *J. Am. Chem. Soc.* **2008**, *130*, 17755.
(16) Olmstead, M. M.; de Bettencourt-Dias, A.; Duchamp, J. C.; Stevenson, S.; Marciu, D.; Dorn, H. C.; Balch, A.L. *Angew. Chem., Int. Ed.* **2001**, *40*, 1223.
(17) Wakahara, T.; Iiduka, Y.; Ikenaga, O.; Nakahodo, T.; Sakuraba, A.; Tsuchiya, T.; Maeda, Y.; Kako, M.; Akasaka, T.; Yoza, K.; Horn, E.; Mizorogi, N.; Nagase, S. *J. Am. Chem. Soc.* **2006**, *128*, 9919.
(18) Lee, H. M.; Olmstead, M. M.; Iezzi, E.; Duchamp, J. C.; Dorn, H. C.; Balch, A. L. *J. Am. Chem. Soc.* **2002**, *124*, 3494.
(19) Samuel, E.; Harrod, J. F.; Gourier, D.; Dromzee, Y.; Robert, F.; Jeannin, Y. *Inorg. Chem.* **1992**, *31*, 3252.
(20) Runyan, Jr., C. E.; Hughbanks, T. *J. Am. Chem. Soc.* **1994**, *116*, 7909-7910.
(21) Martinsen, A.; Songstad, J. *Acta Chem. Scand.* A 31 **1977**, 645-650.
(22) Brevard, C.; Granger, P.; Handbook of High Resolution Multinulear NMR, J. Wiley and Sons: New York, 1981.

Chapter 3

Synthesis, Structure, and Density Functional Theory of the First Scandium Dinitrogen Complex, $[(C_5Me_4H)_2Sc]_2(\mu\text{-}\eta^2\text{:}\eta^2\text{-}N_2)$

Introduction

Although numerous examples of dinitrogen complexes of the early transition metals are known,[1] no dinitrogen complex of scandium has been isolated. Since scandium is the first transition metal with the lowest atomic number, its dinitrogen complexes would be the simplest transition metal compounds to analyze by theoretical methods. However, the small size of scandium along with its electropositive nature also makes it one of the more experimentally challenging metals[2,3] to use to explore dinitrogen chemistry.

An attractive synthetic route to a scandium dinitrogen complex is the method used with yttrium and lanthanide complexes to access divalent-like "Ln^{2+}" reactivity by combining complexes of trivalent metal ions with alkali metals as shown in eq 3.1 where Z is defined as a monoanionic ligand that allows these reactions to occur.[4,5]

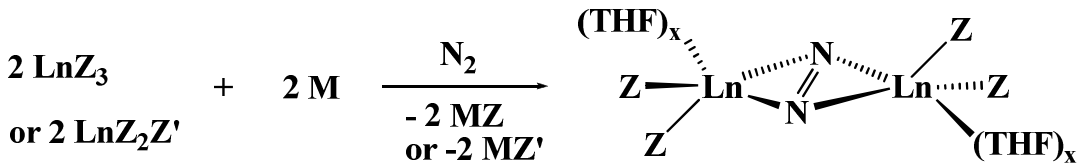

(3.1)

Ln = La, Ce, Pr, Nd, Gd, Tb, Dy, Ho, Er, Y, Tm, Lu
Z = $N(SiMe_3)_2$, C_5Me_4H, C_5Me_5, $C_5H_2(CMe_3)_3$, $OC_6H_3(^tBu)_2$-2,6
Z' = BPh_4, I; x = 0-2
M = K, KC_8, Na

With dinitrogen as a substrate, these reactions provide $[Z_2(THF)_xLn]_2(\mu\text{-}\eta^2\text{:}\eta^2\text{-}N_2)$ products with a co-planar arrangement of the bridging side-on bound dinitrogen and the two metals as shown in eq 3.1. These complexes have N-N bond distances of 1.233(5)-1.305(6) Å and can be considered to be complexes of $(N_2)^{2-}$.[4-10] Since scandium in some complexes is

known to have oxidation states lower than 3+ (subvalent scandium),[11-13] this appeared to be a reasonable way to access scandium dinitrogen chemistry.

Tetraphenylborate salts of yttrium and lanthanide metallocene cations of general formula $[(C_5Me_4R)_2Ln][(\mu\text{-}\eta^2{:}\eta^1\text{-Ph})_2BPh_2]$ (R = Me, H),[5,14] e.g. Figure 3.1a, have proven to be excellent starting materials for the formation of $[(C_5Me_4R)_2(THF)_xLn]_2(\mu\text{-}\eta^2{:}\eta^2\text{-}N_2)$ products. These complexes are molecular species that are soluble in arene solvents and contain an easily displaced leaving group since the tetraphenylborate is only loosely coordinated to the metal center via agostic interactions involving two of the phenyl groups. When the scandium example of this class was crystallographically characterized,[15] it displayed a new type of $(BPh_4)^{1-}$ bonding mode involving dihapto coordination from a single phenyl group, i.e. $[(C_5Me_5)_2Sc][(\mu\text{-}\eta^2{:}\eta^1\text{-Ph})BPh_3]$, Figure 3.1b. However, unlike the $[(C_5Me_4R)_2M][(\mu\text{-}\eta^2{:}\eta^1\text{-Ph})_2BPh_2]$ complexes (R = Me, H) of the lanthanides and uranium,[16] the $[(C_5Me_5)_2Sc][(\mu\text{-}\eta^2{:}\eta^1\text{-Ph})BPh_3]$ complex has minimal solubility in arene solvents.

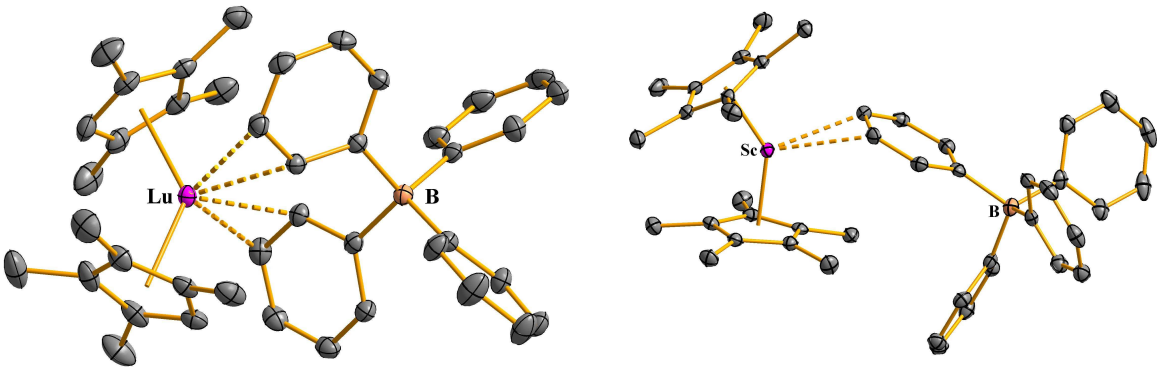

Figure 3.1. Binding modes of $(BPh_4)^{1-}$ in (*a*) $[(C_5Me_4H)_2Lu][(\mu\text{-}\eta^2{:}\eta^1\text{-Ph})_2BPh_2]$[5] and (*b*) $[(C_5Me_5)_2Sc][(\mu\text{-}\eta^2{:}\eta^1\text{-Ph})BPh_3]$.[15]

The synthesis of a $[Z_2Sc]_2(\mu\text{-}\eta^2{:}\eta^2\text{-}N_2)$ analogue of the complexes in eq 3.1 with Z = C_5Me_5 appeared challenging not only because the cationic precursor had low solubility, but also because the small size of scandium could make it sterically difficult to form such a

complex. Hence, a sterically less crowded target was chosen with Z = C_5Me_4H. This chapter reports the synthetic chemistry needed to make the previously unknown $(C_5Me_4H)_2ScX$ precursors and $[(C_5Me_4H)_2Sc][(\mu\text{-Ph})BPh_3]$, as well as its reductive chemistry with potassium graphite.

Experimental

The manipulations described below were performed under nitrogen or argon with rigorous exclusion of air and water using Schlenk, vacuum line, and glovebox techniques. Solvents were saturated with UHP grade argon (Airgas) and dried by passage through Glasscontour[17] drying columns before use. NMR solvents were dried over Na/K alloy, degassed, and vacuum transferred before use. Allylmagnesium chloride (2.0 M in THF) was purchased from Aldrich and used as received. 1,4-Dioxane was purchased from Aldrich and used as received. 1,2,3,4-Tetramethylcyclopentadiene ($C_5Me_4H_2$) was purchased from Aldrich, distilled onto 4 Å molecular sieves, and degassed by three freeze-pump-thaw cycles prior to use. Potassium bis(trimethylsilyl)amide (Aldrich) was dissolved in toluene and the mixture was centrifuged and decanted. Solvent was removed from the supernatant before use as a white solid. KC_5Me_4H was prepared as described for KC_5Me_5.[18] $[HNEt_3][BPh_4]$[19] and KC_8[18] were prepared according to the literature. ^1H and ^{13}C NMR spectra were recorded on Bruker GN500 or CRYO500 MHz spectrometers. ^{45}Sc NMR spectra were recorded on a Bruker Avance 600 spectrometer operating at 145 MHz for ^{45}Sc. The ^{45}Sc NMR spectra were referenced to $[Sc(H_2O)_6]^{3+}$ in D_2O. ^{15}N NMR spectra were recorded with an Avance 600 MHz spectrometer operating at 61 MHz for ^{15}N and calibrated using an external reference, ^{15}N-formamide in DMSO (-268 ppm with respect to nitromethane at 0 ppm). IR samples were prepared as KBr pellets, and the spectra were obtained on a Varian 1000 FT-IR system. Elemental analyses were performed using a PerkinElmer Series II 2400 CHNS elemental analyzer.

$(C_5Me_4H)_2ScCl(THF)$, 6. In a nitrogen filled glovebox, KC_5Me_4H (2.623 g, 16 mmol) was slowly added to a stirred white slurry of $ScCl_3$ (1.237 g, 8 mmol) in 100 mL of THF. After the mixture was stirred for 48 h, the suspension was centrifuged to separate insoluble materials, presumably KCl, the supernatant was decanted, and the solution was evaporated to dryness. The resulting pale-orange powder was extracted with toluene to give a bright orange solution that was evaporated to dryness to yield a pale-orange powder (2.482 g). Washing this powder with hexane leaves $(C_5Me_4H)_2ScCl(THF)$, **6**, as a pale-yellow powder (2.126 g, 66%). Crystals suitable for X-ray diffraction were grown from a concentrated THF solution at –35 ºC over the course of 72 h. ^{1}H NMR (500 MHz, THF-d_8): δ 5.62 (s, 2H, C_5Me_4H), 1.98 (s, 12H, C_5Me_4H), 1.85 (s, 12H, C_5Me_4H). ^{13}C NMR (126 MHz, THF-d_8): δ 123.99 (C_5Me_4H), 117.96 (C_5Me_4H), 112.43 (C_5Me_4H), 13.92 (C_5Me_4H), 12.44 (C_5Me_4H). ^{45}Sc NMR (145 MHz, THF-d_8): δ 55 ($\Delta\nu_{1/2}$ = 400 Hz). Anal. Calcd for $C_{22}H_{34}ClOSc$: C, 66.91; H, 8.68. Found: C, 66.42; H, 8.83. The desolvated derivative, $(C_5Me_4H)_2ScCl$, is described in the Appendix.

$(C_5Me_4H)_2Sc(\eta^3\text{-}C_3H_5)$, 7. In a nitrogen-filled glovebox, allylmagnesium chloride (0.53 mL, 1.06 mmol) was added to a stirred orange slurry of **6** (0.420 g, 1.06 mmol) in 100 mL of toluene. A yellow solution immediately formed. After the mixture was stirred for 24 h, the solution was evaporated to dryness to yield a pale yellow powder. This material was treated with 2% 1,4-dioxane in hexane (75 mL) and the mixture centrifuged to separate a white precipitate. The yellow supernatant was decanted and removal of solvent under vacuum yielded $(C_5Me_4H)_2Sc(\eta^3\text{-}C_3H_5)$, **7**, (0.337 g, 96%) as a yellow powder. Crystals suitable for X-ray analysis were grown from a concentrated toluene solution of **7** at –35 ºC over the course of 24 h.[56] ^{1}H NMR (500 MHz, benzene-d_6): δ 7.10 (m, 1H, CH_2CHCH_2), 5.93 (s, $\Delta\nu_{1/2}$ = 9 Hz, 2H, C_5Me_4H), 3.81 (s, $\Delta\nu_{1/2}$ = 102 Hz, 2H, allyl *anti* CH_2), 1.95 (s, 12H, C_5Me_4H), 1.64 (s, $\Delta\nu_{1/2}$ = 12 Hz, 12H, C_5Me_4H). ^{13}C NMR (126 MHz, benzene-d_6): δ 157.3 (CH_2CHCH_2), 121.2 (C_5Me_4H), 116.6 (C_5Me_4H), 112.6 (C_5Me_4H), 70.6 (CH_2CHCH_2), 13.4

(C_5Me_4H), 12.3 (C_5Me_4H). ^{1}H NMR (500 MHz, toluene-d_8): δ 7.0 (m, 1H, CH_2CHCH_2), 5.88 (s, $\Delta\nu_{1/2}$ = 9 Hz, 2H, C_5Me_4H), 3.70 (s, $\Delta\nu_{1/2}$ = 98 Hz, 2H, allyl *anti* CH_2), 1.93 (d, 12H, C_5Me_4H), 1.62 (s, $\Delta\nu_{1/2}$ = 12 Hz, 12H, C_5Me_4H). ^{1}H NMR (500 MHz, toluene-d_8, 228 K): δ 7.06 (m, 1H, CH_2CHCH_2), 6.07 (s, 1H, C_5Me_4H), 5.73 (s, 1H, C_5Me_4H), 3.82 (d, 2H, allyl *anti* CH_2), 2.07 (d, 2H, allyl *syn* CH_2), 1.96 (d, 12H, C_5Me_4H), 1.79 (s, 6H, C_5Me_4H), 1.42 (s, 6H, C_5Me_4H). ^{1}H NMR (500 MHz, toluene-d_8, 373 K): δ 7.01 (m, 1H, CH_2CHCH_2), 5.85 (s, 2H, C_5Me_4H), 2.84 (d, $\Delta\nu_{1/2}$ = 25.7 Hz, 4H, allyl CH_2), 1.92 (s, 12H, C_5Me_4H), 1.64 (s, 12H, C_5Me_4H). ^{13}C NMR (126 MHz, toluene-d_8): δ 157.1 (CH_2CHCH_2), 120.8 (C_5Me_4H), 116.2 (C_5Me_4H), 112.3 (C_5Me_4H), 70.2 (CH_2CHCH_2), 13.0 (C_5Me_4H), 11.9 (C_5Me_4H). ^{45}Sc NMR (145 MHz, benzene-d_6): δ 153 ($\Delta\nu_{1/2}$ = 350 Hz). IR 3078w, 3062w, 2963m, 2909s, 2860s, 2726w, 1663w, 1555w, 1485m, 1435m, 1382m, 1329w, 1253w, 1176w, 1147w, 1028m, 974w, 834m, 794vs, 702s, 614w, 594w cm^{-1}. Anal. Calcd for $C_{21}H_{31}Sc$: C, 76.80; H, 9.51; Sc, 13.69. Found: C, 76.60; H, 9.45; Sc, 14.02.

[(C_5Me_4H)$_2$Sc][(μ-Ph)BPh$_3$], 8. In an argon-filled glovebox free of coordinating solvents, [$HNEt_3$][BPh_4] (0.185 g, 0.435 mmol) was added to a stirred yellow solution of **7** (0.119 g, 0.362 mmol) in 20 mL of toluene. After the mixture was stirred for 3 h, the yellow solution was filtered to remove insoluble yellow-white material. Evaporation of the solution yielded an oily product that crystallized after at least 2 h under vacuum (10^{-3} torr). The thoroughly dried material was washed with hexane to give a yellow crystalline solid. The hexane washing cycle of this yellow crystalline material was repeated until the supernatant was colorless. This yielded **8** as a yellow crystalline powder (0.165 g, 75%). Anal. Calcd for $C_{42}H_{46}BSc$: C, 83.16; H, 7.64. Found: C, 83.00; H, 7.79. Single crystals suitable for X-ray analysis were grown from a concentrated toluene solution at -35 °C over the course of 48 h.[56] ^{1}H NMR (500 MHz, benzene-d_6): δ 8.02 (m, 8H, C_6H_5), 7.21 (m, 8H, C_6H_5), 7.12 (m, 4H, C_6H_5), 5.17 (s, 2H, C_5Me_4H), 1.49 (s, 12H, C_5Me_4H), 1.35 (s, 12H, C_5Me_4H). ^{13}C NMR (126 MHz, benzene-d_6): δ 136.2 (C_6H_5), 134.1 (C_6H_5), 131.9 (C_5Me_4H), 128.9 (C_5Me_4H), 128.8

(C_6H_5), 127.7 (C_6H_5), 125.7 (C_6H_5), 124.2 (C_6H_5), 120.4 (C_5Me_4H), 13.5 (C_5Me_4H), 12.2 (C_5Me_4H). ^{45}Sc NMR (145 MHz, benzene-d_6): δ 190 ($\Delta\nu_{1/2}$ = 7800 Hz). IR: 3122w, 3088w, 3051m, 3040m, 2997m, 2983m, 2911m, 2861m, 2732w, 1933w, 1873w, 1807w, 1759w, 1581m, 1568m, 1479s, 1426s, 1385s, 1376m, 1328w, 1286w, 1267w, 1240m, 1184m, 1157m, 1150m, 1066m, 1031m, 1022s, 978w, 910w, 895m, 837s, 824s, 764m, 744vs, 730vs, 705vs, 624m, 605vs cm^{-1}.

[(C_5Me_4H)$_2$Sc(THF)$_2$][BPh$_4$], 9. In a nitrogen-filled glovebox, **8** (100 mg, 0.133 mmol) was dissolved in 2 mL of THF to give a yellow solution. Single crystals of [(C_5Me_4H)$_2$Sc(THF)$_2$][BPh$_4$] suitable for X-ray diffraction were grown from a concentrated THF solution at –35 ºC over the course of 3 d.

[(C_5Me_4H)$_2$Sc]$_2$(μ-η^2:η^2-N$_2$), 10. In a nitrogen-filled glovebox, KC_8 (0.032 g, 0.25 mmol) was added to a stirred solution of **8** (0.150 g, 0.25 mmol) in 5 mL of THF. After the reaction mixture was stirred for 20 min, black and white insoluble materials (presumably graphite and $KBPh_4$) were removed by centrifugation and filtration. The green filtrate was stored at -35 °C for 4 d to afford **10** as a dark red microcrystalline solid (22 mg, 30%). Red crystals of **10** suitable for X-ray analysis were obtained in an NMR tube from a concentrated benzene-d_6 solution at 25 °C over the course of 6 d. ^{1}H NMR (500 MHz, benzene-d_6): δ 6.01 (s, 4H, C_5Me_4H), 2.01 (s, 24H, C_5Me_4H), 2.00 (s, 24H, C_5Me_4H). ^{13}C NMR (126 MHz, benzene-d_6): δ 119.8 (C_5Me_4H), 118.4 (C_5Me_4H), 114.5 (C_5Me_4H), 12.6 (C_5Me_4H), 11.9 (C_5Me_4H). ^{15}N NMR (61 MHz, benzene-d_6, referenced to $MeNO_2$): δ 385. ^{45}Sc NMR (145 MHz, benzene-d_6): δ 143 ($\Delta\nu_{1/2}$ = 2700 Hz). IR: 2971m, 2908s, 2861s, 2724w, 1746w, 1641w, 1485w, 1444m, 1383m, 1370m, 1332w, 1149w, 1110w, 1020w, 973w, 825vs, 773m, 700w, 619m cm^{-1}. UV-Vis (benzene, nm (ε)): 592 (60), 447 sh (200). Anal. Calcd for $C_{36}H_{52}N_2Sc_2$: C, 71.74; H, 8.70; N, 4.65. Found: C, 71.33; H, 9.15; N, 4.37.

X-ray Crystallographic Data. Information on X-ray data collection, structure determination, and refinement for **6-11** are given in Table 1. Details for X-ray data collection, structure solution and refinement are given in the Appendix.

Table 3.1. X-ray Data Collection Parameters for $(C_5Me_4H)_2ScCl(THF)$, **6**, $(C_5Me_4H)_2Sc(\eta^3\text{-}C_3H_5)$, **7**,[56] $[(C_5Me_4H)_2Sc][(\mu\text{-Ph})BPh_3]$, **8**,[56] $[(C_5Me_4H)_2Sc(THF)_2][BPh_4]$, **9**, $[(C_5Me_4H)_2Sc]_2(\mu\text{-}\eta^2\text{:}\eta^2\text{-}N_2)$, **10**, and $\{[(C_5Me_4H)_2Sc]_2(\mu\text{-}\eta^2\text{:}\eta^2\text{-}N_2)[(C_5Me_4H)_2Sc]_2(\mu\text{-O})\}$, **11**.

Complex	**6**	**7**	**8**	**9**	**10**	**11**
Empirical formula	$C_{22}H_{34}ClOSc$	$C_{21}H_{31}Sc$	$C_{42}H_{46}BSc$	$C_{50}H_{62}BO_2Sc$ · ½ (C_4H_8O)	$C_{36}H_{52}N_2Sc_2$	$[C_{36}H_{52}N_2Sc_2]$ $[C_{36}H_{52}OSc_2]$
Fw	394.90	328.42	606.56	786.82	602.72	1193.41
Temperature (K)	153(2)	153(2)	163(2)	148(2)	98(2)	148(2)
Crystal system	monoclinic	monoclinic	triclinic	triclinic	monoclinic	monoclinic
Space group	$P2_1/n$	$P2_1/n$	$P\bar{1}$	$P\bar{1}$	$P2_1/n$	Pn
a (Å)	8.6644(5)	8.7813(8)	11.8363(13)	15.513(5)	8.4928(9)	8.8370(14)
b (Å)	14.8610(9)	14.7244(13)	11.9868(13)	17.197(5)	10.1010(10)	21.042(3)
c (Å)	16.4746(10)	14.1177(13)	12.4080(13)	17.467(5)	18.4580(18)	17.909(3)
α (deg)	90	90	100.450(2)	102.366(5)	90	90
β (deg)	97.4774(7)	92.186(2)	98.128(2)	101.371(4)	90.3390(10)	91.485(2)
γ (deg)	90	90	100.555(2)	101.285(4)	90	90
Volume ($Å^3$)	2103.3(2)	1824.1(3)	1674.0(3)	4323(2)	1583.4(3)	3329.1(9)
Z	4	4	2	4	2	2
ρ_{calcd} (Mg/m^3)	1.247	1.196	1.203	1.209	1.264	1.191
μ (mm^{-1})	0.484	0.399	0.248	0.212	0.455	0.433
R1 [I > 2.0σ(I)][a]	0.0333	0.0282	0.0517	0.1200	0.0327	0.0675
wR2 (all data)[a]	0.0913	0.0798	0.1239	0.3774	0.0885	0.1647

[a] Definitions: $wR2 = [\Sigma[w(F_o^2\text{-}F_c^2)^2] / \Sigma[w(F_o^2)^2]]^{1/2}$, $R1 = \Sigma||F_o|\text{-}|F_c|| / \Sigma|F_o|$

Computational Details. The structure of **10** was initially optimized using the TPSSH[20] hybrid meta-GGA functional and split valence basis sets with polarization functions on non-hydrogen atoms (SV(P)).[21] TPSSH was chosen due to its established performance for transition metal[22,23] and lanthanide compounds.[24] Fine quadrature grids (size m4)[25] were used throughout except for the final TZVP optimization. Vibrational frequencies were computed at the TPSSH/SV(P) level[26] and scaled by a factor of 0.95 to account for anharmonicity and basis set incompleteness; this factor was chosen to approximately fit the computed vibrational frequency of free N_2 to the gas phase value[27] of 2359 cm^{-1}. All structures were found to be minima. Natural population analyses[28] and plots were also obtained at the TPSSH/SV(P) level; the contour values were 0.08 for molecular orbital plots. The structural parameters reported in the text are the result of re-optimization using larger triple-zeta valence basis sets with two sets of polarization functions (def2-TZVP)[29] and fine quintature grids (size m5). The differences between the SV(P) and the TZVP structures were found to be small, typically amounting to 0.01 Å in bond lengths or less. The electronic stability of the ground state was tested by performing open shell calculations. No spin symmetry breaking was found. The triplet excited state was computed to be 32 kcal/mol above the singlet ground state. All computations were performed using the TURBOMOLE program package.[30]

Results and Discussion

Synthesis. The synthetic sequence used to obtain $[(C_5Me_4H)_2Sc][(\mu\text{-Ph})BPh_3]$, **8**, shown in eq 3.2-3.4, is similar to the route used to make $[(C_5Me_4R)_2M][(\mu\text{-Ph})_2BPh_2]$ complexes (M = Y, lanthanides; R = Me, H).[5,14] and has many parallels in earlier studies of scandium metallocene chemistry.[2,3,31,32] Individual steps in the synthetic procedure are described in the following paragraphs.

$$ScCl_3 + 2\ KC_5Me_4H \xrightarrow[-\ 2\ KCl]{THF} (C_5Me_4H)_2ScCl(THF) \quad (3.2)$$

6

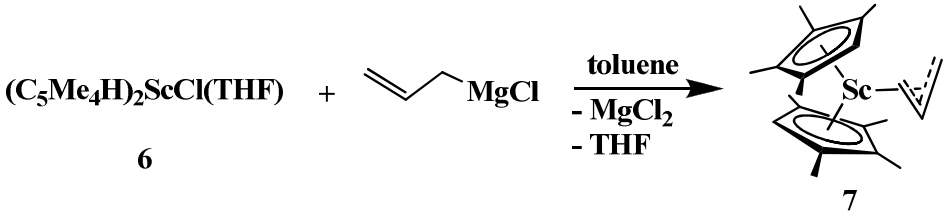

(3.3)

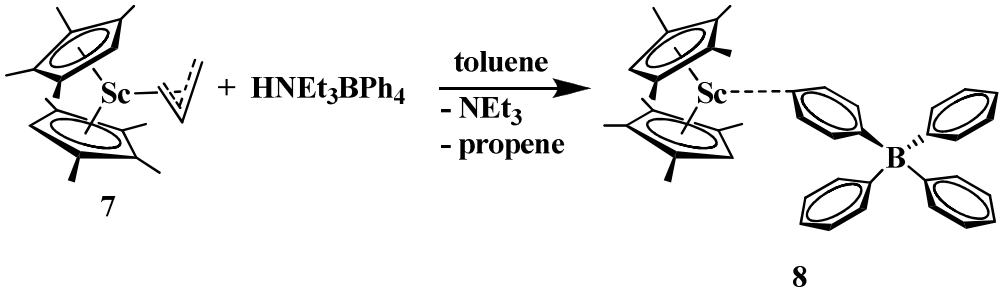

(3.4)

$(C_5Me_4H)_2ScCl(THF)$, 6. Two equiv of KC_5Me_4H react with $ScCl_3$ in THF to form $(C_5Me_4H)_2ScCl(THF)$, **6**, eq 2, in a reaction similar to the preparation of $(C_5Me_5)_2ScCl(THF)$ from $ScCl_3(THF)_3$ with LiC_5Me_5 in xylene at reflux.[3] These complexes can be obtained without any observed complications of forming an "ate" salt, *i.e.* $(C_5Me_4H)_2ScCl_2K(THF)_x$, as is typical for yttrium and the lanthanides.[33,34] Scandium metallocene ate salts can form as demonstrated by the lithium ansa complex, $\{Me_2Si[C_5H_2\text{-}2,4\text{-}(CHMe_2)_2]_2\}Sc(\mu\text{-}Cl)_2Li(THF)_2$,[31] but this is not observed with **6** which has a larger (ring centroid)-Sc-(ring centroid) angle and larger alkali metal. Single crystals of **6** can be obtained from THF, Figure 3.2, and the structural details are described below. Unsolvated $(C_5Me_4H)_2ScCl$ can be obtained from **6** by sublimation in a procedure analogous to the synthesis of $(C_5Me_5)_2ScCl$.[3]

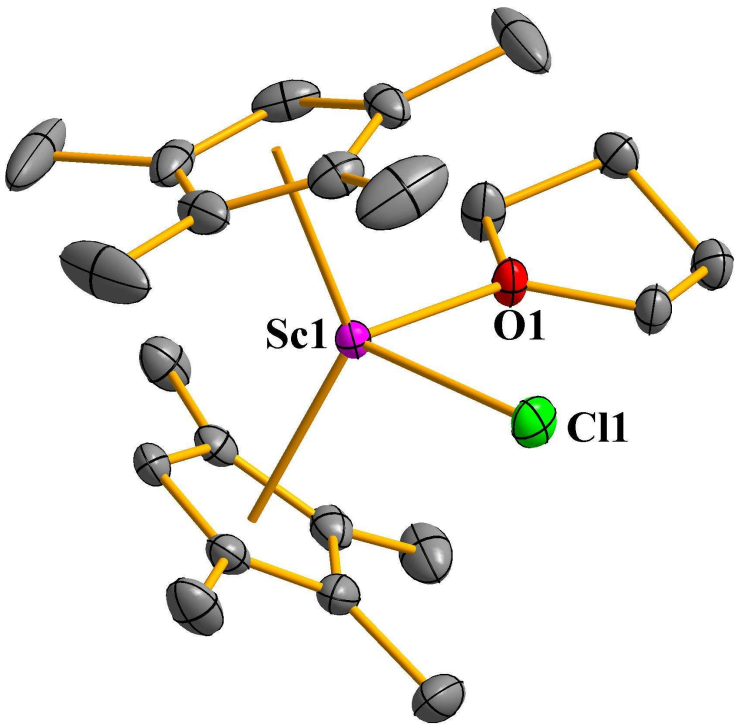

Figure 3.2. Thermal ellipsoid plot of $(C_5Me_4H)_2ScCl(THF)$, **6**, drawn at the 50% probability level. Hydrogen atoms are omitted for clarity.

$(C_5Me_4H)_2Sc(\eta^3\text{-}C_3H_5)$, 7. As shown in eq 3, complex **6** reacts with allylmagnesium chloride to form $(C_5Me_4H)_2Sc(\eta^3\text{-}C_3H_5)$, **7**, which was characterized by ^1H, ^{13}C, and ^{45}Sc NMR spectroscopy as well as by X-ray diffraction, Figure 3.3. An analogous reaction was used to make $\{Me_2Si[C_5H_2\text{-}2,4\text{-}(CHMe_2)_2]_2\}Sc(\eta^3\text{-}C_3H_5)$[31] whereas $(C_5Me_5)_2Sc(C_3H_5)$[3] and $\{Me_2Si(C_5H_3\text{-}3\text{-}CMe_3)_2\}Sc(\eta^3\text{-}C_3H_5)$[32] were made from an allene and the corresponding metallocene hydrides. Like other scandium, yttrium, and lanthanide metallocene allyl complexes,[32,35] **7** displays fluxional behavior in solution, Figure 3.4. A single set of cyclopentadienyl resonances is observed for **7** at room temperature in toluene-d_8, but these split at low temperature. The coalescence temperature for the methyl resonances, 268 K, Figure 3.5, fits in well with the 318 K, 283 K, and 257 K analogues for $(C_5Me_5)_2Y(C_3H_5)$,[35] $(C_5Me_5)_2Lu(C_3H_5)$[35] and $(C_5Me_5)_2Sc(C_3H_5)$,[3] respectively. This series shows a good correlation with steric crowding based on the size of the metal and the cyclopentadienyl

ligand. The fluxional behavior in solution of **7** is also observable at higher temperatures, Figure 3.6.

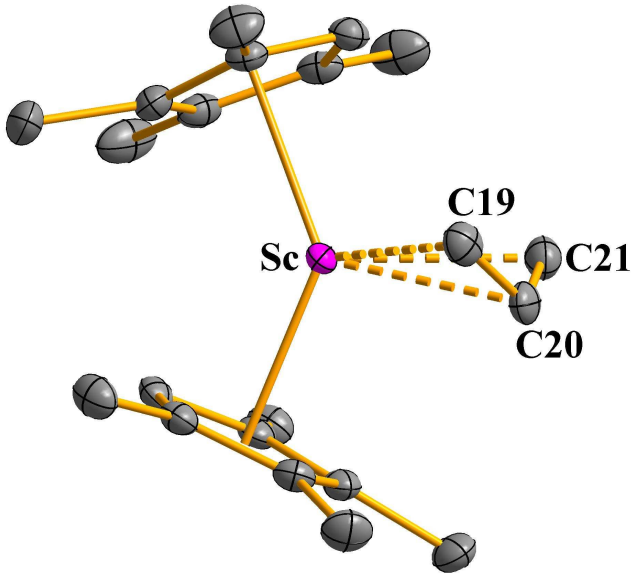

Figure 3.3. Thermal ellipsoid plot of $(C_5Me_4H)_2Sc(\eta^3\text{-}C_3H_5)$, **7**, drawn at the 50% probability level. Hydrogen atoms are omitted for clarity.

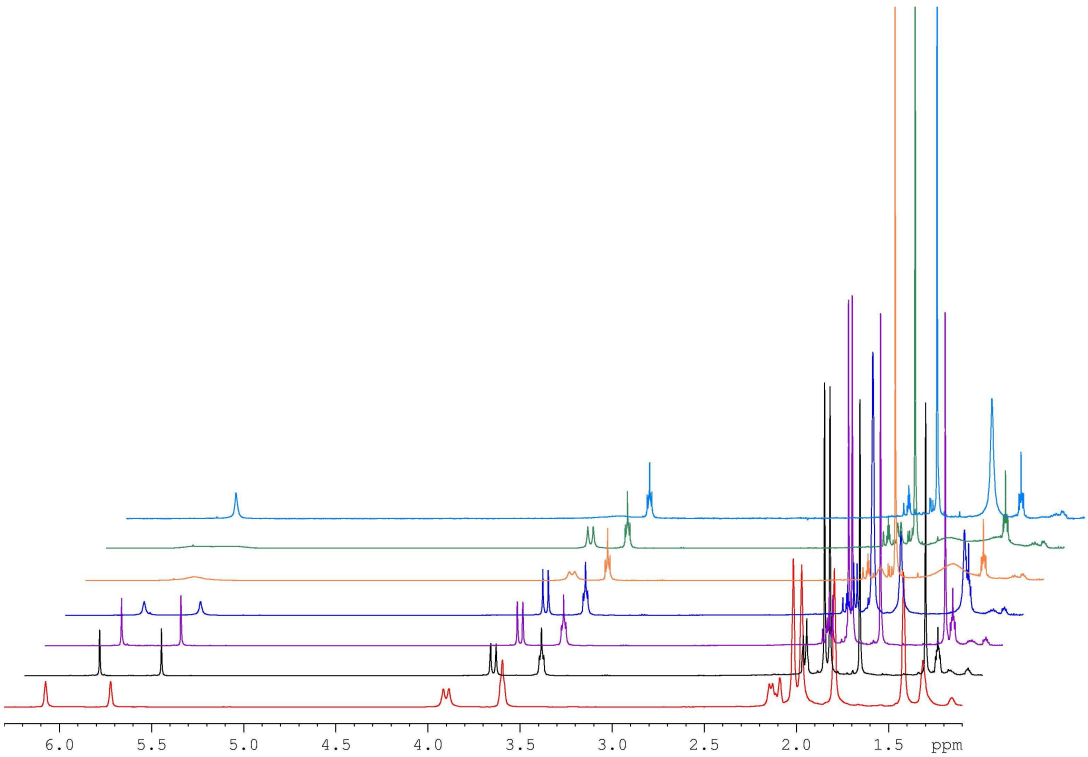

Figure 3.4. Extract of the ^{1}H NMR spectrum (in toluene-d_8) of $(C_5Me_4H)_2Sc(\eta^3\text{-}C_3H_5)$, **7**, at 188 K (bottom), 208 K, 228 K, 248 K, 268 K, 278 K, 298 K (top).

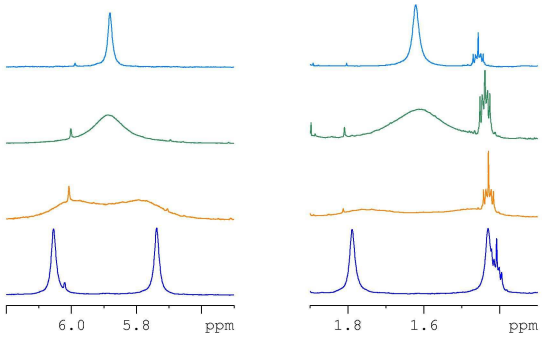

Figure 3.5. Extract of the ^{1}H NMR spectrum (in toluene-d_8) of $(C_5Me_4H)_2Sc(\eta^3\text{-}C_3H_5)$, **7**, at 248 K (bottom), 268 K, 278 K, 298 K (top), showing the coalescence temperature at 268 K.

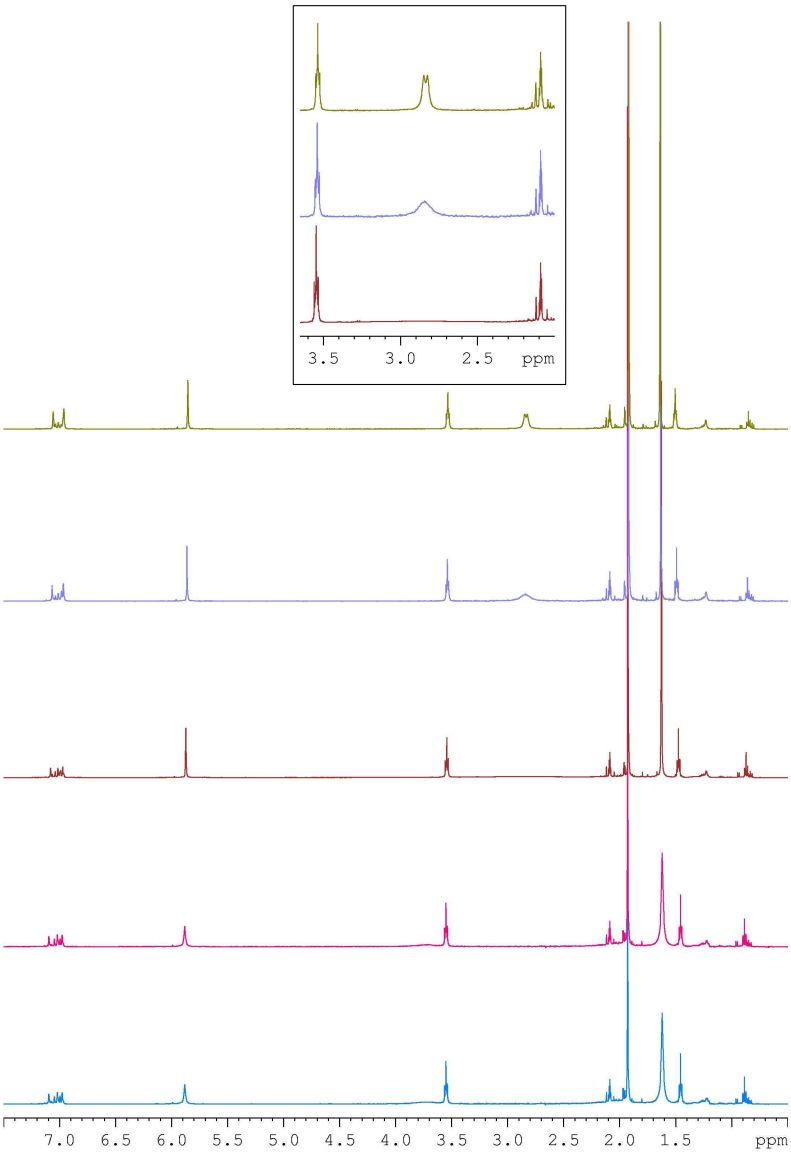

Figure 3.6. ^{1}H NMR spectrum (in toluene-d_8) of $(C_5Me_4H)_2Sc(\eta^3\text{-}C_3H_5)$, **7**, at 298 K (bottom), 323 K, 348 K and 373 K (top).

[($C_5Me_4H)_2Sc$][(μ-Ph)BPh_3], 8. Complex **2** reacts with [$HNEt_3$][BPh_4] to form the tetraphenylborate salt, [($C_5Me_4H)_2Sc$][(μ-Ph)BPh_3], **8**, eq 3.4. This synthesis is similar to that of [($C_5Me_5)_2Sc$][(μ-η^2:η^1-Ph)BPh_3] from the reaction of ($C_5Me_5)_2ScMe$ with [$PhNMe_2H$][BPh_4] in toluene (67% yield).[15] Both complex **8** and the $(C_5Me_5)^{1-}$ analog have very limited solubility in arene solvents. Single crystals of **8** suitable for X-ray diffraction were obtained from toluene and gave the structure shown in Figure 3.7. Complex **8** is not thermally stable: yellow solutions of **8** in toluene, as well as the isolated solid, readily go colorless at room temperature. Hence, samples were routinely stored at -35 °C.

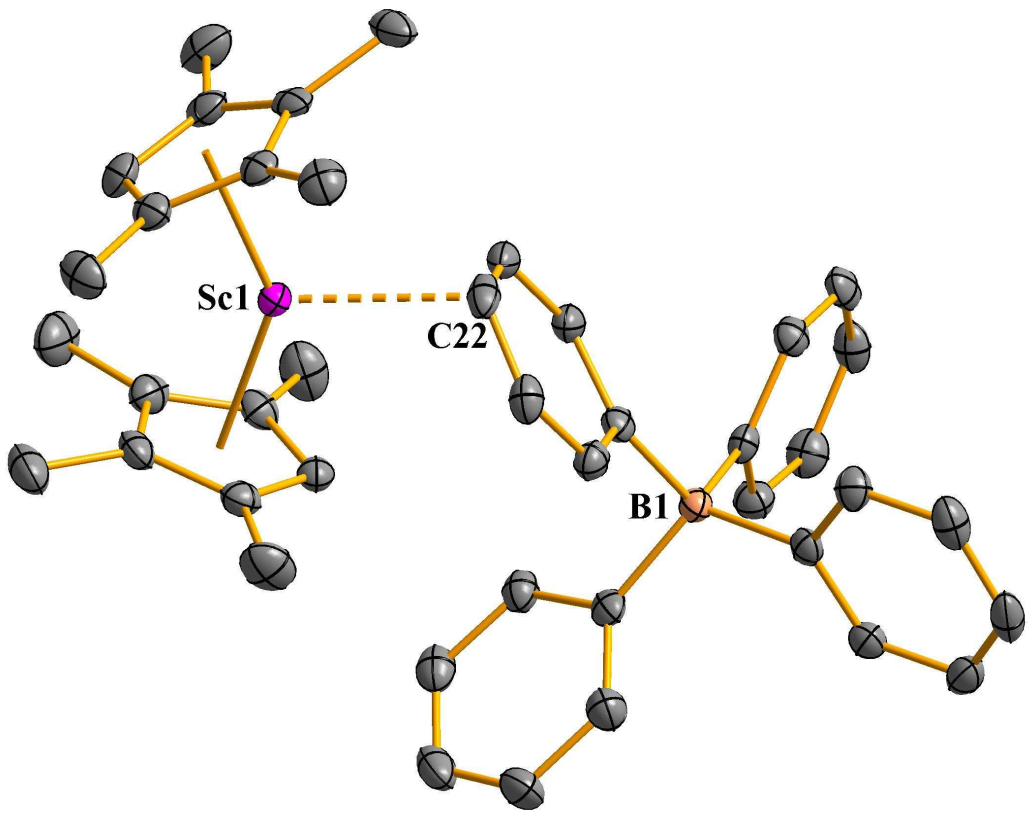

Figure 3.7. Thermal ellipsoid plot of [($C_5Me_4H)_2Sc$][(μ-Ph)BPh_3], **8**, drawn at the 50% probability level. Hydrogen atoms are omitted for clarity.

[($C_5Me_4H)_2Sc(THF)_2$][BPh_4], 9. In THF, complex **8** converts to the solvated complex [($C_5Me_4H)_2Sc(THF)_2$][BPh_4] which was identified by X-ray crystallography in THF, Figure 3.8.

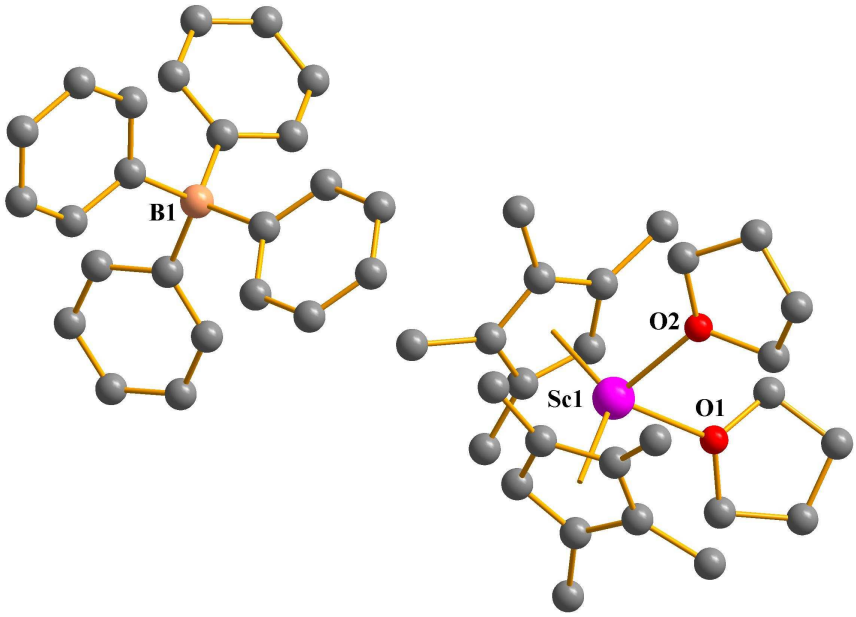

Figure 3.8. Ball-and-stick plot of $[(C_5Me_4H)_2Sc(THF)_2][BPh_4]$, **9**. Hydrogen atoms and independent THF molecules are omitted for clarity.

$[(C_5Me_4H)_2Sc]_2(\mu\text{-}\eta^2\text{:}\eta^2\text{-}N_2)$, 10. Following the reductive method shown in eq 1,[4,5] complex **8** was treated with KC_8 in THF under dinitrogen to generate the scandium dinitrogen complex $[(C_5Me_4H)_2Sc]_2(\mu\text{-}\eta^2\text{:}\eta^2\text{-}N_2)$, **10**, eq 3.5, Figure 3.9.

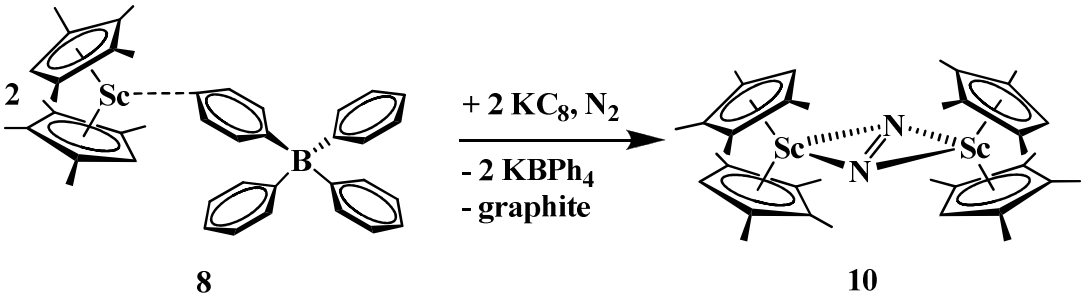

(3.5)

Short, 20 minute reaction times are favored for this procedure as other byproducts begin to appear if the reaction mixture is in solution for longer time periods. Crystallization from THF was also found to be preferable to isolation from toluene, since **10** is not very soluble in toluene. Solutions of **10** in THF are green and benzene solutions are yellow green, but the complex is red in the solid state.

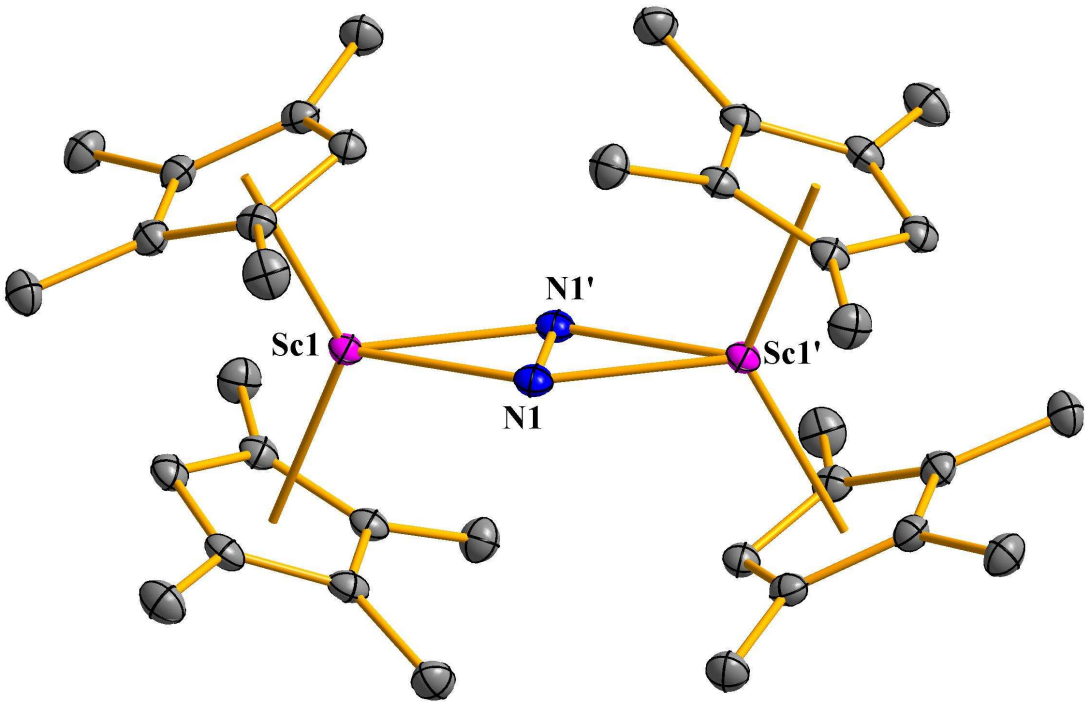

Figure 3.9. Thermal ellipsoid plot of $[(C_5Me_4H)_2Sc]_2(\mu\text{-}\eta^2\text{:}\eta^2\text{-}N_2)$, **10**, drawn at the 50% probability level. Hydrogen atoms are omitted for clarity.

Both ^{45}Sc NMR and ^{15}N NMR data were obtained for **10**. Although ^{45}Sc NMR data have been reported for a variety of complexes,[36-40] relatively few data are available on scandium metallocenes. Hence, reported shifts function mainly as fingerprint spectra that show purity. McGlinchey showed as early as 1985 that there was considerable variation in ^{45}Sc NMR shifts for simple cyclopentadienyl metallocenes as a function of composition.[36] Table 3.2 shows those data as well as similar results for the tetramethylcyclopentadienyl complexes in this study.

The ^{15}N NMR shift of **10** is lower than those observed for the $[(C_5Me_4H)_2Ln]_2(\mu\text{-}\eta^2\text{:}\eta^2\text{-}N_2)$ complexes (ppm): Ln = Lu, 521;[5] La, 495;[7] Y, 468;[41] Sc, 385 (complex **10**). The Sc-Y-La values show an increase in shift as the principal quantum number increases, but the difference between Sc and Y is much larger than that between Y and La. The shifts do not correlate with metal size since Lu is slightly smaller than Y. There are also no correlations in this series of complexes with the experimentally determined N-N bond distances which are

indistinguishable (Å): Ln = Lu, 1.243(12) Å;[5] La, 1.233(5) Å;[7] Y, 1.252(5) Å;[41] Sc, 1.239(3) (see below).

Table 3.2. ^{45}Sc NMR chemical shifts and line width at half height in scandium metallocenes

Complex	Chemical shift (ppm)	Line width at half height (Hz)
$(C_5H_5)_2ScCl$	-9.5	85
$(C_5H_5)_3Sc$	13.5	280
$(C_5Me_4H)_2ScCl(THF)$	55	400
$(C_5H_5)_2ScBH_4$	67.5	250
$[(C_5Me_4H)_2Sc]_2(\mu\text{-}\eta^2\text{:}\eta^2\text{-}N_2)$	143	2700
$(C_5Me_4H)_2Sc(\eta^3\text{-}C_3H_5)$	153	350
$[(C_5Me_4H)_2Sc][(\mu\text{-}Ph)BPh_3]$	190	7800

$\{[(C_5Me_4H)_2Sc]_2(\mu\text{-}\eta^2\text{:}\eta^2\text{-}N_2)[(C_5Me_4H)_2Sc]_2(\mu\text{-}O)\}$, 11. During one attempt to make the ^{15}N analog of **10**, golden crystals of a decomposition product were isolated. X-ray crystallography revealed this to be $\{[(C_5Me_4H)_2Sc]_2(\mu\text{-}\eta^2\text{:}\eta^2\text{-}N_2)[(C_5Me_4H)_2Sc]_2(\mu\text{-}O)\}$, **11**, Figure 3.10. Evidently, the oxide, $[(C_5Me_4H)_2Sc]_2(\mu\text{-}O)$, a common type of decomposition product with f-element metallocenes,[42,43] formed and co-crystallized with **10** into a single crystal of **11**. This co-crystallization may be facilitated by the fact that **10** and the oxide both have compact dianionic ligands coordinated to the two metallocenes. Although **11** was only isolated in a single case, it was included here to show that oxides and reduced dinitrogen complexes can co-crystallize.

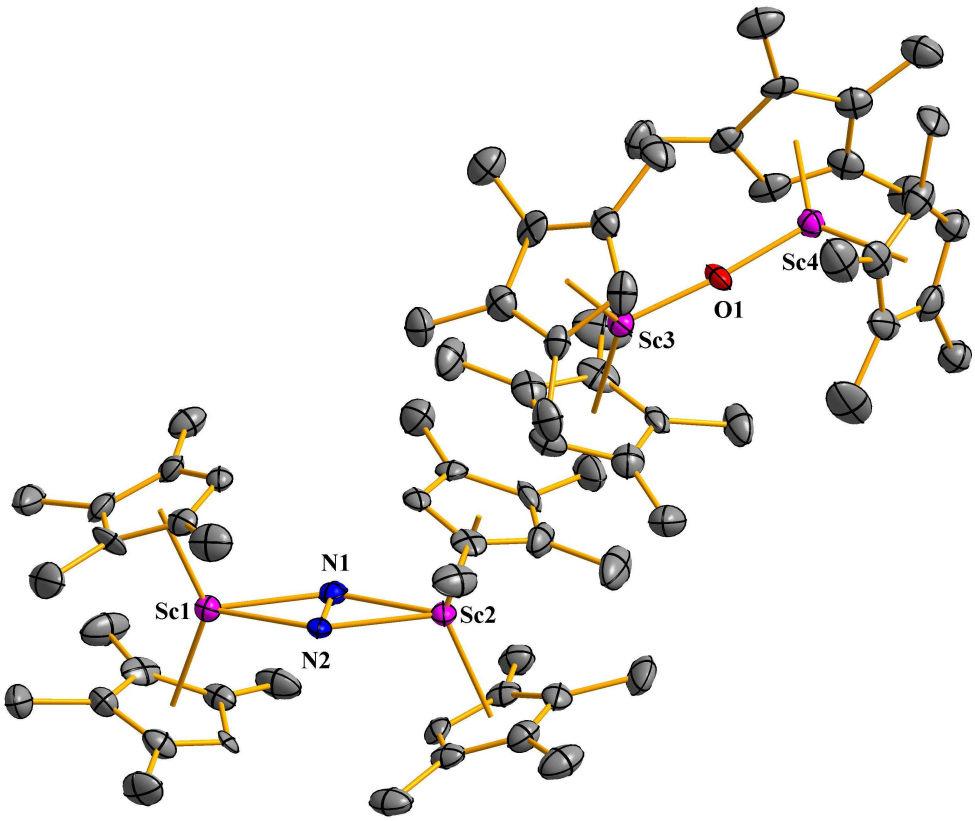

Figure 3.10. Thermal ellipsoid plot of $\{[(C_5Me_4H)_2Sc]_2(\mu\text{-}\eta^2\text{:}\eta^2\text{-}N_2)[(C_5Me_4H)_2Sc]_2(\mu\text{-}O)\}$, **11**, drawn at the 50% probability level. Hydrogen atoms are omitted for clarity.

Structural Studies

$(C_5Me_4H)_2ScCl(THF)$, **6**, and **$(C_5Me_4H)_2Sc(\eta^3\text{-}C_3H_5)$**, **7**. The structures of **6** and **7** are not unusual compared to analogs when the differences in ligands and metals are taken into account. This is shown for **6** in Table 3.3 where its data are compared to those of $(C_5Me_4H)(C_5H_4CH_2CH_2NMe_2)ScCl$, **12**,[44] and $(C_5Me_5)_2YCl(THF)$, **13**.[45] The structure of **7** is compared with the scandium ansa complex, *rac*-$Me_2Si[\eta^5\text{-}C_5H_2\text{-}2,4\text{-}(CHMe_2)_2]_2Sc(\eta^3\text{-}C_3H_5)$, **14**,[32] and the yttrium analog, $(C_5Me_4H)_2Y(\eta^3\text{-}C_3H_5)$, **15**,[41] in Table 3.4.

Table 3.3. Selected Bond Distances (Å) and Angles (deg) for $(C_5Me_4H)_2ScCl(THF)$, **6**, $(C_5Me_4H)(C_5H_4CH_2CH_2NMe_2)ScCl$, **12**,[44] and $(C_5Me_5)_2YCl(THF)$, **13**.[45]

	6	**12**	**13**
M	**Sc**	**Sc**	**Y**
(Cnt)-M-Cnt)[a]	133.0	132.43(7)	136.2(4), 136.6(4)
(Cnt)-M-Cl	108.4,	108.12(6),	106.0(3), 106.0(3),
	106.4	107.30(6)	105.4(3), 105.5(3)
M-(Cnt)	2.222,	2.193(2),	2.382(1), 2.379(1),
	2.219	2.199(2)	2.373(1), 2.388(1)
M-Cl	2.4332(4)	2.4574(12)	2.579(3), 2.577(3)
M-O	2.2557(10)	-	2.410(7), 2.410(7)
M-N	-	2.396(3)	-

[a]Cnt = centroid of the cyclopentadienyl ring

Table 3.4. Selected Bond Distances (Å) and Angles (deg) for $(C_5Me_4H)_2Sc(\eta^3\text{-}C_3H_5)$, **7**, *rac*-$Me_2Si[\eta^5\text{-}C_5H_2\text{-}2,4\text{-}(CHMe_2)_2]_2Sc(\eta^3\text{-}C_3H_5)$, **14**,[32] and $(C_5Me_4H)_2Y(\eta^3\text{-}C_3H_5)$, **15**.[41]

	7	**14**	**15**
M	**Sc**	**Sc**	**Y**
(Cnt)-M-(Cnt)	134.6	128.5(2)	134.5, 134.7
M-(Cnt(1))	2.204	2.188(1)	2.347, 2.348
M-(Cnt(2))	2.190	2.189(1)	2.334, 2.341
M-C(terminal allyl)	2.4702(11)	2.487(3)	2.585(3), 2.590(3)
M-C(terminal allyl)	2.4774(11)	2.469(3)	2.592(3), 2.594(3)
M-C(internal allyl)	2.4618(11)	2.465(5)[#] 2.436(7)[°]	2.603(3), 2.603(3)

[#] Sc-centroid3A (C13-C14A-C15, major rotamer)
°Sc-centroid3B (C13-C14B-C15, minor rotamer)

$[(C_5Me_4H)_2Sc][(\mu\text{-}Ph)BPh_3]$, 8. The structure of **8** differs from lanthanide and actinide analogs[14,16] exemplified by $[(C_5Me_4H)_2Lu][(\mu\text{-}\eta^2\text{:}\eta^1\text{-}Ph)_2BPh_2]$, **16**, Figure 3.1a, in that the anion in **8** interacts with the cation through one not two phenyl groups. This [(μ-

Ph)BPh_3]$^{1-}$ type of attachment had previously been observed in the $(C_5Me_5)^{1-}$ scandium analog, $[(C_5Me_5)_2Sc][(\mu\text{-}\eta^2:\eta^1\text{-Ph})BPh_3]$, **17**, which had Sc-C(phenyl) distances of 2.679(2) and 2.864(2) Å. In **8**, the disparity in Sc-C distances of the two closest carbon atoms of the single phenyl bridge is even greater: 2.568(2) and 2.889(2) Å such that this structure is approaching an $[(\mu\text{-}\eta^1:\eta^1\text{-Ph})BPh_3]^{1-}$ orientation. Comparisons of the metrical parameters of **8**, **16**, and **17** are presented in Table 3.5.

Table 3.5. Selected Bond Distances (Å) and Angles (deg) for $[(C_5Me_4H)_2Sc][(\mu\text{-Ph})BPh_3]$, **8**, $[(C_5Me_4H)_2Lu][(\mu\text{-}\eta^2:\eta^1\text{-Ph})_2BPh_2]$, **16**,[5] and $[(C_5Me_5)_2Sc][(\mu\text{-}\eta^2:\eta^1\text{-Ph})BPh_3]$, **17**.[15]

	8	**16**	**17**
M	**Sc**	**Lu**	**Sc**
M-(Cnt(1))	2.122	2.302	2.1516(10)
M-(Cnt(2))	2.137	2.301	2.1587(9)
M-C(*o*-phenyl)	3.895(2)	2.668(2)	4.048(2)
	4.263(2)	2.800(2)	4.740
M-C(*m*-phenyl)	2.889(2)	2.947(2)	2.864(2)
	3.382(3)	3.237(2)	3.788(2)
M-C(*p*-phenyl)	2.568(2)	3.952(2)	2.679(2)
		4.379(2)	
Cnt(1)-M-Cnt(2)	139.4	133.4	140.94
Cnt(1)-M-C(*o*-phenyl)	84.8	102.9	125.0
	91.0	114.9	120.3
Cnt(1)-M-C(*m*-phenyl)	96.6	100.6	115.5
	107.5	102.3	108.4
Cnt(1)-M-C(*p*-phenyl)	114.3	86.4	105.0
		111.9	
Cnt(2)-M-C(*o*-phenyl)	134.9	103.6	93.4
	126.0	113.7	96.2
Cnt(2)-M-C(*m*-phenyl)	120.9	99.4	100.8
	110.2	100.6	108.7
Cnt(2)-M-C(*p*-phenyl)	105.9	89.6	113.3
		113.1	

The fact that only one phenyl substituent is oriented towards the metal center in **8** is reasonable compared to **16** since the Sc^{3+} metal center is 0.107 Å smaller than the Lu^{3+} metal center according to 8-coordinate Shannon ionic radii.[46] The smaller size of the $(C_5Me_4H)^{1-}$ ligands in **8** compared to the $(C_5Me_5)^{1-}$ ligands in **17** apparently allows a single phenyl carbon to get in closer to the metal cation and make a Sc-C connection 0.1 Å shorter than that in **17**. However, these structures may also be influenced by crystal packing effects as was found with the tris-ring complexes, $(C_5Me_5)Ln[(\eta^6\text{-}Ph)_2BPh_2]$ (Ln = Eu, Sm, Yb) where the pyramidal Eu and Sm complexes differed from the trigonal planar Yb analog.[47]

$[(C_5Me_4H)_2Sc(THF)_2][BPh_4]$, 9. Recrystallization of **8** from THF gave the solvated complex $[(C_5Me_4H)_2Sc(THF)_2][BPh_4]$, **9**, Figure 3.8. Structural comparisons with analogous solvated lanthanide species were not possible since the crystal quality of **9** only provided connectivity.

$[(C_5Me_4H)_2Sc]_2(\mu\text{-}\eta^2\text{:}\eta^2\text{-}N_2)$, 10. The scandium dinitrogen complex **10** differs from most of the $[Z_2(THF)_xLn]_2(\mu\text{-}\eta^2\text{:}\eta^2\text{-}N_2)$ lanthanide and yttrium complexes previously characterized by X-ray crystallography (Z = $N(SiMe_3)_2$, $OC_6H_2{}^tBu_2Me$, C_5Me_5, C_5Me_4H, x = 0-2)[4,5,7,10,24,48,49] in that it is unsolvated. The only other unsolvated examples are $[(C_5Me_5)_2Sm]_2(\mu\text{-}\eta^2\text{:}\eta^2\text{-}N_2)$,[50] which had an unusually short 1.088(12) Å N-N distance, $[(C_5Me_5)_2Tm]_2(\mu\text{-}\eta^2\text{:}\eta^2\text{-}N_2)$[8] and $\{[C_5H_3(SiMe_3)_2]_2Dy\}_2(\mu\text{-}\eta^2\text{:}\eta^2\text{-}N_2)$[9] for which good crystallographic data were not obtained, and $[(C_5H_2{}^tBu_3)_2Nd]_2(\mu\text{-}\eta^2\text{:}\eta^2\text{-}N_2)$[6] and $\{[C_5H_3(SiMe_3)_2]_2Tm\}_2(\mu\text{-}\eta^2\text{:}\eta^2\text{-}N_2)$,[8] which had 1.23 and 1.259(4) Å N-N distances, respectively. The structure of **10** is also unusual in that the four $(C_5Me_4H)^{1-}$ ring centroids define a square plane rather than a tetrahedron. Hence, the dihedral angle between the planes defined by the two ring centroids and Sc for each metallocene is 0° rather than the 90° common for bimetallic metallocene complexes with small bridging ligands such as $[(C_5Me_5)_2Sm]_2(\mu\text{-}\eta^2\text{:}\eta^2\text{-}N_2)$,[50] $[(C_5Me_5)_2Sm]_2(\mu\text{-}H)_2$,[51] and $[(C_5Me_5)_2Sm]_2(\mu\text{-}O)$.[42] The C-H

components of the $(C_5Me_4H)^{1-}$ rings are arranged such that they are staggered within a metallocene with one C-H over the $(N_2)^{2-}$ ligand in the open part of the wedge and the other where the two rings have their closest approach. The dihedral angle between the two planes defined by the ring carbon attached to H, the ring centroid, and Sc is 177.2°.

Despite this unconventional arrangement of ancillary ligands, the $Sc_2(\mu\text{-}\eta^2\text{:}\eta^2\text{-}N_2)$ unit in **10** is planar as it is in the $[Z_2(THF)_xLn]_2(\mu\text{-}\eta^2\text{:}\eta^2\text{-}N_2)$ complexes. The 1.239(3) Å N-N distance is in the broad 1.233(5)-1.305(6) Å range found for the lanthanide and yttrium examples and is indistinguishable from those of the $[(C_5Me_4H)_2Ln(THF)]_2(\mu\text{-}\eta^2\text{:}\eta^2\text{-}N_2)$ complexes (Ln = Lu, 1.243(12) Å;[5] La, 1.233(5) Å;[7] Y, 1.252(5) Å[41]). The 2.216(1) and 2.220(1) Å Sc-N(N_2) distances are about 0.1 Å shorter than those in $\{[(Me_3Si)_2N]_2(THF)Y\}_2(\mu\text{-}\eta^2\text{:}\eta^2\text{-}N_2)$, **18**,[24] and $[(C_5Me_4H)_2Lu(THF)]_2(\mu\text{-}\eta^2\text{:}\eta^2\text{-}N_2)$, **19**.[5] This is consistent with the smaller size of scandium. Comparisons of the metrical parameters of **10**, **18**, and **19** are presented in Table 3.6.

Table 3.6. Selected Bond Distances (Å) and Angles (deg) for $[(C_5Me_4H)_2Sc]_2(\mu\text{-}\eta^2\text{:}\eta^2\text{-}N_2)$, **10**, $\{[(Me_3Si)_2N]_2(THF)Y\}_2(\mu\text{-}\eta^2\text{:}\eta^2\text{-}N_2)$, **18**,[24] and $[(C_5Me_4H)_2Lu(THF)_2]_2(\mu\text{-}\eta^2\text{:}\eta^2\text{-}N_2)$, **19**.[5]

	10	**12**	**13**
M	**Sc**	**Y**	**Lu**
Cnt1-M(1)-Cnt2	131.0	117.44(6)	129.9
M(1)-Cnt1	2.195	2.2443(15)	2.369
M(1)-Cnt2	2.196	2.2640(15)	2.385
M(1)-N(1)	2.216(1)	2.2958(17)	2.290(6)
M(1)-N(1´)	2.220(1)	2.3170(16)	2.311(6)
N(1)-N(1´)	1.239(3)	1.268(3)	1.243(12)

Detailed comparisons of the structure of **10** with the analogous component in $\{[(C_5Me_4H)_2Sc]_2(\mu\text{-}\eta^2\text{:}\eta^2\text{-}N_2)[(C_5Me_4H)_2Sc]_2(\mu\text{-}O)\}$, **11**, are not possible since the crystal quality of **11** provided connectivity only. The structure of the $[(C_5Me_4H)_2Sc]_2(\mu\text{-}\eta^2\text{:}\eta^2\text{-}N_2)$ component of **11** is similar to that one of **10** in that the dihedral angle between the planes defined by the two ring centroids and Sc for each metallocene is 5.2°. The $[(C_5Me_4H)_2Sc]_2(\mu\text{-}O)$ component of **11** differs in that the dihedral angle between the planes defined by the two ring centroids and Sc for each metallocene is 83.3° rather than the 0°. This gives a tetrahedral arrangement of rings more common for bimetallic metallocenes. An overlay of the two components of **11** in Figure 3.11 shows that one metallocene and the bridging ligand line up well for the two structures, but the square planar vs. tetrahedral difference in arrangement of the four $(C_5Me_4H)^{1-}$ rings is evident when the other metallocene components are compared.

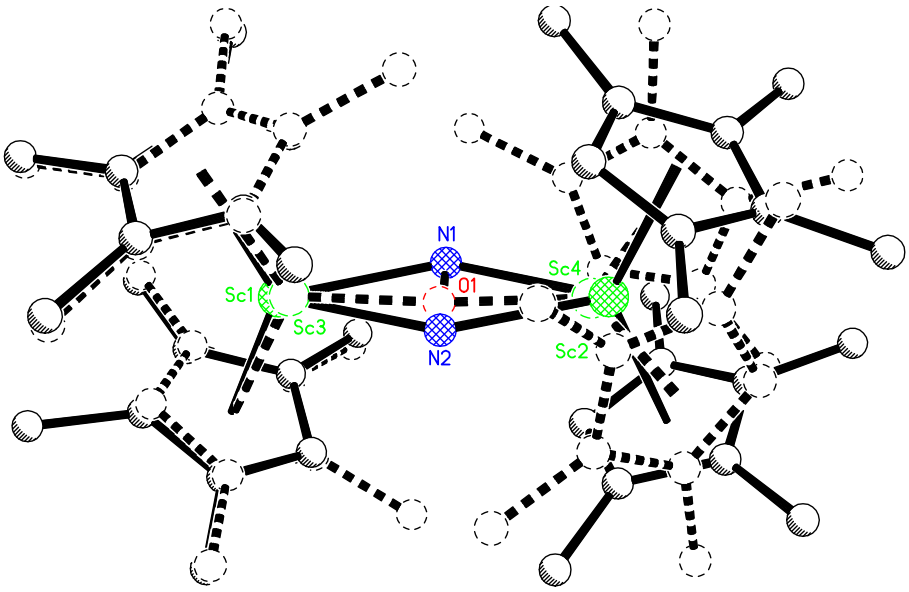

Figure 3.11. Overlay of the $[(C_5Me_4H)_2Sc]_2(\mu\text{-}\eta^2\text{:}\eta^2\text{-}N_2)$ and $[(C_5Me_4H)_2Sc]_2(\mu\text{-}O)$ components of **11**.

The possibility that bimetallic $(N_2)^{2-}$ and $(O)^{2-}$ complexes could be structurally similar and co-crystallize to give unusual metrical parameters à la bond stretch isomerism[52,53] is generally a concern in these complexes. In the case of **11**, the two units have very different

dihedral angles between the planes defined by the two ring centroids and Sc for each metallocene and do not disorder.

Theoretical Studies

The experimentally determined structure of **10** was evaluated with density functional calculations using the Tao-Perdew-Staroverov-Scuseria hybrid (TPSSH) functional.[20] The calculations were similar to those done on $\{[(Me_3Si)_2N]_2(THF)Y\}_2(\mu\text{-}\eta^2\text{:}\eta^2\text{-}N_2)$, **18**.[24] The optimized calculated N-N bond distance of 1.226 Å for **10** agrees well with the crystallographic value of 1.239(3) Å as does the calculated 2.223 Å Sc-N bond (vs 2.216(1) and 2.220(1) Å). The DFT results are consistent with an N-N bond order of 2 in **10**.

To check against the possibility that **10** was the peroxide complex $[(C_5Me_4H)_2Sc]_2(\mu\text{-}\eta^2\text{:}\eta^2\text{-}O_2)$, calculations on this species were also carried out. An O-O bond distance of 1.51 Å was calculated for $[(C_5Me_4H)_2Sc]_2(\mu\text{-}\eta^2\text{:}\eta^2\text{-}O_2)$ that is clearly different from the distances observed in **10** and similar to the experimental values of 1.543(4) Å in $Yb_2[N(SiMe_3)_2]_4(\mu\text{-}\eta^2\text{:}\eta^2\text{-}O_2)(THF)_2$[54] and 1.517(7)-1.603(8) Å in $[Yb_2(\mu\text{-}\eta^2\text{:}\eta^2\text{-}O_2)L_2Cl_2](ClO_4)_2$, where L is 2,14-dimethyl-3,6,10,13,19-pentaazabicyclo[13.3.1]-nonadeca-1(19),2,13,15,17-pentaene.[55]

Inspection of the computed Kohn-Sham molecular orbitals explains the observed bond lengths. The dinitrogen-Sc bonding in **10** results from a strong interaction between a scandium 3*d* orbital and the antibonding π* orbital of N_2 in the ScN_2Sc plane, Figure 3.7. The computed natural population analysis (NPA) for N_2 gives a charge of -0.75 and a scandium 3*d* population of 1.57 along with the fairly short observed Sc-N bond distance of 2.223 Å. This indicates the presence of a polar covalent interaction corresponding to a two-electron-four-center bond between two $(C_5Me_4H)_2Sc$ fragments and N_2, each with a nearly neutral actual charge. The initial reduction of the N≡N triple bond to a formal N=N double bond in **10** is possible because the occupied 3*d* orbital of scandium is high enough in energy and large enough to form a d_π-π* back bond. This is the main basis of the bonding since the occupied

bonding σ and π orbitals of N_2 are too low in energy to interact with the metal atoms. The lowest unoccupied molecular orbital of **10** is the essentially unperturbed π* orbital of N_2 perpendicular to the ScN_2Sc plane, Figure 3.12.

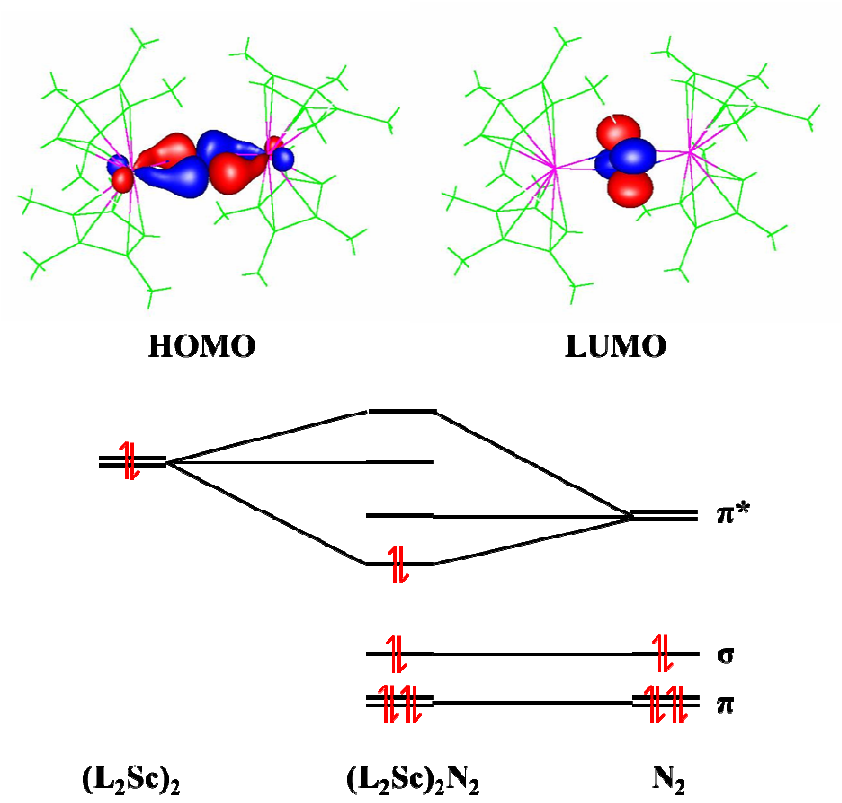

Figure 3.12. Simplified molecular orbital scheme of $[(C_5Me_4H)_2Sc]_2(\mu\text{-}\eta^2\text{:}\eta^2\text{-}N_2)$, **10**.

The orientation of the four cyclopentadienyl rings in **10** was also probed by DFT. The initial calculations gave a structure with a square planar arrangement of the four ring centroids as was found experimentally. Since it was possible that this was a local minimum obtained because the starting point was the experimental coordinates for **10**, a calculation starting with the rings in a tetrahedral arrangement was also carried out. As the energy in this calculation was minimized, the rings began to rotate from tetrahedral to square planar. However, a minimum was reached when the dihedral angle between the planes defined by the two C_5Me_4H ring centroid planes and Sc for each metallocene unit was 54°. Since the energy of this structure is 2.7 kcal/mol higher than that with the square planar rings, it appears that

unfavorable interactions between the rings prevent the model from moving them completely to square planar and the global minimum. In support of this, a calculation with $(C_5H_5)^{1-}$ rings starting in a tetrahedral conformation, ended with the rings square planar in the lowest energy structure. In summary, the calculations support the square planar arrangement of rings found in **10** and **11** to be the lowest in energy.

Conclusion

A reduced dinitrogen complex of the smallest transition metal, scandium, can be obtained by using the tetramethylcyclopentadienyl group as the ancillary ligand. The necessary scandium metallocene precursors $(C_5Me_4H)_2ScCl(THF)$, **6**, $(C_5Me_4H)_2Sc(\eta^3\text{-}C_3H_5)$, **7**, and $[(C_5Me_4H)_2Sc][(\mu\text{-Ph})BPh_3]$, **8**, can be synthesized in a manner similar to those of the larger lanthanides. The reductive method in which a trivalent salt is combined with an alkali metal that was successful with yttrium and the lanthanides in reducing dinitrogen also applies to scandium and provides $[(C_5Me_4H)_2Sc]_2(\mu\text{-}\eta^2\text{:}\eta^2\text{-}N_2)$, **10**, from **8**. Complex **10** has the $M_2(\mu\text{-}\eta^2\text{:}\eta^2\text{-}N_2)$ coordination mode observed with larger metals and in solvated complexes and has an N-N bond distance consistent with $(N{=}N)^{2-}$. Density functional theory shows how this moiety is stabilized by scandium via polar covalent bonding.

References

(1) Reviews and leading references include: (a) Fryzuk, M. D. *Acc. Chem. Res.* **2009**, *42*, 127-133. (b) Special issue: Dedicated to dinitrogen chemistry, *Can. J. Chem.* **2005**, *83*, 277-402. (c) Chirik, P. J. *Dalton Trans.* **2007**, 16-25. (d) Pun, D.; Leopold, S. M.; Bradley, C. A.; Lobkovsky, E.; Chirik, P. J. *Organometallics* **2009**, *28*, 2471-2484. (e) Nikiforov, G. B.; Vidyaratne, I.; Gambarotta, S.; Korobkov, I.; *Angew. Chem. Int. Ed.* **2009**, *48*, 7415-7419. (f) Hirotsu, M.; Fontaine, P. P.; Zavalij, P. Y.; Sita, L. R. *J. Am. Chem. Soc.* **2007**, *129*, 12690-12692. (g) Knobloch, D. J.; Benito-Garagorri, D.; Bernskoetter, W. H.; Keresztes, I.; Lobkovsky, E.; Toomey, H.; Chirik, P. J. *J. Am. Chem. Soc.* **2009**, *131*, 14903-14912. (h) Knobloch, D. J.; Lobkovsky, E.; Chirik, P. J. *Nat. Chem.* **2009**, *2*, 30-35. (i) Chirik, P. J. *Nat. Chem.* **2009**, *1*, 520-522.
(2) Piers, W. E.; Shapiro, P. J.; Bunel, E. E.; Bercaw, J. E. *Synlett* **1990**, 74-84.
(3) Thompson, M. E.; Baxter, S. M.; Bulls, A. R.; Burger, J. B.; Nolan, M. C.; Santarsiero, B. D.; Schaefer, W. P.; Bercaw, J. E. *J. Am. Chem. Soc.* **1987**, *109*, 203-219.
(4) Evans, W. J.; Lee, D. S.; Rego, D. B.; Perotti, J. M.; Kozimor, S. A.; Moore, E. K.; Ziller, J. W. *J. Am. Chem. Soc.* **2004**, *126*, 14574-14582.
(5) Evans, W. J.; Lee, D. S.; Johnston, M. A.; Ziller, J. W. *Organometallics* **2005**, *24*, 6393-6397.
(6) Jaroschik, F.; Momin, A.; Nief, F.; Goff, X. L.; Deacon, G. B.; Junk, P. C. *Angew. Chem. Int. Ed.* **2009**, *48*, 1117-1121.

(7) Evans, W. J.; Lee, D. S.; Lie, C.; Ziller, J. W. *Angew. Chem. Int. Ed.* **2004**, *43*, 5517-5519.
(8) Evans, W. J.; Allen, N. T.; Ziller, J. W. *J. Am. Chem. Soc.* **2001**, *123*, 7927-7928.
(9) Evans, W. J.; Allen, N. T.; Ziller, J. W. *Angew. Chem. Int. Ed.* **2002**, *41*, 359-361.
(10) Evans, W. J.; Zucchi, G.; Ziller, J. W. *J. Am. Chem. Soc.* **2003**, *125*, 10-11.
(11) Cloke, F. G. N.; Khan, K.; Perutz, R. N. *J. Chem. Soc., Chem. Commun.* **1991**, 1372-1373.
(12) Arnold, P. L.; Cloke, F. G. N.; Hitchcock, P. B.; Nixon, J. F. *J. Am. Chem. Soc.* **1996**, *118*, 7630-7631.
(13) Clentsmith, G. K. B.; Cloke, F. G. N.; Green, J. C.; Hanks, J., Hitchcock, P. B.; Nixon, J. F. *Angew. Chem. Int. Ed.* **2003**, *42*, 1038-1041.
(14) Evans, W. J.; Seibel, C. A., Ziller, J. W. *J. Am. Chem. Soc.* **1998**, *120*, 6745-6752.
(15) Bouwkamp, M. W.; Budzelaar, P. H. M.; Gercama, J.; Morales, I. Del H.; de Wolf, J.; Meetsma, A.; Trojanov, S. I.; Teuben, J. H.; Hessen, B. *J. Am. Chem. Soc.* **2005**, *127*, 14310-14319.
(16) Evans, W. J.; Nyce, G. W.; Forrestal, K. J.; Ziller, J. W. *Organometallics*, **2002**, *21*, 1050-1055.
(17) http://www.glasscontoursolventsystems.com/
(18) Evans, W. J.; Kozimor, S. A.; Ziller, J. W.; Kaltsoyannis, N. *J. Am. Chem. Soc.* **2004**, *126*, 14533-14547.
(19) Evans, W. J.; Johnston, M. A.; Greci, M. A.; Gummersheimer, T. S.; Ziller, J. W. *Polyhedron* **2003**, *22*, 119-126.
(20) Staroverov, V. N.; Scuseria, G. E.; Tao, J.; Perdew, J. P. *J. Chem. Phys.* **2003**, *119*, 12129-12137.
(21) Schäfer, A.; Horn, H.; Ahlrichs, R. *J. Chem. Phys.* **1992**, *97*, 2571-2577.
(22) Furche, F.; Perdew, J. P. *J. Chem. Phys.* **2006**, *124*, 044103-27.
(23) Waller, M. P.; Braun, H.; Hojdis, N.; Bühl, M. *J. Chem. Theor. Comput.* **2007**, *3*, 2234-2242.
(24) Evans, W. J.; Fang, M.; Zucchi, G.; Furche, F.; Ziller, J. W.; Hoekstra, R. M.; Zink, J. I. *J. Am. Chem. Soc.* **2009**, *131*, 11195-11202.
(25) Treutler, O.; Ahlrichs, R. *J. Chem. Phys.* **1995**, *102*, 346-354.
(26) Deglmann, P.; Furche, F.; Ahlrichs, R. *Chem. Phys. Lett.* **2002**, *362*, 511-518.
(27) Huber, K. P. & Herzberg, G. *Constants of Diatomic Molecules* (data prepared by *Gallagher*, J. W. & Johnson, R. D. III) in NIST Chemistry WebBook, NIST Standard Reference Database Number 69, Eds. Linstrom, P. J. & Mallard, W. G. National Institute of Standards and Technology, Gaithersburg MD, 20899, http://webbook.nist.gov, (retrieved December 6, 2009).
(28) Reed, A. E.; Weinstock, R. B.; Weinhold, F. *J. Chem. Phys.* **1985**, *83*, 735-746.
(29) Weigend, F.; Ahlrichs, R. *Phys. Chem. Chem. Phys.* **2005**, *18*, 3297-3305.
(30) TURBOMOLE V6-0, TURBOMOLE GmbH, Karlsruhe, 2008, http://www.turbomole.com.
(31) Yoder, J. C.; Day, M. W.; Bercaw, J. E. *Organometallics* **1998**, *17*, 4946-4958.
(32) Abrams, M. B.; Yoder, J. C.; Loeber, C.; Day, M. W.; Bercaw, J. E. *Organometallics* **1999**, *18*, 1389-1401.
(33) Evans, W. J.; Boyle, T. J.; Ziller, J. W. *Inorg. Chem.* **1992**, *31*, 1120-1122.
(34) Evans, W. J.; Keyer, R. A.; Ziller, J. W. *Organometallics* **1993**, *12*, 2618-2633.
(35) Evans, W. J.; Kozimor, S. A.; Brady, J. C.; Davis, B. L.; Nyce, G. W.; Seibel, C. A.; Ziller, J. W.; Doedens, R. J. *Organometallics* **2005**, *24*, 2269-2278.
(36) Bougeard, P.; Mancini, M.; Sayer, B. G.; McGlinchey, M. J. *Inorg. Chem.* **1985**, *24*, 93-95.
(37) Kirakosyan, G. A.; Tarasov, V. P.; Buslaev, Y. A. *Magn. Reson. Chem.* **1989**, *27*, 103-111.
(38) Neculai, A. M.; Roesky, H. W.; Neculai, D.; Magull, J. *Organometallics* **2001**, *20*, 5501-5503.
(39) Neculai, A. M.; Neculai, D.; Roesky, H. W.; Magull, J.; Baldus, M.; Andronesi, O.; Jansen, M. *Organometallics* **2002**, *21*, 2590-2592.
(40) Neculai, A. M.; Cummins, C. C.; Neculai, D.; Roesky, H. W.; Bunkoczi, G.; Walfort, B.; Stalke, D. *Inorg. Chem.* **2003**, *42*, 8803-8810.
(41) Lorenz, S. E.; Schmiege, B. M; Lee, D. S.; Ziller, J. W.; Evans, W. J. *Inorg. Chem.* **2010**, *49*, 6655-6663.
(42) Evans, W. J.; Grate, J. W.; Bloom, I.; Hunter, W. E.; Atwood, J. L. *J. Am. Chem. Soc.* **1985**, *107*, 405-409.
(43) Evans, W. J.; Davis, B. L.; Nyce, G. W.; Perotti, J. M.; Ziller, J. W. *J. Organomet. Chem.* **2003**, *677*, 89-95.
(44) Schumann, H.; Erbstein, F.; Herrmann, K.; Demtschuk, J.; Weimann, R. J. *J. Organomet. Chem.* **1998**, *562*, 255-262.
(45) Evans, W. J.; Grate, J. W.; Levan, K. R.; Bloom, I.; Peterson, T. T.; Doedens, R. J.; Zhang, H.; Atwood, J. L. *Inorg Chem.* **1986**, *25*, 3614-3619.
(46) Shannon, R. D. *Acta Cryst.* **1976**, *A32*, 751-767.
(47) Evans, W. J.; Walensky, J. R.; Furche, F.; DiPasquale, A. G.; Rheingold, A. L. *Organometallics* **2009**, *28*, 6073-6078.
(48) Evans, W. J.; Lee, D. S.; Ziller, J. W. *J. Am. Chem. Soc.* **2004**, *126*, 454-455.
(49) Evans, W. J.; Rego, D. B.; Ziller, J. W. *Inorg. Chem.* **2006**, *45*, 10790-10798.
(50) Evans, W. J.; Ulibarri, T. A.; Ziller, J. W. *J. Am. Chem. Soc.* **1988**, *110*, 6877.
(51) Evans, W. J.; Bloom, I.; Hunter, W. E.; Atwood, J. L. *J. Am. Chem. Soc.* **1983**, *105*, 1401-1403.
(52) Parkin, G. *Acc. Chem. Res.* **1992**, *25*, 455-460.
(53) Labinger, J. A. *C. R. Chimie* **2002**, *5*, 235-244.
(54) Niemeyer, M. *Z. Anorg. Allg. Chem.* **2002**, *628*, 647-657.

(55) Patroniak, V.; Kubicki, M.; Mondry, A.; Lisowski, J.; Radecka-Paryzek, W. *Dalton Trans.* **2004**, 3295-3304.
(56) Sara E. Lorenz, Dissertation 2009, University of California Irvine.

Chapter 4

Synthesis, Structure, and Reactivity of Scandium and Yttrium Metallocene Borohydride Complexes: Comparisons of $(BH_4)^{1-}$ vs $(BPh_4)^{1-}$ as Counteranions

Introduction

One of the effective ways to expand reactivity options with the trivalent lanthanide ions is to use Ln^{3+} complexes as precursors in LnZ_3/K reduction reactions that provide access to "Ln^{2+}" reactivity even if the divalent ion has not been isolated in solution.[1] For example, dinitrogen complexes previously obtainable only with the divalent ions like Sm^{2+},[2] Tm^{2+},[3,4] Dy^{2+},[4,5] and Nd^{2+},[4] can be obtained for lanthanides from La to Lu, eq 4.1.[6,7,8] When trivalent LnZ_3 are challenging to synthesize, e.g. when Z = $(C_5Me_5)^{1-}$,[9-13] LnZ_2Z' precursors such as $[(C_5Me_5)_2Ln][(\mu\text{-Ph})_2BPh_2]$ can be used.[14] When desirable LnZ_3 complexes are made from LnZ_2Z' precursors as is the case of $(C_5Me_4H)_3Y$, which is synthesized from $[(C_5Me_4H)_2Y][(\mu\text{-Ph})_2BPh_2]$,[15] the LnZ_2Z' complexes are the more efficient starting materials for the reductive chemistry.

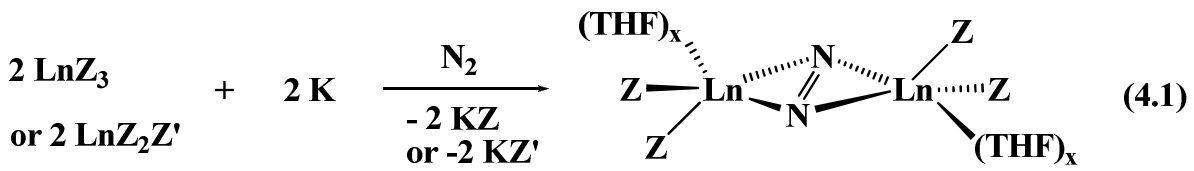

(4.1)

Ln = La, Ce, Pr, Nd, Gd, Tb, Dy, Ho, Er, Y, Tm, Lu
Z = $N(SiMe_3)_2$, C_5Me_4H, C_5Me_5, $C_5H_2(CMe_3)_3$, $OC_6H_3(^tBu)_2$-2,6
Z' = BPh_4, I; x = 0-2

The tetraphenylborate complexes $[(C_5Me_5)_2Ln][(\mu\text{-Ph})_2BPh_2]$[14] and $[(C_5Me_4H)_2Ln][(\mu\text{-Ph})_2BPh_2]$[16] have proven to be excellent reagents for LnZ_2Z'/K reactions in part since the $(BPh_4)^{1-}$ anions are only loosely ligated to the metal via agostic interactions

involving two phenyl groups. Although these complexes are effective precursors, they require multiple steps for synthesis as shown in Scheme 4.1.

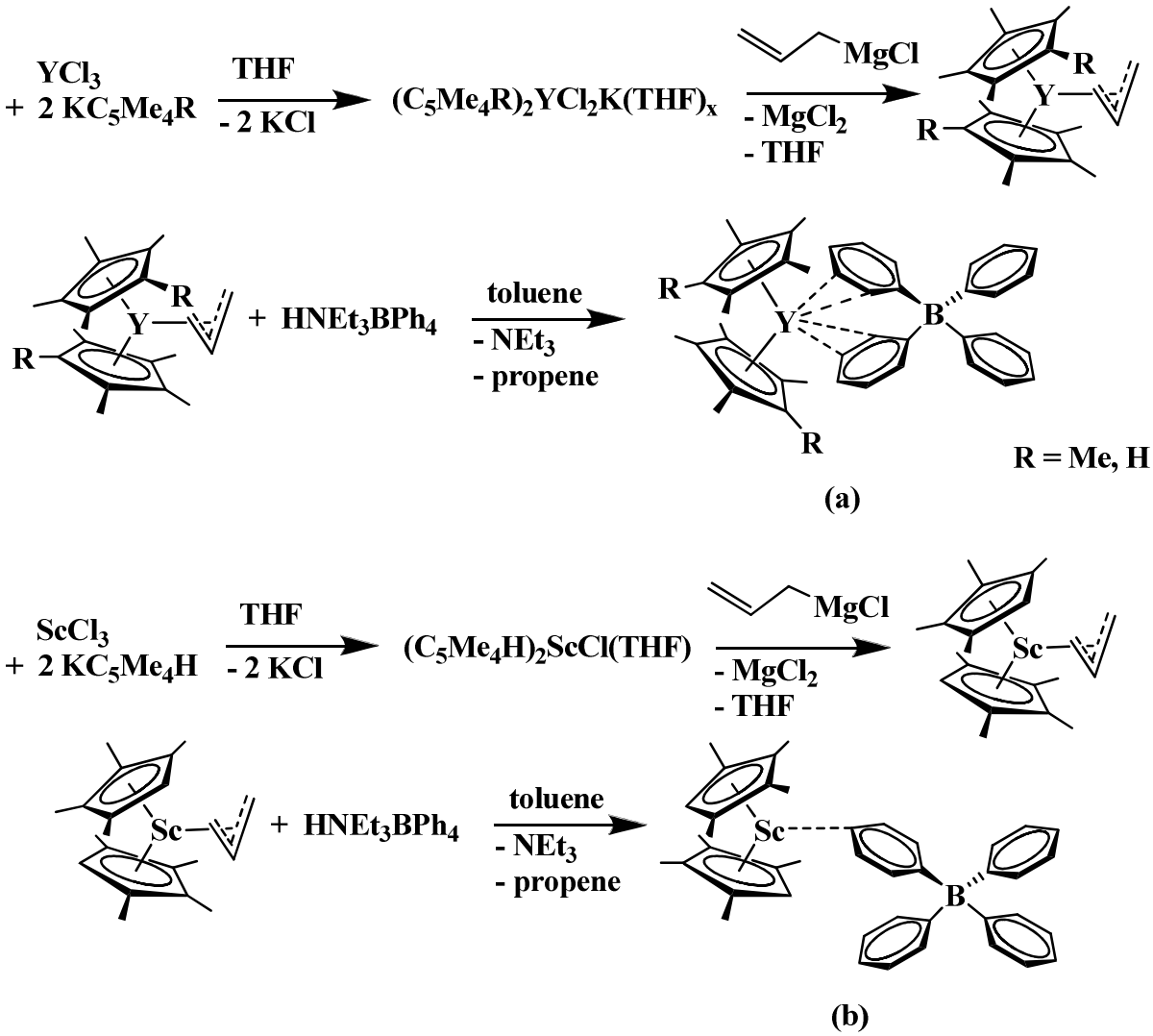

Scheme 4.1. Typical synthesis of rare earth metal tetraphenyl borate complexes. a) $[(C_5Me_4R)_2Y][(\mu\text{-Ph})_2BPh_2]$ (R=H, Me) showing interactions involving two of the phenyl groups and b) $(C_5Me_4H)_2Sc(\mu\text{-Ph})BPh_3)$ showing only one interaction with one of the phenyl groups (see Chapter 3 for more information).

In efforts to find precursors for LnZ_2Z'/K reactions that could be synthesized more directly, the borohydride complexes $(C_5Me_5)_2Ln(BH_4)$ and $(C_5Me_4H)_2Ln(BH_4)$ were attractive since *Schumann et al.* had reported that they could be directly synthesized from $LnCl_3$, eq 4.2.[17]

$$\mathbf{LnCl_3(THF)x + 2\ Na[C_5Me_4R] + NaBH_4 \longrightarrow [(C_5Me_4R)_2Ln(BH_4)(THF)] + 3\ NaCl} \quad \mathbf{(4.2)}$$

R = H, Ln = Y, Sm, Lu; R = Me, Ln = Y, Sm, Lu;
R = Et, Ln = Y, Sm, Lu; R = ^{i}Pr, Ln = Y, Sm, Lu

Since borohydride ligands typically bind to lanthanides via bridging hydride connections that are more direct than the agostic interactions found with their phenyl analogs, it was unlikely that they could be displaced as easily as the $(BPh_4)^{1-}$ ions. On the other hand, the structures of these complexes were unknown and the success of the LnZ_2Z'/K reactions depends in part on only the relative attraction of Z' for Ln^{3+} vs K^{1+}, since the byproduct is KZ′. To evaluate the borohydrides as precursors for LnZ_2Z'/K reactions, the structures of $(C_5Me_4H)_2Y(BH_4)(THF)$, **20**, and $(C_5Me_5)_2Y(BH_4)(THF)$, **21**, were determined, their utility in reductive reactions was examined, and the preference of $[(C_5Me_4R)_2Y]^{1+}$ cations for $(BH_4)^{1-}$ vs $(BPh_4)^{1-}$ was investigated. Structural comparisons of **20** and **21** with the reported tetraphenylborate complexes, $[(C_5Me_4H)_2Y][(\mu\text{-}Ph)_2BPh_2]$, **22**,[15] and $[(C_5Me_5)_2Y][(\mu\text{-}Ph)_2BPh_2]$, **23**,[13] were carried out. In addition, $(C_5Me_4H)_2Sc(BH_4)$, **24**, and $(C_5Me_5)_2Sc(BH_4)$, **25a**, were prepared and their structures were compared to their $(BPh_4)^{1-}$ analogs. Unfortunately, complex **25a** could only be crystallized contaminated with the scandium chloride component $(C_5Me_5)_2ScCl(THF)$, **26**, as $(C_5Me_5)_2Sc(BH_4)_{0.5}(Cl)_{0.5}(THF)$, **27**, in which $(BH_4)^-$ and Cl^- are assigned with site-occupany factors of 0.50.

Experimental

The syntheses and manipulations described below were conducted under argon or nitrogen with rigorous exclusion of air and water using glovebox, vacuum line and Schlenk techniques. Solvents were dried over columns containing Q-5 and molecular sieves. NMR solvents were dried over Na/K alloy, degassed, and vacuum transferred prior to use. Allylmagnesium chloride (2.0 M in THF) was purchased from Aldrich and used as received. 1,4-Dioxane was purchased from Aldrich and used as received. 1,2,3,4-

tetramethylcyclopentadiene ($C_5Me_4H_2$) was purchased from Aldrich, distilled onto 4 Å molecular sieves, and degassed by three freeze-pump-thaw cycles prior to use. Potassium bis(trimethylsilyl)amide (Aldrich) was recrystallized from toluene prior to use. KC_5Me_4H was prepared as described for KC_5Me_5.[18] ^{1}H and ^{13}C NMR spectra were recorded on Bruker GN500 or CRYO500 MHz spectrometers. IR samples were prepared as KBr pellets, and the spectra were obtained on a Varian 1000 FT-IR system. Elemental analyses were performed using a PerkinElmer Series II 2400 CHNS elemental analyzer. Complexes **20** and **22** were prepared by slight modifications of the literature procedure.[17]

$(C_5Me_4H)_2Y(BH_4)(THF)$, 20. In a nitrogen-filled glove box, KC_5Me_4H (2.01 g, 12.5 mmol) was slowly added to a stirred white slurry of YCl_3 (1.22 g, 6.25 mmol) in 100 mL of THF. After the mixture was stirred for 24 h, $NaBH_4$ (270 mg, 7.14 mmol) was added and the mixture was stirred for another 24 h. The solution was then evaporated to dryness to yield a white powder. After this material was stirred in 100 mL of hexane for 24 h, the white precipitate was removed via centrifugation and filtration to yield a colorless solution. Evaporation of the solvent left a white crystalline material, **20** (1.47g, 56%). Crystals suitable for X-ray analysis were grown from a concentrated toluene solution of **20** at 25 °C over the course of 24 h. ^{1}H NMR (500 MHz, benzene-d_6): δ 5.63 (s, 2H, C_5Me_4H), 3.45 (s, 4H, THF), 2.07 (s, 24H, C_5Me_4H), 0.77 (s, 1H, B*H*), 0.62 (s, 1H, B*H*), 0.43 (s, 1H, B*H*), 0.28 (s, 1H, B*H*). ^{13}C NMR (126 MHz, benzene-d_6): δ 121.55 (C_5Me_4H), 118.36 (C_5Me_4H), 110.98 (C_5Me_4H), 13.83 (C_5Me_4H), 12.00 (C_5Me_4H).

$(C_5Me_5)_2Y(BH_4)(THF)$, 21. As described for **20**, **21** was obtained as a colorless crystalline solid (0.776 g, 53 %) from NaC_5Me_5 (1.00 g, 6.32 mmol), YCl_3 (0.636 g, 3.26 mmol) and $NaBH_4$ (0.166 g, 4.39 mmol) in THF (100 mL). Colorless crystals suitable for X-ray analysis were grown from a concentrated hexane solution of **21** at 25 °C over the course of 48 h. ^{1}H NMR (500 MHz, benzene-d_6): δ 3.52 (s, 4H, THF), 2.00 (s, 30H, C_5Me_5),

0.83 (s, 1H, B*H*), 0.66 (s, 1H, B*H*), 0.49 (s, 1H, B*H*), 0.33 (s, 1H, B*H*). ^{13}C NMR (126 MHz, benzene-d_6): δ 118.54 (C_5Me$_5$), 12.41 (C$_5$*Me*$_5$).

(C$_5$Me$_4$H)$_2$Sc(BH$_4$), 24. As described for **20**, **24** was obtained as a pale yellow crystalline solid (0.085 g, 45 %) from KC$_5$Me$_4$H (0.200 g, 1.25 mmol), ScCl$_3$ (0.094 g, 0.62 mmol) and NaBH$_4$ (0.024 g, 0.62 mmol) in THF (20 mL). Colorless crystals suitable for X-ray analysis were grown from a concentrated hexane solution of **24** at -35 °C over the course of 24 h.

Alternative Synthesis of 24. In a nitrogen-filled glove box, NaBH$_4$ (0.058 g, 0.15 mmol) was added to a yellow solution of [(C$_5$Me$_4$H)$_2$Sc][(μ-Ph)BPh$_3$], **8**,[Ch.3] (0.311 g, 0.513 mmol) in 20 mL of THF. After the mixture was stirred for 24 h, the solution was evaporated to dryness to yield a pale yellow powder. After this material was stirred in 20 mL of hexane for 2 h, the white precipitate was removed via centrifugation and filtration to yield a colorless solution. Evaporation of the solvent left a white crystalline material, **24** (134 mg, 86%). ^{1}H NMR (500 MHz, benzene-d_6): δ 6.19 (s, 2H, C$_5$Me$_4$*H*), 1.98 (s, 12H, C$_5$*Me*$_4$H), 1.70 (s, 12H, C$_5$*Me*$_4$H), 1.83 (m, 2H, B*H*$_2$), 1.59 (m, 2H, B*H*$_2$). ^{13}C NMR (126 MHz, benzene-d_6): δ 126.3 (C_5Me$_4$H), 121.1 (C_5Me$_4$H), 115.9 (C_5Me$_4$H), 13.4 (C$_5$*Me*$_4$H), 12.4 (C$_5$*Me*$_4$H). Anal. Calcd for C$_{18}$H$_{30}$BSc: C, 71.54; H, 10.01. Found: C, 72.04; H, 10.61.

(C$_5$Me$_5$)$_2$Sc(BH$_4$), 25a. In a nitrogen-filled glove box, NaBH$_4$ (0.010 g, 0.264 mmol) was added to a yellow solution of [(C$_5$Me$_5$)$_2$Sc][(μ-η^2:η^1-Ph)BPh$_3$] (0.040 g, 0.066 mmol) in 20 mL of THF. After the mixture was stirred for 24 h, the solution was evaporated to dryness to yield a pale yellow powder. After this material was stirred in 20 mL of hexane for 2 h, the white precipitate was removed via centrifugation and filtration to yield a colorless solution. Evaporation of the solvent left a white crystalline material (0.010 g, 48%). ^{1}H NMR (500 MHz, benzene-d_6): δ 2.30 (m, 4H, BH$_4$), 1.89 (s, 30H, C$_5$*Me*$_5$).

(C$_5$Me$_5$)$_2$Sc(Cl)$_{0.5}$(BH$_4$)$_{0.5}$(THF), 27. In a nitrogen-filled glove box, KC$_5$Me$_5$ (0.20 g, 1.3 mmol) was slowly added to a stirred white slurry of ScCl$_3$ (0.094 g, 0.62 mmol) in 20 mL

of THF. After the mixture was stirred for 24 h, $NaBH_4$ (25 mg, 0.66 mmol) was added and the mixture was stirred for another 24 h. The solution was then evaporated to dryness to yield a white powder. After this material was stirred in 20 mL of hexane for 24 h, the white precipitate was removed via centrifugation and filtration to yield a colorless solution. Evaporation of the solvent left a white crystalline material (70 mg). Crystals suitable for X-ray analysis were grown from a concentrated hexane solution of **27** at -35 °C over the course of 24 h.

X-ray Crystallographic Data. X-Ray data collection parameters of **20, 21, 24** and **27** are given in Table 4.1. Details for X-ray data collection, structure determination and refinement are given in the Appendix.

Results and Discussion

$(C_5Me_4H)_2Y(BH_4)$, **20**, and $(C_5Me_5)_2Y(BH_4)$, **21**, can be made directly from YCl_3, a cyclopentadienyl salt, and $NaBH_4$ as previously reported.[17] Complex **20** can be prepared starting with either NaC_5Me_4H as originally reported[17] or with KC_5Me_4H. However, the synthesis of **21** appeared to require that both reagents be sodium salts. Attempts to use complexes **20** and **21** as precursors to yield $[(C_5Me_4H)_2Y(THF)]_2(\mu\text{-}\eta^2\text{:}\eta^2\text{-}N_2)$ and $[(C_5Me_5)_2Y(THF)]_2(\mu\text{-}\eta^2\text{:}\eta^2\text{-}N_2)$ via the LnZ_2Z'/K reactions were unsuccessful. The results of the LnZ_2Z'/K reactions suggested that the borohydride ligands were more tightly bound than the tetraphenylborates as originally anticipated. To obtain more information on this point, complexes **22** and **23** were treated with $NaBH_4$ to determine whether anion substitution would occur. As shown in eq 4.3, in both cases the borohydride displaces the tetraphenylborate.

$$\mathbf{(C_5Me_4R)Y(BPh_4) + NaBH_4 \xrightarrow[\text{THF}]{} [(C_5Me_4R)_2YBH_4(THF)] + NaBPh_4} \qquad \mathbf{(4.3)}$$

R=H, Me

Table 4.1. X-ray Data Collection Parameters for $(C_5Me_4H)_2Y(BH_4)(THF)$, **20**, $(C_5Me_5)_2Y(BH_4)(THF)$, **21**, $(C_5Me_4H)_2Sc(BH_4)$, **24**, and $[(C_5Me_4H)_2Sc(BH_4)(THF)]$ $[(C_5Me_4H)_2Sc(Cl)(THF)]$, **27**.

	20	**21**	**24**	**27**
formula	$C_{22}H_{38}BOY$	$C_{24}H_{42}BOY$	$C_{18}H_{30}BSc$	$[C_{24}H_{38}OScBH_4]$ $[C_{24}H_{38}OScCl]$
fw	418.24	446.30.	302.19	412.65
space group	$P\bar{1}$	$P\bar{1}$	$P2_1/n$	$P\bar{1}$
crystal system	Triclinic	Triclinic	Monoclinic	Triclinic
a (Å)	8.6457(3)	8.5431(10)	12.5375(5)	8.4949(4)
b (Å)	16.8105(6)	17.102(2)	11.2389(4)	16.6454(8)
c (Å)	16.8419(6)	18.187(2)	12.6035(5)	17.7827(8)
α (deg)	65.9645(4)	62.5943(13)	90	63.7179(5)
β (deg)	87.0262(5)	88.1152(16)	102.9693(4)	87.6483(5)
γ (deg)	81.1176(5)	85.9470(16)	90	87.2937(6)
V (Å^3)	2208.56(14)	2353.1(5)	1730.63(12)	2251.47(18)
Z	4	4	4	2
ρ_{calcd} (Mg/m^3)	1.258	1.260	1.160	1.217
μ (mm^{-1})	2.647	2.489	0.414	0.397
temp (K)	103(2)	153(2)	98(2)	153(2)
R1 [I > 2σ(I)][a]	0.0274	0.0324	0.0272	0.0399
wR2 (all data)[a]	0.0666	0.0766	0.0765	0.1053

[a] Definitions: $wR2 = [\Sigma[w(F_o^2-F_c^2)^2] / \Sigma[w(F_o^2)^2]]^{1/2}$, $R1 = \Sigma||F_o|-|F_c|| / \Sigma|F_o|$.

In order to have a structural comparison to the yttrium borohydride complexes **20** and **21**, the scandium analogs $(C_5Me_4H)_2Sc(BH_4)$, **24**, and $(C_5Me_5)_2Sc(BH_4)$, **25a**, have been synthesized, using the same method as described in eq 4.2. Surprisingly, these reactions proceeded not as clean as the analogous synthesis of **20** and **21**. For this reason, complex **25a** could not be formed cleanly, but it crystallized as the solvated $(C_5Me_5)_2ScCl(BH_4)(THF)$, **25**,

together with the respective chloride $(C_5Me_5)_2ScCl(THF)$, **26**, to give $(C_5Me_5)_2Sc(Cl)_{0.5}(BH_4)_{0.5}(THF)$, **27**, in one single crystal. The alternative synthesis by using tetraphenylborate salts of a scandium metallocene as described in eq 4.3 for the yttrium complexes worked much better to yield pure **24** and **25a** according to ^{1}H NMR spectoscopy.

Structural Studies

$(C_5Me_4H)_2Y(BH_4)$, 20, and $(C_5Me_5)_2Y(BH_4)$, 21. As shown in Figures 4.1 and 4.2, respectively, **20** contains a $[(\mu\text{-H})_3BH]^{1-}$ ligand and **21**, which has the more substituted cyclopentadienyl rings, has $[(\mu\text{-H})_2BH_2]^{1-}$ coordination. The metrical parameters are shown in Table 4.2 along with data for $[(C_5Me_4H)_2Y][(\mu\text{-Ph})_2BPh_2]$, **22**,[15] Figure 4.3a, and $[(C_5Me_5)_2Y][(\mu\text{-Ph})_2BPh_2]$, **23**,[13] Figure 4.3b.

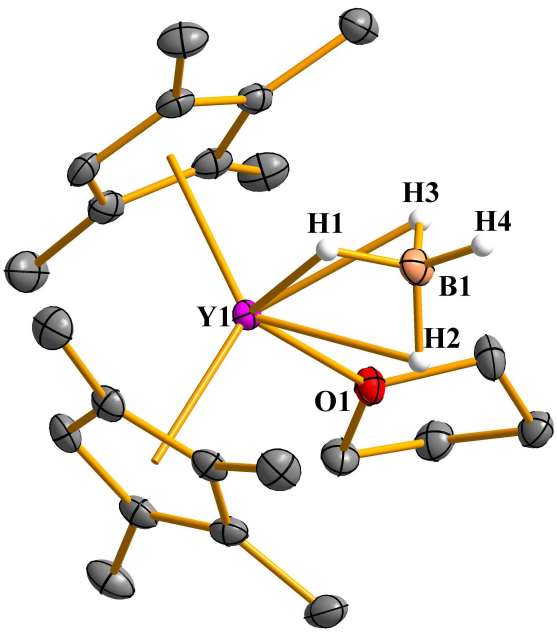

Figure 4.1. Thermal ellipsoid plot of $(C_5Me_4H)_2Y(BH_4)(THF)$, **20**, drawn at the 50% probability level. Hydrogen atoms except for H1, H2, H3 and H4 are omitted for clarity.

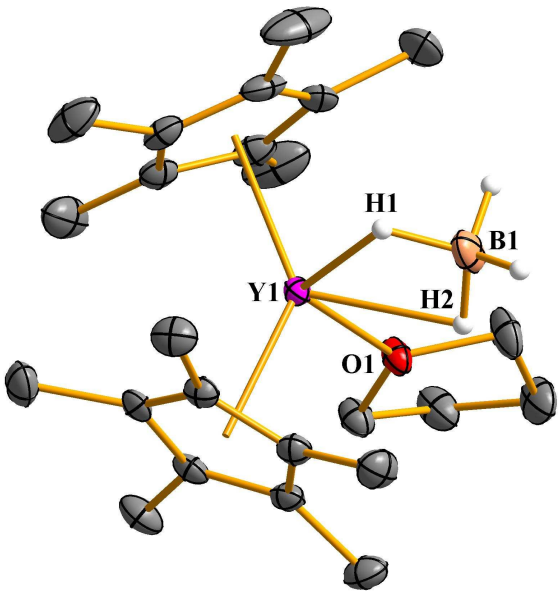

Figure 4.2. Thermal ellipsoid plot of $(C_5Me_5)_2Y(BH_4)(THF)$, **21**, drawn at the 50% probability level. Hydrogen atoms except H1 and H2 are omitted for clarity.

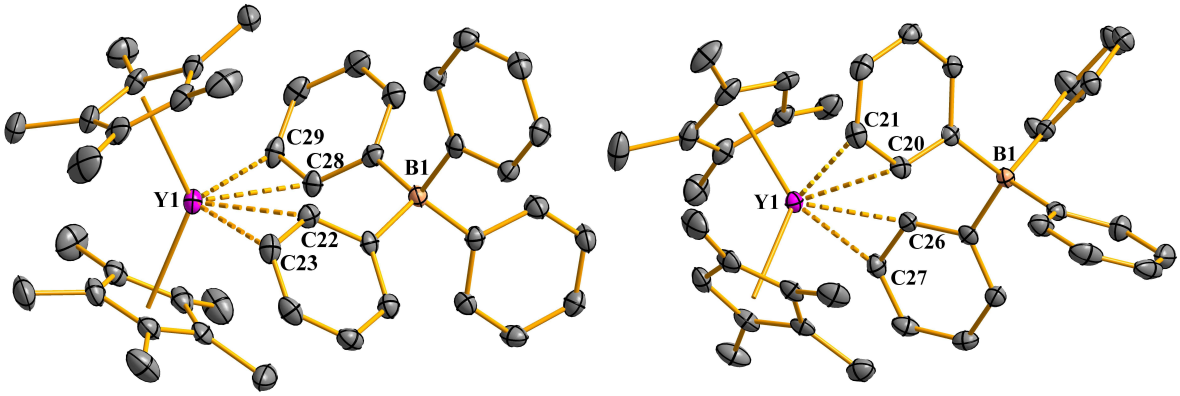

Figure 4.3. Agostic interactions between the metal and the tetraphenylborate anion in (a) $[(C_5Me_4H)_2Y][(\mu\text{-}Ph)_2BPh_2]$, **22**,[15] and (b) $[(C_5Me_5)_2Y][(\mu\text{-}Ph)_2BPh_2]$, **23**.[13] Hydrogen atoms are omitted for clarity.

Table 4.2. Selected Bond Distances (Å) and Angles (deg) for $(C_5Me_4H)_2Y(BH_4)(THF)$, **20**, $(C_5Me_5)_2Y(BH_4)(THF)$, **21**. $[(C_5Me_4H)_2Y][(\mu\text{-}Ph)_2BPh_2]$, **22**,[15] and $[(C_5Me_5)_2Y][(\mu\text{-}Ph)_2BPh_2]$, **23**.[13] The unit cells of **20** and **21** contain two crystallographically independent molecules, the metrical parameters of which are very similar. Only one is discussed in detail here. For more information see supplementary information.

	20	**21**	**22**	**23**
Cnt1-Y1-Cnt2	127.3	135.0	132.8	134.3
Cnt1-Y(1)-O(1)	105.5	103.8	-	-
Cnt1-Y(1)-B(1)	110.8	107.4	-	-
Cnt1-Y(1)-$(H1_b)^*$	102.1	97.2	-	-
Cnt1-Y(1)-$(H2_b)^*$	135.6	126.8	-	-
Cnt1-Y(1)-$(H3_b)^*$	92.2	-	-	-
Y1-Cnt1	2.383	2.386	2.353	2.363
Y1-Cnt2	2.377	2.388	2.353	2.375
Y1-$(H1_b)^*$	2.24(2)	2.25(2)	-	-
Y1-$(H2_b)^*$	2.43(2)	2.30(3)	-	-
Y1-$(H3_b)^*$	2.40(2)	-	-	-
Y1-B1	2.547(2)	2.643(3)	4.349	4.442
Y1-O1	2.3783(12)	2.3951(15)	-	-
Y1-C20#	-	-	2.718(2)	-
Y1-C22#			-	2.819(3)
Y1-C21#	-	-	2.976(2)	-
Y1-C23#			-	3.152(3)
Y1-C26#	-	-	2.829(2)	-
Y1-C28#			-	2.813(3)
Y1-C27#	-	-	3.223(2)	-
Y1-C29#				3.118(3)

* (H_b) = bridging hydrogen atoms
# C = phenyl carbon atoms interact agostic with the metal center

Since the unit cells of **20** and **21** consist of two crystallographically independent molecules whose structural data are similar, only one is considered for discussion here. The (C_5Me_4R ring centroid)-Y-(C_5Me_4R ring centroid) (R = H, Me) angle in **20**, 127.3°, is smaller than the ones in **21**, **22** and **23** with 135.0°, 132.8° and 134.3° due to the $[(\mu\text{-H})_3BH]^{1-}$ coordination of the ligand plus THF coordination to the metal atom and hence a sterically more crowded Y atom in **20**. The Y-(C_5Me_4R ring centroid) distances in **20**, and **21**, 2.383, 2.377, 2.386 and 2.388 Å are within the range with those observed for **22** and **23**, 2.353, 2.353, 2.375 and 2.363 Å. The Y1-H1 bond distance in **20**, 2.24(2) Å, is significantly shorter than the other two Y-H bond distances Y1-H2 and Y1-H3, 2.43(2) and 2.40(2) Å. By contrast, both Y-H bond distances in **21** are closer, 2.25(2) and 2.30(3) Å. The shortest Y-B distance is observed in **20**, 2.547(2) Å, whereas the Y-B bond distance in **21** is approximately 0.1 Å longer. These Y-B bond distances in the yttrium borohydrides **20** and **21** are, as expected, much smaller than the Y–B bond distances in the yttrium tetraphenylborate complexes, **22** and **23**. The Y-B distance in **22**, 4.34(9) Å, is slightly shorter than the Y-B bond distance in **23**, 4.44(2) Å. This comparison shows that the boron atom in the yttriumborohydrides through the hydrogen atoms has a stronger bond to yttrium than in the corresponding tetraphenylborate complexes. For this reason, an easy displacement of the borohydride ligand was not feasible.

$(C_5Me_4H)_2Sc(BH_4)$, 24, and $(C_5Me_5)_2Sc(Cl)_{0.5}(BH_4)_{0.5}(THF)$, 27. As shown in Figures 4.4 and 4.5, respectively, **24** and **27** contain a $[(\mu\text{-H})_2BH_2]^{1-}$ ligand. The metrical parameters are shown in Table 4.3 along with data for $[(C_5Me_4H)_2Sc][(\mu\text{-Ph})BPh_3]$, **8**,[Ch.3] $[(C_5Me_5)_2Sc][(\mu\text{-}\eta^2\text{:}\eta^1\text{-Ph})BPh_3]$, **17**,[19] $[\{C_5H_3(SiMe_3)_2\}_2Sc][(\mu\text{-H})_2BH_2]$, **28**,[20] and $(C_5Me_4H)_2ScCl(THF)$, **6**.[Ch.3]

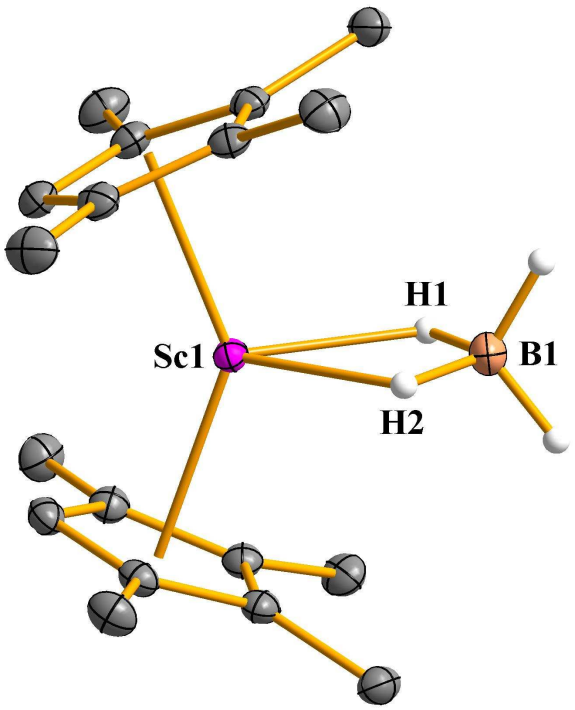

Figure 4.5. Thermal ellipsoid plot of $[(C_5Me_4H)_2Sc][(\mu\text{-}H)_2BH_2]$, **24**, drawn at the 50% probability level. Hydrogen atoms except for H1 and H2 are omitted for clarity.

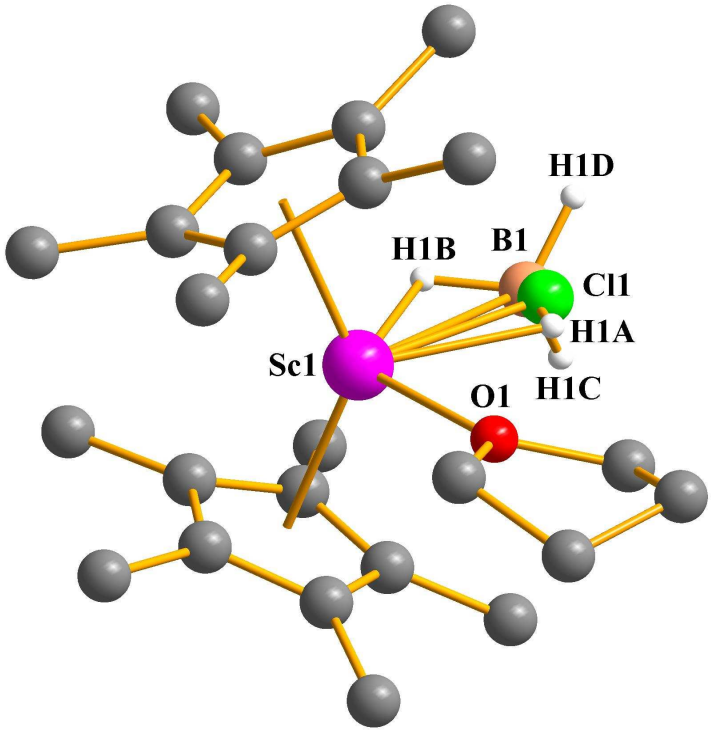

Figure 4.6. Ball-and-Stick plot of **27**, drawn at the 50% probability level, containing the scandium borhydride and chloride complexes, $(C_5Me_5)_2Sc(BH_4)(THF)$, **25**, and $(C_5Me_5)_2Sc(Cl)(THF)$, **26**, in a single crystal. Hydrogen atoms except the hydrogens of the borhydride component are omitted for clarity.

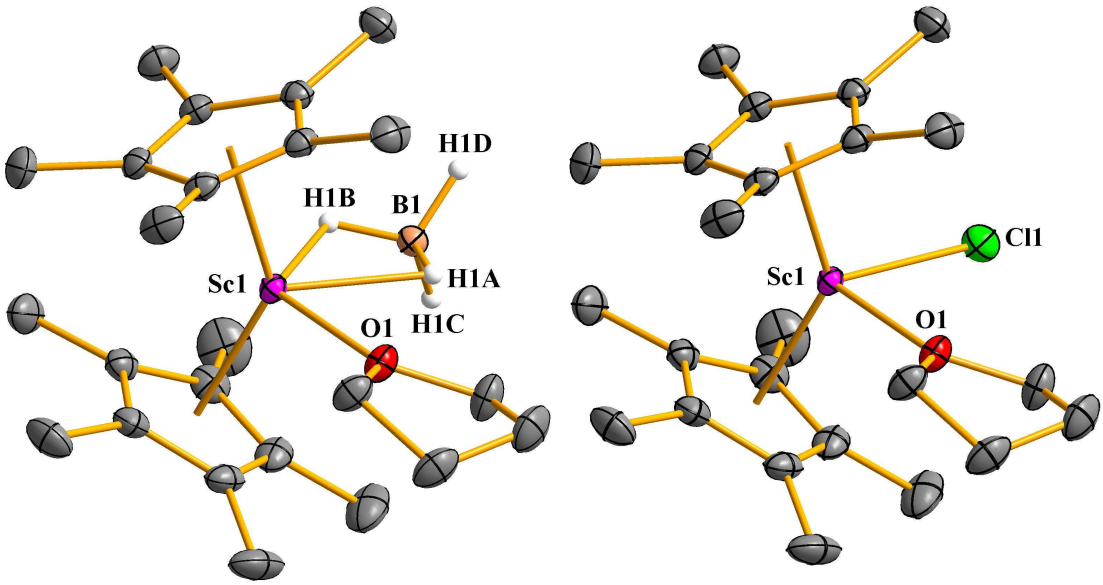

Figure 4.7. Thermal ellipsoid plot of the scandium borohydride and chloride components of **27**, $(C_5Me_5)_2Sc(BH_4)(THF)$, **25**, and $(C_5Me_5)_2Sc(Cl)(THF)$, **26**, drawn at the 50% probability level. Hydrogen atoms except the hydrogens of the borohydride component are omitted for clarity.

The structure of **24** differs from those of **20** and **21** in that it is unsolvated, although the same reaction conditions were chosen. Evidently, **24** prefers to be unsolvated due to its small size. Compared to reported related compounds, the unsolvated analog was not unexpected. The complex $[\{C_5H_3(SiMe_3)_2\}_2Sc][(\mu\text{-}H)_2BH_2]$, **28**, containing sterically less bulky $[C_5H_3(SiMe_3)_2]^-$ units and a borohydride ligand, tends to be unsolvated.[14] The more surprising fact is that $(C_5Me_5)_2Sc(Cl)_{0.5}(BH_4)_{0.5}(THF)$, **27**, bearing the bulkier $(C_5Me_5)^-$ ligand, could be crystallized. Despite the bulkiness of the ligand set as well as the small size of scandium, **27** possesses a coordinated THF molecule.

Furthermore, the structure of **24** differs from that of **20** in that it shows a $[(\mu\text{-}H)_2BH_2]^{1-}$ coordination, while **20** possesses a $[(\mu\text{-}H)_3BH]^{1-}$ ligand in addition to a THF molecule. Also in this case, the small size of scandium could offer an explanation for this difference in both

structures, **20** and **24**, although having used the $(C_5Me_4H)^-$ ligand in both cases. The outcome of this is an eight coordinate complex for scandium, whereas yttrium is ten coordinate.

Table 4.3. Selected Bond Distances (Å) and Angles (deg) for $(C_5Me_4H)_2Sc(BH_4)$, **24**, $[(C_5Me_4H)_2Sc][(\mu\text{-Ph})BPh_3]$, **8**,[Ch.3] $[(C_5Me_5)_2Sc(BH_4)(THF)]$ $[(C_5Me_5)_2Sc(Cl)(THF)]$, **27**, $[(C_5Me_5)_2Sc][(\mu\text{-}\eta^2{:}\eta^1\text{-Ph})]$, **17**,[19] $[\{C_5H_3(SiMe_3)_2\}_2Sc][(\mu\text{-H})_2BH_2]$, **28**,[20] and $(C_5Me_4H)_2ScCl(THF)$, **6**.[Ch.3] The unit cell of **24** and 27, respectively, contains two crystallographically independent molecules, the metrical parameters of which are very similar. Only one is discussed in detail here. For more information see supplementary chapter.

	24	**8**	**27**	**17**	**28**	**6**
Cnt1-Sc1-Cnt2	138.8	139.4	136.5	140.94	136.0	133.0
(Cnt)-Sc(1)-$(H_b)^*$	109.2, 106.0	-	108.4, 95.4	-	110.3, 108.5	-
(Cnt)-Sc(1)-Cl(1)	-	-	106.0, 107.2	-	-	108.4, 106.4
(Cnt)-Sc(1)-B(1)	111.0, 110.1	-	105.3, 103.1	-	112.0, 112.0	-
Sc1-Cnt1	2.139	2.122	2.243	2.1516(10)	2.159	2.222
Sc1-Cnt2	2.146	2.137	2.233	2.1587(9)	2.159	2.219
Sc1-B1	2.5433(11)	6.406	2.556(4)	6.024	2.52(3)	-
Sc1-Cl1	-	-	2.4753(10)	-	-	2.4332(4)
Sc(1)-O(1)	-	-	2.2979(11)	-	-	2.2557(10)
Sc1-$(H_b)^*$	2.066(15), 2.033(15)	-	2.18(3), 2.07(2)	-	2.024(4), 2.024(4)	-
Sc1-C(*p*-phenyl)	-	2.568(2)	-	2.679(2)	-	-

* (H_b) = bridging hydrogen atoms

The structure of **27** reveals that a borohydride ligand is about the same size as a chloride ligand. A comparison of the unit cells of complex **27**, Table 4.1, and complex **6**, Table 3.3,[Ch.3] shows that these are pretty much identical in size. The unit cell of **27** contains two crystallographically independent molecules, the metrical parameters of which are very similar. Only one of the independent molecules is discussed in detail here. The (C_5Me_4R ring centroid)-Sc-(C_5Me_4R ring centroid) (R = H, Me) angle in **27,** 136.5°, is smaller than the ones in **8**, **17** and **24** with 138.8°, 139.4° and 140.94°, respectively. This could be due to a sterically more crowded Sc atom in **27** due to the bulkiness of the $(C_5Me_5)^-$ ligand, the $[(\mu\text{-}H)_2BH_2]^{1-}$ coordination of the borohydride ligand and a chloride coordination, respectively, and a THF coordination to the metal center. The Sc-(C_5Me_4R ring centroid) distances in **24**, 2.139 and 2.146 Å, are somewhat shorter, approximately 0.1 Å, than those observed for **27**, 2.243 and 2.233 Å, but, similar to those observed in **8**, 2.122 and 2.137 Å. In contrast, the Sc-C_5Me_4R ring centroid distances in **27**, 2.243 and 2.233 Å, are still longer than those observed in **17**, 2.1516(10) and 2.1587(9) Å.

The component **25** of **27** shows longer Sc-O and Sc-Cl bond distances, 2.2979(11) and 2.4753(10) Å, as observed in **6**, 2.2557(10) and 2.4332(4) Å. Furthermore, the Sc-C_5Me_4R ring centroid distances in **25**, 2.243 and 2.233 Å, are slightly longer than obtained in **6**, 2.222 and 2.219 Å.

The Sc1-H1A bond distance in **27**, 2.18(3) Å, is significantly longer than the Sc1-H1B bond distance in **27**, 2.07(2) Å, and both of the scandium hydrogen bond distances in **25**, 2.033(15) and 2.066(15) Å. Overall, the scandium hydrogen bond distances in the range of 2.033(15)-2.18(3) Å are shorter compared to the yttrium analogs 2.242-2.432 Å, Table 4.2, but in the same range of 2.03(4) Å as observed in $[\{C_5H_3(SiMe_3)_2\}_2Sc][(\mu\text{-}H)_2BH_2]$, **28**.[20]

The Sc-B bond distances in **24** and **25**, 2.5433(11) and 2.556(4) Å, are longer than in **28**, 2.52(3) Å. Since scandium is bonded over hydride bridges to boron, the Sc-B distances in **24** and **25** are, as expected, much smaller than the Sc–B distances in the respective

tetraphenylborate complexes, **8** and **17**. In these complexes, the scandium atom is far away from the boron center. Interestingly, the Sc–B distance in **8** is, 6.406 Å, thus almost 0.4 Å longer than the Sc-B distance in **17**, 6.024 Å, but both of these show about 2 Å longer metal boron distances than observed in the yttrium tetraphenylborates, **22** and **23**, due to the μ-Ph bridging between M and $[BPh_4]^-$ in **8** and **17** vs a μ-Ph_2 bridging in **22** and **23**. The borohydride ligand is strongly bonded to the metal center in **24** and **25**, overall similar to the yttrium complexes **20** and **21** which raises the assumption of similar reactivity of rare earth borohydride complexes.

Conclusion

Although the borohydride complexes $(C_5Me_4H)_2Y(BH_4)(THF)$, **20** $(C_5Me_5)_2Y(BH_4)(THF)$, **21**, can be made directly from YCl_3, they are not useful precurors in LnZ_2Z'/K reactions like their tetraphenylborate analogs. The polydentate hydride bridges of the borohydride ligands appear to attach to yttrium too strongly to be lost as KZ′ byproducts in the reductive reaction.

The scandium borohydride complexes $(C_5Me_4H)_2Sc(BH_4)$, **24**, and $(C_5Me_5)_2Sc(BH_4)$, **25a**, can also be obtained from a one-pot-synthesis using $ScCl_3$, the potassium salts KC_5Me_4H and KC_5Me_5, respectively, and $NaBH_4$. However, these reactions do not give clean products, in contrast to the alternative synthesis route via scandium tetraphenylborate complexes and $NaBH_4$. The unsolvated structure of $(C_5Me_4H)_2Sc(BH_4)$, **24**, shows a $[(\mu\text{-}H)_2BH_2]^{1-}$ coordination of the borohydride ligand whereas the bigger yttrium captures a tenfold coordination having a $[(\mu\text{-}H)_3BH]^{1-}$ ligand in $(C_5Me_4H)_2Y(BH_4)(THF)$, **20**. Thus, this structurally subtle difference in **24** and **20** shows again how metal size can affect the coordination sphere of the metal centers in complexes. In addition, the structure of $(C_5Me_5)_2Sc(Cl)_{0.5}(BH_4)_{0.5}(THF)$, **27**, proves that a rare earth metallocene chloride and borohydride can cocrystallize in one single crystal.

References

(1) Evans, W. J.; Lee, D. S. *Can. J. Chem.* **2005**, *83*, 375.
(2) Evans, W. J.; Ulibarri, T. A.; Ziller, J. W. *J. Am. Chem. Soc.* **1988**, *110*, 6877.
(3) Evans, W. J.; Allen, N. T.; Ziller, J. W. *J. Am. Chem. Soc.* **2001**, *123*, 7927-7928.
(4) Evans, W. J.; Zucchi, G.; Ziller, J. W. *J. Am. Chem. Soc.* **2003**, *125*, 10-11.
(5) Evans, W. J.; Allen, N. T.; Ziller, J. W. *Angew. Chem., Int. Ed.* **2002**, *41*, 359.
(6) Evans, W. J.; Lee, D. S.; Rego, D. B.; Perotti, J. M.; Kozimor, S. A.; Moore, E. K.; Ziller, J. W. *J. Am. Chem. Soc.* **2004**, *126*, 14516.
(7) Evans, W. J.; Lee, D. S.; Lie, C.; Ziller, J. W. *Angew. Chem., Int. Ed.* **2004**, *43*, 5517-5519.
(8) Evans, W. J.; Lee, D. S.; Ziller, J. W. *J. Am. Chem. Soc.* **2004**, *126*, 454-455.
(9) Evans, W. J.; Perotti, J. M.; Kozimor, S. A.; Champagne, T. M.; Davis, B. L.; Nyce, G. W.; Fujimoto, C. H.; Clark, R. D.; Johnston, M. A.; Ziller, J. W. *Organometallics* **2005**, *24*, 3916-3931.
(10) Evans, W. J.; Gonzales, S. L.; Ziller, J. W. *J. Am. Chem. Soc.* **1991**, *113*, 7423.
(11) Evans, W. J.; Nyce, G. W.; Clark, R. D.; Doedens, R. J.; Ziller, J. W. *Angew. Chem. Int. Ed.* **1999**, *38*, 1801.
(12) Evans, W. J.; Davis, B. L.; Ziller, J. W. *Inorg. Chem.* **2001**, *40*, 6341-6348.
(13) Evans, W. J.; Davis, B. L.; Champagne, T. M.; Ziller, J. W. *Proc. Natl. Acad. Sci. U. S. A.* **2006**, *103*, 12678.
(14) Evans, W. J.; Rego, D. B.; Ziller, J. W. *Inorg. Chem.* **2006**, *45*, 10790.
(15) Lorenz, S. E.; Schmiege, B. M.; Lee, D. S.; Ziller, J. W.; Evans, W. J. *Inorg. Chem.* **2010**, *49*, 6655-6663.
(16) Evans, W. J.; Lee, D. S.; Johnston, M. A.; Ziller, J. W. *Organometallics* **2005**, *24*, 6393-6397.
(17) Schumann, H.; Keitsch, M. R.; Demtschuk, J.; Muehle, S. *Z. Anorg. Allg. Chem.* **1998**, *624*, 1811.
(18) Evans, W. J.; Kozimor, S. A.; Ziller, J. W.; Kaltsoyannis, N. *J. Am. Chem. Soc.* **2004**, *126*, 14533-14547.
(19) Bouwkamp, M. W.; Budzelaar, P. H. M.; Gercama, J.; Morales, I. del H.; de Wolf, J.; Meetsma, A.; Trojanov, S. I.; Teuben, J. H.; Hessen, B. *J. Am. Chem. Soc.* **2005**, *127*, 14310-14319.
(20) Lappert, M. F.; Singh, A.; Atwood, J. L.; Hunter, W. E. *J. Chem. Soc., Chem. Comm.* **1983**, 206-207.

Chapter 5

Scandium Metallocene Borane Chemistry:

Isolation of 9-BBN Coordination Complexes,

$(C_5Me_4R)_2Sc(\mu\text{-}H)_2BC_8H_{14}$ (R = H, Me) and $(C_5Me_4H)_2Sc(\mu\text{-}O)BC_8H_{14}$

Introduction

In general, little is known about the alkylborane chemistry of rare earth metallocenes,.[1-6] Recent investigations have been directed to yttrium metallocene borane complexes, which revealed that yttrium allyl compounds are useful precursors for the formation of 9-BBN (9-borabicyclo[3.3.1]nonane) containing borane substituted allyl complexes and borohydride complexes, respectively. Both of these components, namely $(C_5Me_4H)_2Sc[\eta^3\text{-}C_3H_4(BC_8H_{14})]$ and $(C_5Me_4H)_2Sc(\mu\text{-}H)_2BC_8H_{14}$, cocrystallized in one single crystal.[6] The yttrium allyl complex, $(C_5Me_5)_2Y(\eta^3\text{-}C_3H_5)$, was used as it enables easy access to M-C bond reactivity.[6] In this chapter, the goal was to make the analogous scandium borohydride complex $(C_5Me_5)_2Sc(\mu\text{-}H)_2BC_8H_{14}$, **29**, via the same synthetic route. After its successful isolation, the ligand has been changed from $(C_5Me_5)^-$ to $(C_5Me_4H)^-$ to determine whether the analogous complex, $(C_5Me_4H)_2Sc(\mu\text{-}H)_2BC_8H_{14}$, **30**, can be synthesized since ligand changes sometimes affect the observed reactivity. Oxygen contamination of **30** provided access to a scandium 9-BBN oxide, $(C_5Me_4H)_2Sc(\mu\text{-}O)BC_8H_{14}$, **31**, which features an unusual metallocene containing a M-O-BBN unit.

Experimental

The syntheses and manipulations described below were conducted under argon or nitrogen with rigorous exclusion of air and water using glovebox, vacuum line and Schlenk

techniques. Solvents were dried over columns containing Q-5 and molecular sieves. NMR solvents were dried over Na/K alloy, degassed, and vacuum transferred prior to use. Allylmagnesium chloride (2.0 M in THF) and 1,4-dioxane were purchased from Aldrich and used as received. 1,2,3,4-tetramethylcyclopentadiene ($C_5Me_4H_2$) was purchased from Aldrich, distilled onto 4 Å molecular sieves and degassed by three freeze-pump-thaw cycles prior to use. Potassium bis(trimethylsilyl)amide (Aldrich) was dissolved in toluene, centrifuged and filtered to remove insolubles and dried under reduced pressure. KC_5Me_4H was prepared as described for KC_5Me_5.[7] ^{1}H and ^{13}C NMR spectra were recorded on Bruker GN500 or CRYO500 MHz spectrometers operating at 126 MHz for ^{13}C. ^{11}B NMR spectra were recorded on a Bruker Avance 600 spectrometer operating at 192.5 MHz and referenced to external $BF_3{\cdot}OEt$. ^{45}Sc NMR spectra were recorded on a Bruker Avance 600 spectrometer operating at 145 MHz and referenced to $[Sc(H_2O)_6]^{3+}$ in D_2O. IR samples were prepared as KBr pellets, and the spectra were obtained on a Varian 1000 FT-IR system. Elemental analyses were performed using a PerkinElmer Series II 2400 CHNS elemental analyzer. $(C_5Me_5)_2Sc(\eta^3\text{-}C_3H_5)$, **32**, was prepared by another route compared to the literature procedure,[8] which is explained in Chapter 8.

$(C_5Me_5)_2Sc(\mu\text{-}H)_2BC_8H_{14}$, 29. In a nitrogen-filled glove box free of coordinating solvents, a yellow solution of $(C_5Me_5)_2Sc(\eta^3\text{-}C_3H_5)$, **32**, (0.169 g, 0.47 mmol) in 15 ml of toluene was added to 9-BBN dimer (0.116 g, 0.47 mmol). After the mixture was stirred for 24 h, the yellow solution was evaporated to dryness to yield a yellow tacky solid. This was washed with hexane and evaporated to dryness to yield a still tacky yellow residue (0.17 g, 82%). Yellow crystals suitable for X-ray analysis were grown from a concentrated hexane solution of **29** at −35 °C over the course of 48 h. ^{1}H NMR (500 MHz, benzene-d_6): δ 2.40-1.51 [m, α- β- and γ-H of (BC_8H_{14})], 1.99 (s, 1H, C_5Me_5), 1.57 (s, 30H, C_5Me_5), 1.04 {b, 2H, μ-H of $[(\mu\text{-}H)_2BC_8H_{14}]$}.

$(C_5Me_4H)_2Sc(\mu\text{-}H)_2BC_8H_{14}$, 30. In a nitrogen-filled glove box free of coordinating solvents, a yellow solution of $(C_5Me_4H)_2Sc(\eta^3\text{-}C_3H_5)$, 7, (0.14 g, 0.43 mmol) in 15 ml of toluene was added to 9-BBN dimer (0.10 g, 0.41 mmol). After the mixture was stirred for 24 h, the pale yellow solution was evaporated to dryness to yield a yellow tacky solid. This was washed with hexane and evaporated to dryness to yield a pale yellow powder (0.15 g, 84%). Crystals suitable for X-ray analysis were grown from a concentrated hexane solution of **30** at −35 °C over the course of 24 h. ^{1}H NMR (500 MHz, benzene-d_6): δ 6.49 (s, 2H, C_5Me_4H), 2.41 (m, 2H of $\{BC_8H_{14}\}$), 2.28 (m, 4H of $\{BC_8H_{14}\}$), 2.17 (m, 4H of $\{BC_8H_{14}\}$), 1.98 (s, 12H, C_5Me_4H), 1.56 (s, 12H, C_5Me_4H), 0.76 (br d, 2H, μ-H of $\{(\mu\text{-}H)_2BC_8H_{14})\}$). ^{13}C NMR (126 MHz, benzene-d_6): δ 125.5 (C_5Me_4H), 120.8 (C_5Me_4H), 116.9 (C_5Me_4H), 34.9 (BC_8H_{14}), 25.9 (BC_8H_{14}), 12.4 (C_5Me_4H), 12.2 (C_5Me_4H). $^{11}B\{^1H\}$ NMR (192.5 MHz, benzene-d_6): δ 7.02. ^{45}Sc NMR (145 MHz, benzene-d_6): δ 128.64. IR: 2978m, 2911s, 2870s, 2827s, 2728w, 2043w, 1987w, 1961m, 1911s, 1867w, 1821m, 1769w, 1678w, 1481w, 1445m, 1385m, 1361s, 1323s, 1280w, 1204w, 1149w, 1108w, 1038w, 1023w, 974w, 929w, 918w, 827w, 813m, 796m, 613w cm^{-1}. Anal. Calcd for $C_{42}H_{46}BSc$: C, 76.10; H, 10.32. Found: C, 75.65; H, 10.70.

$(C_5Me_4H)_2Sc(\mu\text{-}O)BC_8H_{14}$, 31. Oxygen contamination of **30** provided **31**. Colorless crystals suitable for X-ray analysis were grown from a concentrated benzene-d_6 solution of **31** at room temperature over the course of three weeks.

X-ray Crystallographic Data. X-Ray data collection parameters of **29, 30** and **31** are given in Table 5.1. Details for X-ray data collection, structure, solution and refinement are given in the Appendix.

Table 5.1. X-ray Data Collection Parameters for $(C_5Me_5)_2Sc(\mu\text{-}H)_2BC_8H_{14}$, **29**, $(C_5Me_4H)_2Sc(\mu\text{-}H)_2BC_8H_{14}$, **30**, and $(C_5Me_4H)_2Sc(\mu\text{-}O)BC_8H_{14}$ **31**.

	29	**30**	**31**
formula	C_{28} H_{46} B Sc	C_{26} H_{42} B Sc	C_{26} H_{40} B O Sc
fw	438.42	410.37	424.35
space group	$P\bar{1}$	$P\bar{1}$	$P2_1/c$
crystal system	Triclinic	Triclinic	Monoclinic
a (Å)	9.1910(5)	10.7158(4)	13.7353(10)
b (Å)	15.1368(8)	13.6441(5)	17.9060(12)
c (Å)	19.9838(11)	17.6253(6)	10.2837(7)
α (deg)	69.3342(6)	102.9444(5)	90
β (deg)	77.1285(7)	99.0856(5)	106.2385(9)
γ (deg)	87.1072(7)	104.3286(5)	90
V (Å^3)	2534.7(2)	2370.41(15)	2428.3(3)
Z	4	4	4
ρ_{calcd} (Mg/m^3)	1.149	1.150	1.161
μ (mm^{-1})	0.303	0.319	0.317
temp (K)	143(2)	88(2)	148(2)
R1 [I > 2σ(I)][a]	0.0463	0.0468	0.0355
wR2 (all data)[a]	0.1225	0.1210	0.0974

[a] Definitions: $wR2 = [\Sigma[w(F_o^2-F_c^2)^2] / \Sigma[w(F_o^2)^2]]^{1/2}$, $R1 = \Sigma||F_o|-|F_c|| / \Sigma|F_o|$.

Results and Discussion

$(C_5Me_5)_2Sc(\eta^3\text{-}C_3H_5)$, **32**, reacts with 1 eq of 9-BBN in toluene during 24 h to give a yellow powder of $(C_5Me_5)_2Sc(\mu\text{-}H)_2BC_8H_{14}$, **29**, in 82% yield, eq 5.1. The analogous reaction with $(C_5Me_4H)_2Sc(\eta^3\text{-}C_3H_5)$, **7**, gives after 24 h $(C_5Me_4H)_2Sc(\mu\text{-}H)_2BC_8H_{14}$, **30** in 84% yield, eq 5.1. Although the topology of the complexes **29** and **30** is the same, the structures are not isomorphous. The difference is that in **29** two conformers of BBN exist, while complex **30** shows only conformer. This is discussed in the structural section.

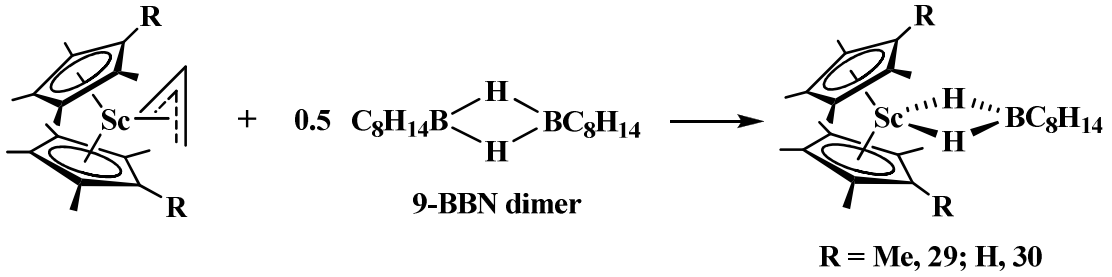

(5.1)

One conceivable route to the generation of complexes **29** and **30** is formulated in eq 5.2 and 5.3 on the basis of the proposed mechanism to form the analogous compound $(C_5Me_5)_2Y(\mu\text{-}H)_2BC_8H_{14}$, **33**.[6] The first step comprises a regular addition of 9-BBN to an olefin, eq 5.2.[9] This is remarkable since according to this mechanism the allyl group would need to adopt an η^1-coordination mode, $(C_5Me_4R)_2Sc(\eta^1\text{-}CH_2CH{=}CH_2)$ (R = H, Me), complex **I**. This means that the η^1-allyl reactivity in this scandium metallocene (and yttrium metallocene, respectively) arises from the olefin and not, as typical for the rare earth metallocenes, from the M-C sigma bond. Furthermore, it is postulated that the resulting alkyl complex, **II**, could β-hydrogen eliminate to produce a 9-BBN substituted olefin as a leaving group and a scandium hydride metallocene, $[(C_5Me_4R)_2ScH]$ (R = H, Me[8]). This hydride complex could have been trapped by another 9-BBN molecule to give the observed products **31** and **32**, eq 5.3.

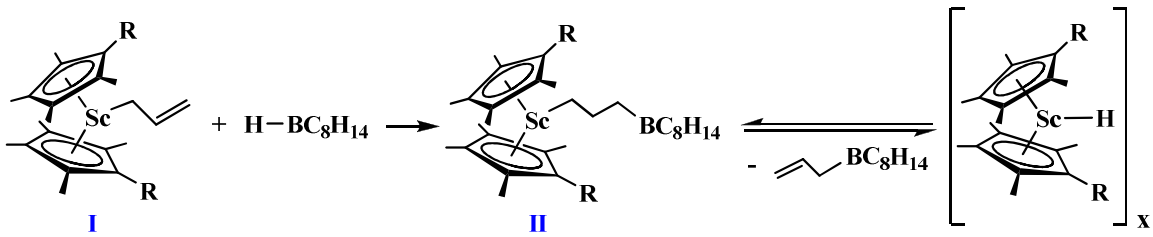

(5.2)

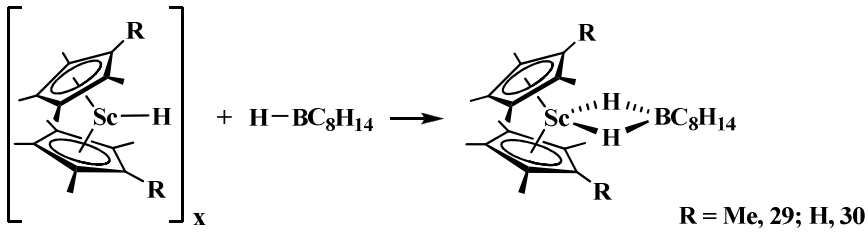

(5.3)

Structural Studies

$(C_5Me_5)_2Sc(\mu\text{-}H)_2BC_8H_{14}$, 29 and $(C_5Me_4H)_2Sc(\mu\text{-}H)_2BC_8H_{14}$, 30. Crystals of **29** and **30** suitable for X-ray diffraction were obtained from hexane solutions. As shown in Figures 5.1 and 5.2, respectively, **29** and **30** have $[(\mu\text{-}H)_2BBN]^{1-}$ coordination. The metrical parameters are shown in Table 5.2 along with data for $(C_5Me_4H)_2Sc(\mu\text{-}O)BC_8H_{14}$, **31**, $(C_5Me_5)_2Y(\mu\text{-}H)_2(BC_8H_{14})$, **33**,[6] and $[(C_5H_5)_2Zr(\mu\text{-}H)(\mu\text{-}O)(BC_8H_{14})]_2$, **34.**[17]

The unit cell of **29** differs from **30** in that each independent molecule possesses a distinguishable BBN conformer, Figure 5.3. The reported complex $RuH[(\mu\text{-}H)_2BBN](\eta^2\text{-}H_2)(PCy_3)_2$ shows a disorder on a carbon for which reason it has been resolved as two possible conformations. Both of these would be structurally similar to the observed two conformations in **29**.[10]

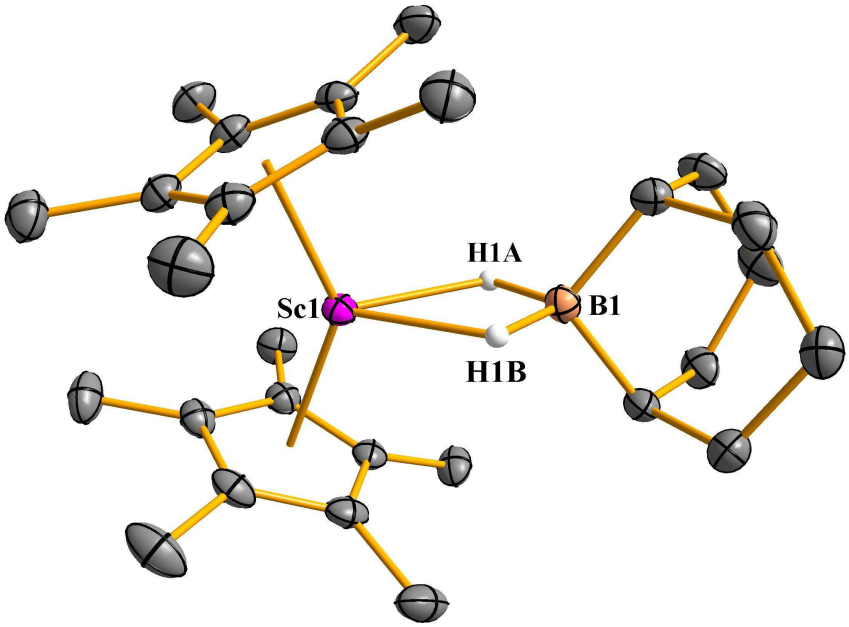

Figure 5.1. Thermal ellipsoid plot of $(C_5Me_5)_2Sc(\mu\text{-}H)_2BC_8H_{14}$, **29**, drawn at the 50% probability level. Hydrogen atoms except the bridging hydrogens of the BBN component are omitted for clarity.

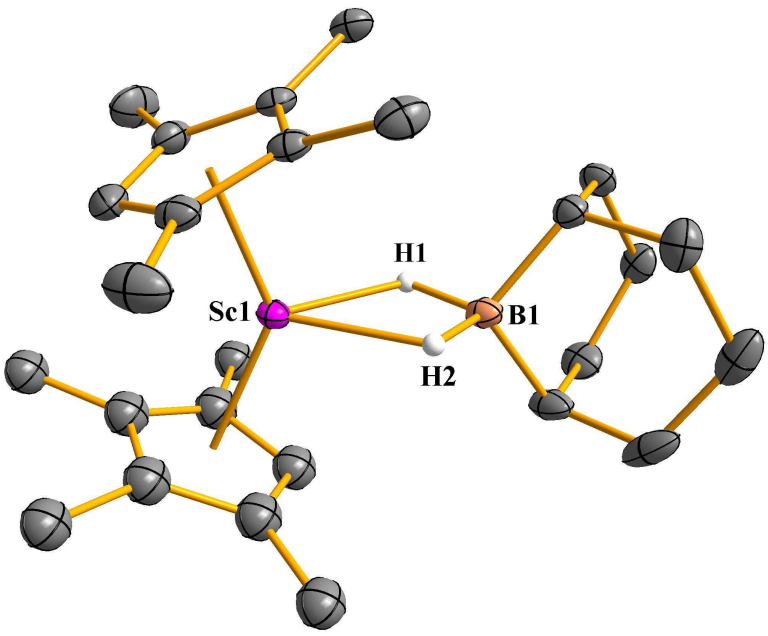

Figure 5.2. Thermal ellipsoid plot of $(C_5Me_4H)_2Sc(\mu\text{-}H)_2BC_8H_{14}$, **30**, drawn at the 50% probability level. Hydrogen atoms except the bridging hydrogens of the BBN component are omitted for clarity.

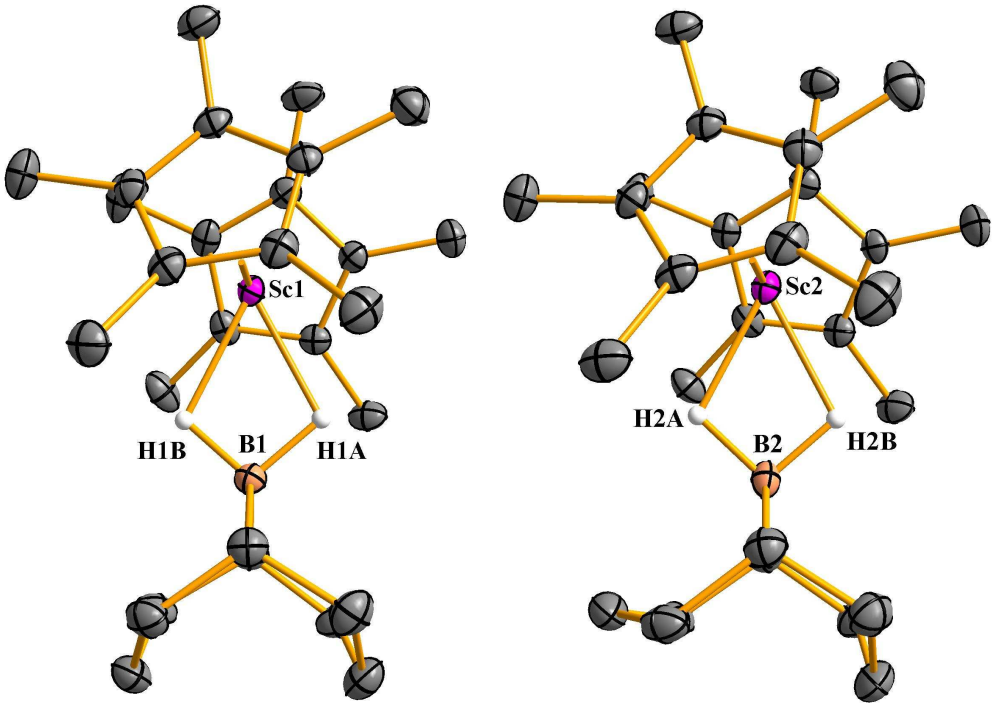

Figure 5.3. Thermal ellipsoid plot of the two crystallographically independent molecules in $(C_5Me_5)_2Sc(\mu\text{-}H)_2BC_8H_{14}$, **29**, drawn at the 50% probability level, showing two distinguishable BBN conformers. Hydrogen atoms except the bridging hydrogen atoms of the BBN component are omitted for clarity.

Table 5.1. Selected Bond Distances (Å) and Angles (deg) for $(C_5Me_5)_2Sc(\mu\text{-}H)_2BC_8H_{14}$, **29**, $(C_5Me_4H)_2Sc(\mu\text{-}H)_2BC_8H_{14}$, **30**, $(C_5Me_4H)_2Sc(\mu\text{-}O)BC_8H_{14}$, **31**, $(C_5Me_5)_2Y(\mu\text{-}H)_2BC_8H_{14}$, **33**,[6] and $[(C_5H_5)_2Zr(\mu\text{-}H)(\mu\text{-}O)(BC_8H_{14})]_2$, **34.**[17] The unit cells of **29** and **30** contain two crystallographically independent molecules, the metrical parameters of which are very similar. Only one is discussed in detail here. For more information see in the Appendix.

	29	**30**	**31**	**33**	**34**
M	**Sc**	**Sc**	**Sc**	**Y**	**Zr**
Cnt1-M(1)-Cnt2	138.5	136.3	137.3	137.1	126.1
Cnt1- M(1)-O(1)	-	-	111.3	-	116.1
Cnt2- M(1)-O(1)	-	-	111.4	-	115.4
(Cnt)-M(1)-O(1)'	-	-	-	-	104.5, 104.4
Cnt1- M(1)-B(1)	111.2	113.0	-	111.0	107.3
Cnt2- M(1)-B(1)	110.3		-	112.7	106.3
Cnt1-M(1)-$(H_b)^*$	104.4, 112.1	111.3, 107.8	-	116.2, 103.5	96.0
M(1)-Cnt1	2.189	2.159	2.137	2.334	2.250
M(1)-Cnt2	2.185	2.152	2.145	2.354	2.261
M(1)-O(1)	-	-	1.9390(11)	-	2.1182(10)
M(1)-O(1)'			-		2.1352(10)
O(1)-B(1)	-	-	1.323(2)	-	1.485(2)
M(1)-$(H_b)^*$	2.05(2), 2.03(2)	2.00(2), 2.02(2)	-	2.152(5), 2.279(5)	1.959(16)
M(1)-B(1)	2.626(2)	2.592(2)	-	2.767(52)	2.654(2)
B(1)-$(H_b)^*$	1.269(0), 1.222(0)	1.23(2), 1.24(2)	-	1.158(5), 1.307(5)	1.309(16)
B(1)-$(C_b)^\#$	1.621(3), 1.609(3)	1.612(3), 1.616(3)	1.590(2), 1.591(2)	1.621(7), 1.616(9)	1.622(2), 1.620(2)

* (H_b) = bridging hydrogen atoms
$^\#$ (C_b) = BBN carbon atoms bridging to boron atom

The (C_5Me_4R ring centroid)-M-(C_5Me_4R ring centroid) (R = H, Me) angle in **29**, 138.5°, is slightly larger than the angles observed in **30**, **31** and **33** with 136.3°, 137.3° and 137.1°. The M-(C_5Me_4H ring centroid) distances in **29**, 2.189 and 2.185 Å, **30**, 2.159 and 2.152 Å, **31**, 2.137 and 2.145 Å, are shorter than in **33**, 2.334 and 2.354 Å, which is consistent with the differences in ionic radii of these two metals according to Shannon. The Sc-H bond distances in **29**, 2.03(2) and 2.05(2) Å, are very similar to those in **30**, 2.00(2) and 2.02(2) Å, and are also consistent with the Sc-H bond distances observed in **24**, 2.033(15) and 2.066(15) Å, and **28**, 2.03(4) Å. As a result of the small size of scandium, expectedly, both hydride bridges in **29** and **30** are shorter than those in **33**, 2.152(5) and 2.279(5) Å. In this context, it is noticeable that the metal hydrogen bond lengths are in **29** and **30** more similar than in **33**. The Sc-B distance in **29**, 2.626(2) Å, is longer than the Sc-B bond distances in **30**, **31** and **27**, 2.592(2), 2.5433(11) and 2.556(4) Å, and shorter than the Y-B bond distance in **33**, 2.767(52) Å.

$(C_5Me_4H)_2Sc(\mu\text{-}O)BC_8H_{14}$, 31. A suitable crystal of **31** for X-ray diffraction was obtained from benzene solution.

The (C_5Me_4R ring centroid) - M - (C_5Me_4R ring centroid) (R = H, Me) angle in **31**, 177.35(11)°, is almost linear. The coordination number of scandium is seven in complex **31**, for which no comparable seven coordinate scandium metallocene possessing a Sc-O bond is known. The Sc-O bond distance in **31** is 1.9390(11) Å, that is expectedly shorter than the Sc-O bond distances observed in eight-coordinate scandium metallocenes: 2.167(3) and 2.176(3) Å (2.172 Å av.) in $(C_5Me_5)_2Sc(O_2C)C_6H_4CH_3$,[11] 2.067(2) and 2.331(2) Å in $(C_5H_5)Co(\mu^2,\eta^1,\eta^1\text{-}CO)(=C(CH_3)OSc(C_5Me_5)_2$,[12] 2.216(3) Å in $(C_5H_5)_2Sc[Si(SiMe_3)_3](THF)$,[13] 2.2964(14) and 2.2652(14) Å in $[(C_5Me_5)_2Sc(THF)_2][BPh_4]$,[14] or 2.2557(10) Å in **6**.[Ch.3] However, the comparison of the Sc-O bond distance of 1.9390(11) Å in **31** with Sc-O bond distances in seven-coordinate scandium complexes which do not feature a metallocene unit reveals that it is even slightly shorter than in [$ScCl_2$(18-crown-

6)](SbCl$_6$) with 2.190(5)-2.229(5) Å, and in [Sc(dapsc)(H$_2$O)$_2$][NO$_3$]$_2$[OH] with an average Sc-O bond distance of 2.110 Å [dapse = 2.6-diacetylpyridinebis(semi-carbazone). When complex **31** is compared to six-coordinate scandium complexes the Sc-O bond distance is slightly longer than for instance found in alkoxides: 1.889(5), 1.854(5) and 1.865(5) Å in [Sc(OC$_6$H$_2$Me-$_4$-Bu$^t_2$-2,6]$_3$,[15] or about the same length as in salicylaldiminato-N,O-scandium complexes with 1.985(3) and 1.920(3) Å.[16]

There are no rare earth metallocene oxo borabicyclononanes known to compare with **31**. The only transition metal oxo borabicyclononane is [(C$_5$H$_5$)$_2$Zr(μ-H)(μ-O)(BC$_8$H$_{14}$)]$_2$, **34**,[17] which is in fact an organohydroborate dimer compared to **31**. The Sc-O bond distance is 1.9390(11) Å in **31**, whereas the Zr-O bond distances are 2.1182(10) and 2.1352(10) Å, respectively, in **34**. Two organohydroborate ligands link two (C$_5$Me$_5$)$_2$Zr units in a Zr(μ-H)(μ-O)B mode that causes a nonlinear Zr-O-B angle of 93.19(8)° vs 177.35(11)° found in **31**. The B-O distance of 1.485(2) Å is in **34** much longer than the observed 1.323(2) Å in **31**.

The B-C bond distances in the compounds **29**, **30**, **31**, **33** and **34** lie within the range 1.590(2) to 1.622(2) Å.

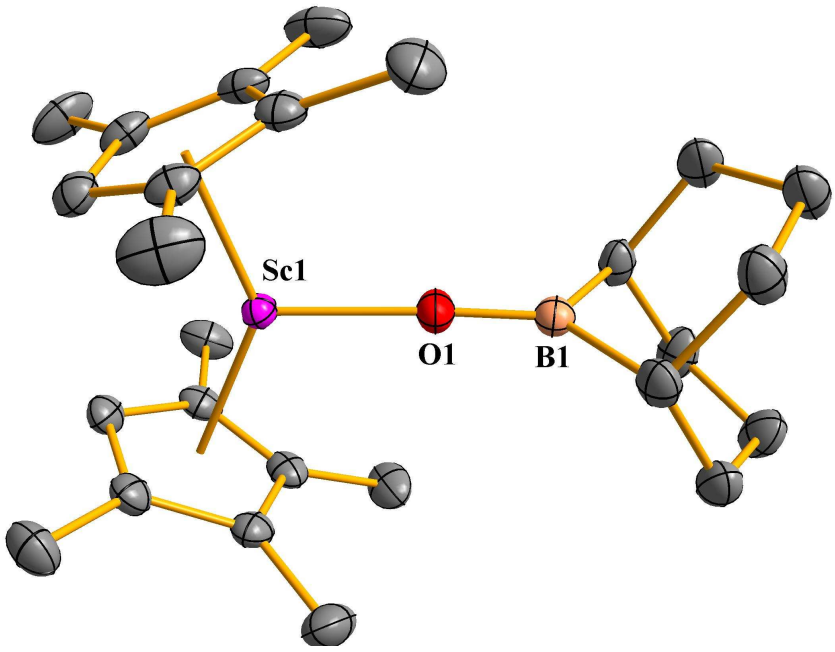

Figure 5.4. Thermal ellipsoid plot of (C$_5$Me$_4$H)$_2$Sc(μ-O)BC$_8$H$_{14}$, **31**, drawn at the 50% probability level. Hydrogen atoms are omitted for clarity.

Conclusion

The borohydride complexes $(C_5Me_5)_2Sc(\mu\text{-}H)_2BC_8H_{14}$, **29** and $(C_5Me_4H)_2Sc(\mu\text{-}H)_2BC_8H_{14}$, **30**, were synthesized from reactions of $(C_5Me_4R)_2Sc(\eta^3\text{-}C_3H_5)$ (R = H, **7**; Me, **32**) and 9-BBN. Switching the $(C_5Me_5)^-$ ligand, which have been shown to be reactive towards 9-BBN,[6] to a $(C_5Me_4H)^-$ ligand, has evidently not limited its reactivity. Complex **29** shows two distinguishable conformers of the BBN ligand, while **30** and **31** have only one type of BBN conformer. Oxygen contamination of **30** provided an unusual monomeric metallocene organoborane oxide $(C_5Me_4H)_2Sc(\mu\text{-}O)BC_8H_{14}$, **31**. This is the first scandium metallocene complex with a seven coordinate scandium containing an $OBBN^-$ ligand. The Sc-O bond distance is short with 1.9390(11) Å.

References

(1) Chen, X.; Lim, S.; Plecˇnik, C. E.; Liu, S.; Du, B.; Meyers, E. A.; Shore, S. G. *Inorg. Chem.* **2004**, *43*, 692.
(2) Galler, J. L.; Goodchild, S.; Gould, J.; McDonald, R.; Sella, A. *Polyhedron* **2004**, *23*, 253.
(3) Chen, X.; Lim, S.; Plecˇnik, C. E.; Liu, S.; Du, B.; Meyers, E. A.; Shore, S. G. *Inorg. Chem.* **2005**, *44*, 6052.
(4) Evans, W. J.; Perotti, J. M.; Ziller, J. W. *Inorg. Chem.* **2005**, *44*, 5820.
(5) Shen, H.; Chan, H.-S.; Xie, Z. *Organometallics* **2006**, *25*, 2617.
(6) Evans, W. J.; Lorenz, S. E.; Ziller, J. W. *Chem. Comm.* **2007**, 4662-4664.
(7) Evans, W. J.; Kozimor, S. A.; Ziller, J. W.; Kaltsoyannis, N. *J. Am. Chem. Soc.* **2004**, *126*, 14533-14547.
(8) Thompson, M. E.; Baxter, S. M.; Bulls, A. R.; Burger, B. J.; Nolan, M. C.; Santasiero, B. D.; Schaefer, W. P.; Bercaw, J. E. *J. Am. Chem. Soc.* **1987**, *109*, 203-219.
(9) Pelter, A.; Smith, K.; Brown, H. C. *Borane Reagents* **1988**, Academic Press: New York.
(10) Lachaize, S.; Essalah, K.; Montiel-Palma, V.; Vendier, L.; Chaudret, B.; Barthelat, J.-C.; Sabo-Etienne, S. *Organometallics* **2005**, *24*, 2935-2943.
(11) St. Clair, M. A.; Santarsiero, B. D. *Acta Cryst. Sect. C* **1989**, *45*, 850-852.
(12) St. Clair, M. A.; Santarsiero, B. D.; Bercaw. J. E. *Organometallics* **1989**, *8*, 17-22.
(13) Campion, B. K.; Heyn, R. H.; Tilley, T. D. *Organometallics* **1993**, *12*, 2584-2590.
(14) Bouwkamp, M. W.; Budzelaar, P. H. M.; Gercama, J.; Morales, I. Del H.; de Wolf, J.; Meetsma, A.; Trojanov, S. I.; Teuben, J. H.; Hessen, B. *J. Am. Chem. Soc.* **2005**, *127*, 14310-14319.
(15) Hitchcock, P. B.; Lappert, M. F.; Singh. A. *Chem. Comm.* **1983**, 1499-1501.
(16) Emslie, D. J. H.; Piers, W. E.; Parvez, M.; McDonald, R. *Organometallics* **2002**, *21*, 4226-4240.
(17) Chung, J.-H.; Shore, S. G. *Bull. Korean Chem. Soc.* **2005**, *26*, 707.

Chapter 6

Synthesis and Structure of the Elusive Monohapto Tetramethylcyclopentadienyl Metallocene Complex (η^5-$C_5Me_4H)_2Sc(\eta^1$-$C_5Me_4H)$

Introduction

One of the unusual developments in organometallic metallocene chemistry in recent years has been the isolation of a series of sterically crowded complexes containing three pentahapto pentamethylcyclopentadienyl rings: (η^5-$C_5Me_5)_3M$.[1-6] Since the cone angle of (η^5-$C_5Me_5)^{1-}$ had previously been estimated to be approximately 142°,[7] the existence of these complexes was not thought to be possible. Isolation of (η^5-$C_5Me_5)_3M$ complexes as well as the more crowded (η^5-$C_5Me_5)_3MX$, (η^5-$C_5Me_5)_3ML$, and (η^5-$C_5Me_5)_3ML_2$ species (X = F,[8] Cl,[8] Me,[9] H;[10] L = CO,[11] N_2,[12] RNC,[13] RCN[13,14]), where M = lanthanide metals, yttrium, thorium, and uranium, showed that the cone angle for (η^5-$C_5Me_5)^{1-}$ could be reduced to 120° by moving the ligand further away from the metal. In each of these complexes, the M–C(η^5-C_5Me_5) distances are approximately 0.1 Å or more longer than any previously observed analogous distances.[15]

Associated with the long distances in these tris(pentamethylcyclopentadienyl) complexes was unusual reactivity of the normally inert ancillary (η^5-$C_5Me_5)^{1-}$ ligands. For example, (η^5-$C_5Me_5)_3Sm$ was found to ring open THF,[16] polymerize ethylene,[6] undergo insertion reactivity with CO,[2] and react by sigma bond metathesis with dihydrogen,[6] Scheme 6.1. None of these reactions had previously been observed with the (η^5-$C_5Me_5)^{1-}$ ligands, but they were common with alkyl lanthanides.[17]

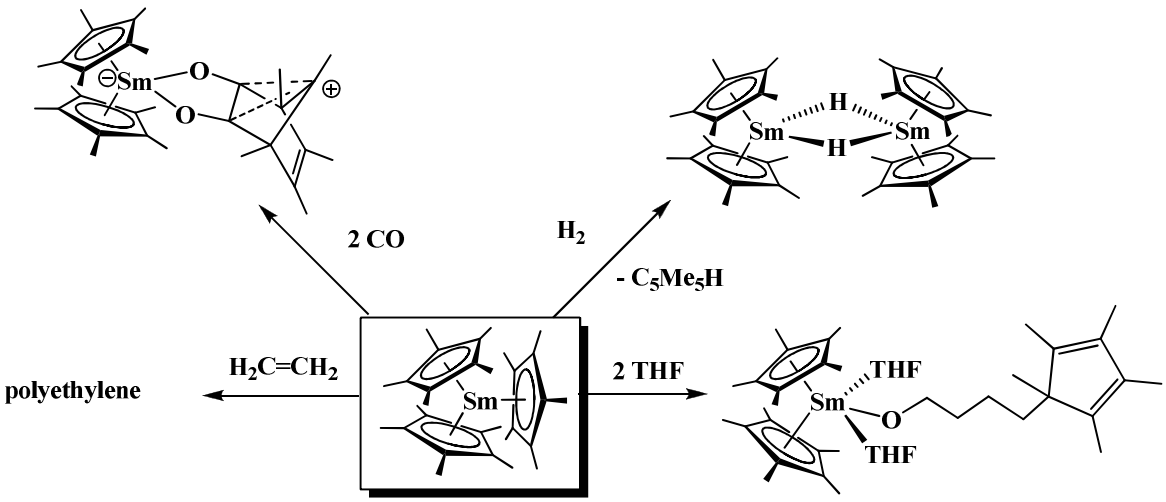

Scheme 6.1. Some examples of high reactivity of $(C_5Me_5)_3Sm$ towards various substrates.

This led to the speculation that $(\eta^5\text{-}C_5Me_5)_3M$ complexes could have access to a monohapto form, $(\eta^5\text{-}C_5Me_5)_2M(\eta^1\text{-}C_5Me_5)$, that engaged in these alkyl-like reactions, eq 6.1. Flexibility in the hapticity of cyclopentadienyl ligands is well known,[18] but it was unclear if such an η^5 to η^1 transformation could occur in these crowded $(\eta^5\text{-}C_5Me_5)_3M$ complexes.

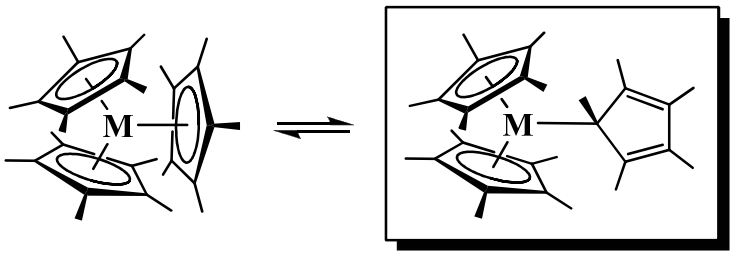

(6.1)

Numerous efforts have been made since $(\eta^5\text{-}C_5Me_5)_3Sm$ was first discovered[4] to obtain spectroscopic evidence on the existence of a $(\eta^5\text{-}C_5Me_5)_2M(\eta^1\text{-}C_5Me_5)$ complex.[19] No evidence was obtained by low temperature spectroscopy and reactions with bases designed to trap a $(\eta^5\text{-}C_5Me_5)_2M(\eta^1\text{-}C_5Me_5)L$ complex suitable for crystallization. This led to a new type of reaction for the $(\eta^5\text{-}C_5Me_5)_3M$ complexes, a reduction reaction called sterically induced reduction (SIR).[20] Base adducts were eventually isolated, namely $(\eta^5\text{-}C_5Me_5)_3ML$[11,12,13] and $(\eta^5\text{-}C_5Me_5)_3ML_2$,[13,14] but the cyclopentadienyl rings in these complexes were found to bind in

a pentahapto mode in the solid state. Hence, even in the presence of a base, there was no evidence for the (η^1-C_5Me_5) coordination that would lead to alkyl-like reactivity.

This chapter describes the first structurally characterizable example of an (η^5-C_5R_5)$_2$M(η^1-C_5R_5) complex. The discovery arose from investigations of the $(C_5Me_4H)^{1-}$ chemistry of Sc^{3+} designed to make the first reduced dinitrogen complex of scandium.[21] The $(C_5Me_4H)^{1-}$ ligand was chosen instead of $(C_5Me_5)^{1-}$ due to the small size of scandium. The synthesis of the dinitrogen complex, $[(C_5Me_4H)_2Sc]_2(\mu\text{-}\eta^2\text{:}\eta^2\text{-}N_2)$, **10**, required the tetraphenylborate complex $[(C_5Me_4H)_2Sc][(\mu\text{-Ph})BPh_3]$, **8**, as a precursor.[Ch.3,21] This complex also is a viable precursor to $(C_5Me_4H)_3Sc$ via the most common synthetic route to $(C_5R_5)_3M$ complexes, namely reaction of a tetraphenylborate salt of a metallocene with an alkali metal cyclopentadienide, eq 6.2. When this reaction was conducted with the scandium and $(C_5Me_4H)^{1-}$ combination, it provided evidence on the previously elusive [bis(pentahapto)](monohapto) orientation for the three cyclopentadienyl rings.

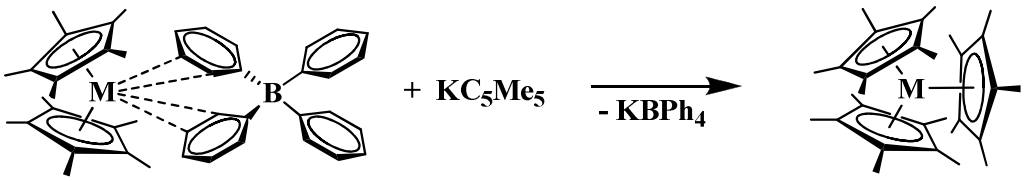

(6.2)

M = La, Ce, Pr, Nd, Sm, Gd, U

Experimental

The manipulations described below were conducted under argon with rigorous exclusion of air and water using Schlenk, vacuum line, and glovebox techniques. Solvents were sparged with UHP argon and dried over columns containing Q-5 and molecular sieves. NMR solvents (Cambridge Isotope Laboratories) were dried over Na/K alloy, degassed, and vacuum-transferred before use. The preparation of $(C_5Me_4H)_2Sc(\eta^3\text{-}C_3H_5)$, **7**, is described in Chapter 3. ^{1}H NMR and ^{13}C NMR spectra were recorded on a Bruker DRX500 spectrometer at 25 °C. ^{45}Sc NMR spectra were recorded on a Bruker Avance 600 spectrometer operating at

145 MHz for ^{45}Sc. The ^{45}Sc NMR spectra were referenced to $[Sc(H_2O)_6]^{3+}$ in D_2O. Infrared spectra were recorded as KBr pellets on a Varian 1000 FTIR spectrophotometer at 25 °C. Elemental analyses were performed on a Perkin Elmer 2400 Series II CHNS analyzer. Mass spectrometry analysis was performed on a Thermo Trace MS+ GCMS.

(η^5-$C_5Me_4H)_2Sc(\eta^1$-$C_5Me_4H)$, 35. In an argon-filled glovebox, KC_5Me_4H (0.040 g, 0.25 mmol) was added to a stirred yellow slurry of $[(C_5Me_4H)_2Sc][(\mu\text{-Ph})BPh_3]$ (0.152 g, 0.25 mmol) in 10 mL of benzene. After the mixture was stirred for 1 h, the orange slurry was centrifuged, filtered, and the solvent was removed under reduced pressure to yield $(C_5Me_4H)_2Sc(\mu^1\text{-}C_5Me_4H)$, **35**, as a bright orange crystalline solid (0.084 g, 82 %, crystalline yield). Yellow crystals suitable for X-ray analysis were grown from a concentrated toluene solution of **35** at -35°C over the course of 2 days. ^{1}H NMR (500 MHz, benzene-d_6): δ 5.62 (2H, $C_5Me_4\mathit{H}$), 2.09 (12H, $C_5\mathit{Me}_4H$), 1.71 (12H, $C_5\mathit{Me}_4H$). ^{13}C NMR (126 MHz, benzene-d_6): δ 125.9 (C_5Me_4H), 120.6 (C_5Me_4H), 111.0 (C_5Me_4H), 13.5 ($C_5\mathit{Me}_4H$), 12.7 ($C_5\mathit{Me}_4H$). ^{1}H NMR (500 MHz, toluene-d_8): δ 5.55 (2H, $C_5Me_4\mathit{H}$), 2.07 (12H, $C_5\mathit{Me}_4H$), 1.69 (12H, $C_5\mathit{Me}_4H$). ^{13}C NMR (126 MHz, toluene-d_8): δ 125.5 (C_5Me_4H), 120.1 (C_5Me_4H), 110.7 (C_5Me_4H), 13.0 ($C_5\mathit{Me}_4H$), 12.3 ($C_5\mathit{Me}_4H$). ^{45}Sc NMR (145 MHz, toluene-d_8): δ 227 ($\Delta_{1/2}$ = 3300 Hz). IR: 3096w, 3075w, 3033w, 2975m, 2904s, 2858s, 2726w, 1662w, 1548w, 1481m, 1432m, 1331w, 1266m, 1106w, 1024m, 974w, 834s, 808s, 728w, 670vs, 623s, 613s cm^{-1}. Anal. Calcd for $C_{27}H_{39}Sc$: C, 79.37; H, 9.62 Found: C, 79.40; H, 9.80.

VT NMR of 35. In order to test the η^1-coordination mode of the $(C_5Me_4H)^-$ ligand in **35** in solution, variable temperature NMR has been taken in toluene-d_8 on a Bruker GN500 spectrometer. The spectrum was initially taken at 298 K to make sure that **35** is pure and that there are no decomposition products observable at room temperature. Subsequently, the sample was cooled down to 243 K and again a ^{1}H NMR spectrum was taken. This procedure was repeated at each of the following temperatures: 223 K, 188 K and finally at 183 K. During this cooling procedure, no splitting of the peaks was observable in the ^{1}H NMR

spectra. Upon warming to 273 K, the peaks for **35** were once again observed. The sample was heated to investigate the thermal stability of **35**. ^{1}H NMR spectra were obtained at 313 K, 333 K and finally at 353 K. The ^{1}H NMR spectrum at 353 K does not show the formation of any decomposition products. Cooling back down to 298 K yielded a ^{1}H NMR spectra which was identical to the initially measured one.

X-Ray Crystallographic Data. X-Ray data collection parameters of **35** is given in Table 6.1. Details for X-ray data collection, structure solution and refinement are given in the Appendix.

Results and Discussion

The reaction of KC_5Me_4H with $[(C_5Me_4H)_2Sc][(\mu\text{-Ph})BPh_3]$[21] was examined in analogy to the reactions of $[(C_5Me_5)_2M][(\mu\text{-Ph})_2BPh_2]$ complexes with KC_5Me_5 that have been shown to form $(C_5Me_5)_3M$ complexes with M = La,[1] Ce,[2] Pr,[2] Nd,[3] Sm,[27] Gd,[5] U,[6] eq 2. Although this reaction has been successful in these cases, it was uncertain if it also would form a tris(cyclopentadienyl) complex with the smaller Sc^{3+} ion even with $(C_5Me_4H)^{1-}$. However, a reaction occurs within 1 h and yellow crystals of **35** with an elemental analysis consistent with $(C_5Me_4H)_3Sc$ were isolated in 82% yield. The ^{1}H and ^{13}C NMR spectra of **35** showed a single type of $(C_5Me_4H)^{1-}$ environment in solution down to –80 °C in toluene, but X-ray crystallography revealed that in the solid state, **35** had a [bis(pentahapto)](monohapto) metallocene structure, $(\eta^5\text{-}C_5Me_4H)_2Sc(\eta^1\text{-}C_5Me_4H)$, **35**, eq 6.3, Figure 6.3. The X-ray diffraction data of **35** clearly showed the monohapto nature of the C1–C5 ring.

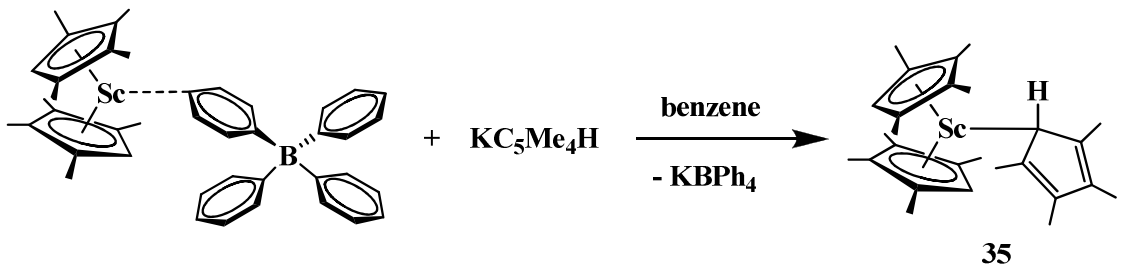

(6.3)

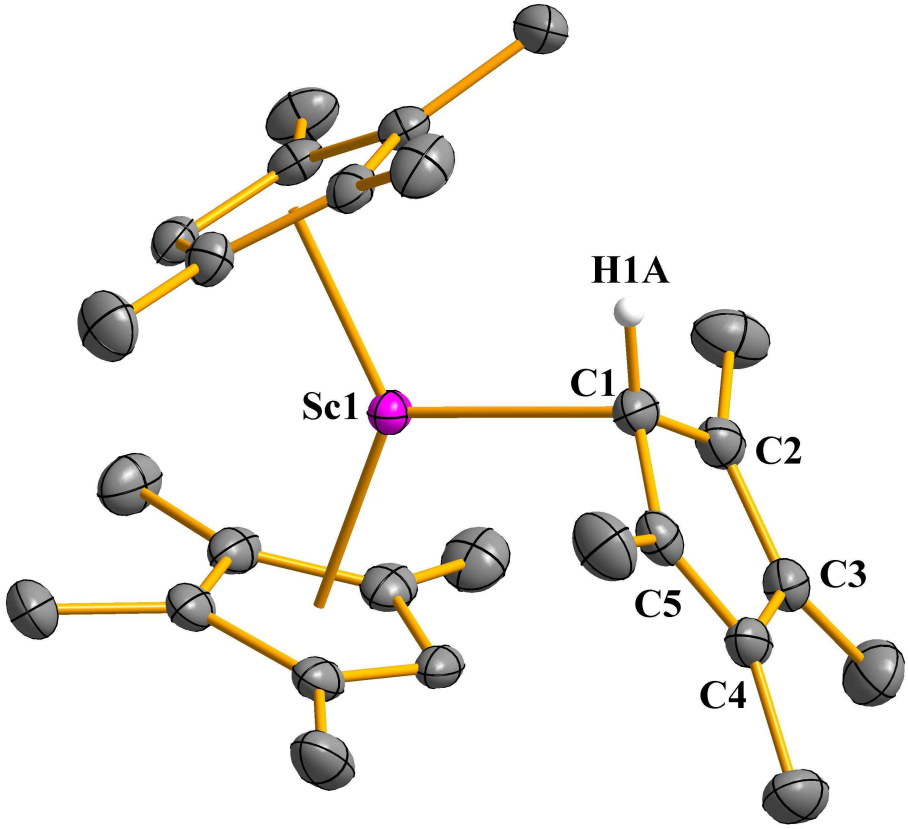

Figure 6.1. Thermal ellipsoid plot of $(C_5Me_4H)_2Sc(\mu^1\text{-}C_5Me_4H)$, **35**, drawn at the 50% probability level. The second independent molecule of **35** and hydrogen atoms except for H1A are omitted for clarity.

Table 6.1. X-ray Data Collection Parameters for $(C_5Me_4H)_2Sc(\mu^1\text{-}C_5Me_4H)$, **35**.

Complex	**35**
Empirical formula	$C_{27}H_{39}Sc$
Fw	408.54
Temperature (K)	148(2)
Crystal system	monoclinic
Space group	$P2_1/c$
a (Å)	16.9583(9)
b (Å)	17.2189(9)
c (Å)	17.1638(9)
α (deg)	90
β (deg)	112.7633(7)
γ (deg)	90
Volume (Å^3)	4621.5(4)
Z	8
ρ_{calcd} *(Mg/m^3)*	1.174
μ *(mm^{-1})*	0.328
*R1 [*I > *2.0*σ*(*I*)]*^{a}	0.0368
wR2 (all data)^a	0.1025

[a] Definitions: $wR2 = [\Sigma[w(F_o^2-F_c^2)^2] / \Sigma[w(F_o^2)^2]]^{1/2}$, $R1 = \Sigma||F_o|-|F_c|| / \Sigma|F_o|$

Structural studies

$(\eta^5\text{-}C_5Me_4H)_2Sc(\eta^1\text{-}C_5Me_4H)$, 35. The X-ray diffraction data of **35** clearly showed the monohapto nature of the C1–C5 ring. Selected bond distances and angles are given in Table 6.2. The unit cell of **35** contains two crystallographically independent molecules, the metrical parameters of which are very similar. Only one is discussed in detail here. For more information see in the Appendix.

Table 6.2. Selected Bond Distances (Å) and Angles (deg) for $(C_5Me_4H)_2Sc(\mu^1\text{-}C_5Me_4H)$, **35**.

	35		**35**
(Cnt)-Sc-Cnt)[a]	135.4	Sc(1)-C(1)	2.3744(15)
Cnt1-Sc(1)-C(1)	106.8	C(1)-C(2)	1.442(2)
Cnt2-Sc(1)-C(1)	117.6	C(1)-C(5)	1.443(2)
Sc-C(η^5-C_5Me_4H)	2.423(2)-2.544(1)	C(2)-C(3)	1.388(2)
Sc(1)-Cnt1	2.178	C(3)-C(4)	1.427(2)
Sc(1)-Cnt2	2.163	C(4)-C(5)	1.380(2)

[a]Cnt = centroid of the cyclopentadienyl ring

The 1.380(2) Å C4–C5 and 1.388(2) Å C2–C3 distances are shorter than the other three C–C distances in the ring, 1.442(2), 1.443(2) and 1.427(2) Å respectively, which is consistent with a localized diene structure. The 2.374(2) Å Sc1–C1 distance is much longer than the 2.243(11), 2.278(2), and 2.286(4) Å Sc–C(alkyl) single bonds in $(C_5Me_5)_2ScMe$,[22] $(C_5Me_5)_2ScCH_2CMe_3$,[23] and $(C_5Me_5)_2ScCH_2SiMe_3$,[24] respectively, but it is shorter than the 2.423(2)-2.544(2) Å range of Sc–C(η^5-C_5Me_4H) distances in **35**. The 135.4° (C10–C14 ring centroid)–Sc–(C19–C23 ring centroid) angle is similar to the 139.4° value in $[(C_5Me_4H)_2Sc][(\mu\text{-Ph})BPh_3]$, **8**,[21,Ch.3] and smaller than the 144.65° analog in $(C_5Me_5)_2ScMe$. The 2.171 Å average Sc–(C_5Me_4H ring centroid) distance is longer than the 2.130 Å value in $[(C_5Me_4H)_2Sc][(\mu\text{-Ph})BPh_3]$ and identical to the 2.171 Å analog in $(C_5Me_5)_2ScMe$. The C–H positions of the η^5-rings in the metallocene are 3° away from being completely staggered.

Conclusion

The first example of an $(\eta^5\text{-}C_5R_5)_2M(\eta^1\text{-}C_5R_5)$ (R = Me, H) complex, an elusive structural type that has been postulated in numerous reactions of $(C_5R_5)_3M$ compounds, has been synthesized and structurally characterized using the combination of M = Sc and C_5R_5 = C_5Me_4H. $[(C_5Me_4H)_2Sc][(\mu\text{-Ph})BPh_3]$ reacts with KC_5Me_4H to form $(\eta^5\text{-}C_5Me_4H)_2Sc(\eta^1\text{-}$

C_5Me_4H), **35**, which has a 2.374(2) Å Sc–C single bond distance in the monohapto ring and 2.423(2)-2.544(2) Å Sc–C bond distances in the pentahapto rings.

References

(1) Evans, W. J.; Davis, B. L.; Ziller, J. W. *Inorg. Chem.* **2001**, 40, 6341.
(2) Evans, W. J.; Perotti, J. M.; Kozimor, S. A.; Champagne, T. M.; Davis, B. L.; Nyce, G. W.; Fujimoto, C. H.; Clark, R. D.; Johnston, M. A.; Ziller, J. W. *Organometallics* **2005**, *24*, 3916.
(3) Evans, W. J.; Seibel, C. A.; Ziller, J. W. *J. Am. Chem. Soc.* **1998**, *120*, 6745.
(4) Evans, W. J.; Gonzales, S. L.; Ziller, J. W. *J. Am. Chem. Soc.* **1991**, *113*, 7423.
(5) Evans, W. J.; Davis, B. L.; Champagne, T. M.; Ziller, J. W. *Proc. Natl. Acad. Sci.* **2006**, *103*, 12678.
(6) Evans, W. J.; Forrestal, K. J.; Ziller, J. W. *Angew. Chem. Int. Ed. Engl.* **1997**, *36*, 774.
(7) Davies, C. E.; Gardiner, I. M.; Green, J. C.; Green, M. L. H.; Hazel, N. J.; Grebenik, P. D.; Mtetwa, V. S. B.; Prout, K. *J. Chem. Soc., Dalton Trans.* **1985**, 669.
(8) Evans, W. J.; Nyce, G. W.; Johnston, M. A.; Ziller, J. W. *J. Am. Chem. Soc.* **2000**, *122*, 12019.
(9) Evans, W. J.; Kozimor, S. A.; Ziller, J. W. *Organometallics* **2005**, *24*, 3040.
(10) Evans, W. J.; Nyce, G. W.; Ziller, J. W. *Organometallics*, **2001**, 20, 5489.
(11) Evans, W. J.; Kozimor, S. A.; Nyce, G. W.; Ziller, J. W. *J. Am. Chem. Soc.* **2003**, *125*, 13831.
(12) Evans, W. J.; Kozimor, S. A.; Ziller, J. W. *J. Am. Chem. Soc.* **2003**, *125*, 14264.
(13) Evans, W. J.; Mueller, T. J.; Ziller, J. W. *Chem. Eur. J.* **2010**, *16*, 964.
(14) Evans, W. J.; Mueller, T. J.; Ziller, J. W. *J. Am. Chem. Soc.* **2009**, *131*, 2678.
Evans, W. J.; Davis, B. L. *Chem. Rev.* **2002**, *102*, 2119.
(15) a) Evans, W. J.; Ulibarri, T. A.; Chamberlain, L. R.; Ziller, J. W.; Albarez, D. Jr. *Organometallics*, **1990**, *9*, 2124. b) Schumann, H.; Glanz, M.; Hemling, H.; Görlitz, F. H. *J. Organomet. Chem.*, **1993**, *462*, 155. c) Evans, W. J.; Forrestal, K. J.; Ziller, J. W. *J. Am. Chem. Soc.* **1998**, *120*, 2180.
(16) Edelmann, F. T. Complexes of Group 3 and Lanthanide Elements. In *Comprehensive Organometallic Chemistry III*; Robert, H. C.; Mingos, D. M. P.; Elsevier: Oxford, 2007; Chapter 4.01, pp 1-190.
(17) Crabtree, Robert H. *The Organometallic Chemistry of the Transition Metals*, 4th ed.; Wiley & Sons: New York, 2005.
(18) Evans, W. J.; Forrestal, K. J.; Ziller, J. W. *J. Am. Chem. Soc.* **1998**, *120*, 9273.
(19) Evans, W. J. *Coord. Chem. Rev.* **2000**, *206*, 263.
(20) Demir, S.; Lorenz, S. E.; Fang, M.; Furche, F.; Meyer, G.; Ziller, J. W.; Evans, W. J. *J. Am. Chem. Soc.* **2010**, *132*, 11151-11158.
(21) Evans, W. J.; Forrestal, K. J.; Leman, J. T.; Ziller, J. W. *Organometallics* **1996**, *15*, 527.
(22) Thompson, M. E.; Baxter, S. M.; Bulls, A. R.; Burger, B. J.; Nolan, M. C.; Santarsiero, B. D.; Schaefer, W. P.; Bercaw, J. E. *J. Am. Chem. Soc.* **1987**, *109*, 203.
(23) Sadow, A. D.; Tilley, T. D. *J. Am. Chem. Soc.* **2003**, *125*, 7971.
(24) Minasian, S. G.; Rinehart, J. D.; Bazinet, P.; Seitz, M. *Acta. Cryst.* **2006**, *E62*, m1823.

Chapter 7

Sigma Bond Metathesis Reactivity of $(C_5Me_4H)_2Sc(\eta^3\text{-}C_3H_5)$ with Diphenyldichalcogenides, PhEEPh (E = S, Se, Te) and Dipyridyldisulfide, PySSPy

Introduction

The synthesis of sterically crowded complexes containing three pentamethylcyclopentadienyl rings, $(\eta^5\text{-}C_5Me_5)_3M$,[1-6] demonstrated that it was possible to make series of complexes in which all the metal ligand bonds are longer than those previously observed.[7] Although this result makes an important point in synthesis and structure, these complexes also have substantial implications in reactivity. The long bonds translate into high reactivity and demonstrate a method to activate the normally inert $(\eta^5\text{-}C_5Me_5)^{1-}$ groups extensively used as ancillary ligands. Until recently, three general types of unexpected $(C_5Me_5)^{1-}$ reactivity have been observed with these sterically crowded $(C_5Me_5)_3M$ complexes depending on the substrate: (a) η^1-like $(C_5Me_5)^{1-}$ reactivity[2,6,8,9,10] (b) a one electron reduction process called sterically induced reduction (SIR),[2,11,12] and (c) displacement of a pentahapto $(\eta^5\text{-}C_5Me_5)^{1-}$ ligand by a ligand of lower hapticity.[9,13] Each of these reactions typically gives a single product in high yield.

Recently, however, in reactions with diphenyldichalcogenide substrates, PhEEPh (E = S, Se, Te), it was found that the $(C_5Me_5)_3M$ complexes could react along two pathways.[15] These reactions formed a single type of metallocene product, $[(C_5Me_5)_2M(EPh)]_2$, but mixtures of two types of byproducts were observed depending on M and E. $(C_5Me_5)_2$, the byproduct of sterically induced reduction, eq 7.1, was predominant in some cases, but C_5Me_5EPh, the byproduct of sigma bond metathesis, eq 7.2, was the major product in other reactions. The latter reaction could be envisaged to occur via a pseudo-alkyl intermediate,

(η^5-$C_5Me_5)_2M(\eta^1$-$C_5Me_5)$, although no evidence for such a structure had been observed even in base adduct species, $(C_5Me_5)_3ML$ and $(C_5Me_5)_3ML_2$.[15-17]

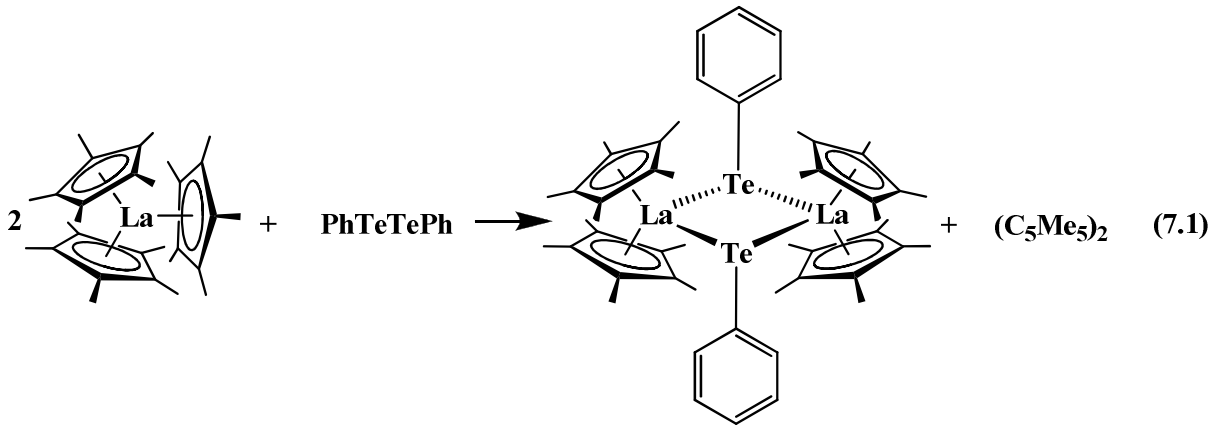

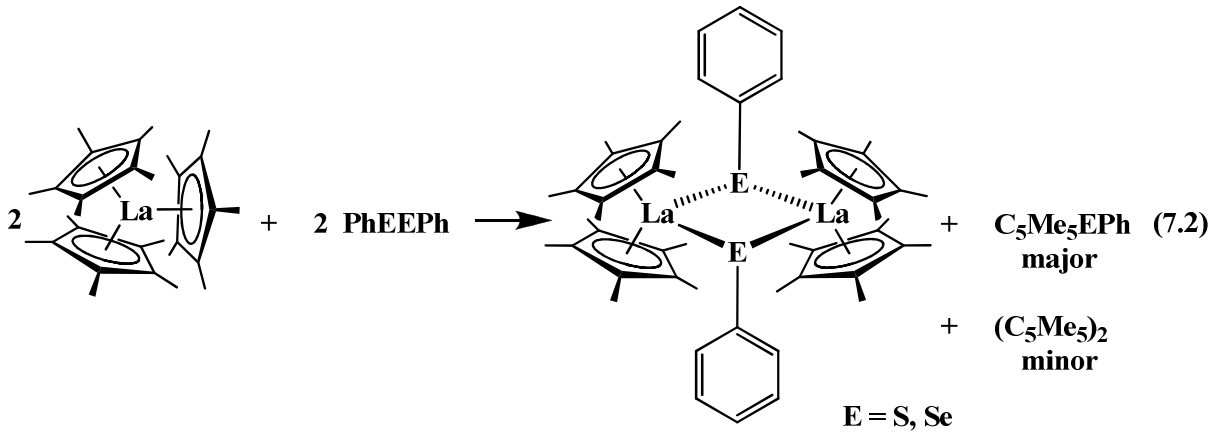

Chapter 6 describes the first structurally characterizable example of a (η^5-$C_5R_5)_2M(\eta^1$-$C_5R_5)$ complex that was discovered with the combination of Sc^{3+} and $(C_5Me_4H)^{1-}$. (η^5-$C_5Me_4H)_2Sc(\eta^1$-$C_5Me_4H)$ provided the first chance to test sigma bond metathesis reactivity in a tris(polyalkylcyclopentadienyl) complex with demonstrated access to a (η^1-$C_5Me_4H)^{1-}$ ligand. However, the viability of sigma bond metathesis of PhEEPh with more conventional scandium alkyl complexes had not yet been established. Sigma bond metathesis usually occurs with substrates that can put H or Si in the position diagonal to the metal.

To provide information on sigma bond metathesis between Sc-C and PhEEPh in a $(C_5Me_4H)^{1-}$ metallocene, reactions with $(C_5Me_4H)_2Sc(\eta^3$-$C_3H_5)$, **7**, were studied.

$(C_5Me_4H)_2Sc(\eta^3\text{-}C_3H_5)$ was chosen for these reactions not only because it is the only hydrocarbyl scandium $(C_5Me_4H)^{1-}$ metallocene in the literature so far, but also because metallocene allyl complexes of the lanthanides have proven to be conveniently synthesized and reliable sources of M-C bond reactivity.[18,19] In this chapter, the reactivity of **7** with PhEEPh is described here as well as a comparison to reactions with $(\eta^5\text{-}C_5Me_4H)_2Sc(\eta^1\text{-}C_5Me_4H)$, **35**.

Experimental

The manipulations described below were conducted under argon with rigorous exclusion of air and water using Schlenk, vacuum line, and glovebox techniques. Solvents were sparged with UHP argon and dried over columns containing Q-5 and molecular sieves. NMR solvents (Cambridge Isotope Laboratories) were dried over Na/K alloy, degassed, and vacuum-transferred before use. PhSSPh, PhSeSePh, and PhTeTePh were purchased from Aldrich and sublimed prior to use. $(C_5Me_4H)_2Sc(\eta^3\text{-}C_3H_5)$, **7**,[Ch.3] and $(C_5Me_4H)_2Sc(\eta^1\text{-}C_5Me_4H)$, **35**,[Ch.6] were prepared as described in the corresponding chapters. ^{1}H NMR and ^{13}C NMR spectra were recorded on a Bruker DRX500 spectrometer at 25 °C. Infrared spectra were recorded as KBr pellets on a Varian 1000 FTIR spectrophotometer at 25 °C. Elemental analyses were performed on a Perkin Elmer 2400 Series II CHNS analyzer. Mass spectrometry analysis was performed on a Thermo Trace MS+ GCMS.

$[(C_5Me_4H)_2ScSPh]_2$, 36. In an argon-filled glovebox, PhSSPh (0.099 g, 0.45 mmol) was added to a yellow solution of $(C_5Me_4H)_2Sc(\eta^3\text{-}C_3H_5)$, **7**, (0.149 g, 0.45 mmol) in 10 mL of toluene. After the mixture was stirred for 24 h, the solution was evaporated to dryness to yield a yellow powder. This was washed with a small amount of cold hexane in order to remove $(\eta^1\text{-}C_3H_5)SPh$ to give yellow crystalline $[(C_5Me_4H)_2ScSPh)]_2$, **36**, (0.279 g, 78 %, crystalline yield). Yellow crystals suitable for X-ray analysis were grown from a concentrated toluene solution of **36** at -35 °C over the course of 2 d. ^{1}H NMR (500 MHz,

benzene-d_6): δ 7.65 (d, 2H, C_6H_5), 7.20 (m, 2H, C_6H_5), 7.03 (m, 1H, C_6H_5), 6.23 (s, 2H, C_5Me_4H), 2.08 (s, 12H, C_5Me_4H), 1.57 (s, 12H, C_5Me_4H). (η^1-C_3H_5)SPh ^{1}H NMR (500 MHz, benzene-d_6): δ 7.24 (m, 2H, C_6H_5), 7.00 (m, 3H, C_6H_5), 5.69 (m, 1H, CH_2CHCH_2), 4.91 (d, 1H, $CH_2CH{=}CH_2$ *anti* CH_2), 4.83 (d, 1H, $CH_2CH{=}CH_2$ *syn* CH_2), 3.19 (d, 2H, $CH_2CH{=}CH_2$). HRMS (GC-MS) m/z calcd for $[M]^+$ 150.0503, found 150.0510.

$(C_5Me_4H)_2ScSePh$, 37. In an argon-filled glovebox, PhSeSePh (0.148 g, 0.47 mmol) was added to a yellow solution of $(C_5Me_4H)_2Sc(\eta^3$-$C_3H_5)$, **7**, (0.156 g, 0.47 mmol) in 10 mL of toluene. After the mixture was stirred for 24 h, the solution was evaporated to dryness to yield a yellow powder. This was washed with a small amount of cold hexane in order to remove (η^1-C_3H_5)SePh to give colorless crystalline $(C_5Me_4H)_2ScSePh$, **37**, (0.161 g, 76 % crystalline yield). Colorless crystals suitable for X-ray analysis were grown from a concentrated toluene solution of **37** at -35 °C over the course of 2 d. ^{1}H NMR (500 MHz, benzene-d_6): δ 7.91 (d, 2H, C_6H_5), 7.15 (m, 2H, C_6H_5), 7.07 (m, 1H, C_6H_5), 6.35 (s, 2H, C_5Me_4H), 2.08 (s, 12H, C_5Me_4H), 1.53 (s, 12H, C_5Me_4H). ^{13}C NMR (126 MHz, benzene-d_6): δ 140.7 (C_6H_5), 137.0 (C_6H_5), 129.0 (C_6H_5), 125.5 (C_5Me_4H), 125.1 (C_6H_5), 121.3 (C_5Me_4H), 118.5 (C_5Me_4H), 12.6 (C_5Me_4H), 12.3 (C_5Me_4H). IR: 3112w, 3072w, 3060w, 3043w, 2976m, 2901m, 2860m, 2728w, 1664w, 1575s, 1470s, 1449s, 1435s, 1385s, 1372s, 1323m, 1176w, 1156m, 1114w, 1071s, 1061m, 1024s, 998m, 975w, 943w, 904w, 842vs, 824vs, 738vs, 694s, 667m, 629w, 615m cm^{-1}. Anal. Calcd for $C_{24}H_{31}ScSe$: C, 65.01; H, 7.05 Found: C, 64.90; H, 7.55.

$(C_5Me_4H)_2ScTePh$, 38. As described for **37**, **38** was obtained as a yellow crystalline solid (0.101 g, 73 % crystalline yield) from PhTeTePh (0.115 g, 0.28 mmol) and $(C_5Me_4H)_2Sc(\eta^3$-$C_3H_5)$, **7**, (0.092 g, 0.028 mmol) in toluene (10 mL). Yellow crystals suitable for X-ray analysis were grown from a concentrated toluene solution of **38** at -35 °C over the course of 1 d. ^{1}H NMR (500 MHz, benzene-d_6): δ 8.21 (m, 2H, C_6H_5), 7.09 (m, 3H, C_6H_5), 6.59 (s, 2H, C_5Me_4H), 2.04 (s, 12H, C_5Me_4H), 1.48 (s, 12H, C_5Me_4H). ^{13}C NMR (126

MHz, benzene-d_6): δ 142.8 (C_6H_5), 129.3 (C_6H_5), 126.1 (C_6H_5), 125.6 (C_5Me_4H), 121.7 (C_5Me_4H), 118.3 (C_5Me_4H), 115.3 (C_6H_5), 13.1 (C_5Me_4H), 12.5 (C_5Me_4H). IR: 3105w, 3070w, 3056m, 3037w, 2974m, 2900s, 2859s, 2724m, 2660m, 1640w, 1596w, 1571s, 1469s, 1433s, 1385s, 1373s, 1323m, 1297w, 1260w, 1113w, 1061m, 1018s, 991m, 836vs, 822s, 733vs, 694s, 652w, 628w, 614m cm^{-1}. Anal. Calcd for $C_{24}H_{31}ScTe$: C, 58.58; H, 6.35 Found: C, 58.28; H, 6.29. CH_2CHCH_2TePh. ^1H NMR (500 MHz, benzene-d_6): δ 7.64 (m, 2H, C_6H_5), 7.00 (m, 1H, C_6H_5), 6.92 (m, 2H, C_6H_5), 5.88 (m, 1H, CH_2CHCH_2), 4.61 (d, 1H, $CH_2CH=CH_2$ *anti* CH_2), 4.57 (d, 1H, $CH_2CH=CH_2$ *syn* CH_2), 3.27 (d, 2H, $CH_2CH=CH_2$).

$(C_5Me_4H)_2ScSPh(THF)$, 39. In a nitrogen-filled glovebox, PhSSPh (0.072 g, 0.33 mmol) was added to a yellow solution of $(C_5Me_4H)_2Sc(\eta^3\text{-}C_3H_5)$, **7**, (0.108 g, 0.33 mmol) in 10 mL of toluene and spiked with 0.1 ml of THF. After the mixture was stirred for 24 h, the solution was evaporated to dryness to yield a yellow white tacky residue of $(C_5Me_4H)_2ScSPh(THF)$ and $(\eta^1\text{-}C_3H_5)SPh$. Both compounds are soluble in hexane. Colorless crystals of **39** (0.107, 69 % crystalline yield) suitable for X-ray analysis were grown from a concentrated hexane solution at room temperature over the course of 1 week. ^1H NMR (500 MHz, benzene-d_6): δ 7.66 (d, 2H, C_6H_5), 7.23 (m, 2H, C_6H_5), 7.04 (m, 1H, C_6H_5), 5.95 (s, 2H, C_5Me_4H), 1.96 (s, 12H, C_5Me_4H), 1.91 (s, 12H, C_5Me_4H). ^{13}C NMR (126 MHz, benzene-d_8): δ 151.5 (C_6H_5), 137.2 (C_6H_5), 128.9 (C_6H_5), 123.5 (C_6H_5), 122.7 (C_5Me_4H), 119.0 (C_5Me_4H), 115.6 (C_5Me_4H), 13.6 (C_5Me_4H), 12.7 (C_5Me_4H). IR: 3090w, 3070w, 2968m, 2906m, 2861m, 2722w, 1580m, 1567w, 1509w, 1471s, 1450m, 1434m, 1373m, 1337w, 1295w, 1240w, 1177w, 1146w, 1111w, 1087s, 1064m, 1015s, 949w, 923m, 861s, 837s, 800s, 735vs, 699s, 690s, 619m. Anal. Calcd for $C_{28}H_{39}OScS$: C, 71.76; H, 8.39 Found: C, 71.35; H, 8.88.

$(C_5Me_4H)_2ScSePh(THF)$, 40. In a nitrogen-filled glovebox, PhSeSePh (0.078 g, 0.25 mmol) was added to a yellow solution of $(C_5Me_4H)_2Sc(\eta^3\text{-}C_3H_5)$, **7**, (0.082 g, 0.25 mmol) in 10 mL of toluene and spiked with 0.1 ml of THF. After the mixture was stirred for 24 h, the

solution was evaporated to dryness to yield a yellow-white tacky residue of $(C_5Me_4H)_2ScSePh(THF)$ and $(\eta^1\text{-}C_3H_5)SePh$. Since $(C_5Me_4H)_2ScSePh(THF)$ is also slightly soluble in hexane, the product was washed with a minimal amount of cold hexane to remove $(\eta^1\text{-}C_3H_5)SePh$ to give a colorless solid. Colorless crystals of **40** (0.081 g, 63 % crystalline yield) suitable for X-ray analysis were grown from a concentrated toluene solution of **40** at -35 °C over the course of 72 h. ^{1}H NMR (500 MHz, benzene-d_6): δ 7.89 (d, 2H, C_6H_5), 7.17 (m, 2H, C_6H_5), 7.08 (m, 1H, C_6H_5), 6.15 (s, 2H, C_5Me_4H), 3.61 (s, 8H, C_4H_8O), 2.00 (s, 12H, C_5Me_4H), 1.77 (s, 12H, C_5Me_4H), 1.26 (s, 8H, C_4H_8O). ^{13}C NMR (126 MHz, benzene-d_6): δ 141.7 (C_6H_5), 137.0 (C_6H_5), 128.8 (C_6H_5), 124.6 (C_6H_5), 123.5 (C_5Me_4H), 119.9 (C_5Me_4H), 116.5 (C_5Me_4H)), 72.8 (C_4H_8O), 25.9 (C_4H_8O), 13.3 (C_5Me_4H), 12.7 (C_5Me_4H). IR: 3112w, 3062w, 2970m, 2909m, 2860m, 2729m, 1644w, 1575s, 1470s, 1435s, 1450s, 1384s, 1372s, 1325w, 1242w, 1176w, 1112w, 1070s, 1022s, 1012s, 925m, 905m, 857s, 841s, 824s, 809s, 738vs, 695s, 667m, 615m. Anal. Calcd for $C_{28}H_{39}OScSe$: C, 65.23; H, 7.63 Found: C, 64.81; H, 7.30.

$(C_5Me_4H)_2ScTePh(THF)$, 41. As described for **40**, **41** was obtained as a colorless crystalline solid (0.267 g, 65 % crystalline yield) from PhTeTePh (0.299 g, 0.73 mmol) and $(C_5Me_4H)_2Sc(\eta^3\text{-}C_3H_5)$ (0.240 g, 0.73 mmol) in toluene (10 mL) and spiked with 0.1 ml of THF. Crystals suitable for X-ray analysis were grown from a concentrated benzene-d_6 solution of **41** at room temperature over the course of 1 week. ^{1}H NMR (500 MHz, benzene-d_6): δ 8.19 (m, 2H, C_6H_5), 7.09 (m, 3H, C_6H_5), 6.36 (s, 2H, C_5Me_4H), 3.58 (s, 4H, C_4H_8O), 1.97 (s, 12H, C_5Me_4H), 1.70 (s, 12H, C_5Me_4H), 1.29 (s, 4H, C_4H_8O).

$(C_5Me_4H)_2ScSpy$, 42. In a nitrogen-filled glovebox, PySSPy (0.097 g, 0.44 mmol) was added at -30 °C to a precooled (-35 °C) yellow solution of $(C_5Me_4H)_2Sc(\eta^3\text{-}C_3H_5)$ (0.144 g, 0.44 mmol) in 10 mL of toluene. The reaction mixture was allowed to warm up while stirring together both components. After the mixture was stirred for 24 h, the solution was evaporated to dryness to yield a yellow white tacky residue of $(C_5Me_4H)_2ScSpy$ and (η^1-

C_3H_5)SPy. The product was washed with cold hexane to remove (η^1-C_3H_5)SPy and dried to give $(C_5Me_4H)_2$ScSpy, **42**, as a colorless solid (0.137 g, 79 %, crystalline yield). Crystals of **42** suitable for X-ray analysis were grown in an NMR tube from a concentrated benzene-d_6 solution at room temperature over the course of 2 weeks. ^{1}H NMR (500 MHz, benzene-d_6): δ 7.19 (m, 2H, C_5H_4N), 6.66 (m, 1H, C_5H_4N), 6.15 (m, 1H, C_5H_4N), 6.02, (s, 1H, C_5Me_4H), 1.99 (s, 6H, C_5Me_4H), 1.91 (s, 6H, C_5Me_4H), 1.86 (s, 6H, C_5Me_4H), 1.41 (s, 6H, C_5Me_4H). ^{13}C NMR (126 MHz, benzene-d_6): δ 145.4 (C_4H_4NCS), 136.4, (C_4H_4NCS), 123.8 (C_5Me_4H), 121.5 (C_5Me_4H), 119.3 (C_5Me_4H), 117.2 (C_5Me_4H), 115.2 (C_4H_4NCS), 112.1 (C_5Me_4H), 14.2 (C_5Me_4H), 13.9 (C_5Me_4H), 12.7 (C_5Me_4H), 11.2(C_5Me_4H). The quartenary carbon of the pyridylring could not be located in the ^{13}C NMR. IR: 3092w, 3077w, 3060w, 3044w, 2962m, 2934m, 2903m, 2860m, 2721w, 2660w, 1731w, 1591vs, 1538s, 1479w, 1447s, 1413vs, 1380s, 1368s, 1326m, 1263m, 1183m, 1136vs, 1086m, 1022m, 1003m, 986w, 868w, 802s, 756vs, 728s, 644m, 617m cm^{-1}. Anal. Calcd for $C_{23}H_{30}$NSSc: C, 69.49; H, 7.61; N, 3.52 Found: C, 69.22; H, 7.54; N, 3.53. CH_2CHCH_2Spy ^{1}H NMR (500 MHz, benzene-d_6): δ 6.84 (m, 1H, py), 6.79 (m, 1H, py), 6.38 (m, 1H, py), the fourth pyridyl resonance was not found, 5.95 (m, 1H, CH_2CHCH_2), 5.15 (d, 1H, $CH_2CH{=}CH_2$ *anti* CH_2), 4.93 (d, 1H, $CH_2CH{=}CH_2$ *syn* CH_2), 3.84 (d, 2H, $CH_2CH{=}CH_2$).

$[(C_5Me_4H)Sc]_3[SePh]_3$, 43. As described for **40**, $(C_5Me_4H)_2$ScSePh(THF) is slightly soluble in hexane. The yellow hexane wash solution which contained $(C_5Me_4H)_2$ScSePh(THF) and (η^1-C_3H_5)SePh, was concentrated and filtered to give a clear yellow solution. Yellow crystals of **43** were obtained from this concentrated hexane solution at room temperature over the course of 10 d.

Reactions with $(C_5Me_4H)_2Sc(\eta^1$-$C_5Me_4H)$, 35. In an argon-filled glovebox, PhSSPh (0.005 g, 0.02 mmol) was added to an orange solution of **35** (0.010 g, 0.02 mmol) in 2 mL of toluene. After the mixture was stirred for 24 h, the pale orange solution was evaporated to dryness to yield a tacky yellow-orange material. ^{1}H-NMR spectroscopy showed that this was

a 2:1:3 mixture of $[(C_5Me_4H)_2Sc(\mu\text{-SPh})]_2$, **36**, unreacted **35**, and resonances at 6.04, 1.98, 1.97 ppm previously attributed to $[(C_5Me_4H)_2Sc]_2(\mu\text{-O})$ (that was also observed in Chapter 3 as a byproduct). In addition, resonances at 1.94 and 3.59 ppm that could not be assigned to a known compound.

Following the procedure above, **35** reacts with PhSeSePh to form a mixture of $(C_5Me_4H)_2Sc(SePh)$, **37** and $[(C_5Me_4H)_2Sc]_2(\mu\text{-O})$ in a 3:1 ratio with a peak at 1.46 ppm that could not be assigned to a known compound.

The analogous reaction of **35** with PhTeTePh form $(C_5Me_4H)_2Sc(TePh)$, **38** and a product with a resonance at 1.43 ppm that could not be assigned to a known compound.

X-ray Crystallographic Data. Information on X-ray data collection, structure determination, and refinement for **36-43** are given in Table 7.1 and Table 7.2. Details for X-ray data collection, structure solution and refinement are given in the Appendix.

Results and Discussion

Reactivity of $(C_5Me_4H)_2Sc(\eta^3\text{-}C_3H_5)$, 7, with PhEEPh (E = S, Se, Te). Complex **7** reacts with PhSSPh to yield dimeric $[(C_5Me_4H)_2Sc(SPh)]_2$, **36**, eq 7.3, and with PhSeSePh and PhTePh to afford monomeric $(C_5Me_4H)_2Sc(SePh)$, **37**, and $(C_5Me_4H)_2Sc(TePh)$, **38**, respectively, as shown in eq 7.4. In each case, C_3H_5EPh was isolated as the byproduct.

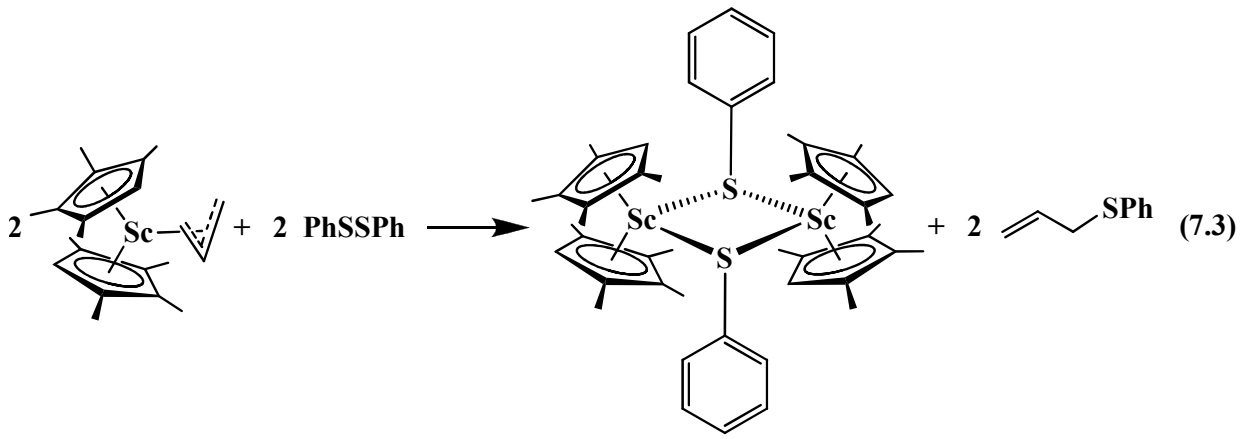

(7.3)

36

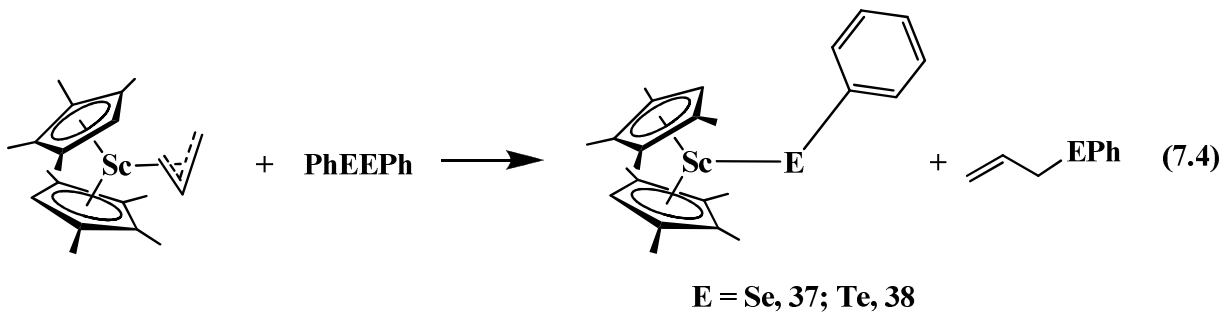

Table 7.1. X-ray Data Collection Parameters for $[(C_5Me_4H)_2ScSPh]_2$, **36**, $(C_5Me_4H)_2ScSePh$, **37** and $(C_5Me_4H)_2ScTePh$, **38**.

Complex	**36**	**37**	**38**
Empirical formula	$C_{48}H_{62}S_2Sc_2 \bullet C_7H_8$	$C_{24}H_{31}ScSe \bullet C_7H_8$	$C_{24}H_{31}ScTe \bullet C_7H_8$
Fw	885.15	535.54	584.18
Temperature (K)	143(2)	148(2)	143(2)
Crystal system	monoclinic	Orthorhombic	Orthorhombic
Space group	$P2_1/n$	*Pnma*	*Pnma*
a (Å)	9.1827(5)	11.2833(5)	11.5128(11)
b (Å)	15.5610(8)	11.7599(6)	11.8430(11)
c (Å)	16.4433(9)	19.9881(10)	20.2121(19)
α (deg)	90	90	90
β (deg)	98.9859(6)	90	90
γ (deg)	90	90	90
Volume ($Å^3$)	2320.8(2)	2652.2(2)	2755.8(4)
Z	2	4	4
ρ_{calcd} (Mg/m^3)	1.267	1.341	1.408
μ (mm^{-1})	0.419	1.667	1.321
R1 $[I > 2.0\sigma(I)]^a$	0.0346	0.0469	0.0406
wR2 (all data)[a]	0.0963	0.1570	0.1340

[a] Definitions: $wR2 = [\Sigma[w(F_o^2-F_c^2)^2] / \Sigma[w(F_o^2)^2]]^{1/2}$, $R1 = \Sigma||F_o|-|F_c|| / \Sigma|F_o|$

Table 7.2. X-ray Data Collection Parameters for $(C_5Me_4H)_2ScTePh(THF)$, **39**, $(C_5Me_4H)_2ScSPh(THF)$, **40**, $(C_5Me_4H)_2ScSePh(THF)$, **41**, $(C_5Me_4H)_2Sc(Spy)$, **42**, and $[(C_5Me_4H)Sc]_3[SePh]_3$, **43**.

Complex	**39**	**40**	**41**	**42**	**43**
Empirical formula	$C_{28}H_{39}OSSc$	$C_{28}H_{39}OScSe$	$C_{28}H_{39}OScTe$	$C_{23}H_{30}NSSc$	$C_{63}H_{69}Sc_3Se_6$
Fw	468.61	515.51	564.15	397.50	1434.82
Temperature (K)	148(2)	148(2)	93(2)	93(2)	143(2)
Crystal system	Triclinic	Triclinic	Triclinic	Monoclinic	Monoclinic
Space group	$P\bar{1}$	$P\bar{1}$	$P\bar{1}$	$P2_1/c$	$P2_1/c$
a (Å)	8.9008(4)	8.8672(5)	9.3570(3)	16.3661(5)	12.8462(7)
b (Å)	9.4443(5)	9.7827(6)	16.8480(6)	8.4809(3)	22.0977(12)
c (Å)	15.9737(8)	15.3323(9)	18.5223(6)	15.8932(5)	21.2071(12)
α (deg)	81.1952(5)	94.6992(7)	67.1803(4)	90	90
β (deg)	75.3670(5)	102.8106(7)	79.3325(4)	108.00	93.7394(7)
γ (deg)	71.1870(5)	97.2083(7)°	76.4365(4)	90	90
Volume ($Å^3$)	1226.05(10)	1278.34(13)	2601.89(15)	2097.98(12)	6007.3(6)
Z	2	2	4	4	4
ρ_{calcd} *(Mg/m^3)*	1.269	1.339	1.440	1.258	1.586
μ *(mm^{-1})*	0.403	1.729	1.399	0.457	4.002
R1 [I > 2.0σ(I)][a]	0.0302	0.0248	0.0217	0.0304	0.0434
wR2 (all data)[a]	0.0817	0.0681	0.0549	0.0841	0.1113

[a] Definitions: $wR2 = [\Sigma[w(F_o^2-F_c^2)^2] / \Sigma[w(F_o^2)^2]]^{1/2}$, $R1 = \Sigma||F_o|-|F_c|| / \Sigma|F_o|$

For E = S and Se, C_3H_5EPh was characterized by mass spectroscopy and NMR that is consistent with the NMR spectra of the known C_3H_5EPh.[20,21] For the less stable C_3H_5TePh, only NMR evidence was obtained that shows similar chemical shifts to those reported for C_3H_5TePh.[22] Complexes **36-38** could be isolated in crystalline form in at least 60% yield and were characterized by X-ray crystallography, Figure 7.1-7.3. Structural details are discussed below.

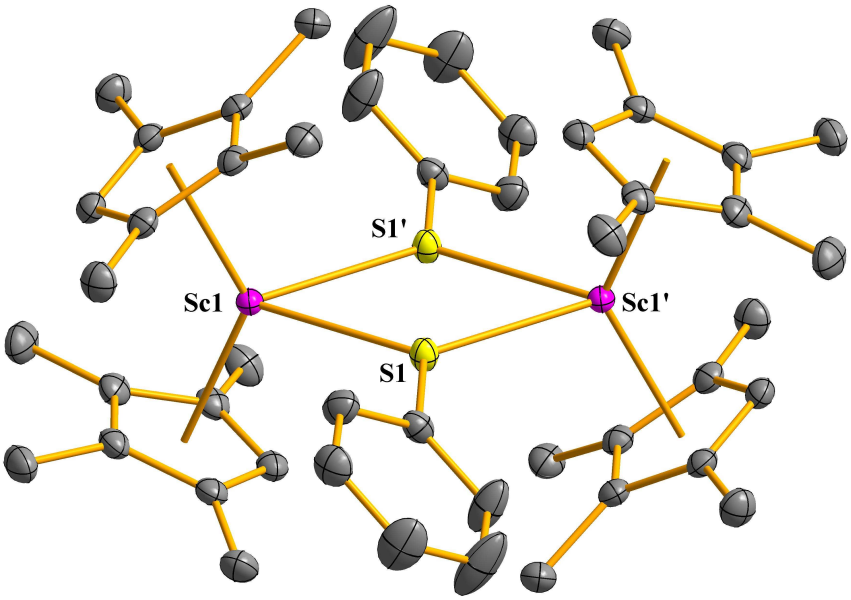

Figure 7.1. Thermal ellipsoid plot of $[(C_5Me_4H)_2ScSPh]_2$, **36**, drawn at the 50% probability level. Hydrogen atoms are omitted for clarity.

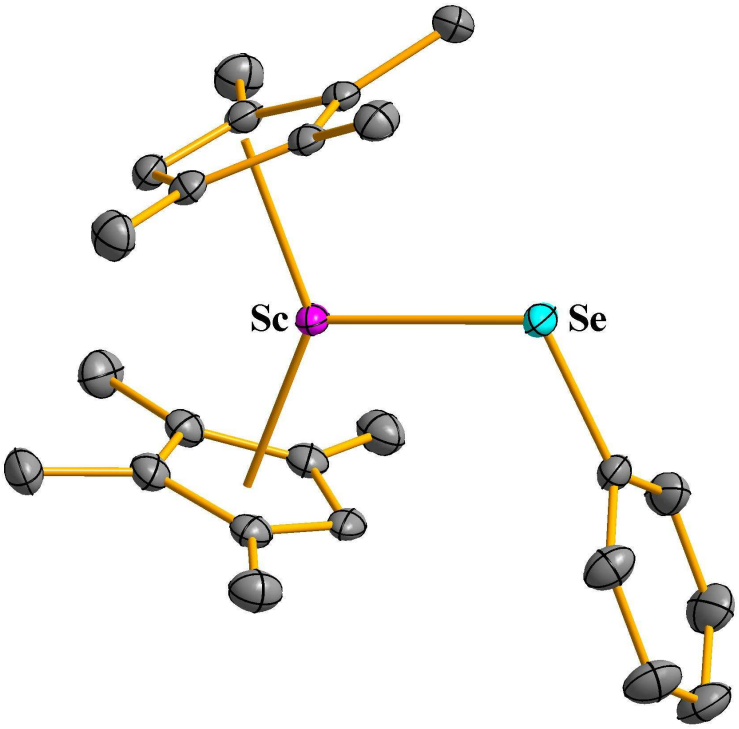

Figure 7.2. Thermal ellipsoid plot of $(C_5Me_4H)_2ScSePh$, **37**, drawn at the 50% probability level. Hydrogen atoms are omitted for clarity.

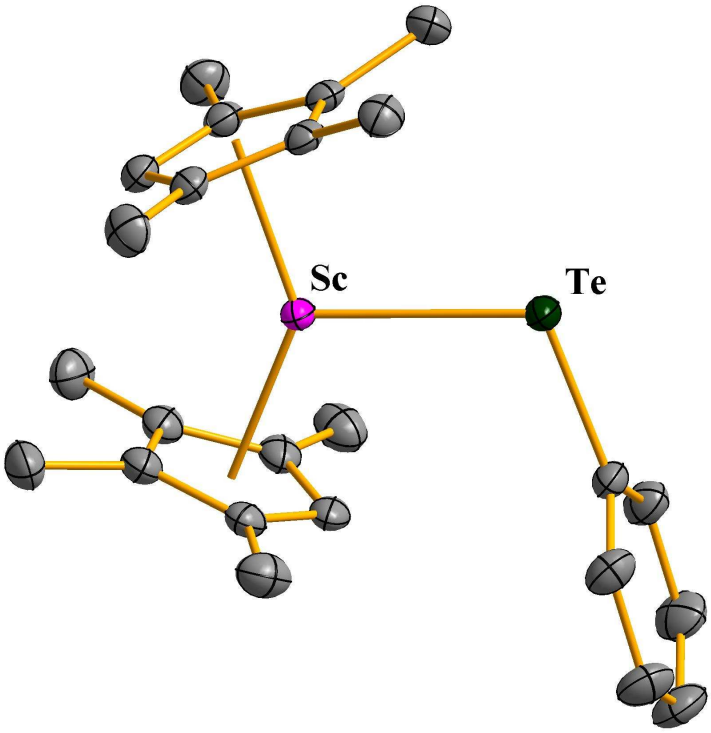

Figure 7.3. Thermal ellipsoid plot of $(C_5Me_4H)_2ScTePh$, **38**, drawn at the 50% probability level. Hydrogen atoms are omitted for clarity.

When the reaction of $(C_5Me_4H)_2Sc(\eta^3\text{-}C_3H_5)$ with PhEEPh is performed in the presence of THF, the THF adducts $(C_5Me_4H)_2Sc(EPh)(THF)$ (E = S, **39**; Se, **40**; Te, **41**) are isolated, eq 7.5. C_3H_5EPh again is observed as the byproduct and each scandium complex was characterized by X-ray crystallography, Figure 7.4-7.6.

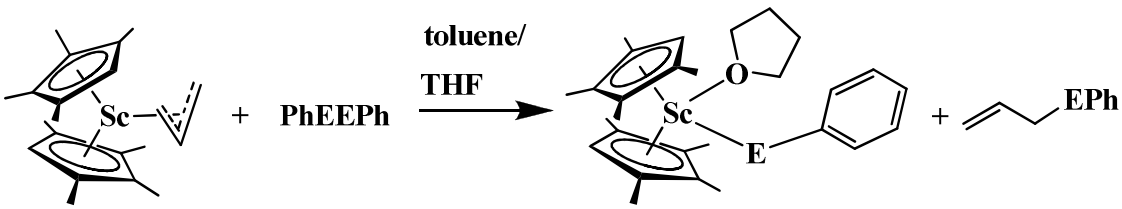

(7.5)

E = S, 39; Se, 40; Te, 41

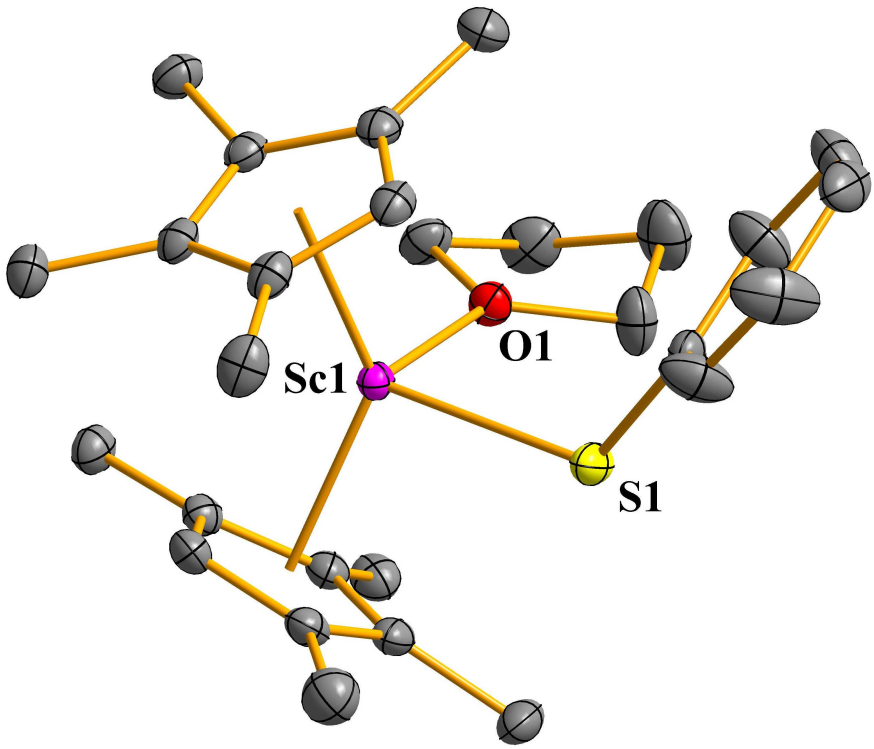

Figure 7.4. Thermal ellipsoid plot of $(C_5Me_4H)_2ScSPh(THF)$, **39**, drawn at the 50% probability level. Hydrogen atoms are omitted for clarity.

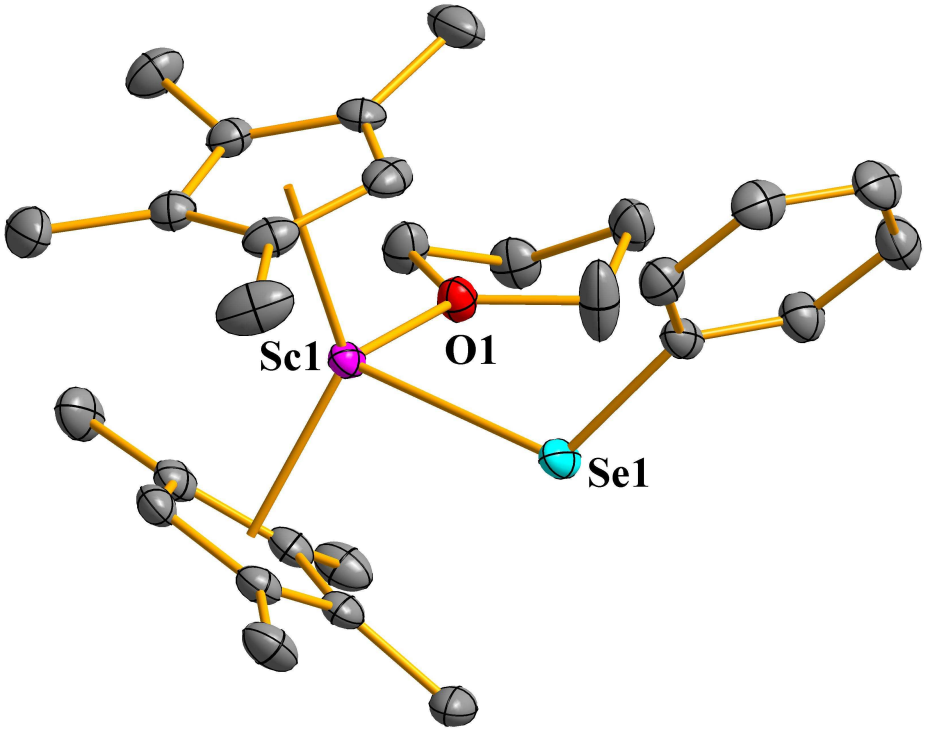

Figure 7.5. Thermal ellipsoid plot of $(C_5Me_4H)_2ScSePh(THF)$, **40**, drawn at the 50% probability level. Hydrogen atoms are omitted for clarity.

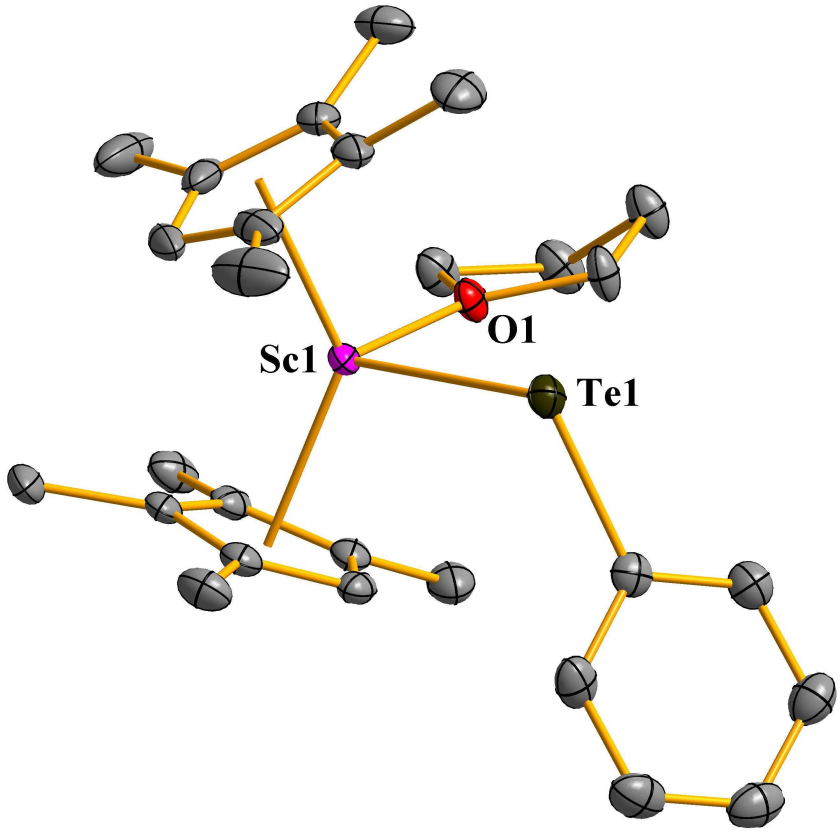

Figure 7.6. Thermal ellipsoid plot of $(C_5Me_4H)_2ScTePh(THF)$, **41**, drawn at the 50% probability level. Hydrogen atoms are omitted for clarity.

Consistent with the formation of the THF adducts **39-41**, a pyridyl analog $(C_5Me_4H)_2Sc(Spy)$, **42**, can be obtained from $(C_5Me_4H)_2Sc(\eta^3\text{-}C_3H_5)$, **7**, and dipyridyldisulfide, pySSpy, eq 7.6, and structurally characterized, Figure 7.7. The byproduct of this reaction is C_3H_5Spy.[20c]

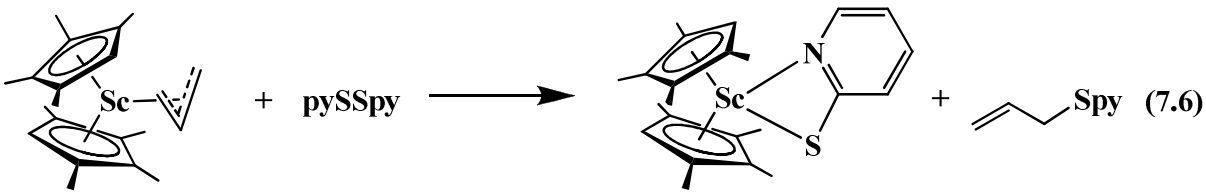

42

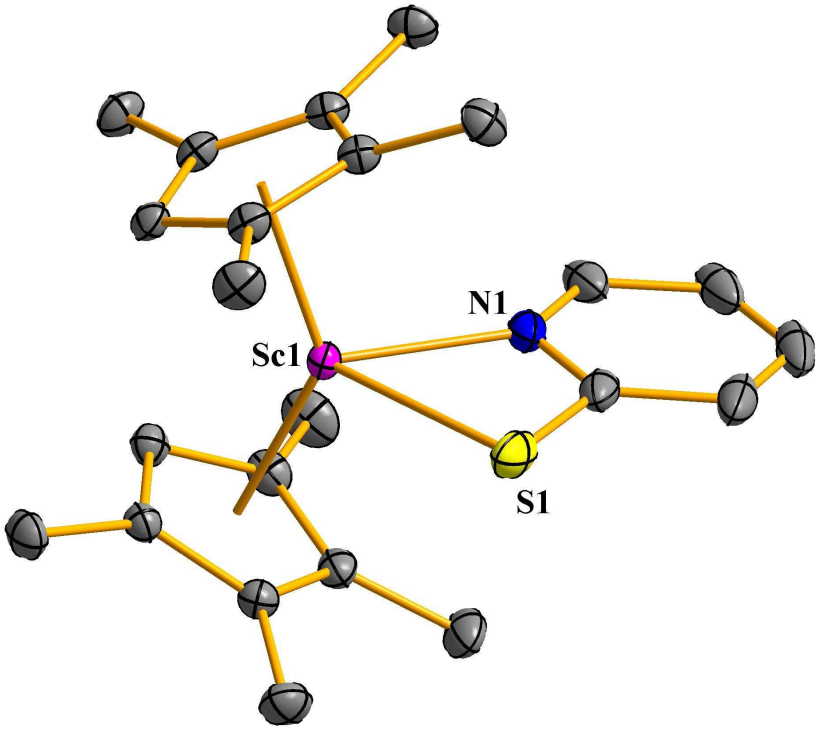

Figure 7.7. Thermal ellipsoid plot of $(C_5Me_4H)_2ScSPy$, **42**, drawn at the 50% probability level. Hydrogen atoms are omitted for clarity.

In addition, when the product $(C_5Me_4H)_2Sc(SePh)(THF)$, **40**, was washed with hexane and this hexane washing solution was kept at room temperature, over the course of 10 days an unprecedented scandium selenium cluster compound was formed, $[(C_5Me_4H)Sc]_3[SePh]_3$, **43**, eq 7.7, that was structurally characterized, Figure 7.8. Scandium lost the coordinated THF ligand and presumably through ligand redistribution formed the trimetallic complex **43** that has shown to be reproducible.

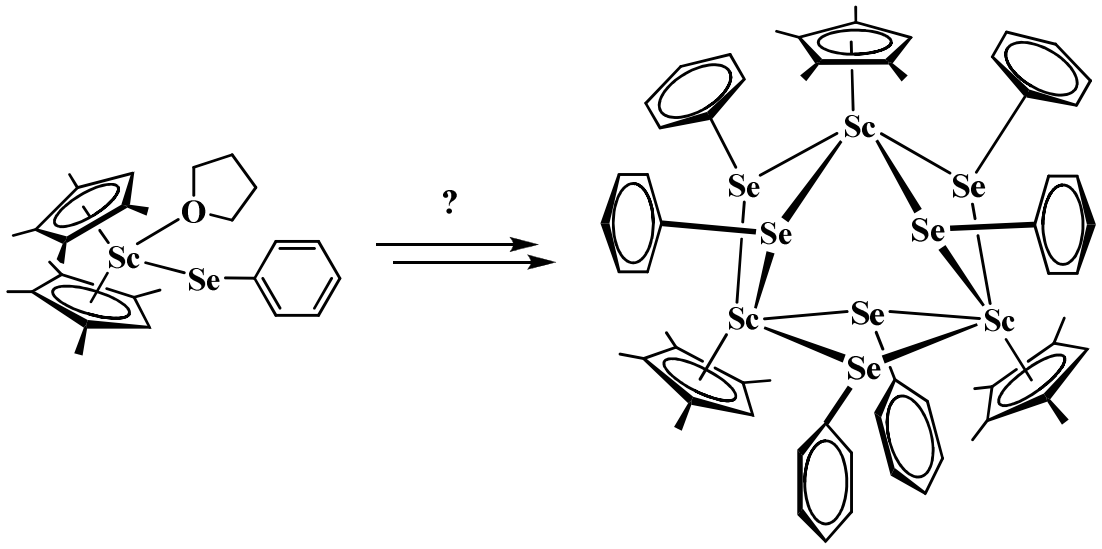

(7.7)

43

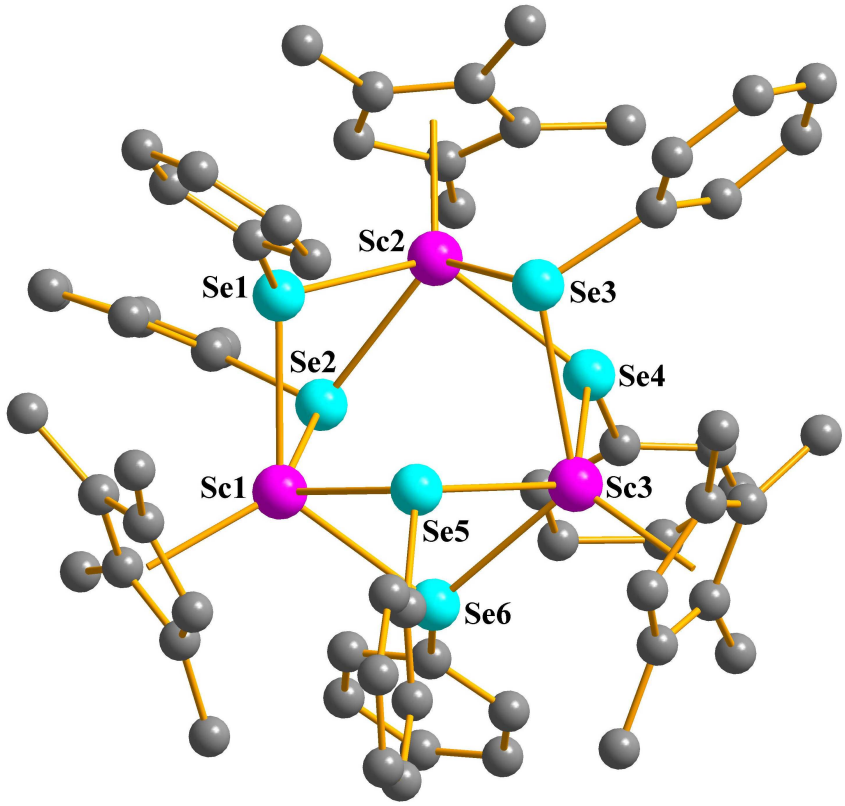

Figure 7.8. Ball-and-Stick plot of $[(C_5Me_4H)Sc]_3[SePh]_3$, **43**. Hydrogen atoms are omitted for clarity.

Reactivity of (η^5-$C_5Me_4H)_2Sc(\eta^1$-C_5Me_4H), 35, with PhEEPh (E = S, Se, Te). (η^5-$C_5Me_4H)_2Sc(\eta^1$-C_5Me_4H), **35**, reacts with PhEEPh in toluene to generate the same scandium metallocenes obtained from **7**, namely $(C_5Me_4H)_2Sc(EPh)$ (E = S, **36**; Se, **37**; Te, **38**) as shown in eq 7.8 and 7.9. The reaction with E = Te is the cleanest. For E = S and Se, the reactions do not go to completion within 24 h and a byproduct is present that is thought to be the oxide, $[(C_5Me_4H)_2Sc]_2(\mu$-O), on the basis of ^{1}H NMR resonances and prior studies.[Ch.3] Specifically, a complex of this composition has been identified crystallographically in a mixed crystal of the composition $\{[(C_5Me_4H)_2Sc]_2(\mu$-η^2:η^2-$N_2)[(C_5Me_4H)_2Sc]_2(\mu$-O)$\}$, **11**.[Ch.3,35] This set of resonances is frequently seen in reactions involving $(C_5Me_4H)^-$ metallocenes of Sc^{3+} as is common with early metal and lanthanide metallocene chemistry in which $[(C_5R_5)_2M]_2(\mu$-O) oxides are almost ubiquitous byproducts.[23,24] However, a direct synthesis and full characterization of the scandium oxide complex has been elusive.

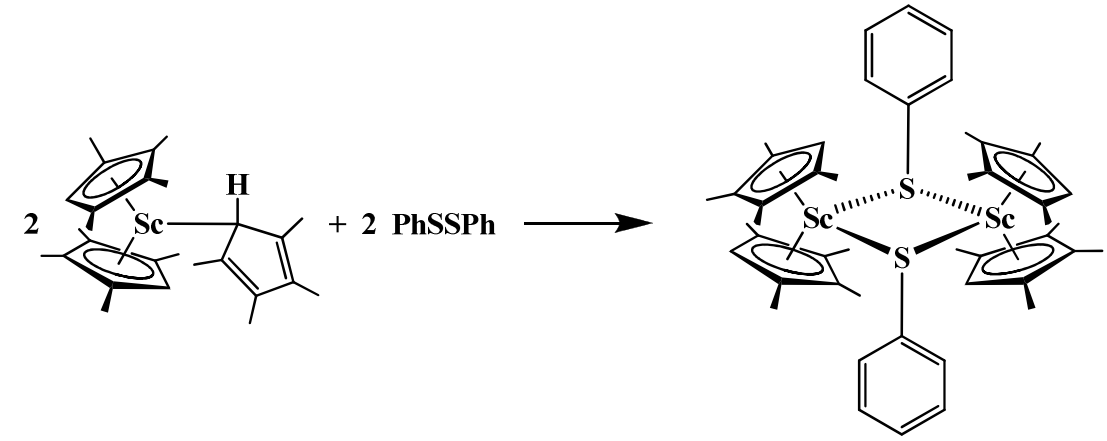

36 **(7.8)**

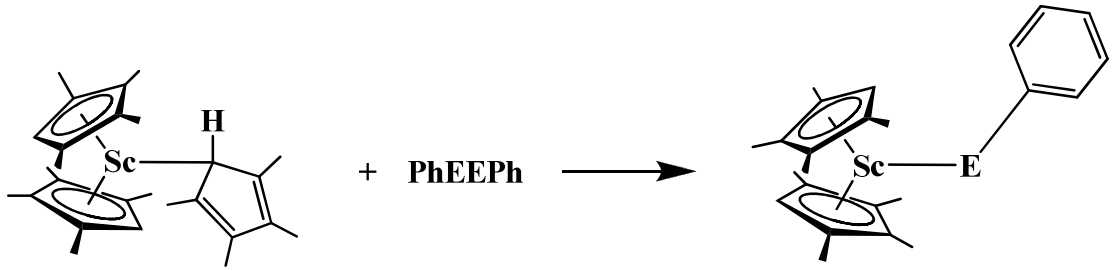

E = Se, 37; Te, 38 **(7.9)**

Structural Studies

$[(C_5Me_4H)_2Sc(EPh)]_x$, 36-38. The structure of $[(C_5Me_4H)_2Sc(SPh)]_2$, **36**, is dimeric whereas the structures of $(C_5Me_4H)_2Sc(SePh)$, **37**, and $(C_5Me_4H)_2Sc(TePh)$, **38**, are monomeric. Disorder in the toluene molecule in the lattices of isomorphous **37** and **38** prevents detailed metrical analysis, but data on Sc-Se and Sc-Te bonds is discussed below with the THF adducts. The metrical data of $[(C_5Me_4H)_2Sc(SPh)]_2$, **36**, is compared with those of $[(C_5Me_5)_2Y(SPh)]_2$, **44**,[25] and $[(C_5Me_5)_2Sm(SPh)]_2$, **45**,[26] Table 7.3, that are the closest reported compounds.

Table 7.3. Selected Bond Distances (Å) and Angles (deg) for $[(C_5Me_4R)_2MSPh]_2$ complexes (M = Sc, **36**, R = H; Y[25], **44**, R = Me; Sm[26], **45**, R = Me).

	Sc, **36**	Y,[25] **44**	Sm,[26] **45**
Eight-coordinate ionic radius[27]	0.870	1.019	1.079
M(1)-S(1)	2.7114(4)	2.8931(6)	2.9341(6)
M(1)-S(1)'	2.7335(4)	2.9031(6)	2.9388(6)
S(1)-C^{ipso}	1.7718(14)	1.766(2)	1.765(2)
M(1)-Cnt1	2.220	2.370	2.429
M(1)-Cnt2	2.202	2.402	2.464
S(1)-M(1)-S(1)'	66.778(14)	61.59(2)	61.99(2)
Cnt1-M(1)-S(1)	111.9	107.4	106.7
Cnt2-M(1)-S(1)	109.9	116.0	116.4
Cnt1-M(1)-S(1)'	112.6	108.9	108.5
Cnt2-M(1)-S(1)'	108.0	115.3	115.5
Cnt1-M(1)-Cnt2	130.1	128.5	128.6
C^{ipso}-S(1)-M(1)	121.07(5)	117.02(8)	124.82(8)
M(1)-S(1)-M(1)'	113.222(14)	118.41(2)	118.01(2)

In the crystal structure of **36** a disordered toluene molecule is present that is evidently not influencing the metrical parameters of **36**. The structure of **36** differs from the structures of **44** and **45** in that it is dimeric. The Shannon ionic radius for eight-coordinate scandium is 0.870 Å, thus much smaller than for eight-coordinate yttrium, 1.019 Å, and samarium, 1.079 Å.[27] Due to the smaller size of scandium, there are some subtle differences in distances and angles between **36** and the complexes **44** and **45** containing the larger yttrium and samarium. For example, the metal-sulfur bond distances for **36** are 2.7114(4) and 2.7335(4) Å, about 0.2 Å shorter than those observed for **44**, 2.8931(6) and 2.9031(6) Å, and for **45**, 2.9341(6) and 2.9388(6) Å. The same applies for the ring centroid-metal bond distances that are 2.220 and 2.202 Å in **36**, thus also about 0.2 Å shorter than in **44**, 2.370 and 2.402 Å, and **45**, 2.429 and 2.464 Å, respectively. Complex **36** contains $(C_5Me_4H)^-$ ligands which could arrange closer to each other resulting in a smaller (ring centroid)-metal-(ring centroid) angle. This angle is 130.1°, slightly larger than those in **44** and **45**, 128.5° and 128.6°, respectively, which is probably again an outcome of the small size of scandium. Furthermore, the metal-sulfur-metal angle in **36** is 66.778(14)° which is significantly larger than 61.59(2)° and 61.99(2)° in **44** and **45**, respectively. In contrast, the data for the $(SPh)^{1-}$ ligand in all three structures are very similar with S-C distances of 1.7718(14), 1.766(2) and 1.765(2) Å in **36**, **44** and **45**, respectively.

The small size of scandium might also effect the arrangement of the $(SPh)^{1-}$ ligands in the molecule. The phenyl rings in **36** are more perpendicular to the plane defined by the scandium, sulfur and ipso-carbon atoms in all three compounds **36**, **44**, and **45**, Figure 7.9. This dihedral angle of 34.7(1)° in **36** is much bigger than the dihedral angles found in **44**, 16.7(1)°, and in **45**, 17.3(1)°.

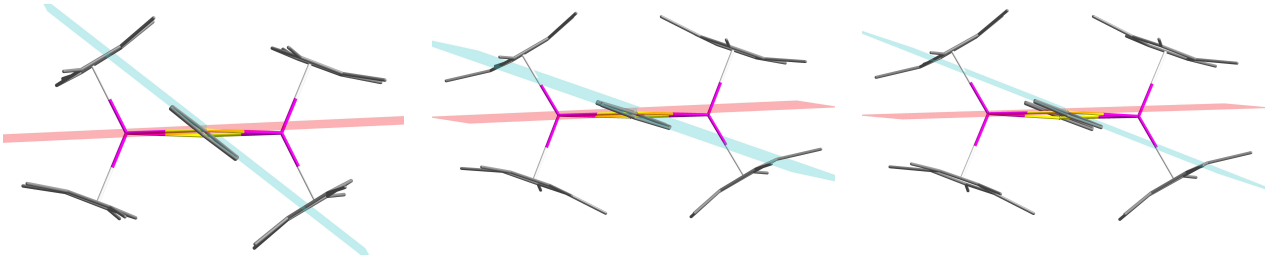

36 (34.7°) **44** (16.1°) **45** (17.3°)

Figure 7.9. The dihedral angle between metal and thiophenyl ligand in $[(C_5Me_4H)_2ScSPh]_2$, **36** in comparison with the dihedral angles in $[(C_5Me_5)_2YSPh]_2$, **44**, and $[(C_5Me_5)_2SmSPh]_2$, **45**.

There are no structural data for a cyclopentadienide containing scandium-sulfur compound known to compare with **36**.

Although the data of **37** and **38** are not good enough to discuss, it becomes clear that the structures are monomeric, which is likely to be the effect of the small size of scandium. The larger samarium analog, even with the larger $(C_5Me_5)^-$ ligand, makes the dimeric complexes, $[(C_5Me_5)_2Sm(SePh)]_2$ and $[(C_5Me_5)_2Sm(TePh)]_2$ possible.[26] There are no structures in terms of a closer progression with selenium or tellurium rare earth metallocene known to compare with.

$(C_5Me_4H)_2Sc(EPh)(THF)$, 39-41. In this series, complexes **39** and **40** are isomorphous but not complex **41**, Figure 7.4-7.6. Their metrical parameters are compared with $(C_5Me_5)_2SmEPh(THF)$ (E = S, **46**; Se, **47**; Te, **48**), Table 7.4.

The Sc-E bond distances follow progression with 2.5222(4), 2.6836(3) and 2.9393(3) Å in **39**, **40** and **41**, respectively. This progression is expected based on size of the chalcogens when compared with the observed Sm-E bond distances of 2.7605(12), 2.8837(6) and 3.1279(3) Å in **46**, **47** and **48**, respectively. The Sc-O bond distances in **39**, **40**, and **41** are all within the same range: 2.2425(9), 2.6836(3) and 2.2407(12) Å, and overall about 0.2 Å shorter than the Sm-O bond distances 2.445(3), 2.443(3) and 2.4490(15) Å found in **46**, **47**

and **48**, respectively. In general, the structures of **39**, **40** and **41**, are not unusual compared to the samarium metallocenes **46**, **47** and **48** when the differences in ligands and ionic radii of the metals are taken into account.

Table 7.4. Selected Bond Distances (Å) and Angles (deg) for $(C_5Me_4H)_2ScSPh(THF)$, **39**, $(C_5Me_4H)_2ScSePh(THF)$, **40**, $(C_5Me_4H)_2ScTePh(THF)$, **41**, $(C_5Me_5)_2SmSPh(THF)$, **46**,[26] $(C_5Me_5)_2SmSePh(THF)$, **47**,[26] and $(C_5Me_5)_2SmTePh(THF)$, **48**.[26] There are two independent molecules of **41** in the crystal structure. The distances and angles of the second independent molecule of **41** are omitted for clarity.

	39	**40**	**41**	**46**	**47**	**48**
E	S	Se	Te	S	Se	Te
M(1)-O(1)	2.2425(9)	2.2397(10)	2.2407(12)	2.445(3)	2.443(3)	2.4490(15)
M(1)-E(1)	2.5222(4)	2.6836(3)	2.9393(3)	2.7605(12)	2.8837(6)	3.1279(3)
M(1)-Cnt(1)	2.244	2.234	2.230	2.442	2.448	2.448
M(1)-Cnt(2)	2.217	2.217	2.213	2.452	2.445	2.445
E(1)-C(19)	1.7689(13)	1.9155(14)	2.1294(17)	-	-	-
E(1)-C(21)	-	-	-	1.759(5)	1.913(4)	2.127(2)
Cnt1-M-Cnt2	133.5	134.1	134.2	133.7	134.1	135.2
Cnt1-M(1)-E(1)	100.7	99.5	101.1	99.5	98.7	100.0
Cnt2-M(1)-E(1)	110.7	111.2	109.0	114.4	114.8	113.1
Cnt1-M(1)-O(1)	104.8	106.1	105.1	104.6	105.7	104.1
Cnt2-M(1)-O(1)	107.2	105.2	106.0	106.1	105.1	103.7
C(19)-E(1)-M(1)	119.93(4)	117.72(4)	112.54(4)	-	-	-
C(21)-E(1)-M(1)	-	-	-	120.82(17)	118.51(14)	112.49(6)
O(1)-M(1)-E(1)	92.16(3)	93.44(3)	94.46(3)	89.72(9)	89.35(8)	92.51(4)

[a]Cnt = centroid of the cyclopentadienyl ring

Scandium has a coordination number of eight in complexes **39-41**. The only known reported structures of selenium and tellurium scandocenes are those of seven coordinate

scandium in $[(C_5Me_5)_2Sc]_2(\mu\text{-Se})$,[28] $[(C_5Me_5)_2Sc]_2(\mu\text{-Te})$,[28] $(C_5Me_5)_2ScTeCH_2C_6H_5$,[28] and $\{(CH_3)_2Si[(t\text{-}C_4H_9)C_5H_3]\}_2Sc(PMe_3)\}_2(\mu\text{-Te})\cdot C_6H_6$.[29] The Sc-Se bond distance in **40** is 2.6836(3) Å. This is expected due to the higher coordination number of the metal and it is longer than 2.5425(16) Å as observed in $[(C_5Me_5)_2Sc]_2(\mu\text{-Se})$.[28] Furthermore, the 2.9393(3) Å Sc-Te bond distance in **41** is also longer than the 2.7528(12) Å distance in $[(C_5Me_5)_2Sc]_2(\mu\text{-Te})$,[28] 2.8337(14) Å in $(C_5Me_5)_2ScTeCH_2C_6H_5$,[28] and 2.8798(5) Å in $\{(CH_3)_2Si[(t\text{-}C_4H_9)C_5H_3]\}_2Sc(PMe_3)\}_2(\mu\text{-Te})\cdot C_6H_6$[29] because of the eight-coordinate scandium. Unfortunately, the poor quality of the data of **37** and **38**, due to a highly disordered solvent molecule, does not favor a detailed comparison with these seven-coordinate scandocenes. However, if for example only the Sc-Te bond distance of 2.8399(10) Å in **38** is taken in account, then this one agrees well with the mentioned Sc-Te bond distances for seven-coordinate scandium.

Figure 7.10 shows the unit cells of $[(C_5Me_4H)_2ScSPh]_2 \cdot C_7H_8$, **36** $\cdot C_7H_8$, and $(C_5Me_4H)_2ScSePh \cdot C_7H_8$, **37** $\cdot C_7H_8$.

In the crystal structure of **36** $\cdot C_7H_8$, the scandium thiophenyl dimers $[(C_5Me_4H)_2ScSPh]_2$, **36**, are located on the cell edges and the center of the cell. There is one disordered toluene molecule per $[(C_5Me_4H)_2ScSPh]_2$, present which fills up the cavities between dimeric $[(C_5Me_4H)_2ScSPh]_2$ molecules. The solvent was disordered about an inversion center and there were no π-stacking interactions between the toluene molecules observed.

In the crystal structure of $(C_5Me_4H)_2ScSePh \cdot C_7H_8$, **37** $\cdot C_7H_8$, there is one disordered toluene molecule per $(C_5Me_4H)_2ScSePh$, **37**, present which fills up the cavities by forming solvent channels between monomeric $(C_5Me_4H)_2ScSePh$ molecules. There was one molecule of toluene solvent present and it was located on a mirror plane and was disordered. There were no π-stacking interactions between the toluene molecules observed.

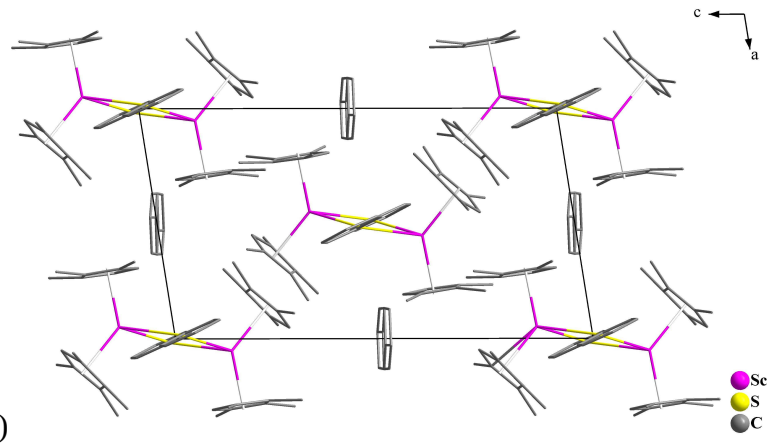

(**a**)

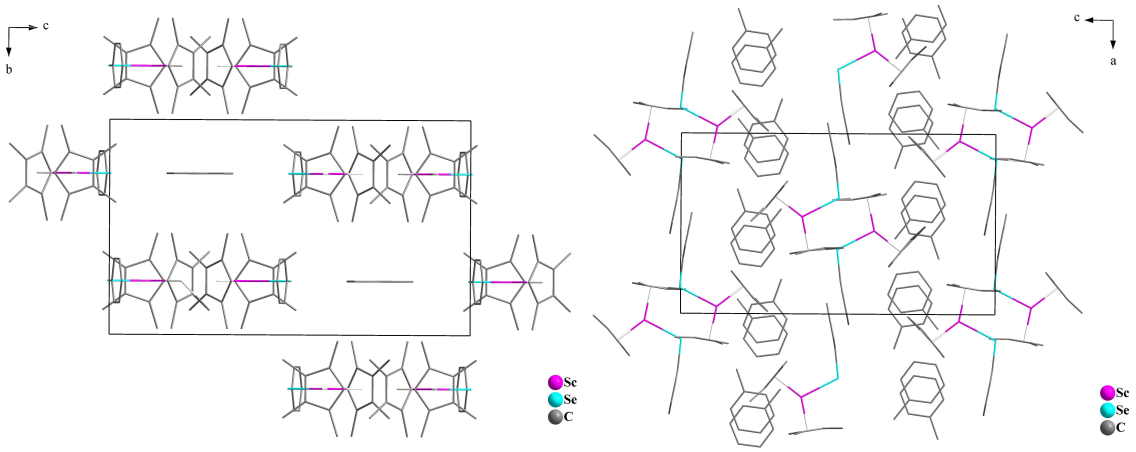

(**b**)

Figure 7.10. (**a**) Unit cell of $[(C_5Me_4H)_2ScSPh]_2 \bullet C_7H_8$, **36** • C_7H_8. View along the b-axis. (**b**) Unit cell of $(C_5Me_4H)_2ScSePh \bullet C_7H_8$, **37** • C_7H_8. View along the a- and b-axes.

$(C_5Me_4H)_2Sc(Spy)$, 42. There are no related structures of (cyclopentadienyl) rare earth metal thiopyridyl complexes known to compare with complex **42**. The structure of **42** is compared with the molybdenum complex $[(C_5H_5)_2Mo(2\text{-}Spy)][PF_6]$, **49**,[30] whose cationic part shows a similar structural feature, Table 7.5.

Table 7.5. Selected Bond Distances (Å) and Angles (deg) for $(C_5Me_4H)_2ScSPy$, **42** and $[(C_5H_5)_2Mo(2\text{-}Spy)][PF_6]$, **49**.

	42	**49**[30b]
(Cnt)-M-(Cnt)[a]	134.6	137.460(18)
(Cnt)-M-E	109.3, 110.2	107.140(29), 108.469(38)
(Cnt)-M-N	108.3, 107.9	107.688(85), 108.002(84)
(Cnt)-M-C[b]	111.8, 113.0	112.331(81), 110.057(87)
C[b]-S-M	78.08(4)	81.219(146)
N-C[b]-M	116.23(9)	109.466(299)
M-(Cnt)	2.179, 2.181	1.9709(6), 1.9709(5)
M-E	2.6158(4)	2.5006(14)
M-N	2.2487(10)	2.1570(35)

[a]Cnt = centroid of the cyclopentadienyl ring
[b]Carbon binding nitrogen and sulfur

The structure of **42** resembles the structure of the metallocene part of **49** in that both metal atoms are eight-coordinate. However, scandium is trivalent whereas molybdenum is tetravalent. Hence, it is not expected that both compounds feature very similar metrical parameters. The metal-sulfur bond distance of 2.6158(4) Å in **42** is slightly longer than 2.5006(14) Å in **49**. Similarly, the metal-nitrogen bond distance of 2.2487(10) Å in **42** is longer than 2.1570(35) Å in **49**. Overall, the structure of **42** is not unusual compared to complex **49** when the differences in ligands and metals are considered.

In contrast, the only structurally characterized metallocene compound featuring an f-block metal and a thiopyridyl ligand is the uranium complex $(C_5Me_5)_2[(^iPr)NC(Me)N(^iPr)\text{-}\kappa^2N,N']U(Spy)$, **50**,[31] in which uranium has an oxidation state of 4+ and is ten-coordinate. As expected, complex **50** shows big differences in bond distances and angles when compared to **42**. For example, the U-N and U-S bond distances in **50** are 2.572(2) Å and 2.7997(6) Å, respectively, whereas the Sc-N and Sc-S bond distances in **42** are 2.2487(10) Å and 2.6158(4) Å.

$[(C_5Me_4H)_2Sc(SPh)]_2$, 36, $(C_5Me_4H)_2ScSPh(THF)$, 39, $(C_5Me_4H)_2ScSpy$, 42. Since there is no structural data for a (cyclopentadienyl) scandium sulfur complex available, a comparison between the metrical data for $[(C_5Me_4H)_2Sc(SPh)]_2$, **36**, $(C_5Me_4H)_2ScSPh(THF)$, **39**, and $(C_5Me_4H)_2ScSpy$, **42**, was undertaken, Table 7.6. The scandium atoms in all three compounds are eight-coordinate which facilitates a comparison of the metrical data.

Table 7.6. Selected Bond Distances (Å) and Angles (deg) for $[(C_5Me_4R)_2ScSPh]_2$, **36**, $(C_5Me_4H)_2ScSPh(THF)$, **39**, and $(C_5Me_4H)_2ScSPy$, **42**.

	36	**39**	**42**
(Cnt)-Sc(1)-(Cnt)[a]	130.1	133.5	134.6
(Cnt)-Sc(1)-S(1)	111.9, 109.9	100.7, 110.7	109.3, 110.2
(Cnt)-Sc(1)-S(1)'	112.6, 108.0		
Sc(1)-(Cnt)	2.220, 2.202	2.244, 2.217	2.179, 2.181
Sc(1)-S(1)	2.7114(4)	2.5222(4)	2.6158(4)
Sc(1)-S(1)'	2.7335(4)		

[a]Cnt = centroid of the cyclopentadienyl ring

The scandium-sulfur bond distance is 2.5222(4) Å in **39** which is substantially shorter than those in **42**, 2.6158(4) Å, and in **36**, 2.7114(4) and 2.7335(4) Å. Thus, the chelate affects a longer scandium-sulfur bond distance in **42** compared to the solvated **39**. However, in this comparison, the longest scandium-sulfur bond distances are observed in **36**, which might be due to the formation of a dimeric molecule. The shortest (ring centroid)-scandium bond distances are found in **42**, 2.179 and 2.181 Å, presumably due to a less crowded complex compared to **36** and **39**. In contrast, the ring centroid-scandium bond distances in **36**, 2.202 and 2.220 Å, more closely resemble the observed values in **42**, 2.217 and 2.244 Å. The smallest (ring centroid)-scandium-(ring centroid) angle exists in **36**, 130.1°, due to the more crowded system, compared to the observed angles for **39** and **42**, 133.5° and 134.6°,

respectively. The (ring centroid)-scandium-sulfur angles in **36** are similar to each other, 109.9° and 111.9° as well as 108.0° and 112.6°, respectively, and within complex **42**, with 109.3° and 110.2°. In contrast, in complex **39** the (ring centroid)-scandium-sulfur angles are 100.7° and 110.7°, quite different from each other.

In general, the observed Sc-S bond distances of 2.5222(4) and 2.6158(4) Å, as well as 2.7114(4) and 2.7335(4) Å in **39**, **42** and **36** agree well with found Sc-S distances as seen by the 2.674(3) Å distance in $[Li(thf)_4][ScCl_3S_2CCH(N_2C_3H\text{-}3,5\text{-}Me_2)_2]$.[32]

$[(C_5Me_4H)Sc]_3(\mu\text{-}SePh)_3$, 43. The metrical paramaters of **43** are given in Table 7.7. There are no other scandium selenium cluster complexes available for comparison.

Interestingly, ligand redistribution resulted in only one $(C_5Me_4H)^-$ ligand and two $(SePh)^-$ ligands per scandium which makes the metal in complex **43** seven-coordinate. Based on this, **43** should be more comparable to $[(C_5Me_5)_2Sc]_2(\mu\text{-}Se)$[28] in which scandium is seven-coordinate as well. However, it has to be considered that **43** is not a metallocene compound by reason of only one $(C_5Me_4H)^-$ ligand per scandium. The Sc-Se bond distance in **43** is within the range of 2.6840(9)-2.8633(9) Å (2.758 Å avg.) which is much longer than the observed value of 2.5425(16) Å in $[(C_5Me_5)_2Sc]_2(\mu\text{-}Se)$.[28] The mean Sc-Se bond distance of 2.758 Å in **43,** in which the scandium is seven-coordinate, is even longer compared to 2.6836(3) Å found in **40** featuring an eight-coordinate scandium. One can assume that the concurrent interactions with one $(C_5Me_4H)^-$ ligand and four relatively bulky $(SePh)^-$ ligands push the selenium atoms further away from the metal causing longer Sc-Se bonds than in **40**. But, there is one of the twelve Sc-Se bond distances in **43**, namely 2.6840(9) Å, which agrees well with 2.6836(3) Å noted in **40**. However, complex **43** is less likely to be overcrowded since the $(C_5Me_4H)^-$ ligand is presumably more strongly bound to the metal as observed by shorter ring centroid-Sc bond distances of 2.141, 2.146 and 2.150 Å in **43** than in **40**, 2.217 and 2.234 Å. The scandium atoms construct a triangular shape in which the average Sc-Sc

distance is 4.038 Å, thus too long to be considered as direct interactions between the metal atoms. This metal triangle is bridged by two selenium atoms per edge and the resulting cavity is empty. The ring centroid-Sc-Se angles are between 115.0-125.8° in **43**, bigger than the observed angles in **40**, 99.5° and 111.2°. The Sc-Se-Se angles in **43** are within the range of 90.52(2)° and 96.60(3)°, hence almost perpendicular.

Table 7.7. Selected Bond Distances (Å) and Angles (deg) for $[(C_5Me_4H)Sc]_3[SePh]_3$, **43**.

	43
Cnt(1)-Sc(1)-(Se)	116.6, 125.8, 113.9, 116.7
Cnt(2)-Sc(2)-(Se)	116.1, 116.1, 121.7, 115.0
Cnt(3)-Sc(3)-(Se)	118.0, 117.8, 115.0, 117.9
C(28)[c]-Se(1)-(Sc)	119.19(14), 127.42(14)
C(34)[c]-Se(2)-(Sc)	111.18(16), 116.10(18)
C(40)[c]-Se(3)-(Sc)	112.47(12), 112.89(12)
C(46)[c]-Se(4)-(Sc)	118.67(14), 125.82(14)
C(46B)[c]-Se(4)-(Sc)	115.5(2), 130.4(2)
C(52)[c]-Se(5)-(Sc)	109.92(13), 115.00(15)
C(58)[c]-Se(6)-(Sc)	118.77(14), 127.77(13)
Sc(1)-(Se)-(Sc)	96.60(3), 93.88(2), 94.07(2), 94.52(3)
Sc(2)-(Se)-(Sc)	96.60(3), 93.88(2), 90.52(2), 95.33(3)
Sc(3)-(Se)-(Sc)	90.52(2), 94.52(3), 94.07(2), 95.33(3)
(Sc)-(Cnt)	2.150, 2.146, 2.141
Sc(1)-(Se)	2.7042(10), 2.7471(9), 2.7498(9), 2.8022(9)
Sc(2)-(Se)	2.7125(9), 2.7501(9), 2.7518(8), 2.7713(9)
Sc(3)-(Se)	2.6840(9), 2.7734(9), 2.7907(10), 2.8633(9)
(Se)-(C)[c]	1.936(4), 1.926(4), 1.938(4), 1.926(6), 1.933(4), 1.932(4), 1.930(4)

[c] ipso-Carbon atom of phenyl group

Discussion

The diphenyldichalcogenides readily participate in sigma bond metathesis reactions (SBM)[33] with allyl scandium metallocenes. Equation 7.10 shows the presumed four-center transition state for these reactions based on previous studies of SBM.[14,34]

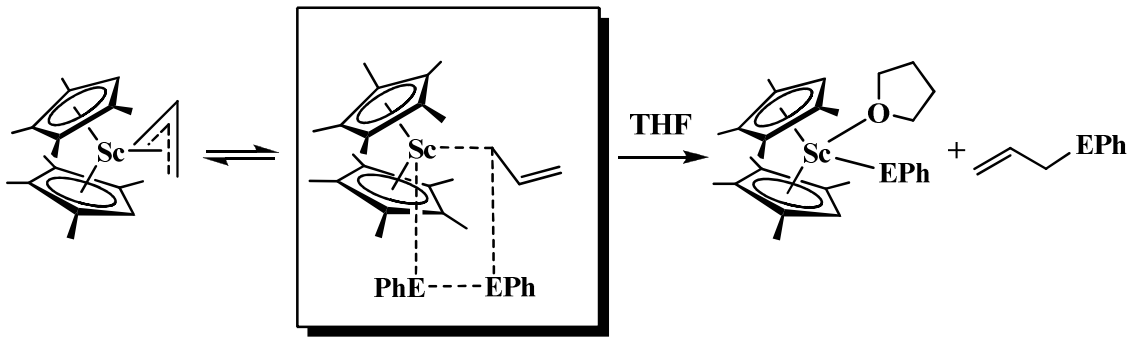

(7.10)

In each of the reactions with the allyl complexes, $(C_5Me_4H)_2Sc(\eta^3\text{-}C_3H_5)$, both in toluene and toluene/THF, the expected allyl phenyl chalcogenide byproduct, C_3H_5EPh, was isolated. In each of these reactions, the allyl complex is acting as a mono-hapto alkyl ligand. Hence, the diphenyldichalcogenide reaction is a good measure of Sc-C bond reactivity.

Examination of the reactions of PhEEPh with $(\eta^5\text{-}C_5Me_4H)_2Sc(\eta^1\text{-}C_5Me_4H)$, **35**, gave the same $[(C_5Me_4H)_2ScEPh]_x$ (x = 0, 1) products as observed with $(C_5Me_4H)_2Sc(\eta^3\text{-}C_3H_5)$, but the reactions were not as clean and the oxide complex, $[(C_5Me_4H)_2Sc]_2(\mu\text{-O})$, was a constant byproduct in the reactions with PhEEPh (E = S, Se). The $(\eta^5\text{-}C_5Me_4H)_2Sc(\eta^1\text{-}C_5Me_4H)$, and $(C_5Me_4H)_2Sc(\eta^3\text{-}C_3H_5)$, reactions were run under analogous conditions, but the allyl reactions were much cleaner. This is consistent with the high reactivity found for $(\eta^5\text{-}C_5R_5)_3M$ complexes. Oxide complexes are often byproducts despite extreme efforts to avoid oxygen in the systems. Hence it can be concluded that although $(\eta^5\text{-}C_5Me_4H)_2Sc(\eta^1\text{-}C_5Me_4H)$, **35**, can react as an η^1-alkyl, it might have other reaction channels that are accessible. The idea that a mono-hapto structure leads to pseudo-alkyl reactivity is sound.

Conclusion

$(C_5Me_4H)_2Sc(\eta^3\text{-}C_3H_5)$, **7**, reacts with PhEEPh (E = S, Se, Te) to form in at least 60 % yield the sigma bond metathesis products C_3H_5EPh and $[(C_5Me_4H)_2Sc(SPh)]_2$, **36**, $(C_5Me_4H)_2Sc(SePh)$, **37**, and $(C_5Me_4H)_2Sc(TePh)$, **38**, respectively, in toluene and $(C_5Me_4H)_2Sc(EPh)(THF)$ (E = S, **39**, Se, **40**, Te, **41**) in toluene/THF. Complex **7** reacts with pySSpy to make the monometallic sulfur derivative $(C_5Me_4H)_2Sc(Spy)$, **42**. A trimetallic ligand redistribution product, $[(C_5Me_4H)Sc(\mu\text{-}SePh)_2]_3$, **43**, was isolated as a byproduct of the PhSeSePh reaction in toluene/THF. In addition, $(C_5Me_4H)_3Sc$, which has a $(\eta^5\text{-}C_5Me_4H)_2Sc(\eta^1\text{-}C_5Me_4H)$ structure in the solid state, was reacted with PhEEPh (E = S, Se, Te) in toluene and these reactions were compared to those of **7** in the respective solvent. It turned out that with $(\eta^5\text{-}C_5Me_4H)_2Sc(\eta^1\text{-}C_5Me_4H)$, the cleanest reaction proceeded with PhTeTePh.

References

(1) Evans, W. J.; Davis, B. L.; Ziller, J. W. *Inorg. Chem.* **2001**, 40, 6341.
(2) Evans, W. J.; Perotti, J. M.; Kozimor, S. A.; Champagne, T. M.; Davis, B. L.; Nyce, G. W.; Fujimoto, C. H.; Clark, R. D.; Johnston, M. A.; Ziller, J. W. *Organometallics* **2005**, *24*, 3916.
(3) Evans, W. J.; Seibel, C. A.; Ziller, J. W. *J. Am. Chem. Soc.* **1998**, *120*, 6745.
(4) Evans, W. J.; Gonzales, S. L.; Ziller, J. W. *J. Am. Chem. Soc.* **1991**, *113*, 7423.
(5) Evans, W. J.; Davis, B. L.; Champagne, T. M.; Ziller, J. W. *Proc. Natl. Acad. Sci.* **2006**, *103*, 12678.
(6) Evans, W. J.; Forrestal, K. J.; Ziller, J. W. *Angew. Chem. Int. Ed. Engl.* **1997**, *36*, 774-776.
(7) a) Evans, W. J.; Ulibarri, T. A.; Chamberlain, L. R.; Ziller, J. W.; Albarez, D. Jr. *Organometallics*, **1990**, *9*, 2124. b) Schumann, H.; Glanz, M.; Hemling, H.; Görlitz, F. H. *J. Organomet. Chem.*, **1993**, *462*, 155. c) Evans, W. J.; Forrestal, K. J.; Ziller, J. W. *J. Am. Chem. Soc.* **1998**, *120*, 2180.
(8) Evans, W. J.; Forrestal, K. J.; Ziller, J. W. *J. Am. Chem. Soc.* **1995**, *117*, 12635-12636.
(9) Evans, W. J.; Mueller, T. J.; Ziller, J. W. *J. Am. Chem. Soc.* **2009**, *131*, 2678-2686.
(10) W. J. Evans, K. J. Forrestal and J. W. Ziller, *J. Am. Chem. Soc.* **1998**, *120*, 9273.
(11) Evans, W. J.; Nyce, G. W.; Clark, R. D.; Doedens, R. J.; Ziller, J. W. *Angew. Chem. Int. Ed.* **1999**, *38*, 1801.
(12) Evans, W. J.; Davis, B. L. *Chem. Rev.* **2002**, *102*, 2119.
(13) Evans, W. J.; Kozimor, S. A.; Ziller, J. W.; Kaltsoyannis, N. *J. Am. Chem. Soc.* **2004**, *126*, 14533-14547.
(14) Mueller, T. J.; Ziller, J. W.; Evans, W. J. *Dalton Trans.* **2010**, *39*, 6767-6773.
(15) Evans, W. J.; Kozimor, S. A.; Nyce, G. W.; Ziller, J. W. *J. Am. Chem. Soc.* **2003**, *125*, 13831.
(16) Evans, W. J.; Kozimor, S. A.; Ziller, J. W. *J. Am. Chem. Soc.* **2003**, *125*, 14264.
(17) Evans, W. J.; Mueller, T. J.; Ziller, J. W. *Chem. Eur. J.* **2010**, *16*, 964.
(18) Evans, W. J.; Montalvo, E.; Champagne, T. M.; Ziller, J. W.; DiPasquale, A. G.; Rheingold, A.; *Organometallics* **2008**, *27*, 3582-3586.
(19) Evans, W. J.; Lorenz, S. E.; Ziller, J. W. *Chem. Comm.* **2007**, 4662-4664.

(20) (a) Kwart, H.; Schwartz, J. L. *J. Org. Chem.* **1974**, *39*, 1575-1583. (b) Kwart, H.; Miles, W. H.; Horgan, A. G.; Kwart, L. D. *J. Am. Chem. Soc.* **1981**, *103*, 1757-1760. (c) Saha, A.; Ranu, B. C. *Tetrahedron Lett.* **2010**, *51*, 1902-1905.
(21) Yu, M.; Zhang, Y.; Bao, W. *Synthetic Commun.* **1997**, *27(4)*, 609-613.
(22) Deryagina, E. N.; Korchevin, N. A. *Russ. Chem. Bull.* **1996**, *45*, 223-225.
(23) Evans, W. J.; Grate, J. W.; Bloom, I.; Hunter, W. E.; Atwood, J. L. *J. Am. Chem. Soc.* **1985**, *107*, 405-409.
(24) Evans, W. J.; Davis, B. L.; Nyce, G. W.; Perotti, J. M.; Ziller, J. W. *J. Organomet. Chem.* **2003**, *677*, 89-95.
(25) Evans, W. J.; Schmiege, B. M.; Lorenz, S. E.; Miller, K. A.; Champagne, T. M.; Ziller, J. W.; DiPasquale, A. G.; Rheingold, A. L. *J. Am. Chem. Soc.* **2008**, *113*, 8555-8563.
(26) Evans, W. J.; Miller, K. A.; Lee, D. S.; Ziller, J. W. *Inorg. Chem.* **2005**, *44*, 4326.
(27) Shannon, R. D. *Acta Cryst*. **1976**, *A32*, 751-767.
(28) Piers, W. E.; Parks, D. J.; MacGillivray, L. R.; Zaworotko, M. J. *Organometallics* **1994**, *13*, 4547-4558.
(29) Piers, W. E.; Ferguson, G., Gallagher, J. F. *Inorg. Chem.* **1994**, *33*, 3784-3787.
(30) De C. T. Carrondo, M. A. A. F; Dias, A. R.; Garcia, H.; Mirpuri, A.; Fátima, M.; Piedade, M.; Salema, M. S. *Polyhedron* **1989**, *8*, 2439-2447. (b) Distances and Angles were determined from the published cif-file by the use of Diamond.
(31) Evans, W. J.; Walensky, J. R.; Ziller, J. W. *Inorg. Chem.* **2010**, *49*, 1743–1749.
(32) Otero, A.; Fernandez-Baeza, J.; Antinolo, A.; Tejeda, J.; Lara-Sanchez, A.; Sanchez-Barba, L.; Martinez-Caballero, E.; Rodriguez, A. M.; Lopez-Solera, I. *Inorg.Chem.* **2005**, *44*, 5336.
(33) Thompson, M. E.; Baxter, S. M.; Bulls, A. R.; Burger, B. J.; Nolan, M. C.; Santarsiero, B. D.; Schaefer, W. P.; Bercaw, J. E.; *J. Am. Chem. Soc.* **1987**, *109*, 203.
(34) Beletskaya, I. P.; Voskoboynikov, A. Z.; Shestakova, A. K.; Yanovsky, A. I.; Fukin, G. K.; Zacharov, L. N.; Struchkov, Y. T.; Schumann, H. *J. Organomet. Chem.* **1994**, *468*, 121.
(35) Demir, S.; Lorenz, S. E.; Fang, M.; Furche, F.; Meyer, G.; Ziller, J. W.; Evans, W. J. *J. Am. Chem. Soc.* **2010**, *132*, 11151-11158.

Chapter 8

Sigma Bond Metathesis Reactivity of $(C_5Me_5)_2Sc(\eta^3\text{-}C_3H_5)$ with Diphenylditelluride, PhTeTePh

Introduction

In chapter 7, it was shown that the scandium allyl complex $(C_5Me_4H)_2Sc(\eta^3\text{-}C_3H_5)$ can undergo a sigma bond metathesis reaction with diphenylditelluride in toluene to form the product $(C_5Me_4H)_2ScTePh$. In order to investigate the ligand size effect in this reaction, the exploration was extended to a starting material containing the slightly larger $(C_5Me_5)^-$ ligand. The analogous reaction of $(C_5Me_5)_2Sc(\eta^3\text{-}C_3H_5)$ and diphenylditelluride in toluene produced an unprecedented scandium tellurium cluster, $\{[(C_5Me_5)Sc]_4(\mu_3\text{-}Te)_4\}$.

Experimental

The manipulations described below were conducted under argon or nitrogen with rigorous exclusion of air and water using Schlenk, vacuum line, and glovebox techniques. Solvents were sparged with UHP argon and dried over columns containing Q-5 and molecular sieves. NMR solvents (Cambridge Isotope Laboratories) were dried over Na/K alloy, degassed, and vacuum-transferred before use. PhTeTePh was purchased from Aldrich and sublimed prior to use. $(C_5Me_5)_2ScCl(THF)$, **26**, was prepared with some modifications of the reported synthesis.[1] An alternative synthesis to the literature method[1] was used for the preparation of $(C_5Me_5)_2Sc(\eta^3\text{-}C_3H_5)$, **32**, see below. ^1H and ^{13}C NMR spectra were recorded on Bruker GN500 or CRYO500 MHz spectrometers at rt.

$(C_5Me_5)_2ScCl(THF)$, 26. In a nitrogen filled glovebox, KC_5Me_5 (1.166 g, 6.689 mmol) was slowly added to a stirred white slurry of $ScCl_3$ (0.519 g, 3.430 mmol) in 80 mL of THF. After the mixture was stirred for 48 h, the suspension was centrifuged to separate insoluble materials, presumably KCl, the supernatant was decanted, and the solution was

evaporated to dryness. The resulting pale-orange powder was extracted with toluene to give a bright orange solution that was evaporated to dryness to yield a pale-orange powder. Washing this powder with hexane leaves $(C_5Me_4H)_2ScCl(THF)$, **26**, as a pale-yellow powder (0.606 g, 42%). Crystals suitable for X-ray diffraction were grown from a concentrated THF solution at –35 ºC over the course of 72 h.

$(C_5Me_5)_2Sc(\eta^3\text{-}C_3H_5)$, 32. In a nitrogen-filled glovebox, allylmagnesium chloride (0.72 mL, 1.4 mmol) was added to a stirred orange slurry of **26** (0.606 g, 1.43 mmol) in 100 mL of toluene. A yellow solution immediately formed. After the mixture was stirred for 24 h, the solution was evaporated to dryness to yield a pale yellow powder. This material was treated with 2% 1,4-dioxane in hexane (75 mL) for 24h and the mixture was centrifuged to separate a white precipitate. The yellow supernatant was decanted and removal of solvent under vacuum yielded $(C_5Me_5)_2Sc(\eta^3\text{-}C_3H_5)$, **32**, (0.372 g, 73%) as a yellow powder. Crystals suitable for X-ray analysis were grown from a concentrated toluene solution of **32** at –35 ºC over the course of 24 h. ^{1}H NMR (500 MHz, benzene-d_6): δ 7.13 (m, 1H, CH_2CHCH_2), 3.29 (s, $\Delta\nu_{1/2}$ = 30 Hz, 2H, allyl *anti* CH_2), 2.14 (1H, allyl *syn* CH_2), 2.15 (1H, allyl *syn* CH_2), 1.86 (s, 30H, C_5Me_5).

$\{[(C_5Me_5)Sc]_4(\mu_3\text{-}Te)_4\}$, 51. In an argon-filled glovebox, PhTeTePh (0.059 g, 0.144 mmol) was added to a yellow solution of $(C_5Me_5)_2Sc(\eta^3\text{-}C_3H_5)$, **32**, (0.050 g, 0.140 mmol) in 10 mL of toluene. After the mixture was stirred for 24 h, the solution was evaporated to dryness to yield a yellow powder. This was washed with a small amount of cold hexane to yield a golden yellow solid (0.028 g, 65%). Crystals of **51** suitable for X-ray analysis were grown in an NMR tube from a concentrated benzene-d_6 solution at room temperature over the course of 2 weeks. ^{1}H NMR (500 MHz, benzene-d_6): δ 1.89 (s, 60H, C_5Me_5).

X-ray Crystallographic Data. Information on X-ray data collection, structure determination, and refinement for **26**, **32** and **51** are given in Table 8.1. Details for X-ray data collection, structure solution and refinement are given in the Appendix.

Table 8.1. X-ray Data Collection Parameters for Complex $(C_5Me_5)_2ScCl(THF)$, **26**, $(C_5Me_5)_2Sc(\eta^3\text{-}C_3H_5)$, **32**, and $\{[(C_5Me_5)Sc]_4(\mu_3\text{-}Te)_4\}$, **51.**

Complex	**26**	**32**	**51**
Empirical formula	C_{24} H_{38} Cl O Sc	C_{23} H_{35} Sc	C_{40} H_{60} Sc_4 Te_4
Fw	422.95	356.47	1231.12
Temperature (K)	148(2)	98(2)	93(2)
Crystal system	Triclinic	Orthorhombic	Triclinic
Space group	$P\bar{1}$	*Cmca*	$P\bar{1}$
a (Å)	8.4353(6)	14.6990(12)	11.4455(8)
b (Å)	16.5792(11)	9.2201(8)	11.6530(8)
c (Å)	18.1925(12)	30.322(3)	18.7846(13)
α (deg)	61.1903(9)	90	86.2700(10)
β (deg)	89.7836(10)	90	86.0220(10)
γ (deg)	87.7080(10)	90	66.6840(10)
Volume $Å^3$	2227.2(3)	4109.5(6)	2293.3(3)
Z	4	8	2
ρ_{calcd} (Mg/m^3)	1.261	1.152	1.783
μ (mm^{-1})	0.462	0.359	3.085
R1 $[I > 2.0\sigma(I)]^a$	0.0777	0.1192	0.1670
wR2 (all data)^a	0.2111	0.3338	0.5016

[a] Definitions: $wR2 = [\Sigma[w(F_o^2-F_c^2)^2] / \Sigma[w(F_o^2)^2]\ ]^{1/2}$, $R1 = \Sigma||F_o|-|F_c|| / \Sigma|F_o|$

Results and Discussion

$(C_5Me_5)_2ScCl(THF)$, 26. The reaction of two equiv of KC_5Me_5 and one equiv of $ScCl_3$ at ambient temperature afforded $(C_5Me_5)_2ScCl(THF)$, **26**, eq 8.1, similar to the preparation of $(C_5Me_5)_2ScCl(THF)$ from $ScCl_3(THF)_3$ and LiC_5Me_5 in xylene at reflux,[1] and analogous to the preparation of $(C_5Me_4H)_2ScCl(THF)$, **6**.[Ch.3] Complex **26** was characterized by X-ray crystallography, Figure 8.1. Unfortunately, the collected data is not of sufficient quality to discuss bond distances and angles.

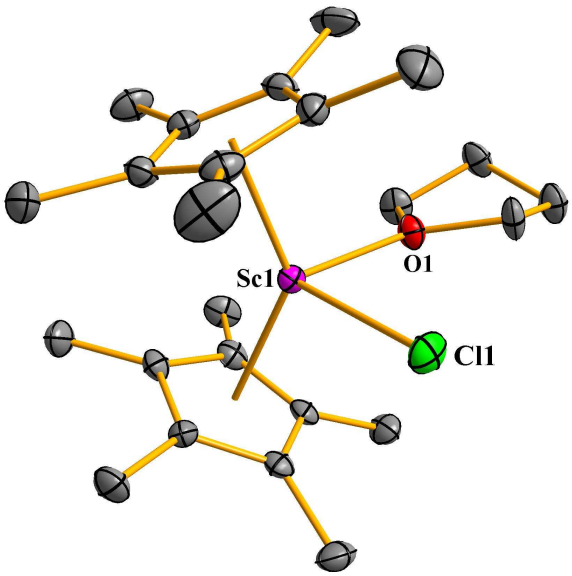

Figure 8.1. Thermal ellipsoid plot of $(C_5Me_5)_2ScCl(THF)$, **26**, drawn at the 50% probability level. Hydrogen atoms are omitted for clarity.

$(C_5Me_5)_2Sc(\eta^3\text{-}C_3H_5)$, 32. The reaction of $(C_5Me_5)_2ScCl(THF)$ with C_3H_5MgCl afforded $(C_5Me_5)_2Sc(\eta^3\text{-}C_3H_5)$, **32**, eq 8.1, thus different to the reported synthesis based on the starting materials of an allene and the corresponding hydride.[1] Complex **32** was characterized by X-ray crystallography, Figure 8.2. The collected data is of poor quality and does not allow a detailed discussion.

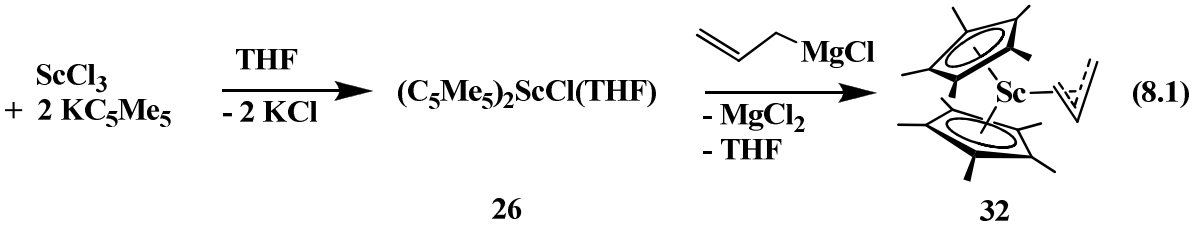

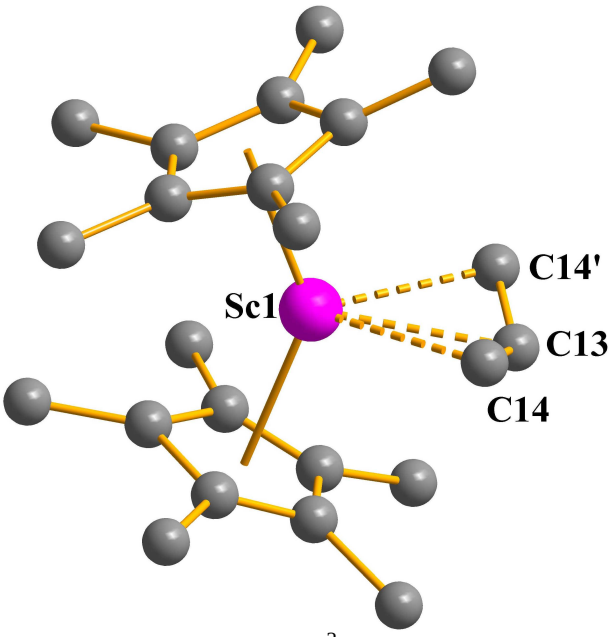

Figure 8.2. Ball-and-Stick plot of $(C_5Me_5)_2Sc(\eta^3\text{-}C_3H_5)$, **32**. Hydrogen atoms are omitted for clarity.

{[(C$_5$Me$_5$)Sc]$_4$(μ_3-Te)$_4$}, 51. $(C_5Me_5)_2Sc(\eta^3\text{-}C_3H_5)$ reacts with PhTeTePh in toluene at ambient temperature to afford a yellow product. The ^{1}H-NMR spectrum of this reaction shows one peak at 1.89 ppm and a few little peaks that could not be assigned. Thus, according to the ^{1}H-NMR spectrum, this reaction does not proceed as cleanly as the analogous reaction of $(C_5Me_4H)_2Sc(\eta^3\text{-}C_3H_5)$ with PhTeTePh in toluene that was discussed in Chapter 7. Complex **51** could be isolated out of this reaction, eq 8.2, Figure 8.3. Since this product was a preliminary result, the mechanism of this reaction is not yet known. Obviously, the reaction must undergo a redox process due to the lack of the phenyl rings of the telluride ligands.

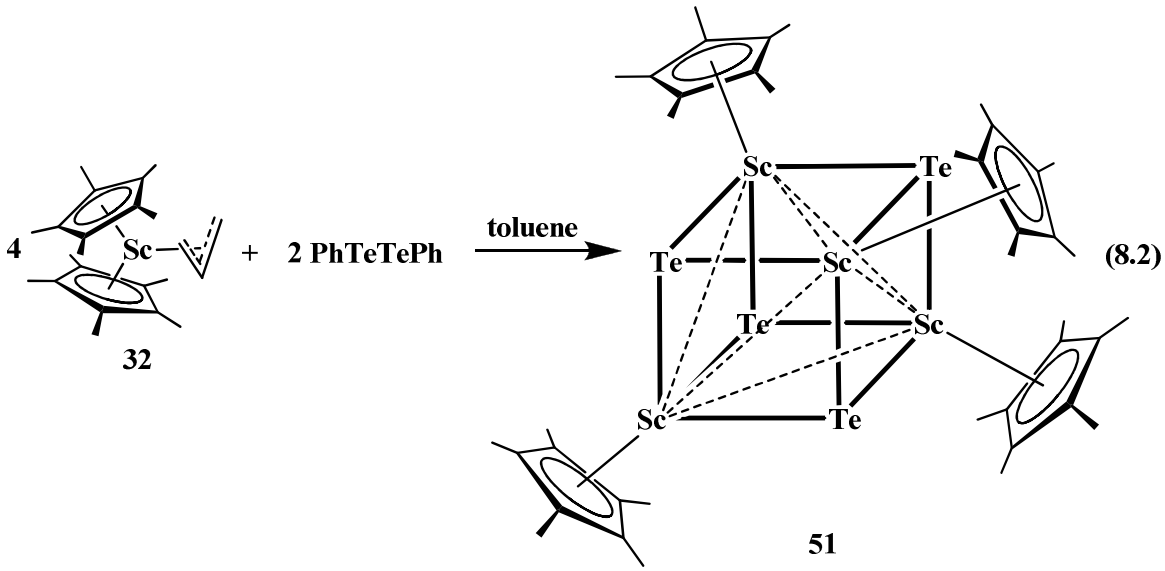

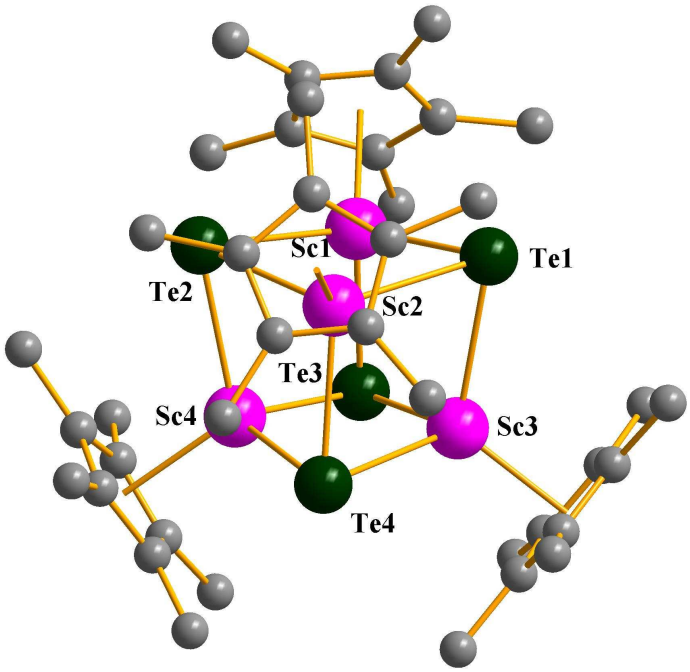

Figure 8.3. Ball-and-Stick plot of {[(C_5Me_5)Sc]$_4$(μ_3-Te)$_4$}, **51**. Hydrogen atoms are omitted for clarity.

In complex **51**, each scandium atom features a coordination number of six. This is different compared to the coordination numbers of the scandocene starting materials (C_5Me_5)$_2$ScCl(THF), **26**, and (C_5Me_5)$_2$Sc(η^3-C_3H_5), **32**. In complex **51**, four (C_5Me_5)Sc units and four μ_3-bridging telluride ligands form a heteronuclear cube, in which all scandium atoms have the oxidation state of +3. The only known compound that can be compared to **51** is a

$(C_5Me_5)^-$ ligated cobalt-tellurium cluster, namely $\{[(C_5Me_5)Co]_4(\mu^3\text{-}Te)_4\}$, **52**,.[2] This could be obtained through the oxidation of the cobalt(II) complex $[(C_5Me_5)CoCl]_2$ with binary Zintl polyanion $[Sn_2Te_6]^{4-}$ in $Li_4Sn_2Te_6 \cdot 8$ *en* (*en* = 1,2-diaminoethane).

The structure of **51** provides only connectivity due to a poor crystal quality, for which reason a detailed structural discussion is neglected. Nonetheless, the interatomic distances between the scandium atoms are about 3.5 Å. Hence, it can be assumed that there are no scandium scandium interactions. This is consistent with the fact that in complex **52**, there are no metal metal interactions as is attested by long Co-Co distances ranging from 3.714(5)-3.876(5) Å. In contrast, the Sc-Te distances seem to lay around 2.8 Å, which would be comparable to the values of 2.7528(12) Å in $[(C_5Me_5)_2Sc]_2(\mu\text{-}Te)$ involving a seven-coordinate scandium.[3] The Te-Sc-Te angles range between 99 and 106° which is an indication for a distortion in the heteronuclear cube. Complex **51** represents the first molecular scandium-tellurium cluster compound.

Conclusion

The complex $(C_5Me_5)_2Sc(\eta^3\text{-}C_3H_5)$, **32**, could be synthesized via a synthetic route using $(C_5Me_5)_2ScCl(THF)$ and C_3H_5MgCl. Compound **32** showed unexpected redox reactivity with PhTeTePh to afford a scandium tellurium cluster complex, namely $\{[(C_5Me_5)Sc]_4(\mu_3\text{-}Te)_4\}$, **51**. This complex represents the first example of a molecular rare earth metal tellurium cluster, whose core features a heteronuclear cube.

References

(1) Thompson, M. E.; Baxter, S. M.; Bulls, A. R.; Burger, B. J.; Nolan, M. C.; Santarsiero, B. D.; Schaefer, W. P.; Bercaw, J. E.; *J. Am. Chem. Soc.* **1987**, *109*, 203.
(2) Zimmermann, C.; Dehnen, S. *Z. Anorg. Allg. Chem.* **2001**, *627*, 847-850.
(3) Piers, W. E.; Parks, D. J.; MacGillivray, L. R.; Zaworotko, M. J. *Organometallics* **1994**, *13*, 4547-4558.

Chapter 9

Facile N_2O Insertion into Metal Carbon Bonds of Lanthanide Allyl Complexes

Introduction

One of the characteristics of organometallic complexes of electropositive metals is that they can readily react with oxygen-containing compounds to make oxide derivatives. In many cases, the source of the oxygen is unknown and it is difficult to isolate and characterize molecular products from these reactions since intractable or insoluble products often form. However, for the metallocenes of yttrium and the lanthanides, oxide complexes of the formula $[(C_5Me_5)_2Ln]_2(\mu\text{-O})$ are often formed that are isolable and fully characterizable.[1-7] Crystallographic data have been obtainable on examples with Ln = La,[3] Ce,[4] Nd,[5] Sm,[1] Y,[2] and Lu[5] as well as several analogs of formula $[(C_5R_5)_2LnL]_2(\mu\text{-O})$ where L = Lewis base.[6-7]

When a new metallocene system of metals of this type is investigated, it is often useful to generate the $[(C_5R_5)_2Ln]_2(\mu\text{-O})$ oxide complex to facilitate identification by NMR spectroscopy in case it is formed as a byproduct. In the case of $[(C_5Me_5)_2Sm]_2(\mu\text{-O})$, the oxide complex was deliberately made with reagents such as pyNO, epoxides, NO, and N_2O.[1] Recent studies of tetramethylcyclopentadienyl complexes of scandium generated a byproduct identified by NMR spectroscopy that was thought to be the analogous oxide in this system, namely $[(C_5Me_4H)_2Sc]_2(\mu\text{-O})$.[8] In efforts to make this complex independently, the reaction of the allyl complex, $(C_5Me_4H)_2Sc(\eta^3\text{-}C_3H_5)$,[8] with N_2O was investigated. However, instead of forming the oxide, N_2O inserted into the Sc-C(allyl) bond. This chapter describes the details of this reaction as well as its extension to allyl yttrium and lanthanide metallocenes.

N_2O has been extensively studied since it is a thermodynamically powerful oxidant, a potent greenhouse gas, and a component in the global nitrogen cycle with its own

metalloenzyme, nitrous oxide reductase, that converts it to dinitrogen and water.[9-11] In reactions with metal complexes, N_2O often functions as an oxo transfer reagent providing either metal oxides or inserting oxygen into metal-ligand bonds.[12-18] Hence, the N_2O insertion reported here is not common. To our knowledge only two isolated examples of N_2O insertion with organometallic complexes of electropositive metals have been reported. In one case, nitrous oxide reacted with $(C_5Me_5)_2M(C_2Ph_2)$ (M = Ti, Zr) to make $(C_5Me_5)_2M[N(O)NCPh{=}CPh]$ in which the $[N(O)NCPh{=}CPh]^{1-}$ ligand surprisingly binds to Ti and Zr only with the nitrogen atoms.[19] In the other example, the samarium complex, $(C_5Me_5)_2Sm(CH_2C_6H_5)(THF)$,[21] reacted with N_2O to generate the dimer as shown in eq 9.1.[20]

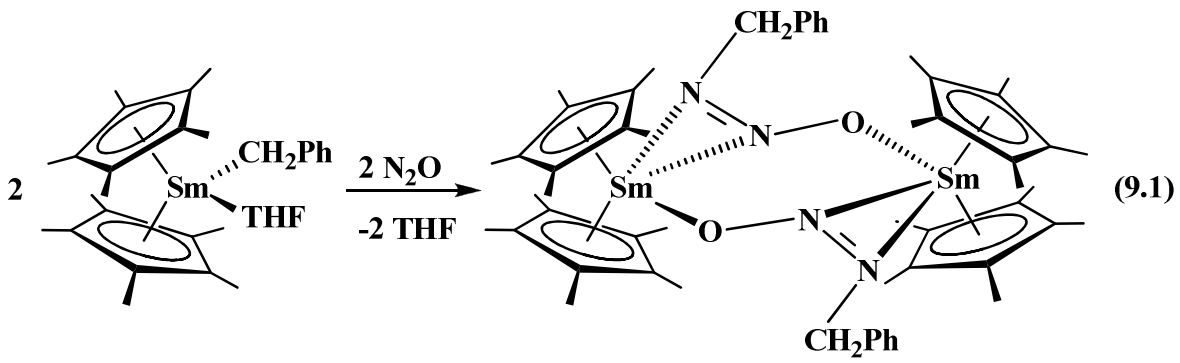

(9.1)

We report here that this N_2O insertion reaction is quite facile with organoscandium, yttrium, and lanthanide allyl metallocenes.

Experimental

The manipulations described below were performed under argon with rigorous exclusion of air and water using Schlenk, vacuum line, and glovebox techniques. Solvents were saturated with UHP grade argon (Airgas) and dried by passage through Glasscontour[27] drying columns before use. NMR solvents (Cambridge Isotope Laboratories) were dried over Na/K alloy, degassed, and vacuum-transferred before use. $(C_5Me_5)_2M(\eta^3\text{-}C_3H_5)$[23] (M = Sm,[22] La, Y[23]) and $(C_5Me_4H)_2M(\eta^3\text{-}C_3H_5)$ (M = Sc,[8] Y[24]) complexes were prepared according to

literature methods. Nitrous oxide (99% Sigma-Aldrich) was used as received. ^{1}H and ^{13}C NMR spectra were recorded on Bruker GN500 or CRYO500 MHz spectrometers. Due to the paramagnetism of samarium, only resonances that could be unambiguously identified are reported. Infrared spectra were recorded as KBr pellets on a Varian 1000 FTIR spectrophotometer at 25 ^{o}C. Elemental analyses were performed on a PerkinElmer 2400Series II CHNS elemental analyzer.

[($C_5Me_4H)_2Sc(\mu$-η^1:η^2-ON=$NC_3H_5)]_2$, 53. A sealable Schlenk flask outfitted with a Teflon stopcock was charged with $(C_5Me_4H)_2Sc(\eta^3$-$C_3H_5)$, **7**, (143 mg, 0.435 mmol) in toluene (10 mL) and a stir bar. The flask was attached to a high vacuum line and the reaction mixture was frozen in liquid nitrogen and placed under vacuum (10^{-5} Torr) for 30 min. One equiv of N_2O was measured into a second, similar Schlenk tube of known volume using a manometer and was subsequently condensed into the first tube. The reaction vessel was sealed and rapidly warmed to room temperature which caused a color change from bright yellow to yellow. Once at room temperature, the reaction flask was returned to the glovebox and the mixture was stirred at room temperature for 4 h. Evaporation of solvent yielded a yellow crystalline material that was washed with hexane until the supernatant was colorless. Complex **53** remained as a yellow crystalline powder (126 mg, 78%). Colorless crystals of **53** suitable for X-ray diffraction were grown over the course of three days from a concentrated toluene solution at -35 °C. ^{1}H NMR (C_6D_6) δ 6.31 (m, 2H, $CH_2C\mathit{H}CH_2$), 5.95 (s, 4H, $C_5Me_4\mathit{H}$), 5.44 (d, 2H, $^{3}J_{trans}$ = 17.0 Hz, $CH_2CH{=}C\mathit{H}_2$ *trans* $C\mathit{H}_2$), 5.18 (d, 2H, $^{3}J_{cis}$ = 10.3 Hz, $CH_2CH{=}C\mathit{H}_2$ *cis* $C\mathit{H}_2$), 4.51 (d, 4H, $^{3}J_{H\text{-}H}$ = 5.8 Hz, $C\mathit{H}_2CH{=}CH_2$), 1.89 (s, 24H, $C_5\mathit{Me}_4H$), 1.69 (s, 24H, $C_5\mathit{Me}_4H$). ^{13}C NMR (C_6D_6) δ 134.8 ($CH_2\mathit{C}HCH_2$), 123.4 (C_5Me_4H), 119.3 (C_5Me_4H), 112.9 (C_5Me_4H), 117.7 ($CH_2CH{=}\mathit{C}H_2$), 56.7 ($\mathit{C}H_2CH{=}CH_2$), 13.3 ($C_5\mathit{Me}_4H$), 10.9 ($C_5\mathit{Me}_4H$). IR: 3083m, 3054m, 3021m, 2969s, 2943s, 2907s, 2860s, 2722m, 2064w, 1941w, 1856w, 1647m, 1603m, 1510m, 1494s, 1451s, 1403s, 1381s, 1331m, 1305m, 1287m, 1184s,

1128s, 1082m, 1021m, 990s, 927s, 823s, 806s, 777s, 730s, 694s, 615m cm^{-1}. Anal. Calcd for $C_{46}H_{74}N_4O_2Sc_2$: C, 67.72; H, 8.39; N; 7.52. Found: C, 67.68; H, 8.85; N, 7.41.

$[(C_5Me_4H)_2Y(\mu\text{-}\eta^1\text{:}\eta^2\text{-ON=NC}_3H_5)]_2$, 54. As described for **53**, **54** was obtained as a colorless crystalline solid (171 mg, 76%) from N_2O (1 equiv) and $(C_5Me_4H)_2Y(\eta^3\text{-}C_3H_5)$, **15**, (200 mg, 0.537 mmol) in toluene (10 mL). Colorless crystals of **54** suitable for X-ray diffraction were grown over the course of three days from a concentrated toluene solution at -35 °C. ^{1}H NMR (C_6D_6) δ 6.17 (m, 2H, $CH_2C\mathit{H}{=}CH_2$), 5.83 (s, 4H, $C_5Me_4\mathit{H}$), 5.15 (m, 4H, $CH_2CH{=}C\mathit{H_2}$), 4.23 (d, 4H, $^3J_{H\text{-}H}$ = 7.0 Hz, $C\mathit{H_2}CH{=}CH_2$), 2.06 (s, 12H, $C_5\mathit{Me}_4H$), 2.00 (s, 12H, $C_5\mathit{Me}_4H$), 1.96 (s, 12H, $C_5\mathit{Me}_4H$), 1.93 (s, 12H, $C_5\mathit{Me}_4H$). ^{13}C NMR (C_6D_6) δ 133.1 ($CH_2\mathit{C}H{=}CH_2$), 120.2 ($CH_2CH{=}\mathit{C}H_2$), 120.0 (C_5Me_4H), 119.5 (C_5Me_4H), 117.9 (C_5Me_4H), 117.3 (C_5Me_4H), 110.6 (C_5Me_4H), 53.5 ($\mathit{C}H_2CH{=}CH_2$), 13.5 ($C_5\mathit{Me}_4H$), 13.4 ($C_5\mathit{Me}_4H$), 12.4 ($C_5\mathit{Me}_4H$), 12.2 ($C_5\mathit{Me}_4H$). IR: 3079m, 3018m, 2966s, 2911s, 2861s, 2725m, 2060w, 1875w, 1646m, 1433s, 1403s, 1382s, 1326m, 1310m, 1288w, 1216s, 1196s, 1134s, 1113m, 1023m, 1013m, 990s, 967m, 936s, 907w, 796s, 785s, 764s, 697w, 620m cm^{-1}. Anal. Calcd for $C_{42}H_{62}N_4O_2Y_2$: C, 60.57; H, 7.50; N, 6.73. Found: C, 60.62; H, 7.46; N, 6.68.

$[(C_5Me_5)_2Y(\mu\text{-}\eta^1\text{:}\eta^2\text{-ON=NC}_3H_5)]_2$, 55. As described for **53**, **55** was obtained as a colorless crystalline solid (106 mg, 87%) from N_2O (1 equiv) and $(C_5Me_5)_2Y(\eta^3\text{-}C_3H_5)$ (110 mg, 0.275 mmol) in toluene (10 mL). Colorless crystals of **55** suitable for X-ray diffraction were grown over the course of 3 d from a concentrated toluene solution at -35 °C. ^{1}H NMR (C_6D_6) δ 6.22 (m, 2H, $CH_2C\mathit{H}{=}CH_2$), 5.19 (m, 4H, $CH_2CH{=}C\mathit{H_2}$), 4.32 (d, 4H, $^3J_{H\text{-}H}$ = 6.8 Hz, $C\mathit{H_2}CH{=}CH_2$), 2.01 (s, 60H, $C_5\mathit{Me}_5$). ^{13}C NMR (C_6D_6) δ 133.2 ($CH_2\mathit{C}H{=}CH_2$), 118.1 (C_5Me_5), 119.8 ($CH_2CH{=}\mathit{C}H_2$), 53.8 ($\mathit{C}H_2CH{=}CH_2$), 12.8 ($C_5\mathit{Me}_5$). IR: 3079m, 2966s, 2905s, 2860s, 2723m, 2063m, 1848w, 1646m, 1496m, 1428s, 1402s, 1380s, 1306m, 1286m, 1211m, 1177s, 1129s, 1061m, 1022m, 989s, 963m, 922s, 795s, 760w, 729w, 672m, 621m cm^{-1}. Anal. Calcd for $C_{46}H_{70}N_4O_2Y_2$: C, 62.16; H, 7.94; N, 6.30. Found: C, 62.31; H, 7.90; N, 6.14.

$[(C_5Me_5)_2Sm(\mu\text{-}\eta^1\text{:}\eta^2\text{-ON=NC}_3H_5)]_2$, 56. As described for **53**, **56** was obtained as a yellow-orange crystalline solid (141 mg, 82%) from N_2O (1 equiv) and $(C_5Me_5)_2Sm(\eta^3\text{-}C_3H_5)$ (157 mg, 0.340 mmol) in toluene (10 mL). ^{1}H NMR (C_6D_6) δ 3.51 (d, 2H, $^3J_{cis}$ = 10.2 Hz, $CH_2CH{=}CH_2$ *cis*), 2.90 (d, 2H, $^3J_{trans}$ = 17.0 Hz, $CH_2CH{=}CH_2$ *trans*), 1.35 (s, 60H, C_5Me_5), -0.29 (d, 4H, $^3J_{H\text{-}H}$ = 6.7 Hz, $CH_2CH{=}CH_2$). ^{13}C NMR (C_6D_6) δ 128.8 ($CH_2CH{=}CH_2$), 117.1 ($CH_2CH{=}CH_2$), 114.0 (C_5Me_5), 46.1 ($CH_2CH{=}CH_2$), 18.6 (C_5Me_5). Anal. Calcd for $C_{50}H_{82}N_4O_2Sm_2$: C, 54.61; H, 6.91; N, 5.54. Found: C, 53.65; H, 7.11; N, 4.85. Although the analytical data give a C:H:N ratio of 12.9:20.4:1 close to the 12.5:20.5:1 ratio expected, the analysis was not as good as that for isomorphous **57**. Crystals of **56** were surprisingly less stable than those of **53**-**55** and **57**.

$[(C_5Me_5)_2La(\mu\text{-}\eta^1\text{:}\eta^2\text{-ON=NC}_3H_5)]_2$, 57. As described for **53**, **57** was obtained as a colorless crystalline solid (121 mg, 73%) from N_2O (1 equiv) and $(C_5Me_5)_2La(\eta^3\text{-}C_3H_5)$ (150 mg, 0.333 mmol) in toluene (10 mL). ^{1}H NMR (C_6D_6) δ 6.19 (m, 2H, $CH_2CH{=}CH_2$), 5.20 (m, 4H, $CH_2CH{=}CH_2$), 4.26 (d, 4H, $^3J_{H\text{-}H}$ = 6.9 Hz, $CH_2CH{=}CH_2$), 2.04 (s, 60H, C_5Me_5). ^{13}C NMR (C_6D_6) δ 133.2 ($CH_2CH{=}CH_2$), 120.1 (C_5Me_5), 119.8 ($CH_2CH{=}CH_2$), 53.4 ($CH_2CH{=}CH_2$), 11.9 (C_5Me_5). IR: 3078m, 2963s, 2909s, 2859s, 2725m, 2062w, 1875w, 1646m, 1496m, 1439s, 1422s, 1398s, 1380s, 1304m, 1286m, 1207m, 1173s, 1129s, 1061m, 1022m, 1003m, 990m, 961m, 935m, 908m, 803w, 788s, 729w, 694w, 619w cm^{-1}. Anal. Calcd for $C_{46}H_{70}N_4O_2La_2$: C, 55.87; H, 7.13; N, 5.67. Found: C, 55.85; H, 7.79; N, 5.26.

X-ray Crystallographic Data. Information on X-ray data collection, structure determination, and refinement for **53** and **54** is given in Table 9.1 and **55, 56** and **57** is given in Table 9.2.

Table 9.1. X-ray Data Collection Parameters for $[(C_5Me_4H)_2Sc(\mu\text{-}\eta^1{:}\eta^2\text{-}ON{=}NC_3H_5)]_2$, **53**, and $[(C_5Me_4H)_2Y(\mu\text{-}\eta^1{:}\eta^2\text{-}ON{=}NC_3H_5)]_2$, **54.**

Complex	**53**	**54**
Empirical formula	$C_{42}H_{62}N_4O_2Sc_2$ •2(C_7H_8)	$C_{42}H_{62}N_4O_2Y_2$ •2(C_7H_8)
Fw	929.14	1017.04
Temperature (K)	143(2)	93(2)
Crystal system	Monoclinic	Monoclinic
Space group	*C*2/*c*	*C*2/*c*
a (Å)	15.7970(13)	15.5705(7)
b (Å)	12.9336(11)	13.2395(6)
c (Å)	26.217(2)	26.4343(12)
α (deg)	90	90
β (deg)	106.2580(10)	105.9252(5)
γ (deg)	90	90
Volume $Å^3$	5142.2(7)	5240.2(4)
Z	4	4
ρ_{calcd} *(Mg/m^3)*	1.200	1.289
μ *(mm^{-1})*	0.308	2.247
R1[a] *[I > 2.0σ(I)]*	0.0924	0.0383
wR2[b] *(all data)*	0.2587	0.0915

[a] $R1 = \Sigma \,|\,|F_o| - |F_c|\,| / \Sigma\,|F_o|$
[b] $wR2 = [\Sigma\,[w\,(F_0^2-F_c^2)^2 / \Sigma[w\,(F_o^2)^2]]^{1/2}$

Table 9.2. X-ray Data Collection Parameters for $[(C_5Me_5)_2Y(\mu\text{-}\eta^1:\eta^2\text{-}ON{=}NC_3H_5)]$, **55**, $[(C_5Me_5)_2Sm(\mu\text{-}\eta^1:\eta^2\text{-}ON{=}NC_3H_5)]$, **56**, and $[(C_5Me_5)_2La(\mu\text{-}\eta^1:\eta^2\text{-}ON{=}NC_3H_5)]$, **57**.

Complex	**55**	**56**	**57**
Empirical formula	$C_{46}H_{70}N_4O_2Y_2$ •$2(C_7H_8)$	$C_{46}H_{70}N_4O_2Sm_2$ •$2(C_7H_8)$	$C_{46}H_{70}N_4O_2La_2$ •$2(C_7H_8)$
Fw	1073.15	1196.03	1173.15
Temperature (K)	183(2)	173(2)	143(2) K
Crystal system	Monoclinic	Monoclinic	Monoclinic
Space group	$P2_1/n$	$P2_1/n$	$P2_1/n$
a (Å)	15.8443(8)	14.8358(6)	14.6563(9)
b (Å)	13.9604(7)	14.0396(5)	14.1978(8)
c (Å)	25.2595(12)	27.3264(10)	27.4602(16)
α (deg)	90	90	90
β (deg)	91.3400(6)	93.5110(10)	93.2795(7)
γ (deg)	90	90	90
Volume Å^3	5585.7(5)	5681.1(4)	5704.8(6)
Z	4	4	4
ρ_{calcd} *(Mg/m^3)*	1.276	1.398	1.366
μ *(mm^{-1})*	2.112	2.090	1.521
R1 [I > 2.0σ(I)]	0.0361	0.0308	0.0261
wR2 (all data)	0.0961	0.0847	0.0641

[a] $R1 = \Sigma \,||F_o| - |F_c|| / \Sigma |F_o|$
[b] $wR2 = [\Sigma [w (F_0^2-F_c^2)^2 / \Sigma[w (F_o^2)^2]]^{1/2}$

Results and Discussion

Recent efforts to make the first dinitrogen complex of scandium focused on the reduction of $[(C_5Me_4H)_2Sc][(\mu\text{-}Ph)BPh_3]$, **8**, with KC_8 under nitrogen.[Ch.3] This generated a highly reactive species, $[(C_5Me_4H)_2Sc]_2(\mu\text{-}\eta^2:\eta^2\text{-}N_2)$, that decomposed in one case to grow a crystal containing both dinitrogen and oxide ligands, $[(C_5Me_4H)_2Sc]_2(\mu\text{-}\eta^2:\eta^2\text{-}$

$N_2)[(C_5Me_4H)_2Sc]_2(\mu\text{-}O)$.[8,Ch.3] To be able to identify $[(C_5Me_4H)_2Sc]_2(\mu\text{-}O)$ by NMR spectroscopy, an independent synthesis was pursued.

Since N_2O is used as a source of oxide[12-18] and since it was previously found that $(C_5Me_5)_2Sm(THF)_2$ reacts with N_2O to make $[(C_5Me_5)_2Sm]_2(\mu\text{-}O)$,[1] the reaction of $(C_5Me_4H)_2Sc(\eta^3\text{-}C_3H_5)$ with N_2O was examined. The allyl complex was chosen since it is one of the more readily accessible reactive M-C bonded species available with electropositive metallocenes.[22] Although this reaction was not analogous to the samarium reaction involving metal based reduction,[1] we assumed that this combination would ultimately form the oxide complex, since metallocene oxides of this type are so readily formed even without any obvious source of oxygen.

As shown in eq 9.2, this reaction did not give an oxide, but instead led to an insertion product $[(C_5Me_4H)_2Sc(\mu\text{-}\eta^1{:}\eta^2\text{-}ON{=}NCH_2CH{=}CH_2)]_2$, **53**, containing an allyl azoxy ligand, figure 9.1. The ^1H NMR spectrum showed resonances consistent with a localized allyl ligand and a single set of $(C_5Me_4H)^-$ resonances that integrated appropriately for **53**. No evidence for any other products containing $(C_5Me_4H)^-$ was observed.

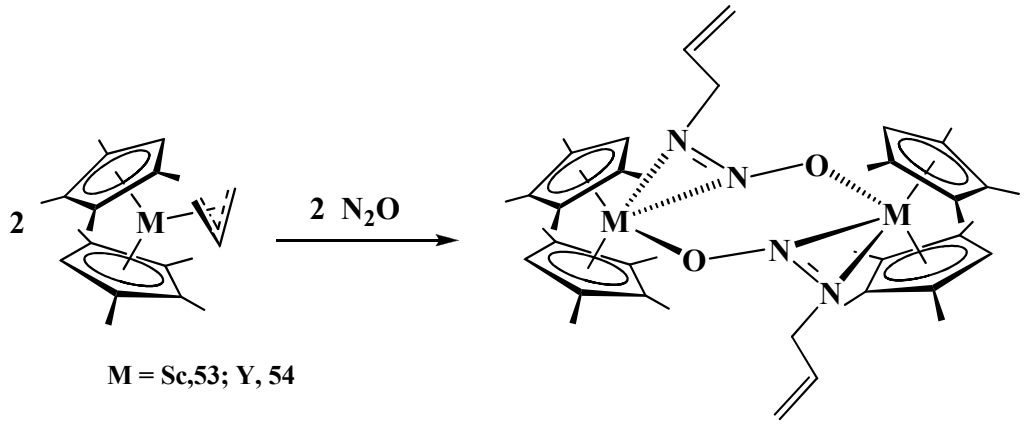

(9.2)

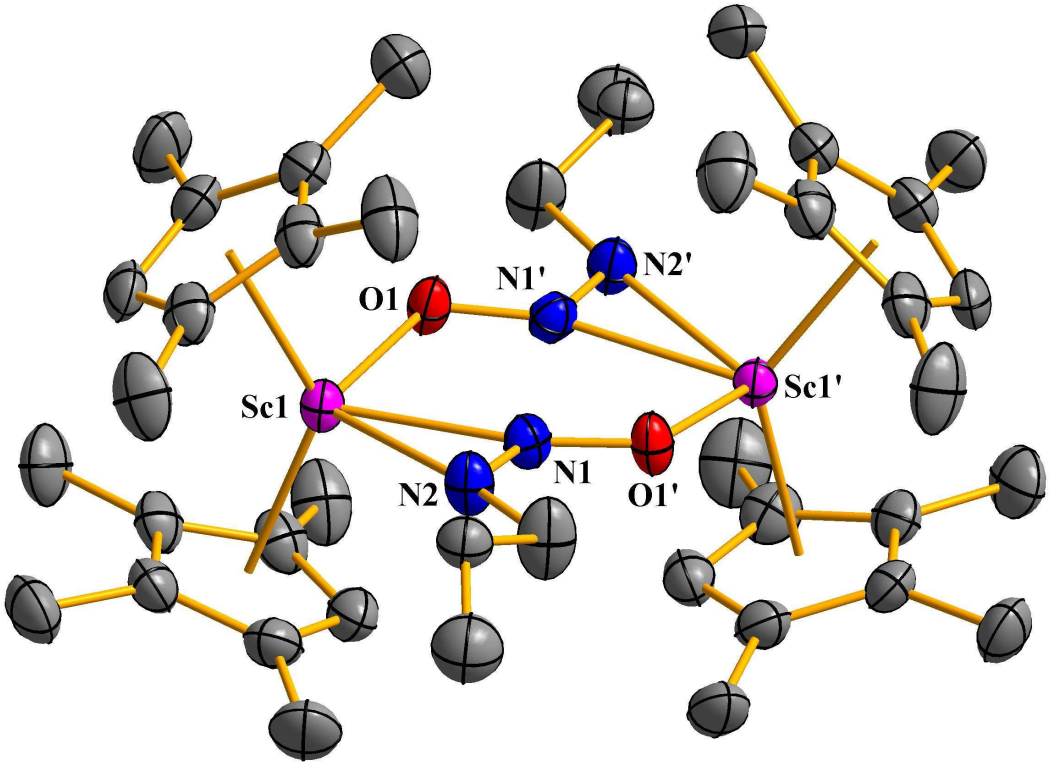

Figure 9.1. Thermal ellipsoid plot of $[(C_5Me_4H)_2Sc(\mu\text{-}\eta^1{:}\eta^2\text{-}ON{=}NC_3H_5)]_2$, **53**, drawn at the 50% probability level with hydrogen atoms omitted for clarity.

Complex **53** was definitively identified by X-ray crystallography which showed that it crystallizes as a dimer in the solid state. The $(RN_2O)^{1-}$ ligands bridge the two metallocenes in a $\mu\text{-}\eta^1{:}\eta^2$-mode, eq. 9.3, analogous to that found in the product of reacting $(C_5Me_5)_2Sm(CH_2C_6H_5)(THF)$[21] with N_2O, eq 9.1.[20]

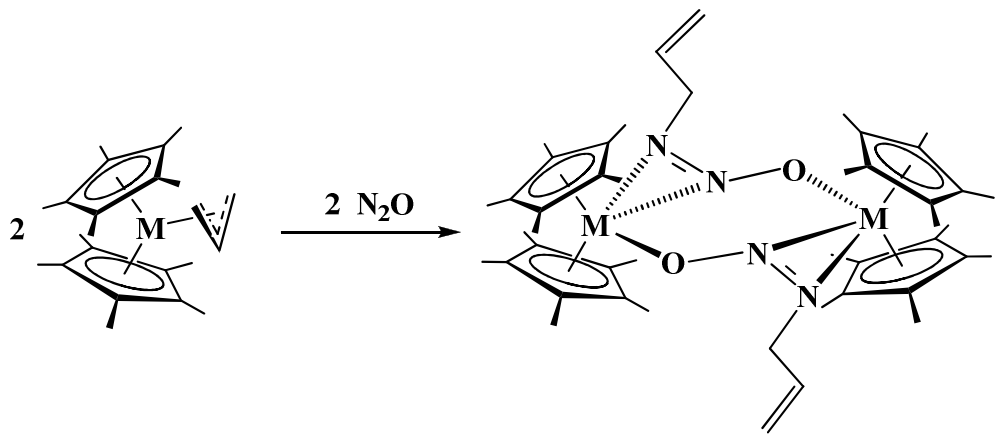

(9.3)

M = Y, 55; Sm, 56; La, 57

To determine the generality of $(RN_2O)^{1-}$ ligand formation with metallocene allyl complexes as a function of metal and ancillary ligand, analogous reactions were examined with $(C_5Me_4H)_2Y(\eta^3\text{-}C_3H_5)$ and $(C_5Me_5)_2M(\eta^3\text{-}C_3H_5)$ (M = Y, Sm, La). As shown in eq 9.3, products analogous to **53** were formed in each case and provided complexes that could be analyzed by X-ray diffraction, Figure 9.2-9.5. In Figure 9.6, a picture of a single crystal of $[(C_5Me_5)_2La(\mu\text{-}\eta^1{:}\eta^2\text{-}ON{=}NC_3H_5)]_2$ is shown.

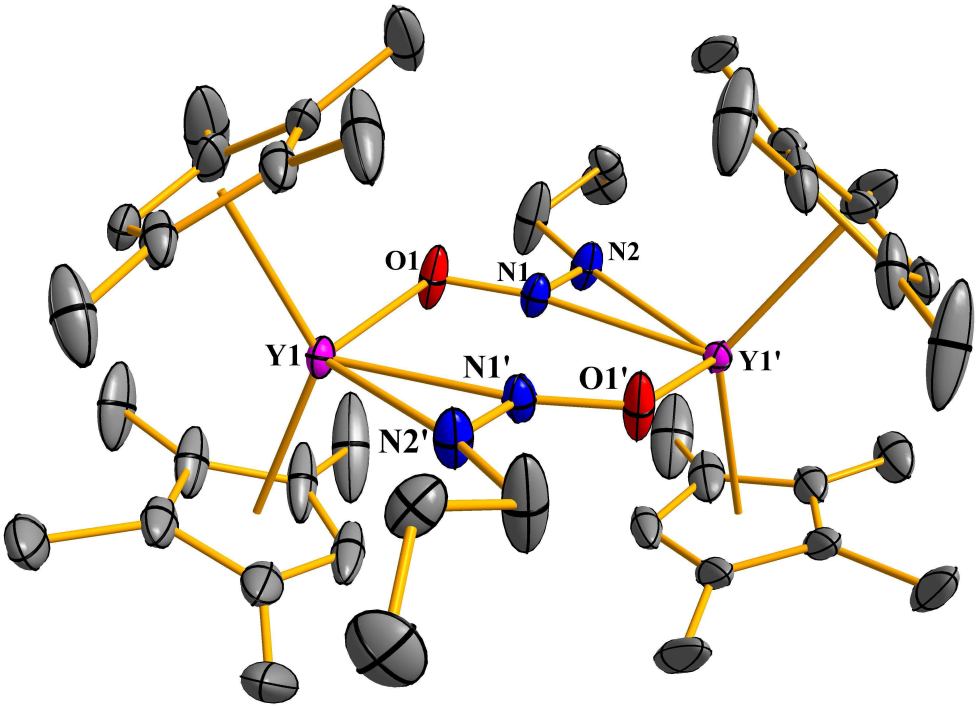

Figure 9.2. Thermal ellipsoid plot of $[(C_5Me_4H)_2Y(\mu\text{-}\eta^1{:}\eta^2\text{-}ON{=}NC_3H_5)]_2$, **54**, drawn at the 50% probability level with hydrogen atoms omitted for clarity.

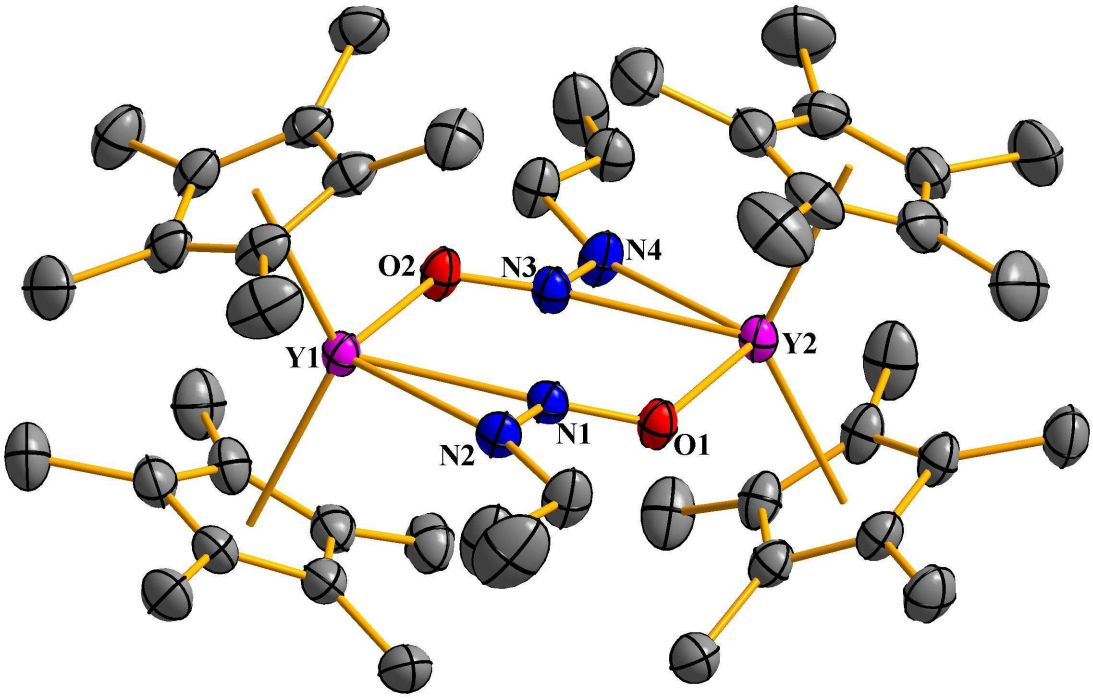

Figure 9.3. Thermal ellipsoid plot of $[(C_5Me_5)_2Y(\mu\text{-}\eta^1{:}\eta^2\text{-}ONNC_3H_5)]_2$, **55**, drawn at the 50% probability level with hydrogen atoms omitted for clarity.

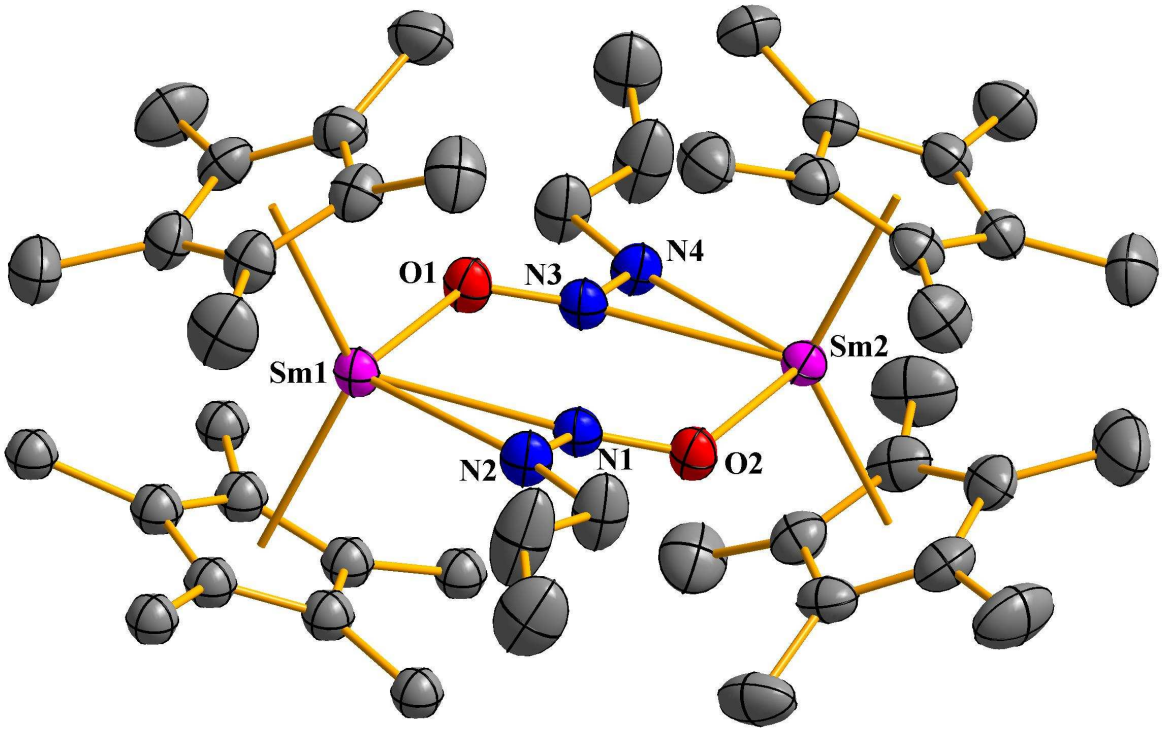

Figure 9.4. Thermal ellipsoid plot of $[(C_5Me_5)_2Sm(\mu\text{-}\eta^1{:}\eta^2\text{-}ON{=}NC_3H_5)]_2$, **56**, drawn at the 50% probability level with hydrogen atoms omitted for clarity.

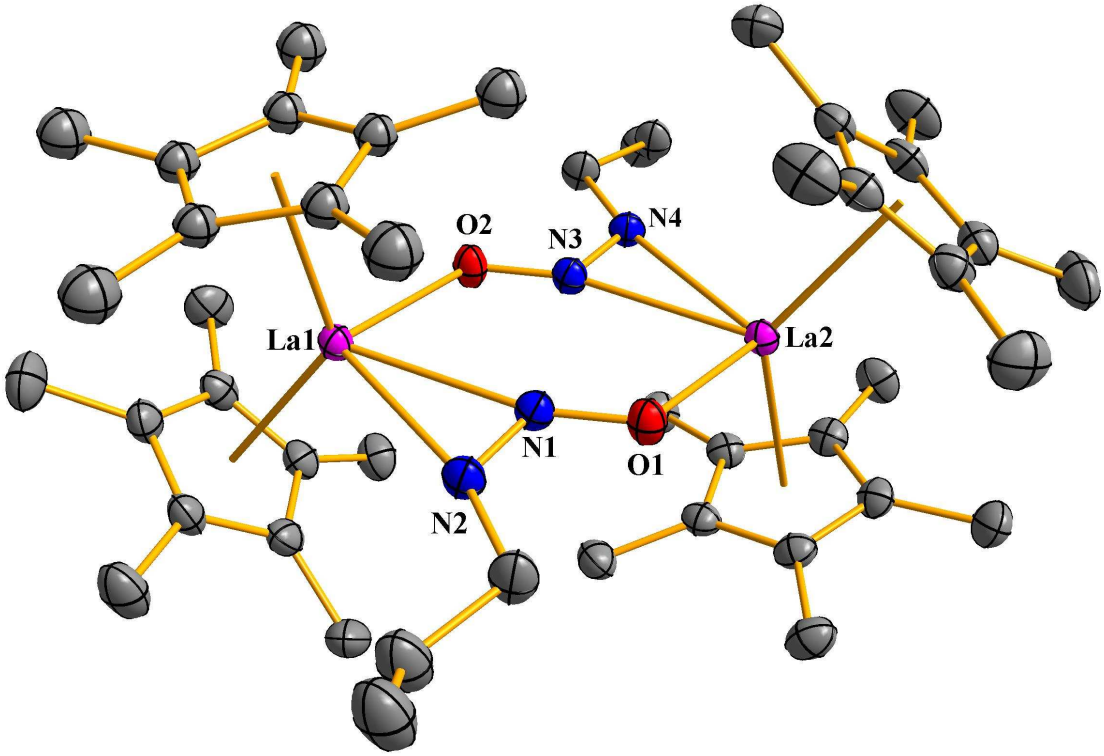

Figure 9.5. Thermal ellipsoid plot of $[(C_5Me_5)_2La(\mu\text{-}\eta^1{:}\eta^2\text{-}ONNC_3H_5)]_2$, **57**, drawn at the 50% probability level with hydrogen atoms omitted for clarity.

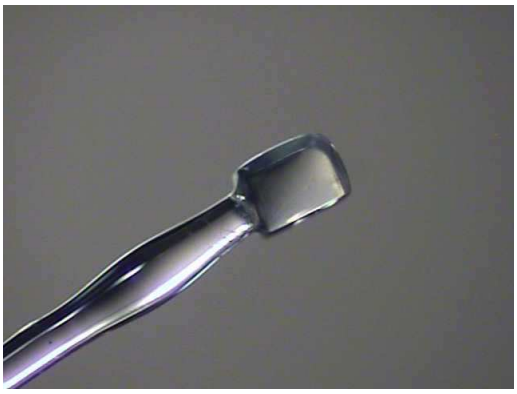

Figure 9.6. Picture of the single crystal $[(C_5Me_5)_2La(\mu\text{-}\eta^1{:}\eta^2\text{-}ONNC_3H_5)]_2 \bullet 2(C_7H_8)$, **57**.

Since the $[(C_5Me_5)_2Ln]_2(\mu\text{-}O)$ oxides are known for Ln = La,[3] Sm,[1] and Y,[2] the formation of an oxide byproduct in these reactions could be determined by NMR spectroscopy. No evidence for oxide formation was found in any of the spectra.

It should be noted that insertion chemistry has also been observed recently with NO and metallocene allyls of these metals.[28] Specifically, the $(C_5Me_5)_2M(\eta^3\text{-}C_3H_5)$ complexes (M = Y, Sm, La) react with NO to form $\{(C_5Me_5)_2M[\mu\text{-}ONN(CH_2CH{=}CH_2)O]\}_2$ products.

Structural Studies

Complexes **53** and **54** are isomorphous as are **55-57**. Each complex contains a nine-coordinate lanthanide metal center ligated by two polyalkylcyclopentadienyl ligands, two nitrogen atoms of one $(RN_2O)^{1-}$ ligand, and an oxygen of the other $(RN_2O)^{1-}$ ligand, Figure 9.1-9.5 show the structures of **53-57**. Selected bond distances and angles for **54-57** are shown in Table 9.3. The data on **53** established connectivity, but was not of sufficient quality to discuss metrical parameters.

In each case the N-N and N-O bond distances in the $(RN_2O)^-$ ligand are in the N=N double and N-O single bond regions, respectively.[25] This suggests that the ligand is more appropriately considered as an allyl substituted azoxy ligand coordinating through the N=N bond rather than an allyl nitroso amide coordinating through a single nitrogen. Further support for this view comes from the bond distances to the metal. The structures of **55-57** each have two similar M-N distances consistent with azo ligation rather than one short and one longer as expected for an amide/amine coordination mode. Surprisingly, **54** has two rather different Y-N distances despite N-N and N-O distances like those in **55-57**.

The C-C bond distances of the allyl substituents in each $(RN_2O)^-$ ligand are consistent with localized C-C single and C=C double bonds.[25] The 2.419(2) Å Sm-O and 2.556(3) and 2.565(3) Å Sm-N bond distances in the samarium complex **56** are equivalent to the corresponding bond distances in the previously reported benzyl complex, $[(C_5Me_5)_2Sm(\mu\text{-}\eta^1{:}\eta^2\text{-}ON{=}NCH_2Ph)]_2$, **58**,[20] [2.422(2) Å Sm-O; 2.557(3) and 2.579(2) Å Sm-N]. These Sm-N distances are considerably longer than the 2.39(1)-2.45(1) Å distances in the azobenzene

complex, $(C_5Me_5)_2Sm(PhNNPh)(THF)$,[26] that has 1.32(1)-1.39(2) Å N-N bond distances (two molecules in the unit cell). The Sm-O distance in **56** is much shorter than the 2.532(8)-2.557(9) Å Sm-O(THF) bond lengths in $(C_5Me_5)_2Sm(PhNNPh)(THF)$.[26]. The fact that the Sm-O bond in **56** is shorter than these latter typical Sm-O(neutral donor ligand) distances is also consistent with the allyl azoxy coordination mode discussed above.

Table 9.3. Selected Bond Distances (Å) and Angles (deg) in $[(C_5Me_4H)_2Y(\mu\text{-}\eta^1{:}\eta^2\text{-}ON{=}NC_3H_5)]_2$, **54**, $[(C_5Me_5)_2Y(\mu\text{-}\eta^1{:}\eta^2\text{-}ON{=}NC_3H_5)]$, **55**, $[(C_5Me_5)_2Sm(\mu\text{-}\eta^1{:}\eta^2\text{-}ON{=}NC_3H_5)]$, **56**, and $[(C_5Me_5)_2La(\mu\text{-}\eta^1{:}\eta^2\text{-}ON{=}NC_3H_5)]$, **57**.

	54	**55**	**56**	**57**
M(1)-Cnt	2.345, 2.366	2.405, 2.389	2.464, 2.486	2.550, 2.559
M(1)-N(1)	2.410(2)	2.484(2)	2.556(3)	2.642(2)
M(1)-N(2)	2.484(2)	2.508(2)	2.565(3)	2.640(2)
M(1)-O(1)	2.324(2)	2.354(2)	2.419(2)	2.490(1)
N(1)-N(2)	1.264(3)	1.264(2)	1.258(3)	1.258(2)
N(1)-O(2)	1.300(2)	1.305(2)	1.306(3)	1.307(2)
N(2)-C(41)	1.474(3)	1.468(3)	1.477(4)	1.476(3)
C(41)-C(42)	1.592(6)	1.498(3)	1.495(5)	1.502(3)
C(42)-C(43)	1.311(9)	1.230(4)	1.205(6)	1.248(4)
Cnt1-M(1)-Cnt2	131.1	129.9	130.9	131.8
M(1)-O(1)-N(3)	117.2(1)	120.9(1)	121.3(2)	120.2(1)
O(1)-N(3)-M(2)	161.1(2)	163.6(1)	163.6(9)	163.3(1)
O(1)-M(1)-N(1)	80.62(6)	74.93(5)	74.72(7)	75.82(5)

Cnt = centroid of the $(C_5Me_5)^{1-}$ or $(C_5Me_4H)^{1-}$ ligand

Complexes **54** and **55** provide an opportunity to compare $(C_5Me_4H)^-$ vs $(C_5Me_5)^-$ analogs. The Y-(ring centroid), Y-N(2), and Y-O(1) distances are 0.02-0.03 Å shorter in the $(C_5Me_4H)^{1-}$ complex. This is consistent with the slightly smaller size of the ligand and its less electron donating nature that may lead to a stronger metal allyl azoxy interation. The Y-N(1) distance in **54** is also shorter, but the difference, 0.07 Å, is larger than for the other bonds. As described above, this distance in **54** is unusual.

Conclusion

N_2O readily reacts with allyl metallocene complexes of Sc, Y, and the lanthanides to make allyl azoxy $(RN_2O)^-$ ligands that can bridge two metal centers to make bimetallic complexes, $[(C_5Me_4R)_2M(\mu\text{-}\eta^1{:}\eta^2\text{-ON=NC}_3H_5)]_2$. Hence, insertion rather than delivery of oxygen is the preferred mode of reaction. Interestingly, NO behaves similarly with metallocene allyls of these metals.

References

(1) Evans, W. J.; Grate, J. W.; Bloom, I.; Hunter, W. E.; Atwood, J. L. *J. Am. Chem. Soc.* **1985**, *107*, 405.
(2) Ringelberg, S. N.; Meetsma, A.; Troyanov, S. I.; Hessen, B.; Teuben, J. H. *Organometallics* **2002**, *21*, 1759.
(3) Evans, W. J.; Davis, B. L.; Nyce, G. W.; Perotti, J. M.; Ziller, J. W. *J. Organomet. Chem.* **2003**, *677*, 89.
(4) Evans, W. J.; Rego, D. B.; Ziller, J. W. *Inorg. Chem.* **2006**, *45*, 10790.
(5) Deposited in the Cambridge Crystallographic Data Base.
(6) Evans, W. J.; Drummond, D. K.; Hughes, L. A.; Zhang, H.; Atwood, J. L. *Polyhedron* **1988**, *7*, 1693.
(7) Deelman, B. J.; Booij, M.; Meetsma, A.; Teuben, J. H.; Kooijman, H.; Spek, A. L. *Organometallics* **1995**, *14*, 2306.
(8) Demir, S.; Lorenz, S. E.; Fang, M.; Furche, F.; Meyer, G.; Ziller, J. W.; Evans, W. J. *J. Am. Chem. Soc.* **2010**, *132*, 11151-11158.
(9) Tolman, W. B. *Angew. Chem. Int. Ed.* **2010**, *49*, 2-9.
(10) Trogler, W. C. *Coord. Chem. Rev.* **1999**, *187*, 303-327.
(11) Leont'ev, A. V.; Fomicheva, O. A.; Proskurnina, M. V.; Zefirov, N. S. Russ. *Chem. Rev.* **2001**, *37*, 91-104.
(12) Bottomley, F.; Paez, D. E.; White, P. S. *J. Am. Chem. Soc.* **1982**, *104*, 5651-5657.
(13) Hall, K. A.; Mayer, J. M. *J. Am. Chem. Soc.* **1992**, *114*, 10402-10411.
(14) Smith III, M. R.; Matsunaga, P. T.; Andersen, R. A. *J. Am. Chem. Soc.* **1993**, *115*, 7049-7050.
(15) Howard, W. A.; Parkin, G. *J. Am. Chem. Soc.* **1994**, *116*, 606-615.
(16) Baranger, A. M.; Hanna, T. A.; Bergman, R. G. *J. Am. Chem. Soc.* **1995**, *117*, 10041-10046.
(17) List, A. K.; Koo, K.; Rheingold, A. L.; Hillhouse, G. L. *Inorg. Chim. Acta* **1998**, *270*, 399-404.
(18) Yu, H.; Jia, G.; Lin, Z. *Organometallics* **2009**, *28*, 1158-1164 and references therein.
(19) Vaughan, G. A.; Sofield, C. D.; Hillhouse, G. L.; Rheingold, A. L. *J. Am. Chem. Soc.* **1989**, *111*, 5491.
(20) Labahn, T.; Mandel, A.; Magull, J. *Z. Anorg. Allg. Chem.* **1999**, *625*, 1273.
(21) Evans, W. J.; Ulibarri, T. A.; Ziller, J. W. *Organometallics* **1991**, *10*, 134.
(22) Evans, W. J.; Seibel, C. A.; Ziller, J. W. *J. Am. Chem. Soc.* **1998**, *120*, 6745.
(23) Evans, W. J.; Kozimor, S. A.; Brady, J. C.; Davis, B. L.; Nyce, G. W.; Seibel, C. A.; Ziller, J. W.; Doedens, R. J. *Organometallics* **2005**, *24*, 2269.
(24) Lorenz, S. E.; Schmiege, B. M.; Lee, D. S.; Ziller, J. W.; Evans, W. J. *Inorg. Chem.* **2001**, *49*, 6655-6663.

(25) Allen, F. H.; Kennard, O.; Watson, D. G.; Brammer, L.; Orpen, A. G.; Taylor, R. *J. Chem. Soc., Perkin Trans. II* **1987**, S1.
(26) Evans, W. J.; Drummond, D. K.; Chamberlain, L. R.; Doedens, R. J.; Bott, S. G.; Zhang, H.; Atwood, J. L. *J. Am. Chem. Soc.* **1988**, *110*, 4983.
(27) http://www.glasscontoursolventsystems.com/
(28) Casely, I. J.; Suh, Y.; Ziller, J. W.; Evans, W. J. *Organometallics* **2010**, *29*, 5209-5214.

Chapter 10

Carbodiimide Insertion into the Metal Carbon Bond of

$(C_5Me_4H)_2Sc(\eta^3\text{-}C_3H_5)$

Introduction

The insertion of carbodiimides (RNCNR, where R = alkyl, aryl) into metal alkyl bonds provides access to amidinate moieties, that have proven to act as valuable ancillary ligands in their own right.[1]

A growing number of lanthanide and actinide amidinate complexes are known, the synthesis of which is commonly via an ionic metathesis reaction that comprises the use of an amidinate salt. Alternatively, the insertion chemistry of carbodiimides has been examined with yttrium and f-element alkyl,[2] alkynyl,[3] and amide[4] complexes.[5] Equation 10.1 shows one typical example of an insertion reaction into the M-C bond.[2a]

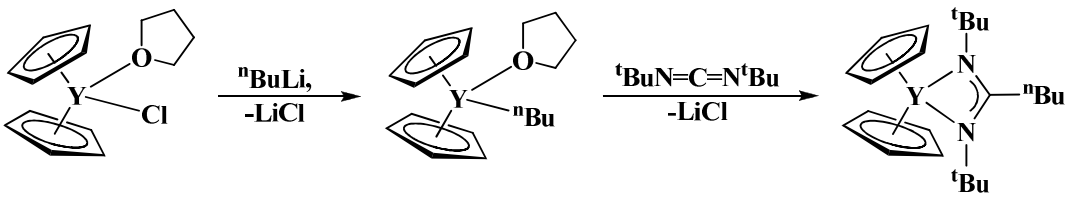

(10.1)

In comparison to these results observed in yttrium, lanthanide and actinide chemistry, there are also some examples known of scandium amidinate complexes. Among those it can be distinguished between mono- and di-amidinate compounds of scandium, for example $\{[(Ar)NC(Ph)N(Ar)\text{-}\kappa^2N,N']Sc(CH_2SiMe_3)(THF)_2\}[BPh_4]$ (Ar = 2,6-diisopropylphenyl)[6] and $\{[(Me_3Si)NC(Ph)N(SiMe_3)\text{-}\kappa^2N,N']_2ScH\}_2$.[7] In contrast, there are no cyclopentadienyl scandium amidinates, featuring a RNCNR (R = alkyl, aryl) known. However, a structurally related compound to metallocene amidinate complexes is the reported example of $(C_5Me_5)_2Sc[(H)NC(Me)N(NMe_2)\text{-}\kappa^2N,N']$.[8] This complex is prepared by the reaction of

$(C_5Me_5)_2ScMe$ with 1 eq 2,2-dimethylhydrazine and subsequent dissolution in acetonitrile, eq 10.2.[8]

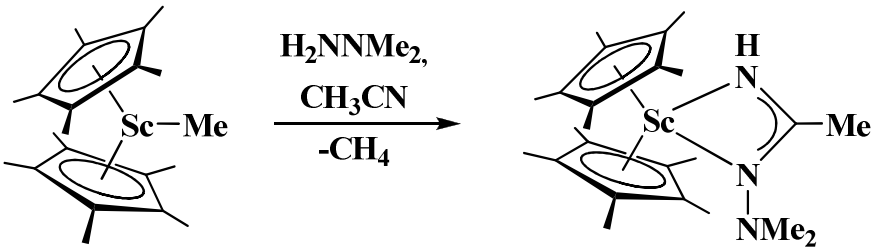

(10.2)

Metallocene allyls of the lanthanides are conveniently prepared stable sources of M-C bond containing complexes and are ideal for studying further reactivity.[8,10] In chapter 9, the facile N_2O insertion reaction into allyl metallocenes of organoscandium, yttrium, and lanthanide complexes was described. On the basis of this type of insertion reaction, the complex $(C_5Me_4H)_2Sc(\eta^3\text{-}C_3H_5)$ has been used as the starting material for the insertion of carbodiimides into the M-C bond in this chapter. The reaction of $(C_5Me_4H)_2Sc(\eta^3\text{-}C_3H_5)$ with $^iPrN{=}C{=}N^iPr$ afforded $(C_5Me_4H)_2Sc[(^iPr)NC(CH_2CH{=}CH_2)N(^iPr)\text{-}\kappa^2N,N']$, **59**.

Experimental

The manipulations described below were conducted under argon with rigorous exclusion of air and water using Schlenk, vacuum line, and glovebox techniques. Solvents were sparged with UHP argon and dried over columns containing Q-5 and molecular sieves. NMR solvents (Cambridge Isotope Laboratories) were dried over Na/K alloy, degassed, and vacuum-transferred before use. $(C_5Me_4H)_2Sc(\eta^3\text{-}C_3H_5)$ was prepared according to literature methods.[Ch.3] ^1H NMR spectrum was recorded on a Bruker DRX500 spectrometer at 25 °C.

$(C_5Me_4H)_2Sc[(^iPr)NC(CH_2CH{=}CH_2)N(^iPr)\text{-}\kappa^2N,N']$, 59. In an argon-filled glovebox, $(C_5Me_4H)_2Sc(\eta^3\text{-}C_3H_5)$ (0.079 g, 0.24 mmol) was dissolved in 10 ml of hexane and

added to ^{i}PrN=C=N^{i}Pr (0.030 g, 0.24 mmol) dissolved in 1 ml of hexane. After the mixture was stirred for 48 h, the solution was evaporated to dryness to yield a yellow powder. This was washed with a small amount of cold hexane in order to remove unreacted $(C_5Me_4H)_2Sc(\eta^3\text{-}C_3H_5)$ to give yellow crystalline $(C_5Me_4H)_2Sc[(^{i}Pr)NC(CH_2CH{=}CH_2)N(^{i}Pr)\text{-}\kappa^2N,N']$ (0.064 g, 59%). Crystals suitable for X-ray analysis were grown from a concentrated hexane solution of **59** at −35 °C over the course of 2 d. ^{1}H NMR (C_6D_6): δ 5.89 (m, 1H, $^3J_{H\text{-}H}$ = 7.0 Hz, $CH_2CH{=}CH_2$), 5.85 (s, 2H, C_5Me_4H), 5.07 (m, 2H, $^3J_{trans}$ = 18.2 Hz, $^3J_{cis}$ = 8.6 Hz, $^3J_{H\text{-}H}$ = 9.6 Hz, $CH_2CH{=}CH_2$), 3.66 (septet, 2H, $CHMe_2$), 3.07 (m, 2H, $^3J_{H\text{-}H}$ = 6.3 Hz, $CH_2CH{=}CH_2$), 2.01 (s, 12H, C_5Me_4H), 1.95 (s, 12H, C_5Me_4H), 1.08 (d, 12H, $CHMe_2$).

X-ray Crystallographic Data. Information on X-ray data collection, structure determination, and refinement for **59** are given in Table 10.1. Details for X-ray data collection, structure solution and refinement are given in the Appendix.

Results and Discussion

Recently is has been shown that carbodiimides RN=C=NR (where R = ^{i}Pr) can readily insert into the M-C bond of actinide alkyl, alkynyl, and aryl complexes. For instance, the insertion reaction of ^{i}PrN=C=N^{i}Pr with $(C_5Me_5)_2AnMe_2$ (An = U, Th) afforded the isomorphous methyl amidinate products $(C_5Me_5)_2AnMe[(^{i}Pr)NC(Me)N(^{i}Pr)\text{-}\kappa^2N,N']$.[5]

$(C_5Me_4H)_2Sc(\eta^3\text{-}C_3H_5)$ reacted with ^{i}PrN=C=N^{i}Pr to give $(C_5Me_4H)_2Sc[(^{i}Pr)NC(CH_2CH{=}CH_2)N(^{i}Pr)\text{-}\kappa^2N,N']$, **59**, eq 10.3., Figure 10.1. This reaction, being a preliminary result, proceeded cleanly according to ^{1}H NMR analysis giving only complex **59** as the product.

Table 10.1. X-ray Data Collection Parameters for Complex $(C_5Me_4H)_2Sc[(^iPr)NC(CH_2CH{=}CH_2)N(^iPr)\text{-}\kappa^2N,N']$, **59**.

Complex	**59**
Empirical formula	$C_{28}H_{45}N_2Sc$
Fw	454.62
Temperature (K)	143(2)
Crystal system	Triclinic
Space group	$P\bar{1}$
a (Å)	9.1685(4)
b (Å)	9.4497(5)
c (Å)	15.0224(7)
α (deg)	94.6362(5)
β (deg)	90.2360(5)
γ (deg)	90.9249(5)
Volume Å^3	1297.09(11)
Z	2
ρ_{calcd} *(Mg/m^3)*	1.164
μ *(mm^{-1})*	0.301
R1 [I > 2.0σ(I)][a]	0.0298
wR2 (all data)[a]	0.0815

[a] Definitions: $wR2 = [\Sigma[w(F_o^2-F_c^2)^2] / \Sigma[w(F_o^2)^2]]^{1/2}$, $R1 = \Sigma||F_o|-|F_c|| / \Sigma|F_o|$

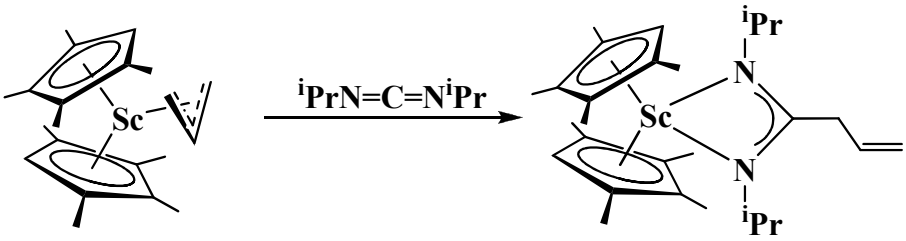

(10.3)

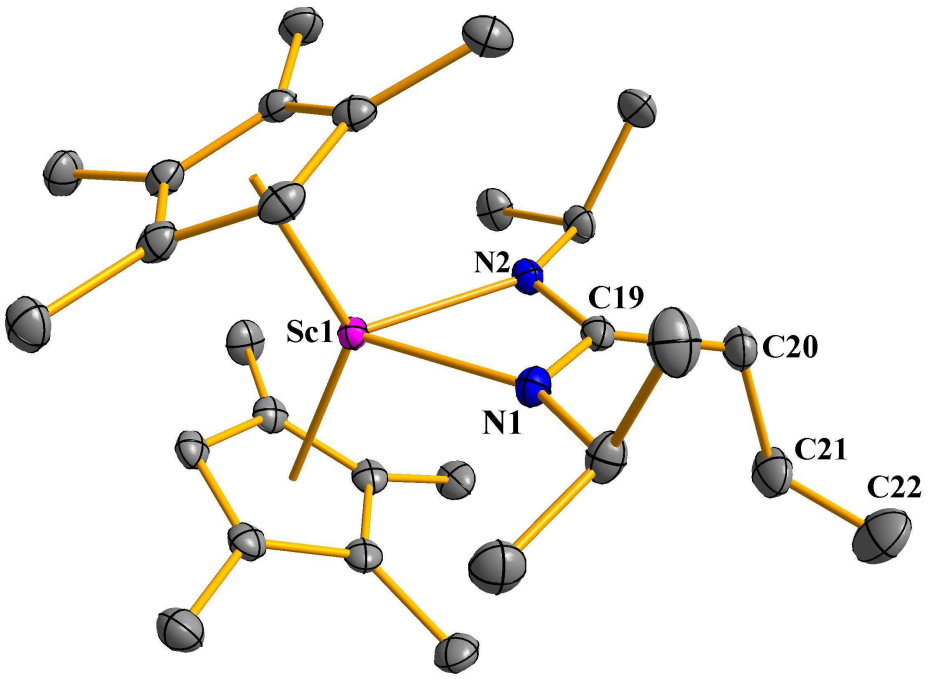

Figure 10.1: Thermal ellipsoid plot of $(C_5Me_4H)_2Sc[^iPrNC(\eta^1\text{-}C_3H_5)N^iPr\text{-}\kappa^2N,N']$, **59**, drawn at the 50% probability level with hydrogen atoms omitted for clarity.

Structural Studies.

Complex **59** contains an eight-coordinate scandium atom ligated by two tetramethylcyclopentadienyl ligands and two nitrogen atoms of the $[(^iPr)NC(CH_2CH{=}CH_2)N(^iPr)$ ligand, Figure 10.1. Selected bond distances and angles for complex **59** are shown in Table 10.2. These are compared to the metrical parameters of $(C_5Me_5)_2Sc[(H)NC(Me)N(NMe_2)\text{-}\kappa^2N,N']$, **60**, Table 10.3.

The (ring centroid)-scandium bond distances of 2.231 Å and 2.233 Å in complex **59** are equivalent to 2.231 Å and 2.232 Å found in complex **60**. Furthermore, the Sc-N bond distances of 2.1872(9) Å and 2.2198(9) Å observed in complex **59** are very similar to those of 2.1615(42) Å and 2.2650(48) Å in compound **60**. The M-N bond lengths of 2.1872(9) Å and 2.2198(9) Å in complex **59** are different compared to those of 2.1615(42) Å and 2.2650(48) Å in **60**. The Sc-C distance of the NCN unit of 2.6159(10) Å in complex **59** is slightly longer

than the value of 2.6057(47) Å found in the NCN unit in complex **60**. The (ring centroid)-Sc-(ring centroid) angle of 132.4° in **59** is, as a consequence of the coordination of a bulkier amidinate ligand to the metal center, smaller than the angle of 137.8° observed in **60**. The (ring centroid)-Sc-N angles ranging between 109.5-112.1° in complex **59** are slightly larger than the range of 105.6-110.6° found in complex **60**. In addition, the (ring centroid)-Sc-$C^{\#}$ ($C^{\#}$ = of the NCN unit) angles are 111.5° and 116.0° in **59**, similar to those in **60** with 106.5° and 115.3°. However, these (ring centroid)-Sc-$C^{\#}$ ($C^{\#}$ = of the NCN unit) angles in complex **59** resemble more each other than the mentioned analogous angles found in **60**.

The observed C-C bond distances of C(19)-C(20) = 1.5251(14) Å and C(20)-C(21) = 1.5023(16) Å in complex **59** are consistent with a single bond, whereas the C-C bond distance of 1.3150(19) Å in complex **60** is expectedly equivalent with a double bond.

Table 10.2. Selected Bond Distances (Å) and Angles (deg) for $(C_5Me_4H)_2Sc[(^iPr)NC(CH_2CH{=}CH_2)N(^iPr)\text{-}\kappa^2N,N']$ **59**.

	59		**59**
Cnt1-Sc(1)-Cnt2	132.4	Sc(1)-N(1)	2.1872(9)
Cnt1-Sc1-N1	109.5	Sc(1)-N(2)	2.2198(9)
Cnt1-Sc1-N2	112.1	Sc(1)-C(19)	2.6159(10)
Cnt1-Sc1-C19	116.0	C(19)-C(20)	1.5251(14)
Sc(1)-Cnt1	2.233	C(20)-C(21)	1.5023(16)
Sc(1)-Cnt2	2.231	C(21)-C(22)	1.3150(19)

Table 10.3. Selected Bond Distances (Å) and Angles (deg) for $(C_5Me_4H)_2Sc[(^iPr)NC(CH_2CH{=}CH_2)N(^iPr)\text{-}\kappa^2N,N']$, **59**, and $(C_5Me_5)_2Sc[(H)NC(Me)N(NMe_2)\text{-}\kappa^2N,N']$, **60**.[8]

	59	**60**
Cnt1-M(1)-Cnt2	132.4	137.8
(Cnt)-M1-(N)	109.5, 112.1, 110.2, 109.5	108.5, 107.4, 110.6, 105.6
Cnt1-M1-(C)[#]	116.0, 111.5	115.3, 106.5
M(1)-(Cnt)	2.233, 2.231	2.232, 2.231
M(1)-(N)[#]	2.1872(9), 2.2198(9)	2.1615(42), 2.2650(48)
M(1)-(C)[#]	2.6159(10)	2.6057(47)

[#] C of N=C=N unit

Conclusion

Facile insertion of the carbodiimide $^iPrN{=}C{=}N^iPr$ into the scandium carbon bond of $(C_5Me_4H)_2Sc(\eta^3\text{-}C_3H_5)$ provided a scandium amidinate complex, $(C_5Me_4H)_2Sc[(^iPr)NC(CH_2CH{=}CH_2)N(^iPr)\text{-}\kappa^2N,N']$, **59**. This complex is, besides the compound $(C_5Me_5)_2Sc[(H)NC(Me)N(NMe_2)\text{-}\kappa^2N,N']$, **60**, only the second cyclopentadienyl scandium metallocene featuring a coordinated NCN unit to the metal center.

References

(1) (a) Barker, J.; Kilner, M. *Coord. Chem. Re*V. **1994**, *133*, 219. (b) Edelmann, F. T. *Coord. Chem. Re*v. **1994**, *137*, 403.
(2) (a) Zhang, J.; Ruan, R.; Shao, Z.; Cai, R.; Weng, L.; Zhou, X. *Organometallics* **2002**, *21*, 1420. (b) Liu, B.; Yang, Y.; Cui, D.; Tang, T.; Chen, X.; Jing, X. *Dalton Trans.* **2007**, 4252. (c) Masuda, J. D.; Jantunen, K. C.; Scott, B. L.; Kiplinger, J. L. *Organometallics* **2008**, *27*, 1299.
(3) Zhang, W.-X.; Nishiura, M.; Hou, Z. *J. Am. Chem. Soc.* **2005**, *127*, 16788.
(4) (a) Zhang, J.; Cai, R.; Weng, L.; Zhou, X. *Organometallics* **2004**, *23*, 3303. (b) Cui, P.; Chen, Y.; Li, G.; Xia, W. *Angew. Chem., Int. Ed.* **2008**, *47*, 9944.
(5) Evans, W. J.; Walensky, J. R.; Ziller, J. W. *Organometallics* **2010**, *29*, 101-107.
(6) Bambirra, S.; Bouwkamp, M. W.; Meetsma, A.; Hessen, B. *J. Am. Chem. Soc.* **2004**, *126*, 9182.
(7) Hagadorn, J. R.; Arnold, J. *Organometallics* **1996**, *15*, 984-991.
(8) Shapiro, P. J.; Henling, L. M.; Marsh, R. E.; Bercaw, J. E. *Inorg. Chem.* **1990**, 29, 4560-4565.
(9) Evans, W. J.; Montalvo, E.; Champagne, T. M.; Ziller, J. W.; DiPasquale, A. G.; Rheingold, A.; *Organometallics* **2008**, *27*, 3582-3586.
(10) Evans, W. J.; Lorenz, S. E.; Ziller, J. W. *Chem. Comm.* **2007**, 4662-4664.

Chapter 11

Isolation of $(C_5Me_4H)_5Sc_5(\mu_5\text{-}O)(\mu_3\text{-}OH)_4(\mu\text{-}OH)_4 \cdot [(C_6H_5)NH]_2$

Introduction

Reactions of samarium metallocene complexes with diphenylhydrazine, PhNHNHPh have been previously examined. Diphenylhydrazine has two reactive hydrogen atoms which are suitable for deprotonation. For instance, this succeeded in a clean reaction with $[(C_5Me_5)_2SmH]_2$ that yielded $(C_5Me_5)_2Sm(PhNHNPh)$ and in THF, $(C_5Me_5)_2Sm(\eta^2\text{-}PhNHNPh)(THF)$, eq 11.1.[1]

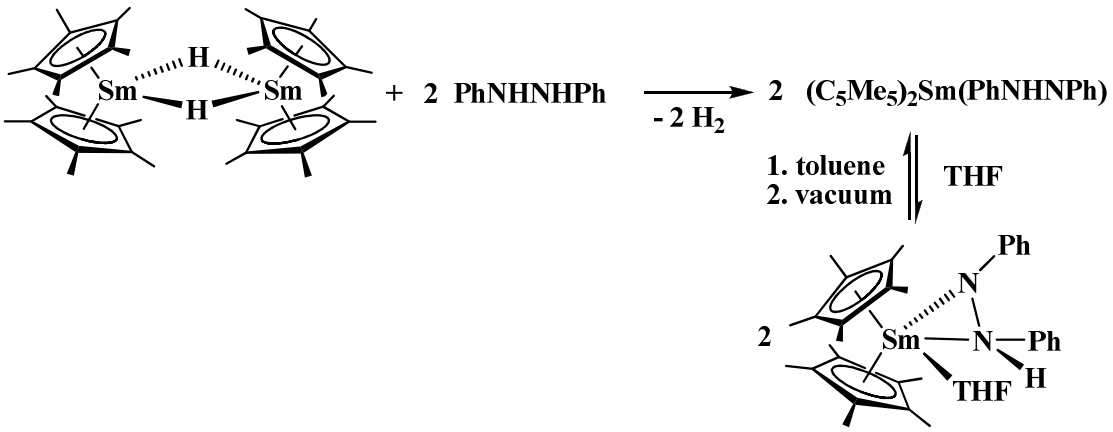

(11.1)

Another way to prepare the same product, $(C_5Me_5)_2Sm(PhNHNPh)$, is the reaction of divalent $(C_5Me_5)_2Sm$ with PhNHNHPh, eq. 11.2, although this reaction was not as clean as the synthetic route using the hydride.[1] The byproduct of this reaction is presumably hydrogen, however it was not isolated.[1]

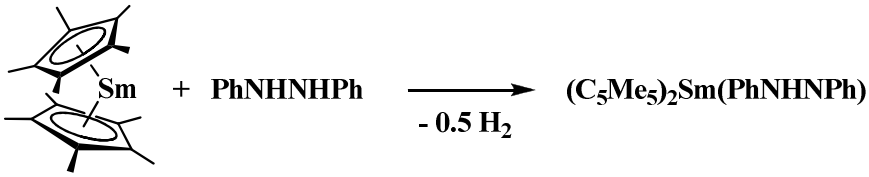

(11.2)

In contrast, the THF coordinated $(C_5Me_5)_2Sm(THF)_2$ reacts with PhNHNHPh by cleaving the N-N bond to give $(C_5Me_5)_2Sm(NHPh)(THF)$, eq. 11.3.

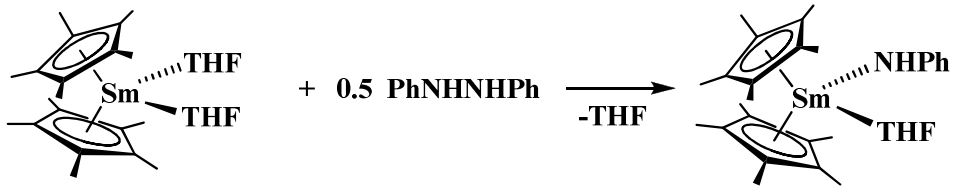

(11.3)

The allyl complex $(C_5Me_4H)_2Sc(\eta^3\text{-}C_3H_5)$ has been proven to be a stable starting material for probing M-C reactivity. It reacts with a range of substrates like $[HNEt_3][BPh_4]$,[Ch.3] PhEEPh (E = S, Se, Te),[Ch.6] pySSpy,[Ch.6] N_2O[Ch.9] and $^iPrN{=}C{=}N^iPr$,[Ch.10] respectively. Therefore, it has been chosen to examine reactivity with further substrates. The aim was to investigate reactivity of scandium metallocene complexes with diphenylhydrazine, PhNHNHPh.

$(C_5Me_4H)_2Sc(\eta^3\text{-}C_3H_5)$ reacts with PhNHNHPh to yield a tacky dark green material that is hexane soluble. The desired product could not be isolated and instead attempts to grow crystals resulted in the isolation of the unexpected scandium hydroxo cluster complex, $(C_5Me_4H)_5Sc_5(\mu_5\text{-}O)(\mu_3\text{-}OH)_4(\mu_2\text{-}OH)_4 \cdot [(C_6H_5)NH]_2$, **61**, most likely formed from oxygen/water impurities. The main structural feature is an oxo-centered scandium pyramid that is capped by hydroxo ligands over each edge and the metal atoms are each coordinated with one $(C_5Me_4H)^-$ ligand. Beside this, a cocrystallized PhNHNHPh is present.

Experimental

The manipulations described below were conducted under argon with rigorous exclusion of air and water using Schlenk, vacuum line, and glovebox techniques. Solvents were sparged with UHP argon and dried over columns containing Q-5 and molecular sieves. NMR solvents (Cambridge Isotope Laboratories) were dried over Na/K alloy, degassed, and vacuum-transferred before use. $(C_5Me_4H)_2Sc(\eta^3\text{-}C_3H_5)$ was prepared according to literature methods.[Ch.3] ^{1}H NMR spectra was recorded on a Bruker DRX500 spectrometer at 25 °C.

Reaction of $(C_5Me_4H)_2Sc(\eta^3\text{-}C_3H_5)$, 7, with PhNHNHPh. In a nitrogen-filled glovebox, an orange solution of PhNHNHPh (0.029 g, 0.16 mmol) in 2 ml of toluene was added to $(C_5Me_4H)_2Sc(\eta^3\text{-}C_3H_5)$ (0.028 g, 0.16 mmol) in 8 ml of toluene. After the mixture was stirred for 24 h, the dark orange solution was evaporated to dryness to yield a tacky green material. ^{1}H NMR (500 MHz, benzene-d_6): δ 8.02 (m, 3H), 7.27 (m, 2H), 6.71 (m, 2H), 6.89 (m, 1H), 6.17 (d, 1H), 6.04 (s, 2H), 6.00 (s, 1H), 5.66 (s, 1H), 5.59 (s, 1H), 2.13 (s, 3H), 2.05 (s, 2H), 2.02 (s, 3H), 1.98 (d, 24H), 1.89 (s, 3H), 1.82 (s, 3H), 1.74 (s, 3H), 1.58 (d, 6H), 1.51 (s, 3H).

$(C_5Me_4H)_5Sc_5(\mu_5\text{-}O)(\mu_3\text{-}OH)_4(\mu\text{-}OH)_4 \cdot [(C_6H_5)NH]_2$, 61. Crystals of **61** suitable for X-ray analysis were grown at rt from a concentrated benzene solution over the course of 6 weeks.

X-ray Crystallographic Data. Information on X-ray data collection, structure determination, and refinement for **61** is given in Table 11.1. Details for X-ray data collection, structure solution and refinement are given in the Appendix.

Results and Discussion

$(C_5Me_4H)_2Sc(\eta^3\text{-}C_3H_5)$, **7**, reacts with PhNHNHPh to give a scandium metallocene product of an unknown composition and a byproduct that is thought to be the oxide, $[(C_5Me_4H)_2Sc]_2(\mu\text{-}O)$, on the basis of ^{1}H NMR resonances and prior studies.[Ch.3] The ^{1}H NMR spectrum of the crude product indicates coordination of the PhNHNHPh ligand to scandium, since the observed peaks belong presumably to the $(C_5Me_4H)^-$ ligand that are shifted compared to the ^{1}H NMR spectrum of the starting material $(C_5Me_4H)_2Sc(\eta^3\text{-}C_3H_5)$. The reaction proceeds to completion within 24 hours. In efforts to crystallize the products of this reaction, oxygen and water impurities presumably reacted with the initial product to form an unprecedented scandium hydroxo cluster, $(C_5Me_4H)_5Sc_5(\mu_5\text{-}O)(\mu_3\text{-}OH)_4(\mu\text{-}OH)_4 \cdot [(C_6H_5)NH]_2$, **61**, eq 11.1, Figure 11.1.

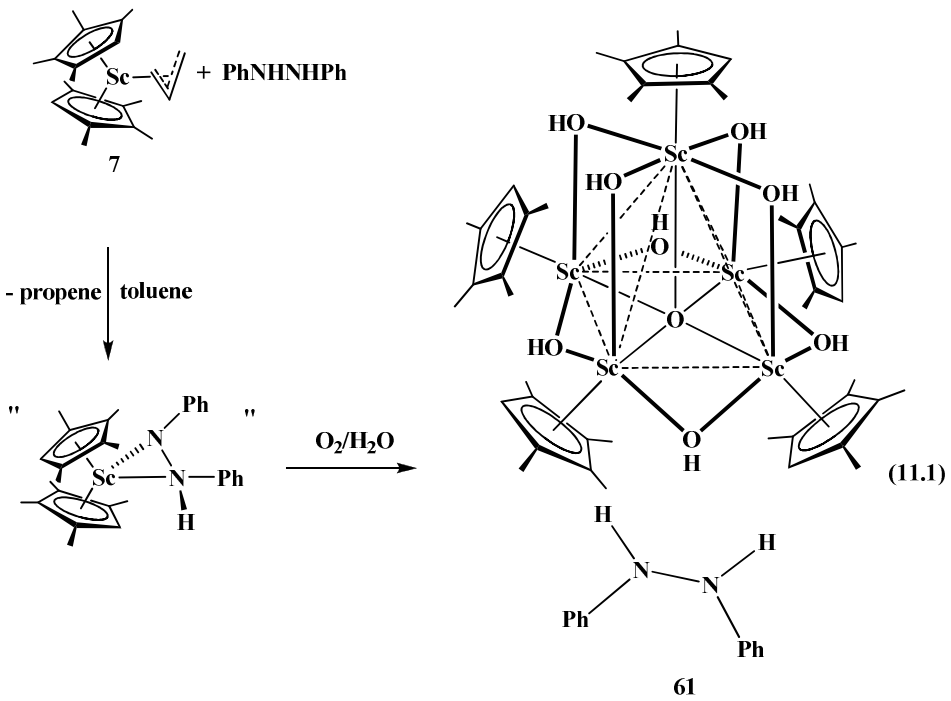

The structure of this unusual complex **61**, is similar to $(C_5Me_5)_5Y_5(\mu_5\text{-O})(\mu_3\text{-OMe})_4(\mu\text{-OMe})_4$, **62**, that was obtained from reaction of $(C_5Me_5)_5YCl(THF)$ and $KOCH_3 \cdot CH_3OH$ at 30 °C for two days.[2]

Furthermore, the core of complex **61** is structurally related to the rare earth metal isopropoxides, $M(OPr^i)_3$ (M = Sc, Y, Er, Yb, Nd), which can be synthesized through different routes, exemplified in eq 11.3 and eq 11.4.[3-5]

$$\mathbf{M + 3\ {}^{i}PrOH \longrightarrow M(OiPr)_3 + 1.5\ H_2} \qquad \mathbf{(11.3)}$$

$$\mathbf{M = Sc, Y}$$

$$\mathbf{NdCl_3(Pr^iOH)_3 + 3\ KOPr^i \longrightarrow Nd(O^iPr)_3 + 3\ KCl + 3\ Pr^iOH} \qquad \mathbf{(11.4)}$$

However, the formation of an isopropoxide compound showing the pattern in Figure 11.3 depends on the reaction conditions. For instance, there is a chlorine-containinig cluster, namely $Nd_6(O^iPr)_{17}Cl$, also reported which was obtained from the reaction of $NdCl_3$ with NaO^iPr.[6]

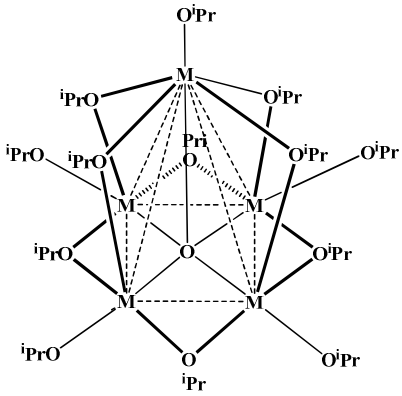

Figure 11.3. Structural feature of rare earth metal alkoxides with M (Sc,Y, Er, Yb, Nd)

Table 11.1. X-ray Data Collection Parameters for Complex $(C_5Me_4H)_5Sc_5(\mu_5\text{-}O)(\mu_3\text{-}OH)_4(\mu\text{-}OH)_4 \cdot [(C_6H_5)NH]_2$, **61**.

Complex	**61**
Empirical formula	$C_{57}\ H_{85}\ N_2\ O_9\ Sc_5 \bullet ½(C_6H_6)$
Fw	1206.12
Temperature (K)	93(2)
Crystal system	Monoclinic
Space group	$P2_1/c$
a (Å)	21.9553(8)
b (Å)	12.6867(5)
c (Å)	21.7649(8)
α (deg)	90
β (deg)	103.9457(5)
γ (deg)	90
Volume Å^3	5883.7(4)
Z	4
ρ_{calcd} *(Mg/m^3)*	1.362
μ *(mm^{-1})*	0.603
*R1 [*I > *2.0*σ*(*I*)]*^{a}	0.0422
wR2 (all data)^a	0.1103

[a] Definitions: $wR2 = [\Sigma[w(F_o^2-F_c^2)^2] / \Sigma[w(F_o^2)^2]\ ]^{1/2}$, $R1 = \Sigma||F_o|-|F_c|| / \Sigma|F_o|$

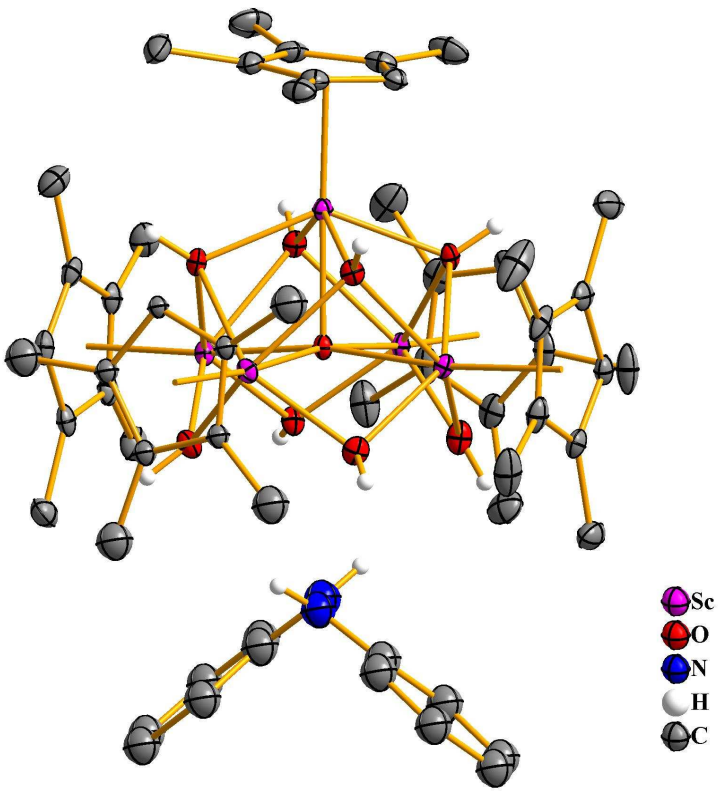

Figure 11.1. Thermal ellipsoid plot of $(C_5Me_4H)_5Sc_5(\mu_5\text{-}O)(\mu_3\text{-}OH)_4(\mu\text{-}OH)_4 \cdot [(C_6H_5)NH]_2$, **61**, drawn at the 50% probability level. Hydrogen atoms, except those of the hydroxo and hydrazine groups, have been omitted for clarity.

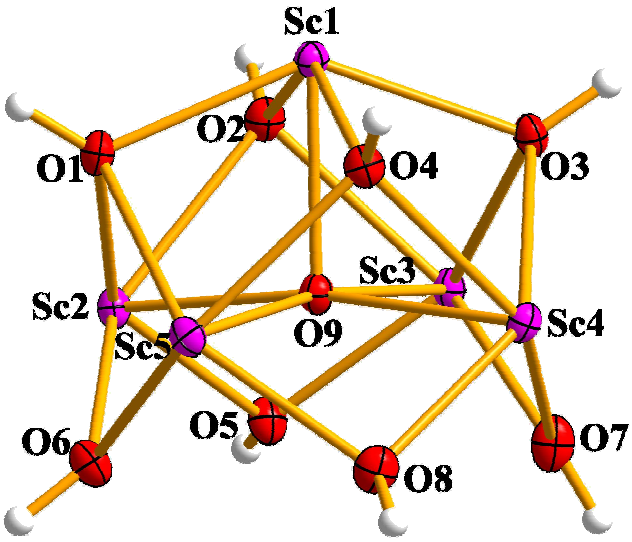

Figure 11.2. Thermal ellipsoid plot of the unit $Sc_5O(OH)_8$ in the compound $(C_5Me_4H)_5Sc_5(\mu_5\text{-}O)(\mu_3\text{-}OH)_4(\mu\text{-}OH)_4 \cdot [(C_6H_5)NH]_2$, **61**, drawn at the 50% probability level. Hydrogen atoms, except those of the hydroxo groups, have been omitted for clarity.

Structural studies

Selected bond distances and angles for $(C_5Me_4H)_5Sc_5(\mu_5\text{-}O)(\mu_3\text{-}OH)_4(\mu\text{-}OH)_4 \cdot [(C_6H_5)NH]_2$, **61** are listed in Table 11.2. The structure of complex **61** is compared to $(C_5Me_5)_5Y_5(\mu_5\text{-}O)(\mu_3\text{-}OMe)_4(\mu\text{-}OMe)_4$, **62**,[2] $Sc(OPr^i_3)$, **63**,[3] and $Y(OPr^i)_3$, **64**,[4] respectively, in Table 11.3. Complex **61** resembles compound **62** in that each metal is coordinated by a cyclopentadienyl ligand, even though **61** contains $(C_5Me_4H)^-$ and **62** $(C_5H_5)^-$ ligands. The core of complex **61** consists of an oxo-centered metal pyramid whose faces and edges, respectively, are capped by hydroxo ligands. This similar structural feature is observed in complex **62** as well, where the capping ligands are $(MeO)^-$. Consequently, the coordination number of the metals in both complexes is eight, thus their metrical parameters are appropriate for comparison. For this reason, complex **62** is the closest related compound to compare with **61**. However, the structural feature of an oxo-centered rare earth metal cluster with a square-pyramidal core of complex **61** resembles generally the structure of rare earth alkoxide compounds of the formula $M(OPr^i)_3$, which are better described as $M_5O(OPr^i)_{13}$ (M = Sc, Y, Er, Yb, Nd). Although the metals are six-coordinate in these complexes, a comparison of the metrical parameters for complex **61** with those of $Sc(OPr^i_3)$, **63**,[3] and $Y(OPr^i)_3$, **64**,[4] is taken into account, to check on similarities. The data for the cocrystallized diphenylhydrazine in complex **61** is neglected in respect of discussion, since because of the large distance of the diphenyldihydrazine to centered oxygen atom of the scandium cluster, N(1)-O(9) = 4.0426(1) Å and N(11)-O(9) = 4.0892(1) Å, there is no direct interaction between the N-N single bond of PhNHNHPh and the scandium cluster.

Table 11.2. Selected Bond Distances (Å) and Angles (deg) for $(C_5Me_4H)_5Sc_5(\mu_5\text{-}O)(\mu_3\text{-}OH)_4(\mu\text{-}OH)_4 \cdot [(C_6H_5)NH]_2$, **61**.

	61		**61**
Sc(1)-Cnt1	2.228	Sc(3)-O(2)	2.2814(15)
Sc(2)-Cnt2	2.245	Sc(4)-O(8)	2.1040(16)
Sc(3)-Cnt3	2.232	Sc(4)-O(7)	2.1107(16)
Sc(4)-Cnt4	2.250	Sc(4)-O(9)	2.2336(14)
Sc(5)-Cnt5	2.229	Sc(4)-O(4)	2.2396(15)
Sc(1)-O(9)	2.1446(15)	Sc(4)-O(3)	2.2409(15)
Sc(1)-O(1)	2.1546(15)	Sc(5)-O(6)	2.0936(15)
Sc(1)-O(2)	2.1634(15)	Sc(5)-O(8)	2.1065(16)
Sc(1)-O(4)	2.1686(15)	Sc(5)-O(9)	2.2247(15)
Sc(1)-O(3)	2.1764(15)	Sc(5)-O(4)	2.2511(15)
Sc(2)-O(6)	2.0910(16)	Sc(5)-O(1)	2.2544(15)
Sc(2)-O(5)	2.0927(15)	Sc(1)-Sc(5)	3.2026(5)
Sc(2)-O(9)	2.1941(14)	Sc(1)-Sc(4)	3.2147(5)
Sc(2)-O(1)	2.2638(15)	Sc(1)-Sc(3)	3.2160(5)
Sc(2)-O(2)	2.2876(15)	Sc(1)-Sc(2)	3.2166(5)
Sc(3)-O(5)	2.0983(15)	Sc(2)-Sc(5)	3.1168(5)
Sc(3)-O(7)	2.1064(16)	Sc(2)-Sc(3)	3.1297(5)
Sc(3)-O(9)	2.2248(15)	Sc(3)-Sc(4)	3.1275(5)
Sc(3)-O(3)	2.2357(15)	Sc(4)-Sc(5)	3.1361(6)
Cnt1-Sc(1)-O(1)	112.0	O(9)-Sc(1)-Sc(5)	43.85(4)
Cnt1-Sc(1)-O(9)	177.3	O(2)-Sc(1)-Sc(5)	102.19(4)
O(9)-Sc(1)-O(1)	69.16(6)	C(4)-Sc(1)-Sc(5)	161.67(5)
O(1)-Sc(1)-O(2)	82.88(6)	Sc(5)-Sc(1)-Sc(4)	58.509(12)
O(2)-Sc(1)-O(4)	138.78(6)	Sc(5)-Sc(1)-Sc(3)	87.425(14)

Table 11.3. Ranges of Selected Bond Distances (Å) and Angles (deg) for $(C_5Me_4H)_5Sc_5(\mu_5\text{-}O)(\mu_3\text{-}OH)_4(\mu\text{-}OH)_4 \cdot [(C_6H_5)NH]_2$, **61**, $(C_5Me_5)_5Y_5(\mu_5\text{-}O)(\mu_3\text{-}OMe)_4(\mu\text{-}OMe)_4$, **62**,[2] $(O^iPr)_5Sc_5(\mu_5\text{-}O)(\mu_3\text{-}O^iPr)_4(\mu\text{-}O^iPr)_4$, **63**,[3] and $(O^iPr)_5Y_5(\mu_5\text{-}O)(\mu_3\text{-}O^iPr)_4(\mu\text{-}O^iPr)_4$, **64**.[4]

	61	**62**	**63**	**64**
ionic radius	0.870 (eight-coord.)	1.019 (eight-coord.)	0.745 (six-coord.)	0.900 (six-coord.)
(M)-(Cnt)	2.228- 2.250	2.387-2.425	-	-
M-O[#]	-	-	1.873(6)-1.890(8)	1.98(4)-2.07(5)
M^{ba}-(μ-O)	2.0910(16)-2.1107(16)	2.209(19)-2.250(20)	2.061(7)-2.095(7)	2.20(4)-2.31(3)
M^{ba}-(μ_3-O)	2.2357(15)-2.2876(15)	2.395(21)-2.457(19)	2.277(7)-2.317(7)	2.38(3)-2.45(4)
M^{ap}-(μ_3-O)	2.1546(15)-2.1764(15)	2.299(19)-2.348(20)	2.154(7)-2.179(7)	2.18(5)-2.32(4)
M-(μ_5-O)	2.1446(15)-2.2336(14)	2.271(17)-2.414(19)	2.159(6)-2.193(7)	2.31(4)-2.39(4)
M^{ap}-M^{ba}	3.2026(5)-3.2166(5)	3.361(5)-3.472(5)	3.183(3)-3.203(3)	3.44(1)-3.47(1)
M^{ba}-M^{ba}	3.1297(5)-3.1361(6)	3.343(5)-3.361(5)	3.059(3)-3.078(3)	3.30(1)-3.34(1)

[#]O: oxygen of the hydroxide and alkoxide, respectively, ligand

The Sc-O bond distances ranging from 2.0910(16)-2.2876(15) Å (2.183 Å av.) in pentametallic complex **61** can be compared to 2.167(3) and 2.176(3) Å (2.172 Å av.) in $(C_5Me_5)_2Sc(O_2C)C_6H_4CH_3$,[7] in which the scandium atoms are also eight-coordinate. The structure of **61** is very regular. The μ_3-OH groups in **61** lie closer to the apical scandium atom, Sc(1), with Sc(1)-O lengths from 2.1546(15)-2.1764(15) Å. In contrast, the longest Sc-O bond distances in complex **61** are observed in the connections of the basal scandium atoms, Sc(2)-Sc(5), with the μ_3-OH groups ranging from 2.2357(15)-2.2876(15) Å. Expectedly, the doubly bridging eight Sc(basal)-O(μ_3-OH) distances are shorter, lying in the range 2.0910(16) to 2.1107(16) Å. The oxygen atom centering the scandium pyramid is closer to the apical scandium showing a Sc(1)-O(9) bond distance of 2.1446(15) Å, than to the basal scandium atoms in which the Sc-O bond distances lie within 2.1941(14)-2.2336(14) Å. The metal-

metal distances between the basal and basal scandium atoms are within a range of 3.1297(5)-3.1361(6) Å., thus shorter than the observed Sc-Sc distances between the apical and basal scandium atoms ranging from 3.2026(5)-3.2166(5) Å.

In general, the structure of complex **61** is not unusual compared to the pentametallic yttrium complex **62**, when the differences in ligands and metals are taken into account. The (ring centroid)-metal bond distances ranging from 2.228-2.250 Å in complex **61** are, expectedly, smaller than 2.387-2.425 Å in complex **62**. Although all bond distances are, due to the larger metal yttrium, about 0.1-0.2 Å longer than found in complex **61**, a similar progression of the yttrium oxygen distances is observed when compared with the sequence in complex **61**.

A comparison of the Sc-O bond distances in complex **61**, in which scandium is eight-coordinate (ionic radius of 0.870 Å), with complex **63**, in which scandium is six-coordinate (ionic radius of 0.745 Å), shows that the observed values are partially very similar, although the coordination number of the metal is different: The ranges of Sc-O bond distances between the basal scandium atoms and the μ_3-bridging oxygen atoms is in complex **61**: 2.2357(15)-2.2876(15) Å and in complex **63**: 2.277(7)-2.317(7) Å. The same progression is visible when the ranges of Sc-O bond distances between the apical scandium atoms and the μ_3-bridging oxygens compared with 2.1546(15)-2.1764(15) Å in complex **61**, and 2.154(7)-2.179(7) Å in **63**. Differences in lengths between both compounds are noticeable when the Sc-O bond distances of the basal scandium atoms to the μ-O are considered: 2.0910(16)-2.1107(16) Å is the range found in **61** wheras the range observed in **63** is with 2.061(7)-2.095(7) Å slightly shorter. The Sc-O bond distance between the apical scandium and the oxygen centering the metal pyramid is with 2.1446(15) Å in complex **61** shorter than 2.159(6) Å in complex **63**. Contrary to this, the Sc-O bond distances between the basal scandium atoms and the oxygen in the center of the pyramid are in complex **61** with a range of 2.1941(14)-2.2336(14) Å longer than and 2.165(6)- 2.193(7) Å range in complex **63**. As expected, the Sc-Sc bond

distances are due to the bulky $(C_5Me_4H)^-$ ligands in **61** with 3.1297(5)-3.1361(6) Å (between apical and basal scandium atoms) and 3.2026(5)-3.2166(5) Å (between basal scandium atoms) are much longer than the observed values in **63**: 3.059(3)-3.078(3) Å (between apical and basal scandium atoms) and 3.183(3)-3.203(3) Å (between basal scandium atoms).

The comparison of the metrical parameters of complexes **63** and **64** shows that the M-O distances increase between 0.1-0.2 Å when moving down the group from scandium to yttrium. This progression in the M-O bond distances is also recognizable when complexes **61** and **62** are compared with each other.

Conclusion

The reaction of $(C_5Me_4H)_2Sc(\eta^3\text{-}C_3H_5)$, **7**, with PhNHNHPh afforded under exposure of oxygen/water a pentametallic scandium hydroxo cluster $(C_5Me_4H)_5Sc_5(\mu_5\text{-}O)(\mu_3\text{-}OH)_4(\mu\text{-}OH)_4 \cdot [(C_6H_5)NH]_2$, **61**. This complex features a scandium square-pyramidal core which is "centered" by an oxygen atom and there is a $(C_5Me_4H)^-$ ligand coordinated at each metal atom. Furthermore, face/edge of this metal pyramid is capped with a hydroxo ligand. This kind of structural feature has been observed before in the yttrium complex $(C_5Me_5)_5Y_5(\mu_5\text{-}O)(\mu_3\text{-}OMe)_4(\mu\text{-}OMe)_4$, **62**.[2] The structural core of **61** resembles also the core of the scandium propoxide $Sc(OPr^i)_3$. Structural comparisons between **61**, **62** and **63** have shown that the core of **61** resembles in some respects the core of **63**, although in **61** the scandium is eight-coordinate and in **63** six-coordinate. Furthermore, **61** and **62** are very similar in terms of progression in their distances, when the differences in ligands and metals are taken into consideration.

References

(1) Evans, W. J.; Kociok-Kohn, G.; Leong, V. S.; Ziller, J. W. *Inorg. Chem.* **1992**, *31*, 3592-3600.
(2) Evans, W. J.; Sollberger, M. S. *J. Am. Chem. Soc.* **1986**, *108*, 6095-6096.
(3) Turevskaya, E. P.; Belokon', A. I.; Starikova, Z. A.; Yanovsky, A. I.; Kiruschenkov, E. N.; Turova, N. Ya. *Polyhedron* **2000**, *19*, 705-711.

(4) Poncelet, O.; Sartain, O. W. J.; Hubert-Pfalzgraf, L. G.; Folting, K.; Caulton, K. G. *Inorg. Chem.* **1989**, *28*, 264.
(5) Kritikos, M.; Moustiakimov, M.; Wijk, M.; Westin, G. *J. Chem. Soc., Dalton Trans.* **2001**, 1931-1938.
(6) Andersen, R. A.; Templeton, D. H.; Zalkin, A. *Inorg. Chem.* **1978**, *17*, 1962-1965.
(7) St. Clair, M. A.; Santarsiero, B. D. *Acta Cryst. Sect. C* **1989**, *45*, 850-852.

Chapter 12

Summary

In this thesis various new scandium complexes, along with some yttrium and lanthanide complexes, have been successfully synthesized and characterized.

The solid scandium metal cluster complex $\{CSc_6\}I_{12}Sc$ reacted with KC_5H_5 in THF under dinitrogen to afford an unprecedented molecular scandium nitride complex $[(C_5H_5)_2ScNSc(C_5H_5)(THF)]_2$, Fig. 12.1a. The reaction of $\{CSc_6\}I_{12}Sc$ with KC_5H_5 in THF under argon, however, resulted in the isolation of a scandium propoxide complex, $[(C_5H_5)_2Sc]_2[\mu\text{-}O(C_3H_7)]_2$, Fig. 12.1b. The mechanism of both of these reactions remains unclear. However, the remarkable fact is that the salt metathesis reaction of the relatively inert $\{CSc_6\}I_{12}Sc$ proceeded to completion with KC_5H_5 in THF at ambient temperature. This is promising in respect of further investigations of solid state compounds with substrates used typically in organometallic synthesis.

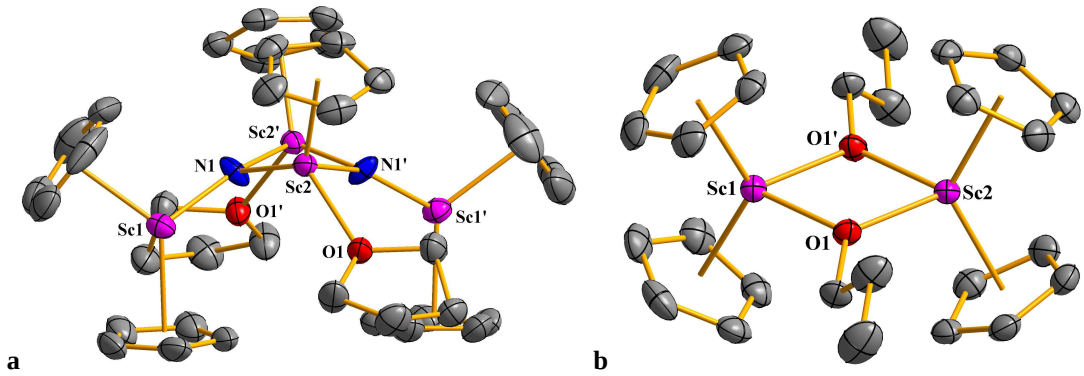

Figure 12.1. Thermal ellipsoid plots of (**a**) $[(C_5H_5)_2ScNSc(C_5H_5)(THF)]_2$ and (**b**) $[(C_5H_5)_2Sc]_2[\mu\text{-}O(C_3H_7)]_2$, drawn at the 50% probability level. Hydrogen atoms are omitted for clarity.

The first reduced dinitrogen complex of scandium was obtained by use of the tetramethylcyclopentadienyl ancillary ligand set, $[(C_5Me_4H)_2Sc]_2(\mu\text{-}\eta^2\text{:}\eta^2\text{-}N_2)$. The synthesis of its precursor compounds involves the preparation of the complexes $(C_5Me_4H)_2ScCl(THF)$, $(C_5Me_4H)_2Sc(\eta^3\text{-}C_3H_5)$, and $[(C_5Me_4H)_2Sc][(\mu\text{-}Ph)BPh_3]$, Figure 12.2a-c.

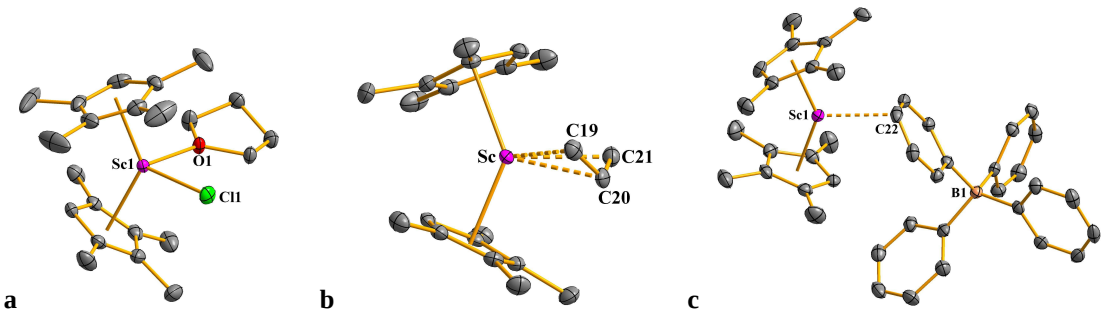

Figure 12.2. Thermal ellipsoid plots of (**a**) $(C_5Me_4H)_2ScCl(THF)$, (**b**) $(C_5Me_4H)_2Sc(\eta^3\text{-}C_3H_5)$, (**c**) $[(C_5Me_4H)_2Sc][(\mu\text{-Ph})BPh_3]$, drawn at the 50% probability level. Hydrogen atoms are omitted for clarity.

The reaction of $ScCl_3$ with 2 equiv of KC_5Me_4H afforded $(C_5Me_4H)_2ScCl(THF)$, which reacted with allylmagnesiumchloride to give $(C_5Me_4H)_2Sc(\eta^3\text{-}C_3H_5)$. This scandium allyl complex was further reacted with $[HNEt_3][BPh_4]$ to yield $[(C_5Me_4H)_2Sc][(\mu\text{-Ph})BPh_3]$, which is structurally different to the analogous lanthanide tetraphenylborate complexes. It shows only one primary Sc-C(phenyl) agostic interaction between the metallocene cation and the tetraphenylborate anion. The reduction of $[(C_5Me_4H)_2Sc][(\mu\text{-Ph})BPh_3]$ with KC_8 under dinitrogen provided the first scandium dinitrogen complex $[(C_5Me_4H)_2Sc]_2(\mu\text{-}\eta^2\text{:}\eta^2\text{-}N_2)$, Figure 12.3a.

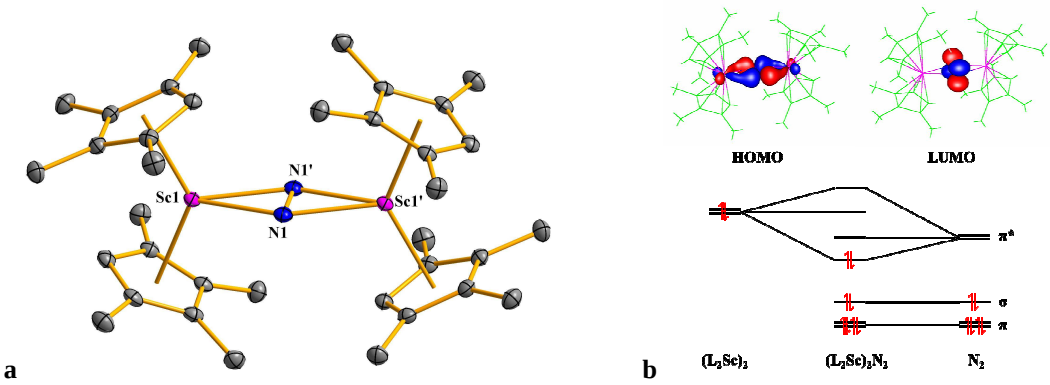

Figure 12.3. (**a**) Thermal ellipsoid plot of $[(C_5Me_4H)_2Sc]_2(\mu\text{-}\eta^2\text{:}\eta^2\text{-}N_2)$, drawn at the 50% probability level. Hydrogen atoms are omitted for clarity. (**b**) Simplified molecular orbital scheme of $[(C_5Me_4H)_2Sc]_2(\mu\text{-}\eta^2\text{:}\eta^2\text{-}N_2)$.

This dinitrogen complex possesses a $M_2(\mu\text{-}\eta^2\text{:}\eta^2\text{-}N_2)$ coordination mode that was previously found with larger metals and with solvated complexes. The observed N=N bond distance of 1.239(3) Å is consistent with $(N{=}N)^{2-}$ and in good agreement with the optimized

calculated value of 1.226 Å, as determined by density functional theory calculations. These also explain how this moiety is stabilized by scandium via polar covalent bonding, Figure 12.3b. The size of the dinitrogen complex is similar to the respective oxide complex so that they can even cocrystallize in a single crystal, as exemplified by the isolation of $\{[(C_5Me_4H)_2Sc]_2(\mu\text{-}\eta^2\text{:}\eta^2\text{-}N_2)[(C_5Me_4H)_2Sc]_2(\mu\text{-}O)\}$, Figure 12.4a. Additionally, the dissolution of $[(C_5Me_4H)_2Sc][(\mu\text{-}Ph)BPh_3]$ in THF afforded $[(C_5Me_4H)_2Sc(THF)_2][BPh_4]$, Figure 12.4b, whose main structural feature is the same as for solvated lanthanide tetraphenylborate complexes.

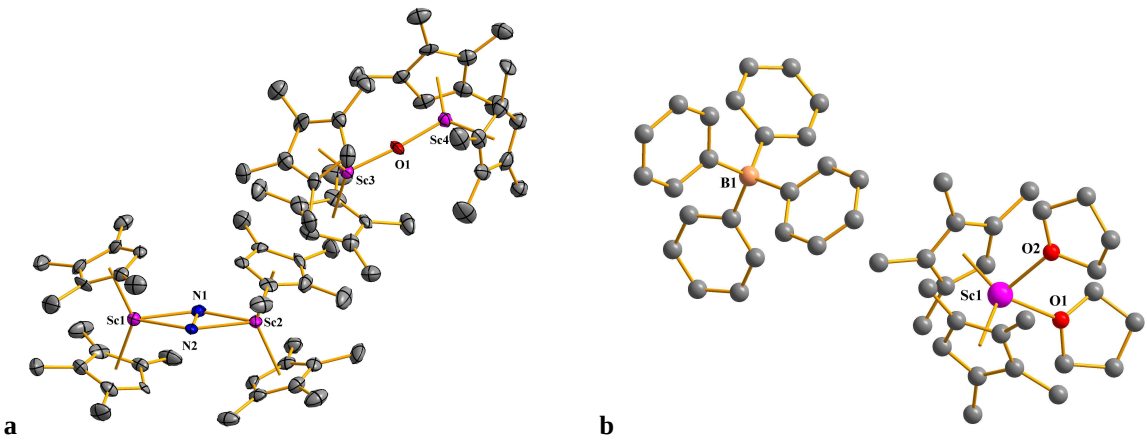

Figure 12.4. (**a**) Thermal ellipsoid plot of $\{[(C_5Me_4H)_2Sc]_2(\mu\text{-}\eta^2\text{:}\eta^2\text{-}N_2)[(C_5Me_4H)_2Sc]_2(\mu\text{-}O)\}$, drawn at the 50% probability level. (**b**) Ball-and-stick plot of $[(C_5Me_4H)_2Sc(THF)_2][BPh_4]$. In (**a**) and (**b**) the hydrogen atoms are omitted for clarity.

Since the isolation of the first scandium dinitrogen complex $[(C_5Me_4H)_2Sc]_2(\mu\text{-}\eta^2\text{:}\eta^2\text{-}N_2)$ succeeded, future work can be directed towards investigations of its reactivity. Due to the small size of scandium, it is conceivable that the reactivity of this complex could be different as compared to lanthanide dinitrogen complexes.

Tetraphenylborate salts of yttrium and the lanthanides have proven to be excellent precursors for the activation of dinitrogen. However, their syntheses require multiple steps. For this reason, borohydride complexes, $(C_5Me_4R)_2Y(BH_4)(THF)$ (R = H, Me) were tested to examine their ability to activate dinitrogen. However, this did not occur, presumably because the borohydride ligand is bound too strongly to yttrium to be eliminated as a KZ′ byproduct in

the reductive (LnZ_2Z'/K) reaction. These yttrium borohydride complexes, and their scandium analogues, were prepared by the reaction of the respective trivalent metal chloride, KC_5Me_4H or NaC_5Me_5 and $NaBH_4$ in a one-pot synthesis. Through this procedure, $(C_5Me_4R)_2Y(BH_4)(THF)$ (R = H, Me) and $(C_5Me_4H)_2Sc(BH_4)$, were secured and their structures determined, Figure 12.5a-c. In these complexes the bridging mode of the borohydride ligand differs due to differences in ligand size.

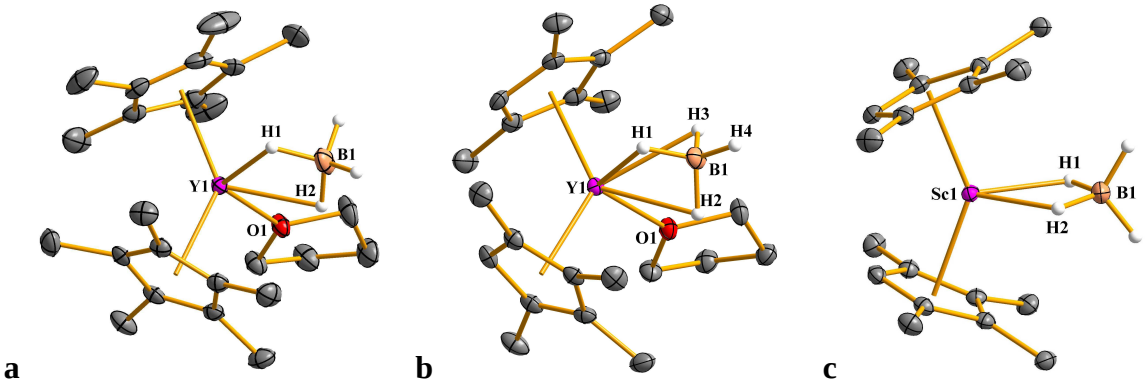

Figure 12.5. Thermal ellipsoid plots of (**a**) $(C_5Me_5)_2Y(BH_4)(THF)$, (**b**) $(C_5Me_4H)_2Y(BH_4)(THF)$, (**c**) $(C_5Me_4H)_2Sc(BH_4)$, drawn at the 50% probability level. Hydrogen atoms except the hydrogens of the borhydride component are omitted for clarity.

Beside these results of borohydride complexes, a chloride contaminated borohydride of scandium, with 50% chloride and 50% borohydride occupancy, was obtained in one single crystal, $[(C_5Me_5)_2Sc(BH_4)(THF)]$ $[(C_5Me_5)_2Sc(Cl)(THF)]$, Figure 12.6a-c.

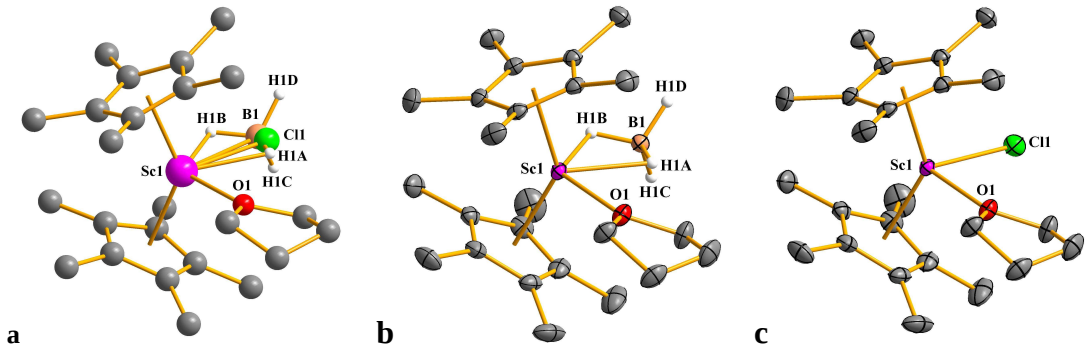

Figure 12.6. (**a**) Ball-and-stick plot of $[(C_5Me_5)_2Sc(BH_4)(THF)]$ $[(C_5Me_5)_2Sc(Cl)(THF)]$. Thermal ellipsoid plots of the scandium borohydride and chloride components of $[(C_5Me_5)_2Sc(BH_4)(THF)]$ $[(C_5Me_5)_2Sc(Cl)(THF)]$: (**b**) $(C_5Me_5)_2Sc(BH_4)(THF)$, and (**c**) $(C_5Me_5)_2Sc(Cl)(THF)$, **26**, drawn at the 50% probability level. Hydrogen atoms except the hydrogens of the borhydride component are omitted for clarity.

In addition, the reactivity of the scandium tetraphenylborate complex $[(C_5Me_4H)_2Sc][(\mu\text{-Ph})BPh_3]$ has been examined by its reaction with KC_5Me_4H that afforded $(\eta^5\text{-}C_5Me_4H)_2Sc(\eta^1\text{-}C_5Me_4H)$. Structure determination gave evidence that this complex is the first example of an η^1-coordination mode for a $(C_5Me_4H)^-$ ligand bound to a rare-earth metal, Figure 12.7.

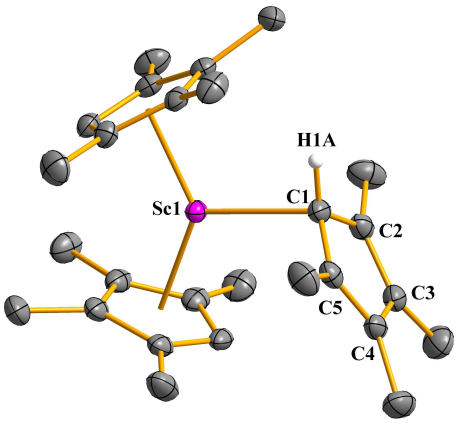

Figure 12.7. Thermal ellipsoid plot of $(\eta^5\text{-}C_5Me_4H)_2Sc(\eta^1\text{-}C_5Me_4H)$, drawn at the 50% probability level. Second independent molecolue of $(C_5Me_4H)_2Sc(\eta^1\text{-}C_5Me_4H)$ and hydrogen atoms except for H1A are omitted for clarity.

The discovery of $(\eta^5\text{-}C_5Me_4H)_2Sc(\eta^1\text{-}C_5Me_4H)$ led us to question whether this complex might react differently compared to the $(\eta^5\text{-}C_5Me_5)_3Ln$ analogues for which a variety of reaction modes has been found. Even if the reaction mode might be the same, the products might be diverse due to the smaller metal. Preliminary results have revealed that this complex shows sigma bond metathesis reactivity towards diphenyldichalcogenides. Future work could be directed to the reactivity of this complex towards a range of small molecules, such as CO, CO_2, nitriles, and other unsaturated substrates.

The scandium allyl complex $(C_5Me_4H)_2Sc(\eta^3\text{-}C_3H_5)$ emerged to be a valuable precursor for various reactions. In addition to the formation of $[(C_5Me_4H)_2Sc][(\mu\text{-Ph})BPh_3]$, reaction with 9-BBN (9-borabicyclo[3.3.1]nonane) led to, depending on the ancillary ligand

($C_5Me_5^-$ vs. $C_5Me_4H^-$), $(C_5Me_5)_2Sc(\mu\text{-}H)_2BC_8H_{14}$, and $(C_5Me_4H)_2Sc(\mu\text{-}H)_2BC_8H_{14}$, respectively, Figure 12.8a-b.

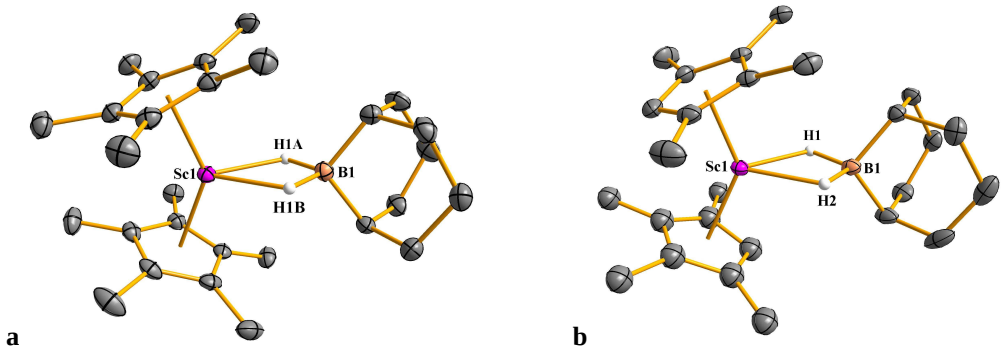

Figure 12.8. Thermal ellipsoid plots of (**a**) $(C_5Me_5)_2Sc(\mu\text{-}H)_2BC_8H_{14}$ and (**b**) $(C_5Me_4H)_2Sc(\mu\text{-}H)_2BC_8H_{14}$, drawn at the 50% probability level. Hydrogen atoms except the brigding hydrogens of the BBN component are omitted for clarity.

Structure determination revealed also that $(C_5Me_5)_2Sc(\mu\text{-}H)_2BC_8H_{14}$ shows two types of 9-BBN conformations, Figure 9a, whereas $(C_5Me_4H)_2Sc(\mu\text{-}H)_2BC_8H_{14}$ consists of only one. Oxygen exposure of $(C_5Me_4H)_2Sc(\mu\text{-}H)_2BC_8H_{14}$ yielded $(C_5Me_4H)_2Sc(\mu\text{-}O)BC_8H_{14}$, Figure 12.9b.

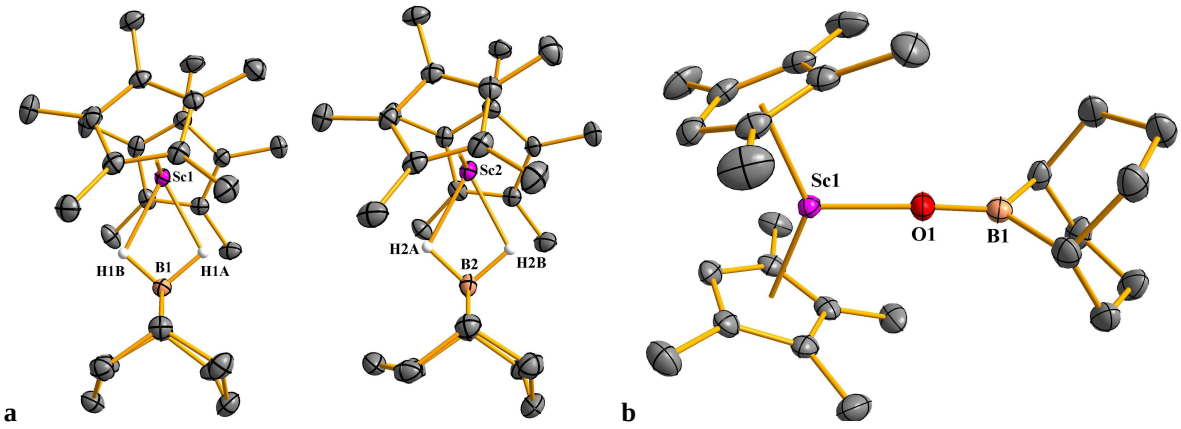

Figure 12.9. Thermal ellipsoid plots of (**a**) $(C_5Me_5)_2Sc(\mu\text{-}H)_2BC_8H_{14}$, showing both BBN conformers, and (**b**) $(C_5Me_4H)_2Sc(\mu\text{-}O)BC_8H_{14}$, drawn at the 50% probability level. Hydrogen atoms except the brigding hydrogens of the BBN component are omitted for clarity.

Furthermore, $(C_5Me_4H)_2Sc(\eta^3\text{-}C_3H_5)$ was found to be reactive towards diphenyldichalogenides. It reacted cleanly via sigma bond metathesis (SBM) with PhEEPh (E = S, Se, Te) in toluene to give $[(C_5Me_4H)_2ScSPh]_2$ and $(C_5Me_4H)_2ScEPh$ (E = Se, Te), Figure

12.10a-c. These products could also be obtained via SBM with $(\eta^5\text{-}C_5Me_4H)_2Sc(\eta^1\text{-}C_5Me_4H)$, but not as cleanly.

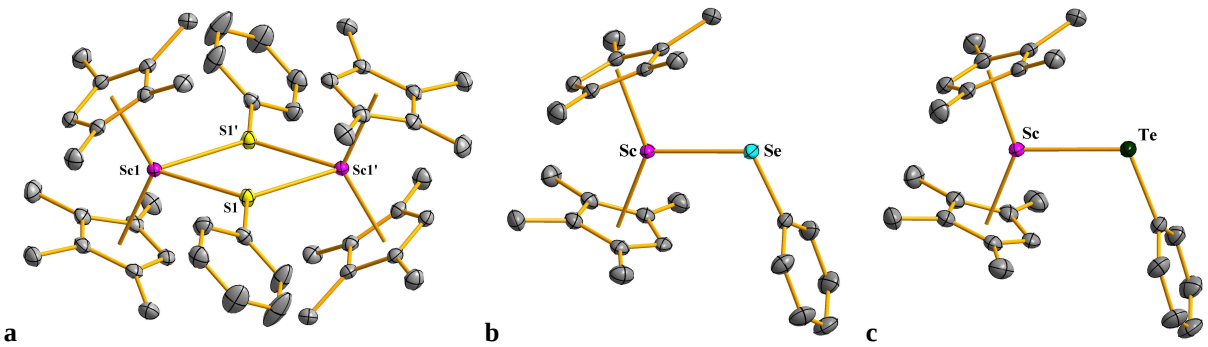

Figure 12.10. Thermal ellipsoid plots of (**a**) $[(C_5Me_4H)_2ScSPh]_2$, (**b**) $(C_5Me_4H)_2ScSePh$ and (**c**) $(C_5Me_4H)_2ScTePh$, drawn at the 50% probability level. Hydrogen atoms are omitted for clarity.

The same reactions were conducted in a mixture of toluene and THF and afforded the solvated $(C_5Me_4H)_2ScEPh(THF)$ (E = S, Se, Te) complexes, Figure 12.11a-c.

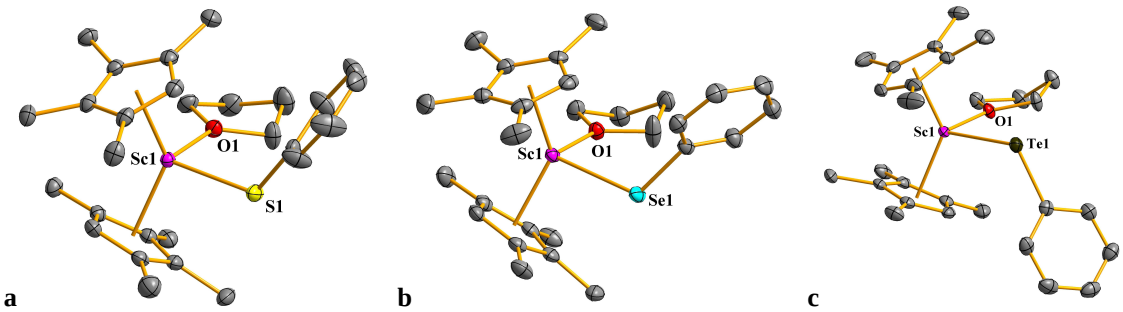

Figure 12.11. Thermal ellipsoid plots of (**a**) $(C_5Me_4H)_2ScSPh(THF)$, (**b**) $(C_5Me_4H)_2ScSePh(THF)$, (**c**) $(C_5Me_4H)_2ScTePh(THF)$, drawn at the 50% probability level. Hydrogen atoms are omitted for clarity.

In addition, the reaction of pySSpy with $(C_5Me_4H)_2Sc(\eta^3\text{-}C_3H_5)$ gave the analogous $(C_5Me_4H)_2ScSpy$ product, Figure 12.12a. A remarkable ligand redistribution of $(C_5Me_4H)_2ScSePh(THF)$, with loss of coordinated THF, formed an unprecedented trimetallic scandium selenium cluster complex, $[(C_5Me_4H)Sc]_3[SePh]_3$, Figure 12.12b.

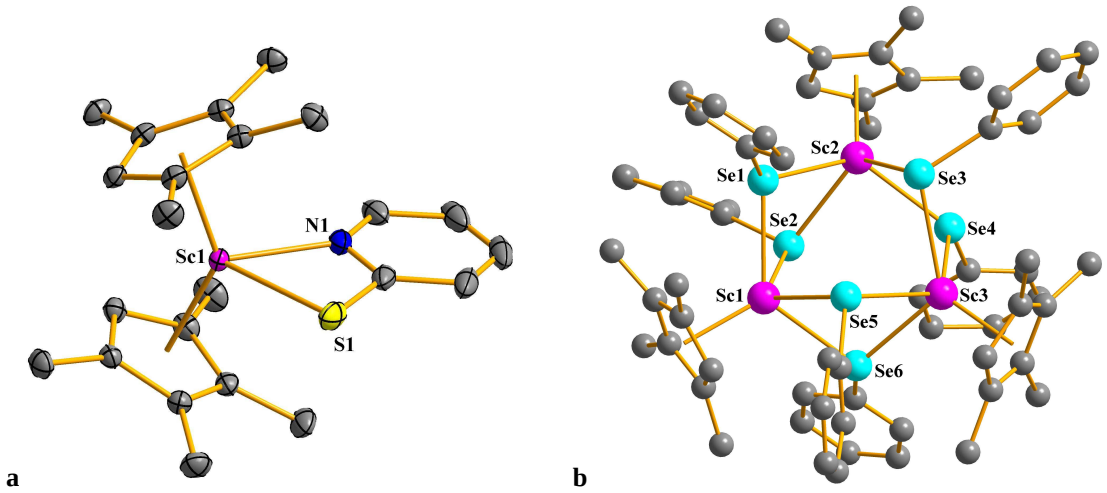

Figure 12.12. Thermal ellipsoid plot of (**a**) $(C_5Me_4H)_2ScSpy$, drawn at the 50% probability level. Ball-and-stick plot of (**b**) $[(C_5Me_4H)Sc]_3[SePh]_3$. Hydrogen atoms are omitted for clarity.

The slightly bulkier ligand $(C_5Me_5)^-$ containing $(C_5Me_5)_2Sc(\eta^3\text{-}C_3H_5)$ was analogously obtained from the reaction of $(C_5Me_5)_2ScCl(THF)$ and C_3H_5MgCl, Figure 12.13a-b. Reactivity studies of PhTeTePh with $(C_5Me_5)_2Sc(\eta^3\text{-}C_3H_5)$ resulted in the isolation of a scandium tellurium cluster complex, $\{[(C_5Me_5)Sc]_4(\mu_3\text{-}Te)_4\}$, Figure 12.13c.

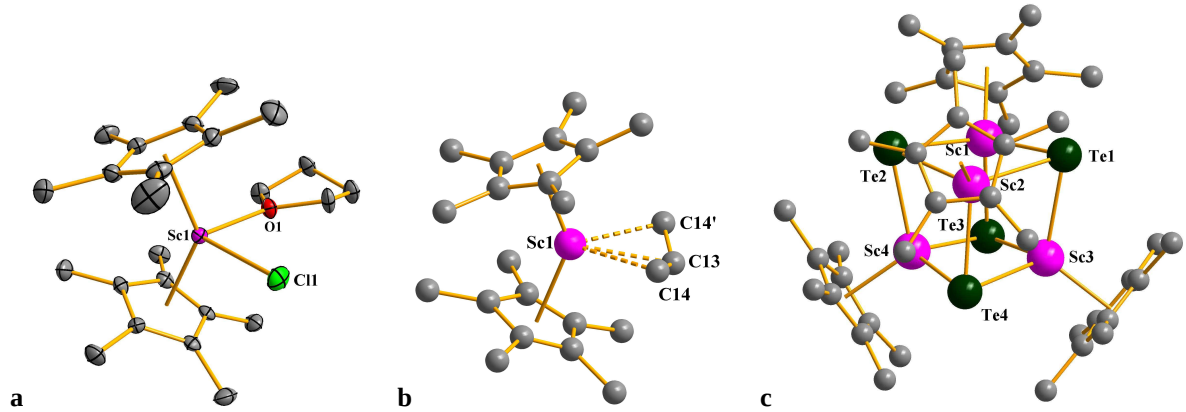

Figure 12.13. Thermal ellipsoid plot of (**a**) $(C_5Me_5)_2ScCl(THF)$ drawn at the 50% probability level. Ball-and-stick plot of (**b**) $(C_5Me_5)_2ScCl(THF)$ and (**c**) $\{[(C_5Me_5)Sc)_4](\mu_3\text{-}Te)_4\}$. Hydrogen atoms are omitted for clarity.

$(C_5Me_4H)_2Sc(\eta^3\text{-}C_3H_5)$ is also a suitable precursor to insert N_2O into the M-C bond to give a $[(C_5Me_4H)_2Sc(\mu\text{-}\eta^1\text{:}\eta^2\text{-}ON{=}NC_3H_5)]_2$ complex, Figure 12.14a. The extension of this reaction to $(C_5Me_4H)_2Y(\eta^3\text{-}C_3H_5)$ to afford $[(C_5Me_4H)_2Y(\mu\text{-}\eta^1\text{:}\eta^2\text{-}ON{=}NC_3H_5)]_2$, Figure

12.14b, and to $(C_5Me_5)_2M(\eta^3\text{-}C_3H_5)$ (M = Y, La, Sm) to yield $[(C_5Me_5)_2M(\mu\text{-}\eta^1{:}\eta^2\text{-}ON{=}NC_3H_5)]_2$, Figure 12.14c-e, was successful.

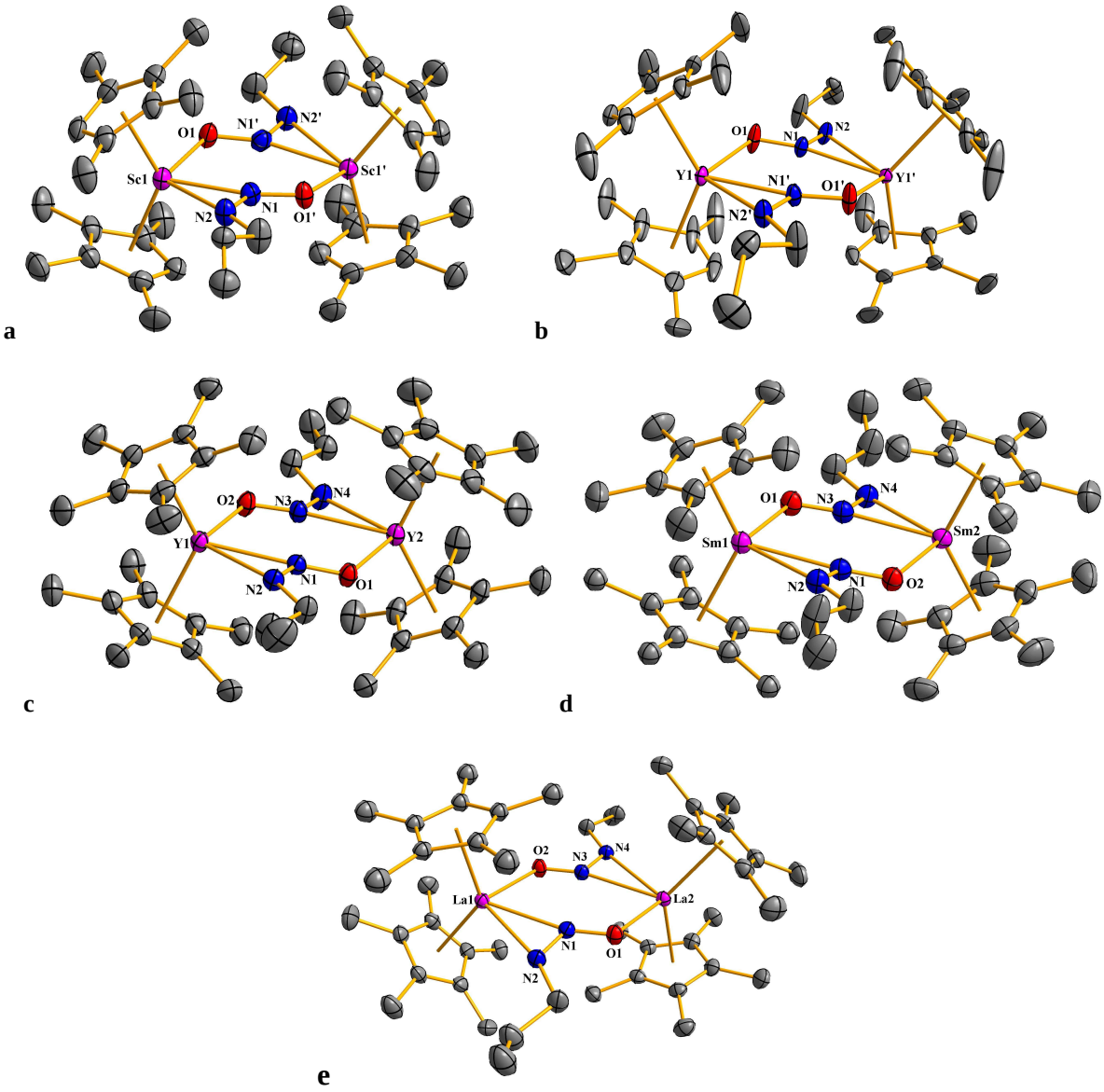

Figure 12.14. Thermal ellipsoid plots of (**a**) $[(C_5Me_4H)_2Sc(\mu\text{-}\eta^1{:}\eta^2\text{-}ON{=}NC_3H_5)]_2$, (**b**) $[(C_5Me_4H)_2Y(\mu\text{-}\eta^1{:}\eta^2\text{-}ON{=}NC_3H_5)]_2$, (**c**) $[(C_5Me_5)_2Y(\mu\text{-}\eta^1{:}\eta^2\text{-}ON{=}NC_3H_5)]_2$, (**d**) $[(C_5Me_5)_2Sm(\mu\text{-}\eta^1{:}\eta^2\text{-}ON{=}NC_3H_5)]_2$, (**e**) $[(C_5Me_5)_2La(\mu\text{-}\eta^1{:}\eta^2\text{-}ON{=}NC_3H_5)]_2$, drawn at the 50% probability level Hydrogen atoms are omitted for clarity.

Another insertion into the Sc-C bond of $(C_5Me_4H)_2Sc(\eta^3\text{-}C_3H_5)$ proceeded with $^iPrN{=}C{=}N^iPr$ to afford the scandium amidinate complex $(C_5Me_4H)_2Sc[(^iPr)NC(CH_2CH{=}CH_2)N(^iPr)\text{-}\kappa^2N,N']$, Figure 12.15.

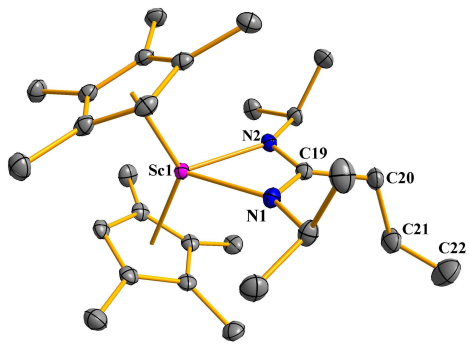

Figure 12.15. Thermal ellipsoid plot of $(C_5Me_4H)_2Sc[(^iPr)NC(CH_2CH{=}CH_2)N(^iPr)\text{-}\kappa^2N,N']$, drawn at the 50% probability level. Hydrogen atoms are omitted for clarity.

Finally, from the attempt to react $(C_5Me_4H)_2Sc(\eta^3\text{-}C_3H_5)$ with diphenylhydrazine, the desired products could not be isolated. Instead, a scandium hydroxo cluster complex, $(C_5Me_4H)_5Sc_5(\mu_5\text{-}O)(\mu_3\text{-}OH)_4(\mu_2\text{-}OH)_4\cdot[(C_6H_5)NH]_2$, crystallized, Figure 12.16.

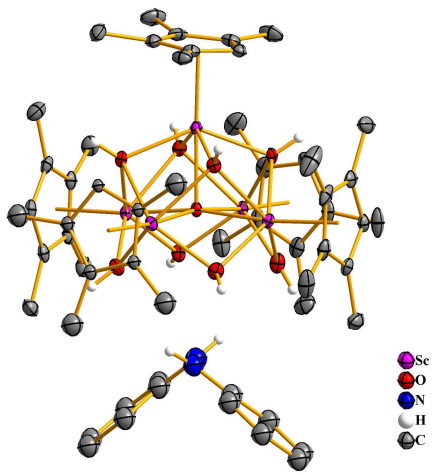

Figure 12.16. Thermal ellipsoid plot of $(C_5Me_4H)_5Sc_5(\mu_5\text{-}O)(\mu_3\text{-}OH)_4(\mu_2\text{-}OH)_4\cdot[(C_6H_5)NH]_2$, drawn at the 50% probability level. Hydrogen atoms, except those of the hydroxo and hydrazine groups, have been omitted for clarity.

The scandium allyl complex, $(C_5Me_4H)_2Sc(\eta^3\text{-}C_3H_5)$, has proven to be an excellent precursor for various reactions, for instance it can either deprotonate substrates or it can undergo insertion or SBM reactions. These properties can be used in future work to investigate further reactions.

Chapter 13

Appendix

13.1. Crystallographic Data for $[(C_5H_5)_2ScNSc(C_5H_5)(THF)]_2$, 2

X-ray Data Collection, Structure Solution and Refinement for **2**.

An orange crystal of approximate dimensions 0.08 x 0.10 x 0.21 mm was mounted on a glass fiber and transferred to a Bruker SMART APEX II diffractometer. The APEX2[1] program package was used to determine the unit-cell parameters and for data collection (60 sec/frame scan time for a sphere of diffraction data). The raw frame data was processed using SAINT[2] and SADABS[3] to yield the reflection data file. Subsequent calculations were carried out using the SHELXTL[4] program. The diffraction symmetry was *mmm* and the systematic absences were consistent with the orthorhombic space group *Pbcn* that was later determined to be correct.

The structure was solved by direct methods and refined on F^2 by full-matrix least-squares techniques. The analytical scattering factors[5] for neutral atoms were used throughout the analysis. Hydrogen atoms were included using a riding model. The molecule was located about a two-fold rotation axis. There were two molecules of THF solvent present per dimeric formula unit.

Least-squares analysis yielded wR2 = 0.1815 and Goof = 1.031 for 253 variables refined against 4500 data (0.80Å), R1 = 0.0612 for those 3213 data with $I > 2.0\sigma(I)$.

References

1. APEX2 Version 2.2-0, Bruker AXS, Inc.; Madison, WI 2007.
2. SAINT Version 7.46a, Bruker AXS, Inc.; Madison, WI 2007.
3. Sheldrick, G. M. SADABS, Version 2008/1, Bruker AXS, Inc.; Madison, WI 2007.
4. Sheldrick, G. M. SHELXTL, Version 2008/4, Bruker AXS, Inc.; Madison, WI 2008.
5. International Tables for X-Ray Crystallography 1992, Vol. C., Dordrecht: Kluwer Academic Publishers.

Table 13.1. Atomic coordinates (x 10^4) and equivalent isotropic displacement parameters ($Å^2$x 10^3) for **2**. U(eq) is defined as one third of the trace of the orthogonalized U^{ij} tensor.

	x	y	z	U(eq)
Sc(1)	-1154(1)	1768(1)	9092(1)	31(1)
Sc(2)	233(1)	2398(1)	8951(1)	26(1)
N(1)	-587(2)	2230(2)	7835(3)	29(1)
O(1)	873(1)	1644(1)	9827(3)	33(1)
C(1)	-1668(3)	2895(3)	9344(8)	76(2)
C(2)	-1700(3)	2587(3)	10528(6)	73(2)
C(3)	-2121(3)	2053(3)	10425(5)	56(1)
C(4)	-2333(2)	2033(3)	9206(6)	60(2)
C(5)	-2064(3)	2539(4)	8547(6)	73(2)
C(6)	-1621(2)	683(2)	8415(5)	51(1)
C(7)	-1011(2)	703(2)	7881(5)	47(1)
C(8)	-563(2)	669(2)	8880(5)	46(1)
C(9)	-906(2)	642(2)	10069(5)	47(1)
C(10)	-1553(2)	639(2)	9770(5)	50(1)
C(11)	756(2)	3074(2)	10712(4)	44(1)

C(12)	104(2)	3249(2)	10712(4)	45(1)
C(13)	-22(2)	3568(2)	9548(4)	40(1)
C(14)	536(2)	3594(2)	8834(4)	37(1)
C(15)	1031(2)	3287(2)	9539(4)	39(1)
C(16)	1565(2)	1674(2)	9607(4)	40(1)
C(17)	1837(2)	1108(2)	10370(5)	43(1)
C(18)	1402(2)	1105(2)	11539(4)	48(1)
C(19)	758(2)	1274(2)	11011(4)	48(1)
O(2)	1312(2)	4590(2)	6569(4)	68(1)
C(20)	922(4)	5135(3)	6698(7)	86(2)
C(21)	1047(5)	5442(4)	7937(7)	114(3)
C(22)	1684(4)	5258(6)	8249(10)	154(5)
C(23)	1842(3)	4683(3)	7414(8)	79(2)

Table 13.2. Anisotropic displacement parameters ($Å^2 x 10^3$) for **2**. The anisotropic displacement factor exponent takes the form: $-2\pi^2[h^2 a^{*2} U^{11} + ... + 2 h k a^* b^* U^{12}]$

	U^{11}	U^{22}	U^{33}	U^{23}	U^{13}	U^{12}
Sc(1)	37(1)	27(1)	29(1)	2(1)	3(1)	-4(1)
Sc(2)	27(1)	22(1)	29(1)	2(1)	6(1)	2(1)
N(1)	36(2)	35(2)	17(1)	0(1)	-2(1)	-18(1)
O(1)	27(1)	32(1)	40(2)	10(1)	4(1)	3(1)
C(1)	43(3)	32(3)	153(7)	13(4)	-1(4)	10(2)
C(2)	53(3)	81(4)	83(4)	-49(4)	-34(3)	43(3)
C(3)	48(3)	58(3)	61(3)	5(3)	19(3)	21(3)
C(4)	36(3)	59(3)	85(4)	-20(3)	-8(3)	7(2)
C(5)	70(4)	93(5)	56(3)	18(3)	-3(3)	40(4)
C(6)	45(3)	37(2)	71(3)	-10(2)	12(2)	-15(2)
C(7)	50(3)	36(2)	54(3)	-11(2)	10(2)	-6(2)
C(8)	42(2)	24(2)	72(3)	5(2)	25(2)	4(2)
C(9)	57(3)	27(2)	56(3)	12(2)	18(2)	4(2)
C(10)	50(3)	32(2)	68(3)	4(2)	29(2)	-8(2)
C(11)	59(3)	35(2)	38(2)	-4(2)	-17(2)	5(2)
C(12)	54(3)	42(2)	38(2)	-14(2)	2(2)	9(2)
C(13)	43(2)	28(2)	48(2)	-14(2)	-9(2)	8(2)
C(14)	50(3)	20(2)	40(2)	1(2)	-10(2)	-3(2)
C(15)	35(2)	28(2)	54(3)	-6(2)	-7(2)	-3(2)
C(16)	30(2)	43(2)	47(2)	7(2)	-2(2)	0(2)
C(17)	37(2)	37(2)	56(3)	9(2)	-3(2)	5(2)
C(18)	54(3)	49(3)	41(2)	12(2)	-5(2)	11(2)
C(19)	40(2)	51(3)	53(3)	28(2)	7(2)	8(2)
O(2)	92(3)	50(2)	63(2)	-5(2)	6(2)	1(2)
C(20)	121(6)	51(3)	87(5)	11(3)	6(4)	28(4)
C(21)	205(10)	63(4)	75(5)	-4(4)	24(6)	57(5)
C(22)	69(5)	262(14)	132(8)	-123(9)	47(5)	-66(7)
C(23)	48(3)	63(4)	127(6)	-7(4)	21(4)	-6(3)

Table 13.3. Hydrogen coordinates ($x 10^4$) and isotropic displacement parameters ($Å^2 x 10^3$) for **2**.

	x	y	z	U(eq)
H(1A)	-1465	3332	9152	91
H(2A)	-1520	2767	11346	87
H(3A)	-2293	1785	11154	67
H(4A)	-2687	1742	8883	72
H(5A)	-2187	2674	7659	88

H(6A)	-2032	624	7929	61
H(7A)	-910	664	6948	56
H(8A)	-88	615	8776	55
H(9A)	-715	559	10934	56
H(10A)	-1911	555	10390	60
H(11A)	998	2890	11459	53
H(12A)	-197	3217	11457	54
H(13A)	-430	3804	9332	48
H(14A)	596	3853	8027	44
H(15A)	1499	3290	9322	47
H(16A)	1743	2101	9907	48
H(16B)	1665	1621	8685	48
H(17A)	2291	1190	10610	52
H(17B)	1808	686	9893	52
H(18A)	1398	664	11951	57
H(18B)	1544	1439	12174	57
H(19A)	510	867	10831	57
H(19B)	514	1548	11629	57
H(20A)	465	5001	6640	103
H(20B)	1012	5455	6001	103
H(21A)	1007	5930	7880	137
H(21B)	742	5277	8591	137
H(22A)	1715	5132	9164	185
H(22B)	1984	5629	8084	185
H(23A)	2239	4773	6919	95
H(23B)	1911	4281	7939	95

13.2. Crystallographic Data for $[(C_5H_5)_2Sc]_2[\mu\text{-}O(C_3H_7)]_2$, 3

X-ray Data Collection, Structure Solution and Refinement for **3**.

A brown crystal of approximate dimensions 0.26 x 0.30 x 0.31 mm was mounted on a glass fiber and transferred to a Bruker SMART APEX II diffractometer. The APEX2[1] program package was used to determine the unit-cell parameters and for data collection (20 sec/frame scan time for a sphere of diffraction data). The raw frame data was processed using SAINT[2] and SADABS[3] to yield the reflection data file. Subsequent calculations were carried out using the SHELXTL[4] program. The diffraction symmetry was 4/*mmm* and the systematic absences were consistent with the tetragonal space group $P4_22_12$ that was later determined to be correct.

The structure was solved by direct methods and refined on F^2 by full-matrix least-squares techniques. The analytical scattering factors[5] for neutral atoms were used throughout the analysis. Hydrogen atoms were included using a riding model. The molecule was located on a two-fold rotation axis. Carbon atoms C(11), C(12), and C(13) were disordered and included using multiple components with partial site-occupancy-factors (approx. 0.85/0.15).

At convergence, wR2 = 0.0856 and Goof = 1.078 for 165 variables refined against 2956 data (0.75Å), R1 = 0.0304 for those 2820 data with I > 2.0σ(I). The absolute structure was assigned by refinement of the Flack parameter[6].

References

1. APEX2 Version 2008.3-0, Bruker AXS, Inc.; Madison, WI 2008.
2. SAINT Version 7.53a, Bruker AXS, Inc.; Madison, WI 2007.
3. Sheldrick, G. M. SADABS, Version 2008/1, Bruker AXS, Inc.; Madison, WI 2008.
4. Sheldrick, G. M. SHELXTL, Version 2008/4, Bruker AXS, Inc.; Madison, WI 2008.
5. International Tables for X-Ray Crystallography 1992, Vol. C., Dordrecht: Kluwer Academic Publishers.
6. Flack, H. D. Acta. Cryst., A39, 876-881, 1983.

Table 13.4. Atomic coordinates (x 10^4) and equivalent isotropic displacement parameters (Å^{2}x 10^3) for sd22. U(eq) is defined as one third of the trace of the orthogonalized U^{ij} tensor.

	x	y	z	U(eq)
Sc(1)	-3333(1)	6667(1)	-5000	22(1)
Sc(2)	-1970(1)	8030(1)	-5000	21(1)
O(1)	-3034(1)	7729(1)	-3898(1)	24(1)
C(1)	-4206(1)	7540(1)	-6736(3)	33(1)
C(2)	-4687(1)	7173(1)	-5569(3)	37(1)
C(3)	-4704(1)	6389(1)	-5933(3)	40(1)
C(4)	-4213(1)	6244(1)	-7302(3)	42(1)
C(5)	-3908(1)	6974(1)	-7804(2)	35(1)
C(6)	-2726(1)	9064(1)	-6522(2)	32(1)
C(7)	-2049(1)	9435(1)	-5861(2)	33(1)
C(8)	-1406(1)	9130(1)	-6703(2)	32(1)
C(9)	-1662(1)	8567(1)	-7833(2)	32(1)
C(10)	-2476(1)	8538(1)	-7738(2)	30(1)
C(11)	-3414(1)	7997(2)	-2410(3)	30(1)
C(12)	-3700(2)	8828(2)	-2573(3)	43(1)
C(13)	-4088(2)	9101(3)	-942(5)	54(1)
C(11A)	-3470(9)	8340(9)	-3130(30)	41(4)
C(12A)	-3706(12)	8062(9)	-1540(20)	46(5)
C(13A)	-4119(13)	8731(11)	-630(30)	43(5)

Table 13.5. Anisotropic displacement parameters (Å^{2}x 10^3) for sd22. The anisotropic displacement factor exponent takes the form: $-2\pi^2[h^2 a^{*2}U^{11} + ... + 2 h k a^* b^* U^{12}]$

	U^{11}	U^{22}	U^{33}	U^{23}	U^{13}	U^{12}
Sc(1)	22(1)	22(1)	22(1)	0(1)	0(1)	-2(1)
Sc(2)	22(1)	22(1)	17(1)	0(1)	0(1)	-2(1)
O(1)	24(1)	26(1)	21(1)	-4(1)	2(1)	-1(1)
C(1)	30(1)	32(1)	38(1)	0(1)	-13(1)	1(1)
C(2)	22(1)	47(1)	43(1)	0(1)	-4(1)	3(1)
C(3)	23(1)	44(1)	52(1)	6(1)	-10(1)	-9(1)
C(4)	41(1)	34(1)	51(1)	-14(1)	-22(1)	3(1)
C(5)	32(1)	48(1)	25(1)	-1(1)	-8(1)	0(1)
C(6)	34(1)	29(1)	34(1)	5(1)	-1(1)	4(1)
C(7)	47(1)	21(1)	31(1)	0(1)	-3(1)	-2(1)
C(8)	35(1)	29(1)	33(1)	8(1)	1(1)	-6(1)
C(9)	42(1)	32(1)	24(1)	6(1)	4(1)	-3(1)
C(10)	39(1)	29(1)	22(1)	6(1)	-6(1)	-3(1)
C(11)	32(1)	37(1)	22(1)	-4(1)	7(1)	-2(1)
C(12)	38(1)	48(2)	42(1)	-15(1)	3(1)	7(1)
C(13)	44(2)	67(2)	52(2)	-26(2)	6(1)	5(2)
C(11A)	45(8)	23(7)	56(11)	-18(8)	8(7)	14(6)
C(12A)	71(11)	31(7)	36(9)	4(6)	13(9)	0(7)
C(13A)	52(10)	33(9)	43(9)	-18(8)	-9(7)	22(9)

Table 13.6. Hydrogen coordinates (x 10^4) and isotropic displacement parameters ($Å^2$x 10^{-3}) for **3**.

	x	y	z	U(eq)
H(1A)	-4100	8081	-6791	40
H(2A)	-4955	7421	-4683	45
H(3A)	-4998	6008	-5354	48
H(4A)	-4107	5753	-7794	50
H(5A)	-3563	7062	-8706	42
H(6A)	-3249	9157	-6196	39
H(7A)	-2037	9818	-5010	40
H(8A)	-881	9281	-6534	39
H(9A)	-1342	8260	-8537	39
H(10A)	-2804	8214	-8390	36
H(11A)	-3046	7963	-1467	36
H(11B)	-3861	7653	-2162	36
H(12A)	-4080	8862	-3495	51
H(12B)	-3257	9173	-2840	51
H(13A)	-4269	9638	-1072	82
H(13B)	-3710	9075	-33	82
H(13C)	-4532	8764	-687	82
H(11C)	-3930	8471	-3817	49
H(11D)	-3145	8812	-3015	49
H(12C)	-3247	7889	-893	55
H(13D)	-4297	8551	465	64
H(13E)	-4567	8904	-1281	64
H(13F)	-3756	9166	-480	64

13.3. Crystallographic Data for $(C_5Me_4H)_2ScCl(THF)$, 6

X-ray Data Collection, Structure Solution and Refinement for **6**.

A colorless crystal of approximate dimensions 0.13 x 0.23 x 0.24 mm was mounted on a glass fiber and transferred to a Bruker SMART APEX II diffractometer. The APEX2[1] program package was used to determine the unit-cell parameters and for data collection (25 sec/frame scan time for a sphere of diffraction data). The raw frame data was processed using SAINT[2] and SADABS[3] to yield the reflection data file. Subsequent calculations were carried out using the SHELXTL[4] program. The diffraction symmetry was 2/*m* and the systematic absences were consistent with the monoclinic space group $P2_1/n$ that was later determined to be correct.

The structure was solved by direct methods and refined on F^2 by full-matrix least-squares techniques. The analytical scattering factors[5] for neutral atoms were used throughout the analysis. Hydrogen atoms were included using a riding model.

At convergence, wR2 = 0.0913 and Goof = 1.034 for 234 variables refined against 4923 data (0.76Å), R1 = 0.0333 for those 4367 data with I > 2.0σ(I).

References

1. APEX2 Version 2.2-0 Bruker AXS, Inc.; Madison, WI 2007.
2. SAINT Version 7.46a, Bruker AXS, Inc.; Madison, WI 2007.
3. Sheldrick, G. M. SADABS, Version 2008/1, Bruker AXS, Inc.; Madison, WI 2008.
4. Sheldrick, G. M. SHELXTL, Version 2008/3, Bruker AXS, Inc.; Madison, WI 2008.
5. International Tables for X-Ray Crystallography 1992, Vol. C., Dordrecht: Kluwer Academic Publishers.

Table 13.7. Atomic coordinates (x 10^4) and equivalent isotropic displacement parameters (Å^{2}x 10^3) for **6**. U(eq) is defined as one third of the trace of the orthogonalized U^{ij} tensor.

	x	y	z	U(eq)
Sc(1)	1329(1)	1313(1)	2386(1)	14(1)
Cl(1)	2464(1)	2813(1)	2468(1)	24(1)
O(1)	3520(1)	843(1)	3160(1)	19(1)
C(1)	2783(2)	889(1)	1230(1)	25(1)
C(2)	1679(2)	1527(1)	898(1)	25(1)
C(3)	187(2)	1141(1)	894(1)	29(1)
C(4)	372(2)	262(1)	1199(1)	31(1)
C(5)	1962(2)	117(1)	1424(1)	28(1)
C(6)	4519(2)	989(2)	1302(1)	60(1)
C(7)	2010(4)	2411(1)	522(1)	57(1)
C(8)	-1320(3)	1535(2)	493(1)	72(1)
C(9)	-860(3)	-458(2)	1148(2)	75(1)
C(10)	-310(2)	500(1)	3267(1)	20(1)
C(11)	419(2)	1156(1)	3815(1)	23(1)
C(12)	-102(2)	2017(1)	3536(1)	24(1)
C(13)	-1158(2)	1906(1)	2814(1)	22(1)
C(14)	-1301(2)	972(1)	2657(1)	19(1)
C(15)	-174(2)	-506(1)	3355(1)	27(1)
C(16)	1457(2)	996(2)	4606(1)	36(1)
C(17)	284(2)	2897(1)	3966(1)	39(1)
C(18)	-2036(2)	2652(1)	2344(1)	34(1)
C(19)	4815(2)	1412(1)	3520(1)	22(1)
C(20)	5908(2)	789(1)	4054(1)	24(1)
C(21)	5605(2)	-119(1)	3636(1)	23(1)
C(22)	3865(2)	-92(1)	3383(1)	26(1)

Table 13.8. Anisotropic displacement parameters (Å^{2}x 10^3) for **6**. The anisotropic displacement factor exponent takes the form: $-2\pi^2[h^2 a^{*2}U^{11} + ... + 2 h k a^* b^* U^{12}]$

	U^{11}	U^{22}	U^{33}	U^{23}	U^{13}	U^{12}
Sc(1)	13(1)	14(1)	17(1)	1(1)	1(1)	0(1)
Cl(1)	26(1)	15(1)	32(1)	1(1)	4(1)	-4(1)
O(1)	15(1)	15(1)	25(1)	1(1)	-3(1)	-1(1)
C(1)	18(1)	38(1)	18(1)	-2(1)	3(1)	2(1)
C(2)	35(1)	23(1)	17(1)	2(1)	4(1)	0(1)
C(3)	22(1)	46(1)	17(1)	-4(1)	-1(1)	9(1)
C(4)	35(1)	37(1)	22(1)	-13(1)	12(1)	-17(1)
C(5)	47(1)	21(1)	18(1)	0(1)	7(1)	10(1)
C(6)	19(1)	132(2)	31(1)	-13(1)	6(1)	0(1)
C(7)	114(2)	31(1)	28(1)	8(1)	19(1)	-12(1)
C(8)	41(1)	146(3)	25(1)	-9(1)	-8(1)	48(2)
C(9)	92(2)	90(2)	51(1)	-46(1)	42(1)	-71(2)
C(10)	16(1)	22(1)	22(1)	2(1)	7(1)	-1(1)
C(11)	18(1)	32(1)	19(1)	0(1)	5(1)	-3(1)
C(12)	22(1)	25(1)	26(1)	-7(1)	8(1)	-3(1)

C(13)	17(1)	21(1)	28(1)	0(1)	7(1)	2(1)
C(14)	13(1)	21(1)	22(1)	-1(1)	4(1)	-2(1)
C(15)	24(1)	22(1)	36(1)	8(1)	9(1)	1(1)
C(16)	29(1)	58(1)	20(1)	4(1)	2(1)	-4(1)
C(17)	39(1)	34(1)	45(1)	-19(1)	14(1)	-9(1)
C(18)	25(1)	26(1)	50(1)	7(1)	8(1)	7(1)
C(19)	18(1)	21(1)	27(1)	-3(1)	-2(1)	-4(1)
C(20)	20(1)	27(1)	24(1)	-2(1)	-3(1)	0(1)
C(21)	20(1)	24(1)	26(1)	1(1)	-1(1)	4(1)
C(22)	23(1)	17(1)	36(1)	4(1)	-6(1)	0(1)

Table 13.9. Hydrogen coordinates (x 10^4) and isotropic displacement parameters ($Å^2$x 10^{3}) for **6**.

	x	y	z	U(eq)
H(5A)	2448	-477	1591	34
H(6A)	5015	532	1678	90
H(6B)	4817	1589	1513	90
H(6C)	4859	912	762	90
H(7A)	3042	2623	759	85
H(7B)	1222	2851	633	85
H(7C)	1984	2338	-70	85
H(8A)	-1466	1380	-90	107
H(8B)	-1293	2191	555	107
H(8C)	-2185	1290	753	107
H(9A)	-1105	-659	580	112
H(9B)	-1801	-214	1339	112
H(9C)	-477	-969	1493	112
H(14A)	-2125	689	2256	22
H(15A)	504	-653	3861	41
H(15B)	272	-755	2886	41
H(15C)	-1208	-766	3374	41
H(16A)	1467	353	4737	53
H(16B)	1064	1336	5046	53
H(16C)	2516	1195	4550	53
H(17A)	53	3393	3577	58
H(17B)	1392	2907	4182	58
H(17C)	-341	2963	4417	58
H(18A)	-2746	2934	2686	50
H(18B)	-2635	2408	1848	50
H(18C)	-1299	3103	2193	50
H(19A)	4434	1899	3853	27
H(19B)	5353	1686	3086	27
H(20A)	5653	775	4622	29
H(20B)	7006	976	4060	29
H(21A)	6173	-177	3154	28
H(21B)	5904	-621	4019	28
H(22A)	3560	-496	2911	31
H(22B)	3303	-278	3842	31

13.4. Crystallographic Data for $[(C_5Me_4H)_2Sc(THF)_2][BPh_4]$, 9

Table 13.10. Atomic coordinates (x 10^4) and equivalent isotropic displacement parameters ($Å^2$x 10^3) for **9**. U(eq) is defined as one third of the trace of the orthogonalized U^{ij} tensor.

	x	y	z	U(eq)
Sc(1)	2697(1)	5888(1)	-546(1)	32(1)
Sc(2)	2280(1)	584(1)	4061(1)	34(1)
O(1)	3269(4)	7239(4)	-346(4)	36(2)
O(2)	1970(4)	5963(4)	-1750(4)	34(2)
O(3)	1745(4)	671(4)	2812(4)	38(2)
O(4)	3083(4)	1890(4)	4265(4)	46(2)
C(1)	2239(6)	6172(6)	769(6)	40(2)
C(2)	1571(6)	6395(6)	215(6)	41(2)
C(3)	1087(6)	5684(6)	-390(6)	39(2)
C(4)	1407(6)	5017(6)	-236(6)	38(2)
C(5)	2128(6)	5324(6)	477(6)	36(2)
C(6)	2815(7)	6688(6)	1573(6)	44(2)
C(7)	1382(7)	7232(7)	325(7)	58(3)
C(8)	220(6)	5593(8)	-1007(7)	55(3)
C(9)	1010(6)	4133(6)	-696(6)	44(2)
C(10)	4095(6)	5505(6)	51(6)	37(2)
C(11)	3505(6)	4737(6)	-439(6)	40(2)
C(12)	3348(6)	4765(6)	-1249(6)	35(2)
C(13)	3868(5)	5546(5)	-1271(6)	32(2)
C(14)	4314(5)	5978(6)	-474(6)	36(2)
C(15)	4492(6)	5701(7)	938(6)	43(2)
C(16)	3259(6)	3987(6)	-159(6)	41(2)
C(17)	2913(6)	4028(6)	-1941(6)	41(2)
C(18)	4026(6)	5807(6)	-2004(6)	41(2)
C(19)	3609(6)	7843(6)	435(6)	44(2)
C(20)	3742(7)	8665(7)	234(7)	57(3)
C(21)	3610(6)	8483(6)	-663(6)	44(3)
C(22)	3693(6)	7610(6)	-882(6)	41(2)
C(23)	1560(6)	6652(6)	-1862(6)	43(2)
C(24)	843(8)	6303(7)	-2634(7)	61(3)
C(25)	1113(8)	5621(7)	-3103(6)	52(3)
C(26)	1633(6)	5295(6)	-2466(6)	39(2)
C(27)	1010(6)	1176(6)	4401(6)	38(2)
C(28)	1641(6)	1286(6)	5154(6)	39(2)
C(29)	1638(6)	501(6)	5271(6)	40(2)
C(30)	1031(6)	-100(6)	4604(6)	41(2)
C(31)	689(6)	330(7)	4072(6)	48(3)
C(32)	649(7)	1828(8)	4090(8)	61(3)
C(33)	2077(7)	2074(7)	5792(7)	54(3)
C(34)	2084(8)	343(7)	6047(6)	53(3)
C(35)	711(8)	-1008(7)	4537(8)	62(3)
C(36)	2585(6)	-805(6)	3653(6)	37(2)
C(37)	3129(6)	-336(6)	3287(6)	41(2)
C(38)	3801(5)	295(6)	3901(7)	43(2)
C(39)	3667(6)	190(6)	4645(6)	42(3)
C(40)	2920(6)	-500(6)	4496(6)	41(2)
C(41)	1883(6)	-1603(6)	3221(7)	45(3)
C(42)	3086(7)	-572(7)	2391(7)	55(3)
C(43)	4573(7)	864(7)	3741(7)	56(3)
C(44)	4250(7)	642(7)	5500(7)	57(3)
C(45)	2334(7)	1079(7)	2366(7)	54(3)
C(46)	1897(9)	700(9)	1518(8)	80(4)
C(47)	919(7)	431(10)	1467(7)	75(4)
C(48)	858(6)	226(8)	2253(7)	57(3)

C(49)	3974(6)	2346(7)	4843(7)	55(3)
C(50)	4353(7)	3012(7)	4481(8)	57(3)
C(51)	3539(8)	3057(7)	3825(7)	55(3)
C(52)	2739(6)	2555(6)	4018(7)	43(2)
B(1)	2601(7)	985(7)	-949(7)	34(2)
B(2)	2236(6)	5273(7)	3734(7)	40(3)
C(53)	3166(6)	1345(6)	4(6)	38(2)
C(54)	3205(6)	2091(6)	498(6)	38(2)
C(55)	3711(7)	2381(6)	1297(6)	48(3)
C(56)	4208(6)	1916(7)	1646(7)	49(3)
C(57)	4209(6)	1161(7)	1161(6)	47(3)
C(58)	3694(6)	879(6)	358(6)	38(2)
C(59)	1789(6)	1438(6)	-1178(6)	35(2)
C(60)	1573(6)	1660(6)	-1880(6)	38(2)
C(61)	813(6)	1987(6)	-2078(6)	43(2)
C(62)	280(6)	2102(6)	-1559(6)	44(3)
C(63)	457(6)	1872(6)	-865(8)	50(3)
C(64)	1205(6)	1538(6)	-665(6)	40(2)
C(65)	3348(5)	1098(6)	-1469(5)	32(2)
C(66)	3741(6)	466(7)	-1748(6)	43(2)
C(67)	4417(6)	592(7)	-2170(6)	49(3)
C(68)	4699(6)	1327(7)	-2336(6)	48(3)
C(69)	4348(6)	1961(7)	-2042(6)	49(3)
C(70)	3681(6)	1848(6)	-1619(6)	40(2)
C(71)	2027(6)	11(6)	-1145(6)	36(2)
C(72)	1768(6)	-323(6)	-538(7)	44(3)
C(73)	1184(6)	-1103(7)	-713(8)	54(3)
C(74)	914(6)	-1601(7)	-1472(8)	54(3)
C(75)	1169(7)	-1284(7)	-2077(8)	57(3)
C(76)	1724(6)	-504(6)	-1919(7)	48(3)
C(77)	1914(5)	4427(6)	2957(6)	39(2)
C(78)	1513(6)	3652(6)	3047(6)	40(2)
C(79)	1277(7)	2961(7)	2418(6)	49(3)
C(80)	1387(6)	2978(7)	1667(6)	47(3)
C(81)	1767(6)	3739(6)	1566(7)	43(2)
C(82)	2000(6)	4433(7)	2200(6)	43(2)
C(83)	3098(6)	5927(7)	3600(6)	43(2)
C(84)	3805(6)	5665(7)	3321(7)	51(3)
C(85)	4531(6)	6227(8)	3231(7)	56(3)
C(86)	4573(6)	7046(7)	3408(7)	52(3)
C(87)	3890(7)	7340(7)	3677(6)	51(3)
C(88)	3166(6)	6770(6)	3769(6)	45(3)
C(89)	1382(6)	5726(6)	3764(6)	41(2)
C(90)	976(6)	5936(6)	3066(7)	48(3)
C(91)	322(6)	6398(6)	3064(8)	51(3)
C(92)	100(6)	6686(7)	3767(8)	53(3)
C(93)	469(7)	6500(7)	4454(8)	57(3)
C(94)	1139(6)	6039(6)	4450(7)	48(3)
C(95)	2563(6)	5014(6)	4574(6)	41(2)
C(96)	1960(6)	4601(6)	4941(6)	42(2)
C(97)	2206(7)	4298(6)	5583(6)	45(3)
C(98)	3146(7)	4412(7)	5927(7)	51(3)
C(99)	3759(7)	4825(6)	5602(6)	45(3)
C(100)	3489(6)	5125(6)	4957(6)	42(2)
O(5)	3123(7)	7332(5)	7115(5)	80(3)
C(101)	3356(9)	6946(8)	6439(8)	70(4)
C(102)	3218(10)	7441(10)	5849(8)	83(5)
C(103)	2914(9)	8181(12)	6285(11)	105(6)
C(104)	3217(9)	8158(8)	7145(8)	70(4)

Table 13.11. Anisotropic displacement parameters ($Å^2 x\ 10^3$) for **9**. The anisotropic displacement factor exponent takes the form: $-2\pi^2[\ h^2\ a^{*2}U^{11} + ...\ + 2\ h\ k\ a^*\ b^*\ U^{12}\ ]$

	U^{11}	U^{22}	U^{33}	U^{23}	U^{13}	U^{12}
Sc(1)	11(1)	40(1)	42(1)	11(1)	3(1)	9(1)
Sc(2)	11(1)	46(1)	43(1)	9(1)	4(1)	9(1)
O(1)	18(3)	45(4)	46(4)	15(3)	6(3)	8(3)
O(2)	17(3)	45(4)	43(4)	16(3)	5(3)	13(3)
O(3)	15(3)	57(4)	44(4)	21(3)	5(3)	8(3)
O(4)	12(3)	49(4)	74(5)	16(4)	7(3)	7(3)
C(1)	26(5)	57(7)	44(6)	17(5)	11(4)	20(4)
C(2)	33(5)	51(6)	52(6)	23(5)	15(5)	22(5)
C(3)	18(4)	63(7)	45(6)	30(5)	7(4)	13(4)
C(4)	15(4)	48(6)	45(6)	15(5)	0(4)	2(4)
C(5)	19(4)	46(6)	39(6)	5(5)	3(4)	9(4)
C(6)	54(6)	43(6)	36(6)	8(5)	15(5)	11(5)
C(7)	35(6)	78(8)	65(8)	10(6)	18(5)	26(5)
C(8)	13(4)	98(9)	65(7)	39(6)	11(4)	19(5)
C(9)	28(5)	57(7)	44(6)	12(5)	4(4)	11(4)
C(10)	22(4)	44(6)	37(5)	-1(5)	-7(4)	17(4)
C(11)	22(4)	48(6)	52(6)	10(5)	7(4)	23(4)
C(12)	30(5)	42(6)	46(6)	25(5)	15(4)	20(4)
C(13)	12(4)	37(5)	52(6)	20(5)	6(4)	10(4)
C(14)	16(4)	33(5)	55(6)	2(5)	6(4)	8(4)
C(15)	23(5)	58(7)	50(6)	18(5)	2(4)	16(4)
C(16)	31(5)	48(6)	53(6)	17(5)	19(4)	17(4)
C(17)	26(5)	49(6)	48(6)	10(5)	7(4)	15(4)
C(18)	13(4)	49(6)	57(6)	16(5)	3(4)	7(4)
C(19)	25(5)	52(6)	48(6)	7(5)	4(4)	6(4)
C(20)	39(6)	61(7)	66(8)	28(6)	-1(5)	5(5)
C(21)	12(4)	51(6)	67(7)	18(5)	3(4)	6(4)
C(22)	29(5)	51(6)	49(6)	28(5)	6(4)	11(4)
C(23)	32(5)	47(6)	54(6)	17(5)	6(4)	21(4)
C(24)	48(7)	70(8)	58(7)	5(6)	-6(5)	28(6)
C(25)	52(7)	59(7)	32(6)	2(5)	-9(5)	16(5)
C(26)	24(5)	44(6)	49(6)	16(5)	4(4)	11(4)
C(27)	19(4)	55(6)	46(6)	14(5)	6(4)	23(4)
C(28)	29(5)	58(7)	39(6)	24(5)	12(4)	16(4)
C(29)	32(5)	57(7)	49(6)	31(5)	20(5)	23(5)
C(30)	34(5)	50(6)	48(6)	21(5)	23(5)	10(5)
C(31)	16(4)	71(8)	49(6)	4(6)	9(4)	4(4)
C(32)	37(6)	86(9)	79(9)	44(7)	23(6)	29(6)
C(33)	48(6)	55(7)	55(7)	0(6)	18(5)	15(5)
C(34)	61(7)	72(8)	49(7)	38(6)	27(5)	33(6)
C(35)	54(7)	57(7)	87(9)	23(7)	44(7)	10(6)
C(36)	21(4)	41(6)	47(6)	9(5)	8(4)	10(4)
C(37)	26(5)	55(6)	42(6)	10(5)	9(4)	12(4)
C(38)	12(4)	58(7)	60(7)	19(5)	7(4)	13(4)
C(39)	11(4)	53(6)	58(7)	13(5)	-3(4)	11(4)
C(40)	26(5)	54(6)	42(6)	6(5)	5(4)	14(4)
C(41)	18(4)	44(6)	65(7)	3(5)	8(4)	1(4)
C(42)	41(6)	60(7)	64(7)	2(6)	14(5)	25(5)
C(43)	31(5)	56(7)	81(8)	10(6)	23(5)	11(5)
C(44)	33(5)	63(7)	62(7)	4(6)	-7(5)	18(5)
C(45)	42(6)	66(7)	56(7)	18(6)	20(5)	8(5)
C(46)	66(9)	86(10)	68(9)	10(7)	10(7)	-10(7)
C(47)	31(6)	148(13)	51(7)	35(8)	2(5)	34(7)
C(48)	9(4)	96(9)	59(7)	21(6)	-3(4)	6(5)
C(49)	20(5)	59(7)	67(7)	-3(6)	-4(5)	5(5)
C(50)	25(5)	54(7)	89(9)	9(6)	21(5)	8(5)
C(51)	54(7)	43(6)	67(8)	14(6)	25(6)	1(5)

C(52)	32(5)	41(6)	59(7)	14(5)	13(5)	11(4)
B(1)	22(5)	40(6)	38(6)	2(5)	11(4)	11(4)
B(2)	6(4)	64(8)	55(7)	22(6)	11(4)	12(4)
C(53)	15(4)	56(6)	47(6)	20(5)	10(4)	8(4)
C(54)	25(5)	40(6)	45(6)	10(5)	6(4)	1(4)
C(55)	43(6)	43(6)	49(7)	8(5)	9(5)	-2(5)
C(56)	16(4)	71(8)	50(7)	20(6)	2(4)	-6(5)
C(57)	20(5)	72(8)	55(7)	27(6)	11(4)	9(5)
C(58)	20(4)	47(6)	49(6)	13(5)	7(4)	14(4)
C(59)	19(4)	44(6)	40(6)	5(5)	9(4)	11(4)
C(60)	26(4)	50(6)	40(6)	17(5)	4(4)	15(4)
C(61)	35(5)	54(6)	41(6)	10(5)	1(4)	23(5)
C(62)	20(4)	50(6)	56(7)	7(5)	2(4)	12(4)
C(63)	20(5)	53(7)	86(9)	22(6)	22(5)	15(4)
C(64)	22(4)	56(6)	54(6)	25(5)	16(4)	18(4)
C(65)	19(4)	46(6)	33(5)	5(4)	4(4)	18(4)
C(66)	22(5)	55(6)	61(7)	27(5)	14(4)	12(4)
C(67)	27(5)	76(8)	58(7)	22(6)	22(5)	27(5)
C(68)	18(4)	81(8)	44(6)	15(6)	10(4)	11(5)
C(69)	24(5)	58(7)	54(7)	8(5)	10(5)	-7(5)
C(70)	24(4)	45(6)	55(7)	15(5)	16(4)	10(4)
C(71)	16(4)	41(6)	56(6)	19(5)	10(4)	12(4)
C(72)	25(5)	41(6)	64(7)	14(5)	8(5)	5(4)
C(73)	25(5)	51(7)	92(9)	21(7)	26(6)	9(5)
C(74)	16(4)	45(6)	93(10)	12(7)	5(5)	6(4)
C(75)	38(6)	43(6)	64(8)	-10(6)	-21(6)	11(5)
C(76)	26(5)	51(7)	58(7)	3(6)	2(5)	8(4)
C(77)	7(4)	63(7)	54(6)	30(5)	7(4)	10(4)
C(78)	16(4)	53(6)	47(6)	19(5)	1(4)	2(4)
C(79)	34(5)	66(7)	51(7)	39(6)	4(5)	-1(5)
C(80)	23(5)	66(7)	51(7)	23(6)	5(4)	5(4)
C(81)	23(5)	59(7)	52(6)	23(6)	14(4)	7(4)
C(82)	31(5)	59(7)	46(6)	31(6)	7(4)	10(5)
C(83)	14(4)	61(7)	51(6)	13(5)	6(4)	7(4)
C(84)	15(4)	68(7)	64(7)	13(6)	5(4)	7(4)
C(85)	12(4)	88(9)	60(7)	17(6)	2(4)	4(5)
C(86)	22(5)	61(8)	59(7)	13(6)	-2(5)	-8(5)
C(87)	37(6)	56(7)	52(7)	18(5)	-1(5)	-2(5)
C(88)	19(4)	54(7)	48(6)	-1(5)	1(4)	3(4)
C(89)	19(4)	50(6)	55(7)	15(5)	5(4)	10(4)
C(90)	30(5)	57(7)	52(7)	17(5)	4(5)	6(5)
C(91)	17(4)	48(6)	77(8)	19(6)	-11(5)	8(4)
C(92)	20(5)	51(7)	81(9)	13(6)	4(5)	11(4)
C(93)	27(5)	69(8)	76(8)	13(6)	16(5)	17(5)
C(94)	29(5)	53(6)	54(7)	9(5)	-4(5)	13(4)
C(95)	22(4)	54(6)	50(6)	17(5)	8(4)	13(4)
C(96)	25(5)	54(6)	49(6)	15(5)	10(4)	9(4)
C(97)	45(6)	46(6)	45(6)	7(5)	19(5)	8(5)
C(98)	42(6)	60(7)	52(7)	14(6)	10(5)	18(5)
C(99)	30(5)	57(7)	48(6)	14(5)	9(4)	11(5)
C(100)	23(5)	44(6)	54(6)	9(5)	4(4)	8(4)
O(5)	123(8)	61(6)	69(6)	18(5)	33(6)	39(5)
C(101)	52(7)	69(9)	79(9)	-6(8)	23(7)	13(6)
C(102)	68(9)	108(12)	61(9)	16(9)	23(7)	-8(8)
C(103)	36(7)	177(18)	139(15)	108(14)	23(8)	39(9)
C(104)	58(8)	78(9)	85(10)	30(8)	17(7)	33(7)

Table 13.12. Hydrogen coordinates (x 10^4) and isotropic displacement parameters ($Å^2$x 10^{3}) for **9**.

	x	y	z	U(eq)
H(5A)	2421	4975	782	43
H(6A)	2805	6364	1971	66
H(6B)	2580	7168	1743	66
H(6C)	3440	6870	1532	66
H(7A)	732	7173	112	87
H(7B)	1729	7548	33	87
H(7C)	1561	7520	902	87
H(8A)	-296	5315	-838	82
H(8B)	241	5268	-1534	82
H(8C)	151	6138	-1049	82
H(9A)	1138	3780	-338	66
H(9B)	1281	4004	-1154	66
H(9C)	352	4037	-897	66
H(14A)	4798	6503	-311	43
H(15A)	5033	5488	1039	65
H(15B)	4044	5447	1194	65
H(15C)	4660	6299	1167	65
H(16A)	3684	3646	-255	62
H(16B)	2641	3676	-458	62
H(16C)	3289	4144	421	62
H(17A)	3248	3604	-1902	61
H(17B)	2921	4178	-2450	61
H(17C)	2284	3815	-1927	61
H(18A)	4134	5350	-2386	61
H(18B)	4556	6276	-1846	61
H(18C)	3491	5965	-2263	61
H(19A)	4190	7774	732	53
H(19B)	3165	7791	769	53
H(20A)	3294	8958	404	68
H(20B)	4360	9012	513	68
H(21A)	4083	8857	-810	53
H(21B)	3004	8529	-933	53
H(22A)	3376	7331	-1454	49
H(22B)	4338	7591	-793	49
H(23A)	2019	7121	-1901	52
H(23B)	1294	6840	-1406	52
H(24A)	247	6105	-2525	73
H(24B)	793	6726	-2935	73
H(25A)	1504	5815	-3444	62
H(25B)	575	5193	-3455	62
H(26A)	1228	4828	-2362	47
H(26B)	2140	5104	-2645	47
H(31A)	180	70	3576	58
H(32A)	44	1814	4183	91
H(32B)	610	1727	3509	91
H(32C)	1057	2369	4375	91
H(33A)	1709	2146	6185	80
H(33B)	2122	2533	5540	80
H(33C)	2686	2059	6068	80
H(34A)	1771	517	6464	79
H(34B)	2721	653	6222	79
H(34C)	2050	-246	5961	79
H(35A)	306	-1085	4895	94
H(35B)	1236	-1228	4697	94
H(35C)	383	-1298	3977	94
H(40A)	2746	-780	4909	50

H(41A)	2122	-1937	2825	68
H(41B)	1330	-1485	2941	68
H(41C)	1741	-1904	3616	68
H(42A)	3306	-1069	2259	83
H(42B)	3467	-122	2254	83
H(42C)	2457	-678	2079	83
H(43A)	4848	546	3364	84
H(43B)	5029	1142	4250	84
H(43C)	4343	1273	3502	84
H(44A)	4882	831	5481	85
H(44B)	4216	268	5851	85
H(44C)	4025	1116	5715	85
H(45A)	2380	1678	2498	65
H(45B)	2952	991	2503	65
H(46A)	2135	223	1314	96
H(46B)	2006	1098	1193	96
H(47A)	626	-57	1004	90
H(47B)	616	877	1396	90
H(48A)	359	415	2451	69
H(48B)	755	-373	2189	69
H(49A)	4385	1977	4898	65
H(49B)	3890	2583	5383	65
H(50A)	4845	2875	4235	68
H(50B)	4597	3543	4899	68
H(51A)	3495	3631	3873	66
H(51B)	3591	2815	3274	66
H(52A)	2547	2886	4461	52
H(52B)	2218	2336	3536	52
H(54A)	2864	2431	282	46
H(55A)	3713	2908	1604	58
H(56A)	4540	2101	2197	58
H(57A)	4565	832	1379	57
H(58A)	3703	358	44	46
H(60A)	1945	1595	-2249	45
H(61A)	677	2125	-2579	52
H(62A)	-214	2343	-1682	52
H(63A)	72	1936	-507	60
H(64A)	1316	1379	-173	49
H(66A)	3550	-56	-1652	52
H(67A)	4684	155	-2344	59
H(68A)	5130	1393	-2650	57
H(69A)	4561	2485	-2126	59
H(70A)	3444	2300	-1426	48
H(72A)	1997	-10	10	53
H(73A)	973	-1284	-290	65
H(74A)	562	-2150	-1584	65
H(75A)	956	-1611	-2621	68
H(76A)	1902	-318	-2353	58
H(78A)	1405	3611	3556	48
H(79A)	1026	2448	2508	59
H(80A)	1213	2493	1233	56
H(81A)	1866	3780	1055	51
H(82A)	2234	4946	2103	52
H(84A)	3789	5096	3191	61
H(85A)	5005	6036	3042	67
H(86A)	5078	7418	3347	63
H(87A)	3911	7910	3796	61
H(88A)	2695	6968	3957	53
H(90A)	1151	5758	2579	58
H(91A)	38	6507	2578	61
H(92A)	-318	7023	3777	63
H(93A)	282	6675	4935	68

H(94A)	1427	5948	4944	58
H(96A)	1329	4527	4723	51
H(97A)	1761	4017	5799	54
H(98A)	3344	4203	6375	61
H(99A)	4389	4906	5829	54
H(10A)	3940	5420	4757	50
H(10B)	2966	6379	6211	84
H(10C)	3997	6918	6577	84
H(10D)	2746	7115	5354	100
H(10E)	3790	7629	5696	100
H(10F)	3223	8701	6193	126
H(10G)	2248	8103	6116	126
H(10H)	3857	8471	7382	84
H(10I)	2834	8394	7474	84

13.5. Crystallographic Data for $[(C_5Me_4H)_2Sc]_2(\mu\text{-}\eta^2\text{:}\eta^2\text{-}N_2)$, 10

X-ray Data Collection, Structure Solution and Refinement for **10**.

A red crystal of approximate dimensions 0.09 x 0.09 x 0.18 mm was mounted on a glass fiber and transferred to a Bruker SMART APEX II diffractometer. The APEX2[1] program package was used to determine the unit-cell parameters and for data collection (30 sec/frame scan time for a sphere of diffraction data). The raw frame data was processed using SAINT[2] and SADABS[3] to yield the reflection data file. Subsequent calculations were carried out using the SHELXTL[4] program. The diffraction symmetry was 2/*m* and the systematic absences were consistent with the monoclinic space group $P2_1/n$ that was later determined to be correct.

The structure was solved by direct methods and refined on F^2 by full-matrix least-squares techniques. The analytical scattering factors[5] for neutral atoms were used throughout the analysis. Hydrogen atoms, with the exception of those associated with C(9), were located from a difference-Fourier map and refined (x,y,z and U_{iso}). Hydrogen atoms H(9A), H(9B) and H(9C) were included using a riding model.

At convergence, wR2 = 0.0885 and Goof = 1.024 for 274 variables refined against 3476 data (0.78Å), R1 = 0.0327 for those 2977 data with I > 2.0σ(I).

References

1. APEX2 Version 2008.3-0, Bruker AXS, Inc.; Madison, WI 2008.
2. SAINT Version 7.53a, Bruker AXS, Inc.; Madison, WI 2007.
3. Sheldrick, G. M. SADABS, Version 2008/1, Bruker AXS, Inc.; Madison, WI 2008.
4. Sheldrick, G. M. SHELXTL, Version 2008/3, Bruker AXS, Inc.; Madison, WI 2008.
5. International Tables for X-Ray Crystallography 1992, Vol. C., Dordrecht: Kluwer Academic Publishers.

Table 13.13. Atomic coordinates (x 10^4) and equivalent isotropic displacement parameters ($Å^2$x 10^3) for **10**. U(eq) is defined as one third of the trace of the orthogonalized U^{ij} tensor.

	x	y	z	U(eq)
Sc(1)	5860(1)	8664(1)	5802(1)	12(1)
N(1)	4324(2)	9930(1)	5118(1)	16(1)
C(1)	4486(2)	6570(2)	5484(1)	16(1)

C(2)	5533(2)	6184(2)	6047(1)	16(1)
C(3)	7100(2)	6348(2)	5795(1)	16(1)
C(4)	7024(2)	6849(2)	5079(1)	16(1)
C(5)	5412(2)	6966(2)	4888(1)	16(1)
C(6)	2720(2)	6482(2)	5524(1)	20(1)
C(7)	5082(2)	5515(2)	6741(1)	21(1)
C(8)	8554(2)	5860(2)	6177(1)	20(1)
C(9)	8424(2)	7146(2)	4606(1)	22(1)
C(10)	5480(2)	9118(2)	7115(1)	15(1)
C(11)	5535(2)	10389(2)	6791(1)	15(1)
C(12)	7068(2)	10574(2)	6503(1)	16(1)
C(13)	7956(2)	9412(2)	6650(1)	16(1)
C(14)	6984(2)	8536(2)	7040(1)	16(1)
C(15)	4096(2)	8581(2)	7529(1)	20(1)
C(16)	4216(2)	11376(2)	6841(1)	20(1)
C(17)	7735(2)	11796(2)	6158(1)	21(1)
C(18)	9670(2)	9218(2)	6465(1)	22(1)

Table 13.14. Anisotropic displacement parameters ($Å^2 x\ 10^3$) for **10**. The anisotropic displacement factor exponent takes the form: $-2\pi^2[\ h^2\ a^{*2}U^{11} + ...\ + 2\ h\ k\ a^*\ b^*\ U^{12}\ ]$

	U^{11}	U^{22}	U^{33}	U^{23}	U^{13}	U^{12}
Sc(1)	13(1)	14(1)	11(1)	-1(1)	0(1)	0(1)
N(1)	19(1)	14(1)	13(1)	-4(1)	-1(1)	0(1)
C(1)	16(1)	13(1)	18(1)	-2(1)	0(1)	-1(1)
C(2)	18(1)	12(1)	16(1)	0(1)	1(1)	0(1)
C(3)	17(1)	14(1)	17(1)	-2(1)	0(1)	3(1)
C(4)	16(1)	16(1)	16(1)	-3(1)	2(1)	2(1)
C(5)	19(1)	15(1)	14(1)	-2(1)	-1(1)	0(1)
C(6)	16(1)	22(1)	23(1)	2(1)	0(1)	-2(1)
C(7)	24(1)	18(1)	20(1)	3(1)	3(1)	-1(1)
C(8)	18(1)	21(1)	22(1)	1(1)	-2(1)	4(1)
C(9)	19(1)	28(1)	19(1)	0(1)	6(1)	2(1)
C(10)	17(1)	18(1)	10(1)	-2(1)	0(1)	-1(1)
C(11)	16(1)	18(1)	11(1)	-3(1)	-1(1)	-1(1)
C(12)	17(1)	19(1)	12(1)	-2(1)	-2(1)	-3(1)
C(13)	15(1)	21(1)	13(1)	-3(1)	-3(1)	0(1)
C(14)	20(1)	18(1)	11(1)	-2(1)	-2(1)	1(1)
C(15)	20(1)	22(1)	18(1)	2(1)	4(1)	-1(1)
C(16)	20(1)	20(1)	21(1)	0(1)	2(1)	3(1)
C(17)	20(1)	22(1)	21(1)	2(1)	0(1)	-4(1)
C(18)	16(1)	29(1)	22(1)	-3(1)	0(1)	1(1)

Table 13.15. Hydrogen coordinates ($x\ 10^4$) and isotropic displacement parameters ($Å^2 x\ 10^{\ 3}$) for **10**.

	x	y	z	U(eq)
H(9A)	8711	8081	4656	33
H(9B)	8154	6957	4099	33
H(9C)	9315	6591	4755	33
H(5A)	5040(20)	7275(19)	4450(11)	20(5)
H(6A)	2210(30)	7320(30)	5575(13)	44(7)
H(6B)	2390(30)	5890(30)	5893(14)	44(7)
H(6C)	2270(30)	6140(20)	5086(14)	40(6)
H(7A)	5010(30)	4600(30)	6667(13)	41(6)
H(7B)	4030(30)	5830(20)	6902(12)	35(6)

H(7C)	5800(30)	5650(20)	7121(12)	30(6)
H(8A)	9460(30)	6320(20)	6049(12)	31(6)
H(8B)	8450(30)	5910(20)	6711(13)	38(6)
H(8C)	8790(30)	4930(20)	6054(12)	36(6)
H(14A)	7330(20)	7690(20)	7217(11)	26(5)
H(15A)	4340(20)	7720(20)	7726(12)	27(5)
H(15B)	3870(30)	9160(20)	7949(13)	36(6)
H(15C)	3180(30)	8510(20)	7217(13)	37(6)
H(16A)	4590(20)	12250(20)	6757(12)	30(6)
H(16B)	3380(30)	11250(20)	6497(13)	33(6)
H(16C)	3720(30)	11320(20)	7298(14)	38(6)
H(17A)	7160(20)	12570(20)	6293(11)	27(5)
H(17B)	8800(30)	11920(20)	6308(12)	31(6)
H(17C)	7670(30)	11770(20)	5630(13)	34(6)
H(18A)	10080(30)	8410(20)	6661(12)	32(6)
H(18B)	10340(30)	9920(20)	6656(13)	43(7)
H(18C)	9860(30)	9210(20)	5931(14)	42(7)

13.6. Crystallographic Data for $\{[(C_5Me_4H)_2Sc]_2(\mu\text{-}\eta^2\text{:}\eta^2\text{-}N_2)[(C_5Me_4H)_2Sc]_2(\mu\text{-}O)\}$, 11

X-ray Data Collection, Structure Solution and Refinement for **11**.

A gold crystal of approximate dimensions 0.07 x 0.08 x 0.17 mm was mounted on a glass fiber and transferred to a Bruker SMART APEX II diffractometer. The APEX2[1] program package was used to determine the unit-cell parameters and for data collection (60 sec/frame scan time for a sphere of diffraction data). The raw frame data was processed using SAINT[2] and SADABS[3] to yield the reflection data file. Subsequent calculations were carried out using the SHELXTL[4] program. The diffraction symmetry was 2/*m* and the systematic absences were consistent with the monoclinic space groups *Pn* and *P*2/*n*. It was later determined that space group *Pn* was correct.

The structure was solved by direct methods and refined on F^2 by full-matrix least-squares techniques. The analytical scattering factors[5] for neutral atoms were used throughout the analysis. Hydrogen atoms were included using a riding model. There were two different independent molecules present (Z = 2).

Least-squares analysis yielded wR2 = 0.1647 and Goof = 1.012 for 744 variables refined against 9526 data (0.90Å), R1 = 0.0675 for those 6548 data with I > 2.0σ(I). The absolute structure was assigned by refinement of the Flack[6] parameter. The data was weak making it necessary to limit refinement to a resolution of 0.90Å.

References

1. APEX2 Version 2.2-0,. Bruker AXS, Inc.; Madison, WI 2007.
2. SAINT Version 7.46a, Bruker AXS, Inc.; Madison, WI 2007.
3. Sheldrick, G. M. SADABS, Version 2008/1, Bruker AXS, Inc.; Madison, WI 2008.
4. Sheldrick, G. M. SHELXTL, Version 2008/3, Bruker AXS, Inc.; Madison, WI 2008.
5. International Tables for X-Ray Crystallography 1992, Vol. C., Dordrecht: Kluwer Academic Publishers.
6. Flack, H. D. Acta. Cryst., A39, 876-881, 1983.

Table 13.16. Atomic coordinates (x 10^4) and equivalent isotropic displacement parameters ($Å^2$x 10^3) for **11**. U(eq) is defined as one third of the trace of the orthogonalized U^{ij} tensor.

	x	y	z	U(eq)
Sc(1)	4819(2)	4296(1)	2326(1)	22(1)
Sc(2)	3056(2)	3029(1)	728(1)	22(1)
N(1)	4597(7)	3641(3)	1372(3)	23(2)
N(2)	3308(7)	3678(3)	1675(3)	19(2)
C(1)	5249(9)	5142(4)	1384(4)	26(2)
C(2)	5931(10)	5376(3)	2073(5)	35(2)
C(3)	4778(9)	5498(4)	2577(5)	30(2)
C(4)	3381(9)	5315(4)	2222(5)	30(2)
C(5)	3672(8)	5112(3)	1503(4)	21(2)
C(6)	6049(10)	5001(4)	671(5)	46(2)
C(7)	7579(10)	5545(4)	2157(6)	52(3)
C(8)	4919(10)	5843(4)	3309(5)	43(2)
C(9)	1845(10)	5389(4)	2561(5)	44(2)
C(10)	6875(9)	3710(4)	3030(4)	27(2)
C(11)	6457(10)	4203(4)	3518(5)	36(2)
C(12)	4924(9)	4093(4)	3716(5)	33(2)
C(13)	4447(9)	3537(4)	3353(4)	27(2)
C(14)	5611(8)	3306(4)	2944(4)	23(2)
C(15)	8421(9)	3625(4)	2703(5)	36(2)
C(16)	7529(11)	4675(4)	3870(5)	50(3)
C(17)	4027(12)	4450(5)	4296(5)	53(3)
C(18)	2884(10)	3225(4)	3478(5)	43(2)
C(19)	3245(9)	3562(4)	-509(4)	26(2)
C(20)	2107(9)	3105(4)	-626(4)	31(2)
C(21)	844(9)	3268(4)	-185(5)	33(2)
C(22)	1253(9)	3824(4)	215(4)	28(2)
C(23)	2703(9)	3997(4)	4(4)	28(2)
C(24)	4761(9)	3588(4)	-891(5)	35(2)
C(25)	2154(11)	2617(4)	-1253(5)	52(3)
C(26)	-684(10)	2974(4)	-199(5)	49(3)
C(27)	236(10)	4184(4)	736(5)	42(2)
C(28)	4673(9)	2135(4)	1202(4)	25(2)
C(29)	3996(10)	1908(4)	522(4)	33(2)
C(30)	2418(10)	1862(4)	630(5)	37(2)
C(31)	2123(9)	2078(3)	1372(4)	29(2)
C(32)	3501(9)	2230(3)	1705(4)	23(2)
C(33)	6344(10)	2209(4)	1348(5)	46(2)
C(34)	4841(12)	1682(5)	-140(5)	53(3)
C(35)	1257(12)	1541(4)	129(5)	58(3)
C(36)	603(9)	2090(4)	1733(5)	46(3)
Sc(3)	999(2)	-702(1)	2057(1)	22(1)
Sc(4)	2094(2)	-2022(1)	702(1)	24(1)
O(1)	1437(6)	-1363(2)	1365(3)	26(1)
C(37)	-214(10)	188(4)	1348(5)	33(2)
C(38)	1072(10)	33(3)	951(4)	29(2)
C(39)	2366(10)	177(4)	1389(5)	35(2)
C(40)	1912(11)	447(4)	2078(5)	36(2)
C(41)	314(10)	444(4)	2049(5)	34(2)
C(42)	-1816(10)	172(4)	1077(5)	47(2)
C(43)	1114(11)	-211(4)	152(4)	44(2)
C(44)	4004(10)	166(5)	1142(6)	60(3)
C(45)	2945(10)	728(4)	2670(5)	45(3)
C(46)	890(9)	-1552(4)	3010(4)	29(2)
C(47)	1611(9)	-1055(4)	3389(4)	29(2)
C(48)	516(9)	-553(4)	3477(4)	32(2)
C(49)	-830(9)	-746(4)	3124(4)	27(2)
C(50)	-610(9)	-1370(4)	2834(4)	32(2)

C(51)	1530(11)	-2208(4)	2853(5)	45(2)
C(52)	3162(10)	-1055(5)	3759(5)	45(2)
C(53)	762(10)	20(4)	3962(5)	40(2)
C(54)	-2329(9)	-403(4)	3138(5)	39(2)
C(55)	4659(8)	-1804(4)	1234(4)	26(2)
C(56)	4588(8)	-2484(4)	1177(5)	27(2)
C(57)	4551(9)	-2633(4)	388(5)	32(2)
C(58)	4530(9)	-2068(4)	-4(5)	31(2)
C(59)	4580(8)	-1566(4)	492(5)	33(2)
C(60)	4873(9)	-1438(4)	1954(5)	41(2)
C(61)	4689(10)	-2957(4)	1811(5)	45(2)
C(62)	4724(10)	-3295(4)	95(5)	45(2)
C(63)	4607(10)	-2012(5)	-856(4)	46(2)
C(64)	443(10)	-2167(4)	-438(5)	40(2)
C(65)	-552(10)	-2055(4)	171(6)	43(2)
C(66)	-420(9)	-2565(4)	686(5)	37(2)
C(67)	626(10)	-2990(4)	396(5)	35(2)
C(68)	1133(11)	-2763(4)	-282(5)	36(2)
C(69)	549(12)	-1761(5)	-1114(5)	60(3)
C(70)	-1612(10)	-1497(5)	254(7)	75(4)
C(71)	-1365(10)	-2657(5)	1356(6)	56(3)
C(72)	1025(11)	-3640(4)	741(5)	40(2)

Table 13.17. Anisotropic displacement parameters ($Å^2 x\ 10^3$) for **11**. The anisotropic displacement factor exponent takes the form: $-2\pi^2[\ h^2\ a^{*2}U^{11} + ...\ + 2\ h\ k\ a^*\ b^*\ U^{12}\ ]$

	U^{11}	U^{22}	U^{33}	U^{23}	U^{13}	U^{12}
Sc(1)	22(1)	21(1)	23(1)	0(1)	0(1)	1(1)
Sc(2)	31(1)	17(1)	18(1)	2(1)	-3(1)	1(1)
N(1)	26(4)	21(4)	23(4)	5(3)	-4(3)	2(3)
N(2)	25(4)	13(4)	19(4)	2(3)	-4(3)	2(3)
C(1)	33(5)	22(5)	22(5)	6(4)	11(4)	7(4)
C(2)	34(5)	13(4)	56(6)	13(4)	-7(4)	-9(4)
C(3)	33(5)	25(5)	32(5)	-6(4)	-1(4)	6(4)
C(4)	31(5)	20(5)	40(6)	0(4)	6(4)	-1(4)
C(5)	28(5)	6(4)	28(5)	-6(3)	-5(4)	4(3)
C(6)	45(6)	44(6)	49(6)	7(5)	18(5)	19(5)
C(7)	32(5)	43(6)	81(8)	19(5)	-18(5)	-11(4)
C(8)	55(6)	30(5)	44(6)	-11(4)	-17(5)	4(4)
C(9)	40(6)	57(7)	37(6)	0(5)	13(5)	19(5)
C(10)	28(5)	38(5)	15(4)	0(4)	-6(3)	5(4)
C(11)	40(5)	39(6)	26(5)	2(4)	-18(4)	-1(4)
C(12)	31(5)	26(5)	43(6)	-8(4)	10(4)	15(4)
C(13)	34(5)	28(5)	19(4)	5(4)	4(4)	5(4)
C(14)	31(5)	17(4)	19(4)	3(3)	-3(4)	0(4)
C(15)	33(5)	39(5)	36(5)	12(4)	-5(4)	-4(4)
C(16)	67(7)	28(6)	54(7)	-1(5)	-32(5)	4(5)
C(17)	80(7)	59(7)	21(5)	-2(5)	2(5)	27(6)
C(18)	42(5)	52(6)	35(5)	11(5)	16(4)	6(5)
C(19)	29(5)	30(5)	19(4)	12(4)	2(4)	3(4)
C(20)	46(6)	17(5)	29(5)	5(4)	-7(4)	0(4)
C(21)	32(5)	34(5)	32(5)	7(4)	-6(4)	-4(4)
C(22)	31(5)	34(5)	18(4)	10(4)	2(4)	8(4)
C(23)	39(5)	28(5)	15(4)	2(4)	-8(4)	2(4)
C(24)	31(5)	43(6)	31(5)	3(4)	2(4)	6(4)
C(25)	84(8)	46(6)	25(5)	-1(4)	-19(5)	0(5)
C(26)	47(6)	48(6)	51(6)	22(5)	-12(5)	-8(5)
C(27)	48(6)	43(6)	37(5)	16(4)	5(4)	16(5)
C(28)	30(5)	19(5)	26(5)	9(4)	-4(4)	6(4)

C(29)	59(6)	12(4)	28(5)	-6(4)	3(4)	6(4)
C(30)	50(6)	25(5)	34(5)	1(4)	-16(4)	-10(4)
C(31)	45(5)	14(4)	29(5)	14(4)	3(4)	0(4)
C(32)	37(5)	13(4)	19(4)	5(3)	-1(4)	4(4)
C(33)	49(6)	50(6)	39(6)	-2(5)	-3(5)	7(5)
C(34)	88(8)	45(6)	27(5)	-7(5)	0(5)	23(6)
C(35)	90(8)	30(6)	52(7)	4(5)	-29(6)	-20(5)
C(36)	40(6)	31(6)	67(7)	15(5)	-7(5)	-8(4)
Sc(3)	27(1)	21(1)	19(1)	2(1)	4(1)	1(1)
Sc(4)	23(1)	26(1)	23(1)	-3(1)	2(1)	1(1)
O(1)	39(3)	16(3)	22(3)	-1(2)	8(2)	7(2)
C(37)	42(5)	29(5)	29(5)	4(4)	2(4)	-6(4)
C(38)	50(6)	11(4)	24(5)	-1(4)	0(4)	5(4)
C(39)	44(5)	19(5)	45(6)	15(4)	16(5)	-6(4)
C(40)	52(6)	25(5)	33(5)	7(4)	6(4)	-8(4)
C(41)	35(5)	26(5)	42(6)	5(4)	8(4)	3(4)
C(42)	52(6)	38(6)	51(6)	0(5)	-14(5)	10(5)
C(43)	74(7)	34(5)	24(5)	-1(4)	10(5)	-2(5)
C(44)	51(6)	42(6)	88(8)	32(6)	25(6)	-6(5)
C(45)	56(6)	33(6)	46(6)	1(5)	-11(5)	-20(5)
C(46)	37(5)	29(5)	22(5)	2(4)	6(4)	0(4)
C(47)	35(5)	46(6)	8(4)	4(4)	9(4)	0(4)
C(48)	37(5)	34(5)	27(5)	1(4)	8(4)	-1(4)
C(49)	33(5)	31(5)	19(4)	-1(4)	2(4)	-5(4)
C(50)	35(5)	40(6)	23(5)	-2(4)	13(4)	-18(4)
C(51)	68(7)	25(5)	42(6)	4(4)	4(5)	3(5)
C(52)	44(6)	57(7)	35(6)	3(5)	-3(4)	-2(5)
C(53)	48(6)	41(6)	32(5)	-10(4)	3(4)	2(4)
C(54)	43(6)	44(6)	31(5)	-9(4)	15(4)	-4(5)
C(55)	12(4)	36(5)	31(5)	2(4)	-1(4)	0(4)
C(56)	8(4)	31(5)	41(5)	7(4)	-6(4)	1(3)
C(57)	21(4)	38(6)	37(5)	3(4)	5(4)	0(4)
C(58)	23(4)	36(5)	36(5)	1(4)	11(4)	4(4)
C(59)	16(4)	46(6)	36(5)	14(5)	4(4)	0(4)
C(60)	31(5)	49(6)	42(6)	-7(5)	-11(4)	-9(4)
C(61)	30(5)	57(7)	48(6)	18(5)	2(4)	3(5)
C(62)	45(6)	42(6)	49(6)	2(5)	11(5)	13(5)
C(63)	50(6)	60(7)	28(5)	11(5)	17(4)	10(5)
C(64)	38(5)	47(6)	34(5)	-6(5)	-15(4)	-6(4)
C(65)	37(5)	24(5)	67(7)	-12(5)	-22(5)	0(4)
C(66)	19(5)	37(6)	55(6)	-15(5)	-3(4)	-7(4)
C(67)	34(5)	40(6)	31(5)	5(4)	-4(4)	-13(5)
C(68)	62(6)	18(5)	29(5)	-5(4)	2(4)	7(4)
C(69)	80(8)	52(7)	46(7)	5(5)	-24(6)	12(6)
C(70)	21(5)	71(8)	133(11)	-43(8)	-17(6)	10(5)
C(71)	38(6)	55(7)	77(8)	-20(6)	5(5)	-4(5)
C(72)	62(6)	15(5)	42(6)	-1(4)	-6(5)	2(4)

Table 13.18. Hydrogen coordinates (x 10^4) and isotropic displacement parameters ($Å^2$x 10^{3}) for **11**.

	x	y	z	U(eq)
H(5A)	2882	5028	1105	25
H(6A)	5396	5119	243	69
H(6B)	6281	4546	646	69
H(6C)	6992	5245	659	69
H(7A)	7769	5944	1893	79
H(7B)	8193	5206	1943	79
H(7C)	7849	5595	2687	79

H(8A)	4559	6280	3246	65
H(8B)	5982	5847	3479	65
H(8C)	4309	5626	3681	65
H(9A)	1402	5796	2405	67
H(9B)	1953	5378	3106	67
H(9C)	1184	5041	2391	67
H(14A)	5624	2879	2699	27
H(15A)	9059	3372	3045	54
H(15B)	8887	4042	2629	54
H(15C)	8318	3406	2221	54
H(16A)	7954	4500	4337	76
H(16B)	6983	5069	3975	76
H(16C)	8349	4765	3528	76
H(17A)	3756	4159	4698	79
H(17B)	3104	4624	4060	79
H(17C)	4644	4798	4503	79
H(18A)	2962	2933	3904	64
H(18B)	2567	2988	3029	64
H(18C)	2136	3555	3580	64
H(23A)	3195	4414	127	33
H(24A)	4598	3546	-1432	53
H(24B)	5405	3240	-708	53
H(24C)	5255	3995	-780	53
H(25A)	2218	2836	-1734	78
H(25B)	1233	2357	-1250	78
H(25C)	3041	2342	-1178	78
H(26A)	-1455	3309	-232	74
H(26B)	-816	2727	258	74
H(26C)	-790	2693	-634	74
H(27A)	-42	4594	511	64
H(27B)	772	4255	1214	64
H(27C)	-682	3935	819	64
H(32A)	3658	2329	2247	27
H(33A)	6638	1980	1806	69
H(33B)	6591	2660	1406	69
H(33C)	6894	2033	927	69
H(34A)	5529	1337	12	80
H(34B)	5427	2034	-343	80
H(34C)	4122	1526	-523	80
H(35A)	1008	1124	335	87
H(35B)	1666	1488	-370	87
H(35C)	341	1803	96	87
H(36A)	162	1663	1720	69
H(36B)	-70	2385	1461	69
H(36C)	728	2231	2253	69
H(41A)	-342	654	2422	41
H(42A)	-1988	510	708	70
H(42B)	-2485	237	1498	70
H(42C)	-2034	-241	846	70
H(43A)	2039	-61	-82	66
H(43B)	228	-53	-132	66
H(43C)	1102	-677	154	66
H(44A)	4259	577	921	90
H(44B)	4131	-171	772	90
H(44C)	4676	85	1576	90
H(45A)	3608	1043	2444	68
H(45B)	3562	390	2900	68
H(45C)	2339	933	3052	68
H(50A)	-1430	-1659	2644	39
H(51A)	1012	-2524	3156	68
H(51B)	2615	-2213	2979	68
H(51C)	1374	-2309	2322	68

H(52A)	3064	-1054	4303	68
H(52B)	3716	-675	3607	68
H(52C)	3716	-1435	3608	68
H(53A)	256	-43	4437	60
H(53B)	341	395	3709	60
H(53C)	1849	81	4058	60
H(54A)	-2998	-618	3485	59
H(54B)	-2796	-403	2636	59
H(54C)	-2163	37	3302	59
H(59A)	4765	-1113	351	39
H(60A)	5935	-1311	2015	61
H(60B)	4592	-1708	2375	61
H(60C)	4229	-1059	1940	61
H(61A)	5511	-3258	1723	68
H(61B)	3730	-3189	1840	68
H(61C)	4890	-2732	2282	68
H(62A)	5801	-3390	39	67
H(62B)	4197	-3331	-391	67
H(62C)	4287	-3597	446	67
H(63A)	5667	-2013	-1002	68
H(63B)	4123	-1615	-1020	68
H(63C)	4078	-2373	-1090	68
H(68A)	1778	-3006	-633	43
H(69A)	-315	-1847	-1452	90
H(69B)	1492	-1856	-1368	90
H(69C)	541	-1313	-967	90
H(70A)	-2641	-1653	331	113
H(70B)	-1600	-1237	-200	113
H(70C)	-1281	-1240	684	113
H(71A)	-2321	-2863	1207	84
H(71B)	-1576	-2243	1583	84
H(71C)	-819	-2926	1720	84
H(72A)	99	-3849	904	60
H(72B)	1717	-3579	1172	60
H(72C)	1515	-3905	368	60

13.7. Crystallographic Data for $(C_5Me_4H)_2Y(BH_4)(THF)$, 20

X-ray Data Collection, Structure Solution and Refinement for **20**.

A colorless crystal of approximate dimensions 0.11 x 0.12 x 0.28 mm was mounted on a glass fiber and transferred to a Bruker SMART APEX II diffractometer. The APEX2[1] program package was used to determine the unit-cell parameters and for data collection (30 sec/frame scan time for a sphere of diffraction data). The raw frame data was processed using SAINT[2] and SADABS[3] to yield the reflection data file. Subsequent calculations were carried out using the SHELXTL[4] program. There were no systematic absences nor any diffraction symmetry other than the Friedel condition. The centrosymmetric triclinic space group $P\bar{1}$ was assigned and later determined to be correct.

The structure was solved by direct methods and refined on F^2 by full-matrix least-squares techniques. The analytical scattering factors[5] for neutral atoms were used throughout the analysis. There were two molecules of the formula unit present (Z = 4). Hydrogen atoms H(1)-H(8) were located from a difference-Fourier map and refined (x,y,z and U_{iso}). The

remaining hydrogen atoms were included using a riding model. Carbon atoms C(42) and C(43) were disordered and included using multiple components with partial site-occupancy-factors.

At convergence, wR2 = 0.0666 and Goof = 1.018 for 498 variables refined against 10477 data (0.75Å), R1 = 0.0274 for those 8804 data with I > 2.0σ(I).

References

1. APEX2 Version 2008.3-0, Bruker AXS, Inc.; Madison, WI 2008.
2. SAINT Version 7.53a, Bruker AXS, Inc.; Madison, WI 2007.
3. Sheldrick, G. M. SADABS, Version 2008/1, Bruker AXS, Inc.; Madison, WI 2008.
4. Sheldrick, G. M. SHELXTL, Version 2008/4, Bruker AXS, Inc.; Madison, WI 2008.
5. International Tables for X-Ray Crystallography 1992, Vol. C., Dordrecht: Kluwer Academic Publishers.

Table 13.19. Atomic coordinates (x 10^4) and equivalent isotropic displacement parameters (Å^{2}x 10^3) for **20**. U(eq) is defined as one third of the trace of the orthogonalized U^{ij} tensor.

	x	y	z	U(eq)
Y(1)	4820(1)	2520(1)	4913(1)	12(1)
O(1)	6627(1)	1798(1)	4220(1)	18(1)
B(1)	2777(2)	1600(1)	4862(1)	19(1)
C(1)	4485(2)	1984(1)	6622(1)	18(1)
C(2)	5552(2)	1288(1)	6548(1)	16(1)
C(3)	6976(2)	1620(1)	6204(1)	17(1)
C(4)	6787(2)	2516(1)	6071(1)	20(1)
C(5)	5254(2)	2737(1)	6332(1)	20(1)
C(6)	2873(2)	1910(1)	7013(1)	26(1)
C(7)	5296(2)	341(1)	6882(1)	22(1)
C(8)	8479(2)	1084(1)	6107(1)	25(1)
C(9)	8052(2)	3100(1)	5792(1)	30(1)
C(10)	3143(2)	4095(1)	4443(1)	17(1)
C(11)	2821(2)	3832(1)	3774(1)	16(1)
C(12)	4221(2)	3789(1)	3301(1)	17(1)
C(13)	5401(2)	4045(1)	3666(1)	18(1)
C(14)	4729(2)	4228(1)	4370(1)	17(1)
C(15)	1971(2)	4272(1)	5066(1)	24(1)
C(16)	1252(2)	3701(1)	3543(1)	24(1)
C(17)	4340(2)	3564(1)	2521(1)	25(1)
C(18)	6965(2)	4274(1)	3282(1)	25(1)
C(19)	6475(2)	949(1)	4198(1)	23(1)
C(20)	7795(2)	787(1)	3628(1)	21(1)
C(21)	9057(2)	1246(1)	3788(1)	23(1)
C(22)	8098(2)	2070(1)	3808(1)	21(1)
Y(2)	1040(1)	7321(1)	192(1)	13(1)
O(2)	2141(1)	8231(1)	700(1)	20(1)
B(2)	-1706(3)	8023(2)	421(2)	24(1)
C(23)	573(2)	7359(1)	-1362(1)	18(1)
C(24)	185(2)	8250(1)	-1489(1)	18(1)
C(25)	1573(2)	8558(1)	-1388(1)	18(1)
C(26)	2840(2)	7859(1)	-1220(1)	18(1)
C(27)	2208(2)	7123(1)	-1202(1)	18(1)
C(28)	-545(2)	6793(1)	-1446(1)	26(1)
C(29)	-1398(2)	8799(1)	-1778(1)	24(1)
C(30)	1672(2)	9490(1)	-1518(1)	24(1)
C(31)	4562(2)	7920(1)	-1234(1)	25(1)
C(32)	372(2)	5739(1)	1199(1)	18(1)
C(33)	885(2)	6031(1)	1807(1)	19(1)
C(34)	2505(2)	6094(1)	1668(1)	20(1)

C(35)	2996(2)	5850(1)	972(1)	18(1)
C(36)	1672(2)	5627(1)	690(1)	18(1)
C(37)	-1257(2)	5549(1)	1135(1)	24(1)
C(38)	-46(3)	6149(1)	2542(1)	27(1)
C(39)	3554(2)	6276(1)	2242(1)	26(1)
C(40)	4647(2)	5757(1)	661(1)	25(1)
C(41)	1353(2)	8595(1)	1296(1)	28(1)
C(42)	2466(4)	9199(3)	1356(3)	26(1)
C(43)	4071(4)	8715(3)	1273(2)	25(1)
C(42B)	2507(8)	8878(6)	1667(6)	30(2)
C(43B)	3679(9)	9158(6)	964(5)	35(2)
C(44)	3746(2)	8426(1)	574(1)	26(1)

Table 13.20. Anisotropic displacement parameters ($Å^2 x 10^3$) for **20**. The anisotropic displacement factor exponent takes the form: $-2\pi^2[h^2 a^{*2} U^{11} + ... + 2 h k a^* b^* U^{12}]$

	U^{11}	U^{22}	U^{33}	U^{23}	U^{13}	U^{12}
Y(1)	11(1)	13(1)	13(1)	-5(1)	0(1)	-2(1)
O(1)	18(1)	17(1)	21(1)	-11(1)	3(1)	-3(1)
B(1)	18(1)	20(1)	20(1)	-7(1)	-1(1)	-8(1)
C(1)	19(1)	22(1)	12(1)	-6(1)	-1(1)	-2(1)
C(2)	16(1)	18(1)	12(1)	-4(1)	-2(1)	-3(1)
C(3)	14(1)	24(1)	13(1)	-6(1)	-2(1)	-3(1)
C(4)	20(1)	24(1)	14(1)	-6(1)	-4(1)	-7(1)
C(5)	26(1)	22(1)	15(1)	-11(1)	-3(1)	-3(1)
C(6)	22(1)	34(1)	20(1)	-8(1)	6(1)	-3(1)
C(7)	23(1)	20(1)	21(1)	-4(1)	-2(1)	-6(1)
C(8)	17(1)	33(1)	21(1)	-8(1)	-3(1)	3(1)
C(9)	32(1)	34(1)	24(1)	-8(1)	-4(1)	-17(1)
C(10)	15(1)	14(1)	20(1)	-6(1)	1(1)	0(1)
C(11)	15(1)	13(1)	18(1)	-3(1)	-2(1)	0(1)
C(12)	18(1)	15(1)	14(1)	-2(1)	0(1)	0(1)
C(13)	16(1)	13(1)	20(1)	-3(1)	2(1)	0(1)
C(14)	17(1)	11(1)	22(1)	-6(1)	-1(1)	-2(1)
C(15)	22(1)	23(1)	28(1)	-12(1)	5(1)	1(1)
C(16)	17(1)	24(1)	27(1)	-7(1)	-6(1)	-1(1)
C(17)	32(1)	25(1)	15(1)	-6(1)	1(1)	-1(1)
C(18)	18(1)	20(1)	31(1)	-3(1)	6(1)	-3(1)
C(19)	25(1)	18(1)	32(1)	-15(1)	5(1)	-6(1)
C(20)	25(1)	22(1)	19(1)	-11(1)	2(1)	-2(1)
C(21)	21(1)	26(1)	24(1)	-12(1)	4(1)	-3(1)
C(22)	21(1)	23(1)	23(1)	-11(1)	8(1)	-9(1)
Y(2)	13(1)	15(1)	13(1)	-6(1)	0(1)	-1(1)
O(2)	18(1)	22(1)	22(1)	-14(1)	1(1)	-2(1)
B(2)	14(1)	31(1)	25(1)	-13(1)	3(1)	2(1)
C(23)	21(1)	22(1)	12(1)	-8(1)	0(1)	-2(1)
C(24)	18(1)	21(1)	12(1)	-5(1)	0(1)	1(1)
C(25)	20(1)	18(1)	13(1)	-4(1)	2(1)	-2(1)
C(26)	17(1)	23(1)	14(1)	-8(1)	3(1)	-3(1)
C(27)	20(1)	21(1)	14(1)	-9(1)	1(1)	2(1)
C(28)	29(1)	30(1)	25(1)	-15(1)	-5(1)	-5(1)
C(29)	22(1)	25(1)	21(1)	-6(1)	-4(1)	3(1)
C(30)	29(1)	19(1)	22(1)	-6(1)	3(1)	-6(1)
C(31)	18(1)	33(1)	26(1)	-13(1)	6(1)	-4(1)
C(32)	22(1)	15(1)	17(1)	-5(1)	1(1)	-4(1)
C(33)	26(1)	15(1)	15(1)	-4(1)	0(1)	-3(1)
C(34)	26(1)	15(1)	16(1)	-4(1)	-6(1)	0(1)
C(35)	18(1)	13(1)	19(1)	-4(1)	-4(1)	2(1)

C(36)	22(1)	14(1)	19(1)	-7(1)	-1(1)	-2(1)
C(37)	24(1)	26(1)	27(1)	-12(1)	5(1)	-9(1)
C(38)	40(1)	24(1)	17(1)	-8(1)	5(1)	-6(1)
C(39)	32(1)	21(1)	22(1)	-7(1)	-10(1)	-1(1)
C(40)	19(1)	21(1)	33(1)	-10(1)	-3(1)	2(1)
C(41)	28(1)	33(1)	30(1)	-22(1)	2(1)	0(1)
C(44)	20(1)	34(1)	28(1)	-17(1)	1(1)	-9(1)

Table 13.21. Hydrogen coordinates (x 10^4) and isotropic displacement parameters ($Å^2$x 10^{3}) for **20**.

	x	y	z	U(eq)
H(1)	2420(30)	2124(15)	5148(15)	36(6)
H(2)	3220(20)	1964(14)	4166(14)	28(6)
H(3)	3790(30)	1174(15)	5249(15)	37(6)
H(4)	1870(30)	1246(15)	4861(15)	39(7)
H(5A)	4870	3286	6424	23
H(6A)	2967	1641	7648	40
H(6B)	2349	1543	6818	40
H(6C)	2258	2498	6825	40
H(7A)	5633	35	7492	33
H(7B)	5906	58	6536	33
H(7C)	4181	315	6834	33
H(8A)	9055	812	6662	38
H(8B)	9118	1468	5659	38
H(8C)	8243	623	5936	38
H(9A)	8871	2876	6243	45
H(9B)	7599	3701	5706	45
H(9C)	8505	3101	5246	45
H(14A)	5224	4524	4678	21
H(15A)	1263	4818	4753	36
H(15B)	2522	4331	5528	36
H(15C)	1364	3781	5321	36
H(16A)	872	4187	2995	36
H(16B)	509	3690	4006	36
H(16C)	1352	3143	3478	36
H(17A)	3706	4028	2042	38
H(17B)	3957	3002	2669	38
H(17C)	5436	3515	2342	38
H(18A)	6869	4908	2922	38
H(18B)	7315	3948	2921	38
H(18C)	7730	4116	3750	38
H(19A)	5447	975	3948	28
H(19B)	6576	474	4790	28
H(20A)	7470	1051	3008	25
H(20B)	8157	150	3808	25
H(21A)	9614	882	4348	27
H(21B)	9825	1388	3311	27
H(22A)	8646	2304	4150	26
H(22B)	7904	2530	3212	26
H(5)	-910(30)	8525(15)	48(15)	36(6)
H(6)	-1190(30)	7653(16)	1107(16)	45(7)
H(7)	-1610(30)	7540(15)	119(15)	40(7)
H(8)	-2860(30)	8330(17)	445(17)	56(8)
H(27A)	2840	6572	-1202	22
H(28A)	-739	6945	-2062	39
H(28B)	-1535	6893	-1166	39
H(28C)	-88	6171	-1163	39
H(29A)	-1307	9281	-2347	36
H(29B)	-1779	9043	-1353	36

H(29C)	-2135	8430	-1821	36
H(30A)	1160	9900	-2069	36
H(30B)	2774	9570	-1530	36
H(30C)	1147	9607	-1039	36
H(31A)	4951	8072	-1828	38
H(31B)	5130	7353	-846	38
H(31C)	4726	8377	-1039	38
H(36A)	1710	5311	297	22
H(37A)	-1373	4960	1570	37
H(37B)	-1429	5578	553	37
H(37C)	-2028	5987	1241	37
H(38A)	229	5630	3084	41
H(38B)	-1166	6221	2419	41
H(38C)	194	6673	2602	41
H(39A)	3793	5747	2780	39
H(39B)	3023	6761	2383	39
H(39C)	4528	6439	1937	39
H(40A)	5243	5212	1073	37
H(40B)	5136	6261	620	37
H(40C)	4638	5738	88	37
H(41A)	1213	8122	1873	34
H(41B)	316	8934	1061	34
H(42A)	2267	9792	878	32
H(42B)	2366	9255	1920	32
H(43A)	4877	9112	1094	30
H(43B)	4407	8206	1823	30
H(42C)	2990	8389	2196	37
H(42D)	2040	9374	1816	37
H(43C)	4711	9146	1201	42
H(43D)	3326	9755	519	42
H(44A)	3856	8900	-7	31
H(44B)	4485	7896	623	31

13.8. Crystallographic Data for $(C_5Me_5)_2Y(BH_4)(THF)$, 21

X-ray Data Collection, Structure Solution and Refinement for 21

A colorless crystal of approximate dimensions 0.19 x 0.23 x 0.27 mm was mounted on a glass fiber and transferred to a Bruker SMART APEX II diffractometer. The APEX2[1] program package was used to determine the unit-cell parameters and for data collection (25 sec/frame scan time for a sphere of diffraction data). The raw frame data was processed using SAINT[2] and SADABS[3] to yield the reflection data file. Subsequent calculations were carried out using the SHELXTL[4] program. There were no systematic absences nor any diffraction symmetry other than the Friedel condition. The centrosymmetric triclinic space group $P\bar{1}$ was assigned and later determined to be correct.

The structure was solved by direct methods and refined on F^2 by full-matrix least-squares techniques. The analytical scattering factors[5] for neutral atoms were used throughout the analysis. Hydrogen atoms H(1)-H(8) were located from a difference-Fourier map and refined (x,y,z and U_{iso}). The remaining hydrogen atoms were included using a riding model.

At convergence, wR2 = 0.0766 and Goof = 1.044 for 539 variables refined against 10240 data, R1 = 0.0324 for those 8393 data with $I > 2.0\sigma(I)$.

References

1. APEX2 Version 2.2-0 Bruker AXS, Inc.; Madison, WI 2007.
2. SAINT Version 7.46a, Bruker AXS, Inc.; Madison, WI 2007.
3. Sheldrick, G. M. SADABS, Version 2008/1, Bruker AXS, Inc.; Madison, WI 2008.
4. Sheldrick, G. M. SHELXTL, Version 2008/3, Bruker AXS, Inc.; Madison, WI 2008.
5. International Tables for X-Ray Crystallography 1992, Vol. C., Dordrecht: Kluwer Academic Publishers.

Table 13.22. Atomic coordinates (x 10^4) and equivalent isotropic displacement parameters ($Å^2$x 10^3) for **21**. U(eq) is defined as one third of the trace of the orthogonalized U^{ij} tensor.

	x	y	z	U(eq)
Y(1)	6269(1)	7461(1)	4883(1)	14(1)
O(1)	7957(2)	6340(1)	5911(1)	20(1)
B(1)	3805(4)	6510(2)	5500(2)	28(1)
C(1)	5575(3)	8115(2)	5949(2)	27(1)
C(2)	4665(3)	8639(2)	5234(2)	27(1)
C(3)	5699(3)	9132(2)	4585(2)	22(1)
C(4)	7250(3)	8900(2)	4900(2)	21(1)
C(5)	7155(3)	8278(2)	5743(2)	24(1)
C(6)	4952(4)	7592(2)	6816(2)	51(1)
C(7)	2908(3)	8757(2)	5184(3)	56(1)
C(8)	5178(4)	9891(2)	3767(2)	39(1)
C(9)	8730(3)	9324(2)	4477(2)	38(1)
C(10)	8504(4)	7965(2)	6351(2)	46(1)
C(11)	7477(3)	6634(2)	4024(1)	19(1)
C(12)	5899(3)	6882(2)	3755(1)	19(1)
C(13)	5736(3)	7817(2)	3320(1)	18(1)
C(14)	7212(3)	8145(2)	3306(1)	18(1)
C(15)	8292(3)	7412(2)	3760(1)	18(1)
C(16)	8168(3)	5699(2)	4441(2)	28(1)
C(17)	4667(3)	6272(2)	3805(2)	29(1)
C(18)	4262(3)	8345(2)	2878(2)	27(1)
C(19)	7694(3)	9058(2)	2732(2)	30(1)
C(20)	10041(3)	7481(2)	3771(2)	27(1)
C(21)	9670(3)	6278(2)	5891(1)	23(1)
C(22)	10173(3)	5665(2)	6773(2)	30(1)
C(23)	8853(3)	5039(2)	7089(2)	32(1)
C(24)	7420(3)	5646(2)	6696(2)	32(1)
Y(2)	1094(1)	2481(1)	183(1)	13(1)
O(2)	2712(2)	3584(1)	-780(1)	19(1)
B(2)	-1480(4)	3583(2)	-223(2)	25(1)
C(25)	-373(3)	1925(2)	-746(1)	18(1)
C(26)	-235(3)	1199(2)	58(1)	18(1)
C(27)	1371(3)	906(1)	198(1)	18(1)
C(28)	2229(3)	1461(2)	-512(1)	19(1)
C(29)	1146(3)	2093(2)	-1098(1)	18(1)
C(30)	-1873(3)	2363(2)	-1203(2)	25(1)
C(31)	-1557(3)	757(2)	637(2)	27(1)
C(32)	2026(3)	39(2)	874(2)	26(1)
C(33)	3930(3)	1264(2)	-662(2)	27(1)
C(34)	1478(3)	2781(2)	-1966(1)	23(1)
C(35)	1405(3)	3050(2)	1322(1)	24(1)
C(36)	555(3)	2280(2)	1708(1)	23(1)
C(37)	1579(3)	1550(2)	1811(1)	20(1)
C(38)	3054(3)	1876(2)	1465(1)	18(1)
C(39)	2943(3)	2800(2)	1171(1)	21(1)
C(40)	849(4)	3949(2)	1223(2)	45(1)
C(41)	-1094(3)	2210(2)	2054(2)	43(1)
C(42)	1248(3)	600(2)	2369(2)	34(1)

C(43)	4564(3)	1347(2)	1502(2)	34(1)
C(44)	4283(4)	3390(2)	880(2)	40(1)
C(45)	4233(3)	3451(2)	-1108(2)	26(1)
C(46)	4580(3)	4336(2)	-1806(2)	35(1)
C(47)	3834(3)	4962(2)	-1503(2)	38(1)
C(48)	2340(3)	4533(2)	-1094(2)	25(1)

Table 13.23. Anisotropic displacement parameters ($Å^2 x\ 10^3$) for **21**. The anisotropic displacement factor exponent takes the form: $-2\pi^2[\ h^2\ a^{*2}U^{11} + ...\ + 2\ h\ k\ a^*\ b^*\ U^{12}\ ]$

	U^{11}	U^{22}	U^{33}	U^{23}	U^{13}	U^{12}
Y(1)	13(1)	14(1)	13(1)	-5(1)	0(1)	0(1)
O(1)	16(1)	22(1)	16(1)	-3(1)	1(1)	1(1)
B(1)	26(2)	31(2)	28(2)	-14(1)	10(1)	-14(1)
C(1)	40(2)	22(1)	23(1)	-15(1)	8(1)	0(1)
C(2)	21(1)	26(1)	44(2)	-26(1)	2(1)	3(1)
C(3)	30(1)	16(1)	23(1)	-12(1)	-7(1)	4(1)
C(4)	24(1)	20(1)	26(1)	-16(1)	-1(1)	-3(1)
C(5)	30(1)	23(1)	24(1)	-15(1)	-8(1)	5(1)
C(6)	86(3)	38(2)	32(2)	-20(1)	28(2)	-10(2)
C(7)	23(2)	56(2)	113(3)	-61(2)	3(2)	5(1)
C(8)	61(2)	22(1)	32(2)	-12(1)	-20(1)	12(1)
C(9)	33(2)	43(2)	53(2)	-33(2)	11(1)	-16(1)
C(10)	60(2)	45(2)	45(2)	-32(2)	-33(2)	21(2)
C(11)	23(1)	20(1)	14(1)	-9(1)	1(1)	4(1)
C(12)	22(1)	21(1)	17(1)	-11(1)	1(1)	-2(1)
C(13)	19(1)	21(1)	14(1)	-8(1)	-2(1)	1(1)
C(14)	23(1)	21(1)	11(1)	-7(1)	3(1)	-2(1)
C(15)	17(1)	25(1)	13(1)	-9(1)	1(1)	0(1)
C(16)	33(1)	23(1)	29(1)	-14(1)	-5(1)	8(1)
C(17)	28(1)	30(1)	33(1)	-19(1)	1(1)	-7(1)
C(18)	24(1)	32(1)	25(1)	-14(1)	-8(1)	6(1)
C(19)	42(2)	26(1)	19(1)	-6(1)	5(1)	-9(1)
C(20)	18(1)	41(2)	24(1)	-16(1)	3(1)	-3(1)
C(21)	17(1)	27(1)	19(1)	-6(1)	1(1)	1(1)
C(22)	23(1)	37(2)	20(1)	-6(1)	-2(1)	7(1)
C(23)	35(2)	26(1)	22(1)	0(1)	-2(1)	6(1)
C(24)	26(1)	32(2)	18(1)	4(1)	2(1)	0(1)
Y(2)	13(1)	14(1)	12(1)	-5(1)	-1(1)	0(1)
O(2)	18(1)	16(1)	19(1)	-5(1)	3(1)	-1(1)
B(2)	23(2)	22(2)	29(2)	-10(1)	-9(1)	4(1)
C(25)	19(1)	20(1)	18(1)	-12(1)	-2(1)	-1(1)
C(26)	20(1)	19(1)	20(1)	-11(1)	-1(1)	-6(1)
C(27)	23(1)	15(1)	18(1)	-8(1)	-4(1)	-1(1)
C(28)	19(1)	19(1)	21(1)	-13(1)	-1(1)	0(1)
C(29)	22(1)	19(1)	16(1)	-10(1)	0(1)	-1(1)
C(30)	24(1)	29(1)	23(1)	-13(1)	-7(1)	1(1)
C(31)	27(1)	30(1)	23(1)	-11(1)	2(1)	-12(1)
C(32)	36(1)	18(1)	25(1)	-10(1)	-7(1)	2(1)
C(33)	24(1)	27(1)	33(1)	-16(1)	2(1)	1(1)
C(34)	28(1)	27(1)	15(1)	-10(1)	2(1)	-2(1)
C(35)	35(1)	23(1)	16(1)	-13(1)	-9(1)	8(1)
C(36)	19(1)	36(1)	14(1)	-13(1)	-1(1)	1(1)
C(37)	23(1)	22(1)	13(1)	-6(1)	-3(1)	-4(1)
C(38)	17(1)	24(1)	13(1)	-8(1)	-6(1)	4(1)
C(39)	26(1)	24(1)	11(1)	-6(1)	-4(1)	-7(1)
C(40)	76(2)	31(2)	31(2)	-20(1)	-17(2)	20(2)
C(41)	23(1)	82(2)	23(1)	-24(2)	1(1)	8(1)
C(42)	50(2)	30(2)	18(1)	-6(1)	-2(1)	-14(1)

C(43)	25(1)	48(2)	28(1)	-19(1)	-11(1)	14(1)
C(44)	48(2)	45(2)	23(1)	-10(1)	-3(1)	-27(1)
C(45)	18(1)	27(1)	30(1)	-12(1)	6(1)	-3(1)
C(46)	29(2)	39(2)	28(1)	-7(1)	9(1)	-9(1)
C(47)	41(2)	24(1)	39(2)	-3(1)	0(1)	-11(1)
C(48)	33(1)	13(1)	24(1)	-4(1)	-1(1)	1(1)

Table 13.24. Hydrogen coordinates (x 10^4) and isotropic displacement parameters ($Å^2$x 10^{3}) for **21**.

	x	y	z	U(eq)
H(1)	3690(30)	7254(16)	4923(15)	20(6)
H(2)	4950(40)	6180(20)	5461(18)	45(9)
H(3)	3680(40)	6610(20)	6030(20)	70(11)
H(4)	2990(40)	6110(20)	5475(18)	46(9)
H(6A)	4763	7980	7076	76
H(6B)	5723	7112	7142	76
H(6C)	3967	7344	6791	76
H(7A)	2554	9264	5275	83
H(7B)	2455	8224	5609	83
H(7C)	2567	8862	4635	83
H(8A)	4549	10335	3868	58
H(8B)	4544	9674	3468	58
H(8C)	6101	10158	3435	58
H(9A)	9269	9514	4828	57
H(9B)	8464	9836	3945	57
H(9C)	9418	8896	4381	57
H(10A)	8488	8325	6643	70
H(10B)	9499	8021	6052	70
H(10C)	8400	7345	6753	70
H(16A)	7821	5380	4152	42
H(16B)	7817	5410	5019	42
H(16C)	9316	5699	4423	42
H(17A)	4585	6272	3268	43
H(17B)	3654	6473	3947	43
H(17C)	4962	5672	4232	43
H(18A)	3924	8134	2494	40
H(18B)	4476	8970	2568	40
H(18C)	3431	8273	3285	40
H(19A)	8238	9054	2251	45
H(19B)	8399	9249	3024	45
H(19C)	6760	9466	2547	45
H(20A)	10431	7783	3201	41
H(20B)	10560	6888	4053	41
H(20C)	10269	7816	4066	41
H(21A)	10086	6867	5700	28
H(21B)	10054	6035	5513	28
H(22A)	10250	5992	7099	36
H(22B)	11194	5345	6791	36
H(23A)	8993	4576	6905	39
H(23B)	8786	4756	7701	39
H(24A)	6599	5322	6602	38
H(24B)	6985	5901	7057	38
H(5)	-1530(30)	2820(17)	211(16)	28(7)
H(6)	-560(50)	3710(30)	-540(30)	89(14)
H(7)	-2460(40)	3830(20)	-630(20)	64(10)
H(8)	-1530(50)	3900(30)	130(30)	117(17)
H(30A)	-2168	2071	-1528	37
H(30B)	-1723	2986	-1574	37
H(30C)	-2708	2317	-805	37

H(31A)	-1546	139	745	40
H(31B)	-2560	1062	382	40
H(31C)	-1428	781	1159	40
H(32A)	2232	-384	652	39
H(32B)	1266	-193	1328	39
H(32C)	3007	129	1082	39
H(33A)	4082	650	-564	41
H(33B)	4600	1354	-284	41
H(33C)	4211	1659	-1236	41
H(34A)	666	2793	-2340	35
H(34B)	2506	2636	-2143	35
H(34C)	1477	3360	-1981	35
H(40A)	1309	4044	1660	67
H(40B)	-298	3986	1264	67
H(40C)	1175	4402	680	67
H(41A)	-1051	2079	2638	65
H(41B)	-1594	1736	2008	65
H(41C)	-1704	2771	1741	65
H(42A)	1152	504	2943	51
H(42B)	2111	213	2328	51
H(42C)	267	467	2198	51
H(43A)	5291	1388	1886	51
H(43B)	5037	1580	949	51
H(43C)	4346	728	1694	51
H(44A)	4755	3411	1354	60
H(44B)	3899	3986	481	60
H(44C)	5073	3160	614	60
H(45A)	4189	3008	-1313	31
H(45B)	5052	3246	-675	31
H(46A)	4096	4430	-2330	42
H(46B)	5724	4399	-1888	42
H(47A)	3603	5556	-1970	46
H(47B)	4521	5013	-1101	46
H(48A)	2034	4672	-636	30
H(48B)	1471	4738	-1500	30

13.9. Crystallographic Data for $(C_5Me_4H)_2Sc(BH_4)$, 24

X-ray Data Collection, Structure Solution and Refinement for **24**.

A colorless crystal of approximate dimensions 0.27 x 0.29 x 0.36 mm was mounted on a glass fiber and transferred to a Bruker SMART APEX II diffractometer. The APEX2[1] program package was used to determine the unit-cell parameters and for data collection (20 sec/frame scan time for a sphere of diffraction data). The raw frame data was processed using SAINT[2] and SADABS[3] to yield the reflection data file. Subsequent calculations were carried out using the SHELXTL[4] program. The diffraction symmetry was 2/*m* and the systematic absences were consistent with the monoclinic space group $P2_1/n$ that was later determined to be correct.

The structure was solved by direct methods and refined on F^2 by full-matrix least-squares techniques. The analytical scattering factors[5] for neutral atoms were used throughout the analysis. Hydrogen atoms were located from a difference-Fourier map and refined (x,y,z and U_{iso}).

At convergence, wR2 = 0.0765 and Goof = 1.029 for 301 variables refined against 4209 data (0.75Å), R1 = 0.0272 for those 3940 data with I > 2.0σ(I).

References

1. APEX2 Version 2008.3-0, Bruker AXS, Inc.; Madison, WI 2008.
2. SAINT Version 7.53a, Bruker AXS, Inc.; Madison, WI 2007.
3. Sheldrick, G. M. SADABS, Version 2008/1, Bruker AXS, Inc.; Madison, WI 2008.
4. Sheldrick, G. M. SHELXTL, Version 2008/3, Bruker AXS, Inc.; Madison, WI 2008.
5. International Tables for X-Ray Crystallography 1992, Vol. C., Dordrecht: Kluwer Academic Publishers.

Table 13.25. Atomic coordinates (x 10^4) and equivalent isotropic displacement parameters (Å^{2}x 10^3) for **24**. U(eq) is defined as one third of the trace of the orthogonalized U^{ij} tensor.

	x	y	z	U(eq)
Sc(1)	7754(1)	8066(1)	284(1)	12(1)
B(1)	9118(1)	8791(1)	1969(1)	20(1)
C(1)	6408(1)	9630(1)	-393(1)	15(1)
C(2)	6569(1)	9665(1)	761(1)	15(1)
C(3)	6194(1)	8566(1)	1109(1)	15(1)
C(4)	5794(1)	7852(1)	171(1)	15(1)
C(5)	5926(1)	8516(1)	-751(1)	15(1)
C(6)	6660(1)	10621(1)	-1099(1)	21(1)
C(7)	6949(1)	10735(1)	1453(1)	19(1)
C(8)	6172(1)	8234(1)	2260(1)	19(1)
C(9)	5213(1)	6679(1)	137(1)	21(1)
C(10)	8072(1)	6042(1)	-316(1)	16(1)
C(11)	9123(1)	6491(1)	201(1)	15(1)
C(12)	9366(1)	7464(1)	-430(1)	16(1)
C(13)	8464(1)	7622(1)	-1333(1)	17(1)
C(14)	7677(1)	6737(1)	-1262(1)	17(1)
C(15)	7531(1)	4961(1)	29(1)	22(1)
C(16)	9874(1)	5951(1)	1180(1)	19(1)
C(17)	10426(1)	8139(1)	-231(1)	22(1)
C(18)	8390(1)	8514(1)	-2240(1)	24(1)

Table 13.26. Anisotropic displacement parameters (Å^{2}x 10^3) for **24**. The anisotropic displacement factor exponent takes the form: $-2\pi^2[h^2 a^{*2}U^{11} + ... + 2 h k a^* b^* U^{12}]$

	U^{11}	U^{22}	U^{33}	U^{23}	U^{13}	U^{12}
Sc(1)	12(1)	14(1)	11(1)	-1(1)	3(1)	0(1)
B(1)	18(1)	23(1)	17(1)	-4(1)	0(1)	2(1)
C(1)	12(1)	18(1)	16(1)	2(1)	4(1)	2(1)
C(2)	12(1)	16(1)	17(1)	-1(1)	4(1)	2(1)
C(3)	13(1)	17(1)	15(1)	-1(1)	5(1)	1(1)
C(4)	12(1)	18(1)	16(1)	-1(1)	5(1)	0(1)
C(5)	12(1)	20(1)	14(1)	0(1)	2(1)	1(1)
C(6)	20(1)	21(1)	22(1)	6(1)	6(1)	1(1)
C(7)	17(1)	17(1)	22(1)	-4(1)	5(1)	0(1)
C(8)	20(1)	22(1)	16(1)	0(1)	8(1)	0(1)
C(9)	19(1)	20(1)	24(1)	-2(1)	6(1)	-4(1)
C(10)	18(1)	15(1)	16(1)	-3(1)	6(1)	1(1)
C(11)	16(1)	16(1)	14(1)	-1(1)	6(1)	3(1)
C(12)	16(1)	18(1)	16(1)	-1(1)	8(1)	1(1)

C(13)	19(1)	19(1)	14(1)	0(1)	7(1)	3(1)
C(14)	17(1)	19(1)	14(1)	-4(1)	4(1)	2(1)
C(15)	25(1)	17(1)	26(1)	-2(1)	10(1)	-3(1)
C(16)	21(1)	21(1)	16(1)	0(1)	4(1)	6(1)
C(17)	17(1)	24(1)	26(1)	-1(1)	10(1)	-2(1)
C(18)	30(1)	26(1)	18(1)	6(1)	11(1)	6(1)

Table 13.27. Hydrogen coordinates (x 10^4) and isotropic displacement parameters ($Å^2$x 10^{3}) for **24**.

	x	y	z	U(eq)
H(1)	8559(13)	7941(13)	1902(12)	30(4)
H(2)	8858(12)	9255(14)	1108(12)	32(4)
H(3)	8941(12)	9390(14)	2592(13)	35(4)
H(4)	9968(13)	8503(14)	2142(13)	33(4)
H(5A)	5691(12)	8261(13)	-1502(12)	26(4)
H(6A)	7431(14)	10856(15)	-884(13)	37(4)
H(6B)	6234(13)	11329(15)	-1002(13)	36(4)
H(6C)	6505(12)	10397(13)	-1854(13)	33(4)
H(7A)	7255(13)	10515(14)	2205(13)	33(4)
H(7B)	7478(13)	11172(14)	1205(12)	32(4)
H(7C)	6360(14)	11271(16)	1441(13)	41(4)
H(8A)	6826(12)	8486(13)	2766(12)	28(4)
H(8B)	6095(12)	7409(15)	2332(12)	29(4)
H(8C)	5552(13)	8568(14)	2474(13)	33(4)
H(9A)	5218(12)	6245(13)	-530(12)	27(3)
H(9B)	5555(12)	6154(14)	730(12)	30(4)
H(9C)	4469(14)	6822(13)	160(13)	34(4)
H(14A)	7009(12)	6628(12)	-1758(11)	21(3)
H(15A)	7407(12)	5020(14)	764(13)	34(4)
H(15B)	6818(13)	4846(14)	-457(13)	35(4)
H(15C)	7998(13)	4259(15)	8(13)	34(4)
H(16A)	9501(12)	5739(14)	1756(13)	35(4)
H(16B)	10440(13)	6480(15)	1497(13)	35(4)
H(16C)	10183(13)	5223(15)	999(13)	37(4)
H(17A)	10694(15)	8242(15)	508(16)	43(5)
H(17B)	10961(13)	7714(15)	-468(13)	36(4)
H(17C)	10337(14)	8886(16)	-568(14)	43(4)
H(18A)	7655(14)	8610(14)	-2645(14)	36(4)
H(18B)	8661(13)	9313(15)	-1981(13)	39(4)
H(18C)	8837(15)	8241(15)	-2740(14)	41(4)

13.10. Crystallographic Data for $(C_5Me_5)_2ScCl(THF)$, 26

X-ray Data Collection, Structure Solution and Refinement for **26**.

A colorless crystal of approximate dimensions 0.09 x 0.10 x 0.27 mm was mounted on a glass fiber and transferred to a Bruker SMART APEX II diffractometer. The APEX2[1] program package and the CELL_NOW[2] were used to determine the unit-cell parameters. Data was collected using a 30 sec/frame scan time for a sphere of diffraction data. The structure was twinned. The raw frame data was processed using SAINT[3] and TWINABS[4] to yield the reflection data file (HKLF5 format)[4]. Subsequent calculations were carried out using the SHELXTL[5] program. There were no systematic absences nor any diffraction

symmetry other than the Friedel condition. The centrosymmetric triclinic space group $P\bar{1}$ was assigned and later determined to be correct.

The structure was solved by direct methods and refined on F^2 by full-matrix least-squares techniques. The analytical scattering factors[6] for neutral atoms were used throughout the analysis. Hydrogen atoms were located from a difference-Fourier map and refined (x,y,z and U_{iso}). Hydrogen atoms were included using a riding model. There were two molecules of the formula unit present.

Least-squares analysis yielded wR2 = 0.2111 and Goof = 1.038 for 507 variables refined against 9086 data (0.80Å), R1 = 0.0777 for those 7178 with I > 2.0σ(I).

References

1. APEX2 Version 2.2-0, Bruker AXS, Inc.; Madison, WI 2007.
2. Sheldrick, G. M. CELL_NOW, Version 2008-2, Bruker AXS, Inc.; Madison, WI 2008.
3. SAINT Version 7.46a, Bruker AXS, Inc.; Madison, WI 2007.
4. Sheldrick, G. M. TWINABS, Version 2007/5, Bruker AXS, Inc.; Madison, WI 2007.
5. Sheldrick, G. M. SHELXTL, Version 2008/3, Bruker AXS, Inc.; Madison, WI 2008.
6. International Tables for X-Ray Crystallography 1992, Vol. C., Dordrecht: Kluwer Academic Publishers.

Table 13.28. Atomic coordinates (x 10^4) and equivalent isotropic displacement parameters ($Å^2$x 10^3) for **26**. U(eq) is defined as one third of the trace of the orthogonalized U^{ij} tensor.

	x	y	z	U(eq)
Sc(1)	8702(1)	2662(1)	4887(1)	13(1)
Cl(1)	10924(1)	2989(1)	5560(1)	23(1)
O(1)	7058(3)	2753(2)	5838(2)	20(1)
C(1)	9557(6)	1017(3)	5946(3)	22(1)
C(2)	10375(5)	1241(3)	5198(3)	22(1)
C(3)	9281(5)	1345(3)	4571(3)	18(1)
C(4)	7751(5)	1217(3)	4921(3)	20(1)
C(5)	7926(6)	997(3)	5767(3)	22(1)
C(6)	10307(7)	718(4)	6781(3)	37(1)
C(7)	12165(5)	1251(4)	5105(4)	36(1)
C(8)	9759(6)	1358(3)	3766(3)	29(1)
C(9)	6216(6)	1154(3)	4521(3)	29(1)
C(10)	6648(7)	638(3)	6420(3)	36(1)
C(11)	7612(5)	4330(3)	4072(2)	16(1)
C(12)	9196(5)	4348(3)	3823(2)	16(1)
C(13)	9359(5)	3826(3)	3402(2)	16(1)
C(14)	7842(5)	3506(3)	3353(3)	18(1)
C(15)	6763(5)	3812(3)	3786(3)	19(1)
C(16)	6927(6)	4878(3)	4469(3)	24(1)
C(17)	10465(5)	4929(3)	3883(3)	25(1)
C(18)	10846(6)	3743(3)	2977(3)	23(1)
C(19)	7339(6)	3190(3)	2750(3)	26(1)
C(20)	4972(5)	3753(3)	3737(3)	25(1)
C(21)	7584(5)	2677(3)	6638(3)	23(1)
C(22)	6125(5)	2897(4)	7003(3)	26(1)
C(23)	4783(5)	2549(4)	6675(3)	26(1)
C(24)	5316(5)	2812(3)	5789(3)	24(1)
Sc(2)	3673(1)	2348(1)	188(1)	13(1)
Cl(2)	5972(1)	1720(1)	-232(1)	24(1)
O(2)	2138(3)	2189(2)	-736(2)	18(1)
C(25)	5184(5)	3790(3)	-724(3)	17(1)
C(26)	5068(5)	3704(3)	86(3)	18(1)
C(27)	3451(5)	3871(3)	214(3)	17(1)
C(28)	2577(5)	4015(3)	-508(3)	18(1)

C(29)	3648(5)	3970(3)	-1089(2)	17(1)
C(30)	6689(5)	3816(3)	-1183(3)	22(1)
C(31)	6435(5)	3567(3)	671(3)	23(1)
C(32)	2826(6)	4099(3)	864(3)	22(1)
C(33)	884(5)	4391(3)	-678(3)	25(1)
C(34)	3296(6)	4157(3)	-1966(3)	24(1)
C(35)	3523(6)	643(3)	1252(3)	21(1)
C(36)	4369(5)	1069(3)	1637(2)	20(1)
C(37)	3299(5)	1672(3)	1757(2)	17(1)
C(38)	1791(5)	1646(3)	1414(2)	17(1)
C(39)	1941(6)	1000(3)	1122(3)	21(1)
C(40)	4151(7)	-135(3)	1119(3)	35(1)
C(41)	6056(6)	826(4)	1969(3)	33(1)
C(42)	3606(6)	2061(3)	2340(3)	25(1)
C(43)	253(5)	2090(3)	1476(3)	25(1)
C(44)	617(6)	622(4)	848(3)	31(1)
C(45)	2605(6)	1692(3)	-1193(3)	26(1)
C(46)	1291(6)	1918(4)	-1834(3)	33(1)
C(47)	-161(6)	2057(4)	-1406(3)	30(1)
C(48)	501(5)	2548(3)	-970(3)	25(1)

Table 13.29. Anisotropic displacement parameters ($Å^2 x\ 10^3$) for **26**. The anisotropic displacement factor exponent takes the form: $-2\pi^2[\ h^2\ a^{*2}U^{11} + ...\ + 2\ h\ k\ a^*\ b^*\ U^{12}\ ]$

	U^{11}	U^{22}	U^{33}	U^{23}	U^{13}	U^{12}
Sc(1)	11(1)	14(1)	13(1)	-6(1)	0(1)	0(1)
Cl(1)	17(1)	26(1)	26(1)	-14(1)	-6(1)	-1(1)
O(1)	18(2)	25(2)	18(2)	-12(1)	0(1)	2(1)
C(1)	33(3)	16(2)	18(2)	-9(2)	-4(2)	1(2)
C(2)	20(2)	15(2)	27(2)	-8(2)	-3(2)	2(2)
C(3)	20(2)	16(2)	17(2)	-6(2)	4(2)	-2(2)
C(4)	25(2)	14(2)	20(2)	-8(2)	2(2)	-2(2)
C(5)	28(3)	13(2)	19(2)	-4(2)	6(2)	-1(2)
C(6)	54(4)	25(3)	24(3)	-7(2)	-14(2)	10(2)
C(7)	15(2)	38(3)	59(4)	-28(3)	-1(2)	4(2)
C(8)	39(3)	26(2)	27(2)	-17(2)	10(2)	-5(2)
C(9)	24(3)	25(2)	40(3)	-16(2)	-3(2)	-4(2)
C(10)	45(3)	19(2)	36(3)	-7(2)	21(2)	-7(2)
C(11)	17(2)	15(2)	11(2)	-3(2)	0(2)	1(2)
C(12)	19(2)	13(2)	12(2)	-2(2)	-1(2)	0(2)
C(13)	18(2)	14(2)	15(2)	-7(2)	2(2)	-4(2)
C(14)	19(2)	19(2)	13(2)	-6(2)	-1(2)	1(2)
C(15)	17(2)	19(2)	15(2)	-5(2)	-4(2)	3(2)
C(16)	27(3)	19(2)	26(2)	-12(2)	2(2)	1(2)
C(17)	27(3)	18(2)	27(2)	-8(2)	-1(2)	-8(2)
C(18)	21(2)	26(2)	23(2)	-12(2)	10(2)	-6(2)
C(19)	31(3)	29(3)	21(2)	-14(2)	-2(2)	-4(2)
C(20)	11(2)	30(3)	27(2)	-9(2)	-4(2)	-1(2)
C(21)	22(2)	39(3)	16(2)	-18(2)	-1(2)	-2(2)
C(22)	22(2)	37(3)	21(2)	-17(2)	2(2)	0(2)
C(23)	21(2)	34(3)	19(2)	-11(2)	5(2)	-2(2)
C(24)	15(2)	34(3)	26(2)	-16(2)	2(2)	0(2)
Sc(2)	13(1)	14(1)	13(1)	-6(1)	1(1)	0(1)
Cl(2)	21(1)	22(1)	28(1)	-12(1)	7(1)	2(1)
O(2)	20(2)	19(2)	20(2)	-12(1)	-1(1)	-1(1)
C(25)	19(2)	16(2)	15(2)	-6(2)	3(2)	-4(2)
C(26)	21(2)	15(2)	19(2)	-9(2)	1(2)	-4(2)
C(27)	20(2)	14(2)	18(2)	-8(2)	3(2)	-2(2)

C(28)	20(2)	11(2)	19(2)	-4(2)	2(2)	1(2)
C(29)	21(2)	15(2)	14(2)	-5(2)	0(2)	-5(2)
C(30)	20(2)	26(2)	21(2)	-11(2)	6(2)	-7(2)
C(31)	17(2)	28(2)	21(2)	-9(2)	0(2)	-6(2)
C(32)	28(2)	19(2)	23(2)	-13(2)	4(2)	-2(2)
C(33)	21(2)	22(2)	31(2)	-12(2)	-2(2)	3(2)
C(34)	28(3)	23(2)	18(2)	-7(2)	-1(2)	-2(2)
C(35)	32(3)	8(2)	18(2)	-3(2)	6(2)	0(2)
C(36)	20(2)	18(2)	10(2)	1(2)	2(2)	-1(2)
C(37)	19(2)	18(2)	12(2)	-5(2)	2(2)	0(2)
C(38)	23(2)	18(2)	10(2)	-5(2)	3(2)	-5(2)
C(39)	24(2)	20(2)	16(2)	-7(2)	3(2)	-7(2)
C(40)	54(4)	18(2)	29(3)	-9(2)	12(2)	1(2)
C(41)	22(3)	37(3)	20(2)	1(2)	-2(2)	6(2)
C(42)	34(3)	25(2)	15(2)	-9(2)	1(2)	-8(2)
C(43)	19(2)	33(3)	23(2)	-12(2)	5(2)	1(2)
C(44)	38(3)	35(3)	23(2)	-14(2)	7(2)	-19(2)
C(45)	30(3)	31(3)	31(2)	-25(2)	5(2)	-5(2)
C(46)	31(3)	50(3)	31(3)	-29(3)	7(2)	-12(2)
C(47)	26(3)	44(3)	27(3)	-21(2)	0(2)	-7(2)
C(48)	21(2)	28(2)	25(2)	-13(2)	-3(2)	0(2)

Table 13.30. Hydrogen coordinates (x 10^4) and isotropic displacement parameters ($Å^2$x 10^{3}) for **26**.

	x	y	z	U(eq)
H(6A)	10770	91	7001	55
H(6B)	9504	728	7167	55
H(6C)	11143	1137	6724	55
H(7A)	12555	677	5123	54
H(7B)	12658	1307	5564	54
H(7C)	12438	1776	4567	54
H(8A)	10442	812	3895	43
H(8B)	10339	1915	3420	43
H(8C)	8808	1356	3459	43
H(9A)	5609	648	4939	44
H(9B)	6460	1039	4052	44
H(9C)	5588	1735	4315	44
H(10A)	6775	-34	6750	54
H(10B)	5603	808	6141	54
H(10C)	6739	909	6791	54
H(16A)	7429	5473	4233	36
H(16B)	7125	4537	5076	36
H(16C)	5781	4980	4355	36
H(17A)	10579	5476	3335	38
H(17B)	11475	4569	4053	38
H(17C)	10167	5119	4300	38
H(18A)	11284	4352	2649	35
H(18B)	10592	3493	2602	35
H(18C)	11629	3329	3401	35
H(19A)	6733	3690	2283	39
H(19B)	6675	2657	3038	39
H(19C)	8281	3015	2532	39
H(20A)	4641	3986	3151	37
H(20B)	4440	4126	3958	37
H(20C)	4682	3110	4069	37
H(21A)	8416	3120	6545	28
H(21B)	8016	2047	7020	28
H(22A)	5985	3568	6800	31
H(22B)	6179	2569	7624	31

H(23A)	4697	1874	7019	31
H(23B)	3751	2858	6668	31
H(24A)	4915	2380	5609	29
H(24B)	4925	3445	5387	29
H(30A)	6951	4458	-1551	34
H(30B)	6537	3509	-1520	34
H(30C)	7558	3498	-776	34
H(31A)	6470	4100	765	35
H(31B)	7430	3503	420	35
H(31C)	6294	3008	1207	35
H(32A)	2502	4755	599	34
H(32B)	3656	3964	1288	34
H(32C)	1909	3728	1133	34
H(33A)	815	4984	-680	37
H(33B)	205	3956	-240	37
H(33C)	531	4479	-1226	37
H(34A)	4094	4558	-2345	36
H(34B)	2241	4462	-2144	36
H(34C)	3324	3575	-1983	36
H(40A)	3939	-723	1614	52
H(40B)	5297	-87	1030	52
H(40C)	3626	-104	626	52
H(41A)	6080	268	2518	50
H(41B)	6474	1335	2028	50
H(41C)	6711	716	1577	50
H(42A)	3786	1554	2913	37
H(42B)	2685	2446	2329	37
H(42C)	4546	2434	2157	37
H(43A)	-323	1649	1965	38
H(43B)	-388	2279	966	38
H(43C)	464	2632	1537	38
H(44A)	310	36	1319	47
H(44B)	974	519	385	47
H(44C)	-296	1062	660	47
H(45A)	2704	1020	-807	32
H(45B)	3632	1901	-1472	32
H(46A)	1163	1405	-1958	40
H(46B)	1501	2486	-2362	40
H(47A)	-1001	2440	-1820	37
H(47B)	-593	1461	-1000	37
H(48A)	471	3221	-1350	30
H(48B)	-119	2421	-465	30

13.11. Crystallographic Data for $(C_5Me_5)_2Sc(BH_4)_{0.5}(Cl)_{0.5}(THF)$, 27

X-ray Data Collection, Structure Solution and Refinement for sd3.

A colorless crystal of approximate dimensions 0.21 x 0.30 x 0.36 mm was mounted on a glass fiber and transferred to a Bruker SMART APEX II diffractometer. The APEX2[1] program package was used to determine the unit-cell parameters and for data collection (25 sec/frame scan time for a sphere of diffraction data). The raw frame data was processed using SAINT[2] and SADABS[3] to yield the reflection data file. Subsequent calculations were carried out using the SHELXTL[4] program. There were no systematic absences nor any diffraction

symmetry other than the Friedel condition. The centrosymmetric triclinic space group $P\bar{1}$ was assigned and later determined to be correct.

The structure was solved by direct methods and refined on F^2 by full-matrix least-squares techniques. The analytical scattering factors[5] for neutral atoms were used throughout the analysis. Hydrogen atom associated with the BH_4 ligands were initially located from a difference-Fourier map and refined (x,y,z and U_{iso}) with fixed boron-hydrogen distances. The remaining hydrogen atoms were included using a riding model. There were two molecules of the formula unit present. In both molecules the BH_4 and chloride ligands were disordered resulting in a refinement with each group assigned site-occupancy-factors of 0.50. The refinement is consistent with a composition of an equal number of the BH_4 and chloride complexes.

At convergence, wR2 = 0.1053 and Goof = 1.012 for 530 variables refined against 10304 data (0.75Å), R1 = 0.0399 for those 9494 data with I > 2.0σ(I).

References

1. APEX2 Version 2.2-0 Bruker AXS, Inc.; Madison, WI 2007.
2. SAINT Version 7.53a, Bruker AXS, Inc.; Madison, WI 2007.
3. Sheldrick, G. M. SADABS, Version 2008/1, Bruker AXS, Inc.; Madison, WI 2008.
4. Sheldrick, G. M. SHELXTL, Version 2008/4, Bruker AXS, Inc.; Madison, WI 2008.
5. International Tables for X-Ray Crystallography 1992, Vol. C., Dordrecht: Kluwer Academic Publishers.

Table 13.31. Atomic coordinates (x 10^4) and equivalent isotropic displacement parameters ($Å^2$x 10^3) for **27**. U(eq) is defined as one third of the trace of the orthogonalized U^{ij} tensor.

	x	y	z	U(eq)
Sc(1)	6292(1)	7482(1)	4856(1)	14(1)
Cl(1)	4061(1)	6485(1)	5529(1)	26(1)
B(1)	3709(5)	6669(3)	5405(3)	16(1)
O(1)	7903(1)	6410(1)	5830(1)	20(1)
C(1)	5845(2)	6842(1)	3811(1)	18(1)
C(2)	7424(2)	6614(1)	4060(1)	18(1)
C(3)	8260(2)	7420(1)	3772(1)	18(1)
C(4)	7188(2)	8146(1)	3326(1)	18(1)
C(5)	5687(2)	7790(1)	3370(1)	18(1)
C(6)	4614(2)	6202(1)	3858(1)	27(1)
C(7)	8095(2)	5671(1)	4461(1)	27(1)
C(8)	10026(2)	7510(1)	3726(1)	26(1)
C(9)	7698(2)	9061(1)	2715(1)	28(1)
C(10)	4214(2)	8296(1)	2939(1)	26(1)
C(11)	5511(2)	8083(1)	5912(1)	25(1)
C(12)	4681(2)	8620(1)	5170(1)	23(1)
C(13)	5787(2)	9112(1)	4537(1)	20(1)
C(14)	7318(2)	8868(1)	4884(1)	21(1)
C(15)	7130(2)	8247(1)	5735(1)	23(1)
C(16)	4785(3)	7561(1)	6768(1)	42(1)
C(17)	2930(2)	8755(2)	5086(2)	42(1)
C(18)	5345(2)	9900(1)	3730(1)	30(1)
C(19)	8842(2)	9308(1)	4484(1)	32(1)
C(20)	8390(3)	7942(1)	6382(1)	39(1)
C(21)	7364(2)	5690(1)	6624(1)	28(1)
C(22)	8812(2)	5096(1)	6994(1)	32(1)
C(23)	10143(2)	5756(1)	6674(1)	30(1)
C(24)	9625(2)	6384(1)	5793(1)	24(1)

Sc(2)	1274(1)	2467(1)	210(1)	14(1)
O(2)	2800(1)	3574(1)	-738(1)	20(1)
Cl(2)	-1050(2)	3496(1)	-199(1)	34(1)
B(2)	-1330(6)	3382(3)	-40(3)	22(1)
C(25)	1350(2)	2146(1)	-1081(1)	18(1)
C(26)	-179(2)	1952(1)	-720(1)	18(1)
C(27)	-58(2)	1214(1)	89(1)	18(1)
C(28)	1552(2)	935(1)	213(1)	18(1)
C(29)	2429(2)	1520(1)	-503(1)	19(1)
C(30)	1694(2)	2836(1)	-1962(1)	25(1)
C(31)	-1674(2)	2360(1)	-1178(1)	25(1)
C(32)	-1409(2)	749(1)	669(1)	25(1)
C(33)	2185(2)	49(1)	857(1)	25(1)
C(34)	4120(2)	1330(1)	-674(1)	28(1)
C(35)	622(2)	2261(1)	1682(1)	20(1)
C(36)	1427(2)	3080(1)	1294(1)	22(1)
C(37)	2998(2)	2883(1)	1130(1)	20(1)
C(38)	3182(2)	1944(1)	1406(1)	18(1)
C(39)	1709(2)	1558(1)	1766(1)	18(1)
C(40)	-1024(2)	2136(1)	2050(1)	33(1)
C(41)	808(3)	3980(1)	1197(1)	37(1)
C(42)	4292(2)	3547(1)	850(1)	31(1)
C(43)	4734(2)	1455(1)	1444(1)	26(1)
C(44)	1443(2)	587(1)	2347(1)	26(1)
C(45)	2316(2)	4518(1)	-1191(1)	30(1)
C(46)	3623(3)	4945(1)	-1839(1)	43(1)
C(47)	5072(2)	4389(1)	-1408(1)	38(1)
C(48)	4431(2)	3455(1)	-968(1)	26(1)

Table 13.32. Anisotropic displacement parameters ($Å^2 x\ 10^3$) for sd3. The anisotropic displacement factor exponent takes the form: $-2\pi^2[\ h^2\ a^{*2}U^{11} + ...\ + 2\ h\ k\ a^*\ b^*\ U^{12}\ ]$

	U^{11}	U^{22}	U^{33}	U^{23}	U^{13}	U^{12}
Sc(1)	13(1)	15(1)	13(1)	-6(1)	1(1)	-1(1)
O(1)	20(1)	20(1)	16(1)	-4(1)	0(1)	2(1)
C(1)	19(1)	20(1)	16(1)	-10(1)	1(1)	-2(1)
C(2)	21(1)	20(1)	15(1)	-9(1)	0(1)	2(1)
C(3)	16(1)	24(1)	14(1)	-9(1)	2(1)	-1(1)
C(4)	20(1)	20(1)	13(1)	-6(1)	2(1)	-2(1)
C(5)	19(1)	20(1)	14(1)	-8(1)	-1(1)	0(1)
C(6)	28(1)	27(1)	30(1)	-15(1)	0(1)	-8(1)
C(7)	32(1)	23(1)	27(1)	-13(1)	-5(1)	8(1)
C(8)	16(1)	40(1)	24(1)	-15(1)	2(1)	-3(1)
C(9)	34(1)	25(1)	21(1)	-5(1)	5(1)	-8(1)
C(10)	23(1)	29(1)	24(1)	-10(1)	-7(1)	4(1)
C(11)	34(1)	22(1)	20(1)	-12(1)	4(1)	4(1)
C(12)	21(1)	23(1)	30(1)	-15(1)	1(1)	5(1)
C(13)	23(1)	16(1)	22(1)	-9(1)	-3(1)	2(1)
C(14)	22(1)	20(1)	25(1)	-14(1)	-3(1)	-1(1)
C(15)	30(1)	22(1)	22(1)	-14(1)	-8(1)	5(1)
C(16)	62(1)	36(1)	25(1)	-13(1)	15(1)	3(1)
C(17)	22(1)	46(1)	59(1)	-24(1)	3(1)	9(1)
C(18)	40(1)	19(1)	28(1)	-8(1)	-9(1)	5(1)
C(19)	25(1)	34(1)	45(1)	-24(1)	2(1)	-9(1)
C(20)	50(1)	39(1)	37(1)	-26(1)	-24(1)	14(1)
C(21)	29(1)	25(1)	20(1)	0(1)	1(1)	1(1)
C(22)	38(1)	26(1)	23(1)	-2(1)	-3(1)	9(1)
C(23)	28(1)	37(1)	21(1)	-9(1)	-5(1)	10(1)
C(24)	20(1)	31(1)	19(1)	-9(1)	-2(1)	3(1)

Sc(2)	14(1)	14(1)	13(1)	-6(1)	-1(1)	1(1)
O(2)	21(1)	16(1)	20(1)	-5(1)	0(1)	0(1)
C(25)	22(1)	20(1)	16(1)	-10(1)	0(1)	-1(1)
C(26)	20(1)	20(1)	16(1)	-9(1)	-3(1)	-1(1)
C(27)	19(1)	18(1)	18(1)	-8(1)	-1(1)	-3(1)
C(28)	21(1)	16(1)	20(1)	-10(1)	-2(1)	1(1)
C(29)	19(1)	20(1)	21(1)	-13(1)	0(1)	1(1)
C(30)	30(1)	30(1)	15(1)	-9(1)	2(1)	-5(1)
C(31)	23(1)	27(1)	24(1)	-10(1)	-8(1)	1(1)
C(32)	23(1)	28(1)	21(1)	-8(1)	1(1)	-8(1)
C(33)	32(1)	18(1)	26(1)	-10(1)	-8(1)	5(1)
C(34)	22(1)	30(1)	35(1)	-18(1)	4(1)	3(1)
C(35)	20(1)	27(1)	14(1)	-10(1)	-1(1)	3(1)
C(36)	30(1)	22(1)	18(1)	-11(1)	-5(1)	5(1)
C(37)	25(1)	20(1)	15(1)	-8(1)	-3(1)	-3(1)
C(38)	18(1)	21(1)	15(1)	-7(1)	-3(1)	0(1)
C(39)	20(1)	20(1)	14(1)	-6(1)	-2(1)	0(1)
C(40)	22(1)	50(1)	26(1)	-17(1)	3(1)	4(1)
C(41)	56(1)	26(1)	32(1)	-17(1)	-6(1)	12(1)
C(42)	40(1)	29(1)	24(1)	-10(1)	-4(1)	-14(1)
C(43)	20(1)	31(1)	25(1)	-10(1)	-4(1)	4(1)
C(44)	33(1)	22(1)	19(1)	-6(1)	0(1)	-5(1)
C(45)	36(1)	16(1)	30(1)	-4(1)	-8(1)	2(1)
C(46)	43(1)	30(1)	36(1)	5(1)	-6(1)	-12(1)
C(47)	34(1)	34(1)	33(1)	-2(1)	2(1)	-13(1)
C(48)	20(1)	28(1)	27(1)	-9(1)	4(1)	-4(1)

Table 13.33. Hydrogen coordinates (x 10^4) and isotropic displacement parameters ($Å^2$x 10^{3}) for sd3.

	x	y	z	U(eq)
H(1A)	4870(16)	6347(15)	5670(15)	24(3)
H(1B)	3900(30)	7311(9)	4839(10)	24(3)
H(1C)	3020(30)	6801(17)	5886(12)	24(3)
H(1D)	3060(30)	6210(14)	5237(15)	24(3)
H(6A)	4626	6148	3331	41
H(6B)	3574	6428	3949	41
H(6C)	4840	5613	4324	41
H(7A)	7646	5323	4203	40
H(7B)	7835	5395	5063	40
H(7C)	9243	5678	4378	40
H(8A)	10366	7857	3140	40
H(8B)	10540	6912	3951	40
H(8C)	10318	7818	4057	40
H(9A)	8295	9022	2249	42
H(9B)	8364	9303	2998	42
H(9C)	6767	9458	2499	42
H(10A)	3772	8000	2630	39
H(10B)	4471	8912	2548	39
H(10C)	3440	8305	3360	39
H(16A)	4317	7976	6976	62
H(16B)	5599	7181	7153	62
H(16C)	3965	7184	6735	62
H(17A)	2602	9312	5118	64
H(17B)	2411	8249	5541	64
H(17C)	2630	8793	4545	64
H(18A)	4715	10338	3852	45
H(18B)	4729	9698	3395	45

H(18C)	6304	10179	3415	45
H(19A)	9405	9442	4882	48
H(19B)	8615	9866	3981	48
H(19C)	9496	8902	4328	48
H(20A)	8320	8311	6686	58
H(20B)	9428	8003	6105	58
H(20C)	8243	7313	6778	58
H(21A)	6540	5347	6527	34
H(21B)	6926	5937	7005	34
H(22A)	8954	4631	6791	39
H(22B)	8746	4803	7615	39
H(23A)	10230	6080	7021	36
H(23B)	11166	5449	6666	36
H(24A)	10031	6990	5617	29
H(24B)	10019	6156	5389	29
H(2A)	-114(14)	3631(16)	-265(15)	24(3)
H(2B)	-1270(30)	2648(5)	338(13)	24(3)
H(2C)	-2080(30)	3567(16)	-595(10)	24(3)
H(2D)	-1820(30)	3713(15)	345(13)	24(3)
H(30A)	930	2797	-2341	38
H(30B)	2761	2726	-2134	38
H(30C)	1617	3435	-1984	38
H(31A)	-1940	2052	-1513	37
H(31B)	-1527	2997	-1549	37
H(31C)	-2531	2299	-772	37
H(32A)	-1409	124	761	37
H(32B)	-2404	1053	418	37
H(32C)	-1293	768	1207	37
H(33A)	2480	-339	587	38
H(33B)	1374	-237	1292	38
H(33C)	3114	145	1113	38
H(34A)	4228	725	-638	42
H(34B)	4791	1372	-259	42
H(34C)	4441	1768	-1238	42
H(40A)	-1009	2092	2618	49
H(40B)	-1438	1586	2074	49
H(40C)	-1700	2650	1699	49
H(41A)	1283	4120	1616	55
H(41B)	-340	3967	1280	55
H(41C)	1076	4439	634	55
H(42A)	4579	3666	1319	47
H(42B)	3926	4107	385	47
H(42C)	5215	3301	664	47
H(43A)	5264	1346	1962	39
H(43B)	5398	1820	959	39
H(43C)	4550	882	1438	39
H(44A)	1277	516	2922	39
H(44B)	2367	223	2324	39
H(44C)	512	391	2174	39
H(45A)	2202	4801	-804	35
H(45B)	1298	4583	-1467	35
H(46A)	3431	4902	-2365	51
H(46B)	3728	5582	-1966	51
H(47A)	5920	4425	-1819	45
H(47B)	5479	4582	-1001	45
H(48A)	4481	3163	-1348	32
H(48B)	5044	3081	-462	32

13.12. Crystallographic Data for $(C_5Me_5)_2Sc(\mu\text{-}H)_2BC_8H_{14}$, 29

X-ray Data Collection, Structure Solution and Refinement for **29**.

A yellow crystal of approximate dimensions 0.10 x 0.10 x 0.31 mm was mounted on a glass fiber and transferred to a Bruker SMART APEX II diffractometer. The APEX2[1] program package was used to determine the unit-cell parameters and for data collection (40 sec/frame scan time for a sphere of diffraction data). The raw frame data was processed using SAINT[2] and SADABS[3] to yield the reflection data file. Subsequent calculations were carried out using the SHELXTL[4] program. There were no systematic absences nor any diffraction symmetry other than the Friedel condition. The centrosymmetric triclinic space group $P\bar{1}$ was assigned and later determined to be correct.

The structure was solved by direct methods and refined on F^2 by full-matrix least-squares techniques. The analytical scattering factors[5] for neutral atoms were used throughout the analysis. Hydrogen atoms H(1a), H(1b), H(2a) and H(2b) were located from a difference-Fourier map and refined (x,y,z and U_{iso}). It was necessary to fix the hydrogen-hydrogen distances during refinement to maintain a reasonable geometry about the boron atoms The remaining hydrogen atoms were included using a riding model.

At convergence, wR2 = 0.1225 and Goof = 1.030 for 577 variables refined against 11549 data (0.74Å), R1 = 0.0463 for those 9163 data with I > 2.0σ(I).

References

1. APEX2 Version 2.2-0 Bruker AXS, Inc.; Madison, WI 2007.
2. SAINT Version 7.68a, Bruker AXS, Inc.; Madison, WI 2008.
3. Sheldrick, G. M. SADABS, Version 2008/1, Bruker AXS, Inc.; Madison, WI 2008.
4. Sheldrick, G. M. SHELXTL, Version 2008/4, Bruker AXS, Inc.; Madison, WI 2008.
5. International Tables for X-Ray Crystallography 1992, Vol. C., Dordrecht: Kluwer Academic Publishers.

Table 13.34. Atomic coordinates (x 10^4) and equivalent isotropic displacement parameters ($Å^2$x 10^3) for **29**. U(eq) is defined as one third of the trace of the orthogonalized U^{ij} tensor.

	x	y	z	U(eq)
Sc(1)	1824(1)	355(1)	2034(1)	16(1)
C(1)	-730(2)	-270(1)	2818(1)	19(1)
C(2)	-574(2)	-467(1)	2162(1)	20(1)
C(3)	-528(2)	402(1)	1573(1)	21(1)
C(4)	-543(2)	1141(1)	1857(1)	23(1)
C(5)	-688(2)	727(1)	2627(1)	21(1)
C(6)	-1135(2)	-1022(2)	3563(1)	27(1)
C(7)	-674(2)	-1435(1)	2122(1)	27(1)
C(8)	-823(2)	480(2)	845(1)	32(1)
C(9)	-604(2)	2184(1)	1444(1)	35(1)
C(10)	-945(2)	1272(2)	3141(1)	32(1)
C(11)	4374(2)	20(1)	1459(1)	20(1)
C(12)	3425(2)	41(1)	980(1)	21(1)
C(13)	2981(2)	986(1)	681(1)	22(1)
C(14)	3580(2)	1533(1)	1008(1)	22(1)
C(15)	4487(2)	946(1)	1469(1)	21(1)
C(16)	5233(2)	-827(1)	1809(1)	28(1)
C(17)	3157(2)	-769(2)	743(1)	30(1)
C(18)	2361(2)	1398(2)	6(1)	30(1)
C(19)	3493(2)	2587(1)	814(1)	31(1)

C(20)	5545(2)	1339(2)	1774(1)	28(1)
B(1)	2670(2)	-114(2)	3283(1)	19(1)
C(21)	4339(2)	-322(1)	3431(1)	22(1)
C(22)	4347(2)	-1363(2)	3938(1)	30(1)
C(23)	3237(2)	-1621(2)	4674(1)	32(1)
C(24)	1673(2)	-1245(2)	4617(1)	28(1)
C(25)	1604(2)	-234(1)	4069(1)	21(1)
C(26)	2063(2)	539(2)	4324(1)	28(1)
C(27)	3682(2)	504(2)	4405(1)	29(1)
C(28)	4803(2)	381(2)	3754(1)	27(1)
Sc(2)	2932(1)	4991(1)	2946(1)	17(1)
C(29)	226(2)	5196(1)	3438(1)	22(1)
C(30)	1073(2)	5557(1)	3804(1)	20(1)
C(31)	1763(2)	4795(1)	4255(1)	21(1)
C(32)	1442(2)	3969(1)	4126(1)	23(1)
C(33)	469(2)	4222(1)	3624(1)	23(1)
C(34)	-907(2)	5779(2)	3044(1)	30(1)
C(35)	1025(2)	6550(1)	3807(1)	29(1)
C(36)	2398(2)	4857(2)	4867(1)	29(1)
C(37)	1863(3)	2976(1)	4512(1)	34(1)
C(38)	-250(2)	3525(2)	3402(1)	33(1)
C(39)	5396(2)	5770(1)	2281(1)	20(1)
C(40)	5243(2)	5644(1)	3034(1)	20(1)
C(41)	5276(2)	4660(1)	3429(1)	20(1)
C(42)	5368(2)	4184(1)	2925(1)	20(1)
C(43)	5493(2)	4870(1)	2214(1)	20(1)
C(44)	5595(2)	6715(1)	1671(1)	30(1)
C(45)	5249(2)	6444(1)	3317(1)	28(1)
C(46)	5546(2)	4201(2)	4188(1)	29(1)
C(47)	5524(2)	3137(1)	3092(1)	30(1)
C(48)	5905(2)	4626(2)	1530(1)	31(1)
B(2)	2096(2)	5462(2)	1685(1)	21(1)
C(49)	3112(2)	5950(1)	868(1)	26(1)
C(50)	2462(2)	6913(1)	479(1)	29(1)
C(51)	929(3)	7090(2)	913(1)	33(1)
C(52)	-191(2)	6276(2)	1163(1)	32(1)
C(53)	448(2)	5309(2)	1586(1)	27(1)
C(54)	576(3)	4632(2)	1155(1)	32(1)
C(55)	1609(3)	5009(2)	399(1)	33(1)
C(56)	3133(2)	5284(2)	428(1)	31(1)

Table 13.35. Anisotropic displacement parameters ($Å^2 x\ 10^3$) for **29**. The anisotropic displacement factor exponent takes the form: $-2\pi^2[\ h^2\ a^{*2}U^{11} + ...\ + 2\ h\ k\ a^*\ b^*\ U^{12}\ ]$

	U^{11}	U^{22}	U^{33}	U^{23}	U^{13}	U^{12}
Sc(1)	15(1)	16(1)	17(1)	-5(1)	-3(1)	0(1)
C(1)	12(1)	24(1)	20(1)	-8(1)	-3(1)	0(1)
C(2)	16(1)	21(1)	21(1)	-7(1)	-4(1)	-2(1)
C(3)	17(1)	23(1)	23(1)	-5(1)	-6(1)	-2(1)
C(4)	16(1)	19(1)	33(1)	-6(1)	-9(1)	1(1)
C(5)	14(1)	23(1)	30(1)	-13(1)	-6(1)	3(1)
C(6)	22(1)	35(1)	20(1)	-6(1)	-2(1)	-6(1)
C(7)	28(1)	22(1)	32(1)	-12(1)	-7(1)	-1(1)
C(8)	29(1)	42(1)	23(1)	-4(1)	-9(1)	-9(1)
C(9)	27(1)	19(1)	56(2)	-4(1)	-17(1)	0(1)
C(10)	24(1)	37(1)	47(1)	-28(1)	-11(1)	10(1)
C(11)	16(1)	21(1)	20(1)	-6(1)	2(1)	1(1)
C(12)	22(1)	21(1)	18(1)	-7(1)	2(1)	-3(1)
C(13)	20(1)	24(1)	17(1)	-3(1)	0(1)	-2(1)

C(14)	20(1)	20(1)	22(1)	-5(1)	1(1)	-4(1)
C(15)	16(1)	23(1)	20(1)	-6(1)	1(1)	-3(1)
C(16)	27(1)	27(1)	26(1)	-8(1)	-2(1)	7(1)
C(17)	34(1)	30(1)	28(1)	-15(1)	-2(1)	-2(1)
C(18)	31(1)	32(1)	21(1)	-2(1)	-4(1)	-4(1)
C(19)	30(1)	19(1)	37(1)	-4(1)	-3(1)	-4(1)
C(20)	22(1)	32(1)	28(1)	-9(1)	-3(1)	-8(1)
B(1)	20(1)	19(1)	19(1)	-7(1)	-6(1)	1(1)
C(21)	19(1)	25(1)	22(1)	-8(1)	-3(1)	1(1)
C(22)	25(1)	28(1)	36(1)	-9(1)	-9(1)	9(1)
C(23)	32(1)	26(1)	32(1)	-1(1)	-10(1)	2(1)
C(24)	25(1)	32(1)	21(1)	-3(1)	-4(1)	-2(1)
C(25)	16(1)	27(1)	20(1)	-9(1)	-5(1)	3(1)
C(26)	28(1)	34(1)	26(1)	-17(1)	-9(1)	7(1)
C(27)	30(1)	33(1)	28(1)	-14(1)	-11(1)	1(1)
C(28)	21(1)	32(1)	28(1)	-9(1)	-9(1)	-3(1)
Sc(2)	14(1)	18(1)	18(1)	-8(1)	-1(1)	0(1)
C(29)	14(1)	30(1)	19(1)	-11(1)	1(1)	0(1)
C(30)	16(1)	24(1)	20(1)	-10(1)	0(1)	2(1)
C(31)	18(1)	26(1)	18(1)	-8(1)	1(1)	0(1)
C(32)	20(1)	22(1)	22(1)	-6(1)	4(1)	-3(1)
C(33)	19(1)	26(1)	23(1)	-11(1)	4(1)	-6(1)
C(34)	21(1)	44(1)	25(1)	-13(1)	-4(1)	4(1)
C(35)	29(1)	28(1)	35(1)	-18(1)	-4(1)	5(1)
C(36)	26(1)	41(1)	20(1)	-11(1)	-3(1)	1(1)
C(37)	33(1)	23(1)	35(1)	-4(1)	0(1)	-3(1)
C(38)	31(1)	33(1)	34(1)	-15(1)	1(1)	-12(1)
C(39)	11(1)	22(1)	25(1)	-5(1)	-3(1)	-1(1)
C(40)	14(1)	21(1)	27(1)	-10(1)	-3(1)	1(1)
C(41)	16(1)	22(1)	22(1)	-8(1)	-4(1)	2(1)
C(42)	16(1)	20(1)	24(1)	-8(1)	-4(1)	4(1)
C(43)	14(1)	24(1)	23(1)	-9(1)	-2(1)	2(1)
C(44)	25(1)	25(1)	32(1)	-2(1)	-7(1)	-1(1)
C(45)	23(1)	27(1)	40(1)	-17(1)	-7(1)	0(1)
C(46)	25(1)	35(1)	25(1)	-9(1)	-8(1)	7(1)
C(47)	32(1)	22(1)	37(1)	-12(1)	-8(1)	7(1)
C(48)	28(1)	41(1)	25(1)	-15(1)	-4(1)	10(1)
B(2)	22(1)	18(1)	22(1)	-9(1)	-1(1)	2(1)
C(49)	26(1)	29(1)	22(1)	-10(1)	-4(1)	1(1)
C(50)	34(1)	25(1)	25(1)	-4(1)	-9(1)	0(1)
C(51)	43(1)	30(1)	27(1)	-10(1)	-12(1)	11(1)
C(52)	26(1)	47(1)	26(1)	-16(1)	-10(1)	11(1)
C(53)	25(1)	31(1)	25(1)	-10(1)	-4(1)	1(1)
C(54)	35(1)	33(1)	33(1)	-14(1)	-10(1)	-3(1)
C(55)	44(1)	33(1)	29(1)	-18(1)	-10(1)	6(1)
C(56)	36(1)	36(1)	22(1)	-14(1)	-3(1)	6(1)

Table 13.36. Hydrogen coordinates (x 10^4) and isotropic displacement parameters ($Å^2$x 10^{3}) for **29**.

	x	y	z	U(eq)
H(6A)	-1951	-1426	3578	41
H(6B)	-1455	-725	3934	41
H(6C)	-265	-1405	3664	41
H(7A)	-1673	-1716	2377	40
H(7B)	76	-1834	2356	40
H(7C)	-491	-1385	1608	40
H(8A)	-1869	301	909	48

H(8B)	-170	58	647	48
H(8C)	-625	1133	505	48
H(9A)	-1609	2402	1586	53
H(9B)	-367	2303	916	53
H(9C)	123	2526	1562	53
H(10A)	-1648	1773	2992	48
H(10B)	5	1552	3126	48
H(10C)	-1358	844	3641	48
H(16A)	5720	-1099	1440	42
H(16B)	4547	-1300	2205	42
H(16C)	5993	-633	2009	42
H(17A)	3976	-782	338	45
H(17B)	2212	-686	581	45
H(17C)	3108	-1365	1157	45
H(18A)	3175	1693	-418	46
H(18B)	1636	1876	69	46
H(18C)	1868	897	-73	46
H(19A)	4426	2892	481	46
H(19B)	3337	2741	1261	46
H(19C)	2658	2815	573	46
H(20A)	6178	1841	1376	42
H(20B)	6173	835	2011	42
H(20C)	4975	1599	2136	42
H(21A)	5051	-238	2953	26
H(22A)	4129	-1773	3678	36
H(22B)	5363	-1503	4030	36
H(23A)	3626	-1368	4996	38
H(23B)	3159	-2317	4908	38
H(24A)	1129	-1263	5109	33
H(24B)	1134	-1680	4478	33
H(25A)	554	-127	4004	25
H(26A)	1905	1164	3969	33
H(26B)	1398	480	4803	33
H(27A)	3772	-27	4857	34
H(27B)	3942	1095	4464	34
H(28A)	5752	173	3908	32
H(28B)	5003	1006	3358	32
H(34A)	-1548	6076	3362	45
H(34B)	-1519	5372	2921	45
H(34C)	-391	6270	2594	45
H(35A)	9	6677	4027	44
H(35B)	1315	6995	3302	44
H(35C)	1718	6624	4093	44
H(36A)	1600	4992	5231	43
H(36B)	3165	5365	4670	43
H(36C)	2843	4256	5099	43
H(37A)	958	2591	4797	50
H(37B)	2507	2982	4841	50
H(37C)	2400	2709	4149	50
H(38A)	-658	2979	3838	49
H(38B)	500	3314	3062	49
H(38C)	-1056	3828	3162	49
H(44A)	6261	7124	1764	44
H(44B)	4623	7007	1649	44
H(44C)	6032	6631	1204	44
H(45A)	6154	6841	3057	42
H(45B)	5230	6186	3843	42
H(45C)	4367	6824	3235	42
H(46A)	6593	4025	4158	43
H(46B)	4898	3635	4449	43
H(46C)	5324	4645	4453	43
H(47A)	6520	3015	2847	45

H(47B)	4766	2902	2916	45
H(47C)	5387	2814	3623	45
H(48A)	6862	4308	1515	46
H(48B)	5994	5205	1099	46
H(48C)	5129	4205	1530	46
H(49A)	4154	6055	903	31
H(50A)	3176	7426	404	34
H(50B)	2356	6938	-9	34
H(51A)	1077	7214	1349	40
H(51B)	512	7664	601	40
H(52A)	-490	6229	730	38
H(52B)	-1095	6405	1487	38
H(53A)	-228	5016	2078	32
H(54A)	950	4022	1442	39
H(54B)	-431	4509	1100	39
H(55A)	1704	4519	171	40
H(55B)	1160	5566	86	40
H(56A)	3709	5601	-79	37
H(56B)	3658	4704	653	37
H(1A)	2260(20)	-627(11)	2969(12)	29(6)
H(1B)	2510(20)	656(11)	2832(12)	28(6)
H(2A)	2180(30)	5913(12)	2109(12)	33(6)
H(2B)	2580(30)	4702(12)	2065(12)	34(6)

13.13. Crystallographic Data for $(C_5Me_4H)_2Sc(\mu\text{-}H)_2BC_8H_{14}$, 30

X-ray Data Collection, Structure Solution and Refinement for **30**.

A colorless crystal of approximate dimensions 0.17 x 0.21 x 0.23 mm was mounted on a glass fiber and transferred to a Bruker SMART APEX II diffractometer. The APEX2[1] program package was used to determine the unit-cell parameters and for data collection (20 sec/frame scan time for a sphere of diffraction data). The raw frame data was processed using SAINT[2] and SADABS[3] to yield the reflection data file. Subsequent calculations were carried out using the SHELXTL[4] program. There were no systematic absences nor any diffraction symmetry other than the Friedel condition. The centrosymmetric triclinic space group $P\bar{1}$ was assigned and later determined to be correct.

The structure was solved by direct methods and refined on F^2 by full-matrix least-squares techniques. The analytical scattering factors[5] for neutral atoms were used throughout the analysis. Hydrogen atoms H(1)-H(4) were located from a difference-Fourier map and refined (x,y,z and U_{iso}). The remaining hydrogen atoms were included using a riding model. There were two molecules of the formula unit present. One of the tetramethylcyclopentadienyl ligands on each of the independent molecules was disordered. The disordered ligands were included using multiple components and partial site-occupancy-factors.

At convergence, wR2 = 0.1210 and Goof = 1.037 for 617 variables refined against 10393 data (0.78Å), R1 = 0.0468 for those 8670 data with I > 2.0σ(I).

References

1. APEX2 Version 2008.3-0, Bruker AXS, Inc.; Madison, WI 2008.
2. SAINT Version 7.53a, Bruker AXS, Inc.; Madison, WI 2007.
3. Sheldrick, G. M. SADABS, Version 2008/1, Bruker AXS, Inc.; Madison, WI 2008.
4. Sheldrick, G. M. SHELXTL, Version 2008/3, Bruker AXS, Inc.; Madison, WI 2008.
5. International Tables for X-Ray Crystallography 1992, Vol. C., Dordrecht: Kluwer Academic Publishers.

Table 13.37. Atomic coordinates (x 10^4) and equivalent isotropic displacement parameters ($Å^2$x 10^3) for **30**. U(eq) is defined as one third of the trace of the orthogonalized U^{ij} tensor.

	x	y	z	U(eq)
Sc(1)	7659(1)	7035(1)	9462(1)	16(1)
B(1)	6818(2)	8154(2)	10548(1)	19(1)
C(1)	7767(2)	7508(2)	8202(1)	24(1)
C(2)	6718(2)	7865(1)	8450(1)	18(1)
C(3)	5690(2)	6970(1)	8442(1)	18(1)
C(4)	6108(2)	6063(2)	8187(1)	24(1)
C(5)	7377(2)	6403(2)	8032(1)	26(1)
C(6)	9008(2)	8207(2)	8081(2)	37(1)
C(7)	6683(2)	8984(2)	8591(1)	23(1)
C(8)	4342(2)	6950(2)	8592(1)	24(1)
C(9)	5295(2)	4943(2)	8055(1)	35(1)
C(10)	9922(5)	7211(4)	10087(4)	31(1)
C(11)	9580(5)	6317(5)	9430(3)	27(1)
C(12)	8544(5)	5532(3)	9550(3)	17(1)
C(13)	8252(4)	5928(3)	10289(3)	14(1)
C(14)	9112(5)	6969(4)	10620(3)	21(1)
C(15)	10954(7)	8284(6)	10295(5)	68(2)
C(16)	10375(7)	6244(6)	8805(4)	64(2)
C(17)	8089(5)	4433(4)	9011(3)	38(1)
C(18)	7241(5)	5310(4)	10633(3)	33(1)
C(10B)	9840(4)	7295(3)	10321(3)	12(1)
C(11B)	9846(4)	6650(4)	9577(3)	14(1)
C(12B)	8874(5)	5669(4)	9427(3)	20(1)
C(13B)	8251(5)	5715(4)	10074(3)	25(1)
C(14B)	8859(5)	6716(4)	10638(3)	19(1)
C(15B)	10794(4)	8381(3)	10674(3)	23(1)
C(16B)	10794(5)	6805(4)	9042(3)	30(1)
C(17B)	8602(5)	4644(4)	8802(3)	37(1)
C(18B)	7132(6)	4896(5)	10229(4)	47(1)
C(19)	5839(2)	8854(1)	10403(1)	19(1)
C(20)	4593(2)	8496(2)	10724(1)	29(1)
C(21)	4848(2)	8430(2)	11589(1)	35(1)
C(22)	5933(3)	7927(2)	11788(1)	37(1)
C(23)	7203(2)	8329(2)	11503(1)	28(1)
C(24)	7962(2)	9499(2)	11908(1)	29(1)
C(25)	7278(2)	10292(2)	11689(1)	25(1)
C(26)	6637(2)	10020(1)	10797(1)	23(1)
Sc(2)	3052(1)	7342(1)	5294(1)	17(1)
B(2)	1424(2)	7569(2)	4141(1)	19(1)
C(27)	4187(2)	8848(2)	6449(1)	38(1)
C(28)	2982(2)	9046(2)	6168(1)	28(1)
C(29)	1934(2)	8252(1)	6268(1)	18(1)
C(30)	2492(2)	7560(2)	6605(1)	22(1)
C(31)	3884(2)	7944(2)	6724(1)	35(1)
C(32)	5541(3)	9550(3)	6483(2)	73(1)
C(33)	2893(3)	10008(2)	5911(2)	45(1)
C(34)	496(2)	8195(2)	6154(1)	22(1)
C(35)	1725(2)	6659(2)	6853(1)	33(1)

C(36)	2992(7)	5536(5)	4631(6)	15(1)
C(37)	3810(8)	5720(5)	5391(4)	15(1)
C(38)	4976(6)	6523(5)	5461(4)	16(1)
C(39)	4890(6)	6843(4)	4757(6)	16(1)
C(40)	3663(9)	6232(7)	4238(3)	16(1)
C(41)	1684(4)	4698(3)	4258(3)	31(1)
C(42)	3571(5)	5088(3)	5986(3)	29(1)
C(43)	6199(4)	6842(3)	6130(3)	28(1)
C(44)	5920(4)	7648(4)	4550(3)	33(1)
C(36B)	3104(7)	5540(6)	4953(5)	17(1)
C(37B)	4331(9)	6129(6)	5486(3)	16(1)
C(38B)	5054(6)	6838(4)	5120(6)	16(1)
C(39B)	4294(9)	6671(5)	4343(4)	16(1)
C(40B)	3093(7)	5870(5)	4243(3)	16(1)
C(41B)	2039(4)	4687(3)	5080(3)	27(1)
C(42B)	4840(4)	5902(3)	6252(2)	26(1)
C(43B)	6452(4)	7532(3)	5444(3)	28(1)
C(44B)	4720(4)	7215(3)	3727(2)	23(1)
C(45)	518(2)	8349(2)	4205(1)	25(1)
C(46)	-944(2)	7689(2)	3930(2)	37(1)
C(47)	-1336(2)	6903(2)	3102(2)	38(1)
C(48)	-347(2)	6288(2)	2935(1)	33(1)
C(49)	1124(2)	6947(2)	3207(1)	23(1)
C(50)	1529(2)	7746(2)	2728(1)	26(1)
C(51)	922(2)	8658(2)	2850(1)	28(1)
C(52)	931(3)	9143(2)	3726(1)	33(1)

Table 13.38. Anisotropic displacement parameters ($Å^2 x\ 10^3$) for **30**. The anisotropic displacement factor exponent takes the form: $-2\pi^2[\ h^2\ a^{*2}U^{11} + ...\ + 2\ h\ k\ a^*\ b^*\ U^{12}\ ]$

	U^{11}	U^{22}	U^{33}	U^{23}	U^{13}	U^{12}
Sc(1)	16(1)	15(1)	15(1)	5(1)	1(1)	5(1)
B(1)	25(1)	16(1)	14(1)	4(1)	1(1)	7(1)
C(1)	24(1)	32(1)	18(1)	11(1)	5(1)	10(1)
C(2)	20(1)	20(1)	13(1)	7(1)	1(1)	5(1)
C(3)	20(1)	20(1)	13(1)	5(1)	-2(1)	3(1)
C(4)	32(1)	20(1)	15(1)	4(1)	-2(1)	7(1)
C(5)	37(1)	32(1)	15(1)	7(1)	5(1)	18(1)
C(6)	31(1)	53(2)	40(1)	26(1)	18(1)	14(1)
C(7)	26(1)	21(1)	20(1)	9(1)	2(1)	5(1)
C(8)	18(1)	28(1)	20(1)	8(1)	-1(1)	1(1)
C(9)	45(1)	20(1)	31(1)	4(1)	-9(1)	4(1)
C(19)	22(1)	20(1)	15(1)	5(1)	3(1)	7(1)
C(20)	28(1)	29(1)	28(1)	3(1)	10(1)	6(1)
C(21)	45(1)	27(1)	29(1)	3(1)	20(1)	-1(1)
C(22)	69(2)	24(1)	18(1)	9(1)	13(1)	7(1)
C(23)	45(1)	25(1)	16(1)	6(1)	1(1)	17(1)
C(24)	32(1)	31(1)	17(1)	2(1)	-2(1)	8(1)
C(25)	30(1)	19(1)	22(1)	1(1)	6(1)	3(1)
C(26)	30(1)	18(1)	23(1)	6(1)	6(1)	10(1)
Sc(2)	14(1)	15(1)	17(1)	-1(1)	3(1)	3(1)
B(2)	16(1)	17(1)	23(1)	4(1)	4(1)	4(1)
C(27)	19(1)	38(1)	35(1)	-23(1)	7(1)	-4(1)
C(28)	28(1)	18(1)	29(1)	-8(1)	14(1)	0(1)
C(29)	19(1)	16(1)	16(1)	0(1)	5(1)	5(1)
C(30)	25(1)	26(1)	14(1)	-1(1)	1(1)	12(1)
C(31)	24(1)	50(1)	19(1)	-15(1)	-7(1)	18(1)
C(32)	26(1)	74(2)	68(2)	-48(2)	21(1)	-21(1)

C(33)	69(2)	14(1)	47(1)	-1(1)	37(1)	0(1)
C(34)	20(1)	26(1)	22(1)	9(1)	8(1)	10(1)
C(35)	54(1)	35(1)	23(1)	14(1)	13(1)	25(1)
C(36)	14(2)	12(2)	19(3)	6(3)	2(3)	3(2)
C(37)	18(3)	13(3)	18(3)	7(2)	6(3)	8(2)
C(38)	15(3)	15(2)	20(3)	6(2)	5(2)	5(2)
C(39)	14(3)	17(2)	17(3)	4(3)	2(3)	5(2)
C(40)	20(3)	18(3)	12(2)	5(3)	3(3)	10(2)
C(41)	23(2)	19(2)	40(2)	-1(2)	0(2)	1(2)
C(42)	46(3)	23(2)	30(2)	16(2)	18(2)	20(2)
C(43)	23(2)	29(2)	29(2)	1(2)	-2(2)	14(2)
C(44)	26(2)	33(2)	47(3)	19(2)	20(2)	10(2)
C(36B)	27(4)	14(2)	16(3)	10(3)	7(4)	11(2)
C(37B)	20(3)	15(3)	15(2)	7(3)	4(3)	7(2)
C(38B)	15(2)	16(2)	15(3)	2(3)	1(3)	6(2)
C(39B)	17(3)	11(2)	19(3)	2(2)	6(3)	5(2)
C(40B)	18(3)	10(2)	15(3)	0(2)	2(2)	3(2)
C(41B)	35(2)	16(2)	30(2)	7(2)	11(2)	5(2)
C(42B)	34(2)	31(2)	20(2)	9(2)	2(2)	20(2)
C(43B)	17(2)	31(2)	33(2)	0(2)	2(2)	8(2)
C(44B)	27(2)	22(2)	25(2)	11(2)	13(2)	10(2)
C(45)	34(1)	23(1)	28(1)	13(1)	15(1)	15(1)
C(46)	27(1)	59(2)	50(1)	40(1)	20(1)	27(1)
C(47)	14(1)	53(1)	51(1)	37(1)	1(1)	3(1)
C(48)	28(1)	22(1)	37(1)	12(1)	-12(1)	-3(1)
C(49)	20(1)	21(1)	25(1)	1(1)	-3(1)	8(1)
C(50)	22(1)	32(1)	20(1)	0(1)	5(1)	4(1)
C(51)	37(1)	22(1)	25(1)	9(1)	11(1)	2(1)
C(52)	57(2)	20(1)	30(1)	10(1)	20(1)	15(1)

Table 13.39. Hydrogen coordinates (x 10^4) and isotropic displacement parameters ($Å^2$x 10^{3}) for **30**.

	x	y	z	U(eq)
H(1)	7760(20)	8387(18)	10236(14)	31(6)
H(2)	6360(20)	7217(17)	10158(13)	25(6)
H(5A)	7849	5931	7760	32
H(6A)	8773	8558	7675	56
H(6B)	9575	7779	7902	56
H(6C)	9484	8737	8585	56
H(7A)	7074	9292	8200	34
H(7B)	7188	9390	9132	34
H(7C)	5765	9002	8533	34
H(8A)	3683	6316	8230	36
H(8B)	4125	7575	8496	36
H(8C)	4338	6945	9146	36
H(9A)	4458	4798	7672	53
H(9B)	5114	4838	8564	53
H(9C)	5783	4465	7844	53
H(14A)	9231	7410	11176	25
H(15A)	11745	8287	10662	102
H(15B)	10591	8831	10551	102
H(15C)	11189	8423	9806	102
H(16A)	11094	5956	8967	96
H(16B)	10747	6946	8743	96
H(16C)	9805	5781	8295	96
H(17A)	8731	4061	9143	58
H(17B)	8011	4455	8454	58
H(17C)	7226	4063	9083	58
H(18A)	7590	4800	10842	50

H(18B)	6436	4936	10215	50
H(18C)	7035	5788	11067	50
H(14B)	8727	6925	11194	23
H(15D)	11660	8328	10906	35
H(15E)	10465	8780	11092	35
H(15F)	10877	8741	10254	35
H(16D)	11551	6563	9217	45
H(16E)	11104	7554	9069	45
H(16F)	10347	6400	8491	45
H(17D)	9203	4258	8974	55
H(17E)	8741	4784	8295	55
H(17F)	7686	4222	8730	55
H(18D)	7338	4225	10153	70
H(18E)	6304	4803	9855	70
H(18F)	7038	5136	10778	70
H(19A)	5559	8751	9815	23
H(20A)	4063	8990	10682	35
H(20B)	4053	7794	10374	35
H(21A)	5095	9149	11954	42
H(21B)	4018	8017	11687	42
H(22A)	5575	7157	11546	45
H(22B)	6170	8050	12374	45
H(23A)	7804	7897	11615	34
H(24A)	8122	9614	12494	34
H(24B)	8835	9648	11767	34
H(25A)	7937	10996	11849	30
H(25B)	6590	10332	11999	30
H(26A)	7340	10213	10509	28
H(26B)	6040	10459	10729	28
H(3)	1260(20)	6985(18)	4576(13)	26(6)
H(4)	2630(20)	8031(18)	4431(14)	27(6)
H(31A)	4541	7691	7035	42
H(32A)	5685	10245	6849	109
H(32B)	5597	9623	5947	109
H(32C)	6217	9238	6673	109
H(33A)	3435	10639	6333	67
H(33B)	1971	10017	5812	67
H(33C)	3216	9996	5420	67
H(34A)	221	8188	6658	32
H(34B)	-31	7551	5740	32
H(34C)	360	8808	5990	32
H(35A)	1450	6928	7343	50
H(35B)	2280	6207	6950	50
H(35C)	940	6251	6427	50
H(40A)	3409	6182	3657	19
H(41A)	1842	4039	4000	46
H(41B)	1163	4924	3859	46
H(41C)	1199	4587	4674	46
H(42A)	4006	4533	5901	43
H(42B)	2618	4770	5912	43
H(42C)	3933	5553	6530	43
H(43A)	6573	6252	6107	42
H(43B)	5961	7034	6646	42
H(43C)	6855	7447	6070	42
H(44A)	6557	7320	4340	49
H(44B)	6381	8227	5030	49
H(44C)	5492	7921	4144	49
H(40B)	2408	5531	3733	19
H(41D)	2335	4059	5058	40
H(41E)	1237	4515	4662	40
H(41F)	1848	4928	5604	40
H(42D)	5147	5277	6133	40

H(42E)	4129	5775	6539	40
H(42F)	5576	6505	6586	40
H(43D)	7061	7138	5283	43
H(43E)	6628	7766	6028	43
H(43F)	6579	8146	5231	43
H(44D)	5476	7012	3567	34
H(44E)	4974	7979	3957	34
H(44F)	3985	7005	3259	34
H(45A)	684	8749	4779	30
H(46A)	-1157	7297	4325	45
H(46B)	-1495	8175	3933	45
H(47A)	-1435	7288	2693	45
H(47B)	-2208	6397	3045	45
H(48A)	-543	5950	2354	39
H(48B)	-484	5720	3206	39
H(49A)	1678	6455	3146	28
H(50A)	2504	8042	2876	32
H(50B)	1278	7365	2153	32
H(51A)	-2	8402	2535	34
H(51B)	1416	9213	2640	34
H(52A)	329	9589	3740	40
H(52B)	1833	9608	3998	40

13.14. Crystallographic Data for $(C_5Me_4H)_2Sc(\mu\text{-}O)BC_8H_{14}$, 31

X-ray Data Collection, Structure Solution and Refinement for **31**.

A colorless crystal of approximate dimensions 0.10 x 0.16 x 0.25 mm was mounted on a glass fiber and transferred to a Bruker SMART APEX II diffractometer. The APEX2[1] program package was used to determine the unit-cell parameters and for data collection (25 sec/frame scan time for a sphere of diffraction data). The raw frame data was processed using SAINT[2] and SADABS[3] to yield the reflection data file. Subsequent calculations were carried out using the SHELXTL[4] program. The diffraction symmetry was 2/*m* and the systematic absences were consistent with the monoclinic space group $P2_1/c$ that was later determined to be correct.

The structure was solved by direct methods and refined on F^2 by full-matrix least-squares techniques. The analytical scattering factors[5] for neutral atoms were used throughout the analysis. Hydrogen atoms, with the exception of those associated with C(16), were located from a difference-Fourier map and refined (x,y,z and U_{iso}). The hydrogen atoms attached to C(16) were included using a riding model.

At convergence, wR2 = 0.0974 and Goof = 1.028 for 411 variables refined against 5346 data (0.78Å), R1 = 0.0355 for those 4386 data with I > 2.0σ(I).

References

1. APEX2 Version 2.2-0,. Bruker AXS, Inc.; Madison, WI 2007.
2. SAINT Version 7.46a, Bruker AXS, Inc.; Madison, WI 2007.
3. Sheldrick, G. M. SADABS, Version 2008/1, Bruker AXS, Inc.; Madison, WI 2008.
4. Sheldrick, G. M. SHELXTL, Version 2008/3, Bruker AXS, Inc.; Madison, WI 2008.
5. International Tables for X-Ray Crystallography 1992, Vol. C., Dordrecht: Kluwer Academic Publishers.

Table 13.40. Atomic coordinates (x 10^4) and equivalent isotropic displacement parameters ($Å^2$x 10^3) for **31**. U(eq) is defined as one third of the trace of the orthogonalized U^{ij} tensor.

	x	y	z	U(eq)
Sc(1)	2877(1)	744(1)	1848(1)	17(1)
O(1)	2430(1)	-97(1)	2723(1)	26(1)
B(1)	2127(1)	-690(1)	3272(2)	23(1)
C(1)	4291(1)	358(1)	1001(2)	23(1)
C(2)	3583(1)	-235(1)	686(2)	22(1)
C(3)	2688(1)	31(1)	-258(2)	22(1)
C(4)	2848(1)	789(1)	-547(2)	22(1)
C(5)	3838(1)	982(1)	226(2)	23(1)
C(6)	5334(1)	324(1)	1981(2)	33(1)
C(7)	3765(2)	-1018(1)	1198(2)	35(1)
C(8)	1746(2)	-415(1)	-873(2)	34(1)
C(9)	2127(2)	1278(1)	-1558(2)	33(1)
C(10)	3552(1)	1935(1)	2899(2)	26(1)
C(11)	3186(1)	1551(1)	3868(2)	26(1)
C(12)	2118(1)	1490(1)	3354(2)	25(1)
C(13)	1828(1)	1821(1)	2052(2)	24(1)
C(14)	2715(1)	2100(1)	1789(2)	25(1)
C(15)	4632(2)	2177(1)	3076(3)	42(1)
C(16)	3815(2)	1242(1)	5207(2)	43(1)
C(17)	1416(2)	1155(1)	4073(2)	42(1)
C(18)	767(1)	1886(1)	1133(2)	39(1)
C(19)	2804(1)	-1143(1)	4532(2)	27(1)
C(20)	2314(1)	-1035(1)	5696(2)	33(1)
C(21)	1186(1)	-1251(1)	5353(2)	34(1)
C(22)	536(1)	-970(1)	3976(2)	31(1)
C(23)	1020(1)	-1041(1)	2791(2)	26(1)
C(24)	1125(1)	-1852(1)	2350(2)	31(1)
C(25)	1848(1)	-2342(1)	3419(2)	34(1)
C(26)	2864(1)	-1968(1)	4129(2)	33(1)

Table 13.41. Anisotropic displacement parameters ($Å^2$x 10^3) for **31**. The anisotropic displacement factor exponent takes the form: $-2\pi^2[h^2 a^{*2}U^{11} + ... + 2 h k a^* b^* U^{12}]$

	U^{11}	U^{22}	U^{33}	U^{23}	U^{13}	U^{12}
Sc(1)	18(1)	15(1)	18(1)	-1(1)	7(1)	0(1)
O(1)	33(1)	20(1)	29(1)	0(1)	16(1)	-2(1)
B(1)	26(1)	20(1)	25(1)	-2(1)	11(1)	-1(1)
C(1)	21(1)	30(1)	20(1)	-2(1)	9(1)	5(1)
C(2)	28(1)	22(1)	21(1)	0(1)	12(1)	7(1)
C(3)	25(1)	23(1)	20(1)	-4(1)	9(1)	0(1)
C(4)	24(1)	25(1)	19(1)	1(1)	9(1)	3(1)
C(5)	24(1)	24(1)	23(1)	0(1)	12(1)	-2(1)
C(6)	24(1)	48(1)	25(1)	-4(1)	5(1)	8(1)
C(7)	49(1)	22(1)	37(1)	2(1)	18(1)	11(1)
C(8)	36(1)	34(1)	31(1)	-10(1)	8(1)	-10(1)
C(9)	36(1)	36(1)	24(1)	9(1)	6(1)	8(1)
C(10)	24(1)	17(1)	36(1)	-8(1)	6(1)	0(1)
C(11)	31(1)	21(1)	24(1)	-8(1)	2(1)	4(1)
C(12)	29(1)	21(1)	26(1)	-6(1)	12(1)	3(1)
C(13)	23(1)	19(1)	28(1)	-5(1)	6(1)	4(1)
C(14)	29(1)	16(1)	30(1)	-1(1)	9(1)	3(1)
C(15)	28(1)	30(1)	66(1)	-16(1)	10(1)	-10(1)
C(16)	56(1)	39(1)	26(1)	-8(1)	-3(1)	16(1)

C(17)	52(1)	37(1)	49(1)	-7(1)	35(1)	-1(1)
C(18)	25(1)	42(1)	45(1)	-8(1)	2(1)	11(1)
C(19)	22(1)	28(1)	29(1)	3(1)	4(1)	-7(1)
C(20)	28(1)	44(1)	23(1)	2(1)	1(1)	-11(1)
C(21)	28(1)	50(1)	24(1)	2(1)	7(1)	-11(1)
C(22)	23(1)	40(1)	30(1)	3(1)	7(1)	-5(1)
C(23)	26(1)	29(1)	21(1)	6(1)	4(1)	-2(1)
C(24)	34(1)	31(1)	24(1)	1(1)	4(1)	-9(1)
C(25)	40(1)	23(1)	36(1)	3(1)	5(1)	-4(1)
C(26)	31(1)	26(1)	41(1)	8(1)	6(1)	1(1)

Table 13.42. Hydrogen coordinates (x 10^4) and isotropic displacement parameters ($Å^2$x 10^{3}) for **31**.

	x	y	z	U(eq)
H(16A)	4535	1330	5299	65
H(16B)	3691	705	5243	65
H(16C)	3625	1492	5948	65
H(5A)	4170(13)	1465(10)	248(17)	25(4)
H(6A)	5721(17)	-87(14)	1760(20)	57(7)
H(6B)	5321(16)	228(13)	2900(20)	54(6)
H(6C)	5680(20)	774(15)	1990(30)	67(8)
H(7A)	4010(19)	-1316(14)	590(30)	66(7)
H(7B)	3150(20)	-1240(15)	1280(30)	65(8)
H(7C)	4209(19)	-1015(14)	2070(30)	58(7)
H(8A)	1890(20)	-789(16)	-1480(30)	74(8)
H(8B)	1200(20)	-112(17)	-1450(30)	85(9)
H(8C)	1490(20)	-699(16)	-210(30)	83(9)
H(9A)	2119(16)	1152(12)	-2440(20)	47(6)
H(9B)	2339(16)	1774(14)	-1430(20)	46(6)
H(9C)	1416(17)	1258(12)	-1510(20)	46(6)
H(14A)	2731(14)	2340(10)	950(19)	29(5)
H(15A)	4800(20)	2608(16)	3600(30)	73(8)
H(15B)	4760(20)	2299(15)	2260(30)	68(8)
H(15C)	5100(20)	1777(16)	3460(30)	68(8)
H(17A)	1157(19)	1499(15)	4560(30)	62(7)
H(17B)	1720(20)	768(16)	4690(30)	72(8)
H(17C)	830(20)	925(15)	3460(30)	70(8)
H(18A)	360(20)	2230(17)	1450(30)	83(9)
H(18B)	440(20)	1456(19)	1040(30)	92(11)
H(18C)	770(20)	2065(16)	230(30)	81(9)
H(19A)	3521(14)	-936(10)	4824(18)	29(5)
H(20A)	2681(16)	-1325(12)	6470(20)	42(6)
H(20B)	2392(15)	-498(12)	5950(20)	38(5)
H(21A)	1133(14)	-1817(12)	5383(19)	32(5)
H(21B)	889(16)	-1039(12)	6050(20)	44(6)
H(22A)	367(15)	-432(12)	4090(20)	40(5)
H(22B)	-120(15)	-1241(10)	3742(19)	32(5)
H(23A)	535(14)	-775(10)	1981(19)	28(5)
H(24A)	434(15)	-2099(11)	2052(19)	36(5)
H(24B)	1364(14)	-1840(11)	1527(19)	33(5)
H(25A)	1980(16)	-2805(13)	3000(20)	47(6)
H(25B)	1468(14)	-2496(11)	4110(19)	35(5)
H(26A)	3291(16)	-1994(12)	3530(20)	41(6)
H(26B)	3204(16)	-2265(12)	4920(20)	47(6)

13.15. Crystallographic Data for $(C_5Me_5)_2Sc(\eta^3\text{-}C_3H_5)$, 32

Table 13.43. Atomic coordinates (x 10^4) and equivalent isotropic displacement parameters ($Å^2$x 10^3) for **32**. U(eq) is defined as one third of the trace of the orthogonalized U^{ij} tensor.

	x	y	z	U(eq)
Sc(1)	0	1468(1)	3647(1)	17(1)
C(1)	450(5)	2288(7)	2877(2)	43(2)
C(2)	771(4)	3270(7)	3169(2)	46(2)
C(3)	0	4010(9)	3371(3)	65(4)
C(4)	1095(5)	1439(8)	2562(2)	49(2)
C(5)	1766(5)	3744(9)	3257(3)	61(2)
C(6)	0	5380(13)	3611(4)	90(5)
C(7)	0	155(9)	4382(2)	86(6)
C(8)	778(5)	1096(10)	4376(2)	57(2)
C(9)	455(4)	2510(7)	4382(2)	40(1)
C(10)	0	-1416(13)	4460(4)	250(20)
C(11)	1760(8)	620(20)	4401(3)	153(8)
C(12)	1089(7)	3825(11)	4461(3)	80(3)
C(13)	0	-853(10)	3242(5)	62(3)
C(14)	853(5)	-700(6)	3406(2)	45(2)

Table 13.44. Anisotropic displacement parameters ($Å^2$x 10^3) for **32**. The anisotropic displacement factor exponent takes the form: $-2\pi^2[\, h^2\, a^{*2}U^{11} + \ldots + 2\, h\, k\, a^*\, b^*\, U^{12}\,]$

	U^{11}	U^{22}	U^{33}	U^{23}	U^{13}	U^{12}
Sc(1)	16(1)	17(1)	18(1)	-1(1)	0	0
C(1)	64(4)	36(3)	29(3)	11(2)	12(3)	10(3)
C(2)	23(3)	55(4)	60(4)	39(3)	-8(2)	-12(3)
C(3)	163(13)	13(3)	21(4)	1(3)	0	0
C(4)	51(4)	54(4)	41(3)	6(3)	11(3)	5(3)
C(5)	43(4)	78(5)	63(4)	14(4)	-8(3)	-26(4)
C(6)	174(17)	37(6)	57(7)	1(5)	0	0
C(7)	234(18)	16(4)	9(4)	2(3)	0	0
C(8)	50(4)	100(6)	21(3)	0(3)	-6(2)	40(4)
C(9)	46(3)	50(3)	24(2)	-7(2)	-6(2)	-9(3)
C(10)	690(70)	26(6)	30(6)	5(5)	0	0
C(11)	88(7)	320(20)	49(5)	-43(9)	-26(5)	126(11)
C(12)	96(7)	90(6)	54(4)	-8(4)	-10(4)	-64(6)
C(13)	55(6)	22(4)	109(9)	-20(5)	0	0
C(14)	58(4)	28(3)	50(4)	-11(2)	1(3)	14(3)

13.16. Crystallographic Data for $(\eta^5\text{-}C_5Me_4H)_2Sc(\eta^1\text{-}C_5Me_4H)$, 35

X-ray Data Collection, Structure Solution and Refinement for **35**.

A yellow crystal of approximate dimensions 0.16 x 0.17 x 0.31 mm was mounted on a glass fiber and transferred to a Bruker SMART APEX II diffractometer. The APEX2[1] program package was used to determine the unit-cell parameters and for data collection (25 sec/frame scan time for a sphere of diffraction data). The raw frame data was processed using SAINT[2] and SADABS[3] to yield the reflection data file. Subsequent calculations were carried out using the SHELXTL[4] program. The diffraction symmetry was 2/*m* and the systematic

absences were consistent with the monoclinic space group $P2_1/c$ that was later determined to be correct.

The structure was solved by direct methods and refined on F^2 by full-matrix least-squares techniques. The analytical scattering factors[5] for neutral atoms were used throughout the analysis. Hydrogen atoms were located from a difference-Fourier map and refined (x,y,z and U_{iso}). There were two molecules of the formula unit present (Z = 8).

At convergence, wR2 = 0.1025 and Goof = 1.017 for 817 variables refined against 10523 data (0.77Å), R1 = 0.0368 for those 8144 data with I > 2.0σ(I).

References

1. APEX2 Version 2.2-0,. Bruker AXS, Inc.; Madison, WI 2007.
2. SAINT Version 7.46a, Bruker AXS, Inc.; Madison, WI 2007.
3. Sheldrick, G. M. SADABS, Version 2008/1, Bruker AXS, Inc.; Madison, WI 2008.
4. Sheldrick, G. M. SHELXTL, Version 2008/4, Bruker AXS, Inc.; Madison, WI 2008.
5. International Tables for X-Ray Crystallography 1992, Vol. C., Dordrecht: Kluwer Academic Publishers.

Table 13.45. Atomic coordinates (x 10^4) and equivalent isotropic displacement parameters (Å^{2}x 10^3) for **35**. U(eq) is defined as one third of the trace of the orthogonalized U^{ij} tensor.

	x	y	z	U(eq)
Sc(1)	89(1)	3891(1)	7495(1)	17(1)
C(1)	26(1)	2529(1)	7263(1)	23(1)
C(2)	719(1)	2307(1)	8036(1)	24(1)
C(3)	1368(1)	2006(1)	7822(1)	23(1)
C(4)	1093(1)	2013(1)	6925(1)	23(1)
C(5)	278(1)	2318(1)	6579(1)	23(1)
C(6)	716(1)	2406(1)	8904(1)	37(1)
C(7)	2246(1)	1762(1)	8408(1)	37(1)
C(8)	1644(1)	1757(1)	6465(1)	36(1)
C(9)	-288(1)	2374(1)	5656(1)	35(1)
C(10)	-1303(1)	4529(1)	6707(1)	22(1)
C(11)	-1533(1)	3772(1)	6861(1)	21(1)
C(12)	-1276(1)	3677(1)	7746(1)	21(1)
C(13)	-879(1)	4377(1)	8142(1)	21(1)
C(14)	-909(1)	4905(1)	7497(1)	22(1)
C(15)	-1526(1)	4892(1)	5852(1)	34(1)
C(16)	-2052(1)	3204(1)	6197(1)	31(1)
C(17)	-1490(1)	2991(1)	8168(1)	29(1)
C(18)	-527(1)	4550(1)	9071(1)	31(1)
C(19)	1586(1)	4253(1)	8368(1)	25(1)
C(20)	1159(1)	4971(1)	8095(1)	25(1)
C(21)	880(1)	5012(1)	7205(1)	25(1)
C(22)	1133(1)	4315(1)	6922(1)	25(1)
C(23)	1567(1)	3854(1)	7640(1)	24(1)
C(24)	2045(1)	4008(1)	9271(1)	34(1)
C(25)	1129(1)	5624(1)	8666(1)	33(1)
C(26)	496(1)	5711(1)	6673(1)	34(1)
C(27)	1001(1)	4119(1)	6030(1)	35(1)
Sc(2)	4943(1)	3764(1)	7497(1)	16(1)
C(28)	4875(1)	5140(1)	7398(1)	21(1)
C(29)	4704(1)	5310(1)	8141(1)	22(1)
C(30)	3892(1)	5627(1)	7877(1)	23(1)
C(31)	3546(1)	5685(1)	6976(1)	23(1)
C(32)	4143(1)	5401(1)	6680(1)	22(1)

C(33)	5323(1)	5183(1)	9032(1)	32(1)
C(34)	3400(1)	5843(1)	8412(1)	36(1)
C(35)	2666(1)	5983(1)	6460(1)	35(1)
C(36)	4081(1)	5396(1)	5784(1)	31(1)
C(37)	5879(1)	3199(1)	6843(1)	24(1)
C(38)	6238(1)	3943(1)	7117(1)	22(1)
C(39)	6548(1)	3961(1)	8008(1)	22(1)
C(40)	6385(1)	3229(1)	8297(1)	24(1)
C(41)	5980(1)	2761(1)	7575(1)	23(1)
C(42)	5515(1)	2914(1)	5945(1)	35(1)
C(43)	6367(1)	4568(1)	6568(1)	33(1)
C(44)	7066(1)	4611(1)	8549(1)	34(1)
C(45)	6677(1)	2972(1)	9201(1)	38(1)
C(46)	3929(1)	3370(1)	8127(1)	22(1)
C(47)	4193(1)	2664(1)	7877(1)	21(1)
C(48)	3904(1)	2660(1)	6986(1)	22(1)
C(49)	3462(1)	3367(1)	6680(1)	23(1)
C(50)	3479(1)	3801(1)	7386(1)	22(1)
C(51)	4048(1)	3590(1)	9009(1)	31(1)
C(52)	4602(1)	1996(1)	8453(1)	30(1)
C(53)	3938(1)	1981(1)	6453(1)	30(1)
C(54)	3011(1)	3586(1)	5771(1)	34(1)

Table 13.46. Anisotropic displacement parameters ($Å^2 x 10^3$) for **35**. The anisotropic displacement factor exponent takes the form: $-2\pi^2[h^2 a^{*2} U^{11} + ... + 2 h k a^* b^* U^{12}]$

	U^{11}	U^{22}	U^{33}	U^{23}	U^{13}	U^{12}
Sc(1)	17(1)	15(1)	20(1)	-2(1)	8(1)	-1(1)
C(1)	23(1)	17(1)	34(1)	-1(1)	15(1)	-1(1)
C(2)	30(1)	18(1)	27(1)	-2(1)	15(1)	-3(1)
C(3)	24(1)	17(1)	28(1)	1(1)	11(1)	0(1)
C(4)	28(1)	16(1)	30(1)	-2(1)	17(1)	-2(1)
C(5)	28(1)	17(1)	26(1)	1(1)	11(1)	-4(1)
C(6)	42(1)	43(1)	33(1)	-12(1)	22(1)	-12(1)
C(7)	30(1)	36(1)	41(1)	6(1)	10(1)	6(1)
C(8)	41(1)	33(1)	46(1)	-7(1)	29(1)	-1(1)
C(9)	39(1)	35(1)	29(1)	4(1)	10(1)	-6(1)
C(10)	20(1)	22(1)	22(1)	2(1)	7(1)	3(1)
C(11)	15(1)	21(1)	25(1)	-1(1)	6(1)	2(1)
C(12)	16(1)	22(1)	26(1)	1(1)	10(1)	3(1)
C(13)	17(1)	25(1)	23(1)	-2(1)	9(1)	4(1)
C(14)	19(1)	19(1)	28(1)	-2(1)	9(1)	2(1)
C(15)	36(1)	35(1)	27(1)	8(1)	8(1)	2(1)
C(16)	20(1)	30(1)	34(1)	-9(1)	2(1)	-1(1)
C(17)	26(1)	28(1)	39(1)	8(1)	19(1)	3(1)
C(18)	28(1)	43(1)	23(1)	-6(1)	9(1)	5(1)
C(19)	17(1)	24(1)	34(1)	-5(1)	10(1)	-5(1)
C(20)	20(1)	20(1)	37(1)	-8(1)	14(1)	-5(1)
C(21)	24(1)	18(1)	37(1)	-2(1)	16(1)	-5(1)
C(22)	26(1)	20(1)	37(1)	-4(1)	20(1)	-6(1)
C(23)	19(1)	18(1)	38(1)	-4(1)	16(1)	-2(1)
C(24)	24(1)	37(1)	36(1)	-4(1)	4(1)	-2(1)
C(25)	30(1)	27(1)	43(1)	-15(1)	16(1)	-6(1)
C(26)	36(1)	21(1)	49(1)	5(1)	23(1)	-2(1)
C(27)	48(1)	30(1)	38(1)	-4(1)	29(1)	-7(1)
Sc(2)	16(1)	14(1)	19(1)	0(1)	8(1)	0(1)
C(28)	22(1)	15(1)	28(1)	0(1)	12(1)	0(1)
C(29)	28(1)	16(1)	24(1)	0(1)	11(1)	-5(1)

C(30)	27(1)	15(1)	31(1)	-5(1)	16(1)	-5(1)
C(31)	23(1)	14(1)	31(1)	-1(1)	10(1)	-2(1)
C(32)	26(1)	15(1)	25(1)	-1(1)	11(1)	-4(1)
C(33)	35(1)	33(1)	27(1)	6(1)	10(1)	-7(1)
C(34)	39(1)	31(1)	48(1)	-8(1)	29(1)	-4(1)
C(35)	24(1)	28(1)	48(1)	-1(1)	9(1)	1(1)
C(36)	39(1)	30(1)	26(1)	-4(1)	13(1)	-8(1)
C(37)	22(1)	24(1)	27(1)	-3(1)	13(1)	3(1)
C(38)	18(1)	23(1)	29(1)	2(1)	13(1)	2(1)
C(39)	15(1)	22(1)	29(1)	-1(1)	8(1)	2(1)
C(40)	19(1)	26(1)	28(1)	4(1)	9(1)	7(1)
C(41)	22(1)	18(1)	33(1)	1(1)	14(1)	4(1)
C(42)	32(1)	47(1)	31(1)	-13(1)	16(1)	-2(1)
C(43)	35(1)	31(1)	42(1)	10(1)	27(1)	5(1)
C(44)	21(1)	31(1)	45(1)	-10(1)	7(1)	-2(1)
C(45)	36(1)	47(1)	29(1)	12(1)	10(1)	12(1)
C(46)	22(1)	17(1)	29(1)	-2(1)	14(1)	-4(1)
C(47)	22(1)	16(1)	28(1)	1(1)	12(1)	-2(1)
C(48)	21(1)	17(1)	30(1)	-4(1)	12(1)	-4(1)
C(49)	18(1)	20(1)	29(1)	-1(1)	7(1)	-4(1)
C(50)	18(1)	17(1)	32(1)	-1(1)	11(1)	-1(1)
C(51)	40(1)	28(1)	31(1)	-4(1)	22(1)	-5(1)
C(52)	33(1)	21(1)	41(1)	8(1)	19(1)	3(1)
C(53)	31(1)	23(1)	40(1)	-11(1)	17(1)	-6(1)
C(54)	26(1)	37(1)	29(1)	2(1)	2(1)	-5(1)

Table 13.47. Hydrogen coordinates (x 10^4) and isotropic displacement parameters ($Å^2$x 10^{3}) for **35**.

	x	y	z	U(eq)
H(1A)	-553(12)	2479(10)	7201(11)	34(5)
H(6A)	616(15)	2920(15)	9034(15)	67(7)
H(6B)	1232(15)	2296(13)	9323(14)	55(7)
H(6C)	284(13)	2118(12)	8973(12)	44(6)
H(7A)	2694(15)	2088(13)	8336(14)	60(7)
H(7B)	2363(15)	1247(14)	8327(14)	59(7)
H(7C)	2337(15)	1800(13)	8997(15)	66(7)
H(8A)	2138(15)	2071(14)	6597(14)	62(7)
H(8B)	1825(15)	1235(14)	6581(14)	61(7)
H(8C)	1351(14)	1797(13)	5841(15)	63(7)
H(9A)	-528(17)	2883(16)	5497(16)	81(8)
H(9B)	-7(17)	2292(15)	5299(16)	80(8)
H(9C)	-844(15)	2062(13)	5501(14)	62(7)
H(14A)	-712(10)	5455(10)	7590(10)	25(4)
H(15A)	-1261(14)	4640(13)	5501(14)	58(6)
H(15B)	-1308(13)	5413(13)	5881(12)	50(6)
H(15C)	-2170(14)	4890(12)	5525(13)	54(6)
H(16A)	-1998(17)	3261(15)	5702(17)	79(9)
H(16B)	-1920(15)	2684(15)	6347(14)	66(7)
H(16C)	-2598(17)	3268(14)	6079(15)	69(8)
H(17A)	-2053(14)	2999(12)	8053(13)	51(6)
H(17B)	-1168(13)	3008(11)	8772(13)	43(6)
H(17C)	-1365(14)	2491(14)	7952(13)	59(7)
H(18A)	-417(15)	5083(15)	9165(14)	65(7)
H(18B)	12(16)	4287(14)	9361(15)	67(7)
H(18C)	-883(18)	4413(16)	9315(17)	91(9)
H(23A)	1785(10)	3355(10)	7611(10)	25(4)
H(24A)	2572(13)	4331(11)	9530(12)	43(5)
H(24B)	1702(14)	4067(13)	9638(14)	56(6)

H(24C)	2188(13)	3458(13)	9295(12)	48(6)
H(25A)	1597(15)	5939(13)	8777(14)	62(7)
H(25B)	623(14)	5937(12)	8412(13)	52(6)
H(25C)	1127(13)	5415(12)	9218(14)	53(6)
H(26A)	82(12)	5972(11)	6856(12)	39(5)
H(26B)	188(12)	5576(11)	6069(13)	41(5)
H(26C)	928(14)	6066(12)	6695(12)	48(6)
H(27A)	410(13)	4201(11)	5639(12)	40(5)
H(27B)	1133(12)	3581(12)	5984(12)	43(6)
H(27C)	1358(14)	4439(13)	5824(14)	62(7)
H(28A)	5442(11)	5215(9)	7398(10)	22(4)
H(33A)	5523(13)	4631(13)	9133(13)	52(6)
H(33B)	5080(14)	5307(13)	9438(14)	58(7)
H(33C)	5838(13)	5486(11)	9161(12)	42(5)
H(34A)	3747(13)	5798(12)	9016(14)	48(6)
H(34B)	3220(14)	6373(13)	8306(13)	53(6)
H(34C)	2910(14)	5508(13)	8319(13)	56(6)
H(35A)	2560(14)	6020(13)	5821(15)	58(7)
H(35B)	2573(13)	6499(13)	6623(13)	54(6)
H(35C)	2234(14)	5656(13)	6483(13)	56(6)
H(36A)	4006(16)	4921(16)	5530(16)	80(8)
H(36B)	3640(20)	5704(18)	5412(19)	108(11)
H(36C)	4605(16)	5571(14)	5746(14)	64(7)
H(41A)	5792(11)	2219(10)	7572(10)	28(4)
H(42A)	4983(15)	3192(13)	5596(14)	62(7)
H(42B)	5922(17)	2903(14)	5717(15)	76(8)
H(42C)	5344(15)	2359(15)	5923(14)	68(7)
H(43A)	5972(15)	4540(13)	6018(15)	58(7)
H(43B)	6335(14)	5084(14)	6768(13)	58(6)
H(43C)	6909(16)	4542(13)	6564(14)	66(7)
H(44A)	6805(12)	5115(12)	8398(11)	41(5)
H(44B)	7587(16)	4664(13)	8498(14)	66(7)
H(44C)	7169(13)	4533(12)	9134(13)	45(6)
H(45A)	6493(18)	3305(17)	9536(17)	95(10)
H(45B)	6448(16)	2430(16)	9258(15)	76(8)
H(45C)	7317(15)	2957(12)	9477(13)	53(6)
H(50A)	3244(10)	4304(10)	7386(10)	22(4)
H(51A)	4633(14)	3533(12)	9392(13)	46(6)
H(51B)	3898(12)	4139(12)	9030(12)	37(5)
H(51C)	3664(13)	3278(12)	9201(13)	51(6)
H(52A)	4149(14)	1654(13)	8491(13)	58(6)
H(52B)	4935(12)	2163(11)	9022(13)	41(6)
H(52C)	4953(12)	1711(11)	8239(11)	37(5)
H(53A)	3497(13)	1654(12)	6390(12)	46(6)
H(53B)	4471(13)	1713(11)	6696(12)	38(5)
H(53C)	3889(13)	2148(12)	5894(13)	43(6)
H(54A)	2482(14)	3244(13)	5495(13)	55(6)
H(54B)	3389(14)	3544(12)	5438(13)	56(6)
H(54C)	2834(13)	4134(12)	5726(12)	42(5)

13.17. Crystallographic Data for $[(C_5Me_4H)_2ScSPh]_2$, 36

X-ray Data Collection, Structure Solution and Refinement for **36**.

A yellow crystal of approximate dimensions 0.23 x 0.23 x 0.24 mm was mounted on a glass fiber and transferred to a Bruker SMART APEX II diffractometer. The APEX2[1] program package was used to determine the unit-cell parameters and for data collection (20

sec/frame scan time for a sphere of diffraction data). The raw frame data was processed using SAINT[2] and SADABS[3] to yield the reflection data file. Subsequent calculations were carried out using the SHELXTL[4] program. The diffraction symmetry was 2/*m* and the systematic absences were consistent with the monoclinic space group $P2_1/n$ that was later determined to be correct.

The structure was solved by direct methods and refined on F^2 by full-matrix least-squares techniques. The analytical scattering factors[5] for neutral atoms were used throughout the analysis. The molecule was located about an inversion center. Hydrogen atoms were located from a difference-Fourier map and refined (x,y,z and U_{iso}). There was one molecule of toluene solvent present. The solvent was disordered about an inversion center and refined with anisotropic thermal parameters and the FLAT command[4]. The hydrogen atoms associated with the disordered solvent were not located or included in the refinement.

At convergence, wR2 = 0.0963 and Goof = 1.059for 404 variables refined against 5424 data (0.76Å), R1 = 0.0346 for those 4871 data with I > 2.0σ(I).

References

1. APEX2 Version 2.2-0, Bruker AXS, Inc.; Madison, WI 2007.
2. SAINT Version 7.46a, Bruker AXS, Inc.; Madison, WI 2007.
3. Sheldrick, G. M. SADABS, Version 2008/1, Bruker AXS, Inc.; Madison, WI 2008.
4. Sheldrick, G. M. SHELXTL, Version 2008/3, Bruker AXS, Inc.; Madison, WI 2008.
5. International Tables for X-Ray Crystallography 1992, Vol. C., Dordrecht: Kluwer Academic Publishers.

Table 13.48. Atomic coordinates (x 10^4) and equivalent isotropic displacement parameters ($Å^2$x 10^3) for **36**. U(eq) is defined as one third of the trace of the orthogonalized U^{ij} tensor.

	x	y	z	U(eq)
Sc(1)	9483(1)	102(1)	1304(1)	14(1)
S(1)	10175(1)	-952(1)	108(1)	18(1)
C(1)	11209(2)	-430(1)	2542(1)	18(1)
C(2)	12174(2)	-178(1)	1990(1)	18(1)
C(3)	12036(2)	724(1)	1872(1)	18(1)
C(4)	10982(2)	1033(1)	2350(1)	18(1)
C(5)	10496(2)	318(1)	2767(1)	18(1)
C(6)	11114(2)	-1298(1)	2934(1)	25(1)
C(7)	13314(2)	-728(1)	1679(1)	23(1)
C(8)	13019(2)	1257(1)	1422(1)	22(1)
C(9)	10604(2)	1953(1)	2500(1)	25(1)
C(10)	6952(2)	729(1)	1060(1)	20(1)
C(11)	7202(2)	535(1)	1911(1)	20(1)
C(12)	7323(2)	-372(1)	1998(1)	20(1)
C(13)	7140(2)	-740(1)	1203(1)	19(1)
C(14)	6918(2)	-58(1)	627(1)	19(1)
C(15)	6650(2)	1606(1)	692(1)	26(1)
C(16)	7074(2)	1163(1)	2590(1)	29(1)
C(17)	7346(2)	-864(1)	2787(1)	28(1)
C(18)	7021(2)	-1684(1)	1018(1)	25(1)
C(19)	10236(2)	-2082(1)	243(1)	18(1)
C(20)	10819(2)	-2441(1)	1001(1)	24(1)
C(21)	10828(2)	-3322(1)	1124(1)	27(1)
C(22)	10267(3)	-3865(1)	493(1)	39(1)
C(23)	9702(3)	-3519(1)	-270(1)	53(1)
C(24)	9690(2)	-2637(1)	-392(1)	35(1)
C(25)	4716(5)	5377(3)	4(2)	38(1)
C(26)	3680(3)	4890(2)	-120(1)	58(1)

C(27)	3726(5)	3938(3)	-238(2)	39(1)
C(28)	5286(5)	3644(2)	-137(2)	72(1)
C(29)	6303(5)	4125(4)	-3(2)	51(1)

Table 13.49. Anisotropic displacement parameters ($Å^2 x 10^3$) for **36**. The anisotropic displacement factor exponent takes the form: $-2\pi^2[h^2 a^{*2} U^{11} + ... + 2 h k a^* b^* U^{12}]$

	U^{11}	U^{22}	U^{33}	U^{23}	U^{13}	U^{12}
Sc(1)	13(1)	15(1)	13(1)	0(1)	2(1)	0(1)
S(1)	23(1)	15(1)	16(1)	0(1)	5(1)	0(1)
C(1)	18(1)	21(1)	15(1)	0(1)	-1(1)	0(1)
C(2)	15(1)	22(1)	16(1)	-2(1)	-2(1)	0(1)
C(3)	16(1)	20(1)	15(1)	-2(1)	-1(1)	-3(1)
C(4)	18(1)	20(1)	15(1)	-3(1)	-1(1)	-2(1)
C(5)	18(1)	23(1)	13(1)	-1(1)	1(1)	-1(1)
C(6)	30(1)	23(1)	22(1)	5(1)	4(1)	1(1)
C(7)	17(1)	26(1)	25(1)	-2(1)	3(1)	3(1)
C(8)	20(1)	25(1)	22(1)	-2(1)	4(1)	-6(1)
C(9)	30(1)	20(1)	24(1)	-4(1)	4(1)	0(1)
C(10)	13(1)	25(1)	22(1)	1(1)	5(1)	2(1)
C(11)	15(1)	26(1)	21(1)	-2(1)	6(1)	1(1)
C(12)	14(1)	27(1)	18(1)	3(1)	4(1)	-2(1)
C(13)	13(1)	24(1)	20(1)	1(1)	4(1)	-3(1)
C(14)	14(1)	25(1)	18(1)	1(1)	2(1)	-1(1)
C(15)	23(1)	25(1)	32(1)	5(1)	9(1)	6(1)
C(16)	25(1)	37(1)	25(1)	-9(1)	8(1)	4(1)
C(17)	25(1)	39(1)	19(1)	6(1)	5(1)	-5(1)
C(18)	25(1)	23(1)	28(1)	1(1)	7(1)	-6(1)
C(19)	18(1)	16(1)	21(1)	1(1)	6(1)	1(1)
C(20)	28(1)	24(1)	21(1)	2(1)	0(1)	-4(1)
C(21)	30(1)	25(1)	25(1)	8(1)	3(1)	1(1)
C(22)	63(1)	17(1)	36(1)	4(1)	1(1)	4(1)
C(23)	102(2)	20(1)	31(1)	-7(1)	-14(1)	3(1)
C(24)	62(1)	21(1)	20(1)	0(1)	-4(1)	4(1)
C(25)	67(3)	32(2)	17(2)	1(1)	11(2)	-1(2)
C(26)	70(2)	82(2)	24(1)	13(1)	17(1)	27(1)
C(27)	55(2)	41(2)	21(2)	4(1)	8(2)	-7(2)
C(28)	146(3)	40(1)	32(1)	6(1)	24(2)	24(2)
C(29)	46(2)	83(4)	23(2)	6(2)	6(2)	30(2)

Table 13.50. Hydrogen coordinates ($x 10^4$) and isotropic displacement parameters ($Å^2 x 10^3$) for **36**.

	x	y	z	U(eq)
H(5A)	9860(20)	329(12)	3159(11)	21(4)
H(6A)	12110(30)	-1587(14)	3014(14)	43(6)
H(6B)	10350(30)	-1676(15)	2628(14)	45(6)
H(6C)	10820(20)	-1250(15)	3457(15)	44(6)
H(7A)	14160(20)	-403(15)	1636(13)	36(5)
H(7B)	12990(20)	-952(14)	1136(14)	40(6)
H(7C)	13600(30)	-1208(15)	2042(15)	47(6)
H(8A)	13960(30)	997(14)	1417(14)	41(6)
H(8B)	13170(30)	1789(16)	1662(14)	47(6)
H(8C)	12660(20)	1331(14)	842(14)	40(6)
H(9A)	11430(30)	2337(15)	2410(14)	48(6)
H(9B)	10400(20)	2027(15)	3059(14)	45(6)

H(9C)	9720(20)	2160(14)	2154(13)	38(6)
H(14A)	6750(20)	-118(12)	42(13)	28(5)
H(15A)	5730(30)	1793(16)	786(16)	56(7)
H(15B)	6690(20)	1604(15)	114(15)	45(6)
H(15C)	7330(30)	2054(17)	969(16)	56(7)
H(16A)	6110(30)	1161(17)	2750(17)	63(8)
H(16B)	7250(30)	1740(20)	2427(19)	83(10)
H(16C)	7710(30)	1107(17)	3060(17)	59(8)
H(17A)	6370(30)	-933(15)	2938(15)	51(7)
H(17B)	7940(30)	-635(16)	3227(16)	51(7)
H(17C)	7690(30)	-1450(17)	2769(15)	49(7)
H(18A)	6080(30)	-1879(14)	1132(13)	42(6)
H(18B)	7810(20)	-2018(14)	1367(13)	37(6)
H(18C)	7050(20)	-1808(14)	429(14)	39(6)
H(20A)	11240(20)	-2081(13)	1443(13)	32(5)
H(21A)	11270(20)	-3538(13)	1646(13)	35(5)
H(22A)	10270(30)	-4447(17)	585(15)	52(7)
H(23A)	9350(30)	-3880(19)	-729(19)	73(9)
H(24A)	9290(30)	-2397(15)	-905(15)	49(6)

13.18. Crystallographic Data for $(C_5Me_4H)_2ScSePh$, 37

X-ray Data Collection, Structure Solution and Refinement for **37**.

A colorless crystal of approximate dimensions 0.31 x 0.33 x 0.45 mm was mounted on a glass fiber and transferred to a Bruker SMART APEX II diffractometer. The APEX2[1] program package was used to determine the unit-cell parameters and for data collection (15 sec/frame scan time for a sphere of diffraction data). The raw frame data was processed using SAINT[2] and SADABS[3] to yield the reflection data file. Subsequent calculations were carried out using the SHELXTL[4] program. The diffraction symmetry was *mmm* and the systematic absences were consistent with the orthorhombic space groups *Pnma* and $Pna2_1$. It was later determined that the molecule is best described using space group *Pnma* although the structure could also be solved and refined with similar results using the alternate noncentrosymmetric space group.

The structure was solved by direct methods and refined on F^2 by full-matrix least-squares techniques. The analytical scattering factors[5] for neutral atoms were used throughout the analysis. Hydrogen atoms were included using a riding model. The molecule was located on a mirror plane. There was one molecule of toluene solvent present. The solvent was also located on a mirror plane and was disordered. The solvent was included using multiple components, partial site-occupancy factors, equivalent isotropic thermal parameters and geometrical constraints.

Least squares analysis yielded wR2 = 0.1570 and Goof = 1.119 for 132 variables refined against 3069 data (0.78Å), R1 = 0.0469 for those 2806 data with $I > 2.0\sigma(I)$.

References

1. APEX2 Version 2.2-0, Bruker AXS, Inc.; Madison, WI 2007.
2. SAINT Version 7.46a, Bruker AXS, Inc.; Madison, WI 2007.
3. Sheldrick, G. M. SADABS, Version 2008/1, Bruker AXS, Inc.; Madison, WI 2008.
4. Sheldrick, G. M. SHELXTL, Version 2008/3, Bruker AXS, Inc.; Madison, WI 2008.
5. International Tables for X-Ray Crystallography 1992, Vol. C., Dordrecht: Kluwer Academic Publishers.

Table 13.51. Atomic coordinates (x 10^4) and equivalent isotropic displacement parameters ($Å^2$x 10^3) for **37**. U(eq) is defined as one third of the trace of the orthogonalized U^{ij} tensor.

	x	y	z	U(eq)
Sc(1)	4616(1)	2500	6147(1)	16(1)
Se(1)	3564(1)	2500	4974(1)	20(1)
C(1)	2650(5)	2500	6619(3)	22(1)
C(2)	3214(4)	3479(4)	6878(2)	22(1)
C(3)	4131(4)	3107(4)	7309(2)	21(1)
C(4)	2894(4)	4693(4)	6729(2)	29(1)
C(5)	4856(4)	3848(5)	7764(2)	30(1)
C(6)	6343(3)	3103(4)	5448(2)	18(1)
C(7)	6538(3)	3481(4)	6114(2)	20(1)
C(8)	6665(5)	2500	6519(3)	20(1)
C(9)	6327(4)	3838(4)	4834(2)	23(1)
C(10)	6684(5)	4696(4)	6332(3)	29(1)
C(11)	1877(6)	2500	5077(3)	20(1)
C(12)	1253(4)	3519(4)	5138(3)	28(1)
C(13)	45(4)	3515(5)	5280(3)	33(1)
C(14)	-569(6)	2500	5347(4)	36(2)
C(15)	9320(6)	7500	7044(4)	142(5)
C(16)	10290(6)	7500	6615(4)	142(5)
C(17)	11432(6)	7500	6875(4)	142(5)
C(18)	11605(6)	7500	7564(4)	142(5)
C(19)	10635(6)	7500	7992(4)	142(5)
C(20)	9492(6)	7500	7733(4)	142(5)
C(21)	8101(6)	7500	6799(4)	142(5)
C(22)	10263(6)	7500	7708(4)	142(5)
C(23)	10111(6)	7500	7018(4)	142(5)
C(24)	11094(6)	7500	6599(4)	142(5)
C(25)	12228(6)	7500	6870(4)	142(5)
C(26)	12381(6)	7500	7560(4)	142(5)
C(27)	11398(6)	7500	7979(4)	142(5)
C(28)	9200(6)	7500	8184(4)	142(5)

Table 13.52. Anisotropic displacement parameters ($Å^2$x 10^3) for **37**. The anisotropic displacement factor exponent takes the form: $-2\pi^2[h^2 a^{*2}U^{11} + ... + 2 h k a^* b^* U^{12}]$

	U^{11}	U^{22}	U^{33}	U^{23}	U^{13}	U^{12}
Sc(1)	12(1)	23(1)	14(1)	0	1(1)	0
Se(1)	13(1)	32(1)	16(1)	0	0(1)	0
C(1)	14(3)	38(3)	14(3)	0	4(2)	0
C(2)	19(2)	29(2)	17(2)	0(2)	6(2)	1(2)
C(3)	21(2)	28(2)	16(2)	0(2)	3(2)	-2(2)
C(4)	29(2)	30(2)	28(2)	4(2)	6(2)	4(2)
C(5)	29(2)	40(3)	20(2)	-7(2)	-1(2)	-4(2)
C(6)	11(2)	25(2)	19(2)	1(2)	2(1)	-1(2)
C(7)	13(2)	25(2)	21(2)	-2(2)	0(1)	-2(2)
C(8)	14(3)	29(3)	18(3)	0	-2(2)	0
C(9)	20(2)	28(2)	22(2)	6(2)	2(2)	-2(2)
C(10)	30(2)	27(2)	30(2)	-4(2)	-1(2)	-5(2)
C(11)	14(3)	27(3)	18(3)	0	-2(2)	0
C(12)	22(2)	27(2)	34(2)	8(2)	-1(2)	0(2)
C(13)	24(2)	34(3)	42(3)	7(2)	0(2)	9(2)
C(14)	15(3)	46(4)	46(4)	0	1(3)	0

Table 13.53. Hydrogen coordinates (x 10^4) and isotropic displacement parameters ($Å^2$x 10^{3}) for **37**.

	x	y	z	U(eq)
H(1)	1997	2500	6320	27
H(4A)	3612	5120	6615	43
H(4B)	2519	5034	7123	43
H(4C)	2341	4717	6351	43
H(5A)	5685	3598	7754	44
H(5B)	4551	3788	8222	44
H(5C)	4805	4639	7614	44
H(8)	6811	2500	6987	25
H(9A)	5751	3534	4513	35
H(9B)	7117	3843	4629	35
H(9C)	6103	4615	4957	35
H(10A)	6109	5175	6096	44
H(10B)	7489	4954	6228	44
H(10C)	6549	4752	6816	44
H(12)	1656	4221	5082	33
H(13)	-364	4216	5332	40
H(14)	-1395	2500	5437	43
H(16)	10172	7500	6145	170
H(17)	12095	7500	6582	170
H(18)	12386	7500	7741	170
H(19)	10753	7500	8463	170
H(20)	8830	7500	8026	170
H(21A)	7553	7500	7179	213
H(21B)	7965	6820	6526	213
H(21C)	7965	8180	6526	213
H(23)	9335	7500	6833	170
H(24)	10990	7500	6127	170
H(25)	12900	7500	6583	170
H(26)	13156	7500	7745	170
H(27)	11502	7500	8451	170
H(28A)	8464	7500	7923	213
H(28B)	9227	8180	8467	213
H(28C)	9227	6820	8467	213

13.19. Crystallographic Data for $(C_5Me_4H)_2ScTePh$, 38

X-ray Data Collection, Structure Solution and Refinement for **38**.

A yellow crystal of approximate dimensions 0.22 x 0.29 x 0.32 mm was mounted on a glass fiber and transferred to a Bruker SMART APEX II diffractometer. The APEX2[1] program package was used to determine the unit-cell parameters and for data collection (20 sec/frame scan time for a sphere of diffraction data). The raw frame data was processed using SAINT[2] and SADABS[3] to yield the reflection data file. Subsequent calculations were carried out using the SHELXTL[4] program. The diffraction symmetry was *mmm* and the systematic absences were consistent with the orthorhombic space groups *Pnma* and $Pna2_1$. Although the structure could be solved and refined using both space groups, the refinement was better (geometric and thermal considerations) using the centrosymmetric space group *Pnma*.

The structure was solved by direct methods and refined on F^2 by full-matrix least-squares techniques. The analytical scattering factors[5] for neutral atoms were used throughout

the analysis. Hydrogen atoms were included using a riding model. The molecule was located on a mirror plane. There was one molecule of toluene solvent present which was also located on a mirror plane. Unrestrained refinement of the solvent molecule resulted in high thermal parameters and poorly defined geometric parameters. This was possibly due to the solvent's location on the mirror plane. It was necessary to apply geometric (DFIX)[4] restraints to the solvent molecule during refinement. Thermal parameters were set equal with U_{iso} fixed at 0.1500.

At convergence, wR2 = 0.1340 and Goof = 1.131 for 145 variables (18 restraints) refined against 3471 data (0.75Å), R1 = 0.0406 for those 3135 data with I > 2.0σ(I).

References

1. APEX2 Version 2.2-0, Bruker AXS, Inc.; Madison, WI 2007.
2. SAINT Version 7.46a, Bruker AXS, Inc.; Madison, WI 2007.
3. Sheldrick, G. M. SADABS, Version 2008/1, Bruker AXS, Inc.; Madison, WI 2008.
4. Sheldrick, G. M. SHELXTL, Version 2008/3, Bruker AXS, Inc.; Madison, WI 2008.
5. International Tables for X-Ray Crystallography 1992, Vol. C., Dordrecht: Kluwer Academic Publishers.

Table 13.54. Atomic coordinates (x 10^4) and equivalent isotropic displacement parameters (Å^{2}x 10^3) for **38**. U(eq) is defined as one third of the trace of the orthogonalized U^{ij} tensor.

	x	y	z	U(eq)
Sc(1)	-4745(1)	2500	6176(1)	18(1)
Te(1)	-3633(1)	2500	4922(1)	22(1)
C(1)	-6455(3)	3100(3)	5499(2)	20(1)
C(2)	-6627(3)	3475(3)	6158(2)	22(1)
C(3)	-6738(4)	2500	6561(3)	23(1)
C(4)	-6461(3)	3838(4)	4895(2)	27(1)
C(5)	-6771(4)	4686(3)	6375(2)	32(1)
C(6)	-4224(3)	3106(3)	7319(2)	25(1)
C(7)	-3341(3)	3468(3)	6880(2)	24(1)
C(8)	-2793(4)	2500	6617(2)	24(1)
C(9)	-4929(4)	3842(4)	7772(2)	34(1)
C(10)	-3030(4)	4679(4)	6724(2)	35(1)
C(11)	-1817(5)	2500	5082(2)	23(1)
C(12)	-1214(3)	1487(4)	5165(2)	30(1)
C(13)	-34(4)	1488(4)	5328(2)	37(1)
C(14)	542(5)	2500	5411(4)	41(2)
C(15)	377(7)	2500	3122(4)	150
C(16)	658(7)	2500	2453(4)	150
C(17)	-219(9)	2500	1980(4)	150
C(18)	-1377(8)	2500	2176(5)	150
C(19)	-1657(6)	2500	2845(5)	150
C(20)	-780(8)	2500	3318(4)	150
C(21)	1349(10)	2500	3645(6)	150

Table 13.55. Anisotropic displacement parameters (Å^{2}x 10^3) for **38**. The anisotropic displacement factor exponent takes the form: $-2\pi^2[h^2 a^{*2}U^{11} + ... + 2 h k a^* b^* U^{12}]$

	U^{11}	U^{22}	U^{33}	U^{23}	U^{13}	U^{12}
Sc(1)	14(1)	24(1)	16(1)	0	0(1)	0
Te(1)	16(1)	32(1)	18(1)	0	0(1)	0
C(1)	12(1)	24(2)	24(2)	1(1)	-1(1)	2(1)

C(2)	16(1)	26(2)	24(2)	-2(1)	0(1)	2(1)
C(3)	16(2)	29(3)	23(2)	0	3(2)	0
C(4)	25(2)	30(2)	25(2)	5(2)	-2(1)	4(2)
C(5)	34(2)	27(2)	33(2)	-4(2)	2(2)	7(2)
C(6)	23(2)	32(2)	20(2)	-2(1)	-3(1)	0(2)
C(7)	22(2)	33(2)	19(2)	-1(1)	-5(1)	-4(2)
C(8)	18(2)	38(3)	18(2)	0	-4(2)	0
C(9)	34(2)	45(2)	24(2)	-8(2)	2(2)	4(2)
C(10)	37(2)	36(2)	33(2)	4(2)	-8(2)	-8(2)
C(11)	16(2)	32(3)	21(2)	0	2(2)	0
C(12)	22(2)	30(2)	37(2)	-5(2)	3(2)	2(2)
C(13)	24(2)	39(2)	47(2)	-5(2)	1(2)	9(2)
C(14)	16(2)	57(4)	51(4)	0	2(2)	0

Table 13.56. Hydrogen coordinates (x 10^4) and isotropic displacement parameters ($Å^2$x 10^{3}) for **38**.

	x	y	z	U(eq)
H(3)	-6864	2500	7026	27
H(4A)	-5934	3522	4562	40
H(4B)	-6204	4599	5015	40
H(4C)	-7250	3873	4714	40
H(5A)	-6784	4722	6859	47
H(5B)	-7501	4986	6199	47
H(5C)	-6120	5136	6207	47
H(8)	-2162	2500	6314	29
H(9A)	-5723	3548	7801	51
H(9B)	-4946	4614	7599	51
H(9C)	-4577	3843	8214	51
H(10A)	-3718	5075	6559	53
H(10B)	-2419	4695	6386	53
H(10C)	-2750	5052	7126	53
H(12)	-1610	789	5110	36
H(13)	370	794	5381	44
H(14)	1342	2500	5527	50
H(16)	1449	2500	2319	180
H(17)	-28	2500	1523	180
H(18)	-1976	2500	1853	180
H(19)	-2448	2500	2979	180
H(20)	-971	2500	3775	180
H(21A)	1905	1896	3546	225
H(21B)	1011	2374	4084	225
H(21C)	1750	3230	3639	225

13.20. Crystallographic Data for $(C_5Me_4H)_2ScSPh(THF)$, 39

X-ray Data Collection, Structure Solution and Refinement for **39**.

A colorless crystal of approximate dimensions 0.21 x 0.22 x 0.34 mm was mounted on a glass fiber and transferred to a Bruker SMART APEX II diffractometer. The APEX2[1] program package was used to determine the unit-cell parameters and for data collection (20 sec/frame scan time for a sphere of diffraction data). The raw frame data was processed using SAINT[2] and SADABS[3] to yield the reflection data file. Subsequent calculations were carried

out using the SHELXTL[4] program. There were no systematic absences nor any diffraction symmetry other than the Friedel condition. The centrosymmetric triclinic space group $P\bar{1}$ was assigned and later determined to be correct.

The structure was solved by direct methods and refined on F^2 by full-matrix least-squares techniques. The analytical scattering factors[5] for neutral atoms were used throughout the analysis. Hydrogen atoms were located from a difference-Fourier map and refined (x,y,z and U_{iso}). At convergence, wR2 = 0.0817 and Goof = 1.054 for 436 variables refined against 5563 data (0.76Å), R1 = 0.0302 for those 5060 data with I > 2.0σ(I).

References

1. APEX2 Version 2.2-0 Bruker AXS, Inc.; Madison, WI 2007.
2. SAINT Version 7.46a, Bruker AXS, Inc.; Madison, WI 2007.
3. Sheldrick, G. M. SADABS, Version 2008/1, Bruker AXS, Inc.; Madison, WI 2008.
4. Sheldrick, G. M. SHELXTL, Version 2008/3, Bruker AXS, Inc.; Madison, WI 2008.
5. International Tables for X-Ray Crystallography 1992, Vol. C., Dordrecht: Kluwer Academic Publishers.

Table 13.57. Atomic coordinates (x 10^4) and equivalent isotropic displacement parameters ($Å^2$x 10^3) for **39**. U(eq) is defined as one third of the trace of the orthogonalized U^{ij} tensor.

	x	y	z	U(eq)
Sc(1)	7015(1)	7135(1)	2729(1)	14(1)
S(1)	4929(1)	8473(1)	1834(1)	22(1)
O(1)	8508(1)	8705(1)	2166(1)	20(1)
C(1)	4484(2)	7653(2)	3937(1)	20(1)
C(2)	4806(2)	9057(1)	3741(1)	20(1)
C(3)	6289(2)	8904(1)	3973(1)	18(1)
C(4)	6924(2)	7393(1)	4288(1)	18(1)
C(5)	5790(2)	6634(1)	4268(1)	19(1)
C(6)	2951(2)	7360(2)	3882(1)	28(1)
C(7)	3658(2)	10520(2)	3477(1)	28(1)
C(8)	6910(2)	10193(2)	3998(1)	24(1)
C(9)	8379(2)	6778(2)	4693(1)	22(1)
C(10)	9231(2)	5472(1)	1644(1)	21(1)
C(11)	9653(2)	4934(1)	2462(1)	19(1)
C(12)	8426(2)	4330(1)	2988(1)	19(1)
C(13)	7212(2)	4537(1)	2514(1)	21(1)
C(14)	7732(2)	5224(1)	1684(1)	21(1)
C(15)	10240(2)	6075(2)	858(1)	27(1)
C(16)	11260(2)	4743(2)	2679(1)	25(1)
C(17)	8562(2)	3400(2)	3831(1)	24(1)
C(18)	5690(2)	4066(2)	2803(1)	27(1)
C(19)	5185(2)	7936(1)	782(1)	20(1)
C(20)	4112(2)	7285(2)	621(1)	36(1)
C(21)	4230(2)	6909(3)	-205(1)	47(1)
C(22)	5431(2)	7167(2)	-883(1)	32(1)
C(23)	6509(2)	7808(2)	-738(1)	34(1)
C(24)	6387(2)	8200(2)	83(1)	34(1)
C(25)	8077(2)	10039(2)	1572(1)	30(1)
C(26)	9581(2)	10572(2)	1303(1)	38(1)
C(27)	10304(2)	10129(2)	2104(1)	32(1)
C(28)	9994(2)	8634(2)	2422(1)	24(1)

Table 13.58. Anisotropic displacement parameters ($Å^2 x 10^3$) for **39**. The anisotropic displacement factor exponent takes the form: $-2\pi^2[h^2 a^{*2}U^{11} + ... + 2 h k a^* b^* U^{12}]$

	U^{11}	U^{22}	U^{33}	U^{23}	U^{13}	U^{12}
Sc(1)	14(1)	15(1)	14(1)	-1(1)	-4(1)	-4(1)
S(1)	18(1)	28(1)	17(1)	-3(1)	-6(1)	-1(1)
O(1)	18(1)	20(1)	22(1)	1(1)	-4(1)	-7(1)
C(1)	17(1)	27(1)	15(1)	-3(1)	-1(1)	-7(1)
C(2)	19(1)	22(1)	15(1)	-4(1)	-2(1)	-2(1)
C(3)	20(1)	19(1)	15(1)	-4(1)	-2(1)	-4(1)
C(4)	19(1)	20(1)	14(1)	-2(1)	-4(1)	-5(1)
C(5)	21(1)	21(1)	15(1)	0(1)	-2(1)	-8(1)
C(6)	20(1)	43(1)	23(1)	0(1)	-4(1)	-14(1)
C(7)	26(1)	25(1)	25(1)	-5(1)	-8(1)	4(1)
C(8)	29(1)	20(1)	22(1)	-5(1)	-4(1)	-8(1)
C(9)	23(1)	24(1)	21(1)	-2(1)	-9(1)	-4(1)
C(10)	22(1)	19(1)	20(1)	-6(1)	-4(1)	-1(1)
C(11)	18(1)	17(1)	21(1)	-5(1)	-5(1)	0(1)
C(12)	22(1)	14(1)	22(1)	-3(1)	-8(1)	-2(1)
C(13)	24(1)	15(1)	25(1)	-4(1)	-10(1)	-4(1)
C(14)	25(1)	18(1)	21(1)	-6(1)	-9(1)	-2(1)
C(15)	27(1)	29(1)	21(1)	-4(1)	-1(1)	-4(1)
C(16)	18(1)	26(1)	29(1)	-3(1)	-7(1)	-2(1)
C(17)	28(1)	19(1)	25(1)	1(1)	-11(1)	-5(1)
C(18)	30(1)	23(1)	35(1)	0(1)	-15(1)	-12(1)
C(19)	19(1)	20(1)	18(1)	0(1)	-7(1)	-2(1)
C(20)	26(1)	56(1)	31(1)	-16(1)	2(1)	-20(1)
C(21)	29(1)	78(1)	45(1)	-32(1)	-4(1)	-21(1)
C(22)	34(1)	38(1)	22(1)	-9(1)	-12(1)	1(1)
C(23)	47(1)	35(1)	20(1)	1(1)	0(1)	-18(1)
C(24)	41(1)	44(1)	24(1)	-4(1)	0(1)	-27(1)
C(25)	38(1)	28(1)	30(1)	11(1)	-16(1)	-17(1)
C(26)	43(1)	37(1)	38(1)	10(1)	-9(1)	-23(1)
C(27)	26(1)	30(1)	43(1)	-1(1)	-7(1)	-14(1)
C(28)	16(1)	26(1)	31(1)	-2(1)	-5(1)	-6(1)

Table 13.59. Hydrogen coordinates ($x 10^4$) and isotropic displacement parameters ($Å^2 x 10^3$) for **39**.

	x	y	z	U(eq)
H(5A)	5859(19)	5605(19)	4469(11)	25(4)
H(6A)	2020(20)	7960(20)	4275(12)	37(5)
H(6B)	3000(20)	6320(20)	4028(12)	42(5)
H(6C)	2750(20)	7610(20)	3314(14)	44(5)
H(7A)	3320(30)	11200(30)	3888(19)	86(9)
H(7B)	2740(40)	10370(30)	3406(19)	102(10)
H(7C)	4140(30)	11010(30)	2953(17)	73(8)
H(8A)	6180(20)	10850(20)	4408(13)	41(5)
H(8B)	7020(20)	10780(20)	3441(12)	35(5)
H(8C)	7910(20)	9860(20)	4186(12)	37(5)
H(9A)	8130(30)	6260(30)	5211(17)	69(7)
H(9B)	8680(30)	7600(30)	4846(15)	65(7)
H(9C)	9330(30)	6160(30)	4351(15)	63(7)
H(14A)	7156(19)	5465(18)	1227(11)	23(4)
H(15A)	11320(30)	5400(30)	695(15)	59(6)
H(15B)	10390(30)	7020(30)	924(14)	52(6)
H(15C)	9700(30)	6290(20)	399(14)	52(6)
H(16A)	11830(20)	3720(20)	2787(12)	40(5)
H(16B)	11180(20)	5300(20)	3158(13)	41(5)

H(16C)	11930(20)	5110(20)	2237(12)	34(5)
H(17A)	9380(20)	2460(20)	3727(12)	41(5)
H(17B)	7550(20)	3210(20)	4148(11)	33(4)
H(17C)	8840(20)	3843(19)	4234(11)	30(4)
H(18A)	5840(20)	3110(20)	2572(12)	39(5)
H(18B)	4800(20)	4790(20)	2574(12)	40(5)
H(18C)	5330(20)	3990(20)	3432(13)	34(5)
H(20A)	3310(30)	7080(20)	1084(14)	55(6)
H(21A)	3520(30)	6480(30)	-287(15)	65(7)
H(22A)	5510(20)	6890(20)	-1421(13)	38(5)
H(23A)	7300(30)	8000(20)	-1195(14)	52(6)
H(24A)	7120(30)	8700(20)	173(14)	55(6)
H(25A)	7090(20)	10830(20)	1902(13)	45(5)
H(25B)	7820(20)	9720(20)	1107(12)	38(5)
H(26A)	9290(30)	11600(30)	1149(14)	56(6)
H(26B)	10370(30)	9990(20)	797(13)	46(5)
H(27A)	11440(30)	10040(20)	2012(13)	43(5)
H(27B)	9700(20)	10880(20)	2529(12)	38(5)
H(28A)	10850(20)	7825(18)	2152(10)	24(4)
H(28B)	9820(20)	8438(18)	3043(11)	28(4)

13.21. Crystallographic Data for $(C_5Me_4H)_2ScSePh(THF)$, 40

X-ray Data Collection, Structure Solution and Refinement for **40**.

A colorless crystal of approximate dimensions 0.24 x 0.25 x 0.34 mm was mounted on a glass fiber and transferred to a Bruker SMART APEX II diffractometer. The APEX2[1] program package was used to determine the unit-cell parameters and for data collection (20 sec/frame scan time for a sphere of diffraction data). The raw frame data was processed using SAINT[2] and SADABS[3] to yield the reflection data file. Subsequent calculations were carried out using the SHELXTL[4] program. There were no systematic absences nor any diffraction symmetry other than the Friedel condition. The centrosymmetric triclinic space group $P\bar{1}$ was assigned and later determined to be correct.

The structure was solved by direct methods and refined on F^2 by full-matrix least-squares techniques. The analytical scattering factors[5] for neutral atoms were used throughout the analysis. Hydrogen atoms were located included using a riding model. Carbon atoms C(26) and C(27) were disordered (70:30) and included using multiple components and partial site-occupancy-factors. At convergence, wR2 = 0.0681 and Goof = 1.044 for 306 variables refined against 5837 data (0.75Å), R1 = 0.0248 for those 5452 data with $I > 2.0\sigma(I)$.

References

1. APEX2 Version 2.2-0 Bruker AXS, Inc.; Madison, WI 2007.
2. SAINT Version 7.46a, Bruker AXS, Inc.; Madison, WI 2007.
3. Sheldrick, G. M. SADABS, Version 2008/1, Bruker AXS, Inc.; Madison, WI 2008.
4. Sheldrick, G. M. SHELXTL, Version 2008/3, Bruker AXS, Inc.; Madison, WI 2008.
5. International Tables for X-Ray Crystallography 1992, Vol. C., Dordrecht: Kluwer Academic Publishers.

Table 13.60. Atomic coordinates (x 10^4) and equivalent isotropic displacement parameters ($Å^2$x 10^3) for **40**. U(eq) is defined as one third of the trace of the orthogonalized U^{ij} tensor.

	x	y	z	U(eq)
Sc(1)	7405(1)	7928(1)	2315(1)	16(1)
Se(1)	4598(1)	6336(1)	1953(1)	22(1)
O(1)	8628(1)	6170(1)	1954(1)	20(1)
C(1)	5836(2)	9404(2)	1270(1)	21(1)
C(2)	6033(2)	8288(2)	676(1)	21(1)
C(3)	7645(2)	8354(2)	705(1)	21(1)
C(4)	8468(2)	9499(2)	1329(1)	22(1)
C(5)	7332(2)	10141(2)	1670(1)	22(1)
C(6)	4292(2)	9808(2)	1359(1)	29(1)
C(7)	4757(2)	7354(2)	2(1)	28(1)
C(8)	8284(2)	7461(2)	73(1)	30(1)
C(9)	10182(2)	10058(2)	1491(1)	31(1)
C(10)	8834(2)	7410(2)	3851(1)	22(1)
C(11)	9664(2)	8672(2)	3720(1)	22(1)
C(12)	8651(2)	9695(2)	3699(1)	22(1)
C(13)	7180(2)	9040(2)	3780(1)	25(1)
C(14)	7311(2)	7628(2)	3874(1)	25(1)
C(15)	9488(2)	6086(2)	4045(1)	36(1)
C(16)	11397(2)	8975(2)	3788(1)	31(1)
C(17)	9177(2)	11223(2)	3755(1)	33(1)
C(18)	5768(2)	9714(2)	3820(1)	40(1)
C(19)	4188(2)	5110(2)	2813(1)	21(1)
C(20)	3744(2)	5573(2)	3595(1)	24(1)
C(21)	3301(2)	4638(2)	4160(1)	28(1)
C(22)	3268(2)	3230(2)	3954(1)	31(1)
C(23)	3692(2)	2759(2)	3178(1)	31(1)
C(24)	4163(2)	3687(2)	2617(1)	26(1)
C(25)	7884(2)	4732(2)	1798(2)	41(1)
C(26)	9226(3)	3890(2)	1780(2)	28(1)
C(27)	10279(4)	4864(3)	1357(2)	27(1)
C(26B)	8877(7)	3985(6)	1185(5)	32(1)
C(27B)	10437(9)	4623(8)	1755(6)	33(2)
C(28)	10245(2)	6221(2)	1878(1)	26(1)

Table 13.61. Anisotropic displacement parameters ($Å^2$x 10^3) for **40**. The anisotropic displacement factor exponent takes the form: $-2\pi^2[h^2 a^{*2}U^{11} + ... + 2 h k a^* b^* U^{12}]$

	U^{11}	U^{22}	U^{33}	U^{23}	U^{13}	U^{12}
Sc(1)	15(1)	17(1)	16(1)	5(1)	4(1)	2(1)
Se(1)	18(1)	25(1)	22(1)	10(1)	3(1)	-1(1)
O(1)	18(1)	18(1)	25(1)	4(1)	6(1)	2(1)
C(1)	22(1)	22(1)	21(1)	10(1)	6(1)	6(1)
C(2)	25(1)	22(1)	16(1)	9(1)	4(1)	2(1)
C(3)	26(1)	22(1)	19(1)	9(1)	8(1)	6(1)
C(4)	22(1)	22(1)	22(1)	10(1)	8(1)	2(1)
C(5)	26(1)	18(1)	22(1)	7(1)	6(1)	3(1)
C(6)	27(1)	32(1)	34(1)	16(1)	11(1)	13(1)
C(7)	31(1)	30(1)	20(1)	8(1)	0(1)	-3(1)
C(8)	40(1)	33(1)	24(1)	9(1)	15(1)	13(1)
C(9)	24(1)	33(1)	36(1)	13(1)	10(1)	-2(1)
C(10)	26(1)	26(1)	13(1)	5(1)	1(1)	4(1)
C(11)	20(1)	27(1)	16(1)	2(1)	2(1)	2(1)
C(12)	24(1)	24(1)	16(1)	1(1)	3(1)	3(1)

C(13)	22(1)	36(1)	16(1)	1(1)	5(1)	5(1)
C(14)	25(1)	34(1)	15(1)	6(1)	4(1)	-3(1)
C(15)	52(1)	31(1)	25(1)	10(1)	2(1)	12(1)
C(16)	21(1)	40(1)	29(1)	-1(1)	3(1)	1(1)
C(17)	43(1)	24(1)	27(1)	0(1)	3(1)	2(1)
C(18)	28(1)	63(1)	28(1)	-4(1)	7(1)	16(1)
C(19)	16(1)	24(1)	22(1)	9(1)	5(1)	1(1)
C(20)	20(1)	26(1)	27(1)	4(1)	7(1)	3(1)
C(21)	24(1)	39(1)	24(1)	6(1)	10(1)	1(1)
C(22)	32(1)	35(1)	28(1)	14(1)	8(1)	-3(1)
C(23)	37(1)	23(1)	35(1)	8(1)	10(1)	1(1)
C(24)	29(1)	25(1)	26(1)	5(1)	9(1)	3(1)
C(25)	29(1)	19(1)	79(2)	0(1)	23(1)	-1(1)
C(26)	29(1)	20(1)	36(1)	3(1)	6(1)	5(1)
C(27)	24(1)	26(1)	31(2)	3(1)	9(1)	8(1)
C(26B)	27(3)	24(3)	45(4)	0(3)	10(3)	8(2)
C(27B)	28(3)	26(3)	47(5)	0(3)	10(4)	10(2)
C(28)	18(1)	25(1)	34(1)	2(1)	7(1)	3(1)

Table 13.62. Hydrogen coordinates (x 10^4) and isotropic displacement parameters ($Å^2$x 10^{3}) for **40**.

	x	y	z	U(eq)
H(5A)	7537	11074	2028	26
H(6A)	3720	10029	777	44
H(6B)	4472	10622	1807	44
H(6C)	3678	9036	1553	44
H(7A)	4556	7756	-569	43
H(7B)	3802	7252	228	43
H(7C)	5080	6441	-92	43
H(8A)	7834	7613	-549	45
H(8B)	8012	6483	151	45
H(8C)	9424	7702	205	45
H(9A)	10425	10283	922	46
H(9B)	10806	9358	1735	46
H(9C)	10428	10898	1922	46
H(14A)	6526	6955	4058	30
H(15A)	10046	6167	4679	54
H(15B)	10212	5924	3661	54
H(15C)	8631	5308	3921	54
H(16A)	11898	9590	4340	47
H(16B)	11582	9425	3265	47
H(16C)	11839	8105	3802	47
H(17A)	9808	11562	4362	49
H(17B)	8262	11704	3626	49
H(17C)	9807	11402	3315	49
H(18A)	5574	9706	4425	59
H(18B)	4858	9204	3378	59
H(18C)	5946	10674	3684	59
H(20A)	3744	6536	3740	29
H(21A)	3019	4970	4693	34
H(22A)	2958	2593	4340	38
H(23A)	3659	1792	3027	38
H(24A)	4471	3349	2094	31
H(25A)	7093	4552	1219	50
H(25B)	7369	4498	2289	50
H(25C)	6809	4655	1480	50
H(25D)	7932	4340	2356	50
H(26A)	9764	3731	2393	34
H(26B)	8855	2988	1403	34

H(27A)	11350	4622	1454	32
H(27B)	9839	4865	705	32
H(26C)	8701	2962	1163	38
H(26D)	8690	4260	567	38
H(27C)	11284	4479	1447	40
H(27D)	10655	4243	2341	40
H(28A)	10967	6321	2480	31
H(28B)	10546	7007	1553	31
H(28C)	10959	6695	2413	31
H(28D)	10413	6676	1369	31

13.22. Crystallographic Data for $(C_5Me_4H)_2ScTePh(THF)$, 41

X-ray Data Collection, Structure Solution and Refinement for 41.

A colorless crystal of approximate dimensions 0.10 x 0.21 x 0.38 mm was mounted on a glass fiber and transferred to a Bruker SMART APEX II diffractometer. The APEX2[1] program package was used to determine the unit-cell parameters and for data collection (20 sec/frame scan time for a sphere of diffraction data). The raw frame data was processed using SAINT[2] and SADABS[3] to yield the reflection data file. Subsequent calculations were carried out using the SHELXTL[4] program. There were no systematic absences nor any diffraction symmetry other than the Friedel condition. The centrosymmetric triclinic space group $P\bar{1}$ was assigned and later determined to be correct.

The structure was solved by direct methods[5] and refined on F^2 by full-matrix least-squares techniques. The analytical scattering factors[6] for neutral atoms were used throughout the analysis. Hydrogen atoms were included using a riding model. There were two molecules of the formula unit present (Z = 4).

At convergence, wR2 = 0.0549 and Goof = 1.039 for 575 variables refined against 12449 data (0.74Å), R1 = 0.0217 for those 11172 data with I > 2.0σ(I).

References

1. APEX2 Version 2008.3-0 / 2.2-0 Bruker AXS, Inc.; Madison, WI 2007.
2. SAINT Version 7.53a / 7.46a, Bruker AXS, Inc.; Madison, WI 2007.
3. Sheldrick, G. M. SADABS, Version 2008/1, Bruker AXS, Inc.; Madison, WI 2008.
4. Sheldrick, G. M. SHELXTL, Version 2008/3, Bruker AXS, Inc.; Madison, WI 2008.
5. M. C. Burla, R. Caliandro, M. Camalli, B. Carrozzini, G. L. Cascarano, L. De Caro, Giacovazzo, G. Polidori and R. Spagna, SIR2004: an improved tool for crystal structure determination and refinement, J. Appl. Cryst. (2005), vol. 38, pp. 381-388.
6. International Tables for X-Ray Crystallography 1992, Vol. C., Dordrecht: Kluwer Academic Publishers.

Table 13.63. Atomic coordinates (x 10^4) and equivalent isotropic displacement parameters ($Å^2$x 10^3) for **41**. U(eq) is defined as one third of the trace of the orthogonalized U^{ij} tensor.

	x	y	z	U(eq)
Te(1)	-51(1)	3002(1)	7630(1)	19(1)
Sc(1)	3025(1)	2434(1)	7072(1)	15(1)
O(1)	4000(1)	2965(1)	7770(1)	19(1)
C(1)	2050(3)	3248(1)	5749(1)	31(1)

C(2)	2204(2)	3930(1)	5979(1)	22(1)
C(3)	3715(2)	3879(1)	6015(1)	23(1)
C(4)	4519(2)	3151(1)	5816(1)	32(1)
C(5)	3475(3)	2777(1)	5648(1)	35(1)
C(6)	649(3)	3114(2)	5559(1)	50(1)
C(7)	1016(2)	4694(1)	6020(1)	33(1)
C(8)	4352(2)	4555(1)	6128(1)	34(1)
C(9)	6170(3)	2920(2)	5677(2)	52(1)
C(10)	3877(2)	1048(1)	8201(1)	19(1)
C(11)	4906(2)	1009(1)	7541(1)	20(1)
C(12)	4127(2)	934(1)	6987(1)	20(1)
C(13)	2622(2)	948(1)	7288(1)	20(1)
C(14)	2482(2)	1021(1)	8038(1)	19(1)
C(15)	4185(2)	1033(1)	8975(1)	26(1)
C(16)	6565(2)	880(1)	7486(1)	27(1)
C(17)	4851(2)	710(1)	6280(1)	29(1)
C(18)	1430(2)	823(1)	6921(1)	28(1)
C(19)	-768(2)	2096(1)	8738(1)	20(1)
C(20)	-948(2)	2298(1)	9415(1)	24(1)
C(21)	-1547(2)	1753(1)	10132(1)	29(1)
C(22)	-1947(2)	986(1)	10186(1)	32(1)
C(23)	-1756(2)	774(1)	9520(1)	32(1)
C(24)	-1184(2)	1323(1)	8801(1)	26(1)
C(25)	3112(2)	3532(1)	8184(1)	24(1)
C(26)	4210(2)	3892(1)	8428(1)	26(1)
C(27)	5575(2)	3172(1)	8519(1)	27(1)
C(28)	5564(2)	2882(1)	7842(1)	24(1)
Te(2)	-1026(1)	3279(1)	2873(1)	21(1)
Sc(2)	1957(1)	2927(1)	2086(1)	14(1)
O(2)	2968(1)	3453(1)	2787(1)	18(1)
C(29)	682(2)	3790(1)	848(1)	19(1)
C(30)	802(2)	4438(1)	1138(1)	18(1)
C(31)	2321(2)	4451(1)	1104(1)	18(1)
C(32)	3160(2)	3801(1)	810(1)	19(1)
C(33)	2134(2)	3406(1)	644(1)	20(1)
C(34)	-739(2)	3629(1)	705(1)	26(1)
C(35)	-451(2)	5101(1)	1311(1)	23(1)
C(36)	2898(2)	5126(1)	1254(1)	22(1)
C(37)	4813(2)	3651(1)	607(1)	25(1)
C(38)	3100(2)	1509(1)	3081(1)	19(1)
C(39)	4054(2)	1573(1)	2374(1)	17(1)
C(40)	3236(2)	1518(1)	1826(1)	17(1)
C(41)	1774(2)	1439(1)	2182(1)	19(1)
C(42)	1708(2)	1429(1)	2957(1)	20(1)
C(43)	3489(2)	1459(1)	3855(1)	24(1)
C(44)	5710(2)	1500(1)	2263(1)	23(1)
C(45)	3908(2)	1376(1)	1072(1)	23(1)
C(46)	556(2)	1309(1)	1833(1)	27(1)
C(47)	-1349(2)	2157(1)	3888(1)	19(1)
C(48)	-2114(2)	1554(1)	3866(1)	29(1)
C(49)	-2272(2)	796(1)	4511(1)	35(1)
C(50)	-1672(2)	624(1)	5194(1)	32(1)
C(51)	-931(2)	1223(2)	5228(1)	36(1)
C(52)	-777(2)	1983(1)	4582(1)	29(1)
C(53)	2111(2)	3926(1)	3294(1)	24(1)
C(54)	3222(2)	4287(1)	3527(1)	26(1)
C(55)	4638(2)	3625(1)	3508(1)	24(1)
C(56)	4544(2)	3412(1)	2798(1)	21(1)

Table 13.64. Anisotropic displacement parameters ($Å^2 x 10^3$) for **41**. The anisotropic displacement factor exponent takes the form: $-2\pi^2[h^2 a^{*2}U^{11} + ... + 2 h k a^* b^* U^{12}]$

	U^{11}	U^{22}	U^{33}	U^{23}	U^{13}	U^{12}
Te(1)	15(1)	19(1)	21(1)	-8(1)	-3(1)	1(1)
Sc(1)	18(1)	11(1)	14(1)	-5(1)	0(1)	0(1)
O(1)	14(1)	18(1)	25(1)	-12(1)	-1(1)	1(1)
C(1)	58(1)	19(1)	15(1)	-2(1)	-10(1)	-10(1)
C(2)	34(1)	14(1)	16(1)	-2(1)	-4(1)	-2(1)
C(3)	31(1)	15(1)	18(1)	-2(1)	1(1)	-4(1)
C(4)	40(1)	18(1)	20(1)	1(1)	12(1)	1(1)
C(5)	73(2)	14(1)	14(1)	-5(1)	4(1)	-5(1)
C(6)	90(2)	39(1)	30(1)	1(1)	-31(1)	-28(1)
C(7)	36(1)	21(1)	31(1)	-1(1)	-6(1)	5(1)
C(8)	43(1)	22(1)	33(1)	-2(1)	-6(1)	-13(1)
C(9)	47(1)	30(1)	45(1)	4(1)	25(1)	4(1)
C(10)	22(1)	12(1)	18(1)	-3(1)	-3(1)	1(1)
C(11)	19(1)	11(1)	25(1)	-4(1)	0(1)	1(1)
C(12)	26(1)	9(1)	20(1)	-4(1)	2(1)	-1(1)
C(13)	24(1)	12(1)	21(1)	-4(1)	-2(1)	-2(1)
C(14)	19(1)	12(1)	19(1)	-2(1)	1(1)	-1(1)
C(15)	32(1)	21(1)	22(1)	-4(1)	-6(1)	-1(1)
C(16)	18(1)	18(1)	40(1)	-9(1)	-1(1)	1(1)
C(17)	42(1)	15(1)	25(1)	-9(1)	6(1)	0(1)
C(18)	32(1)	20(1)	34(1)	-8(1)	-9(1)	-6(1)
C(19)	12(1)	21(1)	24(1)	-8(1)	-3(1)	0(1)
C(20)	22(1)	24(1)	27(1)	-10(1)	-5(1)	-2(1)
C(21)	26(1)	35(1)	23(1)	-8(1)	-3(1)	-3(1)
C(22)	22(1)	31(1)	32(1)	-2(1)	1(1)	-3(1)
C(23)	21(1)	26(1)	47(1)	-11(1)	2(1)	-7(1)
C(24)	17(1)	31(1)	35(1)	-18(1)	2(1)	-5(1)
C(25)	16(1)	29(1)	32(1)	-22(1)	-1(1)	1(1)
C(26)	20(1)	27(1)	36(1)	-19(1)	-7(1)	0(1)
C(27)	19(1)	26(1)	40(1)	-16(1)	-9(1)	1(1)
C(28)	14(1)	23(1)	35(1)	-14(1)	-2(1)	0(1)
Te(2)	15(1)	19(1)	24(1)	-5(1)	4(1)	-2(1)
Sc(2)	14(1)	12(1)	14(1)	-4(1)	1(1)	-1(1)
O(2)	16(1)	19(1)	20(1)	-10(1)	2(1)	-3(1)
C(29)	23(1)	15(1)	15(1)	-2(1)	-2(1)	-2(1)
C(30)	20(1)	12(1)	16(1)	-2(1)	0(1)	-1(1)
C(31)	22(1)	13(1)	15(1)	-2(1)	1(1)	-2(1)
C(32)	21(1)	15(1)	15(1)	-2(1)	3(1)	-1(1)
C(33)	26(1)	14(1)	15(1)	-4(1)	0(1)	-1(1)
C(34)	28(1)	24(1)	24(1)	-5(1)	-7(1)	-5(1)
C(35)	22(1)	16(1)	25(1)	-4(1)	0(1)	2(1)
C(36)	24(1)	17(1)	23(1)	-4(1)	1(1)	-5(1)
C(37)	23(1)	22(1)	22(1)	-5(1)	7(1)	-3(1)
C(38)	23(1)	12(1)	17(1)	-3(1)	-1(1)	2(1)
C(39)	17(1)	11(1)	19(1)	-5(1)	0(1)	1(1)
C(40)	20(1)	10(1)	20(1)	-5(1)	-2(1)	1(1)
C(41)	20(1)	10(1)	25(1)	-4(1)	-3(1)	-1(1)
C(42)	21(1)	11(1)	21(1)	-2(1)	2(1)	-1(1)
C(43)	33(1)	18(1)	18(1)	-6(1)	-4(1)	0(1)
C(44)	17(1)	21(1)	29(1)	-11(1)	-2(1)	1(1)
C(45)	28(1)	18(1)	22(1)	-10(1)	-2(1)	0(1)
C(46)	25(1)	20(1)	35(1)	-8(1)	-6(1)	-5(1)
C(47)	13(1)	22(1)	20(1)	-8(1)	4(1)	-4(1)
C(48)	27(1)	35(1)	25(1)	-6(1)	-5(1)	-15(1)
C(49)	35(1)	30(1)	39(1)	-6(1)	1(1)	-17(1)
C(50)	23(1)	30(1)	27(1)	2(1)	5(1)	0(1)
C(51)	30(1)	54(1)	18(1)	-7(1)	-4(1)	-8(1)

C(52)	30(1)	40(1)	24(1)	-15(1)	0(1)	-14(1)
C(53)	21(1)	28(1)	29(1)	-18(1)	6(1)	-6(1)
C(54)	24(1)	28(1)	30(1)	-18(1)	3(1)	-7(1)
C(55)	22(1)	27(1)	24(1)	-11(1)	-1(1)	-6(1)
C(56)	15(1)	24(1)	22(1)	-9(1)	1(1)	-4(1)

Table 13.65. Hydrogen coordinates (x 10^4) and isotropic displacement parameters ($Å^2$x 10^3) for **41**.

	x	y	z	U(eq)
H(5A)	3704	2283	5492	42
H(6A)	476	3491	5015	76
H(6B)	-184	3263	5919	76
H(6C)	742	2500	5619	76
H(7A)	1090	5193	5523	50
H(7B)	1143	4857	6455	50
H(7C)	43	4530	6108	50
H(8A)	4217	5101	5670	50
H(8B)	5409	4345	6185	50
H(8C)	3847	4663	6603	50
H(9A)	6516	3307	5154	79
H(9B)	6450	2311	5708	79
H(9C)	6624	2993	6079	79
H(14A)	1588	1047	8375	23
H(15A)	4261	434	9361	39
H(15B)	3379	1418	9164	39
H(15C)	5117	1238	8904	39
H(16A)	7006	368	7340	40
H(16B)	6863	788	7997	40
H(16C)	6906	1401	7085	40
H(17A)	5385	104	6452	44
H(17B)	5547	1105	5976	44
H(17C)	4095	774	5949	44
H(18A)	1366	200	7122	42
H(18B)	1665	1028	6348	42
H(18C)	482	1158	7055	42
H(20A)	-657	2813	9387	29
H(21A)	-1684	1906	10586	35
H(22A)	-2347	612	10676	38
H(23A)	-2018	248	9554	39
H(24A)	-1073	1173	8347	32
H(25A)	2511	3193	8652	28
H(25B)	2442	4014	7832	28
H(26A)	3842	3984	8932	31
H(26B)	4421	4451	8019	31
H(27A)	6485	3403	8467	32
H(27B)	5490	2686	9032	32
H(28A)	6055	3260	7350	28
H(28B)	6079	2268	7957	28
H(33A)	2385	2955	430	24
H(34A)	-1242	4166	327	38
H(34B)	-1378	3459	1203	38
H(34C)	-522	3159	493	38
H(35A)	-642	5605	824	35
H(35B)	-189	5294	1697	35
H(35C)	-1340	4837	1524	35
H(36A)	2659	5696	836	33
H(36B)	3972	4959	1263	33
H(36C)	2439	5163	1763	33

H(37A)	5089	4156	157	37
H(37B)	5126	3123	473	37
H(37C)	5299	3576	1061	37
H(42A)	859	1376	3332	24
H(43A)	3522	859	4237	36
H(43B)	2740	1859	4056	36
H(43C)	4458	1625	3776	36
H(44A)	6164	1036	2054	34
H(44B)	6069	1359	2770	34
H(44C)	5972	2058	1892	34
H(45A)	4502	787	1194	34
H(45B)	4539	1811	769	34
H(45C)	3119	1440	761	34
H(46A)	629	684	1945	40
H(46B)	650	1624	1262	40
H(46C)	-404	1536	2065	40
H(48A)	-2536	1663	3400	34
H(49A)	-2798	392	4482	42
H(50A)	-1769	101	5634	39
H(51A)	-521	1114	5697	43
H(52A)	-269	2391	4618	35
H(53A)	1610	3525	3766	29
H(53B)	1354	4407	3005	29
H(54A)	2927	4312	4060	31
H(54B)	3336	4879	3146	31
H(55A)	5523	3884	3439	28
H(55B)	4659	3098	3995	28
H(56A)	4944	3843	2309	25
H(56B)	5107	2820	2849	25

13.23. Crystallographic Data for $(C_5Me_4H)_2ScSpy$, 42

X-ray Data Collection, Structure Solution and Refinement for **42**.

A colorless crystal of approximate dimensions 0.28 x 0.30 x 0.34 mm was mounted on a glass fiber and transferred to a Bruker SMART APEX II diffractometer. The APEX2[1] program package was used to determine the unit-cell parameters and for data collection (15 sec/frame scan time for a sphere of diffraction data). The raw frame data was processed using SAINT[2] and SADABS[3] to yield the reflection data file. Subsequent calculations were carried out using the SHELXTL[4] program. The diffraction symmetry was 2/*m* and the systematic absences were consistent with the monoclinic space group $P2_1/c$ that was later determined to be correct.

The structure was solved by direct methods and refined on F^2 by full-matrix least-squares techniques. The analytical scattering factors[5] for neutral atoms were used throughout the analysis. Hydrogen atoms associated with C(8) were included using a riding model. The remaining hydrogen atoms were located from a difference-Fourier map and refined (x,y,z and U_{iso}).

At convergence, wR2 = 0.0841 and Goof = 1.029 for 344 variables refined against 5195 data (0.74Å), R1 = 0.0304 for those 4859 data with I > 2.0σ(I).

References

1. APEX2 Version 2008.3-0, Bruker AXS, Inc.; Madison, WI 2008.
2. SAINT Version 7.53a, Bruker AXS, Inc.; Madison, WI 2007.
3. Sheldrick, G. M. SADABS, Version 2008/1, Bruker AXS, Inc.; Madison, WI 2008.
4. Sheldrick, G. M. SHELXTL, Version 2008/3, Bruker AXS, Inc.; Madison, WI 2008.
5. International Tables for X-Ray Crystallography 1992, Vol. C., Dordrecht: Kluwer Academic Publishers.

Table 13.66. Atomic coordinates (x 10^4) and equivalent isotropic displacement parameters ($Å^2$x 10^3) for **42**. U(eq) is defined as one third of the trace of the orthogonalized U^{ij} tensor.

	x	y	z	U(eq)
Sc(1)	2706(1)	917(1)	3211(1)	14(1)
S(1)	1692(1)	-605(1)	1857(1)	27(1)
N(1)	1981(1)	2446(1)	2067(1)	23(1)
C(1)	2065(1)	2522(1)	4144(1)	19(1)
C(2)	1413(1)	1438(2)	3700(1)	19(1)
C(3)	1699(1)	-102(1)	4008(1)	17(1)
C(4)	2526(1)	26(1)	4637(1)	16(1)
C(5)	2747(1)	1644(1)	4717(1)	17(1)
C(6)	2021(1)	4289(2)	4077(1)	29(1)
C(7)	549(1)	1841(2)	3066(1)	28(1)
C(8)	1187(1)	-1599(2)	3780(1)	26(1)
C(9)	3021(1)	-1300(2)	5193(1)	24(1)
C(10)	4233(1)	1804(1)	3751(1)	16(1)
C(11)	3990(1)	2002(1)	2822(1)	16(1)
C(12)	3809(1)	492(1)	2419(1)	16(1)
C(13)	3939(1)	-651(1)	3100(1)	17(1)
C(14)	4200(1)	161(1)	3920(1)	17(1)
C(15)	4563(1)	3082(2)	4429(1)	22(1)
C(16)	3984(1)	3528(1)	2343(1)	21(1)
C(17)	3595(1)	180(2)	1446(1)	22(1)
C(18)	3834(1)	-2403(1)	2978(1)	23(1)
C(19)	1521(1)	1346(2)	1504(1)	26(1)
C(20)	931(1)	1816(2)	686(1)	36(1)
C(21)	830(1)	3386(2)	478(1)	41(1)
C(22)	1300(1)	4511(2)	1063(1)	37(1)
C(23)	1871(1)	3993(2)	1851(1)	28(1)

Table 13.67. Anisotropic displacement parameters ($Å^2$x 10^3) for **42**. The anisotropic displacement factor exponent takes the form: $-2\pi^2[h^2 a^{*2}U^{11} + ... + 2 h k a^* b^* U^{12}]$

	U^{11}	U^{22}	U^{33}	U^{23}	U^{13}	U^{12}
Sc(1)	13(1)	14(1)	13(1)	0(1)	2(1)	0(1)
S(1)	22(1)	35(1)	21(1)	-8(1)	3(1)	-8(1)
N(1)	17(1)	32(1)	19(1)	7(1)	6(1)	4(1)
C(1)	23(1)	16(1)	19(1)	1(1)	9(1)	3(1)
C(2)	16(1)	23(1)	18(1)	3(1)	6(1)	4(1)
C(3)	17(1)	18(1)	17(1)	0(1)	6(1)	0(1)
C(4)	17(1)	17(1)	15(1)	2(1)	5(1)	2(1)
C(5)	19(1)	18(1)	15(1)	-2(1)	5(1)	-1(1)
C(6)	40(1)	16(1)	33(1)	1(1)	16(1)	6(1)
C(7)	18(1)	41(1)	25(1)	7(1)	5(1)	9(1)
C(8)	25(1)	25(1)	29(1)	-2(1)	8(1)	-8(1)
C(9)	24(1)	23(1)	23(1)	8(1)	7(1)	6(1)
C(10)	13(1)	16(1)	20(1)	-2(1)	3(1)	-1(1)
C(11)	14(1)	14(1)	20(1)	-1(1)	6(1)	0(1)

C(12)	16(1)	15(1)	19(1)	-1(1)	6(1)	0(1)
C(13)	16(1)	13(1)	21(1)	0(1)	5(1)	1(1)
C(14)	13(1)	17(1)	19(1)	1(1)	2(1)	1(1)
C(15)	20(1)	21(1)	22(1)	-7(1)	4(1)	-4(1)
C(16)	23(1)	15(1)	27(1)	2(1)	10(1)	0(1)
C(17)	27(1)	21(1)	19(1)	-3(1)	10(1)	-1(1)
C(18)	25(1)	13(1)	30(1)	-1(1)	7(1)	0(1)
C(19)	15(1)	47(1)	17(1)	2(1)	5(1)	2(1)
C(20)	18(1)	71(1)	18(1)	2(1)	4(1)	6(1)
C(21)	23(1)	79(1)	23(1)	22(1)	10(1)	21(1)
C(22)	26(1)	55(1)	35(1)	26(1)	17(1)	19(1)
C(23)	21(1)	37(1)	30(1)	15(1)	12(1)	10(1)

Table 13.68. Hydrogen coordinates (x 10^4) and isotropic displacement parameters ($Å^2$x 10^{3}) for **42**.

	x	y	z	U(eq)
H(8A)	1535	-2413	3615	39
H(8B)	668	-1405	3282	39
H(8C)	1025	-1955	4293	39
H(5A)	3283(11)	2060(20)	5110(11)	25(4)
H(6A)	2579(13)	4770(20)	4099(13)	44(5)
H(6B)	1600(13)	4630(20)	3551(13)	39(5)
H(6C)	1876(13)	4740(30)	4560(14)	49(6)
H(7A)	367(16)	1090(30)	2635(17)	61(7)
H(7B)	556(14)	2830(30)	2774(15)	56(6)
H(7C)	134(14)	1990(30)	3349(14)	51(6)
H(9A)	3574(13)	-920(20)	5568(13)	34(5)
H(9B)	3103(11)	-2200(20)	4856(12)	33(5)
H(9C)	2718(12)	-1730(20)	5613(12)	37(5)
H(14A)	4320(9)	-317(19)	4497(10)	18(4)
H(15A)	4622(10)	2720(20)	5006(11)	25(4)
H(15B)	4165(12)	4000(20)	4331(12)	34(5)
H(15C)	5129(12)	3420(20)	4429(12)	34(5)
H(16A)	3587(12)	3560(20)	1776(13)	32(4)
H(16B)	3836(12)	4370(20)	2655(12)	34(5)
H(16C)	4518(14)	3770(20)	2258(13)	43(5)
H(17A)	4096(13)	460(20)	1236(13)	41(5)
H(17B)	3109(13)	760(20)	1096(13)	38(5)
H(17C)	3479(12)	-900(20)	1317(13)	36(5)
H(18A)	3784(14)	-2900(30)	3498(15)	55(6)
H(18B)	4281(14)	-2860(30)	2839(14)	52(6)
H(18C)	3287(14)	-2670(20)	2524(14)	50(6)
H(20A)	642(12)	990(20)	338(12)	29(4)
H(21A)	438(13)	3730(20)	-62(14)	42(5)
H(22A)	1224(13)	5620(20)	922(14)	42(5)
H(23A)	2233(11)	4730(20)	2306(11)	28(4)

13.24. Crystallographic Data for $[(C_5Me_4H)Sc]_3[SePh]_3$, 43

X-ray Data Collection, Structure Solution and Refinement for **43**.

A yellow crystal of approximate dimensions 0.32 x 0.37 x 0.41 mm was mounted on a glass fiber and transferred to a Bruker SMART APEX II diffractometer. The APEX2[1] program package was used to determine the unit-cell parameters and for data collection (20 sec/frame scan time for a sphere of diffraction data). The raw frame data was processed using SAINT[2] and SADABS[3] to yield the reflection data file. Subsequent calculations were carried out using the SHELXTL[4] program. The diffraction symmetry was 2/*m* and the systematic absences were consistent with the monoclinic space group $P2_1/c$ that was later determined to be correct.

The structure was solved by direct methods and refined on F^2 by full-matrix least-squares techniques. The analytical scattering factors[5] for neutral atoms were used throughout the analysis. Hydrogen atoms were included using a riding model. Carbon atoms C(19)-C(27) and C(46)-C(51) were disordered and included using multiple components, partial site-occupancy-factors and isotropic thermal parameters.

At convergence, wR2 = 0.1113 and Goof = 1.025 for 640 variables refined against 14236 data (0.74Å), R1 = 0.0434 for those 11110 data with I > 2.0σ(I).

References

1. APEX2 Version 2.2-0,. Bruker AXS, Inc.; Madison, WI 2007.
2. SAINT Version 7.46a, Bruker AXS, Inc.; Madison, WI 2007.
3. Sheldrick, G. M. SADABS, Version 2008/1, Bruker AXS, Inc.; Madison, WI 2008.
4. Sheldrick, G. M. SHELXTL, Version 2008/3, Bruker AXS, Inc.; Madison, WI 2008.
5. International Tables for X-Ray Crystallography 1992, Vol. C., Dordrecht: Kluwer Academic Publishers.

Table 13.69. Atomic coordinates (x 10^4) and equivalent isotropic displacement parameters ($Å^2$x 10^3) for **43**. U(eq) is defined as one third of the trace of the orthogonalized U^{ij} tensor.

	x	y	z	U(eq)
Sc(1)	4367(1)	4672(1)	2316(1)	39(1)
Sc(2)	1897(1)	3537(1)	2460(1)	34(1)
Sc(3)	1914(1)	5142(1)	3322(1)	38(1)
Se(1)	4037(1)	3506(1)	2632(1)	39(1)
Se(2)	2751(1)	4198(1)	1511(1)	38(1)
Se(3)	2064(1)	3901(1)	3704(1)	32(1)
Se(4)	591(1)	4491(1)	2560(1)	38(1)
Se(5)	4042(1)	4919(1)	3558(1)	40(1)
Se(6)	2946(1)	5601(1)	2317(1)	34(1)
C(1)	6278(3)	4636(3)	2513(2)	58(1)
C(2)	6082(3)	4379(3)	1906(2)	61(2)
C(3)	5632(4)	4842(3)	1502(2)	61(2)
C(4)	5572(4)	5381(3)	1854(3)	59(1)
C(5)	5974(3)	5251(3)	2478(2)	58(1)
C(6)	6795(4)	4324(3)	3086(3)	69(2)
C(7)	6446(4)	3770(3)	1718(3)	79(2)
C(8)	5408(4)	4780(3)	795(2)	74(2)
C(9)	5297(4)	5999(3)	1605(3)	73(2)
C(10)	1940(4)	2436(2)	2349(3)	57(1)
C(11)	1085(4)	2562(2)	2702(3)	57(1)
C(12)	307(4)	2890(2)	2322(3)	59(1)
C(13)	706(5)	2953(2)	1746(3)	61(2)

C(14)	1716(5)	2673(2)	1758(3)	71(2)
C(15)	2861(5)	2049(3)	2589(4)	83(2)
C(16)	951(5)	2317(3)	3340(3)	76(2)
C(17)	-785(4)	3054(3)	2468(4)	90(2)
C(18)	154(6)	3235(3)	1167(3)	95(3)
C(19)	1847(6)	5643(4)	4336(3)	30(2)
C(20)	1635(7)	6098(4)	3850(4)	44(2)
C(21)	631(7)	5961(4)	3507(3)	32(2)
C(22)	238(7)	5477(4)	3793(4)	41(2)
C(23)	933(6)	5269(4)	4278(4)	42(2)
C(24)	2651(7)	5612(4)	4841(4)	60(2)
C(25)	2307(9)	6648(5)	3752(5)	68(3)
C(26)	-16(9)	6256(5)	3035(5)	56(3)
C(27)	-863(10)	5270(7)	3619(6)	89(4)
C(19B)	1862(11)	6247(7)	3673(7)	58(3)
C(20B)	970(10)	6063(5)	3552(5)	37(3)
C(21B)	676(11)	5561(6)	4004(6)	56(3)
C(22B)	1518(11)	5498(6)	4366(5)	44(3)
C(23B)	2293(11)	5918(6)	4158(6)	59(3)
C(24B)	2336(12)	6796(7)	3356(7)	70(4)
C(25B)	312(12)	6409(7)	3035(7)	56(3)
C(26B)	-361(11)	5274(6)	4078(7)	65(4)
C(27B)	1731(11)	5101(6)	4949(6)	65(4)
C(28)	4868(3)	3152(2)	3332(2)	48(1)
C(29)	5519(4)	2676(3)	3194(3)	64(1)
C(30)	6211(4)	2437(3)	3664(4)	80(2)
C(31)	6252(4)	2675(3)	4262(3)	77(2)
C(32)	5601(4)	3137(3)	4404(3)	64(2)
C(33)	4896(4)	3378(2)	3942(2)	50(1)
C(34)	3168(5)	3678(2)	844(2)	56(1)
C(35)	4067(5)	3338(3)	884(2)	63(1)
C(36)	4371(6)	3027(3)	358(3)	82(2)
C(37)	3757(7)	3029(3)	-199(3)	107(3)
C(38)	2782(7)	3328(3)	-226(3)	105(3)
C(39)	2487(6)	3658(3)	296(2)	79(2)
C(40)	891(3)	3646(2)	4170(2)	36(1)
C(41)	1132(4)	3386(2)	4749(2)	54(1)
C(42)	336(5)	3160(3)	5104(2)	68(2)
C(43)	-677(4)	3185(2)	4877(3)	61(1)
C(44)	-911(4)	3452(3)	4312(3)	68(2)
C(45)	-125(3)	3693(2)	3953(2)	57(1)
C(46)	-173(3)	4785(2)	1806(2)	34(2)
C(47)	-1229(3)	4884(2)	1870(2)	66(3)
C(48)	-1814(11)	5123(7)	1328(7)	84(4)
C(49)	-1447(8)	5256(5)	845(5)	59(3)
C(50)	-474(9)	5122(6)	777(6)	68(3)
C(51)	231(4)	4919(3)	1249(3)	54(3)
C(46B)	-197(4)	4945(3)	1916(3)	26(2)
C(47B)	-1213(4)	5120(3)	2013(3)	40(3)
C(48B)	-1797(8)	5411(5)	1545(5)	44(3)
C(49B)	-1348(15)	5553(10)	985(10)	95(6)
C(50B)	-248(12)	5382(8)	852(7)	66(4)
C(51B)	279(9)	5063(7)	1331(6)	48(3)
C(52)	4860(4)	5613(2)	3840(2)	45(1)
C(53)	5548(4)	5522(2)	4360(2)	51(1)
C(54)	6189(4)	5990(3)	4586(2)	62(1)
C(55)	6141(5)	6543(3)	4295(3)	67(2)
C(56)	5448(5)	6638(3)	3779(2)	67(2)
C(57)	4805(5)	6172(2)	3551(2)	61(2)
C(58)	2342(3)	5897(2)	1519(2)	42(1)
C(59)	1594(4)	6340(3)	1511(2)	66(2)
C(60)	1226(6)	6584(4)	933(3)	102(3)

C(61)	1599(6)	6395(4)	381(3)	96(2)
C(62)	2327(5)	5956(3)	390(2)	68(2)
C(63)	2708(4)	5703(2)	954(2)	48(1)

Table 13.70. Anisotropic displacement parameters ($Å^2 x 10^3$) for **43**. The anisotropic displacement factor exponent takes the form: $-2\pi^2[h^2 a^{*2} U^{11} + ... + 2 h k a^* b^* U^{12}]$

	U^{11}	U^{22}	U^{33}	U^{23}	U^{13}	U^{12}
Sc(1)	33(1)	50(1)	33(1)	9(1)	2(1)	-2(1)
Sc(2)	39(1)	33(1)	29(1)	-3(1)	-7(1)	-3(1)
Sc(3)	55(1)	36(1)	22(1)	-1(1)	2(1)	7(1)
Se(1)	39(1)	45(1)	34(1)	4(1)	4(1)	5(1)
Se(2)	51(1)	40(1)	24(1)	-4(1)	4(1)	9(1)
Se(3)	35(1)	36(1)	25(1)	3(1)	1(1)	-2(1)
Se(4)	37(1)	43(1)	33(1)	8(1)	1(1)	1(1)
Se(5)	47(1)	41(1)	30(1)	7(1)	-9(1)	-14(1)
Se(6)	41(1)	36(1)	25(1)	3(1)	-4(1)	-6(1)
C(1)	31(2)	89(4)	54(3)	29(3)	-1(2)	-4(2)
C(2)	30(2)	99(4)	54(3)	22(3)	12(2)	14(2)
C(3)	33(2)	105(5)	45(3)	29(3)	14(2)	10(3)
C(4)	35(2)	85(4)	58(3)	30(3)	5(2)	-8(2)
C(5)	34(2)	85(4)	55(3)	18(3)	2(2)	-17(2)
C(6)	35(2)	110(5)	60(3)	35(3)	-5(2)	-7(3)
C(7)	44(3)	125(6)	70(4)	19(4)	15(3)	30(3)
C(8)	52(3)	126(6)	45(3)	26(3)	16(2)	15(3)
C(9)	44(3)	86(4)	90(4)	43(3)	1(3)	-20(3)
C(10)	60(3)	38(2)	71(3)	-14(2)	-16(3)	-3(2)
C(11)	67(3)	36(2)	64(3)	6(2)	-26(3)	-17(2)
C(12)	53(3)	43(3)	76(4)	3(2)	-26(3)	-16(2)
C(13)	76(4)	36(2)	67(3)	-11(2)	-37(3)	-2(2)
C(14)	92(4)	53(3)	65(3)	-31(3)	-18(3)	-2(3)
C(15)	69(4)	45(3)	130(6)	-17(3)	-27(4)	11(3)
C(16)	85(4)	52(3)	91(5)	7(3)	7(4)	-8(3)
C(17)	50(3)	69(4)	148(7)	-3(4)	-17(4)	-20(3)
C(18)	135(6)	71(4)	72(4)	-3(3)	-62(4)	-10(4)
C(28)	36(2)	52(3)	53(3)	17(2)	-4(2)	-3(2)
C(29)	52(3)	61(3)	78(4)	11(3)	-4(3)	10(2)
C(30)	49(3)	73(4)	114(6)	22(4)	-11(3)	12(3)
C(31)	49(3)	87(5)	92(5)	42(4)	-26(3)	-12(3)
C(32)	52(3)	76(4)	62(3)	32(3)	-14(2)	-23(3)
C(33)	44(2)	57(3)	50(3)	20(2)	-3(2)	-11(2)
C(34)	95(4)	48(3)	27(2)	-4(2)	13(2)	24(3)
C(35)	78(4)	70(3)	42(3)	-14(2)	15(2)	18(3)
C(36)	116(5)	80(4)	52(3)	-8(3)	29(3)	39(4)
C(37)	200(9)	89(5)	33(3)	-2(3)	22(4)	76(6)
C(38)	190(8)	91(5)	31(3)	-7(3)	-8(4)	61(5)
C(39)	128(6)	73(4)	34(2)	-4(2)	-5(3)	45(4)
C(40)	44(2)	31(2)	32(2)	1(2)	12(2)	-4(2)
C(41)	65(3)	62(3)	33(2)	6(2)	-3(2)	-21(2)
C(42)	96(4)	76(4)	32(2)	7(2)	14(3)	-29(3)
C(43)	69(3)	51(3)	67(3)	5(3)	35(3)	-10(3)
C(44)	47(3)	65(3)	96(4)	34(3)	24(3)	6(2)
C(45)	45(3)	61(3)	66(3)	29(3)	12(2)	5(2)
C(52)	52(3)	51(3)	29(2)	3(2)	-8(2)	-24(2)
C(53)	58(3)	61(3)	32(2)	5(2)	-11(2)	-17(2)
C(54)	64(3)	77(4)	43(3)	-3(3)	-19(2)	-21(3)
C(55)	70(4)	70(4)	57(3)	-3(3)	-17(3)	-33(3)
C(56)	91(4)	60(3)	48(3)	8(2)	-18(3)	-42(3)
C(57)	83(4)	63(3)	36(2)	14(2)	-21(2)	-34(3)

C(58)	41(2)	56(3)	27(2)	8(2)	-5(2)	-4(2)
C(59)	61(3)	96(4)	42(3)	10(3)	3(2)	26(3)
C(60)	99(5)	146(7)	60(4)	26(4)	-6(4)	66(5)
C(61)	105(5)	137(7)	43(3)	29(4)	-14(3)	34(5)
C(62)	82(4)	95(4)	28(2)	15(3)	3(2)	4(3)
C(63)	49(3)	63(3)	33(2)	7(2)	5(2)	-3(2)

Table 13.71. Hydrogen coordinates (x 10^4) and isotropic displacement parameters ($Å^2$x 10^{3}) for **43**.

	x	y	z	U(eq)
H(5A)	6028	5531	2818	70
H(6A)	7544	4283	3032	103
H(6B)	6486	3923	3131	103
H(6C)	6690	4565	3464	103
H(7A)	7210	3765	1731	118
H(7B)	6164	3678	1288	118
H(7C)	6203	3465	2010	118
H(8A)	6064	4801	584	110
H(8B)	4946	5109	642	110
H(8C)	5069	4390	701	110
H(9A)	5905	6178	1421	110
H(9B)	5084	6255	1951	110
H(9C)	4721	5967	1280	110
H(14A)	2155	2655	1415	85
H(15A)	2668	1621	2560	124
H(15B)	3055	2153	3031	124
H(15C)	3453	2126	2332	124
H(16A)	759	1888	3308	114
H(16B)	400	2542	3536	114
H(16C)	1607	2358	3600	114
H(17A)	-1282	2820	2195	135
H(17B)	-899	3487	2392	135
H(17C)	-888	2961	2912	135
H(18A)	-422	2973	1011	143
H(18B)	648	3284	837	143
H(18C)	-121	3633	1277	143
H(23)	816	4926	4534	50
H(24A)	2540	5931	5150	89
H(24B)	3334	5666	4668	89
H(24C)	2626	5216	5048	89
H(25A)	2951	6619	4025	102
H(25B)	1926	7015	3859	102
H(25C)	2480	6668	3309	102
H(26A)	-191	5974	2687	84
H(26B)	355	6606	2874	84
H(26C)	-657	6393	3217	84
H(27A)	-1358	5554	3790	134
H(27B)	-968	4866	3795	134
H(27C)	-979	5255	3158	134
H(23B)	2989	5955	4334	71
H(24D)	2232	6756	2896	104
H(24E)	3085	6816	3477	104
H(24F)	1996	7166	3492	104
H(25D)	-180	6676	3233	84
H(25E)	-74	6119	2759	84
H(25F)	773	6651	2784	84
H(26D)	-267	4900	4324	97

H(26E)	-692	5179	3660	97
H(26F)	-805	5553	4298	97
H(27D)	1498	5311	5322	98
H(27E)	2480	5018	5009	98
H(27F)	1350	4718	4892	98
H(29A)	5495	2513	2779	77
H(30A)	6654	2109	3569	95
H(31A)	6734	2517	4578	93
H(32A)	5629	3296	4821	77
H(33A)	4437	3695	4045	60
H(35A)	4479	3316	1272	76
H(36A)	5010	2810	382	98
H(37A)	3987	2832	-563	128
H(38A)	2329	3303	-597	125
H(39A)	1838	3866	280	94
H(41A)	1839	3359	4909	64
H(42A)	505	2988	5508	81
H(43A)	-1213	3017	5111	73
H(44A)	-1619	3478	4154	82
H(45A)	-304	3888	3562	68
H(47A)	-1546	4798	2252	80
H(48A)	-2543	5179	1355	101
H(49A)	-1855	5454	518	71
H(50A)	-227	5168	367	82
H(51A)	954	4877	1188	65
H(47B)	-1502	5038	2406	48
H(48B)	-2502	5515	1601	53
H(49B)	-1755	5770	671	114
H(50B)	56	5485	470	79
H(51B)	963	4918	1275	58
H(53A)	5582	5138	4564	61
H(54A)	6663	5926	4943	75
H(55A)	6585	6862	4447	80
H(56A)	5411	7023	3580	81
H(57A)	4329	6238	3196	74
H(59A)	1332	6479	1894	79
H(60A)	703	6889	925	122
H(61A)	1348	6572	-9	115
H(62A)	2581	5818	4	82
H(63A)	3224	5396	955	58

13.25. Crystallographic Data for {[$(C_5Me_5)Sc)_4$](μ_3-$Te)_4$}, 51

Table 13.72. Atomic coordinates (x 10^4) and equivalent isotropic displacement parameters ($Å^2$x 10^3) for **51**. U(eq) is defined as one third of the trace of the orthogonalized U^{ij} tensor.

	x	y	z	U(eq)
Sc(1)	8215(3)	4525(3)	2508(2)	17(1)
Sc(2)	9529(3)	6763(3)	2334(2)	25(1)
Sc(3)	6899(3)	7314(3)	3499(2)	16(1)
Sc(4)	6624(3)	7470(3)	1683(2)	32(1)
Te(1)	9300(2)	5335(2)	3575(1)	52(1)
Te(2)	8888(2)	5589(2)	1222(1)	64(1)
Te(3)	5636(1)	6151(2)	2722(1)	49(1)
Te(4)	7368(3)	8963(2)	2425(2)	86(1)

C(1)	8642(8)	2452(9)	3091(5)	30(4)
C(2)	7630(9)	2702(10)	2641(5)	29(4)
C(3)	8100(8)	2722(9)	1931(5)	32(4)
C(4)	9403(8)	2483(9)	1942(4)	31(4)
C(5)	9738(8)	2316(8)	2659(4)	27(4)
C(6)	8566(13)	2348(16)	3888(7)	63(7)
C(7)	6289(13)	2911(16)	2877(7)	76(9)
C(8)	7348(13)	2955(15)	1279(7)	52(6)
C(9)	10278(12)	2419(15)	1304(7)	53(6)
C(10)	11031(12)	2043(14)	2916(7)	41(5)
C(11)	10645(13)	8095(11)	1840(6)	61(7)
C(12)	11225(12)	6947(10)	1498(6)	52(6)
C(13)	11868(10)	6015(9)	2014(5)	32(4)
C(14)	11686(10)	6587(9)	2676(5)	29(4)
C(15)	10930(11)	7872(10)	2568(6)	51(6)
C(16)	9860(20)	9334(16)	1491(9)	86(10)
C(17)	11167(19)	6752(15)	722(9)	99(12)
C(18)	12614(15)	4656(13)	1884(7)	42(5)
C(19)	12205(16)	5942(13)	3371(7)	50(6)
C(20)	10505(18)	8833(15)	3128(8)	80(9)
C(21)	5027(12)	8042(11)	4329(7)	52(6)
C(22)	6003(12)	7172(12)	4727(7)	62(7)
C(23)	6935(12)	7653(12)	4782(7)	61(7)
C(24)	6534(12)	8819(12)	4418(7)	45(6)
C(25)	5355(11)	9060(11)	4137(6)	46(6)
C(26)	3847(18)	7908(18)	4141(11)	93(11)
C(27)	6042(19)	5951(18)	5038(11)	76(9)
C(28)	8139(19)	7032(19)	5162(12)	125(16)
C(29)	7239(18)	9657(18)	4342(11)	88(10)
C(30)	4586(18)	10199(18)	3711(11)	86(10)
C(31)	6084(13)	7795(12)	433(7)	56(7)
C(32)	5020(13)	7682(12)	806(7)	60(7)
C(33)	4450(13)	8716(13)	1244(7)	62(7)
C(34)	5160(13)	9467(13)	1142(7)	49(6)
C(35)	6171(13)	8898(13)	641(7)	63(7)
C(36)	6970(20)	6900(19)	-92(12)	95(12)
C(37)	4570(20)	6646(19)	747(11)	93(11)
C(38)	3290(20)	8970(20)	1733(11)	93(11)
C(39)	4890(20)	10660(20)	1503(12)	140(20)
C(40)	7160(20)	9380(20)	376(11)	90(11)

Table 13.73. Anisotropic displacement parameters ($Å^2 x\ 10^3$) for **51**. The anisotropic displacement factor exponent takes the form: $-2\pi^2[\ h^2\ a^{*2}U^{11} + ...\ + 2\ h\ k\ a^*\ b^*\ U^{12}\ ]$

	U^{11}	U^{22}	U^{33}	U^{23}	U^{13}	U^{12}
Sc(1)	13(2)	17(2)	22(2)	-4(1)	7(1)	-6(1)
Sc(2)	22(2)	9(2)	42(2)	-13(1)	-11(2)	0(1)
Sc(3)	15(2)	15(2)	20(2)	-2(1)	0(1)	-8(1)
Sc(4)	23(2)	21(2)	54(2)	-28(2)	28(2)	-13(2)
Te(1)	30(1)	37(1)	86(1)	-17(1)	-4(1)	-8(1)
Te(2)	58(1)	55(1)	76(1)	-20(1)	12(1)	-20(1)
Te(3)	26(1)	54(1)	68(1)	-23(1)	6(1)	-15(1)
Te(4)	86(2)	66(2)	100(2)	-18(1)	11(1)	-24(1)

13.26. Crystallographic Data for $[(C_5Me_4H)_2Sc(\mu\text{-}\eta^1:\eta^2\text{-}ON{=}NC_3H_5)]_2$, 53

Table 13.74. Atomic coordinates (x 10^4) and equivalent isotropic displacement parameters ($Å^2$x 10^3) for **53**. U(eq) is defined as one third of the trace of the orthogonalized U^{ij} tensor.

	x	y	z	U(eq)
Sc(1)	10079(1)	7554(1)	6624(1)	25(1)
O(1)	8997(2)	7373(2)	6992(1)	32(1)
N(1)	10857(2)	7418(3)	7495(1)	28(1)
N(2)	11487(2)	7374(3)	7291(1)	33(1)
C(1)	10624(3)	6308(4)	6062(2)	36(1)
C(2)	10515(3)	5687(3)	6484(2)	36(1)
C(3)	9622(3)	5659(4)	6452(2)	37(1)
C(4)	9156(3)	6257(4)	6010(2)	38(1)
C(5)	9786(3)	6639(4)	5770(2)	36(1)
C(6)	11484(4)	6488(5)	5926(2)	53(1)
C(7)	11236(4)	5067(4)	6861(2)	54(1)
C(8)	9203(4)	5013(5)	6794(2)	55(1)
C(9)	8175(3)	6386(5)	5823(2)	58(2)
C(10)	9332(3)	9301(4)	6484(2)	37(1)
C(11)	9418(3)	9035(3)	5982(2)	35(1)
C(12)	10326(3)	9014(3)	6007(2)	34(1)
C(13)	10808(3)	9256(4)	6532(2)	38(1)
C(14)	10192(3)	9421(3)	6826(2)	37(1)
C(15)	8484(4)	9511(5)	6610(2)	51(1)
C(16)	8671(3)	8973(5)	5479(2)	50(1)
C(17)	10703(4)	8954(4)	5537(2)	50(1)
C(18)	11779(4)	9425(5)	6722(2)	59(2)
C(19)	12392(3)	7298(5)	7652(2)	47(1)
C(20)	13004(6)	6905(9)	7337(4)	34(2)
C(21)	13787(9)	7368(11)	7408(5)	57(3)
C(20B)	13078(7)	7380(10)	7354(4)	44(2)
C(21B)	13781(9)	6896(12)	7453(6)	61(3)
C(22)	9057(5)	13184(7)	5634(5)	89(1)
C(23)	9786(6)	13710(7)	5568(6)	89(1)
C(24)	10613(5)	13246(8)	5715(5)	89(1)
C(25)	10710(5)	12254(9)	5928(6)	89(1)
C(26)	9981(7)	11728(7)	5994(6)	89(1)
C(27)	9155(6)	12192(7)	5847(5)	89(1)
C(28)	8142(6)	13699(10)	5471(6)	89(1)
C(29)	9374(5)	12704(7)	5763(5)	89(1)
C(30)	9651(6)	13629(7)	5592(6)	89(1)
C(31)	10528(6)	13757(7)	5600(6)	89(1)
C(32)	11129(5)	12961(9)	5779(5)	89(1)
C(33)	10852(6)	12036(8)	5950(6)	89(1)
C(34)	9975(6)	11908(7)	5942(6)	89(1)
C(35)	8393(5)	12541(10)	5727(7)	89(1)

Table 13.75. Anisotropic displacement parameters ($Å^2$x 10^3) for **53**. The anisotropic displacement factor exponent takes the form: $-2\pi^2[\, h^2\, a^{*2}U^{11} + \ldots + 2\, h\, k\, a^*\, b^*\, U^{12}\,]$

	U^{11}	U^{22}	U^{33}	U^{23}	U^{13}	U^{12}
Sc(1)	22(1)	31(1)	21(1)	0(1)	6(1)	2(1)
O(1)	25(1)	48(2)	21(1)	-4(1)	5(1)	-3(1)
N(1)	25(2)	33(2)	27(2)	3(1)	6(1)	3(1)
N(2)	26(2)	47(2)	27(2)	2(2)	8(1)	4(2)
C(1)	45(3)	37(2)	30(2)	-3(2)	15(2)	7(2)

C(2)	49(3)	34(2)	28(2)	-1(2)	14(2)	10(2)
C(3)	47(3)	35(2)	31(2)	-5(2)	12(2)	-6(2)
C(4)	43(3)	41(2)	28(2)	-10(2)	6(2)	-8(2)
C(5)	48(3)	40(2)	19(2)	-6(2)	9(2)	1(2)
C(6)	51(3)	72(4)	45(3)	9(3)	27(2)	22(3)
C(7)	73(4)	53(3)	39(3)	9(2)	20(3)	30(3)
C(8)	69(4)	57(3)	41(3)	5(2)	18(3)	-16(3)
C(9)	43(3)	87(4)	34(3)	-3(3)	-2(2)	-19(3)
C(10)	38(2)	37(2)	36(2)	8(2)	12(2)	11(2)
C(11)	40(2)	35(2)	28(2)	9(2)	7(2)	8(2)
C(12)	41(2)	35(2)	30(2)	7(2)	14(2)	0(2)
C(13)	37(2)	36(2)	42(2)	3(2)	11(2)	-9(2)
C(14)	47(3)	33(2)	32(2)	-2(2)	14(2)	-2(2)
C(15)	52(3)	61(3)	43(3)	10(2)	16(2)	28(3)
C(16)	48(3)	66(3)	32(2)	10(2)	2(2)	14(3)
C(17)	64(3)	55(3)	39(3)	9(2)	27(2)	-2(3)
C(18)	48(3)	70(4)	58(3)	0(3)	16(3)	-27(3)
C(19)	25(2)	79(4)	38(2)	3(2)	9(2)	11(2)

Table 13.76. Hydrogen coordinates (x 10^4) and isotropic displacement parameters ($Å^2$x 10^{3}) for **53**.

	x	y	z	U(eq)
H(5)	9661	7055	5459	43
H(6A)	11364	6831	5580	80
H(6B)	11773	5822	5911	80
H(6C)	11871	6925	6199	80
H(7A)	11114	5017	7207	81
H(7B)	11805	5412	6905	81
H(7C)	11257	4372	6717	81
H(8A)	9063	4326	6635	83
H(8B)	8660	5348	6820	83
H(8C)	9613	4944	7150	83
H(9A)	8011	6726	5475	86
H(9B)	7980	6811	6079	86
H(9C)	7892	5706	5794	86
H(14)	10335	9586	7193	44
H(15A)	8297	10223	6509	77
H(15B)	8566	9420	6992	77
H(15C)	8032	9029	6412	77
H(16A)	8153	8670	5558	76
H(16B)	8847	8539	5220	76
H(16C)	8527	9669	5332	76
H(17A)	10673	9638	5372	75
H(17B)	10360	8459	5277	75
H(17C)	11318	8727	5658	75
H(18A)	12080	8901	6565	88
H(18B)	11976	9369	7110	88
H(18C)	11920	10115	6614	88
H(19A)	12402	6817	7947	57
H(19B)	12592	7986	7805	57
H(19C)	12477	7827	7918	57
H(19D)	12463	6639	7827	57
H(20A)	12834	6345	7096	41
H(21A)	13950	7928	7650	68
H(21B)	14180	7136	7216	68
H(20B)	12960	7847	7063	53
H(21C)	13928	6421	7741	73
H(21D)	14174	7001	7242	73

H(23A)	9720	14388	5422	106
H(24A)	11111	13605	5669	106
H(25A)	11275	11937	6028	106
H(26A)	10047	11050	6140	106
H(27A)	8656	11832	5892	106
H(28A)	8190	14389	5328	133
H(28B)	7918	13759	5783	133
H(28C)	7736	13277	5200	133
H(30A)	9240	14174	5470	106
H(31A)	10717	14389	5483	106
H(32A)	11728	13048	5784	106
H(33A)	11262	11491	6072	106
H(34A)	9786	11276	6059	106
H(35A)	8063	13174	5594	133
H(35B)	8333	12377	6080	133
H(35C)	8159	11969	5483	133

13.27. Crystallographic Data for $[(C_5Me_4H)_2Y(\mu\text{-}\eta^1\text{:}\eta^2\text{-}ON{=}NC_3H_5)]_2$, 54

X-ray Data Collection, Structure Solution and Refinement for **54**

A colorless crystal of approximate dimensions 0.16 x 0.19 x 0.22 mm was mounted on a glass fiber and transferred to a Bruker SMART APEX II diffractometer. The APEX2[1] program package was used to determine the unit-cell parameters and for data collection (30 sec/frame scan time for a sphere of diffraction data). The raw frame data was processed using SAINT[2] and SADABS[3] to yield the reflection data file. Subsequent calculations were carried out using the SHELXTL[4] program. The diffraction symmetry was 2/*m* and the systematic absences were consistent with the monoclinic space groups *Cc* and *C*2/*c*. It was later determined that space group *C*2/*c* was correct.

The structure was solved by direct methods and refined on F^2 by full-matrix least-squares techniques. The analytical scattering factors[5] for neutral atoms were used throughout the analysis. Hydrogen atoms were included using a riding model. The molecule was located about a two-fold rotation axis. There were two molecules of toluene solvent (related by two-fold rotation) present per formula unit. Carbon atoms C(20), C(21) and the solvent were disordered and included using multiple components with partial site-occupancy-factors (0.50)

At convergence, wR2 = 0.0915 and Goof = 1.051 for 310 variables refined against 6227 data (0.76Å), R1 = 0.0383 for those 5155 data with I > 2.0σ(I).

References

1. APEX2 Version 2008.3-0, Bruker AXS, Inc.; Madison, WI 2008.
2. SAINT Version 7.53a, Bruker AXS, Inc.; Madison, WI 2007.
3. Sheldrick, G. M. SADABS, Version 2008/1, Bruker AXS, Inc.; Madison, WI 2008.
4. Sheldrick, G. M. SHELXTL, Version 2008/3, Bruker AXS, Inc.; Madison, WI 2008.
5. International Tables for X-Ray Crystallography 1992, Vol. C., Dordrecht: Kluwer Academic Publishers.

Table 13.77. Atomic coordinates (x 10^4) and equivalent isotropic displacement parameters ($Å^2$x 10^3) for **54**. U(eq) is defined as one third of the trace of the orthogonalized U^{ij} tensor.

	x	y	z	U(eq)
Y(1)	114(1)	2444(1)	1609(1)	15(1)
O(1)	-1084(1)	2249(2)	1965(1)	33(1)
N(1)	917(1)	2306(2)	2526(1)	21(1)
N(2)	1546(1)	2288(2)	2309(1)	25(1)
C(1)	688(2)	1146(2)	1031(1)	28(1)
C(2)	574(2)	550(2)	1455(1)	33(1)
C(3)	-344(2)	506(2)	1416(1)	39(1)
C(4)	-810(2)	1071(2)	971(1)	39(1)
C(5)	-166(2)	1457(2)	733(1)	27(1)
C(6)	1555(2)	1346(3)	901(1)	47(1)
C(7)	1295(3)	-13(3)	1846(1)	59(1)
C(8)	-758(3)	-111(3)	1766(1)	68(1)
C(9)	-1805(2)	1196(4)	780(1)	79(2)
C(10)	-658(3)	4238(2)	1464(1)	51(1)
C(11)	-567(2)	3973(2)	961(1)	42(1)
C(12)	348(2)	3967(2)	987(1)	34(1)
C(13)	837(3)	4221(2)	1508(1)	43(1)
C(14)	205(3)	4381(2)	1799(1)	49(1)
C(15)	-1530(3)	4411(4)	1592(1)	92(2)
C(16)	-1329(2)	3873(3)	469(1)	60(1)
C(17)	740(2)	3884(2)	526(1)	43(1)
C(18)	1823(3)	4385(3)	1696(1)	77(2)
C(19)	2468(2)	2218(3)	2651(1)	50(1)
C(20)	3084(3)	1806(5)	2305(2)	25(1)
C(20B)	3131(3)	2417(5)	2346(2)	28(1)
C(21)	3800(5)	2331(6)	2310(3)	37(2)
C(21B)	3827(5)	1855(6)	2426(3)	38(2)
C(22)	369(4)	8028(4)	711(2)	28(1)
C(23)	-441(4)	8517(4)	532(2)	24(1)
C(24)	-1227(4)	8063(4)	540(2)	31(1)
C(25)	-1218(4)	7093(5)	740(2)	38(1)
C(26)	-390(4)	6608(5)	935(2)	38(1)
C(27)	426(5)	7054(5)	926(2)	35(1)
C(28)	1227(4)	8516(5)	695(3)	41(1)
C(29)	-794(4)	8074(4)	688(2)	28(1)
C(30)	-627(5)	7110(5)	904(3)	42(1)
C(31)	202(5)	6737(6)	1012(3)	41(2)
C(32)	939(5)	7277(5)	921(2)	41(1)
C(33)	753(4)	8220(4)	706(2)	29(1)
C(34)	-92(4)	8613(4)	589(2)	23(1)
C(35)	-1728(4)	8498(5)	554(3)	44(2)

Table 13.78. Anisotropic displacement parameters ($Å^2$x 10^3) for **54**. The anisotropic displacement factor exponent takes the form: $-2\pi^2[h^2 a^{*2}U^{11} + ... + 2 h k a^* b^* U^{12}]$

	U^{11}	U^{22}	U^{33}	U^{23}	U^{13}	U^{12}
Y(1)	14(1)	21(1)	12(1)	0(1)	3(1)	3(1)
O(1)	16(1)	71(1)	12(1)	-6(1)	3(1)	2(1)
N(1)	15(1)	32(1)	14(1)	3(1)	3(1)	-1(1)
N(2)	13(1)	46(1)	16(1)	4(1)	4(1)	1(1)
C(1)	48(2)	22(1)	20(1)	2(1)	19(1)	13(1)
C(2)	65(2)	18(1)	20(1)	2(1)	20(1)	9(1)
C(3)	67(2)	36(2)	15(1)	-8(1)	13(1)	-27(1)

C(4)	46(2)	51(2)	16(1)	-9(1)	5(1)	-27(1)
C(5)	42(2)	26(1)	13(1)	-4(1)	8(1)	-4(1)
C(6)	55(2)	63(2)	35(2)	22(2)	31(2)	37(2)
C(7)	116(3)	44(2)	29(2)	19(1)	39(2)	49(2)
C(8)	89(3)	87(3)	21(1)	5(2)	3(2)	-66(2)
C(9)	48(2)	156(5)	24(2)	-1(2)	-6(2)	-58(3)
C(10)	92(3)	46(2)	19(1)	12(1)	20(2)	49(2)
C(11)	67(2)	39(2)	18(1)	8(1)	12(1)	35(2)
C(12)	63(2)	20(1)	20(1)	4(1)	14(1)	4(1)
C(13)	84(2)	22(1)	24(1)	1(1)	15(2)	-14(1)
C(14)	110(3)	18(1)	18(1)	1(1)	17(2)	13(2)
C(15)	125(4)	127(4)	34(2)	30(2)	37(2)	112(3)
C(16)	66(2)	90(3)	20(1)	14(2)	8(2)	53(2)
C(17)	73(2)	34(2)	28(1)	4(1)	23(2)	-6(2)
C(18)	112(4)	80(3)	37(2)	-4(2)	16(2)	-76(3)
C(19)	13(1)	117(3)	21(1)	13(2)	3(1)	0(2)
C(20)	18(3)	29(3)	26(3)	-7(2)	5(2)	4(2)
C(20B)	19(3)	41(3)	26(3)	5(3)	7(2)	1(3)
C(21)	22(3)	47(4)	48(4)	4(3)	18(3)	3(3)
C(21B)	23(3)	48(4)	46(4)	1(3)	15(3)	1(3)

Table 13.79. Hydrogen coordinates (x 10^4) and isotropic displacement parameters (Å^{2}x 10^{3}) for **54**.

	x	y	z	U(eq)
H(5A)	-304	1770	376	32
H(6A)	1784	714	796	71
H(6B)	1991	1622	1211	71
H(6C)	1455	1834	612	71
H(7A)	1244	-736	1765	89
H(7B)	1232	97	2201	89
H(7C)	1880	232	1829	89
H(8A)	-893	-790	1618	102
H(8B)	-1311	215	1791	102
H(8C)	-340	-159	2118	102
H(9A)	-2083	539	668	118
H(9B)	-1953	1666	482	118
H(9C)	-2030	1464	1065	118
H(14A)	343	4692	2157	59
H(15A)	-1760	5083	1469	138
H(15B)	-1436	4367	1973	138
H(15C)	-1963	3897	1417	138
H(16A)	-1506	4545	321	90
H(16B)	-1837	3548	554	90
H(16C)	-1139	3462	211	90
H(17A)	716	4544	355	65
H(17B)	397	3392	273	65
H(17C)	1363	3661	651	65
H(18A)	1972	5040	1568	116
H(18B)	2130	3847	1560	116
H(18C)	2013	4377	2081	116
H(19A)	2492	1753	2947	61
H(19B)	2678	2891	2796	61
H(19C)	2570	1553	2800	61
H(19D)	2548	2696	2933	61
H(20A)	2939	1205	2103	30
H(20B)	3039	2953	2098	34
H(21A)	3932	2930	2514	45

H(21B)	4186	2112	2109	45
H(21C)	3916	1321	2675	46
H(21D)	4254	1973	2235	46
H(23A)	-453	9185	399	28
H(24A)	-1777	8410	409	38
H(25A)	-1758	6765	746	45
H(26A)	-381	5950	1080	45
H(27A)	981	6717	1057	42
H(28A)	1138	9247	650	62
H(28B)	1420	8242	400	62
H(28C)	1685	8380	1025	62
H(30A)	-1096	6723	975	50
H(31A)	305	6077	1157	49
H(32A)	1523	6999	1004	49
H(33A)	1220	8610	636	35
H(34A)	-201	9267	437	28
H(35A)	-1957	8461	864	66
H(35B)	-2115	8103	267	66
H(35C)	-1719	9203	443	66

13.28. Crystallographic Data for $[(C_5Me_5)_2Y(\mu\text{-}\eta^1\text{:}\eta^2\text{-}ON{=}NC_3H_5)]_2$, 55

X-ray Data Collection, Structure Solution and Refinement for **55**.

A colorless crystal of approximate dimensions 0.31 x 0.31 x 0.43 mm was mounted on a glass fiber and transferred to a Bruker SMART APEX II diffractometer. The APEX2[1] program package was used to determine the unit-cell parameters and for data collection (20 sec/frame scan time for a sphere of diffraction data). The raw frame data was processed using SAINT[2] and SADABS[3] to yield the reflection data file. Subsequent calculations were carried out using the SHELXTL[4] program. The diffraction symmetry was 2/*m* and the systematic absences were consistent with the monoclinic space group $P2_1/n$ that was later determined to be correct.

The structure was solved by direct methods and refined on F^2 by full-matrix least-squares techniques. The analytical scattering factors[5] for neutral atoms were used throughout the analysis. Hydrogen atoms were included using a riding model. There were two molecules of toluene solvent present. Carbon atoms C(44), C(45) and C(46) were disordered and included using multiple components and partial site-occupancy-factors (0.50:0.50). One of the toluene molecules was also disordered (0.55:0.45) and included as above but with isotropic thermal parameters.

At convergence, wR2 = 0.0961 and Goof = 1.034 for 626 variables refined against 12296 data (0.78Å), R1 = 0.0361 for those 10126 data with I > 2.0σ(I).

References

1. APEX2 Version 2.2-0, Bruker AXS, Inc.; Madison, WI 2007.
2. SAINT Version 7.46a, Bruker AXS, Inc.; Madison, WI 2007.
3. Sheldrick, G. M. SADABS, Version 2008/1, Bruker AXS, Inc.; Madison, WI 2008.
4. Sheldrick, G. M. SHELXTL, Version 2008/3, Bruker AXS, Inc.; Madison, WI 2008.
5. International Tables for X-Ray Crystallography 1992, Vol. C., Dordrecht: Kluwer Academic Publishers.

Table 13.80. Atomic coordinates (x 10^4) and equivalent isotropic displacement parameters ($Å^2$x 10^3) for **55**. U(eq) is defined as one third of the trace of the orthogonalized U^{ij} tensor.

	x	y	z	U(eq)
Y(1)	640(1)	7258(1)	1523(1)	24(1)
Y(2)	-573(1)	7421(1)	3368(1)	23(1)
O(2)	778(1)	7519(1)	3000(1)	28(1)
O(1)	-716(1)	7217(1)	1884(1)	30(1)
N(1)	883(1)	7362(1)	2496(1)	25(1)
N(2)	1618(1)	7280(1)	2318(1)	27(1)
N(3)	-818(1)	7317(1)	2392(1)	26(1)
N(4)	-1549(1)	7409(2)	2572(1)	31(1)
C(1)	1010(2)	5377(2)	1512(1)	33(1)
C(2)	1591(1)	5820(2)	1170(1)	34(1)
C(3)	1151(2)	6139(2)	713(1)	35(1)
C(4)	283(1)	5941(2)	779(1)	33(1)
C(5)	197(1)	5455(2)	1266(1)	31(1)
C(6)	1269(2)	4803(2)	1988(1)	47(1)
C(7)	2536(2)	5795(2)	1245(1)	54(1)
C(8)	1576(2)	6388(2)	206(1)	50(1)
C(9)	-419(2)	6096(2)	375(1)	47(1)
C(10)	-612(2)	4989(2)	1427(1)	44(1)
C(11)	1164(2)	9066(2)	1553(1)	33(1)
C(12)	1440(2)	8722(2)	1057(1)	34(1)
C(13)	715(2)	8576(2)	725(1)	36(1)
C(14)	-8(2)	8782(2)	1025(1)	35(1)
C(15)	272(2)	9096(2)	1534(1)	34(1)
C(16)	1728(2)	9469(2)	1982(1)	43(1)
C(17)	2346(2)	8656(2)	896(1)	44(1)
C(18)	701(2)	8478(2)	132(1)	48(1)
C(19)	-905(2)	8768(2)	820(1)	47(1)
C(20)	-290(2)	9467(2)	1954(1)	42(1)
C(21)	68(2)	5720(2)	3603(1)	42(1)
C(22)	-234(2)	6030(2)	4089(1)	43(1)
C(23)	-1124(2)	6050(2)	4054(1)	42(1)
C(24)	-1369(2)	5762(2)	3538(1)	41(1)
C(25)	-628(2)	5556(2)	3262(1)	41(1)
C(26)	973(2)	5494(2)	3477(1)	64(1)
C(27)	324(2)	6156(2)	4580(1)	62(1)
C(28)	-1722(2)	6110(3)	4512(1)	63(1)
C(29)	-2271(2)	5585(3)	3361(1)	67(1)
C(30)	-615(2)	5147(2)	2713(1)	59(1)
C(31)	-245(1)	9293(2)	3524(1)	30(1)
C(32)	-86(1)	8838(2)	4018(1)	30(1)
C(33)	-864(1)	8531(2)	4220(1)	32(1)
C(34)	-1502(1)	8740(2)	3836(1)	33(1)
C(35)	-1124(2)	9236(2)	3410(1)	33(1)
C(36)	409(2)	9856(2)	3240(1)	41(1)
C(37)	754(2)	8833(2)	4306(1)	42(1)
C(38)	-1001(2)	8275(2)	4790(1)	45(1)
C(39)	-2436(2)	8583(2)	3894(1)	50(1)
C(40)	-1611(2)	9729(2)	2972(1)	46(1)
C(41)	2343(1)	7377(2)	2687(1)	38(1)
C(42)	3144(2)	7382(2)	2383(1)	53(1)
C(43)	3834(2)	7050(3)	2520(2)	67(1)
C(44)	-2272(10)	7238(7)	2218(6)	33(2)
C(45)	-3090(5)	7341(5)	2504(3)	34(2)
C(46)	-3789(5)	7364(8)	2324(3)	53(2)
C(44B)	-2266(10)	7571(7)	2173(6)	29(2)
C(45B)	-3061(4)	7797(5)	2447(3)	33(1)
C(46B)	-3729(1)	7770(2)	2333(1)	57(3)

C(47)	552(1)	2086(2)	1026(1)	48(1)
C(48)	1012(1)	1290(2)	885(1)	53(1)
C(49)	1816(2)	1390(2)	693(2)	65(1)
C(50)	2179(2)	2277(3)	640(2)	66(1)
C(51)	1721(2)	3073(3)	783(1)	67(1)
C(52)	918(2)	2976(2)	971(1)	56(1)
C(53)	-329(2)	1981(3)	1228(1)	78(1)
C(54)	-1447(2)	11899(3)	4211(2)	43(1)
C(55)	-653(2)	11552(2)	4089(2)	49(3)
C(56)	-13(2)	12185(3)	3959(2)	49(1)
C(57)	-167(2)	13165(2)	3952(2)	57(1)
C(58)	-961(3)	13512(2)	4075(2)	69(2)
C(59)	-1602(2)	12879(3)	4204(2)	56(1)
C(60)	-2125(4)	11192(5)	4351(3)	71(2)
C(61)	-470(2)	12587(3)	4028(2)	48(2)
C(62)	-1049(3)	13317(3)	4109(3)	54(2)
C(63)	-1866(3)	13097(4)	4256(3)	99(3)
C(64)	-2104(3)	12147(4)	4324(3)	80(2)
C(65)	-1524(3)	11417(3)	4244(2)	64(2)
C(66)	-707(3)	11637(3)	4096(2)	49(4)
C(67)	367(5)	12858(6)	3877(4)	76(2)

Table 13.81. Anisotropic displacement parameters ($Å^2 x\ 10^3$) for **55**. The anisotropic displacement factor exponent takes the form: $-2\pi^2[\ h^2\ a^{*2}U^{11} + ...\ + 2\ h\ k\ a^*\ b^*\ U^{12}\ ]$

	U^{11}	U^{22}	U^{33}	U^{23}	U^{13}	U^{12}
Y(1)	20(1)	31(1)	21(1)	-3(1)	2(1)	-1(1)
Y(2)	18(1)	32(1)	20(1)	-1(1)	1(1)	1(1)
O(2)	22(1)	38(1)	23(1)	-3(1)	2(1)	0(1)
O(1)	23(1)	43(1)	23(1)	-4(1)	2(1)	0(1)
N(1)	22(1)	29(1)	24(1)	-1(1)	2(1)	-1(1)
N(2)	19(1)	35(1)	27(1)	-2(1)	2(1)	-2(1)
N(3)	22(1)	33(1)	23(1)	-1(1)	1(1)	0(1)
N(4)	19(1)	49(1)	25(1)	-5(1)	-1(1)	0(1)
C(1)	31(1)	30(1)	37(1)	-9(1)	0(1)	2(1)
C(2)	24(1)	37(1)	41(1)	-12(1)	4(1)	3(1)
C(3)	31(1)	41(1)	32(1)	-11(1)	9(1)	-2(1)
C(4)	28(1)	41(1)	28(1)	-11(1)	0(1)	-2(1)
C(5)	28(1)	33(1)	34(1)	-12(1)	4(1)	-4(1)
C(6)	53(2)	43(2)	44(2)	-2(1)	-2(1)	13(1)
C(7)	25(1)	60(2)	76(2)	-18(2)	3(1)	5(1)
C(8)	54(2)	57(2)	42(2)	-9(1)	22(1)	-3(1)
C(9)	39(2)	64(2)	39(2)	-11(1)	-9(1)	-1(1)
C(10)	36(1)	48(2)	49(2)	-14(1)	11(1)	-12(1)
C(11)	40(1)	29(1)	31(1)	0(1)	6(1)	-5(1)
C(12)	38(1)	34(1)	31(1)	3(1)	7(1)	-7(1)
C(13)	42(1)	38(1)	28(1)	4(1)	5(1)	-1(1)
C(14)	38(1)	38(1)	28(1)	6(1)	1(1)	3(1)
C(15)	42(1)	29(1)	30(1)	3(1)	6(1)	2(1)
C(16)	49(2)	42(2)	39(1)	-6(1)	4(1)	-14(1)
C(17)	40(2)	52(2)	41(2)	-2(1)	11(1)	-12(1)
C(18)	57(2)	59(2)	28(1)	4(1)	4(1)	3(1)
C(19)	41(2)	60(2)	40(2)	7(1)	-4(1)	12(1)
C(20)	49(2)	40(2)	37(1)	-1(1)	10(1)	8(1)
C(21)	38(1)	37(1)	52(2)	15(1)	8(1)	4(1)
C(22)	52(2)	40(2)	36(1)	10(1)	-8(1)	-8(1)
C(23)	52(2)	39(1)	35(1)	3(1)	17(1)	-8(1)
C(24)	38(1)	39(2)	46(2)	2(1)	1(1)	-11(1)
C(25)	57(2)	32(1)	34(1)	2(1)	11(1)	-3(1)

C(26)	50(2)	58(2)	84(2)	23(2)	14(2)	17(2)
C(27)	74(2)	64(2)	46(2)	15(2)	-19(2)	-2(2)
C(28)	74(2)	67(2)	51(2)	-3(2)	33(2)	-16(2)
C(29)	49(2)	80(2)	72(2)	-1(2)	-4(2)	-28(2)
C(30)	93(2)	42(2)	43(2)	-7(1)	19(2)	-4(2)
C(31)	32(1)	31(1)	28(1)	-5(1)	3(1)	2(1)
C(32)	28(1)	35(1)	28(1)	-7(1)	0(1)	2(1)
C(33)	31(1)	40(1)	25(1)	-7(1)	4(1)	3(1)
C(34)	27(1)	44(1)	28(1)	-7(1)	3(1)	9(1)
C(35)	33(1)	38(1)	27(1)	-5(1)	1(1)	11(1)
C(36)	46(2)	38(1)	38(1)	-4(1)	6(1)	-6(1)
C(37)	34(1)	54(2)	37(1)	-5(1)	-8(1)	-4(1)
C(38)	48(2)	58(2)	29(1)	-5(1)	6(1)	-2(1)
C(39)	26(1)	85(2)	41(2)	-2(1)	6(1)	12(1)
C(40)	45(2)	54(2)	38(1)	1(1)	-1(1)	23(1)
C(41)	21(1)	61(2)	32(1)	-5(1)	-1(1)	-3(1)
C(42)	25(1)	93(2)	43(2)	-9(2)	1(1)	-5(1)
C(43)	30(2)	94(3)	77(2)	-23(2)	0(2)	0(2)
C(44)	23(3)	49(6)	27(4)	-4(5)	-1(3)	6(5)
C(45)	27(3)	41(4)	33(3)	-1(3)	2(2)	1(3)
C(46)	27(4)	91(7)	42(4)	12(3)	-2(3)	-6(3)
C(44B)	20(3)	41(6)	26(3)	2(4)	-5(2)	4(5)
C(45B)	22(3)	42(4)	34(3)	-8(3)	-4(2)	4(3)
C(46B)	30(5)	103(9)	38(4)	-10(4)	-1(3)	17(4)
C(47)	58(2)	56(2)	29(1)	5(1)	-8(1)	0(1)
C(48)	62(2)	40(2)	57(2)	8(1)	-13(2)	0(1)
C(49)	59(2)	54(2)	82(2)	-10(2)	-16(2)	16(2)
C(50)	46(2)	76(2)	75(2)	-1(2)	-8(2)	-5(2)
C(51)	79(2)	50(2)	71(2)	-1(2)	-16(2)	-15(2)
C(52)	74(2)	47(2)	48(2)	-12(1)	-14(2)	11(2)
C(53)	70(2)	122(3)	41(2)	6(2)	11(2)	2(2)

Table 13.82. Hydrogen coordinates (x 10^4) and isotropic displacement parameters ($Å^2$x 10^{3}) for **55**.

	x	y	z	U(eq)
H(6A)	1696	4331	1889	70
H(6B)	776	4471	2126	70
H(6C)	1507	5230	2261	70
H(7A)	2760	5227	1069	81
H(7B)	2681	5770	1624	81
H(7C)	2780	6372	1090	81
H(8A)	1900	5835	85	76
H(8B)	1957	6932	267	76
H(8C)	1148	6560	-64	76
H(9A)	-640	5475	256	71
H(9B)	-200	6447	71	71
H(9C)	-872	6468	534	71
H(10A)	-861	4642	1124	66
H(10B)	-1008	5481	1544	66
H(10C)	-497	4539	1718	66
H(16A)	1830	10149	1914	65
H(16B)	2266	9123	1990	65
H(16C)	1456	9397	2325	65
H(17A)	2575	9302	851	66
H(17B)	2378	8304	561	66
H(17C)	2675	8319	1171	66
H(18A)	529	9088	-29	72

H(18B)	299	7977	26	72
H(18C)	1266	8306	14	72
H(19A)	-1103	9427	766	71
H(19B)	-1262	8448	1077	71
H(19C)	-936	8422	483	71
H(20A)	-171	10146	2017	63
H(20B)	-188	9106	2282	63
H(20C)	-882	9391	1839	63
H(26A)	1101	4832	3580	95
H(26B)	1349	5931	3674	95
H(26C)	1056	5573	3097	95
H(27A)	610	5550	4664	93
H(27B)	-23	6347	4878	93
H(27C)	747	6653	4515	93
H(28A)	-1986	5483	4566	95
H(28B)	-2160	6587	4432	95
H(28C)	-1407	6298	4834	95
H(29A)	-2452	4956	3487	100
H(29B)	-2311	5601	2973	100
H(29C)	-2634	6083	3506	100
H(30A)	-433	4476	2730	89
H(30B)	-220	5514	2499	89
H(30C)	-1182	5183	2551	89
H(36A)	705	10280	3492	61
H(36B)	136	10240	2960	61
H(36C)	815	9416	3083	61
H(37A)	889	9483	4428	62
H(37B)	1191	8613	4066	62
H(37C)	730	8401	4611	62
H(38A)	-937	8849	5010	67
H(38B)	-586	7793	4904	67
H(38C)	-1572	8015	4826	67
H(39A)	-2683	9138	4070	76
H(39B)	-2529	8007	4106	76
H(39C)	-2704	8502	3543	76
H(40A)	-2073	10100	3122	68
H(40B)	-1844	9249	2726	68
H(40C)	-1235	10159	2783	68
H(41A)	2351	6836	2941	46
H(41B)	2294	7980	2890	46
H(42A)	3115	7678	2044	64
H(43A)	3903	6746	2854	80
H(43B)	4299	7098	2290	80
H(44A)	-2234	6584	2069	40
H(44B)	-2261	7700	1921	40
H(45A)	-3040	7396	2878	40
H(46A)	-3884	7313	1953	64
H(46B)	-4253	7433	2552	64
H(44C)	-2120	8107	1935	35
H(44D)	-2347	6989	1954	35
H(45B)	-2967	8013	2800	40
H(46C)	-3896	7563	1988	69
H(46D)	-4144	7952	2579	69
H(48A)	773	669	919	64
H(49A)	2123	835	597	78
H(50A)	2733	2341	508	79
H(51A)	1962	3692	752	80
H(52A)	610	3532	1065	68
H(53A)	-570	1373	1104	116
H(53B)	-679	2513	1097	116
H(53C)	-311	1990	1616	116
H(55A)	-548	10882	4094	58

H(56A)	530	11948	3876	59
H(57A)	270	13598	3864	69
H(58A)	-1067	14182	4070	83
H(59A)	-2144	13116	4288	67
H(60A)	-1865	10575	4442	106
H(60B)	-2514	11110	4047	106
H(60C)	-2435	11432	4654	106
H(62A)	-887	13966	4063	65
H(63A)	-2263	13596	4311	118
H(64A)	-2662	11997	4425	96
H(65A)	-1687	10768	4290	76
H(66A)	-311	11138	4041	59
H(67D)	330	13294	3573	114
H(67A)	685	12285	3780	114
H(67B)	656	13181	4175	114

13.29. Crystallographic Data for $[(C_5Me_5)_2Sm(\mu\text{-}\eta^1{:}\eta^2\text{-}ON{=}NC_3H_5)]_2$, 56

X-ray Data Collection, Structure Solution and Refinement for **56**.

An orange crystal of approximate dimensions 0.14 x 0.20 x 0.39 mm was mounted on a glass fiber and transferred to a Bruker SMART APEX II diffractometer. The APEX2[1] program package was used to determine the unit-cell parameters and for data collection (20 sec/frame scan time for a sphere of diffraction data). The raw frame data was processed using SAINT[2] and SADABS[3] to yield the reflection data file. Subsequent calculations were carried out using the SHELXTL[4] program. The diffraction symmetry was 2/*m* and the systematic absences were consistent with the monoclinic space group $P2_1/n$ that was later determined to be correct.

The structure was solved by direct methods and refined on F^2 by full-matrix least-squares techniques. The analytical scattering factors[5] for neutral atoms were used throughout the analysis. Hydrogen atoms were included using a riding model. There were two molecules of toluene solvent present. The pentamethylcyclopentadienyl ring defined be atoms C(11)-C(20) was disordered and included using multiple components, partial site-occupancy-factors (0.60/0.40) and isotropic thermal parameters.

At convergence, wR2 = 0.0847 and Goof = 1.027 for 560 variables refined against 13488 data (0.76Å), R1 = 0.0308 for those 11156 data with I > 2.0σ(I).

References

1. APEX2 Version 2008.3-0, Bruker AXS, Inc.; Madison, WI 2008.
2. SAINT Version 7.53a, Bruker AXS, Inc.; Madison, WI 2007.
3. Sheldrick, G. M. SADABS, Version 2008/1, Bruker AXS, Inc.; Madison, WI 2008.
4. Sheldrick, G. M. SHELXTL, Version 2008/3, Bruker AXS, Inc.; Madison, WI 2008.
5. International Tables for X-Ray Crystallography 1992, Vol. C., Dordrecht: Kluwer Academic Publishers.

Table 13.83. Atomic coordinates (x 10^4) and equivalent isotropic displacement parameters ($Å^2$x 10^3) for **56**. U(eq) is defined as one third of the trace of the orthogonalized U^{ij} tensor.

	x	y	z	U(eq)
Sm(1)	4841(1)	7209(1)	2016(1)	27(1)
Sm(2)	2651(1)	7541(1)	469(1)	27(1)
N(1)	3223(2)	7362(2)	1647(1)	30(1)
N(2)	3126(2)	7161(2)	2089(1)	34(1)
N(3)	4268(2)	7394(2)	838(1)	30(1)
N(4)	4364(2)	7528(2)	388(1)	32(1)
O(1)	4972(1)	7264(2)	1139(1)	34(1)
O(2)	2514(2)	7511(2)	1349(1)	34(1)
C(1)	4701(2)	5299(2)	2221(1)	37(1)
C(2)	5345(2)	5363(2)	1857(1)	37(1)
C(3)	6123(2)	5819(2)	2069(1)	37(1)
C(4)	5983(2)	6010(2)	2565(1)	38(1)
C(5)	5097(2)	5720(2)	2655(1)	39(1)
C(6)	3832(3)	4756(3)	2195(2)	53(1)
C(7)	5297(3)	4930(3)	1353(1)	52(1)
C(8)	6977(3)	5989(3)	1811(2)	58(1)
C(9)	6697(3)	6244(3)	2962(2)	59(1)
C(10)	4690(2)	5731(1)	3143(1)	59(1)
C(11)	4523(1)	9001(1)	2357(1)	38(1)
C(12)	5185(1)	8674(1)	2714(1)	44(2)
C(13)	6014(1)	8583(1)	2485(1)	42(1)
C(14)	5864(1)	8854(1)	1986(1)	36(1)
C(15)	4942(1)	9113(1)	1907(1)	34(1)
C(16)	3545(1)	9197(1)	2441(1)	57(2)
C(17)	5034(1)	8460(1)	3244(1)	55(2)
C(18)	6901(1)	8256(2)	2729(1)	75(2)
C(19)	6562(1)	8865(1)	1607(1)	49(1)
C(20)	4489(1)	9448(1)	1429(1)	50(1)
C(11B)	4532(1)	8893(1)	2505(1)	46(2)
C(12B)	5390(1)	8598(1)	2721(1)	42(2)
C(13B)	6030(1)	8640(1)	2350(1)	46(2)
C(14B)	5568(1)	8960(1)	1906(1)	44(2)
C(15B)	4642(1)	9117(1)	2002(1)	49(2)
C(16B)	3658(1)	8957(1)	2766(1)	82(4)
C(17B)	5587(1)	8293(2)	3250(1)	89(4)
C(18B)	7028(1)	8387(2)	2417(1)	102(5)
C(19B)	5987(1)	9109(1)	1417(1)	93(4)
C(20B)	3905(1)	9463(2)	1633(1)	96(4)
C(21)	2522(2)	5653(2)	606(1)	36(1)
C(22)	1609(2)	5957(2)	525(1)	36(1)
C(23)	1471(2)	6217(2)	28(1)	36(1)
C(24)	2302(2)	6098(2)	-198(1)	37(1)
C(25)	2945(2)	5737(2)	160(1)	37(1)
C(26)	2924(3)	5255(3)	1076(1)	48(1)
C(27)	893(2)	5941(3)	892(1)	51(1)
C(28)	561(2)	6369(3)	-234(1)	54(1)
C(29)	2459(3)	6219(3)	-732(1)	53(1)
C(30)	3881(2)	5397(3)	66(1)	51(1)
C(31)	2530(2)	9019(2)	-187(1)	42(1)
C(32)	1623(2)	8743(2)	-147(1)	44(1)
C(33)	1393(2)	8952(2)	334(1)	42(1)
C(34)	2140(2)	9394(2)	582(1)	38(1)
C(35)	2849(2)	9439(2)	263(1)	38(1)
C(36)	3021(3)	8997(3)	-654(1)	66(1)
C(37)	977(3)	8516(3)	-578(2)	70(1)
C(38)	473(3)	8828(3)	535(2)	71(1)
C(39)	2101(3)	9843(3)	1080(1)	58(1)

C(40)	3727(3)	9963(3)	331(2)	58(1)
C(41)	2201(2)	7078(3)	2256(1)	51(1)
C(42)	2235(3)	6837(4)	2789(1)	74(2)
C(43)	1721(3)	7054(4)	3095(2)	68(1)
C(44)	5291(2)	7542(3)	222(1)	45(1)
C(45)	5265(3)	7592(4)	-326(1)	63(1)
C(46)	5811(3)	7243(4)	-600(2)	63(1)
C(47)	5455(4)	12316(5)	3244(2)	96(2)
C(48)	5467(4)	11445(4)	3011(2)	81(2)
C(49)	5610(3)	11299(3)	2530(2)	66(1)
C(50)	5731(3)	12137(4)	2246(2)	72(1)
C(51)	5710(3)	13016(3)	2461(2)	69(1)
C(52)	5567(4)	13062(5)	2965(3)	99(2)
C(53)	5863(4)	12060(6)	1739(2)	127(3)
C(54)	-2019(3)	8308(4)	428(2)	80(2)
C(55)	-1848(3)	8214(3)	-65(2)	67(1)
C(56)	-1758(3)	7314(3)	-263(2)	59(1)
C(57)	-1828(3)	6524(3)	35(2)	62(1)
C(58)	-1991(4)	6648(4)	520(2)	80(2)
C(59)	-2092(4)	7528(4)	719(2)	86(2)
C(60)	-1578(4)	7192(5)	-788(2)	95(2)

Table 13.84. Anisotropic displacement parameters ($Å^2$x 10^3) for **56**. The anisotropic displacement factor exponent takes the form: $-2\pi^2[h^2 a^{*2}U^{11} + ... + 2 h k a^* b^* U^{12}]$

	U^{11}	U^{22}	U^{33}	U^{23}	U^{13}	U^{12}
Sm(1)	27(1)	34(1)	22(1)	1(1)	3(1)	-1(1)
Sm(2)	27(1)	31(1)	22(1)	1(1)	3(1)	2(1)
N(1)	29(1)	35(1)	25(1)	0(1)	4(1)	0(1)
N(2)	31(1)	45(2)	27(1)	2(1)	6(1)	0(1)
N(3)	29(1)	37(1)	25(1)	1(1)	4(1)	-1(1)
N(4)	29(1)	41(2)	27(1)	1(1)	6(1)	2(1)
O(1)	32(1)	46(1)	25(1)	2(1)	3(1)	2(1)
O(2)	31(1)	45(1)	25(1)	0(1)	3(1)	3(1)
C(1)	38(2)	36(2)	38(2)	10(1)	2(1)	-1(1)
C(2)	43(2)	34(2)	35(2)	2(1)	2(1)	5(1)
C(3)	33(2)	40(2)	40(2)	4(1)	8(1)	8(1)
C(4)	34(2)	46(2)	34(2)	5(1)	-2(1)	4(1)
C(5)	40(2)	46(2)	30(2)	10(1)	3(1)	1(1)
C(6)	49(2)	53(2)	57(2)	18(2)	-2(2)	-14(2)
C(7)	66(2)	49(2)	42(2)	-9(2)	1(2)	13(2)
C(8)	43(2)	65(3)	70(3)	5(2)	22(2)	10(2)
C(9)	55(2)	62(3)	58(2)	-2(2)	-20(2)	6(2)
C(10)	65(3)	79(3)	34(2)	12(2)	14(2)	2(2)
C(21)	44(2)	28(2)	36(2)	0(1)	-1(1)	-1(1)
C(22)	38(2)	36(2)	36(2)	-3(1)	6(1)	-6(1)
C(23)	35(2)	37(2)	34(2)	-4(1)	0(1)	-2(1)
C(24)	41(2)	36(2)	32(2)	-6(1)	1(1)	0(1)
C(25)	40(2)	35(2)	37(2)	-7(1)	2(1)	4(1)
C(26)	59(2)	43(2)	42(2)	4(2)	-6(2)	2(2)
C(27)	46(2)	60(2)	47(2)	-2(2)	12(2)	-12(2)
C(28)	41(2)	64(3)	57(2)	1(2)	-10(2)	-5(2)
C(29)	63(2)	64(2)	33(2)	-6(2)	6(2)	6(2)
C(30)	47(2)	52(2)	55(2)	-10(2)	3(2)	15(2)
C(31)	58(2)	39(2)	29(2)	10(1)	9(1)	10(2)
C(32)	52(2)	38(2)	40(2)	6(1)	-9(2)	8(2)
C(33)	38(2)	39(2)	50(2)	5(1)	6(2)	9(1)
C(34)	50(2)	30(2)	34(2)	1(1)	7(1)	8(1)
C(35)	41(2)	35(2)	38(2)	8(1)	4(1)	3(1)

C(36)	95(3)	67(3)	40(2)	11(2)	23(2)	8(2)
C(37)	85(3)	61(3)	60(3)	7(2)	-31(2)	6(2)
C(38)	44(2)	66(3)	104(4)	1(3)	23(2)	11(2)
C(39)	86(3)	49(2)	40(2)	-4(2)	13(2)	16(2)
C(40)	57(2)	49(2)	67(3)	11(2)	3(2)	-11(2)
C(41)	33(2)	88(3)	33(2)	8(2)	9(1)	0(2)
C(42)	41(2)	144(5)	39(2)	27(3)	12(2)	13(3)
C(43)	64(3)	96(4)	45(2)	15(2)	17(2)	12(2)
C(44)	32(2)	74(3)	30(2)	2(2)	10(1)	1(2)
C(45)	42(2)	114(4)	34(2)	12(2)	9(2)	11(2)
C(46)	51(2)	97(4)	42(2)	-5(2)	13(2)	5(2)
C(47)	85(4)	127(6)	79(4)	-11(4)	28(3)	-9(4)
C(48)	64(3)	82(4)	98(4)	-1(3)	14(3)	-7(3)
C(49)	51(2)	61(3)	85(3)	4(2)	-4(2)	-10(2)
C(50)	39(2)	107(4)	69(3)	4(3)	-8(2)	8(2)
C(51)	50(2)	50(2)	109(4)	11(3)	8(2)	7(2)
C(52)	73(4)	91(4)	135(6)	24(4)	19(4)	3(3)
C(53)	70(4)	222(9)	86(4)	25(5)	-10(3)	11(5)
C(54)	62(3)	69(3)	109(4)	-7(3)	9(3)	5(2)
C(55)	56(3)	48(2)	94(4)	12(2)	-9(2)	9(2)
C(56)	35(2)	73(3)	68(3)	3(2)	-5(2)	2(2)
C(57)	49(2)	49(2)	88(3)	2(2)	9(2)	-2(2)
C(58)	73(3)	77(4)	93(4)	12(3)	24(3)	-1(3)
C(59)	78(4)	103(5)	79(4)	-3(3)	29(3)	8(3)
C(60)	70(4)	144(6)	68(3)	6(3)	-11(3)	3(3)

Table 13.85. Hydrogen coordinates (x 10^4) and isotropic displacement parameters ($Å^2$x 10^{3}) for **56**.

	x	y	z	U(eq)
H(6A)	3834	4301	2467	80
H(6B)	3766	4411	1883	80
H(6C)	3326	5200	2218	80
H(7A)	5302	5438	1107	78
H(7B)	4739	4559	1304	78
H(7C)	5819	4512	1320	78
H(8A)	7365	6434	2003	88
H(8B)	6826	6259	1485	88
H(8C)	7296	5384	1776	88
H(9A)	6842	5672	3156	89
H(9B)	6474	6742	3174	89
H(9C)	7242	6471	2812	89
H(10A)	5052	5332	3374	88
H(10B)	4072	5482	3107	88
H(10C)	4679	6385	3267	88
H(16A)	3282	8643	2597	85
H(16B)	3215	9322	2126	85
H(16C)	3503	9754	2654	85
H(17A)	5256	8993	3449	83
H(17B)	5362	7879	3344	83
H(17C)	4388	8369	3283	83
H(18A)	7090	7664	2575	112
H(18B)	6827	8143	3078	112
H(18C)	7361	8747	2692	112
H(19A)	6305	8582	1302	73
H(19B)	7091	8497	1728	73
H(19C)	6742	9524	1546	73
H(20A)	4347	10128	1453	75
H(20B)	3930	9087	1360	75

H(20C)	4895	9347	1164	75
H(16D)	3692	8533	3052	123
H(16E)	3151	8767	2541	123
H(16F)	3568	9614	2875	123
H(17D)	5556	8849	3465	133
H(17E)	6193	8014	3288	133
H(17F)	5141	7820	3340	133
H(18D)	7106	7703	2362	152
H(18E)	7255	8550	2751	152
H(18F)	7365	8746	2180	152
H(19D)	6443	9614	1451	140
H(19E)	5516	9293	1168	140
H(19F)	6272	8516	1317	140
H(20D)	3998	10140	1565	144
H(20E)	3315	9375	1769	144
H(20F)	3929	9097	1329	144
H(26A)	3108	4594	1025	72
H(26B)	2475	5275	1325	72
H(26C)	3452	5634	1187	72
H(27A)	334	6217	743	76
H(27B)	1096	6313	1181	76
H(27C)	781	5281	989	76
H(28A)	221	5770	-240	81
H(28B)	639	6580	-570	81
H(28C)	229	6856	-61	81
H(29A)	3082	6429	-768	80
H(29B)	2040	6696	-876	80
H(29C)	2359	5609	-902	80
H(30A)	4244	5358	377	77
H(30B)	4164	5845	-153	77
H(30C)	3846	4766	-87	77
H(36A)	2687	9375	-906	99
H(36B)	3068	8337	-767	99
H(36C)	3628	9264	-592	99
H(37A)	424	8237	-461	105
H(37B)	1259	8061	-794	105
H(37C)	826	9101	-761	105
H(38A)	545	8608	875	106
H(38B)	125	8358	337	106
H(38C)	153	9439	522	106
H(39A)	2075	9344	1329	87
H(39B)	1561	10245	1086	87
H(39C)	2641	10235	1149	87
H(40A)	3766	10271	654	86
H(40B)	3760	10448	75	86
H(40C)	4228	9514	310	86
H(41A)	1869	6576	2065	61
H(41B)	1877	7688	2199	61
H(42A)	2734	6457	2904	89
H(43A)	1206	7434	3007	81
H(43B)	1830	6846	3424	81
H(44A)	5615	6959	336	54
H(44B)	5621	8100	363	54
H(45A)	4773	7931	-482	76
H(46A)	6317	6896	-466	75
H(46B)	5724	7322	-945	75
H(47A)	5372	12373	3585	115
H(48A)	5366	10897	3204	97
H(49A)	5628	10679	2392	79
H(51A)	5789	13579	2276	83
H(52A)	5551	13674	3113	119
H(53A)	6092	12666	1619	190

H(53B)	5288	11906	1561	190
H(53C)	6302	11553	1686	190
H(54A)	-2086	8926	563	96
H(55A)	-1794	8763	-264	80
H(57A)	-1763	5901	-95	74
H(58A)	-2035	6103	723	96
H(59A)	-2210	7597	1055	103
H(60A)	-1229	7736	-897	142
H(60B)	-2152	7153	-984	142
H(60C)	-1234	6604	-829	142

13.30. Crystallographic Data for $[(C_5Me_5)_2La(\mu\text{-}\eta^1{:}\eta^2\text{-}ON{=}NC_3H_5)]_2$, 57

X-ray Data Collection, Structure Solution and Refinement for **57**.

A colorless crystal of approximate dimensions 0.11 x 0.22 x 0.23 mm was mounted on a glass fiber and transferred to a Bruker SMART APEX II diffractometer. The APEX2[1] program package was used to determine the unit-cell parameters and for data collection (25 sec/frame scan time for a sphere of diffraction data). The raw frame data was processed using SAINT[2] and SADABS[3] to yield the reflection data file. Subsequent calculations were carried out using the SHELXTL[4] program. The diffraction symmetry was 2/*m* and the systematic absences were consistent with the monoclinic space group $P2_1/n$ that was later determined to be correct.

The structure was solved by direct methods and refined on F^2 by full-matrix least-squares techniques. The analytical scattering factors[5] for neutral atoms were used throughout the analysis. Hydrogen atoms were included using a riding model. Carbon atoms C(1)-C(10) were disordered and included using multiple components with partial site-occupancy-factors (0.60/0.40) and isotropic thermal parameters. There were two molecules of toluene solvent present.

At convergence, wR2 = 0.0641 and Goof = 1.025 for 630 variables refined against 13509 data (0.74Å), R1 = 0.0261 for those 11445 data with I > 2.0σ(I).

References

1. APEX2 Version 2.2-0, Bruker AXS, Inc.; Madison, WI 2007.
2. SAINT Version 7.46a, Bruker AXS, Inc.; Madison, WI 2007.
3. Sheldrick, G. M. SADABS, Version 2008/1, Bruker AXS, Inc.; Madison, WI 2008.
4. Sheldrick, G. M. SHELXTL, Version 2008/3, Bruker AXS, Inc.; Madison, WI 2008.
5. International Tables for X-Ray Crystallography 1992, Vol. C., Dordrecht: Kluwer Academic Publishers.

Table 13.86. Atomic coordinates (x 10^4) and equivalent isotropic displacement parameters ($Å^2$x 10^3) for **57**. U(eq) is defined as one third of the trace of the orthogonalized U^{ij} tensor.

	x	y	z	U(eq)
La(1)	9862(1)	7820(1)	2022(1)	20(1)
La(2)	7600(1)	7438(1)	465(1)	19(1)
O(2)	7441(1)	7484(1)	1367(1)	26(1)
O(1)	10012(1)	7745(1)	1124(1)	27(1)

N(1)	8164(1)	7644(1)	1656(1)	22(1)
N(2)	8074(1)	7881(1)	2093(1)	26(1)
N(3)	9295(1)	7601(1)	830(1)	23(1)
N(4)	9393(1)	7444(1)	384(1)	23(1)
C(1)	9491(3)	6021(3)	2368(2)	26(1)
C(2)	10152(4)	6372(3)	2723(2)	24(1)
C(3)	11008(3)	6431(3)	2497(2)	25(1)
C(4)	10865(3)	6151(3)	2003(2)	25(1)
C(5)	9933(3)	5893(3)	1920(2)	24(1)
C(6)	8530(3)	5767(3)	2470(2)	38(1)
C(7)	10018(3)	6544(3)	3249(2)	39(1)
C(8)	11950(3)	6555(3)	2735(2)	37(1)
C(9)	11569(3)	6069(3)	1629(2)	37(1)
C(10)	9473(3)	5503(3)	1462(1)	33(1)
C(1B)	9543(5)	6101(5)	2505(3)	30(2)
C(2B)	10403(6)	6368(5)	2714(3)	28(2)
C(3B)	11031(5)	6323(5)	2358(3)	31(2)
C(4B)	10588(5)	6008(5)	1930(2)	28(2)
C(5B)	9665(5)	5857(5)	2015(3)	32(2)
C(6B)	8658(5)	5932(6)	2750(3)	57(2)
C(7B)	10509(6)	6540(6)	3258(3)	51(2)
C(8B)	12051(5)	6448(6)	2459(3)	59(2)
C(9B)	11092(6)	5811(7)	1470(3)	63(2)
C(10B)	8985(6)	5451(6)	1635(3)	60(2)
C(11)	9766(2)	9774(2)	2224(1)	26(1)
C(12)	10144(2)	9367(2)	2657(1)	28(1)
C(13)	11036(2)	9059(2)	2575(1)	28(1)
C(14)	11201(2)	9239(2)	2083(1)	27(1)
C(15)	10422(2)	9696(2)	1864(1)	26(1)
C(16)	8872(2)	10301(2)	2182(1)	37(1)
C(17)	9705(2)	9356(2)	3139(1)	42(1)
C(18)	11738(2)	8781(2)	2971(1)	43(1)
C(19)	12064(2)	9036(2)	1829(1)	39(1)
C(20)	10376(2)	10099(2)	1356(1)	35(1)
C(21)	7066(2)	5541(2)	558(1)	27(1)
C(22)	6306(2)	5982(2)	313(1)	29(1)
C(23)	6543(2)	6205(2)	-164(1)	30(1)
C(24)	7460(2)	5929(2)	-209(1)	29(1)
C(25)	7784(2)	5508(2)	235(1)	27(1)
C(26)	7043(2)	5099(2)	1056(1)	40(1)
C(27)	5380(2)	6113(2)	518(1)	46(1)
C(28)	5895(2)	6472(2)	-587(1)	46(1)
C(29)	7959(2)	5979(2)	-670(1)	44(1)
C(30)	8686(2)	5013(2)	312(1)	38(1)
C(31)	7501(1)	9376(2)	596(1)	24(1)
C(32)	6577(1)	9100(2)	516(1)	26(1)
C(33)	6432(1)	8834(2)	20(1)	26(1)
C(34)	7276(2)	8934(2)	-204(1)	27(1)
C(35)	7932(1)	9275(2)	150(1)	25(1)
C(36)	7926(2)	9747(2)	1066(1)	30(1)
C(37)	5858(2)	9123(2)	885(1)	34(1)
C(38)	5508(2)	8669(2)	-232(1)	36(1)
C(39)	7436(2)	8791(2)	-736(1)	36(1)
C(40)	8888(2)	9578(2)	53(1)	33(1)
C(41)	7142(2)	7984(2)	2262(1)	35(1)
C(42)	7193(2)	8286(2)	2787(1)	45(1)
C(43)	6737(2)	7967(2)	3120(1)	48(1)
C(44)	10326(2)	7427(2)	215(1)	28(1)
C(45)	10294(2)	7352(2)	-330(1)	32(1)
C(46)	10786(2)	7860(2)	-610(1)	38(1)
C(47)	6807(2)	2266(2)	241(1)	36(1)
C(48)	6922(2)	3157(2)	50(1)	42(1)

C(49)	7081(2)	3282(2)	-436(1)	48(1)
C(50)	7119(2)	2518(2)	-741(1)	50(1)
C(51)	7005(2)	1627(2)	-554(1)	50(1)
C(52)	6853(2)	1502(2)	-70(1)	41(1)
C(53)	6640(2)	2126(2)	772(1)	54(1)
C(54)	9310(2)	7087(2)	-2249(1)	47(1)
C(55)	9302(2)	7963(2)	-2464(1)	49(1)
C(56)	9429(2)	8050(2)	-2958(1)	62(1)
C(57)	9560(2)	7282(3)	-3244(1)	56(1)
C(58)	9576(2)	6414(2)	-3025(1)	47(1)
C(59)	9448(2)	6296(2)	-2538(1)	41(1)
C(60)	9183(2)	6990(3)	-1721(1)	80(1)

Table 13.87. Anisotropic displacement parameters ($Å^2 x 10^3$) for **57**. The anisotropic displacement factor exponent takes the form: $-2\pi^2[h^2 a^{*2} U^{11} + ... + 2 h k a^* b^* U^{12}]$

	U^{11}	U^{22}	U^{33}	U^{23}	U^{13}	U^{12}
La(1)	20(1)	24(1)	16(1)	-1(1)	2(1)	1(1)
La(2)	19(1)	22(1)	17(1)	-1(1)	2(1)	-1(1)
O(2)	23(1)	34(1)	20(1)	0(1)	2(1)	-2(1)
O(1)	24(1)	37(1)	19(1)	-2(1)	1(1)	-2(1)
N(1)	21(1)	26(1)	20(1)	1(1)	2(1)	1(1)
N(2)	25(1)	34(1)	20(1)	-2(1)	4(1)	2(1)
N(3)	22(1)	26(1)	20(1)	0(1)	2(1)	0(1)
N(4)	22(1)	26(1)	21(1)	-1(1)	3(1)	0(1)
C(11)	26(1)	25(1)	28(1)	-7(1)	0(1)	0(1)
C(12)	28(1)	34(1)	22(1)	-8(1)	2(1)	-3(1)
C(13)	27(1)	33(1)	24(1)	-4(1)	-3(1)	-3(1)
C(14)	25(1)	29(1)	27(1)	-4(1)	3(1)	-5(1)
C(15)	29(1)	24(1)	25(1)	-2(1)	1(1)	-4(1)
C(16)	33(1)	38(1)	40(1)	-12(1)	-1(1)	10(1)
C(17)	43(2)	58(2)	27(1)	-9(1)	10(1)	-4(1)
C(18)	38(1)	51(2)	38(1)	1(1)	-13(1)	-4(1)
C(19)	29(1)	47(2)	43(1)	-4(1)	11(1)	-4(1)
C(20)	41(1)	35(1)	29(1)	4(1)	1(1)	-6(1)
C(21)	34(1)	22(1)	26(1)	-1(1)	5(1)	-5(1)
C(22)	28(1)	26(1)	33(1)	-2(1)	4(1)	-7(1)
C(23)	34(1)	26(1)	28(1)	-3(1)	-3(1)	-5(1)
C(24)	38(1)	27(1)	22(1)	-7(1)	5(1)	-6(1)
C(25)	30(1)	24(1)	26(1)	-7(1)	4(1)	-3(1)
C(26)	57(2)	33(1)	29(1)	3(1)	10(1)	-5(1)
C(27)	32(1)	42(2)	63(2)	-1(1)	16(1)	-6(1)
C(28)	54(2)	42(2)	39(1)	-2(1)	-19(1)	-6(1)
C(29)	61(2)	45(2)	27(1)	-9(1)	16(1)	-8(1)
C(30)	38(1)	32(1)	43(1)	-9(1)	2(1)	5(1)
C(31)	28(1)	20(1)	25(1)	0(1)	2(1)	1(1)
C(32)	26(1)	26(1)	25(1)	3(1)	4(1)	4(1)
C(33)	26(1)	26(1)	25(1)	4(1)	-1(1)	0(1)
C(34)	30(1)	25(1)	25(1)	4(1)	2(1)	0(1)
C(35)	27(1)	22(1)	27(1)	3(1)	3(1)	-1(1)
C(36)	35(1)	27(1)	29(1)	-4(1)	-1(1)	0(1)
C(37)	29(1)	41(1)	33(1)	2(1)	8(1)	6(1)
C(38)	31(1)	41(1)	36(1)	1(1)	-6(1)	2(1)
C(39)	44(1)	41(1)	23(1)	1(1)	7(1)	-6(1)
C(40)	30(1)	30(1)	38(1)	1(1)	5(1)	-7(1)
C(41)	26(1)	55(2)	24(1)	-4(1)	6(1)	1(1)
C(42)	35(1)	68(2)	34(1)	-15(1)	9(1)	-5(1)
C(43)	48(2)	67(2)	31(1)	-11(1)	10(1)	-8(1)

C(44)	24(1)	39(1)	22(1)	-2(1)	6(1)	2(1)
C(45)	28(1)	44(1)	25(1)	-6(1)	4(1)	2(1)
C(46)	36(1)	52(2)	28(1)	1(1)	10(1)	3(1)
C(47)	22(1)	43(2)	42(1)	-1(1)	-5(1)	0(1)
C(48)	32(1)	34(1)	59(2)	-13(1)	-3(1)	-4(1)
C(49)	38(1)	39(2)	67(2)	8(1)	7(1)	-5(1)
C(50)	45(2)	59(2)	48(2)	1(1)	16(1)	-6(1)
C(51)	49(2)	42(2)	61(2)	-15(1)	18(1)	-5(1)
C(52)	33(1)	30(1)	60(2)	0(1)	6(1)	2(1)
C(53)	44(2)	71(2)	46(2)	-1(1)	-8(1)	0(1)
C(54)	28(1)	66(2)	46(2)	-6(1)	-5(1)	-2(1)
C(55)	34(1)	38(2)	76(2)	-14(1)	9(1)	-6(1)
C(56)	48(2)	46(2)	94(3)	4(2)	17(2)	0(2)
C(57)	48(2)	71(2)	51(2)	11(2)	15(1)	4(2)
C(58)	36(1)	47(2)	58(2)	-4(1)	9(1)	2(1)
C(59)	33(1)	41(2)	50(2)	2(1)	0(1)	5(1)
C(60)	49(2)	139(4)	50(2)	-19(2)	-2(2)	-10(2)

Table 13.88. Hydrogen coordinates (x 10^4) and isotropic displacement parameters ($Å^2$x 10^{3}) for **57**.

	x	y	z	U(eq)
H(6A)	8521	5143	2622	57
H(6B)	8152	5757	2164	57
H(6C)	8286	6234	2691	57
H(7A)	9401	6791	3286	59
H(7B)	10470	7002	3377	59
H(7C)	10093	5951	3429	59
H(8A)	12267	5947	2746	56
H(8B)	11903	6794	3067	56
H(8C)	12293	7004	2546	56
H(9A)	12109	6441	1734	56
H(9B)	11315	6306	1315	56
H(9C)	11744	5407	1595	56
H(10A)	9890	5544	1197	50
H(10B)	8919	5867	1377	50
H(10C)	9310	4843	1514	50
H(6B1)	8678	5313	2908	86
H(6B2)	8145	5954	2506	86
H(6B3)	8578	6421	2996	86
H(7B1)	11115	6806	3341	77
H(7B2)	10442	5943	3432	77
H(7B3)	10038	6983	3353	77
H(8B1)	12355	5835	2439	89
H(8B2)	12170	6712	2786	89
H(8B3)	12289	6876	2217	89
H(9B1)	11407	6383	1372	94
H(9B2)	10653	5614	1207	94
H(9B3)	11541	5308	1536	94
H(10D)	9007	5811	1332	90
H(10E)	8368	5487	1755	90
H(10F)	9139	4791	1574	90
H(16A)	8855	10759	2449	56
H(16B)	8366	9856	2203	56
H(16C)	8816	10632	1869	56
H(17A)	10078	9723	3378	63
H(17B)	9657	8705	3254	63

H(17C)	9093	9634	3100	63
H(18A)	11927	9339	3161	65
H(18B)	12271	8507	2824	65
H(18C)	11473	8317	3186	65
H(19A)	12406	9622	1792	59
H(19B)	11907	8766	1506	59
H(19C)	12440	8587	2023	59
H(20A)	10884	10539	1323	53
H(20B)	9795	10433	1295	53
H(20C)	10419	9587	1119	53
H(26A)	6524	4664	1061	59
H(26B)	6978	5592	1301	59
H(26C)	7613	4752	1129	59
H(27A)	4993	5568	433	68
H(27B)	5093	6685	381	68
H(27C)	5453	6171	874	68
H(28A)	5760	5916	-790	69
H(28B)	6176	6959	-782	69
H(28C)	5326	6715	-464	69
H(29A)	7601	5657	-933	66
H(29B)	8556	5672	-620	66
H(29C)	8045	6640	-760	66
H(30A)	8759	4563	47	57
H(30B)	8706	4677	625	57
H(30C)	9182	5477	316	57
H(36A)	8077	10414	1027	46
H(36B)	8484	9391	1154	46
H(36C)	7494	9678	1323	46
H(37A)	5758	9776	986	51
H(37B)	6062	8747	1170	51
H(37C)	5286	8863	740	51
H(38A)	5149	9252	-229	54
H(38B)	5190	8172	-62	54
H(38C)	5583	8476	-570	54
H(39A)	7386	9396	-907	54
H(39B)	6979	8353	-879	54
H(39C)	8049	8530	-769	54
H(40A)	8872	10207	-94	49
H(40B)	9154	9130	-171	49
H(40C)	9262	9594	361	49
H(41A)	6813	7376	2228	42
H(41B)	6800	8459	2061	42
H(42A)	7617	8772	2875	54
H(43A)	6303	7480	3052	58
H(43B)	6824	8210	3442	58
H(44A)	10664	6884	362	34
H(44B)	10651	8010	320	34
H(45A)	9888	6904	-481	38
H(46A)	11198	8314	-470	46
H(46B)	10732	7776	-953	46
H(48A)	6890	3691	257	50
H(49A)	7166	3898	-560	57
H(50A)	7222	2602	-1077	61
H(51A)	7033	1094	-762	60
H(52A)	6778	883	53	49
H(53A)	6279	2654	887	81
H(53B)	7226	2098	961	81
H(53C)	6305	1536	813	81
H(55A)	9210	8509	-2273	59
H(56A)	9423	8659	-3101	75
H(57A)	9638	7346	-3583	67
H(58A)	9680	5873	-3218	56

H(59A)	9452	5683	-2399	50
H(60A)	8878	7553	-1604	120
H(60B)	9780	6919	-1546	120
H(60C)	8807	6434	-1665	120

13.31. Crystallographic Data for $(C_5Me_4H)_2Sc[(^iPr)NC(CH_2CH{=}CH_2)N(^iPr)\text{-}\kappa^2N,N']$, 59

X-ray Data Collection, Structure Solution and Refinement for **59**.

A colorless crystal of approximate dimensions 0.28 x 0.32 x 0.38 mm was mounted on a glass fiber and transferred to a Bruker SMART APEX II diffractometer. The APEX2[1] program package was used to determine the unit-cell parameters and for data collection (20 sec/frame scan time for a sphere of diffraction data). The raw frame data was processed using SAINT[2] and SADABS[3] to yield the reflection data file. Subsequent calculations were carried out using the SHELXTL[4] program. There were no systematic absences nor any diffraction symmetry other than the Friedel condition. The centrosymmetric triclinic space group $P\bar{1}$ was assigned and later determined to be correct.

The structure was solved by direct methods and refined on F^2 by full-matrix least-squares techniques. The analytical scattering factors[5] for neutral atoms were used throughout the analysis. Hydrogen atoms were located from a difference-Fourier map and refined (x,y,z and U_{iso}).

At convergence, wR2 = 0.0815 and Goof = 1.036 for 460 variables refined against 5872 data (0.76Å), R1 = 0.0298 for those 5582 data with I > 2.0σ(I).

References

1. APEX2 Version 2.2-0, Bruker AXS, Inc.; Madison, WI 2007.
2. SAINT Version 7.46a, Bruker AXS, Inc.; Madison, WI 2007.
3. Sheldrick, G. M. SADABS, Version 2008/1, Bruker AXS, Inc.; Madison, WI 2008.
4. Sheldrick, G. M. SHELXTL, Version 2008/3, Bruker AXS, Inc.; Madison, WI 2008.
5. International Tables for X-Ray Crystallography 1992, Vol. C., Dordrecht: Kluwer Academic Publishers.

Table 13.89. Atomic coordinates (x 10^4) and equivalent isotropic displacement parameters (Å^{2}x 10^3) for **59**. U(eq) is defined as one third of the trace of the orthogonalized U^{ij} tensor.

	x	y	z	U(eq)
Sc(1)	2185(1)	2312(1)	2544(1)	12(1)
N(1)	2799(1)	4410(1)	3168(1)	16(1)
N(2)	3074(1)	3930(1)	1692(1)	15(1)
C(1)	-266(1)	1379(1)	3070(1)	17(1)
C(2)	-183(1)	899(1)	2153(1)	17(1)
C(3)	-181(1)	2108(1)	1649(1)	17(1)
C(4)	-271(1)	3337(1)	2249(1)	17(1)
C(5)	-308(1)	2877(1)	3122(1)	18(1)
C(6)	-518(1)	462(1)	3824(1)	23(1)
C(7)	-366(1)	-612(1)	1774(1)	24(1)
C(8)	-300(1)	2032(1)	652(1)	23(1)
C(9)	-427(1)	4841(1)	2015(1)	24(1)

C(10)	3707(1)	237(1)	2030(1)	18(1)
C(11)	4775(1)	1284(1)	2310(1)	18(1)
C(12)	4641(1)	1592(1)	3245(1)	18(1)
C(13)	3499(1)	731(1)	3553(1)	18(1)
C(14)	2933(1)	-100(1)	2800(1)	18(1)
C(15)	3521(2)	-487(1)	1108(1)	26(1)
C(16)	6003(1)	1835(1)	1768(1)	24(1)
C(17)	5671(1)	2548(1)	3800(1)	24(1)
C(18)	3082(1)	596(1)	4508(1)	24(1)
C(19)	3298(1)	4850(1)	2405(1)	15(1)
C(20)	4115(1)	6262(1)	2359(1)	20(1)
C(21)	5663(1)	6241(1)	2688(1)	27(1)
C(22)	6321(2)	7322(2)	3138(1)	38(1)
C(23)	2796(1)	5340(1)	3997(1)	19(1)
C(24)	2651(1)	4442(1)	4791(1)	24(1)
C(25)	1542(1)	6396(1)	4018(1)	26(1)
C(26)	3525(1)	4284(1)	799(1)	18(1)
C(27)	3587(1)	2943(1)	163(1)	24(1)
C(28)	2492(1)	5329(1)	402(1)	23(1)

Table 13.90. Anisotropic displacement parameters ($Å^2 x\ 10^3$) for **59**. The anisotropic displacement factor exponent takes the form: $-2\pi^2[\ h^2\ a^{*2}U^{11} + ...\ + 2\ h\ k\ a^*\ b^*\ U^{12}\ ]$

	U^{11}	U^{22}	U^{33}	U^{23}	U^{13}	U^{12}
Sc(1)	11(1)	11(1)	13(1)	1(1)	1(1)	0(1)
N(1)	16(1)	14(1)	16(1)	0(1)	0(1)	0(1)
N(2)	16(1)	14(1)	16(1)	2(1)	2(1)	0(1)
C(1)	12(1)	22(1)	18(1)	1(1)	2(1)	-2(1)
C(2)	13(1)	19(1)	18(1)	1(1)	0(1)	-3(1)
C(3)	11(1)	21(1)	18(1)	2(1)	-1(1)	-1(1)
C(4)	10(1)	20(1)	21(1)	2(1)	0(1)	1(1)
C(5)	12(1)	21(1)	19(1)	-2(1)	2(1)	1(1)
C(6)	24(1)	26(1)	20(1)	5(1)	5(1)	-3(1)
C(7)	25(1)	21(1)	24(1)	-2(1)	-2(1)	-5(1)
C(8)	22(1)	29(1)	18(1)	3(1)	-3(1)	-3(1)
C(9)	20(1)	21(1)	30(1)	4(1)	-2(1)	5(1)
C(10)	18(1)	14(1)	22(1)	0(1)	2(1)	5(1)
C(11)	13(1)	17(1)	23(1)	3(1)	2(1)	4(1)
C(12)	14(1)	18(1)	22(1)	4(1)	-1(1)	3(1)
C(13)	17(1)	17(1)	20(1)	5(1)	0(1)	4(1)
C(14)	18(1)	12(1)	23(1)	3(1)	1(1)	2(1)
C(15)	33(1)	20(1)	24(1)	-4(1)	4(1)	1(1)
C(16)	15(1)	30(1)	29(1)	5(1)	5(1)	2(1)
C(17)	17(1)	27(1)	28(1)	2(1)	-6(1)	-1(1)
C(18)	26(1)	27(1)	20(1)	8(1)	0(1)	1(1)
C(19)	12(1)	13(1)	21(1)	3(1)	0(1)	1(1)
C(20)	21(1)	14(1)	24(1)	3(1)	1(1)	-3(1)
C(21)	20(1)	22(1)	38(1)	6(1)	2(1)	-3(1)
C(22)	29(1)	42(1)	43(1)	0(1)	-4(1)	-12(1)
C(23)	22(1)	17(1)	19(1)	-3(1)	1(1)	-2(1)
C(24)	28(1)	26(1)	17(1)	-1(1)	0(1)	-1(1)
C(25)	30(1)	18(1)	28(1)	-3(1)	6(1)	3(1)
C(26)	19(1)	18(1)	18(1)	5(1)	3(1)	-1(1)
C(27)	28(1)	23(1)	19(1)	2(1)	6(1)	1(1)
C(28)	26(1)	23(1)	22(1)	8(1)	-1(1)	0(1)

Table 13.90. Hydrogen coordinates (x 10^4) and isotropic displacement parameters ($Å^2$x 10^{-3}) for **59**.

	x	y	z	U(eq)
H(5A)	-378(16)	3477(16)	3665(10)	23(3)
H(6A)	-338(17)	951(16)	4391(11)	28(4)
H(6B)	87(18)	-340(18)	3806(11)	34(4)
H(6C)	-1518(19)	164(18)	3832(11)	38(4)
H(7A)	-176(19)	-1283(19)	2192(12)	41(5)
H(7B)	-1360(20)	-796(19)	1565(12)	46(5)
H(7C)	304(18)	-847(17)	1279(11)	34(4)
H(8A)	-15(17)	2891(18)	420(11)	32(4)
H(8B)	-1284(18)	1787(17)	452(11)	32(4)
H(8C)	325(18)	1319(18)	376(11)	35(4)
H(9A)	-940(20)	5370(20)	2427(14)	56(6)
H(9B)	450(20)	5330(20)	2003(13)	52(5)
H(9C)	-930(30)	4930(30)	1496(16)	75(7)
H(14A)	2135(16)	-817(16)	2829(10)	24(3)
H(15A)	2980(20)	-1330(20)	1103(13)	53(5)
H(15B)	2990(20)	40(20)	709(14)	55(5)
H(15C)	4410(30)	-800(30)	874(17)	82(7)
H(16A)	5919(18)	2829(19)	1672(11)	34(4)
H(16B)	6061(18)	1325(17)	1200(11)	33(4)
H(16C)	6900(20)	1728(18)	2055(11)	39(4)
H(17A)	5550(19)	2444(18)	4413(12)	39(4)
H(17B)	5517(19)	3534(19)	3731(11)	39(4)
H(17C)	6670(20)	2393(18)	3644(12)	41(4)
H(18A)	3890(20)	760(20)	4893(14)	60(6)
H(18B)	2750(20)	-350(20)	4590(13)	54(5)
H(18C)	2290(20)	1210(20)	4708(12)	43(5)
H(20A)	3635(17)	7004(17)	2698(10)	29(4)
H(20B)	4133(16)	6495(16)	1746(10)	27(4)
H(21A)	6170(20)	5370(20)	2511(12)	45(5)
H(22A)	5810(20)	8150(20)	3305(14)	56(6)
H(22B)	7350(20)	7235(19)	3320(12)	44(5)
H(23A)	3740(16)	5867(15)	4067(10)	23(3)
H(24A)	1747(17)	3845(17)	4729(10)	29(4)
H(24B)	3497(17)	3835(17)	4850(10)	30(4)
H(24C)	2590(17)	5028(17)	5327(11)	30(4)
H(25A)	609(18)	5881(17)	4025(10)	32(4)
H(25B)	1566(17)	6959(17)	3504(11)	33(4)
H(25C)	1612(18)	7018(18)	4546(11)	36(4)
H(26A)	4541(15)	4694(15)	819(9)	19(3)
H(27A)	3849(17)	3170(17)	-429(11)	31(4)
H(27B)	2644(19)	2459(17)	119(11)	35(4)
H(27C)	4297(19)	2302(19)	361(11)	40(4)
H(28A)	1561(18)	4875(17)	280(10)	31(4)
H(28B)	2335(17)	6168(17)	777(10)	27(4)
H(28C)	2890(19)	5632(18)	-147(12)	38(4)

13.32. Crystallographic Data for $(C_5Me_4H)_5Sc_5(\mu_5\text{-}O)(\mu_3\text{-}OH)_4(\mu_2\text{-}OH)_4\cdot[(C_6H_5)NH]_2$, 61
X-ray Data Collection, Structure Solution and Refinement for **61**.

A colorless crystal of approximate dimensions 0.06 x 0.23 x 0.34 mm was mounted on a glass fiber and transferred to a Bruker SMART APEX II diffractometer. The APEX2[1] program package was used to determine the unit-cell parameters and for data collection (40 sec/frame scan time for a sphere of diffraction data). The raw frame data was processed using SAINT[2] and SADABS[3] to yield the reflection data file. Subsequent calculations were carried out using the SHELXTL[4] program. The diffraction symmetry was 2/*m* and the systematic absences were consistent with the monoclinic space group $P2_1/c$ that was later determined to be correct.

The structure was solved by direct methods and refined on F^2 by full-matrix least-squares techniques. The analytical scattering factors[5] for neutral atoms were used throughout the analysis. Hydrogen atoms H(1)-H(8) were located from a difference-Fourier map and refined (x,y,z and U_{iso}). The remaining hydrogen atoms were included using a riding model. There was one-half molecule of benzene solvent present per formula unit. The solvent was located about an inversion center and was disordered. The nitrogen atoms and carbons C(37)-C(45) were also disordered. All disordered atoms were included using multiple components, partial site-occupancy-factors and isotropic thermal parameters.

At convergence, wR2 = 0.1103 and Goof = 1.028 for 723 variables refined against 12960 data (0.78Å), R1 = 0.0422 for those 10593 data with I > 2.0σ(I).

References

1. APEX2 Version 2008.3-0,. Bruker AXS, Inc.; Madison, WI 2008.
2. SAINT Version 7.68a, Bruker AXS, Inc.; Madison, WI 2009.
3. Sheldrick, G. M. SADABS, Version 2008/1, Bruker AXS, Inc.; Madison, WI 2008.
4. Sheldrick, G. M. SHELXTL, Version 2008/4, Bruker AXS, Inc.; Madison, WI 2008.
5. International Tables for X-Ray Crystallography 1992, Vol. C., Dordrecht: Kluwer Academic Publishers.

Table 13.91. Atomic coordinates (x 10^4) and equivalent isotropic displacement parameters (Å^{2}x 10^3) for **61**. U(eq) is defined as one third of the trace of the orthogonalized U^{ij} tensor.

	x	y	z	U(eq)
Sc(1)	1372(1)	5058(1)	1590(1)	10(1)
Sc(2)	2474(1)	5360(1)	2853(1)	11(1)
Sc(3)	2424(1)	3281(1)	2068(1)	11(1)
Sc(4)	2465(1)	4618(1)	871(1)	11(1)
Sc(5)	2495(1)	6697(1)	1657(1)	12(1)
O(1)	1753(1)	6369(1)	2190(1)	13(1)
O(2)	1695(1)	4170(1)	2456(1)	14(1)
O(3)	1719(1)	3691(1)	1175(1)	13(1)
O(4)	1763(1)	5885(1)	902(1)	12(1)
O(5)	2997(1)	3975(1)	2879(1)	14(1)
O(6)	3084(1)	6393(1)	2549(1)	15(1)
O(7)	3041(1)	3522(1)	1475(1)	17(1)
O(8)	3055(1)	5932(1)	1132(1)	16(1)
O(9)	2377(1)	4996(1)	1848(1)	12(1)
N(1)	4242(2)	4557(3)	2528(2)	35(1)
N(2)	4272(2)	5373(3)	2105(1)	32(1)
N(1B)	4320(5)	4259(10)	2641(5)	20(3)
N(2B)	4096(5)	4811(9)	2078(5)	24(3)

C(1)	381(1)	5899(2)	963(1)	16(1)
C(2)	299(1)	5904(2)	1587(1)	19(1)
C(3)	257(1)	4842(2)	1779(1)	20(1)
C(4)	317(1)	4180(2)	1273(1)	18(1)
C(5)	390(1)	4837(2)	772(1)	15(1)
C(6)	412(1)	6862(2)	568(1)	21(1)
C(7)	193(1)	6884(2)	1935(1)	29(1)
C(8)	97(1)	4461(2)	2376(1)	32(1)
C(9)	261(1)	3000(2)	1257(1)	28(1)
C(10)	3004(1)	6105(2)	3935(1)	17(1)
C(11)	2818(1)	5079(2)	4064(1)	17(1)
C(12)	2152(1)	5040(2)	3896(1)	16(1)
C(13)	1926(1)	6045(2)	3672(1)	16(1)
C(14)	2452(1)	6695(2)	3693(1)	18(1)
C(15)	3666(1)	6513(2)	4071(1)	24(1)
C(16)	3245(1)	4226(2)	4395(1)	22(1)
C(17)	1760(1)	4124(2)	4009(1)	22(1)
C(18)	1254(1)	6395(2)	3498(1)	25(1)
C(19)	2485(1)	1387(2)	1725(1)	20(1)
C(20)	2952(1)	1499(2)	2294(1)	19(1)
C(21)	2648(1)	1664(2)	2790(1)	19(1)
C(22)	1994(1)	1681(2)	2526(1)	20(1)
C(23)	1898(1)	1520(2)	1868(1)	22(1)
C(24)	2587(2)	1071(2)	1094(1)	29(1)
C(25)	3651(1)	1414(2)	2367(1)	28(1)
C(26)	2968(1)	1664(2)	3480(1)	28(1)
C(27)	1486(1)	1701(2)	2886(1)	31(1)
C(28)	2987(1)	3951(2)	37(1)	15(1)
C(29)	2742(1)	4942(2)	-197(1)	19(1)
C(30)	2077(1)	4876(2)	-345(1)	20(1)
C(31)	1913(1)	3842(2)	-207(1)	18(1)
C(32)	2474(1)	3279(2)	30(1)	15(1)
C(33)	3666(1)	3639(2)	222(1)	25(1)
C(34)	3122(2)	5853(2)	-338(1)	31(1)
C(35)	1621(2)	5706(3)	-671(1)	42(1)
C(36)	1262(1)	3391(2)	-352(1)	32(1)
C(37)	2471(3)	8590(3)	1978(2)	14(1)
C(38)	3049(2)	8470(4)	1791(3)	15(1)
C(39)	2892(2)	8288(3)	1125(2)	13(1)
C(40)	2244(2)	8281(3)	907(2)	13(1)
C(41)	1979(2)	8453(3)	1428(2)	11(1)
C(42)	2402(2)	8912(4)	2613(2)	25(1)
C(43)	3706(2)	8568(4)	2188(2)	30(1)
C(44)	3361(2)	8275(4)	710(2)	29(1)
C(45)	1891(2)	8230(4)	218(2)	26(1)
C(37B)	2101(3)	8564(4)	1815(3)	15(1)
C(38B)	2745(3)	8579(4)	2086(2)	14(1)
C(39B)	3072(3)	8406(5)	1611(3)	16(1)
C(40B)	2612(3)	8295(4)	1031(3)	17(1)
C(41B)	2031(2)	8367(4)	1156(3)	16(1)
C(42B)	1566(3)	8819(6)	2111(3)	37(2)
C(43B)	3013(3)	8863(5)	2777(3)	35(2)
C(44B)	3781(3)	8406(6)	1760(3)	38(2)
C(45B)	2788(3)	8255(6)	414(3)	40(2)
C(46)	4617(1)	4717(3)	3151(1)	34(1)
C(47)	4610(2)	3914(3)	3594(2)	53(1)
C(48)	4957(2)	4001(4)	4191(2)	65(1)
C(49)	5315(2)	4870(3)	4359(2)	54(1)
C(50)	5354(2)	5669(4)	3957(2)	66(1)
C(51)	4981(2)	5603(3)	3299(2)	54(1)
C(52)	4615(1)	5135(3)	1673(1)	44(1)
C(53)	4656(2)	5944(4)	1257(2)	61(1)

C(54)	5014(2)	5854(5)	836(2)	81(2)
C(55)	5341(2)	4960(5)	811(2)	74(2)
C(56)	5316(2)	4133(4)	1214(2)	67(1)
C(57)	4950(1)	4206(3)	1658(2)	49(1)
C(58)	-622(3)	9738(7)	-130(4)	62(2)
C(59)	-272(4)	9732(7)	481(3)	62(2)
C(60)	360(4)	9987(5)	625(3)	53(2)
C(58B)	-565(4)	10189(8)	124(5)	43(3)
C(59B)	-57(6)	10211(10)	618(6)	57(3)
C(60B)	552(6)	10012(9)	469(6)	49(3)

Table 13.92. Anisotropic displacement parameters ($Å^2 x\ 10^3$) for **61**. The anisotropic displacement factor exponent takes the form: $-2\pi^2[\ h^2\ a^{*2}U^{11} + ...\ + 2\ h\ k\ a^*\ b^*\ U^{12}\ ]$

	U^{11}	U^{22}	U^{33}	U^{23}	U^{13}	U^{12}
Sc(1)	12(1)	10(1)	10(1)	0(1)	3(1)	0(1)
Sc(2)	14(1)	9(1)	9(1)	-1(1)	3(1)	0(1)
Sc(3)	15(1)	8(1)	10(1)	0(1)	4(1)	0(1)
Sc(4)	13(1)	9(1)	10(1)	1(1)	5(1)	1(1)
Sc(5)	14(1)	8(1)	13(1)	1(1)	3(1)	-1(1)
O(1)	17(1)	11(1)	13(1)	-2(1)	5(1)	1(1)
O(2)	17(1)	13(1)	13(1)	0(1)	5(1)	0(1)
O(3)	16(1)	10(1)	12(1)	-2(1)	4(1)	-3(1)
O(4)	15(1)	12(1)	11(1)	2(1)	3(1)	0(1)
O(5)	19(1)	13(1)	10(1)	1(1)	2(1)	2(1)
O(6)	18(1)	13(1)	14(1)	0(1)	2(1)	-2(1)
O(7)	27(1)	13(1)	12(1)	3(1)	8(1)	0(1)
O(8)	19(1)	14(1)	15(1)	3(1)	7(1)	0(1)
O(9)	14(1)	11(1)	10(1)	0(1)	4(1)	0(1)
C(1)	10(1)	19(1)	18(1)	0(1)	1(1)	0(1)
C(2)	12(1)	25(1)	19(1)	-2(1)	3(1)	3(1)
C(3)	11(1)	31(1)	19(1)	2(1)	5(1)	-1(1)
C(4)	11(1)	20(1)	22(1)	2(1)	1(1)	-3(1)
C(5)	12(1)	16(1)	15(1)	0(1)	1(1)	0(1)
C(6)	16(1)	17(1)	28(1)	4(1)	2(1)	1(1)
C(7)	23(1)	34(2)	27(1)	-10(1)	3(1)	10(1)
C(8)	22(1)	50(2)	26(1)	7(1)	12(1)	-3(1)
C(9)	22(1)	22(1)	37(2)	4(1)	2(1)	-8(1)
C(10)	24(1)	17(1)	10(1)	-4(1)	4(1)	-2(1)
C(11)	22(1)	18(1)	9(1)	-2(1)	2(1)	2(1)
C(12)	23(1)	16(1)	9(1)	-1(1)	5(1)	0(1)
C(13)	21(1)	18(1)	11(1)	-2(1)	6(1)	3(1)
C(14)	27(1)	15(1)	11(1)	-3(1)	6(1)	1(1)
C(15)	23(1)	27(1)	19(1)	-5(1)	2(1)	-6(1)
C(16)	27(1)	24(1)	15(1)	1(1)	3(1)	7(1)
C(17)	28(1)	22(1)	19(1)	2(1)	9(1)	-2(1)
C(18)	24(1)	32(1)	22(1)	2(1)	8(1)	10(1)
C(19)	38(1)	6(1)	18(1)	0(1)	10(1)	-1(1)
C(20)	27(1)	8(1)	22(1)	3(1)	8(1)	2(1)
C(21)	33(1)	8(1)	17(1)	2(1)	7(1)	0(1)
C(22)	31(1)	8(1)	25(1)	2(1)	13(1)	-3(1)
C(23)	29(1)	9(1)	24(1)	3(1)	2(1)	-5(1)
C(24)	59(2)	12(1)	18(1)	-1(1)	14(1)	-1(1)
C(25)	28(1)	19(1)	37(2)	4(1)	9(1)	7(1)
C(26)	50(2)	16(1)	17(1)	3(1)	5(1)	1(1)
C(27)	39(2)	20(1)	42(2)	5(1)	24(1)	-3(1)
C(28)	19(1)	16(1)	13(1)	-2(1)	7(1)	2(1)
C(29)	30(1)	16(1)	14(1)	0(1)	12(1)	0(1)
C(30)	29(1)	24(1)	10(1)	2(1)	7(1)	11(1)

C(31)	20(1)	26(1)	9(1)	-5(1)	4(1)	1(1)
C(32)	21(1)	15(1)	11(1)	-2(1)	6(1)	-1(1)
C(33)	20(1)	36(1)	20(1)	-5(1)	7(1)	3(1)
C(34)	57(2)	21(1)	22(1)	-1(1)	24(1)	-10(1)
C(35)	61(2)	46(2)	18(1)	10(1)	12(1)	35(2)
C(36)	20(1)	55(2)	20(1)	-14(1)	6(1)	-5(1)
C(46)	23(1)	51(2)	30(1)	-8(1)	12(1)	5(1)
C(47)	45(2)	70(2)	50(2)	2(2)	24(2)	13(2)
C(48)	43(2)	94(3)	60(2)	-1(2)	16(2)	11(2)
C(49)	44(2)	83(3)	37(2)	-12(2)	13(2)	-4(2)
C(50)	28(2)	91(3)	82(3)	-23(3)	18(2)	-13(2)
C(51)	32(2)	72(3)	64(2)	-33(2)	25(2)	-16(2)
C(52)	25(1)	75(2)	26(2)	-9(2)	-2(1)	10(2)
C(53)	44(2)	73(3)	55(2)	-3(2)	-7(2)	-8(2)
C(54)	42(2)	121(5)	75(3)	15(3)	5(2)	-25(3)
C(55)	31(2)	152(5)	41(2)	2(3)	9(2)	-8(3)
C(56)	29(2)	117(4)	49(2)	-21(2)	-2(2)	27(2)
C(57)	31(2)	80(3)	34(2)	-4(2)	1(1)	20(2)

Table 13.93. Hydrogen coordinates (x 10^4) and isotropic displacement parameters ($Å^2$x 10^{3}) for **61**.

	x	y	z	U(eq)
H(1A)	4010	3991	2417	42
H(2A)	4086	5985	2114	38
H(1BA)	4256	3574	2646	24
H(2BA)	3697	4978	1944	29
H(5A)	362	4596	329	18
H(6A)	6	7224	476	31
H(6B)	511	6651	170	31
H(6C)	739	7338	800	31
H(7A)	-212	7197	1725	43
H(7B)	530	7390	1934	43
H(7C)	191	6703	2372	43
H(8A)	-329	4170	2273	47
H(8B)	120	5052	2670	47
H(8C)	396	3913	2572	47
H(9A)	-177	2800	1225	42
H(9B)	527	2704	1646	42
H(9C)	396	2726	890	42
H(14A)	2436	7476	3628	21
H(15A)	3823	6622	4528	35
H(15B)	3674	7184	3850	35
H(15C)	3933	6000	3924	35
H(16A)	3344	4348	4853	33
H(16B)	3634	4230	4249	33
H(16C)	3037	3541	4300	33
H(17A)	1708	4154	4443	34
H(17B)	1969	3464	3947	34
H(17C)	1347	4157	3711	34
H(18A)	1087	6397	3877	38
H(18B)	1008	5911	3184	38
H(18C)	1228	7108	3320	38
H(23A)	1482	1385	1569	26
H(24A)	2670	312	1093	44
H(24B)	2947	1458	1014	44
H(24C)	2211	1237	761	44
H(25A)	3833	968	2733	42
H(25B)	3839	2118	2432	42

H(25C)	3735	1101	1984	42
H(26A)	3053	936	3627	43
H(26B)	2695	2002	3719	43
H(26C)	3364	2053	3547	43
H(27A)	1394	979	2996	47
H(27B)	1106	2020	2621	47
H(27C)	1628	2116	3274	47
H(32A)	2502	2500	98	18
H(33A)	3813	3489	-160	38
H(33B)	3714	3008	489	38
H(33C)	3913	4217	457	38
H(34A)	3199	5765	-760	46
H(34B)	3524	5879	-22	46
H(34C)	2893	6512	-324	46
H(35A)	1535	5607	-1131	62
H(35B)	1802	6406	-561	62
H(35C)	1228	5643	-534	62
H(36A)	1142	3169	-796	47
H(36B)	968	3927	-276	47
H(36C)	1252	2781	-78	47
H(41A)	1525	8598	1399	13
H(42A)	2380	9682	2633	38
H(42B)	2764	8660	2937	38
H(42C)	2017	8605	2689	38
H(43A)	3927	9118	2012	45
H(43B)	3925	7895	2190	45
H(43C)	3695	8755	2623	45
H(44A)	3514	8992	672	43
H(44B)	3155	8006	289	43
H(44C)	3715	7817	903	43
H(45A)	1923	8911	16	39
H(45B)	1449	8068	190	39
H(45C)	2074	7679	3	39
H(41B)	1627	8421	826	19
H(42D)	1532	9585	2148	56
H(42E)	1644	8498	2532	56
H(42F)	1175	8540	1844	56
H(43D)	2907	9596	2849	52
H(43E)	3470	8781	2880	52
H(43F)	2835	8395	3046	52
H(44D)	3939	9097	1928	57
H(44E)	3920	8261	1373	57
H(44F)	3944	7861	2075	57
H(45D)	2839	8974	270	59
H(45E)	2457	7895	102	59
H(45F)	3184	7870	464	59
H(47A)	4357	3306	3471	63
H(48A)	4952	3459	4491	78
H(49A)	5552	4924	4785	65
H(50A)	5617	6259	4097	80
H(51A)	4992	6138	2996	64
H(53A)	4427	6575	1269	73
H(54A)	5036	6421	557	97
H(55A)	5590	4901	512	89
H(56A)	5550	3510	1191	80
H(57A)	4930	3641	1939	59
H(58A)	-1053	9550	-217	75
H(59A)	-466	9549	812	75
H(60A)	604	9973	1050	64
H(58B)	-962	10330	209	52
H(59B)	-91	10346	1037	68
H(60B)	930	10027	794	59

H(1)	1547(11)	6852(16)	2314(13)	25(3)
H(2)	1455(11)	3880(20)	2654(12)	25(3)
H(3)	1497(11)	3243(17)	929(11)	25(3)
H(4)	1545(11)	6210(20)	586(9)	25(3)
H(5)	3140(12)	3660(20)	3221(8)	25(3)
H(6)	3321(11)	6837(17)	2773(11)	25(3)
H(7)	3368(8)	3220(20)	1466(13)	25(3)
H(8)	3257(12)	6240(20)	904(11)	25(3)

List of Abbreviations

BMIM	1-butyl-1-methylimidazolium
°C	degree Celsius
Ch.	chapter
DMA	dimethylacetamide
EA	elemental analysis
Et	ethyl
h	hour
IR	infrared
Ln	lanthanide (La-Lu)
Me	methyl
MeCN	acetonitrile
min	minute
NMR	nuclear magnetic resonance
^{i}Pr	isopropyl
PNP	bis(triphenylphosphineiminium)
py	pyridyl
rt	room temperature
THF	tetrahydrofurane
TMSCN	trimethylsilylcyanide

List of Complexes

Compound	Number
$\{CSc_6\}I_{12}Sc$ #	**1**
$[(C_5H_5)_2ScNSc(C_5H_5)(THF)]_2$	**2**
$[(C_5H_5)_2Sc]_2[\mu\text{-}O(C_3H_7)]_2$	**3**
$Sc_3N@C_{80}$ #	**4**
$[(C_5H_5)_2Ti]_2[\mu\text{-}O(C_2H_5)]_2$ #	**5**
$(C_5Me_4H)_2ScCl(THF)$	**6**
$(C_5Me_4H)_2Sc(\eta^3\text{-}C_3H_5)$	**7**
$[(C_5Me_4H)_2Sc][(\mu\text{-}Ph)BPh_3]$	**8**
$[(C_5Me_4H)_2Sc(THF)_2][BPh_4]$	**9**
$[(C_5Me_4H)_2Sc]_2(\mu\text{-}\eta^2\text{:}\eta^2\text{-}N_2)$	**10**
$\{[(C_5Me_4H)_2Sc]_2(\mu\text{-}\eta^2\text{:}\eta^2\text{-}N_2)[(C_5Me_4H)_2Sc]_2(\mu\text{-}O)\}$	**11**
$(C_5Me_4H)(C_5H_4CH_2CH_2NMe_2)ScCl$ #	**12**
$(C_5Me_5)_2YCl(THF)$ #	**13**
rac-$Me_2Si[\eta^5\text{-}C_5H_2\text{-}2,4\text{-}(CHMe_2)_2]_2Sc(\eta^3\text{-}C_3H_5)$ #	**14**
$(C_5Me_4H)_2Y(\eta^3\text{-}C_3H_5)$ #	**15**
$[(C_5Me_4H)_2Lu][(\mu\text{-}\eta^2\text{:}\eta^1\text{-}Ph)_2BPh_2]$ #	**16**
$[(C_5Me_5)_2Sc][(\mu\text{-}\eta^2\text{:}\eta^1\text{-}Ph)BPh_3]$ #	**17**
$\{[(Me_3Si)_2N]_2(THF)Y\}_2(\mu\text{-}\eta^2\text{:}\eta^2\text{-}N_2)$ #	**18**
$[(C_5Me_4H)_2Lu(THF)]_2(\mu\text{-}\eta^2\text{:}\eta^2\text{-}N_2)$ #	**19**
$(C_5Me_4H)_2Y(BH_4)(THF)$	**20**
$(C_5Me_5)_2Y(BH_4)(THF)$	**21**

$[(C_5Me_4H)_2Y][(\mu\text{-}Ph)_2BPh_2]$ #	**22**
$[(C_5Me_5)_2Y][(\mu\text{-}Ph)_2BPh_2]$ #	**23**
$(C_5Me_4H)_2Sc(BH_4)$	**24**
$(C_5Me_5)_2Sc(BH_4)(THF)$	**25**
$(C_5Me_5)_2Sc(BH_4)$	**25a**
$(C_5Me_5)_2ScCl(THF)$	**26**
$(C_5Me_5)_2Sc(BH_4)_{0.5}(Cl)_{0.5}(THF)$	**27**
$[\{C_3H_3(SiMe_3)_2\}_2Sc][(\mu\text{-}H)_2BH_2]$ #	**28**
$(C_5Me_5)_2Sc(\mu\text{-}H)_2BC_8H_{14}$	**29**
$(C_5Me_4H)_2Sc(\mu\text{-}H)_2BC_8H_{14}$	**30**
$(C_5Me_4H)_2Sc(\mu\text{-}O)BC_8H_{14}$	**31**
$(C_5Me_5)_2Sc(\eta^3\text{-}C_3H_5)$	**32**
$(C_5Me_5)_2Y(\mu\text{-}H)_2BC_8H_{14}$ #	**33**
$[(C_5H_5)_2Zr(H)O(BC_8H_{14})]_2$ #	**34**
$(\eta^5\text{-}C_5Me_4H)_2Sc(\eta^1\text{-}C_5Me_4H)$	**35**
$[(C_5Me_4H)_2ScSPh]_2$	**36**
$(C_5Me_4H)_2ScSePh$	**37**
$(C_5Me_4H)_2ScTePh$	**38**
$(C_5Me_4H)_2ScSPh(THF)$	**39**
$(C_5Me_4H)_2ScSePh(THF)$	**40**
$(C_5Me_4H)_2ScTePh(THF)$	**41**
$(C_5Me_4H)_2ScSpy$	**42**
$[(C_5Me_4H)Sc]_3[SePh]_3$	**43**
$[(C_5Me_5)_2Y(SPh)]_2$ #	**44**
$[(C_5Me_5)_2Sm(SPh)]_2$ #	**45**

$(C_5Me_5)_2SmSPh(THF)$	**46**
$(C_5Me_5)_2ScSmPh(THF)$	**47**
$(C_5Me_5)_2SmTePh(THF)$	**48**
$[(C_5H_5)_2Mo(2\text{-}Spy)][PF_6]$ [#]	**49**
$(C_5Me_5)_2[^iPrNC(Me)N^iPr\text{-}\kappa^2N,N']U(Spy)$ [#]	**50**
$\{[(C_5Me_5)Sc)_4](\mu_3\text{-}Te)_4\}$	**51**
$\{[(C_5Me_5)Co)_4](\mu_3\text{-}Te)_4\}$ [#]	**52**
$[(C_5Me_4H)_2Sc(\mu\text{-}\eta^1{:}\eta^2\text{-}ON{=}NC_3H_5)]_2$	**53**
$[(C_5Me_4H)_2Y(\mu\text{-}\eta^1{:}\eta^2\text{-}ON{=}NC_3H_5)]_2$	**54**
$[(C_5Me_5)_2Y(\mu\text{-}\eta^1{:}\eta^2\text{-}ON{=}NC_3H_5)]_2$	**55**
$[(C_5Me_5)_2Sm(\mu\text{-}\eta^1{:}\eta^2\text{-}ON{=}NC_3H_5)]_2$	**56**
$[(C_5Me_5)_2La(\mu\text{-}\eta^1{:}\eta^2\text{-}ON{=}NC_3H_5)]_2$	**57**
$[(C_5Me_5)_2Sm(\mu\text{-}\eta^1{:}\eta^2\text{-}ON{=}NCH_2Ph)]_2$ [#]	**58**
$(C_5Me_4H)_2Sc[(^iPr)NC(CH_2CH{=}CH_2)N(^iPr)\text{-}\kappa^2N,N']$	**59**
$(C_5Me_5)_2Sc[(H)NC(Me)N(NMe_2)\text{-}\kappa^2N,N']$ [#]	**60**
$(C_5Me_4H)_5Sc_5(\mu_5\text{-}O)(\mu_3\text{-}OH)_4(\mu_2\text{-}OH)_4\cdot[(C_6H_5)NH]_2$	**61**
$(C_5Me_5)_5Y_5(\mu_5\text{-}O)(\mu_3\text{-}OMe)_4(\mu\text{-}OMe)_4$ [#]	**62**
$(O^iPr)_5Sc_5(\mu_5\text{-}O)(\mu_3\text{-}O^iPr)_4(\mu\text{-}O^iPr)_4$ [#]	**63**
$(O^iPr)_5Y_5(\mu_5\text{-}O)(\mu_3\text{-}O^iPr)_4(\mu\text{-}O^iPr)_4$ [#]	**64**

[#] References for the literature compounds are given in the corresponding chapters.

Acknowledgements

First and foremost I would like to acknowledge my supervisor Prof. Dr. Gerd Meyer for his great support throughout the last years, fruitful discussions and providing me with the opportunity of having research stays at the University of California Irvine.

I would like to express my gratitude to Prof. William J. Evans PhD, University of California Irvine, for supporting me during my time in his labs and beyond. I thank you for providing me from the day one with all resources upon which a great part of this dissertation was built and showing me the appeal of organometallic chemistry.

My thank goes also to Prof. Dr. Hans-Günther Schmalz for being chairman.

I am very grateful to Joseph W. Ziller PhD for his contribution to this thesis. I appreciate your ability to mount extremely air-sensitive crystals and solve their structures. Furthermore, I would like to thank Prof. Dr. Filipp Furche and Ming Fang PhD for theoretical studies. In addition, I am grateful to André Uthe and Prof. Dr. Axel Klein for EPR measurements and PD. Dr. Leo van Wüllen for the ^{45}Sc-MAS-NMR measurement.

Furthermore, I would like to thank the members of the Meyer Lab, past and present, for creating a wonderful working atmosphere. Additionally, I would like to make a special note to my lab mates Verena Lingen and Johannes Hermle. You were always very supportive of me. I thank you for making my time in the lab such an enjoyable one.

I am very thankful to the Members of the Evans' Lab for all of their support and fantastic working atmosphere. It was a privilege being a part of this team. I would like to separately

thank Thomas J. Mueller and Ian J. Casely PhD for their willingness to help and teach me in air-sensitive organometallic chemistry.

My special thanks go to my family and friends for their constant support and for reminding me of other crucial aspects of life.

Finally, I would like to thank the Fonds der Chemischen Industrie for providing me a Chemiefonds fellowship.

Erklärung

Ich versichere, dass ich die von mir vorgelegte Dissertation selbstständig angefertigt, die benutzten Quellen und Hilfsmittel vollständig angegeben und die Stellen der Arbeit – einschließlich Tabellen, Karten, Abbildungen -, die anderen Werken im Wortlaut oder dem Sinn nach entnommen sind, in jedem Einzelfall als Entlehnung kenntlich gemacht habe; dass diese Dissertation noch keiner anderen Fakultät oder Universität zur Prüfung vorgelegen hat; dass sie - abgesehen von unten angegebenen Teilpublikationen- noch nicht veröffentlicht worden ist sowie, dass ich eine Veröffentlichung vor Abschluss des Promotionsverfahrens nicht vornehmen werde. Die Bestimmungen der Promotionsverordnung sind mir bekannt. Die von mir vorgelegte Dissertation ist von Prof. Dr. Gerd Meyer betreut worden.

Köln, 24.08.2010

Zur Wahrung der Priorität sind folgende Teile dieser Arbeit bereits publiziert:

Demir, S.; Lorenz, S. E.; Fang, M.; Furche, F.; Meyer, G.; Ziller, J. W.; Evans, W. J. *J. Am. Chem. Soc.* **2010**, *132*, 11151-11158.

Demir, S.; Mueller, T. J.; Ziller, J. W; Evans, W. J. *Angew. Chem. Int. Ed.*, DOI: 10.1002/anie.201005898; *Angew. Chem.*, DOI: 10.1002/ange.201005898.

Demir, S.; Mueller, T. J.; Ziller, J. W.; Evans, W. J. *manuscript in preparation*.

Demir, S.; Montalvo, E.; Ziller, J. W.; Meyer, G.; Evans, W. J. *Organometallics* **2010**, *29*, 6608-6611.